MATEMATISK-FYSISKE
MEDDELELSER

UDGIVET AF

DET KGL. DANSKE VIDENSKABERNES SELSKAB

BIND XXIV

KØBENHAVN

I KOMMISSION HOS EJNAR MUNKSGAARD

1946—50

INDHOLD

DET KGL. DANSKE VIDENSKABERNES SELSKAB
MATEMATISK-FYSISKE MEDDELELSER, BIND XXIV, NR. 1

THE POTENTIAL FUNCTION OF ETHANE

BY

BØRGE BAK

KØBENHAVN
I KOMMISSION HOS EJNAR MUNKSGAARD
1946

CONTENTS

Printed in Denmark.
Bianco Lunos Bogtrykkeri A/S

I. Introduction.

In dealing with the problem of finding the coefficients of the general quadratic potential function of molecules for the internal degrees of freedom it is usually found, that the experimental material available is insufficient for a determination of all the force-constants. The well-known 'valence-force' and 'central-force' models are generally applied means of avoiding this difficulty. However, the use of these models very often is evidently wrong, e. g. as demonstrated by the author as regards benzene[1].

In order to find some relations between the theoretically independent force-constants of the general quadratic potential function, based upon less rigorous assumptions than those laid down in the valence-force or central-force systems, the author looked for such rules in the case of *HCN*, CH_4 and C_2H_2[2] and succeeded in putting forward an 'empirical rule' valid for the three molecules mentioned: If one or more hydrogen atoms connected with the same carbon atom are displaced towards the adjoining carbon atom, the forces acting upon the other atoms of the molecule could as a good approximation be put equal to zero.

To see if a more general validity of this rule could be stated, the potential function of ethane was investigated. Ethane is the prototype of alifatic hydrocarbons with a carbon-chain, which means that the results obtained are of more than special interest. The result of the investigation of ethane may be briefly summarized as follows:

As far as only vibrations, non-degenerate with respect to the threefold axis of ethane, are considered, the 'empirical rule' helps to find a set of force-constants which are probably correct. But

1) B. Bak, Det Kgl. Danske Vidensk. Selskab, mat.-fys. Medd. XXII, 9 (1945).
2) B. Bak, ibid. XXII, 16 (1946).

in the case of degenerate vibrations the application of the rule gives false results. This, of course, means that the rule should be handled with much care as its domain of validity is undetermined.

Even if only a partial knowledge of the potential function of ethane is obtained, such knowledge is of importance, too. It can be foreseen that during the next years the study of the spectra of the partially deuterated ethanes will be among the principal means by which to decide finally whether ethane has the D_{3d} or the D_{3h} configuration[1]. For the interpretation of those spectra even a partial knowledge of the potential function of ethane is of importance as all isotopic molecules obey the same potential function.

II. Symmetry Considerations.

The problem of finding the correct stereochemical model of ethane has been the subject of numerous papers during this decade. It seems to be a firmly established result that no free rotation occurs around the carbon-carbon bond, but that three intermediate positions of minimum potential energy exist. It has not, however, been decided whether the D_{3d} or the D_{3h} configuration is the more correct one. The mathematical technique and the subsequent discussion of the vibrational spectra are approximately the same in both cases, as will appear from the following treatment.

1. Symmetry Coordinates and Potential Function for the D_{3d} Model.

Fig. 1 shows in double projection how the ethane molecule is placed in an xyz-coordinate system.

In table I the characters of the normal modes of vibration for molecules of the ethane type (point group D_{3d}) are given.

[1] A discussion of this problem is given by H. MARK in his book: 'Physical Chemistry of High Polymeric Systems', p. 53, New York 1940.

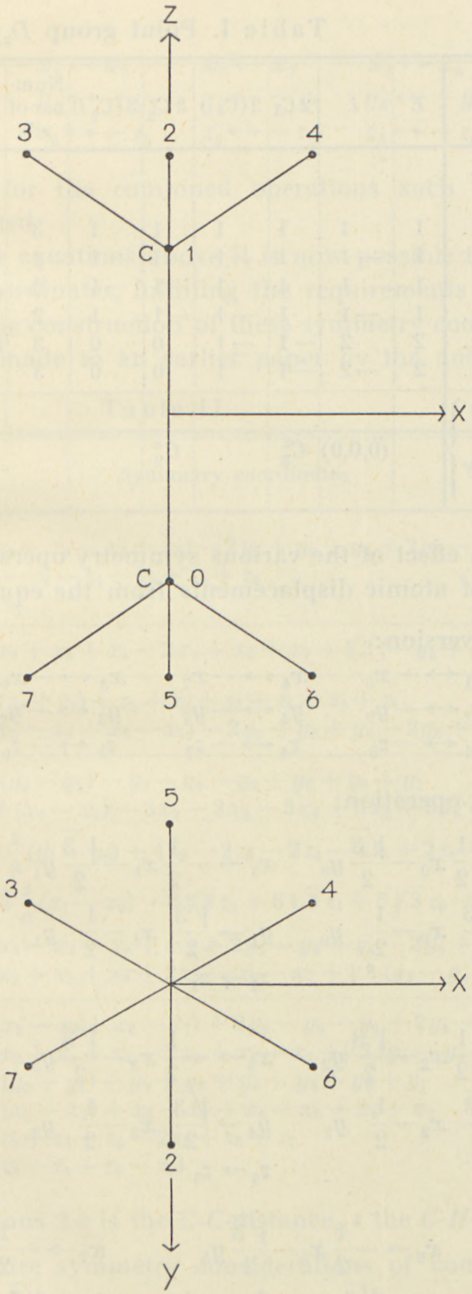

Fig. 1.

Table I. Point group D_{3d}.

Covering operation	E	i	$2C_3$	$2(C_3 i)$	$3C_2'$	$3(C_2' i)$	Number of vib.	Zero freq.	Degree of deg.	Spect. activ.	Frequency desig.
Symmetry class											
A_{1g}	1	1	1	1	1	1	3		1	R	$\nu_1 \nu_2 \nu_3$
A_{1u}	1	−1	1	−1	1	−1	1		1		ν_4
A_{2g}	1	1	1	1	−1	−1	0	R_z	1		
A_{2u}	1	−1	1	−1	−1	1	2	T_z	1	I	$\nu_5 \nu_6$
E_g	2	2	−1	−1	0	0	3	$R_x R_y$	2	R	$\nu_7 \nu_8 \nu_9$
E_u	2	−2	−1	1	0	0	3	$T_x T_y$	2	I	$\nu_{10} \nu_{11} \nu_{12}$
Symmetry elements particularly studied		(0,0,0)	C_3^z		C_2^x						

The effect of the various symmetry operations on the components of atomic displacements from the equilibrium position is:

The inversion:

$$x_1 \leftrightarrow -x_0 \qquad x_4 \leftrightarrow -x_7 \qquad x_3 \leftrightarrow -x_6 \qquad x_2 \leftrightarrow -x_5$$
$$y_1 \leftrightarrow -y_0 \qquad y_4 \leftrightarrow -y_7 \qquad y_3 \leftrightarrow -y_6 \qquad y_2 \leftrightarrow -y_5$$
$$z_1 \leftrightarrow -z_0 \qquad z_4 \leftrightarrow -z_7 \qquad z_3 \leftrightarrow -z_6 \qquad z_2 \leftrightarrow -z_5$$

The C_3^z-operation:

$$x_0 \to -\frac{1}{2} x_0 - \frac{\sqrt{3}}{2} y_0 \qquad x_1 \to -\frac{1}{2} x_1 - \frac{\sqrt{3}}{2} y_1 \qquad x_2 \to -\frac{1}{2} x_4 - \frac{\sqrt{3}}{2} y_4$$
$$y_0 \to \frac{\sqrt{3}}{2} x_0 - \frac{1}{2} y_0 \qquad y_1 \to \frac{\sqrt{3}}{2} x_1 - \frac{1}{2} y_1 \qquad y_2 \to \frac{\sqrt{3}}{2} x_4 - \frac{1}{2} y_4$$
$$z_0 \to z_0 \qquad z_1 \to z_1 \qquad z_2 \to z_4$$

$$x_3 \to -\frac{1}{2} x_2 - \frac{\sqrt{3}}{2} y_2 \qquad x_4 \to -\frac{1}{2} x_3 - \frac{\sqrt{3}}{2} y_3 \qquad x_5 \to -\frac{1}{2} x_7 - \frac{\sqrt{3}}{2} y_7$$
$$y_3 \to \frac{\sqrt{3}}{2} x_2 - \frac{1}{2} y_2 \qquad y_4 \to \frac{\sqrt{3}}{2} x_3 - \frac{1}{2} y_3 \qquad y_5 \to \frac{\sqrt{3}}{2} x_7 - \frac{1}{2} y_7$$
$$z_3 \to z_2 \qquad z_4 \to z_3 \qquad z_5 \to z_7$$

$$x_6 \to -\frac{1}{2} x_5 - \frac{\sqrt{3}}{2} y_5 \qquad x_7 \to -\frac{1}{2} x_6 - \frac{\sqrt{3}}{2} x_6$$
$$y_6 \to \frac{\sqrt{3}}{2} x_5 - \frac{1}{2} y_5 \qquad y_7 \to \frac{\sqrt{3}}{2} x_6 - \frac{1}{2} y_6$$
$$z_6 \to z_5 \qquad z_7 \to z_6.$$

The C_2^x-operation:

$$\begin{array}{llll} x_0 \leftrightarrow x_1 & x_2 \leftrightarrow x_5 & x_3 \leftrightarrow x_7 & x_4 \leftrightarrow x_6 \\ y_0 \leftrightarrow -y_1 & y_2 \leftrightarrow -y_5 & y_3 \leftrightarrow -y_7 & y_4 \leftrightarrow -y_6 \\ z_0 \leftrightarrow -z_1 & z_2 \leftrightarrow -z_5 & z_3 \leftrightarrow -z_7 & z_4 \leftrightarrow -z_6 . \end{array}$$

The equations for the combined operations such as $(C_2 i)$ are easily constructed.

By means of the equations above it is now possible to find a set of symmetry coordinates, fulfilling the requirements of table I. As to details in the construction of these symmetry coordinates reference must be made to an earlier paper by the author[1].

Table II.

Symmetry class	Symmetry coordinates
A_{1g}	$S_1 = \sqrt{3}(x_3 - x_4 - x_6 + x_7) - 2y_2 + y_3 + y_4 + 2y_5 - y_6 - y_7$ $S_2 = -z_2 - z_3 - z_4 + z_5 + z_6 + z_7$ $S_3 = z_0 - z_1$
A_{1u}	$S_4 = -2x_2 + x_3 + x_4 - 2x_5 + x_6 + x_7 + \sqrt{3}(-y_3 + y_4 - y_6 + y_7)$
A_{2u}	$S_5 = -3(z_0 + z_1) + z_2 + z_3 + z_4 + z_5 + z_6 + z_7$ $S_6 = \sqrt{3}(x_3 - x_4 + x_6 - x_7) - 2y_2 + y_3 + y_4 - 2y_5 + y_6 + y_7)$
E_g	$S_{7a} = -b(y_0 - y_1) - y_2 - y_3 - y_4 + y_5 + y_6 + y_7$ $S_{7b} = -3b(x_0 - x_1) - 3x_2 - 3x_3 - 3x_4 + 3x_5 + 3x_6 + 3x_7$ $S_{8a} = 4\sqrt{2}\frac{s}{a}(y_1 - y_0) + 4z_2 - 2z_3 - 2z_4 - 4z_5 + 2z_6 + 2z_7$ $S_{8b} = 12\sqrt{2}\frac{s}{a}(x_1 - x_0) - 6\sqrt{3}z_3 + 6\sqrt{3}z_4 + 6\sqrt{3}z_6 - 6\sqrt{3}z_7$ $S_{9a} = \sqrt{3}(x_3 - x_4 - x_6 + x_7) + 2y_2 - y_2 - y_3 - 2y_5 + y_6 + y_7$ $S_{9b} = -2x_2 + x_3 + x_4 + 2x_5 - x_6 - x_7 + \sqrt{3}(y_3 - y_4 - y_6 + y_7)$
E_u	$S_{10a} = \sqrt{3}(x_3 - x_4 + x_6 - x_7) + 2y_2 - y_3 - y_4 + 2y_5 - y_6 - y_7$ $S_{10b} = -2x_2 + x_3 + x_4 - 2x_5 + x_6 + x_7 + \sqrt{3}(y_3 - y_4 + y_6 - y_7)$ $S_{11a} = -3(y_0 + y_1) + y_2 + y_3 + y_4 + y_5 + y_6 + y_7$ $S_{11b} = -3(x_0 + x_1) + x_2 + x_3 + x_4 + x_5 + x_6 + x_7$ $S_{12a} = -2z_2 + z_3 + z_4 - 2z_5 + z_6 + z_7$ $S_{12b} = \sqrt{3}(z_3 - z_4 + z_6 - z_7)$

In these definitions $2a$ is the C-C-distance, s the C-H-distance and $b = \frac{3a+s}{a}$. Pure symmetry considerations of course only determines each symmetry coordinate except an arbitrary factor,

[1] B. Bak, Det Kgl. Danske Vidensk. Selskab, mat.-fys. Medd. XXII, 16 (1946).

but the factors used in the above expressions are chosen so as to make the potential energy function as simple as possible.

As the potential function must be invariant during any covering operation of the molecule, we find that:

$$2V = a_1S_1^2 + a_2S_2^2 + a_3S_3^2 + a_4S_1S_2 + a_5S_1S_3 + a_6S_2S_3 + a_7S_4^2 + a_8S_5^2 + a_9S_6^2 + a_{10}S_5S_6 + a_{11}(S_{7a}^2 + S_{7b}^2) + a_{12}(S_{8a}^2 + S_{8b}^2) + a_{13}(S_{9a}^2 + S_{9b}^2) + a_{14}(S_{7a}S_{8a} + S_{7b}S_{8b}) + a_{15}(S_{7a}S_{9a} + S_{7b}S_{9b}) + a_{16}(S_{8a}S_{9a} + S_{8b}S_{9b}) + a_{17}(S_{10a}^2 + S_{10b}^2) + a_{18}(S_{11a}^2 + S_{11b}^2) + a_{19}(S_{12a}^2 + S_{12b}^2) + a_{20}(S_{10a}S_{11a} + S_{10b}S_{11b}) + a_{21}(S_{10a}S_{12a} + S_{10b}S_{12b}) + a_{22}(S_{11a}S_{12a} + S_{11b}S_{12b}).$$

2. Symmetry Coordinates and Potential Function for the D_{3h}-Model.

Fig. 2 shows how the ethane molecule is placed in the coordinate system if belonging to the D_{3h} point group.

In table III the characters of the normal modes of vibration are given.

Table III. Point group D_{3h}.

Covering operation	E	σ_h	$2C_3$	$2S_3$	$3C_2$	$3\sigma_v$	Number of vib.	Zero freq.	Degree of deg.	Spect. activ.	Frequency desig.
Symmetry class											
A_1'	1	1	1	1	1	1	3		1	R	$\nu_1\nu_2\nu_3$
A_2'	1	1	1	1	−1	−1	0	R_z	—		
A_1''	1	−1	1	−1	1	−1	1		1		ν_4
A_2''	1	−1	1	−1	−1	1	2	T_z	1	I	$\nu_5\nu_6$
E'	2	2	−1	−1	0	0	3	T_xT_y	2	RI	$\nu_7\nu_8\nu_9$
E''	2	−2	−1	1	0	0	3	R_xR_y	2	R	$\nu_{10}\nu_{11}\nu_{12}$
Symmetry elements particularly studied		σ_z	C_3^z	S_3^z	C_2^y	σ_x					

The effects of the various symmetry operations on the components of atomic displacements from the equilibrium positions are:

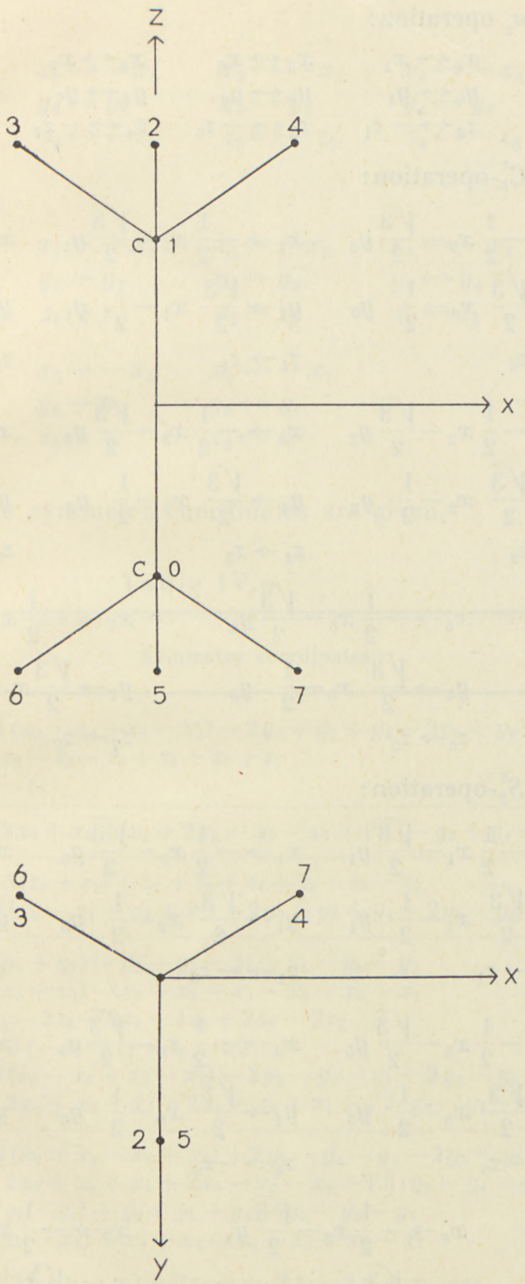

Fig. 2.

The σ_z operation:

$$x_0 \leftrightarrow x_1 \qquad x_3 \leftrightarrow x_6 \qquad x_4 \leftrightarrow x_7 \qquad x_2 \leftrightarrow x_5$$
$$y_0 \leftrightarrow y_1 \qquad y_3 \leftrightarrow y_6 \qquad y_4 \leftrightarrow y_7 \qquad y_2 \leftrightarrow y_5$$
$$z_0 \leftrightarrow -z_1 \qquad z_3 \leftrightarrow -z_6 \qquad z_4 \leftrightarrow -z_7 \qquad z_2 \leftrightarrow -z_5$$

The C_3^z-operation:

$$x_0 \to -\frac{1}{2}x_0 - \frac{\sqrt{3}}{2}y_0 \qquad x_1 \to -\frac{1}{2}x_1 - \frac{\sqrt{3}}{2}y_1 \qquad x_2 \to -\frac{1}{2}x_4 - \frac{\sqrt{3}}{2}y_4$$
$$y_0 \to \frac{\sqrt{3}}{2}x_0 - \frac{1}{2}y_0 \qquad y_1 \to \frac{\sqrt{3}}{2}x_1 - \frac{1}{2}y_1 \qquad y_2 \to \frac{\sqrt{3}}{2}x_4 - \frac{1}{2}y_4$$
$$z_0 \to z_0 \qquad z_1 \to z_1 \qquad z_2 \to z_4$$

$$x_3 \to -\frac{1}{2}x_2 - \frac{\sqrt{3}}{2}y_2 \qquad x_4 \to -\frac{1}{2}x_3 - \frac{\sqrt{3}}{2}y_3 \qquad x_5 \to -\frac{1}{2}x_7 - \frac{\sqrt{3}}{2}y_7$$
$$y_3 \to \frac{\sqrt{3}}{2}x_2 - \frac{1}{2}y_2 \qquad y_4 \to \frac{\sqrt{3}}{2}x_3 - \frac{1}{2}y_3 \qquad y_5 \to \frac{\sqrt{3}}{2}x_7 - \frac{1}{2}y_7$$
$$z_3 \to z_2 \qquad z_4 \to z_3 \qquad z_5 \to z_7$$

$$x_6 \to -\frac{1}{2}x_5 - \frac{\sqrt{3}}{2}y_5 \qquad x_7 \to -\frac{1}{2}x_6 - \frac{\sqrt{3}}{2}y_6$$
$$y_6 \to \frac{\sqrt{3}}{2}x_5 - \frac{1}{2}y_5 \qquad y_7 \to \frac{\sqrt{3}}{2}x_6 - \frac{1}{2}y_6$$
$$z_6 \to z_5 \qquad z_7 \to z_6.$$

The S_3^z-operation:

$$x_0 \to -\frac{1}{2}x_1 - \frac{\sqrt{3}}{2}y_1 \qquad x_1 \to -\frac{1}{2}x_0 - \frac{\sqrt{3}}{2}y_0 \qquad x_2 \to -\frac{1}{2}x_7 - \frac{\sqrt{3}}{2}y_7$$
$$y_0 \to \frac{\sqrt{3}}{2}x_1 - \frac{1}{2}y_1 \qquad y_1 \to \frac{\sqrt{3}}{2}x_0 - \frac{1}{2}y_0 \qquad y_2 \to \frac{\sqrt{3}}{2}x_7 - \frac{1}{2}y_7$$
$$z_0 \to -z_1 \qquad z_1 \to -z_0 \qquad z_2 \to -z_7$$

$$x_3 \to -\frac{1}{2}x_5 - \frac{\sqrt{3}}{2}y_5 \qquad x_4 \to -\frac{1}{2}x_6 - \frac{\sqrt{3}}{2}y_6 \qquad x_5 \to -\frac{1}{2}x_4 - \frac{\sqrt{3}}{2}y_4$$
$$y_3 \to \frac{\sqrt{3}}{2}x_5 - \frac{1}{2}y_5 \qquad y_4 \to \frac{\sqrt{3}}{2}x_6 - \frac{1}{2}y_6 \qquad y_5 \to \frac{\sqrt{3}}{2}x_4 - \frac{1}{2}y_4$$
$$z_3 \to -z_5 \qquad z_4 \to -z_6 \qquad z_5 \to -z_4$$

$$x_6 \to -\frac{1}{2}x_2 - \frac{\sqrt{3}}{2}y_2 \qquad x_7 \to -\frac{1}{2}x_3 - \frac{\sqrt{3}}{2}y_3$$
$$y_6 \to \frac{\sqrt{3}}{2}x_2 - \frac{1}{2}y_2 \qquad y_1 \to \frac{\sqrt{3}}{2}x_3 - \frac{1}{2}y_3$$
$$z_6 \to -z_2 \qquad z_7 \to -z_3$$

The C_2^y-operation:

$$x_0 \leftrightarrow -x_1 \quad x_2 \leftrightarrow -x_5 \quad x_3 \leftrightarrow -x_7 \quad x_4 \leftrightarrow -x_6$$
$$y_0 \leftrightarrow y_1 \quad y_2 \leftrightarrow y_5 \quad y_3 \leftrightarrow y_7 \quad y_4 \leftrightarrow y_6$$
$$z_0 \leftrightarrow -z_1 \quad z_2 \leftrightarrow -z_5 \quad z_3 \leftrightarrow -z_7 \quad z_4 \leftrightarrow -z_6$$

The σ_x-operation:

$$x_0 \rightarrow -x_0 \quad x_1 \rightarrow -x_1 \quad x_2 \rightarrow -x_2 \quad x_3 \leftrightarrow -x_4$$
$$y_0 \rightarrow y_0 \quad y_1 \rightarrow y_1 \quad y_2 \rightarrow y_2 \quad y_3 \leftrightarrow y_4$$
$$z_0 \rightarrow z_0 \quad z_1 \rightarrow z_1 \quad z_2 \rightarrow z_2 \quad z_3 \leftrightarrow z_4$$

$$x_5 \rightarrow -x_5 \quad x_6 \leftrightarrow -x_7$$
$$y_5 \rightarrow y_5 \quad y_6 \leftrightarrow y_7$$
$$z_5 \rightarrow z_5 \quad z_6 \leftrightarrow z_7$$

In table IV the symmetry coordinates are given.

Table IV.

Symmetry class	Symmetry coordinates
A_1'	$S_1 = \sqrt{3}(x_3 - x_4 + x_6 - x_7) - 2y_2 + y_3 + y_4 - 2y_5 + y_6 + y_7$ $S_2 = -z_2 - z_3 - z_4 + z_5 + z_6 + z_7$ $S_3 = z_0 - z_1$
A_1''	$S_4 = -2x_2 + x_3 + x_4 + 2x_5 - x_6 - x_7 + \sqrt{3}(-y_3 + y_4 + y_6 - y_7)$
A_2''	$S_5 = -3(z_0 + z_1) + z_2 + z_3 + z_4 + z_5 + z_6 + z_7$ $S_6 = \sqrt{3}(x_3 - x_4 - x_6 + x_7) - 2y_2 + y_3 + y_4 + 2y_5 - y_6 - y_7$
E'	$S_{7a} = 3(y_0 + y_1) - y_2 - y_3 - y_4 - y_5 - y_6 - y_7$ $S_{7b} = 3(x_0 + x_1) - x_2 - x_3 - x_4 - x_5 - x_6 - x_7$ $S_{8a} = 4z_2 - 2z_3 - 2z_4 - 4z_5 + 2z_6 + 2z_7$ $S_{8b} = 2\sqrt{3}(-z_3 + z_4 + z_6 - z_7)$ $S_{9a} = \sqrt{3}(x_3 - x_4 + x_6 - x_7) + 2y_2 - y_3 - y_4 + 2y_5 - y_6 - y_7$ $S_{9b} = -2x_2 + x_3 + x_4 - 2x_5 + x_6 + x_7 + \sqrt{3}(y_3 - y_4 + y_6 - y_7)$
E''	$S_{10a} = \sqrt{3}(x_3 - x_4 - x_6 + x_7) + 2y_2 - y_3 - y_4 - 2y_5 + y_6 + y_7$ $S_{10b} = -2x_2 + x_3 + x_4 + 2x_5 - x_6 - x_7 + \sqrt{3}(y_3 - y_4 - y_6 + y_7)$ $S_{11a} = b(y_0 - y_1) + y_2 + y_3 + y_4 - y_5 - y_6 - y_7$ $S_{11b} = b(x_0 - x_1) + x_2 + x_3 + x_4 - x_5 - x_6 - x_7$ $S_{12a} = 2\sqrt{2}\frac{s}{a}(y_0 - y_1) - 2z_2 + z_3 + z_4 - 2z_5 + z_6 + z_7$ $S_{12b} = 2\sqrt{2}\frac{s}{a}(x_0 - x_1) + \sqrt{3}(z_3 - z_4 + z_6 - z_7)$

Table

D_{3d} configuration	$\begin{vmatrix} 2a_1 - \frac{m_H}{12}x & a_4 & a_5 \\ a_4 & 2a_2 - \frac{m_H}{3}x & a_6 \\ a_5 & a_6 & 2a_3 - m_C x \end{vmatrix} = 0$	$a_7 = \frac{m_H}{24}x$	$\begin{vmatrix} 2a_8 - \frac{m_H m_C}{3(m_C+3m_H)}x & a_{10} \\ a_{10} & 2a_9 - \frac{m_H}{12}x \end{vmatrix} = 0$
	Roots: x_1 x_2 x_3	x_4	x_5 x_6
Symmetry class	A_{1g}	A_{1u}	A_{2u}
Symmetry class	A_1'	A_1''	A_2''
D_{3h} configuration	Same as above	Same as above	Same as above
	Roots: x_1 x_2 x_3	x_4	x_5 x_6

V.

$$\begin{vmatrix} 2a_{11} - \dfrac{32\left(\dfrac{s}{a}\right)^2 m_H + 24\, m_C}{N_1 m_H m_C} \varkappa & a_{14} + \dfrac{4\sqrt{2}\, sb}{N_1 a m_C} \varkappa & a_{15} \\ a_{14} + \dfrac{4\sqrt{2}\, sb}{N_1 a m_C} \varkappa & 2a_{12} - \dfrac{m_H b^2 + 3\, m_C}{N_1 m_H m_C} \varkappa & a_{16} \\ a_{15} & a_{16} & 2a_{13} - \dfrac{m_H}{12} \varkappa \end{vmatrix} = 0$$

$$N_1 = \frac{m_H\left(24\, b^2 + 96\left(\frac{s}{a}\right)^2\right) + 72\, m_C}{m_C m_H^2}$$

$\varkappa_7 \quad \varkappa_8 \quad \varkappa_9$

$$\begin{vmatrix} 2a_{17} - \dfrac{m_H}{12} \varkappa & a_{20} & a_{21} \\ a_{20} & 2a_{18} - \dfrac{m_H m_C}{3\, M} \varkappa & a_{22} \\ a_{21} & a_{22} & 2a_{19} - \dfrac{m_H}{6} \varkappa \end{vmatrix} = 0$$

M = mass of CH_3.

$\varkappa_{10} \quad \varkappa_{11} \quad \varkappa_{12}$

E_g E_u

E'' E'

$$\begin{vmatrix} 2a_{17} - \dfrac{m_H}{12} \varkappa & a_{20} & a_{21} \\ a_{20} & 2a_{18} - \dfrac{8\left(\dfrac{s}{a}\right)^2 m_H + 6\, m_C}{N_2 m_H m_C} \varkappa & a_{22} + \dfrac{2\sqrt{2}\, sb}{N_2 a m_C} \varkappa \\ a_{21} & a_{22} + \dfrac{2\sqrt{2}\, sb}{N_2 a m_C} \varkappa & 2a_{19} - \dfrac{m_H b^2 + 3\, m_C}{N_2 m_H m_C} \varkappa \end{vmatrix} = 0$$

$$N_2 = \frac{m_H\left(6\, b^2 + 24\left(\frac{s}{a}\right)^2\right) + 18\, m_C}{m_C m_H^2}.$$

$\varkappa_{10} \quad \varkappa_{11} \quad \varkappa_{12}$

$$\begin{vmatrix} 2a_{11} - \dfrac{m_H m_C}{3\, M} \varkappa & a_{14} & a_{15} \\ a_{14} & 2a_{12} - \dfrac{m_H}{24} \varkappa & a_{16} \\ a_{15} & a_{16} & 2a_{13} - \dfrac{m_H}{12} \varkappa \end{vmatrix} = 0$$

M = mass of CH_3.

$\varkappa_7 \quad \varkappa_8 \quad \varkappa_9$

The symmetry coordinates of table IV have been chosen in such a way that the potential function is formulated exactly as in the case of the D_{3d}-model, given on page 8. Formally one can operate with the same potential function in both models but it should be remembered that the physical meaning of the force-constants is not the same in the two cases.

III. Relations between Force-Constants and Vibration Frequencies.

These equations are found in the usual way by means of the Lagrangian equations. The results are given in table V.

As appears from table V the symmetry coordinates have been chosen so as to make all calculations in the non-degenerate classes formally identical. This is a great advantage because this paper mainly deals with these classes. In the degenerate classes there are differences, but there are also fundamental similarities between the equations to be solved.

IV. Numerical Calculations.

1. Experimental Material.

Infrared and Raman data have been published by many authors.

Infrared data.

Levin and Mayer, Journ. Opt. Soc. Am. **16**, 137 (1928)	(C_2H_6)
Benedict, Morikawa, Barnes, and Taylor, J. Chem. Phys. **5**, 1 (1937)	(-)
Barthlomé and Karweil, Naturwis. **25**, 476 (1937)	(-)
Crawford, Avery, and Linnett, J. Chem. Phys. **6**, 682 (1938)	(-)
Fred. Stitt, J. Chem. Phys. **7**, 297 (1939)	(C_2D_6)

Raman data.

Daure, Trans. Far. Soc. **25**, 825 (1929)	(C_2H_6)
Bhagavantam, Ind. Journ. Phys. **6**, 595 (1932)	(-)

Lewis and Houston, Phys. Rev. **44**, 903 (1933) (C_2H_6)
Bhagavantam, Proc. Ind. Acad. Sci. A, **2**, 86 (1935) (-)
Glockler and Renfrew, J. Chem. Phys. **6**, 295 (1938) (-)
Glockler and Renfrew, J. Chem. Phys. **6**, 409 (1938) (-)
Crawford, Avery, and Linnett, J. Chem. Phys. **6**, 682 (1938) (-)
Goubeau and Karweil, Zeits. Phys. Chem. B, **40**, 376 (1938) (-)
Fred Stitt, J. Chem. Phys. **7**, 297 (1939) (C_2D_6)

Fred Stitt was the first to find the very important data from C_2D_6. These highly facilitate the assignment of frequencies. A careful examination of all the available literature reveals that the assignment of frequencies made by Stitt must be considered as far the most probable at present. In table VI the results of Stitt, therefore, are given.

Table VI.

D_{3d} configuration	C_2H_6	C_2D_6	D_{3h} configuration
ν_1	993	852	ν_1
ν_2	1375	1158	ν_2
ν_3	2925	2115	ν_3
ν_4	310	—	ν_4
ν_5	1380	1072	ν_5
ν_6	2925	2100	ν_6
ν_{10}	827	601	ν_7
ν_{11}	1465	1102	ν_8
ν_{12}	2980	2237	ν_9
ν_7	1170	970	ν_{10}
ν_8	1460	1055	ν_{11}
ν_9	2960	2225	ν_{12}

2. Discussion of Various Models.

The frequencies of table VI deviate from the 'harmonical' frequencies of the molecule (the frequencies for zero amplitude). In cases where this deviation could be experimentally determined it has been shown that the harmonical frequencies are roughly about 2 per cent. higher than those experimentally determined for vibrations in which hydrogen and carbon atoms take part.

The deviation is of course greater in the case of C_2H_6 than in the case of C_2D_6 because of the greater amplitudes in the former case. To give an impression of the size of the deviations the 'product rule' of TELLER can be used. The results are given in table VII.

Table VII.

D_{3d}	D_{3h}	Product rule ratio calc.	Experimentally determined
A_{1g}	A_1'	2.00	1.92
A_{1u}	A_1''	1.41	—
A_{2u}	A_2''	1.83	1.79
E_g	E''	2.36	2.22
E_u	E'	2.58	2.44

In papers where force-constants are calculated the experimentally determined frequencies are generally used as if they were 'harmonical', that is, a molecular model carrying out harmonical vibrations with the experimentally determined frequencies is considered, and it is postulated that the conditions of force in such a model are approximately the same as in the real molecule. In the papers hitherto published by the author[1] this procedure has met with no difficulties. In the present case, however, difficulties arise in the degenerate symmetry classes. If the experimentally determined frequencies are used in the calculations in the usual way, imaginary force-constants result. This means that in the case of ethane a model corresponding to those used at the description of other molecules such as benzene, methane, and acetylene does not exist. To get a model with real values of the force-constants we must alter the experimentally determined frequencies slightly before starting the calculations. The set of frequencies used must of course obey the above-mentioned product rule, and they should deviate as little as possible from the experimental ones. But as such correction of the frequencies could be carried through in many different ways, the important question arises what rôle this arbitrariness plays for the numerical size of the force-constants. In this paper we shall try to

[1] loc. cit.

give a partial answer to this problem by making some of the calculations on the basis of two different sets of frequencies that are to be considered beforehand of equal correctness.

The more fundamental problem concerning the difference between the various models and the 'real' molecule cannot be answered until a description of the vibrating molecule by means of a potential function involving higher powers of the symmetry coordinates has been given. But there is no possibility of giving such a description at the present stage of chemical physics.

3. Force-Constants of the Non-Degenerate Classes.

Solving the determinantal equations of the non-degenerate classes with respect to the unknown force-constants we get the eleven equations:

$$a_3 = \frac{m_C}{2}\left(2\sum_1^3 \varkappa_i' - \sum_1^3 \varkappa_i\right) \tag{1}$$

$$a_2 + 4\,a_1 = \frac{m_H}{3}\left(\sum_1^3 \varkappa_i - \sum_1^3 \varkappa_i'\right) \tag{2}$$

$$a_4^2 - 4\,a_1 a_2 = \frac{m_D m_H^2}{36\,(m_D - m_H)}\left(2\sum_1^3 \varkappa_i' \varkappa_j' - \sum_1^3 \varkappa_i \varkappa_j\right)(i \neq j) \tag{3}$$

$$4\,a_2 a_3 + 16\,a_1 a_3 - 4\,a_5^2 - a_6^2 = \frac{m_H m_C}{3}\left(4\sum_1^3 \varkappa_i' \varkappa_j' - \sum_1^3 \varkappa_i \varkappa_j\right)(i \neq j) \tag{4}$$

$$4\,a_1 a_2 a_3 + a_4 a_5 a_6 - a_1 a_6^2 - a_2 a_5^2 - a_3 a_4^2 = \begin{cases} \dfrac{\varkappa_1 \varkappa_2 \varkappa_3 m_C m_H^2}{72} & (5) \\ \dfrac{\varkappa_1' \varkappa_2' \varkappa_3' m_C m_D^2}{72} & (6) \end{cases}$$

$$a_7 = \frac{m_H}{24}\varkappa_4 \tag{7}$$

$$a_8 = \frac{m_C + 3\,m_H}{3\,(m_D - m_H)}\left(2\,(\varkappa_5' + \varkappa_6') - (\varkappa_5 + \varkappa_6)\right) \tag{8}$$

$$a_9 = \frac{m_H}{24}\left(\varkappa_5 + \varkappa_6 + \frac{m_C + 3m_H}{3(m_D - m_H)}(\varkappa_5 + \varkappa_6 - 2(\varkappa'_5 + \varkappa'_6)\right) \quad (9)$$

$$4\,a_8 a_9 - a_{10}^2 = \begin{cases} \dfrac{\varkappa_5 \varkappa_6 m_C m_H^2}{36\,(m_C + 3\,m_H)} & (10) \\ \dfrac{\varkappa'_5 \varkappa'_6 m_C m_D^2}{36\,(m_C + 3\,m_D)} & (11) \end{cases}$$

where $\varkappa_i = 4\pi^2 \nu_i^2$, ν_i being one of the frequencies of the ethane molecule

and $\varkappa'_i = 4\pi^2 \nu'^2_i$, ν'_i being one of the frequencies of the hexadeuteroethane molecule.

By insertion of the numerical values from table VI we get the equations

$$a_3 = 57.85 \cdot 10^4$$

$$4\,a_1 + a_2 = 9.618 \cdot 10^4 \quad (12)$$

$$a_4^2 - 4\,a_1 a_2 = -11.64 \cdot 10^8 \quad (13)$$

$$4\,a_2 a_3 + 16\,a_1 a_3 - 4\,a_5^2 - a_6^2 = 1988 \cdot 10^8 \quad (14)$$

$$4\,a_1 a_2 a_3 + a_4 a_5 a_6 - a_1 a_6^2 - a_2 a_5^2 - a_3 a_4^2 = (5.412 + 5.902)\,\frac{1}{2} \cdot 10^{14} = 5.657 \cdot 10^{14}. \quad (15)$$

$$a_7 = 0.02467 \cdot 10^4;\quad a_8 = 2.5732 \cdot 10^4;\quad a_9 = 1.7651 \cdot 10^4;\quad a_{10} = \pm 2.318 \cdot 10^4.$$

All force-constants are measured in dyne cm^{-1}.

The equations (12) — (15) represent 4 equations with 5 unknowns. It is therefore impossible to find their numerical value without making any physical assumption. We now want to use the 'empirical' rule cited on page 3.

The hydrogen atoms numbers 2, 3 and 4 are displaced towards C (1). The amplitude components are:

$$x_2 = 0 \qquad y_2 = -\frac{2\sqrt{2}}{3} \qquad z_2 = -\frac{1}{3}$$

$$x_3 = \frac{\sqrt{6}}{3} \qquad y_3 = \frac{\sqrt{2}}{3} \qquad z_3 = -\frac{1}{3}$$

$$x_4 = -\frac{\sqrt{6}}{3} \qquad y_4 = \frac{\sqrt{2}}{3} \qquad z_4 = -\frac{1}{3}.$$

By insertion of these values in the definition equations for the symmetry coordinates we get:

$$S_1 = 4\sqrt{2}; \quad S_2 = 1; \quad S_5 = -1; \quad S_6 = 4\sqrt{2}.$$

The remaining symmetry coordinates are equal to zero. If we denote the force acting upon X-atom number i in the direction of the U-axis by $K_{X(i)}(U)$, we may write:

$$\begin{aligned}
K_{H(5)}(Z) &= -a_2 - 2\sqrt{2}\,a_4 + a_8 - 2\sqrt{2}\,a_{10} \\
K_{H(5)}(Y) &= -8\sqrt{2}\,a_1 - a_4 + 8\sqrt{2}\,a_9 - a_{10} \\
K_{H(5)}(X) &= 0 \\
K_{C(0)}(Z) &= -2\sqrt{2}\,a_5 - \frac{1}{2}a_6 - 3\,a_8 + 6\sqrt{2}\,a_{10}.
\end{aligned}$$

Putting these forces equal to zero we get the three equations:

$$a_4 + a_{10} = \frac{a_8 - a_2}{2\sqrt{2}} \qquad (1, f)$$

$$a_4 + a_{10} = 8\sqrt{2}\,(a_9 - a_1) \qquad (2, f)$$

$$4\sqrt{2}\,a_5 + a_6 + 6\,a_8 - 12\sqrt{2}\,a_{10} = 0. \qquad (3, f)$$

('f' means: derived on physical assumption).

Now $(1, f)$, $(2, f)$ and (12) are three equations with three unknowns. We solve them and find

$$a_1 = 1.764 \cdot 10^4 \qquad a_2 = 2.560 \cdot 10^4 \qquad a_4 = \pm 2.318 \cdot 10^4.$$

But a_4 can also be determined from (13) and the values just obtained for a_1 and a_2. We find $a_4 = \pm 2.528 \cdot 10^4$. The consistency between the two ways of calculating a_4 must be considered as a verification of the 'empirical rule' in the present case.

(14) now gives a relation between a_5^2 and a_6^2. $4\,a_5^2 + a_6^2 = 237 \cdot 10^8$. Another relation between the same two constants is available in $(3, f)$. Here two cases arise, dependent upon the sign of a_{10}. The calculations, however, show that $a_{10} < 0$ means that a_5 becomes imaginary. As this possibility must be excluded on physical grounds it only remains that

$$a_5 = 5.950 \cdot 10^4 \quad \text{and} \quad a_6 = -9.763 \cdot 10^4 \quad \text{(case 1)}$$

or

$$a_5 = 1.559 \cdot 10^4 \quad \text{and} \quad a_6 = 15.07 \cdot 10^4 \quad \text{(case 2).}$$

The remaining two possibilities for the numerical values of the force-constants are:

	a_1	a_2	a_3	a_4	a_5	a_6	a_7	a_8	a_9	a_{10}
(Case 1)	1.764	2.559	57.85	−2.528	5.950	−9.762	0.0236	2.5732	1.7651	2.318
(Case 2)	1.764	2.559	57.85	−2.528	1.559	15.07	0.0236	2.5732	1.7651	2.318

A choice between these two possibilities can be made by means of (15). We write (15) as

$$4\,a_1a_2a_3 - a_3a_4^2 - 565.7 \cdot 10^{12} = -a_4a_5a_6 + a_1a_6^2 + a_2a_5^2.$$

In both cases the left-hand side has the value $109.8 \cdot 10^{12}$. In case 1 the right-hand side becomes $111.9 \cdot 10^{12}$, in case 2, $466.7 \cdot 10^{12}$. Thus case 1 must be the correct one and the numerical conformity found is a new confirmation of the validity of the empirical rule in the present case.

We finish this chapter by comparing the experimentally determined frequencies of the non-degenerate vibrations of ethane and hexadeuteroethane with frequencies calculated on the basis of the force-constants of case (1) above.

	Experimentally determined	Calculated in this paper
ν_1	993	1037
ν_2	1375	1344
ν_3	2925	2925
ν_5	1380	1395
ν_6	2925	2917
ν_1'	852	805
ν_2'	1158	1203
ν_3'	2115	2108
ν_5'	1072	1060
ν_6'	2100	2106

4. Effect of the Choice of Model.

In order to see what effect the choice of model has on the numerical values of the force-constants the preceding calculations are repeated on the basis of slightly altered frequency values. At the choice of these values there is an infinite number of possibilities. A special interest would be connected with a model the vibration frequencies of which were derived from the experimental ones by correcting them for anharmonicity. But such correction could not be carried through at present. As the anharmonicity as a rule is greater at hydrogen- than at deuterium-vibrations I have arbitrarily chosen to consider a model with hydrogen frequencies which are 2 per cent. higher than the corresponding values of table VI except in the A_{2u}-class, where only 1 per cent. is added[1]. The deuterium frequencies are taken over without change.

	Theoretical product rule ratio	Ratio for frequencies chosen
A_{1g}	2.00	2.04
A_{2u}	1.83	1.83

The frequency values chosen are more in harmony with the product rule than the experimentally determined ones. But the author wants to stress, that this should not be considered a sign that the molecular model to be built up on the basis of such corrected values is a better approximation to the 'real' molecule, not even if we had succeeded in finding the true 'harmonical' frequencies.

By means of the slightly altered frequency values the calculation of a new set of force-constants could be made in exactly the same way as was shown on pages 18—20. Beneath the force-constants of this second model (model 2) are compared with the force-constants of the model first considered (model 1).

	a_1	a_2	a_3	a_4	a_5	a_6	a_7	a_8	a_9	a_{10}
Model 1 . .	1.764	2.560	57.85	−2.528	5.950	−9.762	0.0236	2.573	1.765	2.318
Model 2 . .	2.084	2.160	41.76	−1.449	2.898	−6.072	0.0240	1.756	2.072	1.229
Deviation per cent. of middle number	8.3	8.5	16.5	27.2	34.6	23.4	1.0	19.0	7.8	31.0

[1] If 2 per cent. are added in this symmetry class, imaginary force-constants result.

Table VIII.

S_i	$\frac{\partial 2V}{\partial S_i}$	Value of $\frac{\partial 2V}{\partial S_i}$ for displacement considered	$\frac{\partial S_i}{\partial y_0}$	$\frac{\partial S_i}{\partial z_0}$	$\frac{\partial S_i}{\partial x_3}$
S_1	$2a_1S_1 + a_4S_2 + a_5S_3$	$8\sqrt{2}\,a_1 + a_4 = \alpha$			$\sqrt{3}$
S_2	$a_4S_1 + 2a_2S_2 + a_6S_3$	$4\sqrt{2}\,a_4 + 2a_2 = \beta$			
S_3	$a_5S_1 + a_6S_2 + 2a_3S_3$	$4\sqrt{2}\,a_5 + a_6 = \gamma$		1	
S_4	$2a_7S_4$	0			1
S_5	$2a_8S_5 + a_{10}S_6$	$-2a_8 + 4\sqrt{2}\,a_{10} = \delta$		-3	
S_6	$a_{10}S_5 + 2a_9S_6$	$-a_{10} + 8\sqrt{2}\,a_9 = \varepsilon$			$\sqrt{3}$
S_{7a}	$2a_{11}S_{7a} + a_{14}S_{8a} + a_{15}S_{9a}$	$4\sqrt{2}\,a_{11} - 4a_{14} - 4\sqrt{2}\,a_{15} = A$	$-b$		
S_{8a}	$a_{14}S_{7a} + 2a_{12}S_{8a} + a_{16}S_{9a}$	$2\sqrt{2}\,a_{14} - 8a_{12} - 4\sqrt{2}\,a_{16} = B$	$-4\sqrt{2}\frac{s}{a}$		
S_{9a}	$a_{15}S_{7a} + a_{16}S_{8a} + 2a_{13}S_{9a}$	$2\sqrt{2}\,a_{15} - 4a_{16} - 8\sqrt{2}\,a_{13} = C$			$\sqrt{3}$
S_{10a}	$2a_{17}S_{10a} + a_{20}S_{11a} + a_{21}S_{12a}$	$-8\sqrt{2}\,a_{17} - 2\sqrt{2}\,a_{20} + 2a_{21} = D$			
S_{11a}	$a_{20}S_{10a} + 2a_{18}S_{11a} + a_{22}S_{12a}$	$-4\sqrt{2}\,a_{20} - 4\sqrt{2}\,a_{18} + 2a_{22} = E$	-3		
S_{12a}	$a_{21}S_{10a} + a_{22}S_{11a} + 2a_{19}S_{12a}$	$-4\sqrt{2}\,a_{21} - 2\sqrt{2}\,a_{22} + 4a_{19} = F$			
		Equation number:	(1)	(2)	(3)

As is seen the 'cross product constants' of the potential function (a_4, a_5, a_6 and a_{10}) are rather badly determined.

5. Attempt to Calculate Force-Constants of Degenerate Classes.

Solving the determinantal equation of e. g. the E_u-class we find that

$$2a_{17} + a_{19} = 2.207 \cdot 10^4$$
$$8a_{17}a_{18} + 4a_{18}a_{19} - 2a_{20}^2 - a_{22}^2 = 51.33 \cdot 10^8$$
$$a_{21}^2 - 4a_{17}a_{19} = 3.233 \cdot 10^8$$
$$4a_{17}a_{18}a_{19} + a_{20}a_{21}a_{22} - a_{17}a_{22}^2 - a_{18}a_{21}^2 - a_{19}a_{20}^2 = 5.240 \cdot 10^{12}$$
$$a_{18} = 5.657 \cdot 10^4$$

This is easily seen to be insufficient knowledge if we want to find the numerical values of the force-constants $a_{19} - a_{22}$. In order to get more information of the force-constants we use the 'empirical rule', displacing a single hydrogen atom towards its

D_{3d}							D_{3h}								
$\frac{\partial S_i}{\partial y_3}$	$\frac{\partial S_i}{\partial z_3}$	$\frac{\partial S_i}{\partial y_5}$	$\frac{\partial S_i}{\partial z_5}$	$\frac{\partial S_i}{\partial x_6}$	$\frac{\partial S_i}{\partial y_6}$	$\frac{\partial S_i}{\partial z_6}$	$\frac{\partial S_i}{\partial y_0}$	$\frac{\partial S_i}{\partial z_0}$	$\frac{\partial S_i}{\partial x_3}$	$\frac{\partial S_i}{\partial y_3}$	$\frac{\partial S_i}{\partial z_3}$	$\frac{\partial S_i}{\partial y_5}$	$\frac{\partial S_i}{\partial z_5}$	$\frac{\partial S_i}{\partial x_0}$	$\frac{\partial S_i}{\partial y_6}$	$\frac{\partial S_i}{\partial z_6}$
1		2		$-\sqrt{3}$	-1				$\sqrt{3}$	1		-2		$\sqrt{3}$	1	
	-1		1			1					-1		1			1
								1								
$-\sqrt{3}$				1	$-\sqrt{3}$				1	$-\sqrt{3}$				-1	$\sqrt{3}$	
	1		1			1		-3			1		1			1
1		-2		$\sqrt{3}$	1				$\sqrt{3}$	1		2		$-\sqrt{3}$	-1	
-1		1			1		3			-1		-1			-1	
	-2		-4			2				0	-2		-4			2
-1		-2		$-\sqrt{3}$	1				$\sqrt{3}$	-1		2		$\sqrt{3}$	-1	
-1		2		$\sqrt{3}$	-1				$\sqrt{3}$	-1		-2		$-\sqrt{3}$	1	
1		1			1		b			1		-1			-1	
	1		-2			1	$2\sqrt{2}\,\frac{s}{a}$				1		-2			1
(4)	(5)	(6)	(7)	(8)	(9)	(10)										

adjoining carbon atom and putting the forces acting upon all the other atoms equal to zero. Thus,

$$x_2 = 0 \quad y_2 = -2\sqrt{2} \quad z_2 = -1,$$

and consequently

$$S_1 = 4\sqrt{2}; \quad S_2 = 1; \quad S_5 = -1;$$

$$S_6 = 4\sqrt{2}; \quad S_{7a} = 2\sqrt{2}; \quad S_{8a} = -4;$$

$$S_{9a} = -4\sqrt{2}; \quad S_{10a} = -4\sqrt{2}; \quad S_{11a} = -2\sqrt{2}; \quad S_{12a} = 2,$$

whether the stereochemical model is D_{3h} or D_{3d}. All other $S_i = 0$.

Table VIII gives a good survey of the way in which to find the relations that could be derived by means of the 'empirical rule'. These relations could all be written in the general form:

$$-2K_{X(i)}(U) = \frac{\partial 2V}{\partial u_i} = \sum_0^7 \frac{\partial 2V}{\partial S_i}\frac{\partial S_i}{\partial u_i}.$$

The ten equations that can be derived from table VIII are (D_{3d}):

$$A \cdot b + 4\sqrt{2}\,\frac{s}{a}B \qquad + 3E \qquad = 0 \quad (1)$$

$$\gamma - 3\delta \qquad = 0 \quad (2)$$

$$\alpha \qquad + \varepsilon \qquad + C \quad + D \qquad = 0 \quad (3)$$

$$\alpha \qquad + \varepsilon - A \qquad - C \quad - D + E \qquad = 0 \quad (4)$$

$$-\beta \quad + \delta \qquad - 2B \qquad + F = 0 \quad (5)$$

$$2\alpha \qquad - 2\varepsilon + A \qquad - 2C + 2D + E \qquad = 0 \quad (6)$$

$$\beta \quad + \delta \qquad - 4B \qquad - 2F = 0 \quad (7)$$

$$-\alpha \qquad + \varepsilon \qquad - C \quad + D \qquad = 0 \quad (8)$$

$$-\alpha \qquad + \varepsilon + A \qquad + C \quad - D + E \qquad = 0 \quad (9)$$

$$\beta \quad + \delta \qquad + 2B \qquad + F = 0 \quad (10)$$

By eliminating the unknown quantities A—F from these equations it could immediately be tested, whether they are correct or not. We get:

$$A = -E; \quad B = \frac{1}{4\sqrt{2}}E; \quad C = \frac{1}{2}E; \quad D = \frac{1}{2}E; \quad F = \frac{-1}{2\sqrt{2}}E$$

and finally derive the following three equations between the wellknown quantities α, β, γ, δ, and ε:

$$-\alpha + \varepsilon = 0 \qquad (4,f)$$

$$\beta + \delta = 0 \qquad (5,f)$$

$$\gamma - 3\delta = 0 \qquad (6,f)$$

$$\alpha + \varepsilon = \sqrt{2}\,(\beta - \delta) \qquad (7,f)$$

Here $(4,f)$, $(5,f)$ and $(6,f)$ simply are identical with the earlier derived equations $(2,f)$, $(1,f)$ and $(3,f)$ (page 19). The consequences of these three equations were shown to be correct. However, $(7,f)$ is certainly wrong. By insertion of the numerical values of the force-constants given on page 21 (model 1) the left-hand side becomes $+35 \cdot 10^4$ while the right-hand side becomes $-24 \cdot 10^4$. This definite inequality is furthermore seen to be independent of the choice of model.

Table IX gives exactly the same result.

6. Difficulties of Further Physical Treatment.

At a first glance it seems peculiar that the first use of the empirical rule made in this paper gives correct results, while the use of the rule just made above leads to at least one false

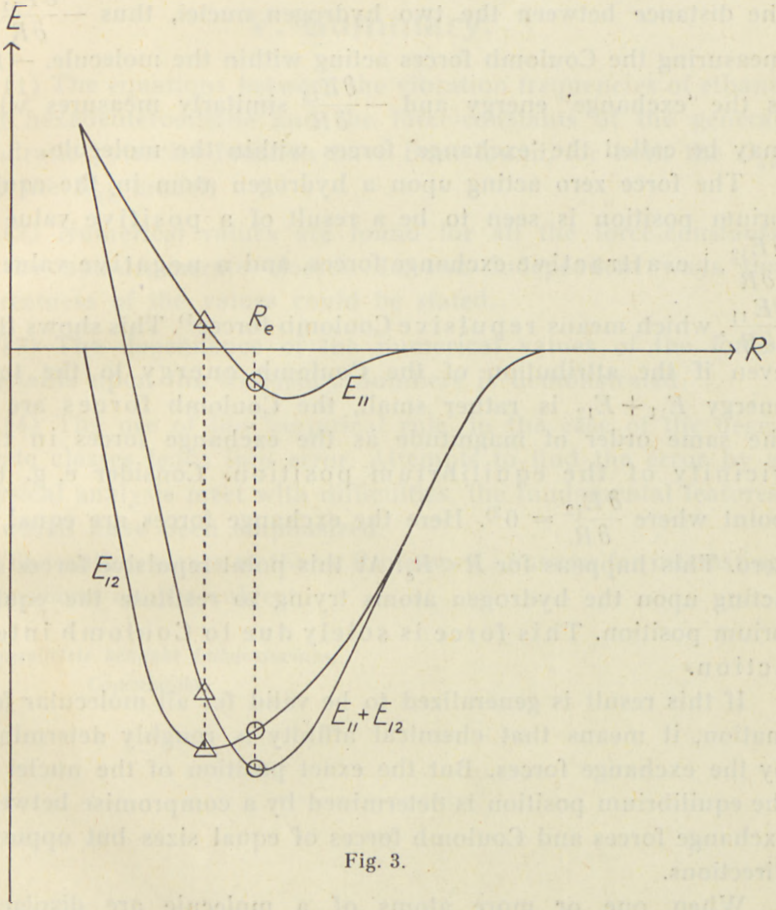

Fig. 3.

equation. *A priori* one would reason that the disturbance of the molecule made by displacing *one* hydrogen atom must be much less than by displacing *three*. If, however, one tries to penetrate deeper into the problem great difficulties are at once met with.

We start with drawing the attention to the original paper by HEITLER and LONDON[1] and by SIUGURA[2] on the prototype of

[1] HEITLER and LONDON, Zeits. f. Physik, **44**, 455 (1927).
[2] SIUGURA, ibid. **45**, 484 (1927).

molecules, the hydrogen molecule. Fig. 3 reproduces the essential features in a figure from the paper of SIUGURA.

E_{11} is the 'Coulomb' integral, which corresponds to the classical interaction energy between the two hydrogen atoms. R is the distance between the two hydrogen nuclei, thus $-\frac{\partial E_{11}}{\partial R}$ is measuring the Coulomb forces acting within the molecule. $-E_{12}$. is the 'exchange' energy and $-\frac{\partial E_{12}}{\partial R}$ similarly measures what may be called the 'exchange' forces within the molecule.

The force zero acting upon a hydrogen atom in the equilibrium position is seen to be a result of a positive value of $\frac{\partial E_{12}}{\partial R}$, i.e. attractive exchange forces, and a negative value of $\frac{\partial E_{11}}{\partial R}$, which means repulsive Coulomb forces[1]. This shows that even if the attribution of the Coulomb energy to the total energy $E_{11}+E_{12}$ is rather small, the Coulomb forces are of the same order of magnitude as the exchange forces in the vicinity of the equilibrium position. Consider e. g. the point where $\frac{\partial E_{12}}{\partial R}=0$[2]. Here the exchange forces are equal to zero. This happens for $R<R_e$. At this point repulsive forces are acting upon the hydrogen atoms trying to restitute the equilibrium position. This force is solely due to Coulomb interaction.

If this result is generalized to be valid for all molecular formation, it means that chemical affinity is roughly determined by the exchange forces. But the exact position of the nuclei in the equilibrium position is determined by a compromise between exchange forces and Coulomb forces of equal sizes but opposite directions.

When one or more atoms of a molecule are displaced from the equilibrium position, the problem, therefore, is to account for the hange in two great forces, exchange and Coulomb forces. Consequently it generally lies beyond the reach of qualitative arguing to give reasons why e. g. the 'empirical rule' could be used with success in one case and not in the other.

1) Points marked with circles.
2) Points marked with triangles.

In future work the author hopes to be able to carry through a quantitative or semi-quantitative treatment of this and similar problems.

V. Summary.

(1) The equations between the vibration frequencies of ethane and hexadeuteroethane and the force-constants of the general quadratic potential function have been found, for both the D_{3d} and the D_{3h} model.

(2) Numerical values are found for all the force-constants of the non-degenerate classes. In two independent ways the correctness of the values could be stated.

(3) The dependence of the numerical values of the force-constants upon the frequency numbers is demonstrated.

(4) The use of the 'empirical rule' in the case of the degenerate classes leads into error. Attempts to find the error by a physical analysis meet with difficulties, the fundamental features of which have been emphasized.

The author wants to thank Professor LANGSETH for interesting discussions on the subject.

Universitetets kemiske Laboratorium,
Copenhagen.

Indleveret til Selskabet den 10. April 1946.
Færdig fra Trykkeriet den 3. September 1946.

DET KGL. DANSKE VIDENSKABERNES SELSKAB
MATEMATISK-FYSISKE MEDDELELSER, BIND XXIV, NR. 2

DIELECTRIC CONSTANT, VISCOSITY, SURFACE TENSION, AND CRITICAL DATA OF BORON TRIBROMIDE, DIOXAN, AND ETHYLENE DICHLORIDE

BY

KRISTIAN HØJENDAHL

KØBENHAVN
I KOMMISSION HOS EJNAR MUNKSGAARD
1946

Printed in Denmark
Bianco Lunos Bogtrykkeri

Although the physical properties of pure liquids have been investigated in a great number of cases, the relationship between these properties of the bulk liquid and the properties of the molecules themselves is not yet completely clear. Presumably the reason is that the actual shape of the molecules is important, i. e. they cannot be regarded as spheres. Again, large molecules are often flexible and, due to the possibility of twisting single bonds, they may take up a number of shapes; ethylene dichloride is a simple example. Ring structures like dioxan must, however, be more rigid. Inorganic molecules are generally simple in shape and rigid, but they have been comparatively little investigated for several reasons, one being that the liquid state is seldom realised at room temperature. Boron tribromide is, however, a liquid at ordinary temperatures, and therefore suitable for study. The three examples quoted are insufficient for a generalisation to be made.

Experimental.

Purification. The purification of ethylene dichloride has been described previously (1). Dioxan marked "Exluan 07" was frozen, dried over sodium and distilled to give four fractions at melting points 11.75, 11.76, 11.80, and 11.55 °C. respectively, According to Timmermans and Roland (2), 11.80 is the correct melting point. Boron tribromide was distilled twice in a stream of pure hydrogen and then a fraction was distilled in vacuo, in a sealed all-glass apparatus, into a conductivity cell and four ampoules. The melting point was found to be —47 °C.; Stock and Kuss (3) found —46 °C.

Dielectric Constant. The dielectric constant of ethylene dichloride has been determined earlier (1); since then Sugden (4)

has made a more accurate determination. The dielectric constant of dioxan has also been determined by several investigators, but that of boron tribromide has not been measured previously. The above conductivity cell of large capacity was used, and the dielectric capacity measured by means of an apparatus described elsewhere (5). It was also proved that boron tribromide is a perfect insulator. The dielectric constants for twice- and thrice-distilled boron tribromide were in agreement; measurements were made at several temperatures between -70 and $+80\,^{\circ}C$. For the liquid state, the following formula was found to be valid:

$$\varepsilon = 2.58 - 0.0028\,t \pm 0.03$$

where ε is the dielectric constant at temperature $t\,^{\circ}C$. The dielectric constant of the solid is not very different from that of the liquid, but the formation of bubbles prevented a very accurate determination. The dipole moment is certainly not larger than $0.15 \cdot 10^{-18}$ e. s. u., and is presumably zero. Zero moment was found for boron trifluoride by WATSON, RAMASWAMY and KANE (6). ANDERSON, LASSETTRE and YOST (7) have studied the Raman spectra of BF_3, BCl_3, and BBr_3 and explain the results on the basis of a plane model in which the three halogen atoms form a regular triangle with the boron atom at the centre. The present data are in accordance with these findings.

Viscosity and Surface Tension. These were both measured by means of the same apparatus. As emphasised by RAASCHOU (8) a modified Ostwald viscometer is very useful for the determination of surface tension by the capillary rise method. The apparatus used here was provided with standard ground joints for the inlet and outlet so that boron tribromide could be distilled into it and kept under dry hydrogen all the time. The liquid was raised by means of hydrogen pressure and then both gas spaces were connected, and the time of outflow of a definite volume between two marks was measured by a stopwatch. After the lapse of some time the meniscus in the narrow tube had attained its equilibrium position, and the capillary rise was measured by means of a cathetometer. The apparatus was calibrated for both purposes by means of water. In the

case of dioxan several different volumes of liquid were used, thus varying both the height of fall in the viscometer and the position of the meniscus for the capillary rise measurements. In this way both viscosity and capillary rise measurements were controlled, and it was proved that the effect of kinetic energy on the viscosity measurements is insignificant. As the walls of the capillary tube are wetted during the flow of liquid, it is fairly certain that the contact angle is zero. The measurements were carried out at several temperatures between -45 and $+70$°C. The viscosity η in gm./cm. sec. was found to vary with the absolute temperature T according to the following logarithmic formulae:

$$\text{Ethylene dichloride} \quad \log_{10}\eta = \frac{532}{T} - 3.88;$$

$$\text{Dioxan} \quad \log_{10}\eta = \frac{625}{T} - 4.02;$$

$$\text{Boron tribromide} \quad \log_{10}\eta = \frac{346}{T} - 3.33;$$

In the case of ethylene dichloride the present values lie between those of THORPE and ROGER (9) and those of FAUST (10). For dioxan the agreement with TIMMERMANS and ROLAND (2) is very good, whereas the data of HERZ and LORENTZ (11) deviate considerably. The viscosity of boron tribromide has not been measured before.

The theory of the logarithmic formula for viscosity has been gradually evolved; in part it dates back to MAXWELL (12) and later contributions are due to RAMAN (13), DUNN (14) and ANDRADE (15). It is in fact a consequence of DEBYE's (16) theory of the "quasicrystalline structure of liquids". The first constant in the formula is a measure of the critical increment of energy required for the mutual passage of molecules, and the second constant is a measure of the velocity with which the molecules move during the passage. Due to its great molecular weight boron tribromide moves more slowly than the other molecules, but the critical increment is smaller because the dimensions of the molecule are small, and the molecule as a whole is of a suitable shape.

The variation of the surface tension γ with the temperature

in °C is not quite linear; for the sake of simplicity, however, a linear formula is given:

Ethylene dichloride $\gamma = 36.3 - 0.14\,t$ (dynes/cm.)
Dioxan $\gamma = 36.1 - 0.14\,t$;
Boron tribromide $\gamma = 32.1 - 0.13\,t$.

These data agree with older data of SCHIFF (17) and TIMMERMANS and ROLAND (2), but not with data of JAEGER (18), WORLEY (19) or HERZ and LORENTZ (11). The surface tension of boron tribromide has not been previously determined.

The Orthobaric Curve. In the T—D (or theT—V) diagram the orthobaric curve gives the relationship between the temperature and the density of saturated vapour or boiling liquid. With the vapour pressure curve in the P—T diagram or the border curve in the P—V diagram it defines the equilibrium between the liquid and gaseous states. Two of these curves determine the third. As will be shown below the orthobaric curve and the vapour pressure curve (to the vicinity of the critical point) may be determined by means of simple devices, whereas the investigation of the border curve requires a complicated apparatus.

The present apparatus for determining the orthobaric curve is constructed by combining suggestions of CENTNERSZWER (20) and GOUY (21). Varying amounts of the material are sealed (air-free) into ampoules 8 cm. long of internal diameter 2 mm. and external diameter 4 mm. An ampoule is placed in the central bore of an electrically heated copper cylinder, and rests on a screw mounted loosely in the cylinder, so that the ampoule may be shaken and moved up and down to make the meniscus visible through the observation hole. Light from an incandescent lamp passes through an inlet into the cylinder, is reflected by the meniscus, and passes out again through the observation hole, which is at an angle to the inlet such that only the reflected image and not the lamp itself is visible. The image is observed during slow heating until it disappears, showing that the meniscus disappears, and the corresponding temperature is read on a thermometer placed in a hole in the copper cylinder. On subsequent slow cooling the temperature of reappearance of the meniscus is also read. The whole arrangement is calibrated by determining the melting points of tin, bismuth and

cadmium contained in glass tubes in place of the ampoule. The ampoules are tested before use, but the observation hole is covered by mica and metal gauze to protect the eye from possible damage due to fragments of an exploding ampoule.

When the meniscus disappears or reappears at the bottom of the ampoule, this is filled with saturated vapour; when it is at the top of the ampoule, this is filled with liquid at the boiling point; and when the meniscus disappears inside the ampoule, the critical state is approached. It follows that the temperature of disappearance of the meniscus, and the density of the contents of the ampoule, are the data to be plotted in a diagram to give points on the orthobaric curve. The weight of the material is obtained by breaking the ampoule into two parts, evaporating the contents, and weighing before and after. The volume of the ampoule is determined by filling the two parts with water and weighing. In this determination, however, the effect of temperature and pressure on the volume is neglected.

Orthobaric curves for ethylene dichloride, dioxan, and boron tribromide obtained in the above manner are shown in Fig. 1. For each density, two temperatures are marked, the higher being for the disappearance and the lower for the appearance of the meniscus; the difference of 2 °C. is a measure of the accuracy. As CENTNERSZWER has emphasised the orthobaric curve is very sensitive to the degree of purity of the material. Slight decomposition of ethylene dichloride at the high temperature used is unavoidable, but dioxan is stable and presumably pure. Most samples of boron tribromide were of twice distilled material only, but four ampoules were filled with thrice distilled material. Of these, only one withstood heating, fortunately one in which the contents had nearly the critical density. The critical temperature of 300 °C. found by means of this sample is considered to be the best value; it is 2 °C. below the maximum of the curve drawn through the other values. The critical density was estimated by means of the law of the rectilinear diameter of CAILLETET and MATHIAS (22). The following critical data have been found:

	t_c	d_c
Ethylene dichloride	290 °C.	0.44
Dioxan	312	0.36
Boron tribromide	300	0.90

Older data are available only for ethylene dichloride; PAWLEWSKI (23) found $t_c = 283\,^{\circ}C.$ and NADEJDINE (24) found $t_c = 288.4\,^{\circ}C.$ and $d_c = 0.419$.

Vapour Pressure. The vapour pressure curve of dioxan shown in Fig. 2 has been determined by a new method de-

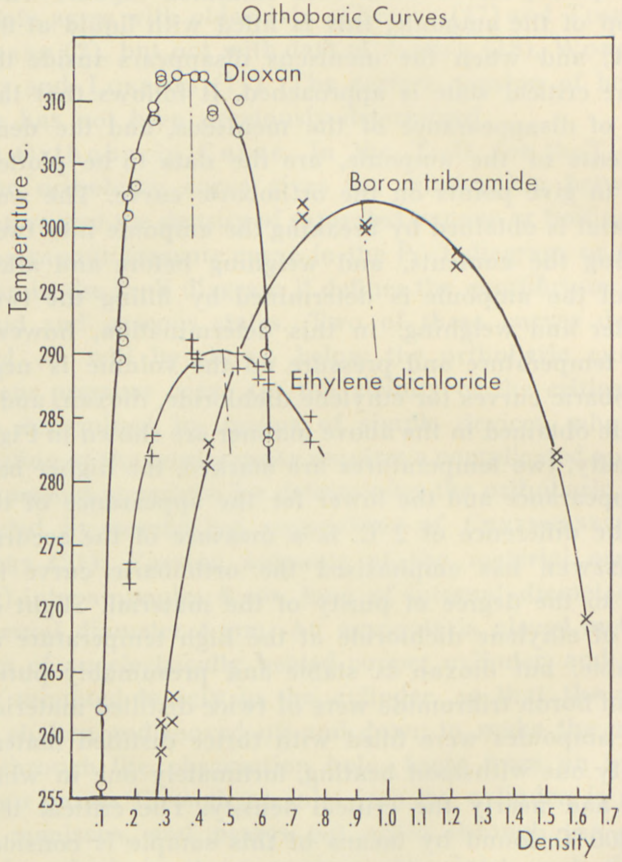

Fig. 1.

pending on a balance of vapour pressures. A U-shaped glass tube is filled with mercury in the bend. The substance to be investigated (here dioxan) is placed on top of the mercury in one branch, and benzene in the other branch. Air is boiled out of each branch before sealing it, and the closed U-tube then contains four phases, namely dioxan liquid, mercury, benzene

liquid, benzene vapour. If now the dioxan branch is heated, a sudden shift will take place at that temperature at which the vapour pressure of the dioxan exceeds that of benzene at room temperature. After the shift the sequence of phases will be:— dioxan vapour, dioxan liquid, mercury, benzene liquid. The difference in height of the mercury column and columns of other liquids will of course exert an influence, but in the vicinity of the critical pressure this will only require a small correction. In the actual measurements each branch of the U-tube was placed in an electrically heated copper cylinder like that described above. For the purpose of following the change of phases the interface benzene-mercury was kept outside, and the temperatures of the two heating baths were raised alternately. When the interface benzene-mercury began to move the heating was reversed, and it was often possible to obtain a balance of pressures with vapour in both branches of the U-tube. The corresponding temperatures of the two heating baths were then read. From the known vapour pressure curve for benzene as determined by YOUNG (25), with a small correction for the heights of the columns of mercury and the other liquids, the vapour pressure curve of dioxan was determined. Systematic errors were to some extent eliminated by interchange of heating baths.

The vapour pressure curve of dioxan is shown in Fig. 2. The difference between the points marked with circles and those marked with crosses lies in the interchange of heating baths. Inside the experimental error of some 2 per cent, the vapour pressure of dioxan may be expressed by the curve shown in the diagram drawn according to the formula:

$$\log_{10} p = 4.69 - \frac{1750}{T}$$

where p is the pressure in bar and T is the absolute temperature. Extrapolating to the critical temperature 312 °C (as determined above), the critical pressure is found to be 50 bar with a possible error of some 3 bar.

Summary.

1. The dielectric constant of liquid and solid boron tribromide has been measured over a wide range of temperatures. The dipole moment is small and presumably zero.

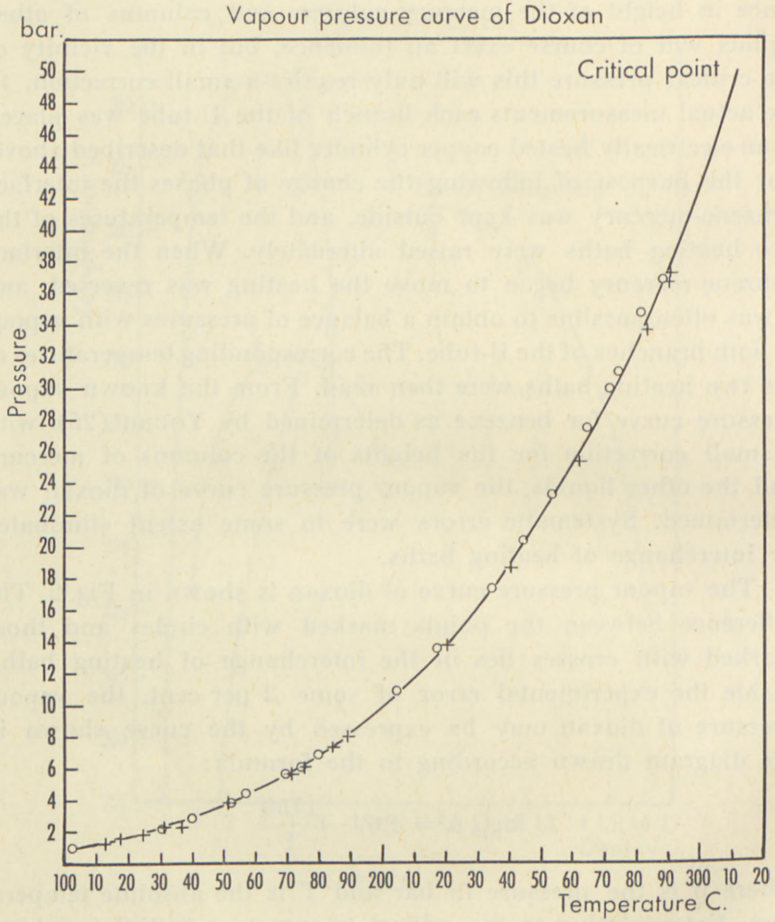

Fig. 2.

2. The surface tension of a sensitive liquid such as boron tribromide is conveniently measured by the capillary rise method in a modified Ostwald viscometer. Viscosity and surface tension data for boron tribromide, dioxan and ethylene dichloride have been obtained over a wide range of temperatures.

3. Simple methods and apparatus have been devised for determining the orthobaric curve and the vapour pressure curve in the vicinity of the critical point. The method of determining the vapour pressure by means of a balance of vapour pressures is particularly new. The bend of a U-tube is filled with mercury, and the substance to be investigated (dioxan) is enclosed (air-free) in one branch and a standard liquid (benzene) in the other. Each branch is placed in a seperate heating bath, and the two are warmed alternately until the visible mercury-benzene interface moves rapidly, showing that vapour is present in both branches. By temperature regulation the motion is brought to a standstill, and the temperature of both baths is read. Knowing the vapour pressure curve of the standard liquid, that of the liquid under investigation may be determined.

This work was carried out in the Chemical Laboratory of the Royal Veterinary and Agricultural College, Copenhagen. I wish to thank the Director of the Laboratory, Professor N. Bjerrum, for his interest, and Dr. A. K. Holliday for help in rendering this paper into English.

Landbohøjskolens kemiske Laboratorium.
Bülowsvej 13. Copenhagen V.

References.

(1) Højendahl, *Z. physikal. Chem. B.* 1933, **20**, 58.
(2) Timmermans and Roland, *J. Chim. Phys.*, 1937, **34**. 725.
(3) Stock and Kuss, *Ber.*, 1914, **47**, 3113.
(4) Sugden, *J. Chem. Soc.*, 1933, 773.
(5) Højendahl, *D. Kgl. Danske Vidensk. Selskab, Mat-fys. Medd.* XVI, 2, 9, 1938.
(6) Watson, Ramaswamy & Kane, *Proc. Roy Soc.*, 1936, A, **156**, 130.
(7) Anderson, Lassettre & Yost, *J. Chem. Physics*, 1936, **4**, 703.
(8) Raaschou, *Ind. Eng. Chem.*, (*Anal*), 1938, **10**, 35.
(9) Thorpe and Roger, *Phil. Trans.*, 1894, **185A**, 397.
(10) Faust, *Z. physikal. Chem.*, 1912, **79**, 101.
(11) Herz and Lorentz, *Z. physikal. Chem. A.*, 1929, **140**, 406.
(12) Maxwell, *Phil. Mag.*, (4) 1868, **35**, 133.
(13) Raman, *Nature*, 1923, **111**, 532.
(14) Dunn, *Trans. Faraday Soc.*, 1926, **22**, 401.
(15) Andrade, *Nature*, 1930, **125**, 309.
(16) Debye, "Der feste Körper", 1938.
(17) Schiff, *Annalen*, 1884, **223**, 72.
(18) Jaeger, *Z. anorg. Chem.*, 1917, **101**, 1.
(19) Worley, *J. Chem. Soc.*, 1914, **105**, 274.
(20) Centnerszwer, *Z. physikal. Chem.*, 1904, **49**, 199.
(21) Gouy, *J. Physique.*, (3), 1897, **6**, 479.
(22) Cailletet and Mathias, *Compt. Rend.*, 1886, **102**, 1202.
(23) Pawlewski, *Ber.*, 1883, **16**, 2633.
(24) Nadejdine, *Rep. d. Physik.*, 1887, **23**, 639.
(25) Young, *J. Chem. Soc.*, 1889, 55, 486.

Indleveret til Selskabet d. 5. Juli 1946.
Færdig fra Trykkeriet d. 31. December 1946.

DET KGL. DANSKE VIDENSKABERNES SELSKAB
MATEMATISK-FYSISKE MEDDELELSER, BIND XXIV, Nr. 3

HINDERED ROTATION IV

THE RAMAN SPECTRUM OF DEUTERATED ETHYL BROMIDES

BY

A. LANGSETH AND B. BAK

KØBENHAVN
I KOMMISSION HOS EJNAR MUNKSGAARD
1947

Printed in Denmark
Bianco Lunos Bogtrykkeri

INTRODUCTION

In classical stereochemistry complete freedom of rotation about single bonds is assumed because it has been impossible to isolate isomers corresponding to different orientations of groups connected by a single bond. Even the simple quantum mechanical conception of the carbon-carbon single bond implies free internal rotation about the bond axis as far as the wave function of the bond is assumed to have rotational symmetry. For the double bond, however, π-electrons have a node coplanar with the plane containing the two carbon atoms and the four adjacent atoms (or groups), thus producing a torsional restriction sufficiently large to make a separation of the contingent rotational isomers possible. It is known that in molecules containing two or more double bonds or aromatic rings the π-electrons may interact, tending to form molecular orbitals covering greater parts of the molecule, which results in a restriction of the internal rotation about bonds represented as single bonds in the classical formular. But even in saturated molecules a similar —though much weaker—rotational hindrance due to interactions between the electrons is to be expected. In ethane, for instance, the mutual perturbation of the two methyl groups will distort the potential curve for their azimuthal orientation. From symmetry reasons it follows that it must exhibit three potential barriers. In fact, strong evidence has in recent times been collected showing that the internal rotation in the ethane molecule is rather strongly restricted. On the basis of entropy measurements KEMP and PITZER[1] found it necessary, in order to obtain agreement between theory and experiment, to assume a

[1] Journ. Amer. Chem. Soc. 59, 276 (1937).

value of about 3000 cal/mol for the height of each barrier. This result was confirmed by KISTIAKOWSKY, LACKER and STITT[1] who from the heat capacity date of C_2H_6 and C_2D_6 found the value 2750 cal/mol. It must be emphazized, however, that the computed height of the barriers depends on the assumed form of the potential function.[2] On the other hand, there seems to be no other possibility of explaining the observed variation of the heat capacity of ethane with temperature than assuming torsional barriers of considerable heights (at least 1500 cal/mol).

The presence of rotational barriers in the ethane molecule involves the existence of certain stable configurations, which will naturally be indistinguishable because of the trigonal symmetry of the methyl groups. Under normal conditions torsional vibrations around the molecule axis will occur, only with occasional jumps over the potential barrier. The frequency of this vibration will be of the order of magnitude of 300 cm^{-1} if the barriers have the computed heights of about 3000 cal/mol. No direct information, however, can be obtained either from the infra-red absorption or from the Raman spectrum, because the fundamental torsional frequency is inactive in both spectra. Theoretically it may, however, appear in combination with other active frequencies or—in the Raman spectrum—as even overtones. In the Raman spectrum of liquid ethane GLOCKLER and RENFREW[3] as well as CRAWFORD, AVERY and LINNETT[4] have reported a faint line at 620 cm^{-1} which might be interpreted as the Raman-active overtone of the torsion frequency. On the basis of a sinusoidal potential function this corresponds to a height of the barrier of ca. 3400 cal/mol in good agreement with the entropy value. Although the molecular spectra of ethane (and hexadeuteroethane) have been very thoroughly investigated and discussed, it has not yet been possible to obtain an unambiguous confirmation of the torsion frequency. Furthermore no conclusive evidence has been gained from the spectroscopical material to permit a choice between the two possible configurations: the

[1] Journ. Chem. Phys. **7**, 289 (1939).
[2] Cf. A. CHARLESBY: Proc. Physic. Soc. **54**, 471 (1942).
[3] Journ. Chem. Phys. **6**, 295, 409 (1938).
[4] Journ. Chem. Phys. **6**, 682 (1938).

D_{3d}-symmetrical ("staggered") or the D_{3h}-symmetrical ("opposed") model.

There is another way of tackling the problem. If substituents are introduced into the two methyl groups of ethane, the presence of a rotational restriction makes the existence of "rotational" isomers possible. Because of the low potential barriers these will be too labile to allow separation and isolation. The Raman spectrum, however, should reveal the coexistence of such isomers and in favorable cases produce a conclusive proof of the rotational restriction. K. W. F. KOHLRAUSCH[1] was the first who on the basis of the Raman spectra of several halogenated paraffins and other alifatic compounds postulated the existence of rotational isomers. Even if in this way—mainly by KOHLRAUSCH and coworkers—it has been possible to collect an extensive material supporting this assumption, still some uncertainty remains because of the great complexity of the spectra. The main difficulty arises from the fact that the various possible rotational isomers may have fairly different thermodynamical stabilities, and that *a priori* very little can be said about the proportion in which they occur in the equilibrium mixture. This difficulty is overcome by the investigation of the spectra of molecules in which the asymmetry responsible for the rotational isomerism is caused by the presence of isotopic atoms. From considerations of symmetry it is evident that for example 1,2-dideutero-ethane, $CH_2D \cdot CH_2D$, must be a mixture of 3 rotational isomers, two of which are mirror-images of one another and therefore will have Raman spectra which are identical, but different from the spectrum of the third. As the three isomers have the same statistical weight their thermodynamical stability must also be approximately the same.[2] The Raman spectrum of the equilibrium mixture should therefore be a superposition of two spectra with an intensity ratio of about 1:2 according to the abundance of the two spectroscopically different molecular species in the mixture.

[1] Zeitschr. phys. Chem. **B, 18**, 61. 217 (1932).—For a compilation of the work done along this line, cf. K. W. F. KOHLRAUSCH: Ramanspektren. Hand- und Jahrb. chem. Phys. Bd. **9**, VI (1943).

[2] A slight difference due to small departures in zero-point energy and moments of inertia is neglected in this connection.

The chance of a successful analysis of the Raman spectrum along this line, however, depends entirely on the possibility of obtaining a spectrum of the best attainable quality and completeness. As there will be great technical difficulties in getting sufficiently good spectra of ethane and its deuterium derivatives, we decided instead to investigate mono-deutero-ethyl bromide, CH_2D-CH_2Br. If there is a restriction of the internal rotation this molecule must exhibit a similar rotational isomerism as CH_2D-CH_2D. From an experimental point of view ethyl bromide is far easier to handle. Its physical properties are convenient for the experimental procedure, it can be prepared in sufficient quantities in a chemically and optically pure state, and the molecule has a comparatively low number of vibrational frequencies to ensure a spectrum which is not too complex for an unambiguous demonstration of the expected effect. Furthermore, ethyl bromide fulfils the important requirement that the rotational problem is not obscured by the effect of interacting dipoles or by steric hindrance as is generally the case with the molecules investigated by KOHLRAUSCH and coworkers.

Experimental Procedure and Results.

All the Raman spectra were taken with a spectrograph of high dispersion and with a Raman apparatus of very high light-gathering power. The positions of the lines were measured against an iron-arc comparison spectrum on photographic enlargements (1:15).

The purified substance under investigation was dried over P_2O_5 and in high vacuum distilled into the Raman tube. The apparatus used is shown in fig. 1. The tube was sealed off at S. By repeated distillation (surface evaporation in the high vacuum) from B to R and pouring back to B by tilting the tube all dust particles were removed from the liquid in R and collected in B. In this way very strongly exposed Raman spectra could be obtained without the continuous background getting too predominant. The Hg-line 4358 Å was used for excitation, the violet Hg-lines being cut off by a $NaNO_2$-filter.

The spectrum of $CH_2D \cdot CH_2Br$ and for comparison those of $CH_3 \cdot CH_2Br$, $CH_3 \cdot CHDBr$, and $CD_3 \cdot CD_2Br$ were measured. The

preparations of these substances are described in the appendix. The observed spectra are given in Tables I and II. The intensities have been estimated visually on an arbitrary scale of 10. Diffuse lines are marked "d", broad lines "b". As mentioned in the appendix we did not succeed in preparing a sample of $CH_2D \cdot CH_2Br$ entirely free from contamination with other isotopic species. In order to identify the spectrum of the pure compound,

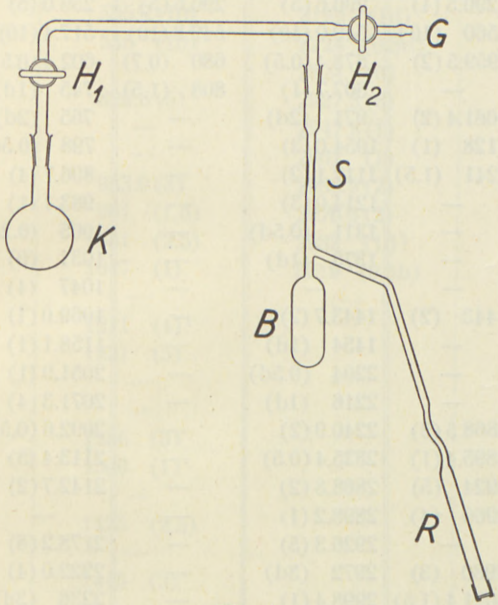

Fig. 1.

it was prepared in three different ways (I, II, III). Intermediate products were in most cases tested for isotopic purity by taking their Raman spectrum. As pointed out in the appendix Preparation I contained as impurities only higher deuterated species, Preparation II only lower deuterated species (i. e. C_2H_5Br), and Preparation III both higher and lower deuterated species. By careful and critical comparison of the spectra all lines due to other isotopic molecules rather than $CH_2D \cdot CH_2Br$ could be eliminated with certainty.

Owing to the improved technique the recorded spectra are more complete than those measured by previous authors.[1]

[1] Cf. K. W. F. Kohlrausch, Smekal-Raman Effekt, Ergänzungsband, p. 206; J. Wagner, Zeitschr. phys. Chem. (B) **40**, 439 (1938); **45**, 69, 341 (1939).

Table I.

Observed Frequencies and Intensities.

$CH_3 \cdot CH_2Br$		$CH_3 \cdot CHDBr$		$CD_3 \cdot CD_2Br$	
Present authors	De Hemptinne	Present authors	De Hemptinne	Present authors	De Hemptinne
—	143.2 (0.5)	—	—	—	—
290.4 (6)	290.5 (4)	290.6 (5)	290.6 (5)	259.0 (5)	259 (2)
560.4 (10)	560 (10)	549.0 (10)	549.8 (10)	517.4 (10)	518 (10)
959.3 (2d)	959.5 (2)	678.4 (0.5)	680 (0.7)	602.4 (0.5)	—
1022 (0.5b)	—	807.7 (1)	808 (1.5)	745 (1d)	—
1062.0 (3)	1061.4 (2)	971 (2d)	—	765 (2d)	—
—	1128 (1)	1054.0 (3)	—	798 (0.5d)	—
1241.5 (2)	1241 (1.5)	1117.1 (2)	—	896.7 (4)	897 (2)
1250 (0.5d)	—	1214.0 (3)	—	983.1 (1)	—
1255 (1d)	—	1311 (0.5d)	—	1005 (0.2d)	—
1348.5 (0.5)	—	1378 (1d)	—	1031 (0)	—
1378.5 (1)	—	—	—	1047 (4)	1050 (1)
1443.3 (2)	1443 (2)	1443.7 (2)	—	1069.0 (1)	—
1453 (1d)	—	1454 (1d)	—	1158.1 (1)	—
2736.9 (1)	—	2204 (0.5d)	—	2051.9 (1)	2051 (0.7)
2825.5 (0.5)	—	2216 (1d)	—	2071.3 (4)	2072 (3)
2867.8 (3)	2868.5 (3)	2240.9 (2)	—	2092.6 (0.5)	2094 (0.7)
2893 (1d)	2895.4 (1)	2825.4 (0.5)	—	2113.4 (5)	2115 (4)
2926.3 (7)	2924 (5)	2868.8 (2)	—	2142.7 (2)	2144 (2)
2961.2 (5)	2960 (4)	2898.2 (1)	—	—	2169 (1)
2970 (1d)	—	2926.3 (5)	—	2178.2 (8)	2181 (5)
2980.2 (3)	2980 (3)	2972 (3d)	—	2222.0 (4)	2222 (2)
3022 (1d)	3021.4 (1.5)	2998.4 (1)	—	2236 (3d)	2235 (1)
				2275 (2d)	—
				2311.1 (2)	—

M. de HEMPTINNE and C. VELGHE[1] have investigated the Raman spectra of several deuterium derivatives of ethyl bromide prepared by a method similar to that used by us in Preparation I (cf. Appendix). They have not, however, succeeded in isolating pure samples of the different derivatives, and the measured spectra are incomplete. For comparison the recorded frequencies are included in Tables I and II. The agreement is generally excellent.

[1] Physica **5**, 958 (1938).

Table II.

$CH_2D \cdot CH_2Br$

Observed Frequencies and Intensities.

Present authors	De Hemptinne	Present authors	De Hemptinne
280.8 (5)	282 (5)	2110 (0.3)	2108 (0.7)
287.0 (3)	—	2167.7 (2)	2167 (5)
536.7 (5)	535.8 (10)	2192 (1d)	2188 (3)
557.5 (10)	556 (10)	2224 (0.5d)	2225 (2)
703.8 (0.5)	—	2824 (0)	—
826.4 (2)	825.6 (5)	2927.3 (6)	2925 (8)
896.8 (0.5)	—	2947.8 (1)	2947 (4)
912.0 (0.3)	—	2961 (1)	—
935.2 (2)	933.9 (3)	2966.5 (2)	2968 (8)
960.8 (1.5)	961 (1.5)	2976.6 (2)	2978 (8)
1031.0 (1.5)	1031 (2.5)	2982 (1d)	—
1046.4 (1)	1047 (1)	3019 (0.5b)	—
1181 (0.5d)	—	—	3076 (2)
1189 (0.5d)	1211 (4)[1]		
1231.2 (3)	1231 (5)		
1247 (0.5d)	—		
1260 (0.5d)	—		
1286.3 (2)	1286 (3)		
1309.9 (0.8)	1309 (1)		
1347 (0.2)	—		
1424.5 (1)	1425 (2.5)		
1437 (0.5d)	—		
1444.5 (2)	1445 (3)		
1453 (1d)	—		

[1] This strong line presumably belongs to some other isotopic molecule (CH_3CHDBr?).

Discussion of Observed Spectra.

As none of the molecules under consideration (viz. $CH_3 \cdot CH_2Br$, $CH_3 \cdot CHDBr$, $CH_2D \cdot CH_2Br$, and $CD_3 \cdot CD_2Br$) can have more than one plane of symmetry all vibrations will be Raman-active. Consequently, there is no need for discussing the symmetries of the molecules and their contingent rotational isomers; all the molecular species must exhibit $(3n - 6) = 18$ Raman lines. Five of these will correspond to hydrogen (or deuterium) stretching vibrations with frequencies $\sim 3000\ cm^{-1}$ (resp. $\sim 2000\ cm^{-1}$). Only 13 Raman lines are to be expected in the region below $1600\ cm^{-1}$.

Table III.

$CH_3 \cdot CH_2Br$	$CH_3 \cdot CHDBr$	$CH_2D \cdot CH_2Br$	
		A	B
290.4 (6)	290.6 (5)	280.8 (5)	287.0 (3)
560.4 (10)	549.0 (10)	557.5 (10)	536.7 (7)
959.3 (2)	678.4 (0.5)	826.4 (2)	703.8 (0.5)
1022 (0.5)	807.7 (1)	896.8 (0.5)	912.0 (0.5)
1062.0 (3)	971 (2)	935.2 (2)	960.8 (1.5)
1241.5 (2)	1054 (3)	1031.0 (1.5)	1046.4 (1)
1250 (0.5)	1117.1 (2)	1181 (0.5)	1189 (0.5)
1255 (1)	1214.0 (3)	1231.2 (3)	1247 (0.5)
1348.5 (0.5)	1311 (0.5)	1286.3 (2)	1260 (0.6)
1378.5 (1)	1378 (1)	1309.9 (0.8)	1347 (0.5)
1443.3 (2)	1443.7 (2)	1444.5 (2)	1424.5 (1)
1453 (1)	1454 (1)	1453 (1)	1437 (0.5)

Table I shows that 12 lines are observed in $CH_3 \cdot CH_2Br$ and in $CH_3 \cdot CHDBr$ and 13 lines in $CD_3 \cdot CD_2Br$. As the 1031 cm^{-1} line found in deuteroethyl bromide probably is an overtone (of the 517.4 frequency), this means that only one fundamental frequency in this region remains unobserved. Table II, however, shows that $CH_2D \cdot CH_2Br$ has a much more complicated spectrum with 24 measured lines. A closer examination of the frequencies reveals that this seems to be due to splitting into pairs of the lines corresponding to those found in the other compounds.

This is exactly the kind of spectrum to be expected if $CH_2D \cdot CH_2Br$ is a mixture of two closely related, but spectroscopically slightly different, molecular species. This difference is not caused simply by the presence of one deuterium atom in the molecule since $CH_3 \cdot CHDBr$ shows no trace of a similar effect. Evidently it is the destruction of the trigonal symmetry of the methyl group by the deuterium atom in $CH_2D \cdot CH_2Br$ that is responsible for the isomerism. The only reasonable explanation seems to be rotational isomerism.

As mentioned above, the equilibrium ratio between the two spectroscopically different rotational isomers should be approximately 1:2. Therefore the intensities of the component lines in each pair should be different. It will depend on the difference in the modes of vibration of the two rotational isomers how

close the observed intensity ratio will be to 1:2. For several of the frequencies there will presumably only be a slight difference. In these cases the intensity ratio should approximately be 1:2. It is seen from Table II that the observed intensity ratios for the two low-frequency pairs (280.8—207.0 and 536.7—557.5 cm^{-1}) are resp. 3:5 and 5:10 in good accordance with the expected ratio. As these lines have fairly isolated positions in the spectrum, we are confident of their assignment as pairs.

On the basis of different intensities an assignment of the spectra corresponding to the two rotational isomers in $CH_2D \cdot CH_2Br$ is tentatively given in Table III. Because of the incompleteness of the spectra—only 12 instead of 13 frequencies being observed—it is impossible to obtain further support of this assignment by the use of TELLER's product rule.

Appendix.

Preparations.

1. C_2H_5Br was made in the usual way and finally purified by a careful fractional distillation through a 60 cm column over P_2O_5. Boiling interval: 38°.45—38°.55 (760 mm).

2. C_2D_5Br was prepared from C_2D_5OD (supplied by "Norsk Hydro"), H_2SO_4 and HBr. The Raman spectrum taken shows that no exchange takes place between the hydrogen in the acids and the deuterium atoms attached to carbon in the C_2D_5-group. The sample was carefully purified as above. Boiling point: 37°.35—37°.45 (760 mm), that is, 1°.1 lower than for C_2H_5Br.

3. $CH_2D \cdot CH_2Br$. In spite of several attempts we have not succeeded in preparing a pure sample of this compound. Raman spectra were taken of the following three preparations:

Preparation I. A dry mixture of ethylene and deuterium bromide in equimolar portions was led through a tube containing a $BiBr_3$-catalyst at 200°. Yield: 15 per cent. The deuterated ethyl bromide formed was condensed and purified as above. Boiling point: 38°.30—38°.70 (760 mm). It is to be expected that this sample must be a mixture of different isotopic molecules because the $BiBr_3$ catalyses the exchange reactions

$$CH_2{=}CH_2 + DBr \rightleftarrows CH_2D \cdot CH_2Br,$$

$$CH_2D \cdot CH_2Br \rightleftarrows CHD{=}CH_2 + HBr,$$

$$CHD{=}CH_2 + DBr \rightleftarrows CHD_2 \cdot CH_2Br, \text{ and so on.}$$

The Raman spectrum taken was fully consistent with this view. As the reaction velocity was rather low at the experimental conditions chosen (hence the low yield), it is seen that the formation of $CH_3 \cdot CH_2Br$ was less probable than the formation of higher deuterated compounds. Actually, no lines from $CH_3 \cdot CH_2Br$ were present in the Raman spectrum.

Preparation II. An ethereal solution of diazomethane (1 mole) (Organic Synt. **15**) was dried for one hour over solid KOH (mechanical stirring). During the drying process a slight decomposition of the diazomethane took place, visible by the evolution of nitrogen, and resulting in the formation of a small quantity of methyl alcohol. Through a separatory funnel the ethereal solution of diazomethane was dropped to the reaction products of D_2O (25 g) and P_2O_5 (15 g). The reaction

$$CH_2N_2 + D_2O = CH_2D \cdot OD + N_2$$

is catalysed by hydrogen ions. The evolution of nitrogen being reduced to a minimum, the ether was distilled off through a 100 cm column. By continuing the fractionation the mixture of $CH_2D \cdot OH$ and $CH_2D \cdot OH$ contaminated with $CH_3 \cdot OD$ and $CH_3 \cdot OH$ was isolated. Yield: 50 per cent. Boiling with constant boiling hydrogen iodide transformed the alcoholic mixture into a mixture of CH_2DJ and CH_3J. Yield: 0.3 mole. By a Grignard reaction $CH_2DMgJ + CH_3MgJ$ was prepared, and the ethereal solution at once dropped to an ethereal solution of methylene iodide at 10°—20°. The evolution of heat during the reactions taking place was considerable.

$$CH_2D \cdot Mg \cdot J + CH_2J_2 = CH_2D \cdot CH_2J + MgJ_2{}^1.$$

The mixture of $CH_2D \cdot CH_2J$ and $CH_3 \cdot CH_2J$ was isolated by fractionated distillation through a 60 cm column. Boiling point: 71°—75°. Yield: 25 per cent.

[1] A corresponding reaction with CH_2Br_2 is not feasible.

Substitution of iodine by bromine was effected by a method mentioned in LASSAR-COHN: Arbeitsmethoden der org. Chem. (1907), p. 382, by which

$$2\,C_2H_5J + 2\,CuBr_2 = 2\,C_2H_5Br + 2\,CuJ + Br_2.$$

The reaction was carried through by boiling for 4 hours under reflux condenser. Yield: 90 per cent. Purification as usual. The sample obtained must be a mixture of $CH_2D \cdot CH_2Br$ and a small amount of $CH_3 \cdot CH_2Br$. There seems to be no possibility of the presence of higher deuterated compounds. These views were fully substantiated by the Raman spectrum.

Preparation III. To 2.5 moles of dimethyl malonate was added $^1/_2$ cc conc. sulphuric acid and 50 cc D_2O. After standing for 15 hours at room temperature methyl alcohol formed by the reaction

$$\begin{matrix} \diagup COOCH_3 \\ CH_2 \\ \diagdown COOCH_3 \end{matrix} + D_2O \rightarrow \begin{matrix} \diagup COOCH_3 \\ CH_2 \\ \diagdown COOD \end{matrix} + CH_3OD \qquad (1)$$

was slowly distilled off through a 60 cm column at 63°—65° (760 mm). Preliminary experiments had shown that under the conditions chosen the saponification only extends to one of the ester groups. At the point at which an evolution of CO_2 starts, the receiver is shifted, thus collecting a mixture of CH_3OD and $CH_2D \cdot COOCH_3$ originating from the reaction

$$\begin{matrix} \diagup COOCH_3 \\ CH_2 \\ \diagdown COOD \end{matrix} \rightarrow CH_2D \cdot COOCH_3 + CO_2. \qquad (2)$$

A preliminary experiment had shown that actually a rather pure sample of $CH_2D \cdot COOCH_3$ is obtained in this way, not being contaminated with $CH_3 \cdot COOCH_3$, $CHD_2 \cdot COOCH_3$, etc. This was clearly demonstrated by the lack of lines originating from these compounds in the Raman spectrum of the sample.

At the present experiment, however, $CH_2D \cdot COOCH_3$ was not isolated, but the mixture of the compound and the accompanying CH_3OD was boiled for 18 hours with 5 n H_2SO_4. The reaction

$$CH_2D \cdot COOCH_3 + H_2O \rightarrow CH_2D \cdot COOH + CH_3OH \qquad (3)$$

having taken place, $CH_2D \cdot COOH$ was distilled off, neutralized and precipitated as $CH_2D \cdot COOAg$, which was filtered, washed with water, alcohol, and ether, and dried to constant weight (227 g) in vacuum. The theoretical yield from 2.5 moles of dimethyl malonate is 420 g.

225 g $CH_2D \cdot COOAg$ suspended in 500 cc dry CCl_4 was gently boiled and a solution of 90 cc dry bromine in 150 cc CCl_4 was added drop by drop. The two gases from the reaction

$$CH_2D \cdot COOAg + Br_2 \rightarrow CH_2DBr + CO_2 + AgBr \qquad (4)$$

were led through 3 wash-bottles with 4 n NaOH, absorbing carbon dioxide. The deuterated methyl bromide was dried and condensed. Afterwards it was fractionated through a 60 cm column. Boiling point: 4°.5—4°.8 (760 mm). The Raman spectrum of this compound showed that during (4) some sort of exchange reaction had taken place which had destroyed the isotopic purity of the sample: it was a mixture of CH_3Br, CH_2DBr, CHD_2Br and a little CD_3Br. The possibility that the exchange should have occurred during (3)—and not during (4)—can be excluded by the following arguments:

(a) If exchange had taken place during (3) and not during (4), a mixture of CH_3COOH and CH_2DCOOH would result from (3)—but not CHD_2COOH, etc.—and subsequently a mixture of CH_3Br and CH_2DBr would be the result.

(b) The fact that no exchange takes place during (1) makes it very unlikely that it should occur during (3).

In spite of this derailment we carried through the reactions

$$CH_2DBr + Mg \rightarrow CH_2D \cdot Mg \cdot Br,$$

$$CH_2D \cdot Mg \cdot Br + CH_2J_2 \rightarrow CH_2D \cdot CH_2J + MgJ_2$$

$$2\,CH_2D \cdot CH_2J + 2\,CuBr_2 \rightarrow 2\,CH_2D \cdot CH_2Br + 2\,CuJ + Br_2$$

and finally got a sample containing $CH_2D \cdot CH_2Br$, CH_3CH_2Br, $CHD_2 \cdot CH_2Br$, and a little $CD_3 \cdot CH_2Br$.

Consequently the Raman spectrum was the least valuable of the three taken. It shows all the lines ascribed to the $CH_2D \cdot CH_2Br$ from the study of the spectra of the preparations number I and II.

4. **$CH_3 \cdot CHDBr$.** A dry ethereal solution of diazoethane (0.5 mole) was prepared by a method quite analogous to the one used for obtaining diazomethane. Owing to the decomposition of the diazoethane during the drying process it is inevitable that this solution should contain a little $CH_3 \cdot CH_2OH$. The ethereal solution was dropped to a mixture of 25 g D_2O and 5 cc conc. H_2SO_4:

$$CH_3 \cdot CHN_3 + DOD \rightarrow CH_3 \cdot CHDOD + N_2.$$

Owing to the use of H_2SO_4 instead of D_2SO_4 about 4 per cent. of the reaction product must be $CH_3 \cdot CH_2OH$.

The evolution of nitrogen having ceased, the reaction flask contains: ether, $CH_3 \cdot CHDOH$, $CH_3 \cdot CHDOD$. $CH_3 \cdot CH_2OH$, $CH_3 \cdot CH_2OD$, and acid esters of sulphuric acid. The ether was fractionated off through a 100 cm column and the esters afterwards saponified. The alcohols were distilled off and transformed into the mixture $CH_3 \cdot CHDBr$ and CH_3CH_2Br in the usual way. Theoretical yield from 0.5 mole diazoethane: 54 g ethyl bromide. We got 18 g of the pure product. Boiling point: 38°.40—38°.60 (760 mm). The considerations concerning the composition of the sample was confirmed by the Raman spectrum.

Summary.

1. The Raman spectra of

$CH_3 \cdot CH_2Br$, $CH_3 \cdot CHDBr$, $CH_2D \cdot CH_2Br$, and $CD_3 \cdot CD_2Br$

are measured and the frequencies recorded.

2. $CH_2D \cdot CH_2Br$ is shown to be a mixture of two spectroscopically different rotational isomers.

3. The intensity ratio of corresponding lines due to the two rotational isomers strongly supports the assumption of a three-minimum potential curve for the internal rotation about the C-C bond.

Universitetets kemiske Laboratorium.

Copenhagen.

Færdig fra Trykkeriet den 12 Juli 1947.

DET KGL. DANSKE VIDENSKABERNES SELSKAB
MATEMATISK-FYSISKE MEDDELELSER, BIND XXIV, NR. 4

UNTERSUCHUNGEN ÜBER DEN EINFLUSS DES AKKOMMODATIONSKOEFFIZIENTEN AUF RADIOMETERERSCHEINUNGEN UND MOLEKULARMANOMETER

VON

SOPHUS WEBER

KØBENHAVN
I KOMMISSION HOS EJNAR MUNKSGAARD
1947

Printed in Denmark.
Bianco Lunos Bogtrykkeri

§ 1. In einer früheren Arbeit[1] habe ich die theoretische Grundlage, insbesondere im MAXWELL'schen Zustande der Gase, für das absolute Manometer von MARTIN KNUDSEN und ähnliche Radiometerkonstruktionen untersucht. Unter Vernachlässigung des Einflusses des Akkommodationskoeffizienten a und des hiervon abhängigen Temperatursprunges wurde für die Radiometerkraft K des absoluten Manometers in der rationellen Ausführung gefunden:

$$K_{\mathrm{cm}^2} = \frac{1}{2} \cdot \frac{p}{T} \cdot \frac{T_1 - T_2}{\frac{\pi}{18 k_1}\left(\frac{d}{\lambda}\right)^2 + \frac{\pi}{3 k_1}\left(k_2 + \frac{m}{6}\right)\left(\frac{d}{\lambda}\right) + \frac{\pi}{3}\frac{k_2}{k_1} m},$$

unter der Voraussetzung, dass die erweiterte MAXWELL'sche Grenzbedingung[2] folgendermassen geschrieben werden kann:

$$w_0 - k_2 \lambda \left(\frac{dw}{dz}\right)_0 = \frac{3}{4} k_1 \frac{\eta}{\varrho T} \cdot \frac{dT}{dr} \cdot \frac{1}{1 + m\frac{\lambda}{d}}.$$

Hier ist d der Abstand zwischen den parallelen Platten mit den Temperaturen T_1 und T_2 und p der Gasdruck. λ ist die mittlere freie Weglänge bei dem Druck p. Die Konstanten k_1 und k_2 sind einander gleich, und zwar etwa $\frac{4}{3}$.

Seit dem Erscheinen jener Arbeit sind einige neue Konstruktionen und Messungen veröffentlicht worden, so dass es von Interesse sein dürfte, die theoretischen Untersuchungen unter Berücksichtigung des Einflusses des Temperatursprunges und des Akkommodationskoeffizienten wieder aufzunehmen und mit den Untersuchungen von E. FREDLUND[3] und von H. KLUMB und

[1] SOPHUS WEBER: D. Kgl. Danske Vidensk. Selskab, Mat.-fys. Medd. XIV, 13, 1937.

[2] SOPHUS WEBER: Comm. Kamerlingh Onnes Lab. Leiden, No. 246[b] S. 7. 1936.

[3] E. FREDLUND: Phil. Mag. S. 7, Vol. XXVI, p. 987, 1938. (a)
— : Arkiv. f. Mat. Astr. Fys. 27 A No. 12, 1940. (b)

H. SCHWARZ[1] zu vergleichen; dies erscheint umso mehr angebracht, als aus den Messungen von E. FREDLUND hervorgeht, dass die mit dem gleichen Apparat gemessenen Radiometerkräfte in den zwei Gasen Wasserstoff und Deuterium, die dieselbe mittlere freie Weglänge λ besitzen, insbesondere bei höherem Druck bedeutend von einander abweichen.

§ 2. Wir wollen erst das absolute Manometer von MARTIN KNUDSEN in der rationellen Ausführung näher betrachten. In dieser Konstruktion, Fig. 1, hat man die feststehende, zirkulare heisse Platte A mit dem Radius r_0, auf der konstanten Temperatur T_1. Die Platte A ist von einem Schutzring von der Temperatur T_2 umgeben. Die bewegliche Platte B hat, wie auch ihre Umgebung, die konstante Temperatur T_2. Der konstante Abstand zwischen den beiden parallelen Platten A und B wird mit d bezeichnet. Während Präzisionsmessungen muss der Abstand d konstant gehalten werden; die Radiometerkraft auf B muss dann in der einen oder anderen Weise kompensiert werden. Liegt die Drehachse D der kalten Platte hinreichend weit von A entfernt, und ist die kalte Platte B gross genug, so wird die Randkorrektion[2] im Knudsen-Zustand des Gases, d. h. wenn $\frac{d}{\lambda} \gtrsim 0$, sehr klein, auch wenn die Bedingung $\frac{d}{2r_0} \ll 1$ nicht besonders gut erfüllt ist.

[1] H. KLUMB & H. SCHWARZ: Z. f. Phys. **122**, 418, 1944.

[2] G. SPIWAK: (Z. f. Phys. **77**, 123, 1932) hat die Grösse der Randkorrektion für zwei quadratische Platten ohne Schutzringe mit Kantlänge b und Abstand d berechnet. Er findet im Knudsen-Zustand des Gases für die Radiometerkraft per cm^2 K:

$$K = \frac{1}{2} p \left(\sqrt{\frac{T_1}{T_2}} - 1 \right) \gamma, \text{ wo } \gamma = \frac{1}{\pi} \left[\frac{2 + \left(\frac{d}{b}\right)^2}{\sqrt{1 + \left(\frac{d}{b}\right)^2}} - \frac{d}{b} \right] \operatorname{arctg} \frac{b}{d},$$

woraus folgt:

$$\gamma = 1 \text{ für } \frac{d}{b} = 0.$$

Durch Reihenentwicklung für γ, wenn $\frac{d}{b} \to 0$, erhält man hieraus:

$$\lim_{\frac{d}{b} \to 0} \gamma = 1 - \left(\frac{1}{2} + \frac{2}{\pi} \right) \left(\frac{d}{b} \right) + \frac{2}{\pi} \left(\frac{d}{b} \right)^2 \cdots .$$

Wir ersehen also, dass für die Konstruktion von SPIWAK die Grösse der Randkorrektion nur ca. 1 % beträgt, wenn $\frac{d}{b} = 0{,}01$.

Bei Verwendung dieses Manometers bei höherem Druck ist es der Konvektionsströmungen wegen am zweckmässigsten, dass die Platten A und B horizontal sind und die heisse Platte oben liegt.

Bei dieser Konstruktion liegt das ganze Temperaturgefälle am Rande der Platte A, und die massgebende Temperaturdifferenz für die bei höherem Druck entstehenden thermischen Gleitströme ist $T_1 - T_2$.

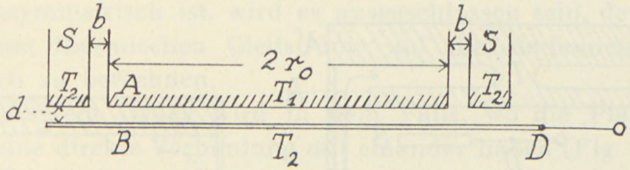

Fig. 1.

In dem Knudsen-Zustand des Gases $\frac{d}{\lambda} = 0$ ist die Theorie dieses Manometers zur Genüge bekannt[1], und man erhält für die Radiometerkraft per cm^2 K:

$$K = \frac{1}{2} p \left(\sqrt{\frac{T_1}{T_2}} - 1 \right) \left\{ 1 + \frac{1}{4} \frac{1-a}{(2-a)^2} \left(\frac{T_1}{T_2} - 1 \right) \left(\sqrt{\frac{T_1}{T_2}} + 1 \right) \right\},$$

wo a den Akkommodationskoeffizienten des Gases den Platten gegenüber bezeichnet, während p der Druck in dem das Radiometersystem umgebenden Raum ist, wo auch die Temperatur T_2 herrscht. Wird nur mit kleinen Temperaturdifferenzen gearbeitet, erhält man hieraus in erster Näherung:

$$K = \frac{1}{2} p \left(\sqrt{\frac{T_1}{T_2}} - 1 \right) \approx \frac{1}{4} p \cdot \frac{T_1 - T_2}{T_2}.$$

Haben die zwei Platten A und B gegenüber dem Gase verschiedene Akkommodationskoeffizienten, nämlich a_1 und a_2, und betrachten wir nur kleine Werte von $T_1 - T_2$, erhalten wir in erster Näherung:

$$K = \frac{1}{4} p \frac{T_1 - T_2}{T} \left\{ 1 + \frac{a_1 - a_2}{a_1 + a_2 - a_1 a_2} \right\}.$$

E. Fredlund hat die Konstruktion von Martin Knudsen etwas abgeändert; er verwendet eine drehbare, sehr dünne Metallscheibe, Radius R, die in der Mitte zwischen zwei grossen

[1] Vgl. J. H. A. ter Heerdt: Dissertation, Utrecht 1923, S. 203.

parallelen Platten A und B auf den Temperaturen T_1 und T_2 aufgehängt ist. Die Scheibe ist in der Gleichgewichtslage parallel zu den grossen Platten. Die Abstände zwischen der Scheibe und den festen Platten sind gleich gross und werden mit d bezeichnet. Aus Konstruktionsgründen liegen die Zentren der grossen Platten und das Zentrum der Scheibe S in der FREDLUND'schen Konstruktion nicht auf einer Gerade. Dies ist im Knudsen-Zu-

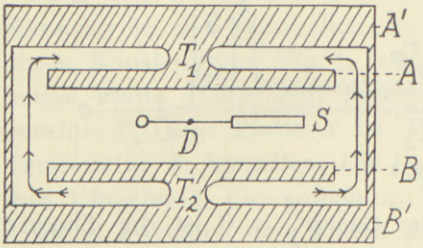

Fig. 2.

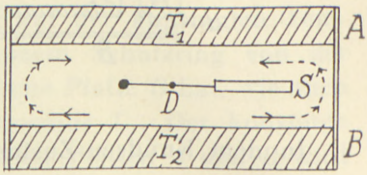

Fig. 3.

stande des Gases ohne Bedeutung; bei höherem Druck wird aber hierdurch der Vergleich zwischen Messungen und Theorie erschwert.

Durch ein magnetisches Kompensationssystem wird die Lage der beweglichen Scheibe während der Messungen unverändert gehalten. In der vorliegenden FREDLUND'schen Ausführung stehen die grossen zirkularen Platten A und B vertikal und haben die Temperaturen T_1 und T_2; die FREDLUND'sche Konstruktion eignet sich jedoch besonders gut für die Arbeit mit horizontaler Plattenaufstellung.

Die praktische Ausführung der FREDLUND'schen Konstruktion bietet zwei Möglichkeiten: die grossen zirkularen Platten A und B können temperaturmässig entweder praktisch unabhängig von einander sein (vgl. Fig. 2) oder in direkter Verbindung mit einander stehen (vgl. Fig. 3). In ersterem Fall, können die am Rande der Platten A' und B' entstehenden thermischen Gleitströme nicht zwischen den Platten A und B und der kleinen Scheibe S eindringen. Diese rationelle Konstruktion ist im Prinzip einer Konstruktion von P. LAZAREFF[1], für die direkte Messung des Temperatursprunges ähnlich. Die vorliegende Konstruktion von FREDLUND entspricht dem zweiten Fall und ist vergleichbar mit der

[1] P. LAZAREFF: Ann. d. Phys. **37**, S. 233, 1912.

von MANDELL und WEST[1] verwendeten Konstruktion für die Wiederholung der LAZAREFF'schen Messungen.

In der FREDLUND'schen Konstruktion (Fig. 3) erhält man bei höherem Druck, unabhängig von dem Verbindungsmaterial, am Rande der grossen Platten thermische Gleitströme, die selbst in einem Apparat mit horizontalen Platten zwischen diesen und der Scheibe eindringen können. Da FREDLUND's Aufstellung ausserdem asymmetrisch ist, wird es ausgeschlossen sein, den Einfluss dieser thermischen Gleitströme auf die Radiometerkraft theoretisch zu berechnen.

Bei höherem Druck wird in dem Falle, wo die Platten A und B keine direkte Verbindung mit einander haben (Fig. 2), die massgebende Temperaturdifferenz hauptsächlich bestimmt durch den Temperaturunterschied der an die Scheibe grenzenden Gasschichten, bezw. durch den Temperatursprung auf beiden Seiten der beweglichen Scheibe; in dem Falle, wo die Platten A und B direkte thermische Verbindung mit einander haben, wird die massgebende Temperaturdifferenz teilweise durch den Temperaturunterschied zwischen den beiden Seiten der Scheibe und teilweise durch die Temperaturdifferenz $T_1 - T_2$ am Rande der grossen Platten bestimmt. Bei höherem Druck und geringem Temperaturunterschied werden aber diese thermischen Gleitströme, jedenfalls wenn der Apparat mit hinreichend grossen, horizontalen Platten gebaut ist, wahrscheinlich nicht sehr tief zwischen den Platten und der Scheibe S eindringen; es wäre daher nicht ganz ausgeschlossen, dass die Dimensionen in einer horizontalen Konstruktion so gewählt werden können, dass diese Gleitströme beinahe ohne Einfluss sind.

Wünscht man aber die grösstmögliche Empfindlichkeit des Instrumentes bei höherem Druck zu erreichen, ist die vorliegende FREDLUND'sche Konstruktion am zweckmässigsten.

In der ersten Untersuchung[2] von FREDLUND war für die Scheibe $\pi R^2 = 1{,}80$ cm^2 und $d = 0{,}485$ cm, also $\frac{d}{R} = 0{,}64$. Diese Versuchsreihe kann also bei höherem Druck kaum als ein absolutes Manometer betrachtet werden.

[1] W. MANDELL and S. WEST: Proc. Phys. Soc. London, 37, p. 20, 1925. Vgl. auch SOPHUS WEBER: D. Kgl. Danske Vidensk. Selskab, Mat.-fys. Medd. XVI, 9, 1939 (Seite 5—7).

[2] E. FREDLUND: loc. cit. (a) S. 996.

In der zweiten Untersuchung von FREDLUND[1] waren die Konstanten des Instrumentes: $\pi R^2 = 3{,}161$ cm^2 und $d = 0{,}042$ cm, also $\frac{d}{R} = 0{,}042$, so dass es sich bei höherem Druck tatsächlich um eine dem absoluten Manometer ähnliche Konstruktion handelt.

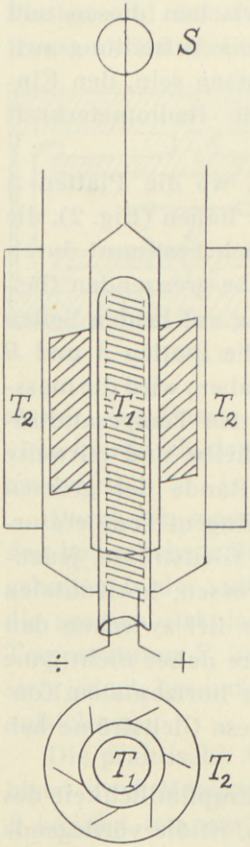

Fig. 4.

In dem Knudsen-Zustand des Gases, d.h. wenn $\frac{d}{\lambda} \rightarrow 0$, sind keine thermischen Gleitströme vorhanden, so dass die beiden Messreihen in diesem Gebiet nebeneinander verwendet werden können.

KLUMB und SCHWARZ[2] haben neuerdings eine interessante Konstruktion eines absoluten Manometers beschrieben und experimentell untersucht; diese hat Ähnlichkeit mit einer Konstruktion von RIEGGER[3], ist aber zweckmässiger und stabiler. Das Manometer von KLUMB und SCHWARZ kann prinzipiell dadurch karakterisiert werden, dass die Grösse der Radiometerkraft auf den beweglichen Radiometerkörper sich durch die Drehung des Radiometerkörpers *nicht* ändert, wodurch eine Kompensation der Radiometerkraft überflüssig wird.

Die Konstruktion ist schematisch in Fig. 4 wiedergegeben. In einer zylindrischen Ringspalte R wird der innere Mantel durch inwendige elektrische Heizung auf einer höheren Temperatur T_1 gehalten, während der äussere Mantel durch Kühlung, z.B. mit Wasser oder flüssiger Luft, auf einer niedrigen Temperatur T_2 gehalten wird. In dem ringförmigen Hohlraum der Ringspalte ist ein leichter und leicht drehbarer zylinderförmiger Radiometerkörper angebracht. Dieser Radiometerkörper besteht aus schiefgestellten Längsschaufeln oder Prallflächen, die unter dem Einfluss der Radiometerkraft ein Drehmoment erfahren.

[1] E. FREDLUND: loc. cit. (b) S. 11.
[2] H. KLUMB und H. SCHWARZ: Z. f. Phys. **122**, 418, 1944.
[3] K. RIEGGER: Z. f. techn. Phys. **1**, 16, 1920.

Der Radiometerkörper ist an einem Quarzfaden oder Wolframdraht aufgehängt, bezw. nach Art der Spannbandlagerung gelagert, wodurch seine Stabilität sehr gross wird.

Das Manometer dieser Konstruktion zeigt weitgehende Linearität der Ausschläge mit dem Druck und ist in dem Knudsen-Gebiet praktisch gesprochen unabhängig von der Gasart, da es nur aus Glas und blankem Platin gebaut ist.

KLUMB und SCHWARZ[1] fanden experimentell in atm. Luft Linearität zwischen 10^{-6} und 10^{-2} Torr, bezw. 0,001 und 13 Bar. Der Apparat zeigt, wie auch zu erwarten war, bei einem bestimmten Druck p_{max} ein Maximum des Ausschlages.

Für einen Apparat mit einem Abstand von etwa 5 mm zwischen dem heissen Mantel und der Mitte der Prallflächen liegt in atm. Luft der maximale Ausschlag bei p_{max} = ca. $3 \cdot 10^{-2}$ Torr = ca. 40 Bar, woraus sich, da $p\lambda = 6{,}2$, ergibt, dass $\frac{d}{\lambda_{max}} = \frac{0{,}5}{6{,}2} \cdot 40$ = ca. 3, in Übereinstimmung mit meinen früheren theoretischen Resultaten.

Der Apparat ist konstruktionsmässig einfach und kann z. B. aus Glas und Platin gebaut werden, so dass er durch Erwärmung leicht zu entgasen ist.

M. E. ist dieser Apparat, versehen mit einer angemessenen Dämpfung, für vakuum-technische Arbeiten und Messungen von kleinen Drücken, eventuell nach Eichung, sehr zweckmässig und vielseitig anwendbar.

Bevor wir zu der theoretischen Behandlung der verschiedenen Manometerkonstruktionen übergehen, wollen wir zwei gleichgrosse, parallele, zirkulare Platten A and B auf den konstanten Temperaturen T_1 und t_1 betrachten (vgl. Fig. 5). Die Platten A und B sind mit Schutzringzylindern umgeben; b ist der Abstand zwischen dem Kupferzylinder A bezw. B und den Schutzringzylindern A' und B' mit den Temperaturen T_2 bezw. t_2. Am Rande der Platten A und B liegen also in den an die Platten grenzenden Gasschichten die Temperaturgradienten

$$\frac{dT}{dr} = \frac{T_1 - T_2}{b} \quad \text{und} \quad \frac{dt}{dr} = \frac{t_1 - t_2}{b},$$

wodurch den Platten entlang thermische Gleitströme entstehen.

[1] KLUMB und SCHWARZ: loc. cit. S. 431.

Haben die Platten die konstanten Temperaturen T_1 und t_1 und liegen die Temperaturgefälle nur am Rande der Platten, können wir annehmen, dass die thermischen Gleitströme am Rande laminar und parallel zu den Platten verlaüfen. Ist der Abstand zwischen den Platten d klein, darf man annehmen, dass die Gleitströmung praktisch gesprochen nicht zwischen den Platten durchdringen wird.

Wenn wir von der Krümmung des Randes absehen, können

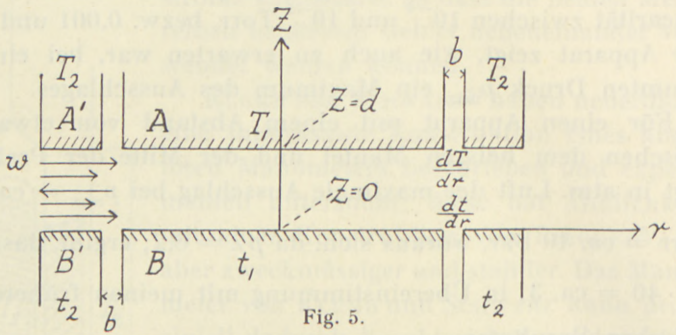

Fig. 5.

wir annehmen, dass der laminare Strömungszustand am Rande der Platten gegeben ist durch:

$$\eta \cdot \frac{d^2 w}{dz^2} = \frac{dp}{dr}, \tag{1}$$

wo w die Strömungsgeschwindigkeit, p der Druck, und η die innere Reibung des Gases bezeichnet. Diese Formel gilt für den stationären Zustand, in welchem auch die gesamte durch den Rand strömende Gasmenge gleich Null sein muss. Da $\frac{dp}{dr}$ für diese laminare Strömung als unabhängig von z angesehen werden kann, erhält man nach Integration für den stationären Zustand:

$$w = A_0 + B_0 z + c_0 z^2, \quad \text{wo} \quad c_0 = \frac{1}{2\eta} \cdot \frac{dp}{dr}. \tag{2}$$

Die Grenzbedingungen an den Oberflächen der Platten A und B sind durch die erweiterte MAXWELL'sche Grenzbedingung

$$w - k_2 \gamma_M \cdot \left(\frac{dw}{dz}\right) = k_1 \cdot \frac{3}{4} \cdot \frac{1}{1 + m\frac{\lambda}{d}} \cdot \frac{\eta}{\varrho T} \cdot \left(\frac{dT}{dr}\right)$$

gegeben.

γ_M ist der MAXWELL'sche Gleitungskoefficient und, wenn λ die mittlere freie Weglänge des Gases nach CHAPMAN bezeichnet, wird:

$$\gamma_M = \sqrt{\frac{\pi}{2}} \cdot \frac{\eta}{p\sqrt{{}_1\varrho}} = \lambda, \quad \text{weil} \quad p\lambda = \sqrt{\frac{\pi}{2}} \cdot \frac{\eta}{\sqrt{{}_1\varrho}} = {}_1\lambda.$$

Die Temperatur T in der MAXWELL'schen Grenzbedingung ist die Temperatur der an die Platte grenzenden Gasschicht, und $\frac{dT}{dr}$ ist der Temperaturgradient in dieser Gasschicht.

Es hat sich aus den Messungen der thermomolekularen Druckdifferenzen in Röhren ergeben, dass die beiden Zahlenfaktoren k_2 und k_1 einander ungefähr gleich sind; annäherungsweise kann $k_1 = k_2 = \frac{4}{3}$ gesetzt werden. m ist, wie früher gezeigt, ein Zahlenfaktor, und wenn der Faktor $\frac{1}{1 + m\frac{\lambda}{d}}$ als eine Gleitungskorrektion auf η aufgefasst werden kann, muss für zwei parallele Platten und den Zustand $\frac{\lambda}{d} \to 0$, $m = 2\,k_2 =$ ca. 2,67 sein.

Für die Randbedingung an den Platten A und B erhalten wir für $z = 0$ und $z = d$ hieraus:

$$w_0 - k_2\gamma_M\left(\frac{dw}{dz}\right)_{z=0} = k_1 \cdot \frac{3}{4} \cdot \frac{\eta}{\varrho\, T} \cdot \frac{1}{1 + m\frac{\lambda}{d}}\left(\frac{dt}{dr}\right) = c_1$$

und

$$w_d + k_2\gamma_M\left(\frac{dw}{dz}\right)_{z=d} = k_1 \cdot \frac{3}{4} \cdot \frac{\eta}{\varrho\, T} \cdot \frac{1}{1 + m\frac{\lambda}{d}}\left(\frac{dT}{dr}\right) = c_2,$$

weil $\left(\frac{dw}{dz}\right)_{z=0}$ und $\left(\frac{dw}{dz}\right)_{z=d}$ entgegengesetzte Vorzeichen haben.

Abgekürzt können wir die Randbedingungen schreiben:

$$w_0 - \varepsilon\left(\frac{dw}{dz}\right)_{z=0} = c_1 \tag{3}$$

und

$$w_d + \varepsilon\left(\frac{dw}{dz}\right)_{z=d} = c_2. \tag{4}$$

Ausserdem gilt in dem stationären Zustand am Rande der Platten:

$$\int_0^d w dz = 0. \tag{5}$$

Hieraus bekommt man nach Einsetzung des Wertes $w = A_0 + B_0 z + c_0 z^2$:

Aus (3) $\quad A_0 = \varepsilon B_0 + c_1$

» (4) $\quad A_0 + B_0 d + c_0 d^2 + \varepsilon (B_0 + 2 c_0 d) = c_2$

» (5) $\quad A_0 + \frac{1}{2} B_0 d + \frac{1}{3} c_0 d^2 = 0.$

Nach Elimination von A_0 und B_0 wird hieraus erhalten:

$$\frac{1}{3} c_0 d^2 \left(1 + 6 \frac{\varepsilon}{d}\right) = c_1 + c_2$$

oder

$$\frac{dp}{dr} = \frac{9}{2} k_1 \cdot \frac{\eta^2}{\varrho T} \cdot \frac{1}{d^2} \cdot \frac{1}{\left(1 + m \frac{\lambda}{d}\right)\left(1 + 6 k_2 \frac{\lambda}{d}\right)} \left(\frac{dT}{dr} + \frac{dt}{dr}\right). \tag{6}$$

Da $p\lambda = \sqrt{\frac{\pi}{2}} \cdot \frac{\eta}{\sqrt{{}_1\varrho}}$, und also $\frac{\pi}{2} \cdot \frac{\eta^2}{{}_1\varrho \cdot p} = p\lambda^2$, wird erhalten:

$$\frac{dp}{dr} = \frac{9}{\pi} k_1 \cdot \frac{p}{T} \cdot \frac{1}{\left(\frac{d}{\lambda} + m\right)\left(\frac{d}{\lambda} + 6 k_2\right)} \sum \frac{dT}{dr}$$

oder

$$\frac{dp}{dr} = \frac{1}{2} \cdot \frac{p}{T} \frac{1}{\frac{\pi}{18 k_1}\left(\frac{d}{{}_1\lambda}\right)^2 p^2 + \frac{\pi}{3 k_1}\left(k_2 + \frac{m}{6}\right)\left(\frac{d}{{}_1\lambda}\right) p + \frac{\pi}{3} \frac{k_2}{k_1} m} \sum \frac{dT}{dr}. \tag{7}$$

Aus dieser Formel erhellt, dass der Druck zwischen den Platten grösser ist als in dem sie umgebenden Gasraum, so dass sich die Platten mit einer senkrecht zu den Platten verlaufenden Kraft abstossen, während sich die Tangentialkräfte auf die Platten infolge der Symmetrie gegenseitig aufheben.

Aus der Formel ist weiter ersichtlich, dass sich die am Rande der Platten liegenden Temperaturgefälle einfach addieren, so

dass die Radiometerkraft grösser wird, wenn mehrere Temperaturgefälle in derselben Richtung vorliegen. Macht also die Platte B — entweder infolge gleichzeitiger Bestrahlung beider Platten oder infolge Wärmeleitung durch das Gas — das Temperaturgefälle der Platte A ganz oder teilweise mit, addieren sich die Kräfte. Dies kann von Bedeutung sein bei der Konstruktion eines hochempfindlichen Zweiplattenradiometers, eines Instrumentes, das in der Strahlungsmessung von Rubens und Nichols[1] verwendet worden ist. —

Wenn wir nur kleine Temperaturdifferenzen haben und folglich nur kleine Druckunterschiede erhalten, ergibt sich aus den Formeln (6) und (7), dass die auf die Platten wirkende Radiometerkraft K folgendermassen geschrieben werden kann:

$$K = \pi R^2 (p_1 - p_2) = \frac{9}{2} k_1 \cdot \frac{\eta^2}{\varrho T} \cdot \frac{1}{d^2} \frac{\pi R^2}{\left(1 + m \frac{\lambda}{d}\right)\left(1 + 6 k_2 \frac{\lambda}{d}\right)} \sum \Delta T \qquad (8)$$

oder

$$K = \frac{1}{2} \cdot \frac{p}{T} \cdot \frac{\pi R^2}{\frac{\pi}{18 k_1}\left(\frac{d}{{}_1\lambda}\right) p^2 + \frac{\pi}{3 k_1}\left(k_2 + \frac{m}{6}\right)\left(\frac{d}{{}_1\lambda}\right) p + \frac{\pi}{3} \frac{k_2}{k_1} m} \sum \Delta T. \qquad (9)$$

p_1 und p_2 ist der Druck zwischen den Platten und in dem sie umgebenden Gasraum; ausserdem ist vorausgesetzt, dass die thermische Gleitströmung praktisch gesprochen nicht zwischen den Platten durchdringt, so dass p_1 zwischen A und B überall konstant ist.

Ist $\frac{dT}{dr} = \frac{dt}{dr}$, wird $\Sigma \Delta T = 2 (T_1 - T_2)$. Wird $\frac{dt}{dr} = 0$ und $t_2 = T_2$ wie im Falle des absoluten Manometers, wird $\Sigma \Delta T = T_1 - T_2$, und wir erhalten dann die früher von mir abgeleitete Formel für K.

Auf Grund der Messungen von Martin Knudsen über den Verlauf der Radiometerkraft in dem absoluten Manometer für das ganze Druckgebiet $0 \leqq \frac{d}{\lambda} \leqq \infty$ ist es wahrscheinlich, dass der Wert von $\mu = \frac{\pi}{3} \frac{k_2}{k_1} m$ in dem Zustande $\frac{d}{\lambda} \to \infty$ ungefähr 2,70 ist.

[1] H. Rubens und E. F. Nichols: Wied. Ann. **60**, 418, 1897. Vgl. auch: G. Hettner: Z. f. Phys. **47**, 499, 1928.

Dies ist in Übereinstimmung mit den Resultaten der umfassenden experimentellen Untersuchungen über die thermomolekularen Druckdifferenzen in Röhren[1], für welche eine analoge Formel gilt. Bei diesen Untersuchungen wurde für den Zustand $\frac{r}{\lambda} \to \infty$ gefunden, dass $\frac{\pi}{6}\frac{k_2}{k_1} m = \frac{1}{2}\mu =$ ca. 1.30, so dass die Übereinstimmung befriedigend ist.

Wenn $\frac{d}{\lambda} = 0$, wird der Grenzwert der Formel (9) für das absolute Manometer

$$K_0 = \frac{1}{2}\frac{p}{T}(T_1 - T_2) \cdot \frac{1}{\mu};$$

demnach muss für $\frac{d}{\lambda} = 0$, $\mu = 2$ gesetzt werden, um mit dem richtigen Grenzwert für $\frac{d}{\lambda} = 0$,

$$K_0 = \frac{1}{2} p \left(\sqrt{\frac{T_1}{T_2}} - 1 \right) \approx \frac{1}{4} \cdot p \frac{T_1 - T_2}{T}$$

übereinzustimmen.

§ 4. Es ist nicht ohne Interesse zu untersuchen, wie die laminare Strömung am Rande der Platten verläuft. Aus dem Ausdruck für die Geschwindigkeit

$$w = A_0 + B_0 z + c_0 z^2$$

erhält man für $z = 0$ und $z = d$:

$$w_{z=0} = A_0 \text{ und } w_{z=d} = A_0 + B_0 d + c_0 d^2,$$

worin

$$c_0 = \frac{3}{d^2} \cdot \frac{c_1 + c_2}{1 + 6\frac{\varepsilon}{d}}$$

$$B_0 = -\frac{2}{d} \cdot \frac{1}{\left(1 + 2\frac{\varepsilon}{d}\right)\left(1 + 6\frac{\varepsilon}{d}\right)} \left\{ c_2 + 2 c_1 \left(1 + 3\frac{\varepsilon}{d}\right) \right\}$$

und

[1] Sophus Weber: Comm. Kamerlingh Onnes Lab. Leiden, No. 246, 1936.

$$A_0 = \frac{c_1\left(1+4\frac{\varepsilon}{d}\right)-c_2\cdot 2\frac{\varepsilon}{d}}{\left(1+2\frac{\varepsilon}{d}\right)\left(1+6\frac{\varepsilon}{d}\right)}.$$

Für das rationelle, absolute Manometer von Martin Knudsen ist $c_2 = 0$, so dass wir erhalten:

$$w = \frac{c_1}{\left(1+2\frac{\varepsilon}{d}\right)\left(1+6\frac{\varepsilon}{d}\right)}\left\{1+4\frac{\varepsilon}{d}-4\left(1+3\frac{\varepsilon}{d}\right)\frac{z}{d}+3\left(1+2\frac{\varepsilon}{d}\right)\left(\frac{z}{d}\right)^2\right\}.$$

Ist das Gleitungsglied $\frac{\varepsilon}{d} \ll 1$, erhält man hieraus:

$$w_0 = A_0 = \frac{c_1}{1+4\frac{\varepsilon}{d}} \quad \text{und} \quad w_d = -2\frac{\varepsilon}{d}\cdot\frac{c_1}{1+8\frac{\varepsilon}{d}},$$

während $w = 0$, wenn $\frac{z}{d} = \frac{1}{3}\left(1+\frac{\varepsilon}{d}\right)$.

Für $\frac{z}{d} = \frac{2}{3}\left(1+\frac{\varepsilon}{d}\right)$ wird $\frac{dw}{dz} = 0$ und $w = -\frac{1}{3}\cdot\frac{c_1}{1+4\frac{\varepsilon}{d}}$.

Der Strömungszustand am Rande wird in diesem Falle wie in Fig. 6 b angegeben, während die Geschwindigkeitsverteilung aus Fig. 6 a zu ersehen ist.

Betrachten wir den einfachen Fall, in dem das Temperatur-

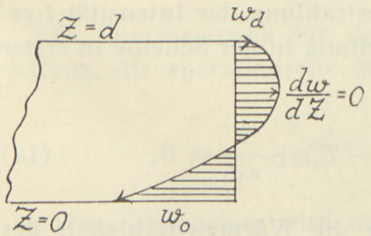

Fig. 6 a.

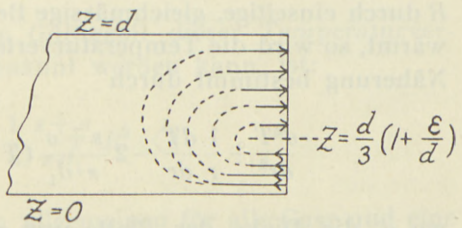

Fig. 6 b.

gefälle in derselben Richtung am Rande der beiden Platten gleich gross ist, erhält man $c_1 = c_2$, und also

$$w_0' = A_0 = \frac{c_1}{1+6\frac{\varepsilon}{d}}, \quad w_d' = w_0' = \frac{c_1}{1+6\frac{\varepsilon}{d}}$$

und

$$w' = \frac{c_1}{1+6\frac{\varepsilon}{d}}\left(1-6\frac{z}{d}+6\left(\frac{z}{d}\right)^2\right).$$

Für $\frac{z}{d} = \frac{1}{2}\left(1 \pm \frac{\sqrt{3}}{3}\right)$ wird $w' = 0$, während für $\frac{z}{d} = \frac{1}{2}$, $\frac{dw'}{dz} = 0$ und $w' = -\frac{1}{2}\frac{c_1}{1+6\frac{\varepsilon}{d}} = -\frac{1}{2}w_0'$.

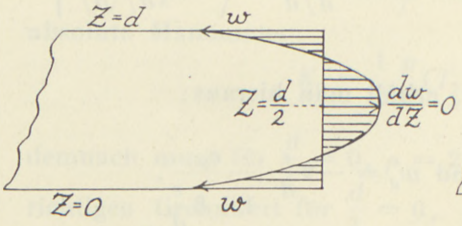

Fig. 7 a.

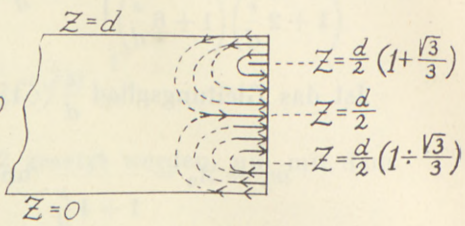

Fig. 7 b.

Der Strömungszustand am Rande ist für diesen Fall in Fig. 7 b, die Geschwindigkeitsverteilung ist in Fig. 7 a wiedergegeben.

§ 5. Wir können nun untersuchen, wie sich die Formel für die Radiometerkraft K ändert, wenn das Temperaturgefälle nicht allein am Rande der Platten, sondern z. B. in den Platten selbst liegt.

Wird z. B. eine dünne, gutleitende Kreisscheibe mit dem Radius R durch einseitige, gleichmässige Bestrahlung der Intensität I erwärmt, so wird die Temperaturverteilung in der Scheibe in erster Näherung bestimmt durch

$$\frac{d^2T}{dr^2}+\frac{1}{r}\frac{dT}{dr}-2\frac{s+\sigma}{\varkappa\cdot d_1}(T-T_0)+\frac{I}{\varkappa d_1}=0, \qquad (10)$$

wo d_1 die Dicke der Platte und $\varkappa$ die Wärmeleitfähigkeit des Plattenmaterials bezeichnet. s ist die äussere Wärmeleitfähigkeit und σ die Strahlungskonstante, wenn die Ausstrahlung proportional mit der Temperaturdifferenz $T-T_0$ angenommen wird.

Wird in dieser Gleichung

$$\frac{I}{2(s+\sigma)} = P, \quad a^2 = \frac{2(s+\sigma)}{\varkappa\cdot d_1}, \text{ und } T' = T-T_0-P$$

gesetzt, erhält man die Differentialgleichung

$$\frac{d^2T'}{dr^2}+\frac{1}{r}\frac{dT'}{dr}-a^2T'=0.$$

Die Lösung hierfür ist, wie bekannt, die Zylinderfunktion $I_0(iar)$ mit komplexem Argument.

Wir finden hieraus: $T'=A\cdot I_0(iar)$, und also, weil für $r=0$, $I_0(iar)=1$:

$$A=\frac{T_1-T_0}{1-I_0(iaR)}$$

und

$$T=T_1-(T_1-T_0)\cdot\frac{1-I_0(iar)}{1-I_0(iaR)}. \tag{11}$$

In dieser Formel sind T_1 und T_0 die Temperaturen im Zentrum und am Rande der Kreisscheibe.

Wird nur die erste Näherung der Reihenentwicklung für $I_0(iar)$ verwendet, erhält man, da

$$I_0(ix)=1+\frac{\left(\frac{1}{2}x\right)^2}{1!^2}+\frac{\left(\frac{1}{2}x\right)^4}{2!^2}+\frac{\left(\frac{1}{2}x\right)^6}{3!^2}+\cdots+\frac{\left(\frac{1}{2}x\right)^{2n}}{n!^2}+\cdots,$$

$$T=T_1-\frac{r^2}{R^2}(T_1-T_0). \tag{12}$$

Die Voraussetzung für die Gültigkeit dieser Temperaturverteilung, die »parabolisch« genannt werden kann, ist:

$$\frac{1}{16}x^2=\frac{1}{8}\frac{s+\sigma}{\varkappa d_1}R^2\ll 1.$$

Diese Bedingung wird im allgemeinen für alle Gase und eine nicht allzugrosse metallische Scheibe hinreichend erfüllt sein.

Bei einer parabolischen Temperaturverteilung auf der heissen Platte

$$T=T_1-\frac{r^2}{R^2}(T_1-T_0)$$

und für die konstante Temperatur T_0 der kalten Platte und

des Schutzringzylinders habe ich[1] früher nachgewiesen, dass man, unter der Voraussetzung, dass $\frac{dp}{dr}$ auch in diesem Falle als unabhängig von z angesehen werden kann, für die totale Radiometerkraft K' zwischen den Platten den folgenden Ausdruck erhält:

$$K' = \frac{9}{4} k_1 \cdot \frac{\eta^2}{\varrho T} \cdot \frac{1}{d^2} \cdot \frac{\pi R^2}{\left(1 + m\frac{\lambda}{d}\right)\left(1 + 6\,k_2 \frac{\lambda}{d}\right)} (T_1 - T_0), \qquad (13)$$

während man für denselben Apparat, wenn der Temperaturunterschied $(T_1 - T_0)$ nur am Rande der heissen Platte liegt, folgenden Ausdruck erhält:

$$K = \frac{9}{2} k_1 \cdot \frac{\eta^2}{\varrho T} \cdot \frac{1}{d^2} \cdot \frac{\pi R^2}{\left(1 + m\frac{\lambda}{d}\right)\left(1 + 6\,k_2 \frac{\lambda}{d}\right)} (T_1 - T_0), \qquad (14)$$

so dass $K' = \frac{1}{2} K$. Dieses Resultat ist in Übereinstimmung damit, dass die mittlere Temperaturdifferenz zwischen den Platten in diesem Falle

$$\frac{1}{\pi R^2} \int_0^R (T - T_0)\, 2\pi r dr = \frac{1}{2} (T_1 - T_0)$$

ist.

Mit einer parabolischen Temperaturverteilung der heissen Platte werden die thermischen Gleitströme nicht allein am Rande der Platten liegen, sondern bis zum Mittelpunkt der Platten durchdringen; in diesem Punkte ist nämlich $\frac{dT}{dr} = 0$.

Die in diesem Falle enstehende, rotationssymmetrische Strömung hat G. Fanselau[2] in seiner Berliner Dissertation behandelt. Ausgehend von den hydrodynamischen Gleichungen für eine nicht zusammendrückbare, zähe Flüssigkeit findet er für den stationären Zustand, dass die Stromlinien für diese Strömung bestimmt sind durch:

$$\psi = r^2 f(z) = r^2 (C_1 z^3 + C_2 z^2 + C_3 z + C_4) = \text{konst.}, \qquad (15)$$

[1] Sophus Weber: loc. cit. S. 37, 1937.
[2] G. Fanselau: Dissertation, Berlin, 1927.

wo $r^2 = x^2 + y^2$, während die Werte von C_1, C_2, C_3 und C_4 in der Weise bestimmt werden müssen, dass die vorgegebenen Randbedingungen erfüllt sind, (vgl. Fig. 8).

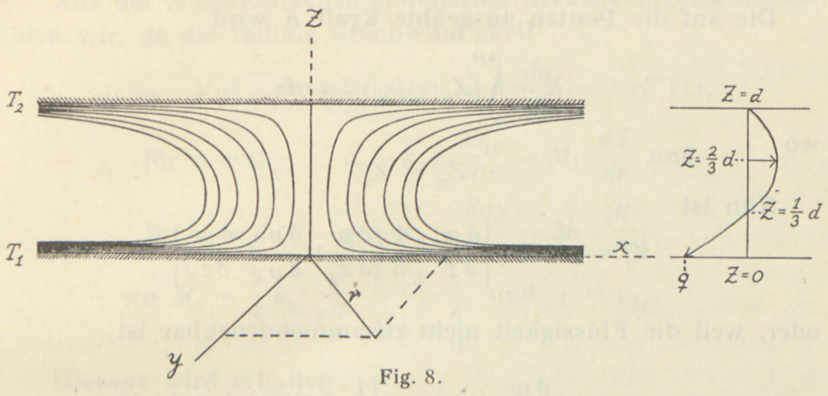

Fig. 8.

Für die Strömungsgeschwindigkeiten in den drei Achsenrichtungen erhält FANSELAU:

$$w = 2f(z), \qquad u = -xf'(z) \quad \text{und} \quad v = -yf'(z) \tag{16}$$

in Übereinstimmung mit der Kontinuitätsbedingung für inkompressible Flüssigkeiten:

$$\frac{\delta u}{\delta x} + \frac{\delta v}{\delta y} + \frac{\delta w}{\delta z} = 0.$$

Vernachlässigt man den Einfluss der Schwere, erhält man aus den hydrodynamischen Gleichungen für den stationären Zustand:

$$\eta \Delta^2 u - \frac{\delta p}{\delta x} = 0$$

$$\eta \Delta^2 v - \frac{\delta p}{\delta y} = 0$$

$$\eta \Delta^2 w - \frac{\delta p}{\delta z} = 0,$$

$$\frac{\delta p}{\delta x}\delta x + \frac{\delta p}{\delta y}\delta y + \frac{\delta p}{\delta z}\delta z = \eta\,[2f''(z)\,\delta z - y f'''(z)\,\delta y - x f'''(z)\,\delta x],$$

woraus:

$$p - p_\infty = -\eta\left[\frac{1}{2} r^2 f'''(z) - 2f'(z)\right], \tag{17}$$

und also:

$$\frac{\delta p}{\delta r} = -r \cdot \eta \, f'''(z) = -6 \, C_1 \cdot \eta \cdot r. \tag{18}$$

Die auf die Platten ausgeübte Kraft K wird

$$K = \int_0^R (Z_n - p_\infty) \, 2 \pi \, r dr,$$

wo

$$Z_n = Z_z.$$

Nun ist

$$Z_z = p - 2 \eta \left[\frac{\delta w}{\delta z} - \frac{1}{3} \left(\frac{\delta u}{\delta x} + \frac{\delta v}{\delta y} + \frac{\delta w}{\delta z} \right) \right]$$

oder, weil die Flüssigkeit nicht zusammendrückbar ist,

$$Z_z = p - 2 \eta \frac{\delta w}{\delta z} = p_\infty - \eta \left[\frac{1}{2} r^2 f'''(z) + 2 f'(z) \right],$$

woraus

$$K = -2 \eta \left[f'(z) + \frac{1}{8} R^2 f'''(z) \right] \cdot \pi R^2. \tag{19}$$

Ausgehend von dieser allgemeinen Behandlung einer rotationssymmetrischen Strömung zwischen zwei parallelen Platten können wir nun annehmen, dass die zwei parallelen Platten Kreisscheiben mit Radius R sind, und dass beide eine parabolische Temperaturverteilung,

$$T = T_1 - \frac{r^2}{R^2} (T_1 - T_2)$$

bezw.

$$t = t_1 - \frac{r^2}{R^2} (t_1 - t_2),$$

besitzen.

Wir erhalten dann:

$$w = 2 f(z), \qquad u = -x f'(z), \qquad v = -y f'(z),$$

wo

$$f(z) = C_1 z^3 + C_2 z^2 + C_3 z + C_4.$$

Da $w = 2 f(z) = 0$ für $z = 0$ und $z = d$, wo d den Abstand der parallelen Platten bezeichnet, erhalten wir die folgenden Bedingungen:

$$\text{für } z = 0, \qquad f(0) = 0, \quad \text{woraus} \quad C_4 = 0,$$

$$\text{und für } z = d, \qquad f(d) = 0, \quad \text{woraus} \quad C_1 d^2 + C_2 d + C_3 = 0.$$

Aus der MAXWELL'schen erweiterten Grenzbedingung bekommen wir, da die radiale Geschwindigkeit

$$q = -\sqrt{u^2 + v^2} = -rf'(z) \text{ und } \frac{dq}{dz} = -rf''(z),$$

$$\text{für } z = 0, \qquad q_0 - k_2 \gamma \cdot \frac{dq_0}{dz} = M_1 \cdot \frac{dT}{dr} \text{ und}$$

$$\text{für } z = d \qquad q_d + k_2 \gamma \cdot \frac{dq_d}{dz} = M_1 \cdot \frac{dt}{dr},$$

$$\text{wo } M_1 = \frac{3}{4} k_1 \cdot \frac{\eta}{\varrho T} \cdot \frac{1}{1 + m\frac{\lambda}{d}} \text{ und } \gamma = \gamma_M.$$

Hieraus wird erhalten:

$$r\left[C_3 - k_2 \gamma 2 C_2\right] = -M_1 \cdot \frac{dT}{dr}$$

und

$$r\left[3 C_1 d^2 + 2 C_2 d + C_3 + k_2 \gamma (6 C_1 d + 2 C_2)\right] = -M_1 \frac{dt}{dr}.$$

Addieren wir diese Ausdrücke, erhalten wir:

$$r\left[3 C_1 d^2 + 2 C_2 d + 2 C_3 + 6 C_1 k_2 \gamma d\right] = -M_1 \sum \frac{dT}{dr},$$

und weil

$$2 C_1 d^2 + 2 C_2 d + 2 C_3 = 0,$$

$$r C_1 d^2 \left[1 + 6 k_2 \frac{\gamma}{d}\right] = -M_1 \cdot \sum \frac{dT}{dr}.$$

Setzen wir $\alpha = C_1 d^2$, erhalten wir:

$$\alpha = -\frac{1}{r} \cdot \frac{M_1}{1 + 6 k_2 \frac{\lambda}{d}} \sum \frac{dT}{dr}, \tag{20}$$

weil $\gamma = \lambda$.

Aus der parabolischen Temperaturverteilung erhält man:

$$\frac{dT}{dr} = -2\frac{r}{R^2}(T_1 - T_2) \text{ und } \frac{dt}{dr} = -2\frac{r}{R^2}(t_1 - t_2),$$

woraus

$$\sum \frac{dT}{dr} = -2\frac{r}{R^2}[(T_1 - T_2) + (t_1 - t_2)] = -2\frac{r}{R^2}\sum \Delta T,$$

und also:

$$\alpha = C_1 d^2 = \frac{3}{2} k_1 \frac{\eta}{\varrho T} \cdot \frac{1}{\left(1 + m\frac{\lambda}{d}\right)\left(1 + 6k_2\frac{\lambda}{d}\right)} \cdot \frac{1}{R^2}\sum \Delta T,$$

woraus erhellt, dass C_1, ebenso wie C_2 und C_3, für die parabolische Temperaturverteilung der Scheiben unabhängig von r ist, so dass der von FANSELAU angegebene Wert für ψ eine befriedigende Lösung des hydrodynamischen Problems ist. — Es ist nun weiter einfach die Werte von C_2 und C_3, in α ausgedrückt, zu berechnen und hieraus mit Hilfe der Formel für K die auf die Platten ausgeübte Kraft zu bestimmen. Wir werden nur die beiden einfachsten Fälle behandeln.

1°. $$\frac{dT}{dr} = \frac{dt}{dr} = -2\frac{r}{R^2}(T_1 - T_2).$$

Der Symmetrie wegen finden wir leicht die Werte von C_2 und C_3. Setzen wir z. B. $q_0 = q_d$, wo $q = -\sqrt{u^2 + v^2} = -rf'(z)$, erhalten wir $C_2 = -\frac{3}{2} C_1 d$ und $C_3 = \frac{1}{2} C_1 d^2$, wodurch

$$f(z) = \alpha\left[\frac{z^3}{d^2} - \frac{3}{2}\frac{z^2}{d} + \frac{1}{2} z\right],$$

und also, weil

$$\sum \frac{dT}{dr} = 2\frac{dT}{dr}:$$

$$\alpha = -\frac{1}{r}\frac{M_1}{1 + 6k_2\frac{\lambda}{d}} \cdot 2\frac{dT}{dr} = 3k_1\frac{\eta}{\varrho T} \cdot \frac{1}{\left(1 + m\frac{\lambda}{d}\right)\left(1 + 6k_2\frac{\lambda}{d}\right)} \frac{T_1 - T_2}{R^2}.$$

Aus der Formel für K erhalten wir für $z = 0$ und $z = d$ denselben Wert, nämlich:

$$K = -2\eta\left[\frac{1}{2} + \frac{3}{4}\frac{R^2}{d^2}\right]\alpha \cdot \pi R^2$$

oder:

$$K_0 = K_d = -\left[3\pi k_1 \frac{\eta^2}{\varrho T} + \frac{9}{2} k_1 \frac{\eta^2}{\varrho T} \cdot \frac{\pi R^2}{d^2}\right] \cdot \frac{T_1 - T_2}{\left(1 + m\frac{\lambda}{d}\right)\left(1 + 6 k_2 \frac{\lambda}{d}\right)}. \qquad (21)$$

Berechnen wir den Strömungszustand am Rande der Platten, erhalten wir in diesem Falle:

$$q = -rf'(z) = -\alpha R\left[3\left(\frac{z}{d}\right)^2 - 3\left(\frac{z}{d}\right) + \frac{1}{2}\right], \text{ woraus}$$

$$q_0 = q_d = -\frac{1}{2}\alpha R, \text{ während } \frac{dq}{dz} = 0 \text{ für } \frac{z}{d} = \frac{1}{2} \text{ mit}$$

$$q_{\max} = \frac{1}{4}\alpha R = -\frac{1}{2} q_0.$$

Weiter finden wir $q = 0$ für $\frac{z}{d} = \frac{1}{2}\left(1 \pm \frac{\sqrt{3}}{3}\right)$, in Übereinstimmung mit der früheren Ableitung S. 16 (vgl. Fig. 7 a und b).

Der Ausdruck für die Kraft K ist aus zwei Gliedern zusammengesetzt. Setzen wir $d = \infty$, und also $\frac{\lambda}{d} = 0$, bleibt nur das erste Glied übrig. Dieses Glied,

$$K_{d=\infty} = -3\pi k_1 \frac{\eta_2}{\varrho T}(T_1 - T_2),$$

ist die Radiometerkraft auf eine Kreisscheibe ohne Gegenplatte, wenn ein Temperaturunterschied $T_1 - T_2$ zwischen Zentrum und Rand der Scheibe besteht. Der Wert für $K_{d=\infty}$ ist in Übereinstimmung mit den Formeln, die P. Epstein[1] und Th. Sexl[2] auf andere Weise hierfür abgeleitet haben.

Ist die Temperaturverteilung auf beiden Seiten der Scheibe dieselbe, wird die Kraft $K_{d=\infty}$ in entgegengesetzter Richtung auf die andere Seite der Scheibe auch ausgeübt, so dass die totale Radiometerkraft für die Scheibe mit Gegenplatte, jedenfalls für $\frac{\lambda}{d} \to 0$,

$$K = -\frac{9}{2} \cdot k_1 \cdot \frac{\eta^2}{\varrho T} \cdot \frac{1}{d^2} \cdot \frac{T_1 - T_2}{\left(1 + m\frac{\lambda}{d}\right)\left(1 + 6 k_2 \frac{\lambda}{d}\right)} \cdot \pi R^2 \qquad (22)$$

wird.

[1] P. Epstein: Z. f. Phys. **54**, 537, 1929.
[2] Th. Sexl: Z. f. Phys. **52**, 249, 1928.

2°. Für das absolute Manometer mit parabolischer Temperaturverteilung hat man

$$\frac{dT}{dr} = \frac{dT}{dr} \quad \text{und} \quad \frac{dt}{dr} = 0.$$

Wir finden in diesem Falle leicht, wenn wir die Gleitung bei der kalten Platte vernachlässigen, wodurch also $f'(d) = 0$,

Fussnote.

Denken wir uns zwei Räume I und II mit den Temperaturen T_1 und T_2, die durch eine Ringspalte $A-B$ (vgl. Fig. 9) mit einander in Ver-

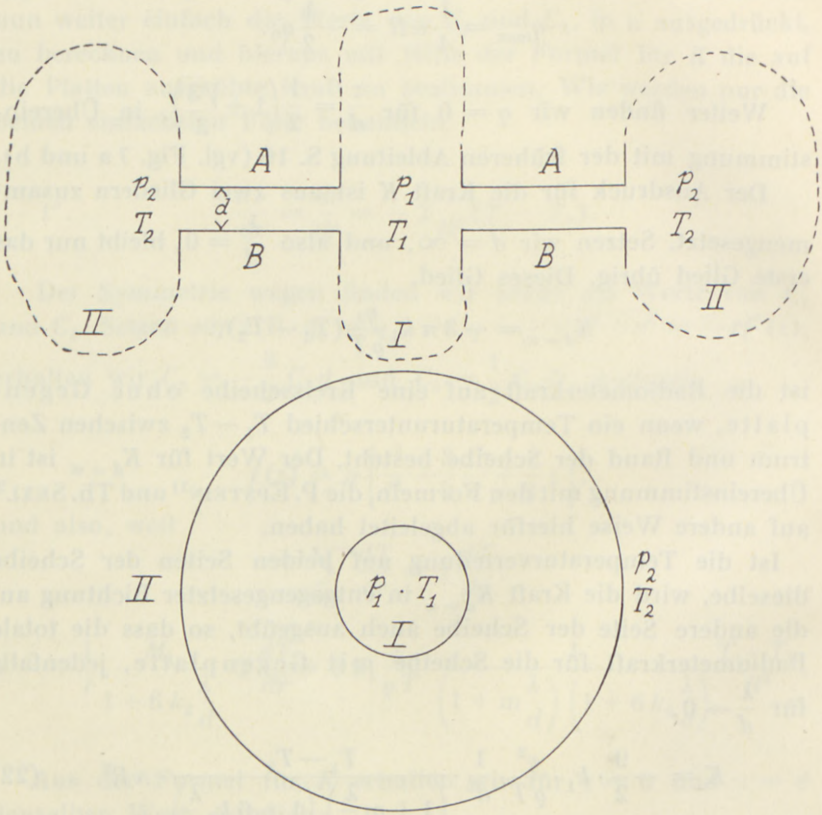

Fig. 9.

bindung stehen, dann wird in den Wänden der Ringspalte ein Temperaturgradient $\frac{dT}{dr}$ liegen.

$$f(z) = \alpha \left[\frac{z^3}{d^2} - 2\,\frac{z^2}{d} + z \right],$$

woraus folgt:

$$\alpha = \frac{3}{2} k_1 \cdot \frac{\eta}{\varrho T} \cdot \frac{1}{\left(1 + m\frac{\lambda}{d}\right)\left(1 + 6\,k_2 \frac{\lambda}{d}\right)} \frac{T_1 - T_2}{R^2}$$

und

$$K_{z=d} = -\frac{9}{4} k_1 \frac{\eta^2}{\varrho T} \cdot \frac{1}{d^2} \cdot \frac{T_1 - T_2}{\left(1 + m\frac{\lambda}{d}\right)\left(1 + 6\,k_2 \frac{\lambda}{d}\right)} \cdot \pi R^2, \qquad (24)$$

in Übereinstimmung mit dem früher abgeleiteten Ausdruck (13). Für die warme Platte erhält man aus der Formel für K:

$$K_{z=0} = -\left[3\,\pi\, k_1 \frac{\eta^2}{\varrho T} + \frac{9}{4} k_1 \frac{\eta^2}{\varrho T} \cdot \frac{\pi R^2}{d^2} \right] \cdot \frac{T_1 - T_2}{\left(1 + m\frac{\lambda}{d}\right)\left(1 + 6\,k_2 \frac{\lambda}{d}\right)},$$

Fortsetzung Fussnote:

Die Gleichgewichtsbedingung wird dann, weil die Temperaturverteilung über die Wände der Ringspalte parabolisch wird

$$\frac{dp}{dr} = -6\,C_1 \cdot \eta \cdot r = -6\,\frac{\alpha}{d^2} \cdot \eta \cdot r.$$

In diesem Falle wird $\sum \frac{dT}{dr} = 2\,\frac{dT}{dr}$, und also:

$$\alpha = -\frac{1}{r} \cdot \frac{M_1}{1 + 6\,k_2 \frac{\lambda}{d}} \cdot 2\,\frac{dT}{dr}$$

oder

$$\frac{dp}{dr} = 6 \cdot \frac{\eta}{d^2} \cdot \frac{3}{4} k_1 \frac{\eta}{\varrho T} \cdot \frac{1}{1 + m\frac{\lambda}{d}} \cdot \frac{1}{1 + 6\,k_2 \frac{\lambda}{d}} \cdot 2\,\frac{dT}{dr},$$

woraus:

$$\frac{dp}{dr} = \frac{1}{2}\frac{p}{T} \cdot \frac{1}{\frac{\pi}{36\,k_1}\left(\frac{d}{\lambda}\right)^2 + \frac{\pi}{6\,k_1}\left(k_2 + \frac{m}{6}\right)\left(\frac{d}{\lambda}\right) + \frac{\pi}{6} \cdot \frac{k_2}{k_1} m} \cdot \frac{dT}{dr}. \qquad (23)$$

Wird für $\frac{d}{\lambda} = 0$, $\mu = \frac{\pi}{6}\frac{k_2}{k_1} \cdot m = 1$, und also $m =$ ca. 2 gesetzt, erhält man für $\frac{d}{\lambda} = 0$: $\frac{dp}{dr} = \frac{1}{2}\frac{p}{T} \cdot \frac{dT}{dr}$ oder $\frac{p_1}{p_2} = \sqrt{\frac{T_1}{T_2}}$ in Übereinstimmung mit der Quadratwurzelformel für die thermomolekulare Druckdifferenz. Für $\frac{\lambda}{d} \to 0$ wird $\mu =$ ca. 2,70. Wünscht man die thermomolekularen Druckdifferenzen für Pumpzwecke zu verwenden, kann eine Ringspalte von angemessenen Dimensionen eine zweckmässige Lösung sein.

weil in dieser Platte die Temperaturdifferenz $(T_1 - T_2)$ zwischen Mittelpunkt und Rand der Scheibe besteht.

Hat die warme Scheibe dieselbe Temperaturverteilung auf der anderen Seite, wird auch die Kraft $-3\pi k_1 \frac{\eta^2}{\varrho T}(T_1 - T_2)$ auf diese Seite ausgeübt, so dass auch in diesem Falle nur das zweite Glied übrigbleibt.

Für den Strömungszustand am Rande der Platten finden wir in Übereinstimmung mit früheren Ergebnissen:

$q = 0$ für $z = d$ und $z = \frac{1}{3}d$; weiter erhalten wir für $z = \frac{2}{3}d$, $\frac{dq}{dz} = 0$ und $q_{\max} = \frac{1}{3}\alpha R$, während für $z = 0$, $q = -\alpha R$ (vgl. Fig. 8 und 6 a, b) wird.

§ 6. Um auch den Einfluss des Akkommodationskoeffizienten zu bestimmen, werden wir nun dazu übergehen, die vorliegenden Konstruktionen des absoluten Manometers laut der hier auseinandergesetzten Theorie näher zu untersuchen. Wir wollen mit dem absoluten Manometer von Martin Knudsen anfangen.

Für ein Manometer dieser Konstruktion in der rationellen Ausführung liegt die massgebende Temperaturdifferenz am Rande der heissen Platte in der an die warme Platte grenzenden Gasschicht. Für den Zustand $\frac{d}{\lambda} \gg 0$ folgt nach dieser Theorie:

$$\frac{dp}{dr} = \frac{9}{2} k_1 \cdot \frac{\eta^2}{{}_1\varrho \cdot p \cdot d^2 \left(1 + 6 k_2 \frac{\lambda}{d}\right)\left(1 + m \frac{\lambda}{d}\right)} \cdot \frac{1}{T} \sum \frac{dT}{dr},$$

oder wenn $\frac{T_1 - T_2}{T} \ll 1$, $k_1 = k_2 = \frac{4}{3}$ und $\frac{\pi}{3}\frac{k_2}{k_1} m = \mu$,

$$\frac{p_1 - p_2}{\Delta r} = \frac{1}{2T} \cdot \frac{p}{\frac{\pi}{24}\left(\frac{d}{{}_1\lambda}\right)^2 \cdot p^2 + \frac{\pi}{4}\left(k_2 + \frac{m}{6}\right)\left(\frac{d}{{}_1\lambda}\right) p + \mu} \sum \frac{dT}{dr}. \qquad (25)$$

Laut der Theorie für den Temperatursprung wird für den Temperaturgradient $\frac{dT}{dr} = \frac{\Delta T}{\Delta r}$ in der an die warme Platte grenzende Luftschicht gefunden (vgl. Fig. 10):

$$\frac{\Delta T}{\Delta r} = \frac{T_1' - T_2}{\Delta r}, \text{ wo } T_1' = T_1 - k \frac{2 - a_1}{2 a_1} \cdot \lambda \frac{dT}{dz}.$$

a_1 ist hier der Akkommodationskoeffizient der warmen Platte dem Gase gegenüber, λ die mittlere freie Weglänge und $k = \frac{15}{4}$. Laut einer meiner früheren Untersuchungen[1] ist

$$\frac{dT}{dz} = \frac{T_1 - T_2}{d} \cdot \frac{1}{1 + \frac{1}{2} k \left[\frac{2 - a_1}{a_1} + \frac{2 - a_2}{a_2}\right] \frac{\lambda}{d}}, \text{ wo}$$

a_2 den Akkommodationskoeffizienten der kalten Platte bezeichnet. Hieraus wird erhalten:

$$\frac{T_1' - T_2}{\Delta r} = \frac{T_1 - T_2}{\Delta r} \cdot \frac{1 + \frac{1}{2} k \cdot \frac{2 - a_2}{a_2} \cdot \frac{\lambda}{d}}{1 + \frac{1}{2} k \left[\frac{2 - a_1}{a_1} + \frac{2 - a_2}{a_2}\right] \frac{\lambda}{d}}. \qquad (26)$$

Ausser diesem massgebenden Temperaturgradient bei der warmen Platte liegt aber auch noch ein Temperaturgradient in

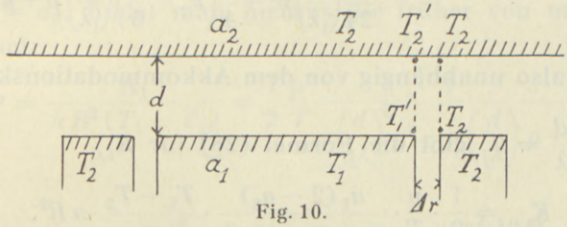

Fig. 10.

der an die kalte Platte grenzenden Gasschicht gegenüber dem Rande der warmen Platte, weil:

$$T_2' - T_2 = k \cdot \frac{2 - a_2}{2\, a_2} \cdot \lambda \cdot \frac{dT}{dz},$$

woraus:

$$\frac{T_2' - T_2}{\Delta r} = \frac{T_1 - T_2}{\Delta r} \cdot \frac{\frac{1}{2} k \cdot \frac{2 - a_2}{a_2} \cdot \frac{\lambda}{d}}{1 + \frac{1}{2} k \left[\frac{2 - a_1}{a_1} + \frac{2 - a_2}{a_2}\right] \frac{\lambda}{d}}.$$

[1] Sophus Weber: D. Kgl. Danske Vidensk. Selskab, Mat.-fys. Medd. XVI, 9, 1939. In Formel (7), S. 31 dieser Abhandlung, ist leider ein Druckfehler, wodurch ein Faktor $\frac{1}{2}$ im Nenner der Formel für $\frac{dT}{dz}$ zuviel steht.

Die Zahlen in Tabelle V, S. 33, sind aber auf Grund der obenstehenden, richtigen Formel berechnet.

Also wird

$$\sum \frac{dT}{dr} = \frac{T_1 - T_2}{\Delta r} \cdot \frac{1 + k \cdot \frac{2 - a_2}{a_2} \cdot \frac{\lambda}{d}}{1 + \frac{1}{2} k \left[\frac{2 - a_1}{a_1} + \frac{2 - a_2}{a_2} \right] \frac{\lambda}{d}}. \tag{27}$$

Für die Radiometerkraft K_1 wird hierdurch erhalten:

$$K_1 = (p_1 - p_2)\pi R^2 =$$

$$\frac{1}{2T} \cdot \frac{1 + k \frac{2 - a_2}{a_2} \cdot \frac{\lambda}{d}}{1 + \frac{1}{2} k \left[\frac{2 - a_1}{a_1} + \frac{2 - a_2}{a_2} \right] \frac{\lambda}{d}} \cdot \frac{p \cdot \pi R^2}{\frac{\pi}{24} \left(\frac{d}{\lambda} \right)^2 p^2 + \frac{\pi}{4} \left(k_2 + \frac{m}{6} \right) \left(\frac{d}{\lambda} \right) p + \mu} \cdot (T_1 - T_2). \tag{28}$$

Für $a_1 = a_2$ geht diese Formel über in die früher von mir abgeleitete Formel:

$$K_1 = (p_1 - p_2)\pi R^2 = \frac{1}{2} \frac{p}{T} \cdot \frac{\pi R^2}{\frac{\pi}{24} \left(\frac{d}{\lambda} \right) p^2 + \frac{\pi}{4} \left(k_2 + \frac{m}{6} \right) \left(\frac{d}{\lambda} \right) p + \mu} (T_1 - T_2)$$

und wird also unabhängig von dem Akkommodationskoeffizienten a.

Wenn $\frac{d}{\lambda} = 0$, gibt die Formel (28) für $K_{1,0}$

$$K_{1,0} = \frac{1}{2} \cdot \frac{p}{T} \cdot \frac{a_1 (2 - a_2)}{a_1 + a_2 - a_1 a_2} \cdot \frac{T_1 - T_2}{\mu} \cdot \pi R^2,$$

während die von Smoluchowski direkt abgeleitete Formel

$$K'_{1,0} = (p_1 - p_2)\pi R^2 = \frac{1}{2} p \left(\sqrt{\frac{T_1}{T_2}} - 1 \right) \cdot \frac{a_1 (2 - a_2)}{a_1 + a_2 - a_1 a_2} \pi R^2,$$

für $\frac{T_1 - T_2}{T_2} \ll 1$ wird:

$$K'_{1,0} = (p_1 - p_2)\pi R^2 = \frac{1}{4} \cdot p \frac{T_1 - T_2}{T} \cdot \frac{a_1 (2 - a_2)}{a_1 + a_2 - a_1 a_2} \pi R^2. \tag{29}$$

Hieraus ist zu ersehen, dass man für das ganze Gebiet $0 \leqq \frac{d}{\lambda} \leqq \infty$ annäherungsweise die Formel für K_1 verwenden kann, wenn für $\frac{d}{\lambda} \to 0$, $\mu_0 = \left(\frac{\pi}{3} \frac{k_2}{k_1} m \right)_{\frac{d}{\lambda} = 0} = 2$ gesetzt wird. Für

grössere Werte von $\frac{d}{\lambda}$, d. h. für $\frac{d}{\lambda} \to \infty$, habe ich früher auf Grund der vorliegenden Messungen von MARTIN KNUDSEN den Wert von $\mu_{\frac{d}{\lambda} \to \infty} = \frac{\pi}{3} \frac{k_2}{k_1} m$ ca. 2,70 gefunden, oder:

$$\mu_\infty = \left(\frac{\pi}{3} \frac{k_2}{k_1} m \right)_{\frac{d}{\lambda} \to \infty} = 2{,}70.$$

Die einfachste Interpolationsformel für μ ist

$$\mu = 2 \cdot \frac{1 + p \cdot \frac{d}{\lambda}}{1 + q \cdot \frac{d}{\lambda}}, \quad \text{wo} \quad \frac{p}{q} = \text{ca. } 1{,}35,$$

wodurch die Formel (28) für K_1 dem ganzen Gebiet $0 \leq \frac{d}{\lambda} \leq \infty$ angepasst ist.

Ist $a_1 = a_2$, findet man hieraus die früher von mir abgeleitete Formel:

$$P = \frac{K_1}{\pi R^2 (T_1 - T_2)} = \frac{1}{2} \frac{p}{T} \frac{1}{\alpha \left(\frac{d}{{}_1\lambda} \right)^2 p^2 + p \left(\frac{d}{{}_1\lambda} \right) p + \mu},$$

woraus

$$P_{\max} = 2 \cdot \frac{{}_1\lambda}{d} \cdot \frac{1}{2\sqrt{\alpha \mu} + \beta}, \quad p_{\max} = \frac{{}_1\lambda}{d} \sqrt{\frac{\mu}{\alpha}}$$

und

$$\frac{d}{\lambda_{\max}} = \sqrt{\frac{\mu}{\alpha}} = \text{ca. } 4{,}54, \quad \text{für} \quad \mu = 2{,}70.$$

Wird λ gross gegenüber d, also $\frac{d}{\lambda} \to 0$, erhält man aus der Formel für P mit $\mu_0 = 2$:

$$P_{\frac{d}{\lambda} \to 0} = \frac{1}{4} \cdot \frac{p}{T} \cdot \frac{1}{1 + \frac{5\pi}{24} \left(\frac{d}{{}_1\lambda} \right) p}. \tag{30}$$

Auf diese Formel werde ich in § 7 zurückkommen.

Einige neue Messreihen mit einem horizontalen absoluten Manometer in der rationellen KNUDSEN'schen Ausführung, in dem der Abstand d während der Messungen durch ein Kompensationsverfahren konstant gehalten wurde, waren für die Theorie von grossem Interesse.

Wir wollen zunächst die FREDLUND'sche Konstruktion näher betrachten, und dann erst die von mir genannte rationelle Konstruktion besprechen, in der die zwei grossen Platten A und B auf den Temperaturen T_1 und T_2 keine direkte thermische oder mechanische Verbindung mit einander haben.

Die Platten A und B können wir dann als unendlich gross annehmen im Vergleich zu den Dimensionen der sehr dünnen, metallischen Scheibe C, die in der Mitte zwischen A und B aufgehängt ist.

Angenommen wird, dass die Platten A und B horizontal liegen, wobei die warme Platte oben ist. Während der Messungen bleibt durch ein Kompensationssystem die Scheibe C auf ihrem Platz. Den Durchmesser der Scheibe C nennen wir $2R_0$ und den Abstand zwischen der Scheibe C und den Platten A und B bezeichnen wir mit d.

Weiter ist für die rationelle Konstruktion

$$\frac{d}{2R_0} \ll 1 \quad \text{und} \quad T_1 > T_2. \quad \text{(Fig. 11)}$$

Die gutleitende, sehr dünne Scheibe und die Gasschicht in der Ebene der Scheibe zwischen den Platten A und B haben die konstante Temperatur $T = \frac{1}{2}(T_1 + T_2)$.

Haben alle Oberflächen in dem Apparat denselben Akkom-

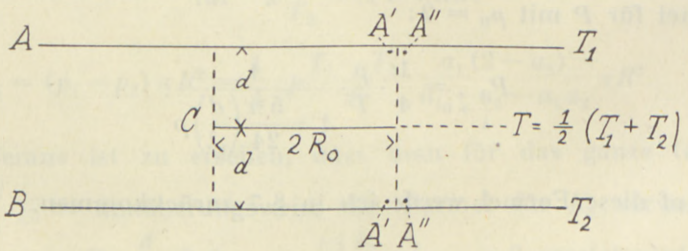

Fig. 11.

modationskoeffizienten a, wird der Temperatursprung an der Oberfläche der Scheibe C:

$$\Delta T_1 = k\frac{2-a}{2a}\lambda\frac{dT}{dz} = \frac{1}{2}\cdot\frac{1}{1+\frac{1}{k}\cdot\frac{a}{2-a}\cdot\frac{d}{\lambda}}(T_1-T), \qquad (31)$$

oder

$$\Delta T_1 = \frac{1}{4}\cdot\frac{1}{1+m_1\cdot\frac{d}{\lambda}}(T_1-T_2), \text{ wo } m_1 = \frac{1}{k}\cdot\frac{a}{2-a} \text{ und } k = \frac{15}{4}.$$

Die Temperatur der an die obere Oberfläche der Scheibe grenzenden Gasschicht wird also:

$$T+\Delta T_1,$$

so dass der horizontale Temperaturgradient am Rande der Scheibe für die obere Seite von C, ΔT_1, und für die untere Seite von C, $-\Delta T_1$ wird.

Ausserdem liegt noch ein Temperaturgradient in den an die grossen Platten A und B grenzenden Gasschichten. Dieser Temperaturgradient rührt von dem Unterschied im Temperatursprung her und liegt gegenüber dem Rande der Scheibe, weil die Temperatur der angrenzenden Gasschicht bei A', $T_1-\Delta T_1$ (Fig. 11) und bei A'', $T_1-\Delta T_2$ ist, wo:

$$\Delta T_1 = \frac{1}{4}\cdot\frac{1}{1+m_1\cdot\frac{d}{\lambda}}(T_1-T_2)$$

und

$$\Delta T_2 = \frac{1}{2}\cdot\frac{1}{1+m_1\cdot\frac{2d}{\lambda}}(T_1-T_2).$$

Der Temperaturunterschied zwischen A' und A'' wird

$$T_1-\Delta T_1-(T_1-\Delta T_2) = \Delta T_2-\Delta T_1 = \Delta T_1'$$

$$= \left[\frac{1}{2}\cdot\frac{1}{1+m_1\frac{2d}{\lambda}} - \frac{1}{4}\cdot\frac{1}{1+m_1\frac{d}{\lambda}}\right](T_1-T_2) = \frac{1}{4}\cdot\frac{T_1-T_2}{\left(1+m_1\frac{d}{\lambda}\right)\left(1+2m_1\frac{d}{\lambda}\right)}.$$

Wir erhalten hieraus $\Delta T_1 > 0$ und $\Delta T_1' > 0$ für alle Werte von $\frac{d}{\lambda}$. Für die untere Seite der Scheibe wird der Zustand ganz analog, nur wird ΔT_1 und $\Delta T_1' < 0$. Da die Gleitströme von Stellen niedriger nach Stellen höherer Temperatur strömen, wird die Strömung am Rande der Scheibe wie in Fig. 12 *a* angegeben.

Verwenden wir nun die entwickelte Theorie, erhalten wir für jede Seite der Scheibe:

$$\Delta p = p - p_\infty = \frac{1}{2T} \cdot \frac{1}{\alpha \left(\frac{d}{{}_1\lambda}\right) p^2 + \beta \left(\frac{d}{{}_1\lambda}\right) p + \mu} \sum \Delta T, \qquad (32)$$

und also für die totale Radiometerkraft auf Scheibe C:

$$K = (p_1 - p_2)\pi R_0^2 = 2 \cdot \frac{1}{2T} \cdot \frac{p}{\alpha \left(\frac{d}{{}_1\lambda}\right)^2 p^2 + \beta \left(\frac{d}{{}_1\lambda}\right) p + \mu} \cdot \pi R_0^2 \sum \Delta T,$$

wo

$$\left.\begin{aligned} \sum \Delta T &= \frac{1}{4} \cdot \frac{T_1 - T_2}{\left(1 + m_1 \frac{d}{\lambda}\right)\left(1 + 2\, m_1 \frac{d}{\lambda}\right)} + \frac{1}{4} \cdot \frac{T_1 - T_2}{1 + m_1 \frac{d}{\lambda}} \\ &= \frac{1}{2} \cdot \frac{1}{1 + 2\, m_1 \frac{d}{\lambda}} (T_1 - T_2). \end{aligned}\right\} \qquad (33)$$

Hieraus entsteht

$$K = \frac{1}{2T} \cdot \frac{p}{\alpha \left(\frac{d}{{}_1\lambda}\right)^2 p^2 + \beta \left(\frac{d}{{}_1\lambda}\right) p + \mu} \cdot \pi R_0^2 \cdot \frac{T_1 - T_2}{1 + 2\, m_1 \left(\frac{d}{{}_1\lambda}\right) p}, \qquad (34)$$

wo

$$\alpha = \frac{\pi}{24}, \quad \beta = \frac{\pi}{4}\left(k_2 + \frac{m}{6}\right) = \frac{5\pi}{12} \quad (\text{für } m = 2),$$

$$2 m_1 = \frac{2}{k} \cdot \frac{a}{2 - a} = \frac{8}{15} \cdot \frac{a}{2 - a} \quad \text{und} \quad 2 \leq \mu \leq 2{,}70.$$

Aus der Formel für K erhellt, dass die Radiometerkraft für die FREDLUND'sche Konstruktion, jedenfalls in der rationellen Ausführung, durch die Formel

$$K = \frac{1}{2\,T} \cdot \pi R_0^2 \cdot \frac{\lambda}{d} \cdot \frac{\frac{d}{\lambda}}{2\,\alpha m_1 \left(\frac{d}{\lambda}\right)^3 + (\alpha + 2\,\beta m_1)\left(\frac{d}{\lambda}\right)^2 + (\beta + 2\,\mu m_1)\left(\frac{d}{\lambda}\right) + \mu} (T_1 - T_2)$$

oder

$$K = A \cdot \frac{p}{\alpha_1 p^3 + \alpha_2 p^2 + \alpha_3 p + \alpha_4} (T_1 - T_2) \qquad (35)$$

dargestellt werden kann, was auch FREDLUND selbst aus seinen Messungen gefunden hat. —

Wir ersehen aus diesem Ausdruck, dass K bei einem bestimmten Wert von $\frac{d}{\lambda}$ ein Maximum K_{max} hat. Der entsprechende Wert für $x = \frac{d}{\lambda}$ wird bestimmt aus der Gleichung

$$4\,\alpha m_1 \left(\frac{d}{\lambda}\right)_{max}^3 + (\alpha + 2\,\beta m_1)\left(\frac{d}{\lambda}\right)_{max}^2 = \mu. \qquad (36)$$

Aus dieser Gleichung folgt, dass der Wert für $\left(\frac{d}{\lambda}\right)_{max}$ von dem Akkommodationskoeffizienten a abhängig wird, was auch bereits von FREDLUND nachgewiesen wurde. Wir erhalten hieraus:

$$\begin{aligned}
\text{Für } a = 1 \quad , \quad & x_{ber} = \left(\frac{d}{\lambda}\right)_{max} = 1{,}60 \\
a = 0{,}70, \quad & x_{ber} = \left(\frac{d}{\lambda}\right)_{max} = 2{,}02 \\
a = 0{,}50, \quad & x_{ber} = \left(\frac{d}{\lambda}\right)_{max} = 2{,}38 \\
a = 0{,}30, \quad & x_{ber} = \left(\frac{d}{\lambda}\right)_{max} = 2{,}88.
\end{aligned}$$

Aus der Formel für K geht hervor, dass die Radiometerkraft K eine Funktion von $\frac{d}{\lambda}$ und von dem Akkommodationskoeffizienten a ist. Dies erklärt, weshalb die Radiometerkraft für denselben Apparat in Deuterium und Wasserstoff bei demselben Wert von $\frac{d}{\lambda}$, bezw. für denselben Druck p, verschieden sein kann, wie FREDLUND experimentell gefunden hat.

Aus dem Ausdruck von K erhalten wir für $\frac{d}{\lambda} \to 0$

$$f_0 = \frac{K_{\text{Deut.}}}{K_{\text{Wass.}}} = 1$$

und für $\frac{d}{\lambda} \to \infty$

$$f_\infty = \frac{K_{\text{Deut.}}}{K_{\text{Wass.}}} = \frac{m_{1,\,\text{W}}}{m_{1,\,\text{D}}} = \frac{a_\text{W}}{2 - a_\text{W}} \cdot \frac{2 - a_\text{D}}{a_\text{D}}. \qquad (37)$$

Der Akkommodationskoeffizient von Deuterium ist m. W. noch nicht experimentell bestimmt[1]. Man kann aber annehmen, dass die Akkommodationskoeffizienten von Helium und Deuterium für dieselbe Oberfläche der Grössenordnung nach angenähert gleich sind. Setzen wir annäherungsweise $a_\text{W} = 0{,}70$ und $a_\text{D} = 1$ für sehr rauhe Oberflächen, erhalten wir für $\frac{d}{\lambda} \to \infty$:

$$f_\infty = \frac{m_{1,\,\text{W}}}{m_{1,\,\text{D}}} = \frac{a_\text{W}}{2 - a_\text{W}} \cdot \frac{2 - a_\text{D}}{a_\text{D}} = \text{ca. } 0{,}54,$$

während Fredlund für $\frac{d}{\lambda} \to \infty$ experimentell

$$f_{\infty,\,\text{obs}} = \text{ca. } 0{,}50 \text{ und } f_{0,\,\text{obs}} = \text{ca. } 1.0$$

gefunden hat.

Um die Fredlund'schen Messungen mit der Theorie vergleichen zu können, müssen wir überlegen, welchen Einfluss eine direkte mechanische bezw. thermische Verbindung zwischen den grossen Platten *A* und *B* haben wird. Durch eine Verbindung werden neue Gleitströme (vgl. Fig. 12 b) von der kalten Platte *B* entlang der Verbindungswand nach der warmen Platte entstehen. Sind die Platten *A* und *B* hinreichend gross verglichen mit den Dimensionen der Scheibe *C* und liegt der Apparat horizontal, ist es möglich, dass diese Gleitströme, jedenfalls bei höherem Druck, praktisch gesprochen nicht zwischen der Scheibe und den grossen Platten durchdringen, und also nur am Rande des Apparates und ausserhalb der Scheibe Wirbelströme bilden, wie in Fig. 12 b angedeutet. In diesem Falle werden die Gleitströme wahrscheinlich nur geringen Einfluss auf die Radiometerkraft ausüben.

Viel komplizierter wird aber der Zustand, wenn der Apparat, wie bei den Fredlund'schen Messungen, vertikal steht, und ausserdem die Scheibe *C* exzentrisch zwischen den grossen

[1] Nach der Beendigung dieser Arbeit hat J. Amdur (Journal of chem. physics, 14, 339, 1946) neue Bestimmungen der Akkommodationskoefficienten der Gase glattem, blankem Platin gegenüber durchgeführt.
Es wurde gefunden für Wasserstoff $a_\infty = 0{,}316$, für Helium $a_\infty = 0{,}409$ und für Deuterium $a_\infty = 0{,}396$.

Platten angebracht ist in der Weise, dass sie an einigen Stellen dicht an den Verbindungsring zwischen den Platten heranreicht. In dieser Aufstellung werden die Rand-Gleitströme zwischen den Platten und der Scheibe durchdringen und, da sie dieselbe Richtung haben, die bestehenden Gleitströme verstärken. Hierdurch wird die gemessene Radiometerkraft grösser als der auf Grund der Formel (34) berechnete Wert. —

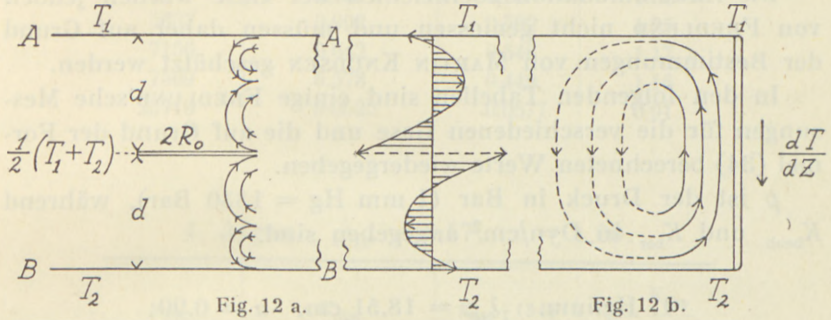

Fig. 12 a. Fig. 12 b.

In diesem Falle muss nämlich in dem Ausdruck für $\sum \Delta T$, Formel (33), noch ein Glied, das aber einer exakten Berechnung nicht zugänglich ist, hinzugefügt werden. Dieses Glied muss jedenfalls proportional mit $(T_1 - T_2)$ sein. Wir können also annäherungsweise schreiben:

$$\sum \Delta T = \frac{1}{2} \cdot \frac{1}{1 + 2\, m_1 \frac{d}{\lambda}} (T_1 - T_2) + \nu \cdot (T_1 - T_2),$$

wo ν von den Dimensionen und wahrscheinlich von $\frac{d}{\lambda}$ abhängen wird.

Wir werden also für $\sum \Delta T$ schreiben:

$$\sum \Delta T = \frac{1}{2} \cdot \frac{1}{1 + 2\, m_1 \frac{d}{\lambda}} (T_1 - T_2) \cdot \varphi;$$

es darf aber nicht erwartet werden, dass φ eine Konstante ist. Aus den FREDLUND'schen Messungen kann also

$$\varphi = \frac{K_{obs}}{K_{ber}}$$

bestimmt werden, wenn K_{ber} aus der Formel (34) berechnet wird.

FREDLUND hat durch Präzisionsmessungen mit seinem zweiten Apparat, in dem alle massgebenden Oberflächen mit Platinschwarz rauh gemacht waren, ein grosses Beobachtungsmaterial für verschiedene Gase gewonnen.

Die Apparatkonstanten waren

$$T_1 - T_2 = 20° \text{ C}, \quad d = 0{,}042 \text{ cm}, \quad \pi R_0^2 = 3{,}161 \text{ cm}^2.$$

Die Akkommodationskoeffizienten der Gase wurden jedoch von FREDLUND nicht gemessen und müssen daher auf Grund der Bestimmungen von MARTIN KNUDSEN geschätzt werden.

In den folgenden Tabellen sind einige FREDLUND'sche Messungen für die verschiedenen Gase und die auf Grund der Formel (34) berechneten Werte wiedergegeben.

p ist der Druck in Bar (1 mm Hg = 1330 Bar), während K_{beob} und K_{ber} in Dyn/cm^2 angegeben sind. —

1. Helium. ${}_1\lambda_{10°} = 18{,}51$ cm, $a = 0{,}90$.

p_{Bar}	K_{obs}	K_{ber} (34)	$\varphi = \frac{K_{obs}}{K_{ber}}$
414.1	13 31	8.11	1.65
825.3	17.13	9.04	1.90
1025	Max. 17.43	8.80	1.98
2809	11.36	5.07	2.24
6800	3.93	1.80	2.18
8783	2.62	1.252	2.09
10620	1.94	0.934	2.08
12630	1.44	0.707	2.04
37090	0.20	0.106	1.90

2. Wasserstoff. ${}_1\lambda_{10°} = 11{,}81$, $a = 0{,}75$.

p_{Bar}	K_{obs}	K_{ber} (34)	$\varphi = \frac{K_{obs}}{K_{ber}}$
319.9	9.34	6.01	1.55
636.0	11.22	6.51	1.72
690	Max. 11.24	6.44	1.74
1865	7.43	3.89	1.91
5758	1.80	1.01	1.79
8186	1.068	0.584	1.83
8640	0.961	0.534	1.80
28580	0.106	0.064	1.66

3. Deuterium. ${}_1\lambda_{10^\circ} = 11{,}81$, $a = 0{,}90$.

p_{Bar}	K_{obs}	K_{ber} (34)	$\varphi = \frac{K_{\text{obs}}}{K_{\text{ber}}}$
287.8	7.43	5.32	1.40
575	Max. 8.76	5.75	1.53
1947	4.687	3.00	1.56
5637	0.992	0.792	1.25
7156	0.642	0.546	1.17
7569	0.578	0.449	1.16
25710	0.0525	0.0577	0.91

4. Argon. ${}_1\lambda_{10^\circ} = 6{,}57$, $a = 1{,}00$.

p_{Bar}	K_{obs}	K_{ber} (34)	$\varphi = \frac{K_{\text{obs}}}{K_{\text{ber}}}$
143.1	4.01	2.68	1.50
280.0	5.12	2.93	1.75
345.0	Max. 5.22	2.85	1.83
687.3	4.26	2.091	2.04
1209	2.556	1.277	2.00
2531	0.830	0.505	1.64
3291	0.491	0.341	1.44
3598	0.410	0.297	1.38
12560	0.0232	0.0336	0.69

5. Stickstoff. ${}_1\lambda_{10^\circ} = 6{,}18$, $a = 1{,}00$.

p_{Bar}	K_{obs}	K_{ber} (34)	$\varphi = \frac{K_{\text{obs}}}{K_{\text{ber}}}$
113.7	2.490	2.373	1.05
226.6	4.518	3.985	1.13
320.0	Max. 4.690	2.683	1.75
555.5	4.060	2.165	1.88
1080	2.320	1.268	1.84
2402	0.668	0.469	1.43
2908	0.456	0.353	1.29
3069	0.405	0.325	1.25
10150	0.0272	0.0419	0.65

Aus diesen Tabellen erhellt, dass die von FREDLUND gemessenen Werte im allgemeinen anderthalb bis zweimal so gross sind wie die aus der Formel (34) berechneten Werte K_{ber}.

Das Verhältnis $\frac{K_{obs}}{K_{ber}} = \varphi$ ist, in Übereinstimmung mit der Erwartung, keine Konstante und ändert sich in dem ganzen Bereich von ca. 1 auf ca. 2. Mit Ausnahme der Werte bei dem höchstem Druck, die nach FREDLUND ziemlich unsicher sind, sind die beobachteten Werte grösser als die nach Formel (34) berechneten, wie auch erwarten werden sollte, da $1 \leqq \varphi$.

Die beobachteten Werte K_{obs} können annäherungsweise durch die empirische FREDLUND'sche Formel

$$K_{obs} = A \frac{p}{1 + b \cdot p + c \cdot p^2 + d \cdot p^3}$$

dargestellt werden.

Die Werte der Konstanten sind in der folgenden Tabelle angegeben.

	$1^{\lambda}{}_{283°.1}$	$A\ (mA)$	$b \cdot 10^3$	$c \cdot 10^6$	$d \cdot 10^9$
Helium	18.51	26.83	1.645	0.511	0.215
Wasserstoff	11.54	26.47	2.615	1.104	0.722
Deuterium	11.54	25.88	3.476	1.369	1.440
Argon	6.57	25.21	5.741	2.914	7.95
Stickstoff	6.18	25.00	6.600	2.424	11.47

Die Einheit für A ist mA, d. h. die in dem Kompensationssystem gemessene Stromstärke in Milliampère. Um A in Dyn/cm^2 anzugeben, muss

$$1\ mA = 2{,}19 \cdot 10^{-3}\ \text{Dyn/cm}^2$$

gesetzt werden. Es wäre wahrscheinlich möglich, die Werte von A, b, c und d durch Ausgleichung nach der Methode der kleinsten Quadrate etwas zu verbessern. Eine weitere Diskussion dieser FREDLUND'schen Messungen, jedenfalls bei höherem Druck, hat m. E. kein Interesse, weil die vertikale Aufstellung des Apparates und die exzentrische Lage der Scheibe eine genauere theoretische Behandlung ausschliessen; ich werde deshalb vorläufig hierauf nicht eingehen.

Aus den obigen Tabellen geht weiter hervor, dass der von FREDLUND gefundene Unterschied zwischen Wasserstoff und Deuterium insbesondere bei höherem Druck einwandfrei durch den Unterschied im Akkommodationskoeffizienten der beiden Gase erklärt werden kann. Für $\frac{d}{\lambda} \rightarrow 0$ ist der Unterschied in der Radiometerkraft sehr gering, um allmählich für $\frac{d}{\lambda} \rightarrow \infty$ bis auf 100 % anzuwachsen, so dass

$$f_\infty = \frac{K_{D,\infty}}{K_{W,\infty}} = \text{ca. } 0{,}5$$

wird, in Übereinstimmung damit dass die Akkommodationskoeffizienten von Wasserstoff und Deuterium für sehr rauhe Oberflächen ca. 0,70 und ca. 1,0 sein werden. Zur Erklärung dieses Unterschieds ist es also nicht nötig, anzunehmen, dass die mittlere freie Weglänge in Wasserstoff und Deuterium verschieden ist. —

Abgesehen von den Verwendungsmöglichkeiten des FREDLUND'schen Manometers in der vorliegenden Ausführung wäre es für die Theorie und für den Einfluss des Akkommodationskoeffizienten auf die Radiometerkraft von Bedeutung, die FREDLUND'sche Konstruktion in der von mir genannten rationellen Ausführung experimentell zu untersuchen und mit der oben angegebenen Theorie zu vergleichen. —

§ 6. Die Theorie der KLUMB-SCHWARZ'schen Manometerausführung wird von den Temperaturen T_1 und T_2, und ausserdem von Anzahl, Lage, Grösse und Form der Prallflächen abhängen; insbesondere wird die gegenseitige Lage der Prallflächen bei niedrigen Drücken von Bedeutung sein, weil hierdurch gegenseitige Schirmwirkungen der Prallflächen entstehen können. Bei dem von KLUMB and SCHWARZ verwendeten, ringförmigen Spalt kann aber die Lage und die Anzahl der Prallflächen so gewählt werden, dass die Schirmwirkung praktisch gesprochen vernachlässsigbar ist.

Die Akkommodationskoeffizienten der verschiedenen Oberflächen den Gasen gegenüber werden auch von Einfluss sein; einfachheitshalber werden wir sie vorläufig für alle Oberflächen in dem Instrument gleich eins setzen, also $a = 1$.

Wir werden also im folgenden von etwaigen Schirmwirkungen bei niedrigem Druck und von dem Einfluss des Akkommodationskoeffizienten absehen und nur ganz kurz die beiden Grenzfälle $\frac{d}{\lambda} = 0$ und $\frac{d}{\lambda} \to \infty$, wo $d = R - r$, näher betrachten; ferner werden wir die Radiometerkraft, bezw. das Drehmoment, auf die Drehachse in P_1 bezogen, auf einen schiefgestellten Planstreifen

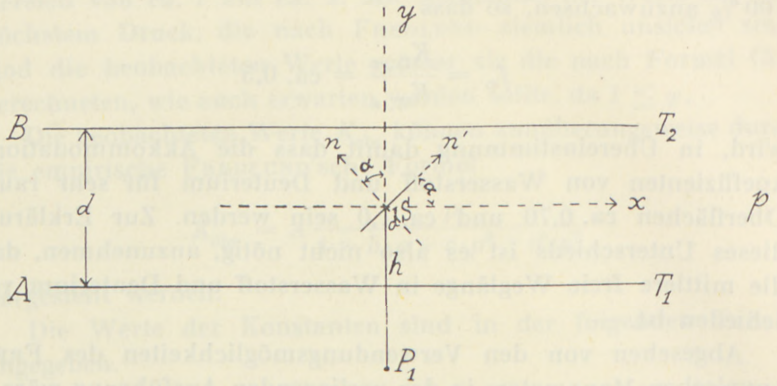

Fig. 13.

zwischen zwei grossen, parallelen Platten auf den Temperaturen T_1 und T_2 berechnen, da eine Ringspalte, für die $\frac{R-r}{r} \ll 1$, in erster Näherung durch zwei parallele Platten ersetzt werden kann.

Wir betrachten erst den Grenzfall $\frac{R-r}{\lambda} = \frac{d}{\lambda} = 0$.

Die beiden grossen, vertikalen Platten A und B stehen parallel und haben die Temperaturen T_1 und T_2, wo $T_1 > T_2$; der Abstand zwischen den Platten ist d. In der Mitte zwischen den Platten steht ein vertikaler Streifen, von dem wir ein Element $dS = 1$ cm^2 betrachten. Den Winkel zwischen der Normale des Streifens und der Y-Achse nennen wir α. Die vertikale Drehachse läuft parallel mit der Z-Achse und schneidet die Y-Achse in dem Punkte P_1 im Abstande h von der Mitte des Elementes dS, Fig. 13.

Wir nehmen an, dass sich in dem Raum des Ringspaltes N_1 Moleküle per cm^3 befinden, die sich mit einer Geschwindigkeit Ω_1 von der Platte A hinweg, und N_2 Moleküle per cm^3, die sich mit der Geschwindigkeit Ω_2 von der Platte B hinweg be-

wegen. Steht der Raum zwischen den Platten A und B mit einem Raum in Verbindung, in dem die Temperatur T_2 und der Druck $p = \frac{1}{3} N m \overline{\Omega_2^2}$ herrschen, hat man, wie bekannt, in der Gleichgewichtslage

$$\frac{1}{2} N_1 \Omega_1 = \frac{1}{2} N_2 \Omega_2 = \frac{1}{4} N \Omega_2$$

und

$$p = \frac{1}{3} N m \overline{\Omega_2^2}.$$

Für beide Seiten des Streifens erhält man nach einer einfachen Berechnung für die totale Komponente der Radiometerkraft K_n in der Richtung der Normale n den Ausdruck:

$$K_n = \frac{2}{3\pi} N_2 m \Omega_2 [\Omega_1 - \Omega_2] \cdot \left[\sin\alpha \cos\alpha + \left(\frac{\pi}{2} - \alpha\right)\right]. \qquad (38)$$

Für die Komponente in der n' Richtung des Elementes dS, $K_{n'}$, wo n' in der XY-Ebene liegt, erhält man für beide Seiten zusammen:

$$K_{n'} = \frac{2}{3\pi} N_2 m \Omega_2 (\Omega_1 - \Omega_2) \sin^2\alpha, \qquad (39)$$

während $K_z = 0$.

Das Drehmoment in Bezug auf die Drehachse in P_1 wird gegeben durch $P = K_x \cdot h$, wo

$$K_x = -K_n \cos\left(\frac{\pi}{2} - \alpha\right) + K_{n'} \cos\alpha,$$

oder

$$K_x = -\frac{1}{2} p \left[\sqrt{\frac{T_1}{T_2}} - 1\right]\left(1 - \frac{2\alpha}{\pi}\right)\sin\alpha, \qquad (40)$$

woraus hervorgeht, dass $K_x = 0$ für $\alpha = 0$ und $\alpha = \frac{\pi}{2}$, ein Resultat das auch einleuchtend ist.

Das Drehmoment P erreicht ein Maximum, wenn $\left(\frac{\pi}{2} - \alpha\right)\sin\alpha$ = Max, d. h. α = ca. 41°.

Aus dem Ausdruck für K_x erhellt, dass die Ablenkung des Radiometersystemes für den Zustand $\frac{d}{\lambda} = 0$ in der negativen Richtung der X-Achse geschieht, solange $\alpha < \frac{\pi}{2}$ ist.

Für den Zustand $\frac{d}{\lambda} \to 0$ erhält man weiter in bekannter Weise (vgl. § 7)

$$K_x = -\frac{1}{2} p \left[\sqrt{\frac{T_1}{T_2}} - 1 \right] \left(1 - \frac{2\alpha}{\pi} \right) \sin \alpha \cdot \frac{1}{1 + \beta \frac{d}{\lambda}},$$

wo d durch die Dimensionen des Radiometersystemes gegeben ist, während λ die mittlere freie Weglänge des Gases bei dem Druck p bezeichnet.

Aus dem Ausdruck für K_x erhellt, dass eine zwischen zwei grossen, parallelen Platten mit verschiedenen Temperaturen T_1 und T_2 aufgehängte Platte oder Scheibe nicht nur einer Radiometerkraft in der Richtung der Normale, sondern auch einer Radiometerkraft in der Richtung n' senkrecht zur Normale n, unterliegt. Die Grösse der Kräfte ist von dem Winkel α abhängig.

Steht die Scheibe parallel zu den grossen Platten, d. h. $\alpha = 0$, heben sich die parallel zur Scheibe wirkenden Radiometerkräfte gegenseitig auf, und also $K_{n'} = 0$ und $K_n = \frac{1}{3} N_2 m \Omega_2 (\Omega_1 - \Omega_2)$ $= \frac{1}{2} p \left(\sqrt{\frac{T_1}{T_2}} - 1 \right)$. Steht die Scheibe aber senkrecht zu den grossen Platten, d. h. $\alpha = \frac{\pi}{2}$, erhält man $K_n = 0$ und $K_{n'}$ $= \frac{2}{3\pi} N_2 m \Omega_2 (\Omega_1 - \Omega_2) = \frac{1}{\pi} \cdot p \left(\sqrt{\frac{T_1}{T_2}} - 1 \right)$, was auch durch eine direkte Berechnung leicht zu beweisen ist.

Diese letztere Anordnung ermöglicht es, ein absolutes Manometer zu konstruieren, für welches der Radiometereffekt in dem Gebiet $0 \leqq \frac{d}{\lambda} \leqq \infty$ unabhängig von der Bewegung der Scheibe, bezw. von dem Ausschlag der Scheibe wird, weil sich die Scheibe in diesem Falle in ihrer eigenen Ebene bewegt.

Wir gehen nun dazu über, den anderen Grenzzustand, d. h. $\frac{d}{\lambda} \to \infty$, zu betrachten; hier sind die durch den Temperaturgradienten entstehenden Gleitströme entlang den Prallflächen massgebend für die auf diesen wirksame Radiometerkraft.

Wenn mehrere Prallflächen vorhanden sind, werden die Gleitströme entlang einer Prallfläche $a\ b$ wahrscheinlich wie in Fig. 14 angegeben verlaufen. Das Gas strömt der Prallfläche entlang in der Richtung von Stellen niedriger Temperatur nach Stellen höherer Temperatur. Wird der Abstand der Prallflächen mit l

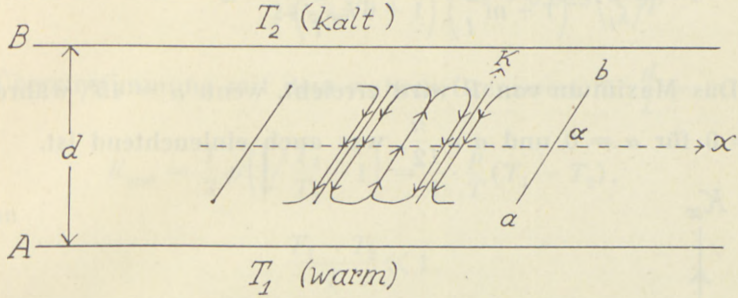

Fig. 14.

bezeichnet, erhalten wir für die Geschwindigkeit w' dieser Gleitströmung (vgl. Seite 16):

$$w' = \frac{c_1}{1 + 6\frac{\varepsilon}{l}}\left(1 - 6\frac{z}{l} + 6\left(\frac{z}{l}\right)^2\right), \text{ wo } c_1 = \frac{3}{4} k_1 \frac{\eta}{\varrho T} \frac{1}{1 + m\frac{\lambda}{l}} \frac{dT}{ds}.$$

Die hierdurch auf die Prallfläche $a\ b$ wirkende Tangentialkraft K in der Richtung der Fläche ist die totale Radiometerkraft per cm^2. Nach einer einfachen Berechnung erhält man für beide Seiten der Prallfläche

$$K_{cm^2} = 2\eta\left(\frac{dw}{dz}\right)_{z=0} = \frac{12}{l} \cdot \frac{3}{4} k_1 \cdot \frac{\eta^2}{\varrho T} \cdot \frac{1}{\left(1 + m\frac{\lambda}{l}\right)\left(1 + 6 k_2 \frac{\lambda}{l}\right)} \cdot \frac{dT}{ds},$$

oder

$$K_{cm^2} = \frac{12}{l} \cdot \frac{\eta^2}{\varrho T} \cdot \frac{1}{\left(1 + m\frac{\lambda}{l}\right)\left(1 + 6 k_2 \frac{\lambda}{l}\right)} \frac{dT}{ds}, \quad \text{wo} \quad \varrho = {}_1\varrho \cdot p,$$

weil $k_1 = k_2 = \frac{4}{3}$, während $\frac{dT}{ds}$ den Temperaturgradienten in der an die Oberfläche der Prallfläche grenzenden Gasschicht bezeichnet.

Setzen wir $\frac{dT}{ds} = \frac{T_1 - T_2}{d} \sin\alpha$, erhalten wir für das Drehmoment, $P = K_x \cdot h$, wo

$$K_x = \frac{12}{l} \cdot \frac{\eta^2}{{}_1\varrho \cdot pT} \cdot \frac{1}{\left(1 + m\frac{\lambda}{l}\right)\left(1 + 6k_2\frac{\lambda}{l}\right)} \cdot \frac{T_1 - T_2}{d} \sin\alpha\cos\alpha. \quad (41)$$

Das Maximum von P wird erreicht, wenn $\alpha = 45°$, während $P = 0$ für $\alpha = 0$ und $\alpha = \frac{\pi}{2}$, was auch einleuchtend ist.

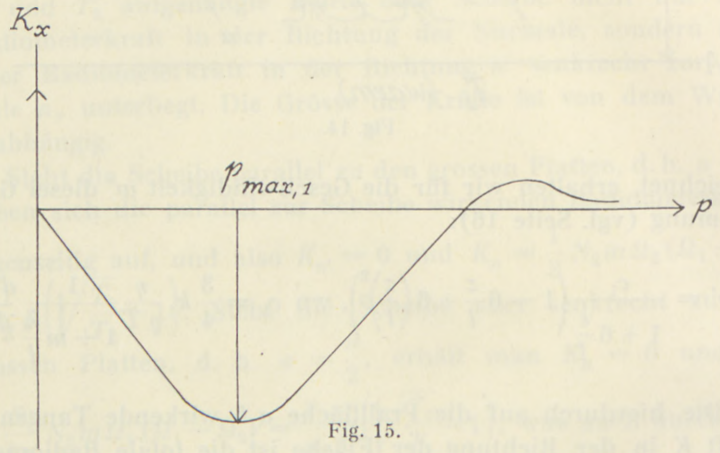

Fig. 15.

Es erhellt hieraus, dass die Ablenkung des Radiometerkörpers in der positiven Richtung der X-Achse erfolgt, solange $\alpha < \frac{\pi}{2}$, d. h. in der entgegengesetzten Richtung wie die Ablenkung im Zustande $\frac{d}{\lambda} \rightarrow 0$.

Für das Manometer von Klumb und Schwarz wird der Verlauf der Radiometerkraft, bezw. des Drehmomentes P, also in dem ganzen Druckgebiet $0 \leqq \frac{d}{\lambda} \leqq \infty$ ungefähr so wie in Fig. 15 angegeben, woraus hervorgeht, dass sich der Apparat am besten für die Messung von niedrigen Drucken eignet.

Die Kurve für K_x in Fig. 15 ist in Übereinstimmung mit den Messungen und Mitteilungen von Klumb und Schwarz.

§ 7. Aus der allgemeinen Formel für das absolute Manometer wird mit $\mu = 2$ für den Zustand $\frac{d}{\lambda} \to 0$ gefunden:

$$K_{cm^2} = \frac{1}{4} \cdot \frac{p}{T} \frac{T_1 - T_2}{1 + \frac{5\pi}{24}\left(\frac{d}{{}_1\lambda}\right) p} = \frac{1}{4} \cdot \frac{p}{T} \frac{T_1 - T_2}{1 + 0{,}625\left(\frac{d}{{}_1\lambda}\right) p},$$

in Übereinstimmung mit dem wahren Grenzwert für $\frac{d}{\lambda} = 0$:

$$K_{cm^2} = \frac{1}{2} p \left(\sqrt{\frac{T_1}{T_2}} - 1 \right) = \frac{1}{4} \cdot \frac{p}{T} (T_1 - T_2),$$

wenn

$$\frac{T_1 - T_2}{T} \ll 1.$$

Bei der Verwendung des absoluten Manometers in dem Druckgebiet $\frac{d}{\lambda} \to 0$ kann es von Interesse sein, diesen Ausdruck mit der Formel zu vergleichen, die man annäherungsweise theoretisch ableiten kann.

In einer früheren Arbeit[1]) habe ich untersucht, wie die Grenzformel

$$K_{cm^2} = \frac{1}{2} p \left(\sqrt{\frac{T_1}{T_2}} - 1 \right)$$

von vereinzelten, gegenseitigen Zusammenstössen der Moleküle zwischen den Platten A und B beeinflusst wird. Einfachheitshalber wurde bei der Ableitung der Akkommodationskoeffizienten des Gases $\alpha = 1$ gesetzt, und ausserdem $\frac{T_1 - T_2}{T} \ll 1$. Für den Wert von K_{cm^2} wurde

$$K_{cm^2} = \frac{1}{2} p \left(\sqrt{\frac{T_1}{T_2}} - 1 \right) \cdot \frac{1}{1 + \alpha\left(\frac{d}{{}_1\lambda}\right) p}, \qquad (42)$$

gefunden, wo $\alpha = \frac{3}{4}$.

${}_1\lambda = \frac{\lambda}{p}$ ist die nach der CHAPMAN'schen Formel berechnete

[1]) SOPHUS WEBER, loc. cit. S. 25. 1937.

freie Weglänge in dem Gase zwischen den Platten, wenn die Gasmasse als einheitliches Gas aufgefasst wird, und also

$$\lambda = \frac{1}{\sqrt{2}\, N \pi \sigma^2},$$

wo $\pi\sigma^2$ den mittleren effektiven Stossquerschnitt der Moleküle bezeichnet. N ist bestimmt durch $p = \frac{1}{3} N m \overline{\Omega_2^2}$, wo p der Druck ausserhalb der Platten ist, während zwischen und am Rande der Platten die folgende Bedingung gilt:

$$\frac{1}{2} N_1 \Omega_1 = \frac{1}{2} N_2 \Omega_2 = \frac{1}{4} N \Omega_2.$$

Bei Berechnung der von den Molekülen übertragenen Bewegungsmenge wurde vorausgesetzt, dass alle gegenseitigen Zusammenstösse gleichwertig sind und dass die direkt von Zusammenstössen in einem Volumenelement kommenden Moleküle gleichmässig verteilt in allen Richtungen ausgestrahlt werden; dies ist der Fall, wenn die Moleküle als harte, elastische Kugeln aufgefasst werden können. Ausserdem ist angenommen, dass ein Molekül höchstens an einem Zusammenstoss zwischen zwei auf einander folgenden Stössen gegen die Wände teilnimmt. Wenn diese Voraussetzungen erfüllt sind, werden die Moleküle, welche infolge von Zusammenstössen die Platten nicht erreichen, durch direkt von Zusammenstössen kommende Moleküle ersetzt.

Die in die Ableitung eingehende Voraussetzung, dass alle gegenseitigen Zusammenstösse der Moleküle gleichwertig sind, verlangt aber eine nähere Überprüfung. Betrachten wir zwei grosse Platten 1 und 2, bezw. das absolute Manometer von Knudsen, mit den Temperaturen T_1 und T_2, die nur wenig von einander abweichen, sieht man, dass man es in dem Raum zwischen den Platten 1 und 2 mit zwei Molekülgruppen 1 und 2 zu tun hat, in welchen sich die Moleküle in entgegengesetzten Richtungen bewegen; für $T_1 = T_2$ bilden die zwei Molekülgruppen zusammen eine homogene Gasmasse im Maxwell'schen Zustand. In dem Zustande $\frac{d}{\lambda} \to 0$ werden vereinzelte Zusammenstösse der Moleküle beider Gruppen einsetzen. Von Platte 1 bezw. 2 geht die Molekülgruppe 1 bezw. 2 aus; die Anzahl der ausgestrahlten Moleküle per Sek. und per cm^2 ist

$$\frac{1}{2} N_1 \Omega_1 \quad \text{bezw.} \quad \frac{1}{2} N_2 \Omega_2.$$

Die von der Platte 1 bezw. 2 ausgestrahlten Moleküle sind gegen die Platte 2, bezw. 1, gerichtet und nach dem Cosinusgesetz

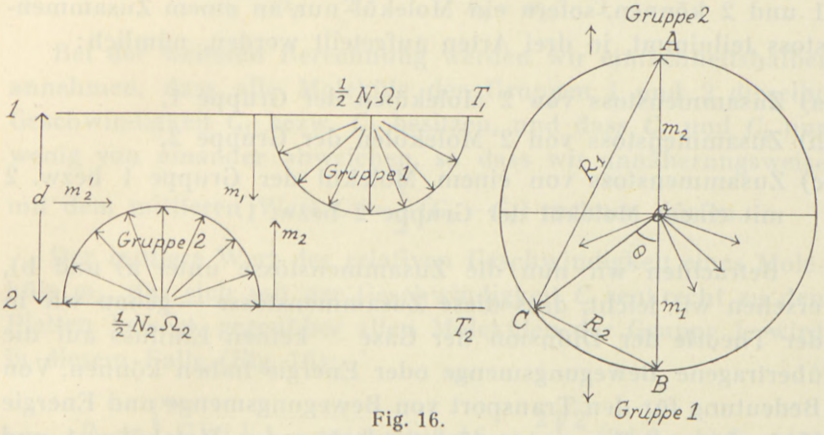

Fig. 16.

verteilt. Die Geschwindigkeitsverteilung für jede Gruppe ist die Maxwell'sche.

In dem Zustand $\frac{d}{\lambda} \to 0$ wird von den von der Platte 1 bezw. 2 ausgestrahlten Molekülen $\frac{1}{2} N_1 \Omega_1$ bezw. $\frac{1}{2} N_2 \Omega_2$ ein Teil $N_1 \Omega_1 \frac{d}{\lambda}$ bezw. $N_2 \Omega_2 \frac{d}{\lambda}$ die Platte 2 bezw. 1 nicht erreichen, weil die Moleküle in dem Raum zwischen den Platten einen Zusammenstoss erlitten haben. Die Anzahl von Molekülen, die per Sek. und per cm^3 zwischen den Platten gegenseitige Zusammenstösse erlitten haben, ist also

$$\frac{N_1 \Omega_1}{\lambda} + \frac{N_2 \Omega_2}{\lambda},$$

wenn ein Molekül höchstens an einem Zusammenstoss teilnimmt. Dies wird der Fall sein für den Zustand $\frac{d}{\lambda} \to 0$, wenn dieser Zustand dem Zustande $\frac{d}{\lambda} = 0$ sehr nahe kommt. In diesem Falle kann auch annäherungsweise für den Zustand $\frac{d}{\lambda} \to 0$, in der obenstehende Summe $N_1 \Omega_1 = N_2 \Omega_2$ gesetzt werden, so

dass die totale Anzahl von Zusammenstössen per Sek. und per cm^3 $\frac{N\Omega_2}{\lambda}$ wird. Die Hälfte dieser Moleküle ist nach den gegenseitigen Zusammenstössen gegen die Platte 1 bezw. 2 gerichtet.

Die gegenseitigen Zusammenstösse der Moleküle der Gruppen 1 und 2 können, sofern ein Molekül nur an einem Zusammenstoss teilnimmt, in drei Arten aufgeteilt werden, nämlich:

a) Zusammenstoss von 2 Molekülen der Gruppe 1,

b) Zusammenstoss von 2 Molekülen der Gruppe 2,

c) Zusammenstoss von einem Molekül der Gruppe 1 bezw. 2 mit einem Molekül der Gruppe 2 bezw. 1.

Betrachten wir nun die Zusammenstösse unter a) und b), ersehen wir leicht, dass diese Zusammenstösse — genau wie in der Theorie der Diffusion der Gase — keinen Einfluss auf die übertragene Bewegungsmenge oder Energie haben können. Von Bedeutung für den Transport von Bewegungsmenge und Energie sind also nur Zusammenstösse zwischen den Molekülen 1 und 2, und wir müssen daher für die verschiedenen Apparate und Konstruktionen die Anzahl der unter c) aufgeführten Zusammenstösse berechnen, da diese Anzahl im allgemeinen von der geometrischen Form des Messapparates abhängig sein wird.

Ist die Temperaturdifferenz zwischen den Molekülgruppen 1 und 2 sehr klein, ist es einleuchtend, dass ein Molekül m_2' (Fig. 16), das sich parallel zu den Platten 1 und 2 bewegt, dieselbe Wahrscheinlichkeit besitzt gegen ein Molekül der Gruppe 1 bezw. 2 zu stossen. — Nennen wir die Anzahl der Stösse gegen Moleküle der Gruppe 1, n_1 und gegen Moleküle der Gruppe 2, n_2, erhalten wir für Moleküle, die sich parallel zu den Platten bewegen

$$\frac{n_1}{n_2} = 1 \text{ oder } \frac{n_1}{n_1 + n_2} = \frac{n_2}{n_1 + n_2} = \frac{1}{2}.$$

Anders liegen die Verhältnisse für ein Molekül, das sich in der Richtung senkrecht zu den Platten bewegt. Betrachten wir ein Molekül m_2, das sich in der Richtung von der Platte 2 nach der Platte 1 und senkrecht zu diesen bewegt, ist es einleuchtend, dass das Molekül m_2 eine grössere Wahrscheinlichkeit besitzt gegen ein Molekül der Gruppe 1 als gegen ein Mole-

kül der Gruppe 2 zu stossen, weil die relative Geschwindigkeit des Moleküls m_2 und der sämtlichen Moleküle der Gruppe 1 grösser ist als die relative Geschwindigkeit des Moleküls m_2 und der sämtlichen Moleküle der Gruppe 2. In diesem Falle wird

$$\frac{n_1}{n_1+n_2} > \frac{1}{2} \quad \text{und} \quad \frac{n_2}{n_1+n_2} < \frac{1}{2}.$$

Bei der weiteren Berechnung werden wir einfachheitshalber annehmen, dass alle Moleküle der Gruppen 1 und 2 dieselbe Geschwindigkeit C_1 bezw. C_2 besitzen, und dass C_1 und C_2 nur wenig von einander abweichen, so dass wir annäherungsweise mit dem mittleren Wert $C = \frac{1}{2}(C_1 + C_2)$ rechnen dürfen.

Der mittlere Wert der relativen Geschwindigkeit eines Moleküls m_2, das sich mit der Geschwindigkeit C senkrecht zu den Platten bewegt, gegenüber allen Molekülen der Gruppe 1, wird in diesem Falle (Fig. 16):

$$R_1 = \int_{\frac{\pi}{2}}^{\pi} C\sqrt{2}\sqrt{1-\cos\theta}\,\sin\theta\,d\theta = \frac{2\sqrt{2}}{3}(2\sqrt{2}-1)\,C \qquad (43)$$

und gegenüber den Molekülen der Gruppe 2:

$$R_2 = \int_{0}^{\frac{\pi}{2}} C\sqrt{2}\sqrt{1-\cos\theta}\,\sin\theta\,d\theta = \frac{2\sqrt{2}}{3}\,C. \qquad (44)$$

Betrachten wir die beiden Gruppen 1 und 2 zusammen, bilden diese ein homogenes Gas, worin sich die Moleküle gleichmässig in allen Richtungen mit der Geschwindigkeit C bewegen (Clausius-Gas); hierfür erhalten wir in derselben Weise den bekannten Ausdruck:

$$R_3 = \frac{1}{2}\int_{0}^{\pi} C\sqrt{2}\sqrt{1-\cos\theta}\,\sin\theta\,d\theta = \frac{4}{3}C. \qquad (45)$$

Wird das MAXWELL'sche Verteilungsgesetz für die Molekulargeschwindigkeiten eingeführt, muss, wie bekannt, der Faktor $\frac{4}{3}$ in R_3 durch $\sqrt{2}$ ersetzt werden.

Bezeichnet in einem homogenen Gas N die Zahl der Moleküle per cm^3, sind die Stosszahlen n_1, n_2 und $(n_1 + n_2)$ in den Gruppen 1, 2 und in dem homogenen Gas durch die relativen Geschwindigkeiten bestimmt. Wir haben hierfür:

$$n_1 = \frac{N}{2} \cdot \pi\sigma^2 \cdot R_1 = N \cdot \pi\sigma^2 \cdot \frac{\sqrt{2}}{3} (2\sqrt{2} - 1) \cdot C$$

$$n_2 = \frac{N}{2} \cdot \pi\sigma^2 \cdot R_2 = N\pi\sigma^2 \cdot \frac{\sqrt{2}}{3} \cdot C \text{ und}$$

$$n_1 + n_2 = N \cdot \pi\sigma^2 \cdot R_3 = N\pi\sigma^2 \cdot \frac{4}{3} \cdot C.$$

Hieraus erhalten wir:

$$\frac{n_1}{n_1 + n_2} = \frac{\sqrt{2}}{3} (2\sqrt{2} - 1) \cdot \frac{3}{4} = \frac{4 - \sqrt{2}}{4} = 0{,}645 = \beta$$

und

$$\frac{n_2}{n_1 + n_2} = \frac{\sqrt{2}}{4} = 0{,}355 = 1 - \beta,$$

während für ein Molekül, das sich parallel zu den Platten bewegt,

$$\frac{n_1}{n_1 + n_2} = \frac{n_2}{n_1 + n_2} = \frac{1}{2} = 0{,}50$$

gilt.

Wird der Winkel zwischen der Bewegungsrichtung des stossenden Moleküls m_2 und der Normale der grossen Platten 1 und 2 mit φ bezeichnet, können wir mit hinreichender Genauigkeit die folgende Interpolationsformel anwenden:

$$\frac{n_1}{n_1 + n_2} = \left(\beta - \frac{1}{2}\right) \cos\varphi + \frac{1}{2} = \frac{1}{2} + \frac{2 - \sqrt{2}}{4} \cos\varphi = S_1;$$

wir finden hieraus im Mittel für den Raum zwischen den beiden Platten:

$$\left(\frac{n_1}{n_1 + n_2}\right)_{\text{mitt}} = \frac{1}{2} + \frac{1}{2}\left(\beta - \frac{1}{2}\right) = \frac{1}{2} + \frac{2 - \sqrt{2}}{8} = 0{,}573 = S_1.$$

In meiner früheren Ableitung der Manometerformel in dem

Gebiet $\frac{d}{\lambda} \to 0$ wurde mit $(n_1 + n_2)$ bezw. $\frac{N\Omega_2}{\lambda}$ effektiven Zusammenstössen per cm^3 zwischen den beiden Platten gerechnet, und es wurde die folgende Formel abgeleitet:

$$K_{cm^2} = \frac{1}{2} p \left(\sqrt{\frac{T_1}{T_2}} - 1 \right) \cdot \frac{1}{1 + \frac{3}{4} \cdot \frac{d}{\lambda}}.$$

Aus dem Vorhergehenden erhellt aber, dass man bei zwei grossen, parallelen Platten nur mit n_1 effektiven gegenseitigen Zusammenstössen zu rechnen hat; hieraus folgt, wie leicht zu sehen ist, dass die Formel geschrieben werden muss:

$$K_{cm^2} = \frac{1}{2} p \left(\sqrt{\frac{T_1}{T_2}} - 1 \right) \cdot \frac{1}{1 + \frac{3}{4} S_1 \left(\frac{d}{\lambda} \right)},$$

oder

$$K_{cm^2} = \frac{1}{2} p \left(\sqrt{\frac{T_1}{T_2}} - 1 \right) \cdot \frac{1}{1 + 0{,}43 \left(\frac{d}{\lambda} \right)}. \qquad (46)$$

Sind die Akkommodationskoeffizienten für die beiden grossen Platten 1 und 2 dieselben, kann man den Einfluss des Akkommodationskoeffizienten auf den Wert von S_1 vernachlässigen. — Ist $\frac{T_1 - T_2}{T_2} \ll 1$, kann die Formel (46) auch folgendermassen geschrieben werden:

$$K_{cm^2} = \frac{1}{4} \cdot p \cdot \frac{1}{1 + \alpha \left(\frac{d}{\lambda} \right) p} \cdot \frac{T_1 - T_2}{T_2},$$

wo $\alpha = 0{,}43$.

Wir können nun diese Formel mit den Messungen von Fredlund vergleichen und wählen hierfür die mit dem zweiten Fredlund'schen Apparat gewonnenen Messreihen mit den Konstanten

$$d = 0{,}042 \text{ cm}, \quad 2R = \text{ca. } 2 \text{ cm} \quad \text{und} \quad T_1 - T_2 = 20° C.$$

Hieraus erhellt, dass $\frac{2R}{d} = \text{ca. } 50$, so dass dieses Instrument als ein absolutes Manometer aufgefasst werden darf, jedenfalls

für den Zustand $\frac{d}{\lambda} \to 0$, wo keine Gleitströme vorhanden sind. —

Um den Einfluss des Akkommodationskoeffizienten weitgehendst zu eliminieren, waren alle massgebenden Oberflächen in diesem Radiometersystem mit Platinschwarz rauh gemacht; ausserdem wurde der Abstand d während der Messungen durch eine elektromagnetische Kompensation der Radiometerkraft konstant gehalten.

Fredlund hat das umfangreiche Beobachtungsmaterial für die Gase Helium, Wasserstoff, Deuterium, Argon und Stickstoff in fünf Tabellen[1] wiedergegeben. Für die in diesen Tabellen aufgeführten Messungen gilt ungefähr:

Für Tabelle V: $0 \leqq \frac{d}{\lambda} \leqq$ ca. 85

» » IV: $0 \leqq \frac{d}{\lambda} \leqq$ » 3,7

» » III: $0 \leqq \frac{d}{\lambda} \leqq$ » 0,95

» » II: $0 \leqq \frac{d}{\lambda} \leqq$ » 0,15

» » I: $0 \leqq \frac{d}{\lambda} \leqq$ » 0,03

Verwenden wir für jede Messreihe und für jedes Gas die Formel

$$\frac{K}{T_1 - T_2} = A \cdot \frac{p}{1 + bp + cp^2 + d \cdot p^3},$$

können wir den Wert von b bestimmen und hieraus den Faktor α berechnen, weil $\alpha = b \cdot \frac{\lambda}{d}$.

	α_V	α_{III}	α_{II}	α_I
	Tabelle V	Tabelle III	Tabelle II	Tabelle I
Helium: He	0.725	0.732	1.08	1.20
Wasserstoff: H_2	0.719	0.779	1.30	1.39
Deuterium: D_2	0.955	0.800	1.32	1.42
Argon: Ar	0.898	0.789	1.33	1.52
Stickstoff: N_2	0.972	0.850	1.37	1.52

[1] E. Fredlund: loc. cit. (b) S. 4—9.

Aus dieser Tabelle geht hervor, dass der beobachtete Wert von α in dem Gebiet $\frac{d}{\lambda} \to 0$ etwas zunimmt und dass der experimentelle Wert von α bedeutend grösser ist als der nach der klassischen kinetischen Theorie berechnete Wert $\alpha = 0{,}43$. Der gefundenen Variation von α, bezw. dem Anwachsen von α für $\frac{d}{\lambda} \to 0$, braucht wahrscheinlich keine grosse Bedeutung zugemessen zu werden, zumal hierfür verschiedene Erklärungen möglich sind, wie z. B. ein minimales Loch in dem Apparat, bezw. bei niedrigen Drucken Anwesenheit oder Abgabe einiger schwerer Dämpfe usw.

Der Unterschied zwischen dem berechneten Wert $\alpha = 0{,}43$ und dem beobachteten, mittleren Wert $\alpha =$ ca. 0,85 ist aber so gross, dass er wahrscheinlich nicht durch den Einfluss eventueller Verunreinigungen der Gase durch schwere Dämpfe, selbst in einem komplizierten Apparat, erklärt werden kann.

Unter der Annahme, dass die entwickelte Theorie für die gegenseitigen Zusammenstösse der Moleküle in den beiden Gruppen annäherend richtig ist, würde sich aus dem Wert $\alpha =$ ca. 0,85 ein Wert von λ ergeben, der nur gleich der Hälfte des klassischen CHAPMAN'schen Wertes ist, d. h. ein Stossquerschnitt der Moleküle von ca. $2\,\pi\sigma^2$, wo $\pi\sigma^2$ den CHAPMAN'schen Stossquerschnitt bezeichnet.

Die Erklärung von diesem Unterschied kann daher vielleicht darin gesucht werden, dass es in dem Gebiet $\frac{d}{\lambda} \to 0$, wo nur vereinzelte Zusammenstösse zwischen den Molekülen stattfinden, nicht erlaubt ist, die Moleküle als harte, elastische Kugeln anzusehen.

Es wird dann in diesem Gebiet, in Übereinstimmung mit den Resultaten der Untersuchungen über Zusammenstösse von nicht-identischen Molekülen in Molekularstrahlen, notwendig, das wellenmechanische Modell der Moleküle zu gebrauchen. — In diesem Falle wird, wie u. a. MASSEY und MOHR[1] gezeigt haben, der effektive Stossquerschnitt grösser und also der Wert von λ in demselben Verhältnis kleiner.

Laut den aus den Untersuchungen mit Molekularstrahlen

[1] H. S. W. MASSEY und C. B. O. MOHR: Proc. Roy. Soc. A 141, 434, 1933.
» » » » A 144, 188, 1934.

für den effektiven Stossquerschnitt gewonnenen Resultaten muss angenommen werden, dass der einzelne Zusammenstoss zwischen zwei Molekülen nach den Gesetzen der Wellenmechanik zu behandeln ist, während es laut der kinetischen Gastheorie erlaubt ist, die klassische Mechanik anzuwenden, wenn es sich um den mittleren Wert von vielen gegenseitigen Zusammenstössen handelt.

Der effektive Stossquerschnitt wird nämlich laut der Wellenmechanik u. a. abhängig von dem Wert der zugeordneten de BROGLIE'schen Wellenlänge λ', und man findet hieraus für den effektiven Stossquerschnitt s_{11} für *identische* Moleküle[1]

$$\text{für } \lambda' = 0, \quad s_{11} = 2\pi\sigma^2 \text{ und}$$

$$\text{für } \lambda' = \infty, \; s_{11} = 8\pi\sigma^2,$$

wo $\pi\sigma^2$ den klassischen CHAPMAN'schen Stossquerschnitt bezeichnet. Hieraus würde folgen, dass der Wert der Hilfsgrösse λ, die mittlere freie Weglänge im Gase, der für den Zustand $\frac{d}{\lambda} \to 0$ in Betracht kommt, bedeutend kleiner ist als der klassische CHAPMAN'sche Wert.

Vollständigkeitshalber muss aber noch erwähnt werden, dass E. FREDLUND mit seiner ersten Manometerkonstruktion, für welche die Konstanten

$$d = 0{,}485 \text{ cm} \quad 2R = \text{ca. } 1{,}50 \text{ cm} \quad \text{und} \quad T_1 - T_2 = 20^\circ \text{C}$$

waren, einen Wert von α für die Gase H_2, N_2 und Ar von im Mittel ca. 0,40 gefunden hat. Das Beobachtungsmaterial in diesen Messreihen ist aber für das Gebiet $\frac{d}{\lambda} \to 0$ nicht sehr gross, und ausserdem muss diese Untersuchung als eine Bestimmung der Radiometerkraft auf eine gut wärmeleitende, kleine Scheibe in einem Temperaturfeld karakterisiert werden. — Es wäre aus theoretischen Gründen von erheblichem Interesse, einige Reihen von neuen Präzisionsmessungen zur Bestimmung des Wertes von α in dem Gebiet $\frac{d}{\lambda} \to 0$ durchzuführen; hierfür würden Unter-

[1] Vgl. EARLE H. KENNARD: Kin. Theory of Gases, 1938, S. 133 und, HARALD WERGELAND: D. Kgl. Danske Vid. Selskab, Mat.-fys. Medd. XXIII, 14, 1945.

suchungen über die molekulare Reibung und die molekulare Wärmeleitfähigkeit in Betracht kommen. Insbesondere ist die molekulare Wärmeleitfähigkeit hierfür geeignet, weil der Einfluss der unbekannten molekularen Streuung der Moleküle nach den gegenseitigen Zusammenstössen bei dem Energietransport in dem Zustande $\frac{d}{\lambda} \to 0$ nur von geringer Bedeutung sein wird, jedenfalls dann, wenn mit parallelen Platten oder grossen coaxialen Zylinderflächen, wofür die Bedingung $\frac{R-r}{r} \ll 1$ erfüllt ist, gearbeitet wird und sehr kleine Temperaturdifferenzen verwendet werden.

Zusammenfassung.

1. In einer früheren Arbeit wurde für die Radiometerkraft per cm^2 in dem absoluten Manometer von MARTIN KNUDSEN die folgende Formel abgeleitet:

$$K'_{cm^2} = \frac{1}{2} \cdot \frac{p}{T} \cdot \frac{T_1 - T_2}{\frac{\pi}{24}\left(\frac{d}{{}_1\lambda}\right)^2 p^2 + \frac{\pi}{3}\left(1 + \frac{m}{8}\right)\left(\frac{d}{{}_1\lambda}\right) p + \frac{\pi}{3} m},$$

unter der Voraussetzung, dass $\frac{d}{\lambda}$ nicht zu klein ist und $\frac{T_1 - T_2}{T_2} \ll 1$. Ausserdem wurde angenommen, dass die Oberflächen des Radiometersystems absolut rauh waren, d. h. dass für alle Gase $a = 1$, wenn a den Akkommodationskoeffizienten des Gases bezeichnet.

d ist die massgebende Abmessung des Radiometersystems; für das absolute Manometer ist d der konstante Abstand der grossen, parallelen Platten mit den Temperaturen T_1 und T_2. ${}_1\lambda = p\lambda$ ist die mittlere freie Weglänge des Gases bei dem Druck 1 Bar. λ wird auf Grund der CHAPMAN'schen Formel berechnet.

Die Formel ist gültig, wenn $\frac{d}{\lambda}$ nicht zu klein ist, und der experimentelle Wert von $\mu = \frac{\pi}{3} \cdot m$ in dem Bereich $\frac{d}{\lambda} \to \infty$ ist $\mu =$ ca. 2,70.

Soll die Formel auch den Grenzwert für $\frac{d}{\lambda} = 0$ befriedigen, muss in diesem Gebiet $\mu = 2$ gesetzt werden. — Laut dieser

Formel muss für zwei Gase mit demselben Wert von λ, z. B. Helium und Deuterium, die Radiometerkraft K für denselben Apparat und bei demselben Druck p die gleiche sein. —

2. E. Fredlund hat aber mit seinem Molekularmanometer experimentell nachgewiesen, dass die Radiometerkräfte in Wasserstoff und Deuterium für denselben Messapparat und bei demselben Druck p verschieden sind.

Für den Zustand $\frac{d}{\lambda} \rightarrow 0$ ist die Radiometerkraft in beiden Gasen, wie auch erwartet werden sollte, praktisch gesprochen die gleiche, während in dem Gebiet $\frac{d}{\lambda} \rightarrow \infty$ die Radiometerkraft in Wasserstoff ca. zweimal so gross wird als in Deuterium.

Bei diesen Untersuchungen von Fredlund waren die Oberflächen des Radiometersystems mit Platinschwarz rauh gemacht.

3. Der Einfluss des Akkommodationskoeffizienten a wird für das absolute Manometer von Martin Knudsen und für das Molekularmanometer von Fredlund in der rationellen Ausführung theoretisch untersucht, und die Manometerformeln werden berechnet. Haben alle Oberflächen des Manometersystems denselben Akkommodationskoeffizienten a, wird für das absolute Manometer von Martin Knudsen gefunden, dass der Einfluss des Akkommodationskoeffizienten auch in dem Gebiet $\frac{d}{\lambda} \rightarrow \infty$ vernachlässigt werden kann.

Für das Fredlund'sche Manometer in der rationellen Ausführung, d. h. eine kleine metallische Kreisscheibe, aufgehängt parallel zu und in der Mitte zwischen zwei grossen, parallelen Platten, die *keine* direkte Verbindung mit einander haben, wurde die folgende Formel gefunden:

$$K_{cm^2} = \frac{1}{2} \cdot \frac{p}{T} \cdot \frac{1}{\frac{\pi}{24}\left(\frac{d}{{}_1\lambda}\right)p^2 + \frac{\pi}{3}\left(1 + \frac{m}{8}\right)\left(\frac{d}{{}_1\lambda}\right)p + \frac{\pi}{3}m} \cdot \frac{1}{1 + 2\,m_1\left(\frac{d}{{}_1\lambda}\right)p}(T_1 - T_2).$$

In dieser Formel ist $2\,m_1 = \frac{8}{15} \cdot \frac{a}{2-a}$ und $2 \leqq \mu = \frac{\pi}{3}m \leqq$ ca. 2,70.

Hieraus erhellt, dass man für zwei Gase mit demselben Wert von ${}_1\lambda$ und mit verschiedenen Akkommodationskoeffizienten a_W und a_D erhält:

$$\text{für } \frac{d}{\lambda} \to 0, \quad f_0 = \left(\frac{K_D}{K_W}\right)_0 = 1 \text{ und}$$

$$\text{für } \frac{d}{\lambda} \to \infty, \quad f_\infty = \left(\frac{K_D}{K_W}\right)_\infty = \frac{a_W}{2 - a_W} \cdot \frac{2 - a_D}{a_D}.$$

Der von FREDLUND gefundene Unterschied in der Radiometerkraft von H_2 und D_2 wird hierdurch einwandfrei erklärt. Wird z. B. für die stark platinierten Oberflächen seines Manometers angenommen, dass a_W = ca. 0,70 und a_D = ca. 1, wird hieraus für $\frac{d}{\lambda} \to \infty$ gefunden, dass $\left(\frac{K_D}{K_W}\right)_\infty$ = ca. $\frac{1}{2}$, in Übereinstimmung mit den experimentellen Resultaten.

Soweit bekannt, ist der Akkommodationskoeffizient für Deuterium noch nicht gemessen[1]. Es darf aber angenommen werden, dass die Akkommodationskoeffizienten für Deuterium und Helium, weil beide Gase dasselbe Molekulargewicht haben, annäherungsweise gleich sind. Auf Grund der Messungen von MARTIN KNUDSEN ist es bekannt, dass für eine stark platinierte Oberfläche, für welche a_W = ca. 0,70, der Akkommodationskoeffizient für Helium ca. 0,95 ist; es ist nicht wahrscheinlich, dass der Akkommodationskoeffizient für reines Deuterium kleiner ist. —

Aus der obenstehenden Formel für die Radiometerkraft K in dem FREDLUND'schen Molekularmanometer geht hervor, dass die Abhängigkeit zwischen K und dem Druck p durch

$$K_{cm^2} = A \cdot \frac{p}{\alpha_1 p^3 + \alpha_2 p^2 + \alpha_3 p + \alpha_4} (T_1 - T_2)$$

gegeben ist.

Diese Druckabhängigkeit zwischen K und p hat FREDLUND auch aus seinen Messungen für alle untersuchten Gase gefunden.

4. Grösse und Verlauf der Radiometerkraft in dem Molekularmanometer von KLUMB und SCHWARZ werden theoretisch untersucht, und die Radiometerkraft auf einer Oberfläche oder Scheibe, die zwischen zwei grossen, parallelen Platten mit verschiedenen Temperaturen T_1 und T_2 aufgehängt ist, wird berechnet. Ist die kleine Scheibe, in der FREDLUND'chen oder die Prallfläche in der KLUMB-SCHWARZ'chen Konstruktion, parallel zu den grossen Platten, wird für den Zustand $\frac{d}{\lambda} = 0$

[1] Vgl. Fussnote S. 34.

die Radiometerkraft in der Richtung der Normale der Scheibe $K_n = \frac{1}{2} p \left[\sqrt{\frac{T_1}{T_2}} - 1 \right]$, während sich die in der Scheibe liegenden Radiometerkräfte gegenseitig aufheben.

Steht die Prallfläche oder kleine Scheibe aber senkrecht zu den grossen Platten mit verschiedenen Temperaturen, wird für den Zustand $\frac{d}{\lambda} = 0$, $K_n = 0$, während die Resultante der in der Scheibe liegenden Radiometerkräfte $K_{n'}$ unter Berücksichtigung beider Seiten der Scheibe

$$K_{n'} = \frac{1}{\pi} \cdot p \left(\sqrt{\frac{T_1}{T_2}} - 1 \right)$$

wird.

Hierdurch wird es möglich ein absolutes Manometer zu konstruieren, in dem der Radiometereffekt von dem Ausschlag unabhängig ist.

5. Für das absolute Manometer von Martin Knudsen wird der Bereich $\frac{d}{\lambda} \to 0$ theoretisch näher untersucht, und zwar von der Voraussetzung ausgehend, dass ein Molekül zwischen zwei auf einander folgenden Stössen gegen die Wände höchstens an einem Zusammenstoss mit anderen Molekülen teilnimmt, und dass die vereinzelten, gegenseitigen Zusammenstösse der Moleküle nicht alle in Bezug auf den Transport von Bewegungsmenge und Energie gleichwertig sind.

Von den grossen Platten 1 und 2 mit den Temperaturen T_1 und T_2 werden die Molekülgruppen 1 bezw. 2 ausgesandt; ein Molekül aus der Gruppe 1 kann nun entweder gegen ein Molekül der Gruppe 1 oder gegen ein Molekül der Gruppe 2 stossen; dasselbe gilt für ein Molekül aus der Gruppe 2. —

Für den Transport von Bewegungsmenge und Energie von der einen Platte nach der anderen sind nur Zusammenstösse zwischen Molekülen aus verschiedenen Gruppen von Bedeutung, während der Zusammenstoss zwischen Molekülen aus derselben Gruppe den Transport von Bewegungsmenge und Energie nicht beeinflusst.

Ausgehend von diesen Betrachtungen wird für den Zustand $\frac{d}{\lambda} \to 0$, und wenn $\frac{T_1 - T_2}{T} \ll 1$, die folgende Formel für die

Radiometerkraft abgeleitet:

$$K_{cm^2} = \frac{1}{4} \cdot \frac{p}{T} \cdot \frac{T_1 - T_2}{1 + \alpha \left(\frac{d}{\lambda}\right)_1 \cdot p}, \quad \text{wo} \quad \alpha = \text{ca. } 0{,}43.$$

Aus dem grossen Beobachtungsmaterial von FREDLUND für das Gebiet $\frac{d}{\lambda} \to 0$ wird aber ein Wert von α gefunden, der ungefähr doppelt so gross ist wie der berechnete Wert $\alpha = 0{,}43$.

Wenn dieser Unterschied reell ist, kann man annehmen, dass der effektive Stossquerschnitt identischer Moleküle in diesem Zustand des Gases doppelt so gross ist wie der klassische CHAPMAN'sche Stossquerschnitt.

Diese Abweichung ist in Übereinstimmung mit den bei den Bestimmungen des effektiven Stossquerschnittes für nicht-identische Moleküle nach der Methode der Molekularstrahlen gefundenen Resultaten. Stellt es sich bei anderen Untersuchungen, z. B. Untersuchungen über die molekulare Reibung und die molekulare Wärmeleitfähigkeit in dem Zustande $\frac{d}{\lambda} \to 0$, heraus, dass der beobachtete Wert von α doppelt so gross ist wie der berechnete, muss man annehmen, dass der einzelne Zusammenstoss zwischen zwei identischen Molekülen auch nach den Gesetzen der Wellenmechanik behandelt werden muss, während nach der kinetischen Gastheorie die Anwendung der klassischen Mechanik erlaubt ist, wenn es sich um den mittleren Effekt von vielen gegenseitigen Zusammenstössen handelt.

Im Hinblick auf dieses Problem wäre es von wesentlichem Interesse, dass neue Präzisionsmessungen über den Verlauf der molekularen Reibung und molekularen Wärmeleitfähigkeit in dem Gebiet $\frac{d}{\lambda} \gtrsim 0$ vorgenommen würden. —

Der Direktion des Dänischen Carlsbergfonds bin ich wieder für gewährte Stütze sehr zu Dank verpflichtet.

Indleveret til Selskabet den 19. Juni 1946.
Færdig fra Trykkeriet den 20. December 1947.

DET KGL. DANSKE VIDENSKABERNES SELSKAB
MATEMATISK-FYSISKE MEDDELELSER, BIND XXIV, NR. 5

THE SHORT-PERIODIC COMETS AND THE HYPOTHESIS OF THEIR CAPTURE BY THE MAJOR PLANETS

BY

ELIS STRÖMGREN †

KØBENHAVN
I KOMMISSION HOS EJNAR MUNKSGAARD
1947

Printed in Denmark
Bianco Lunos Bogtrykkeri

A survey of the motions in our solar system shows that space around our sun is filled with bodies, large and small: the major planets and their satellites, asteroids, and comets; and filled with orbits. Objects that are situated in the outer parts of the system are invisible to us even if they are intrinsically bright; but if they move in very eccentric orbits, so that their perihelion distances are smaller than a certain limit, then they may come within a distance small enough to make them observable. Millions of planets and comets are certainly present in our solar system, but the great majority are never observed from the earth.

Most of the several hundred comets for which orbits have been determined move in very eccentric orbits, very close to parabolic motion. In the case of a few comets, for which slightly hyperbolic motion has been derived, it has been found that this hyperbolicity can be explained as a consequence of the perturbations by the major planets during the motion of the comet towards the inner parts of the solar system. We may maintain that there is not a single comet among those observed for which motion from the outside into our solar system has been established[1].

A small fraction of the comets observed until now move in relatively small ellipses round the sun, and the relation between these comets and the great majority of comets moving in very eccentric orbits has been made the subject of a number of investigations by various authors.

By the investigations of the orbit of the so-called Lexell's comet (comet 1770 I) attention was drawn to the possibility of great changes in the character of the motion of a comet if a near approach to one of the major planets took place. Later it became

[1] Cf. e. g. Publications of the Copenhagen Observatory Nos. 19, 44, 98, 105, 112, 114.

possible to establish by accurate calculations many cases of large changes of cometary orbits caused by one of the major planets (Jupiter). For an example see Publ. Copenhagen Observatory No. 106: H. Q. Rasmusen's calculation of the motion of comet Schwassmann-Wachmann 2 (1929 I). With the increasing knowledge of cometary orbits it became evident that groups of cometary orbits exist which apparently to a certain degree are connected with the major planets: a large group with aphelion distances about equal to the semi-major axis of the orbit of Jupiter, a small group with aphelion distances about equal to the semi-major axis of the orbit of Saturn, and two small groups apparently connected in a similar way with the orbits of Uranus and Neptune. It was supposed that the comets had come from distant regions of the solar system and had been captured by one of the major planets. Later investigations have shown that such an explanation is uncertain in the case of the three groups of comets apparently connected with the planets Saturn, Uranus, and Neptune, while the existence of a group of comets that have a direct mechanical connection with Jupiter may be regarded as an established fact.

How is it possible to establish whether a planet, e. g. Jupiter, has by its attraction captured a comet coming from a great distance, and changed its orbit into an ellipse of relatively small dimensions? The most exact and conclusive method would be that of carrying out for every single comet a calculation of the perturbations as far back in time as the moment when the great change of the orbit due to the close approach between planet and comet took place. The amount of work involved in carrying out this program would, however, be prohibitive, not only because the number of comets to be treated would, nowadays, be very large, but especially because it is not possible *a priori* to see how many revolutions would have to be calculated before the required situation of capture were reached and—still worse—how many times in the past a comet has had near approaches to the planet from the capture up to our time. It has, therefore, been necessary to be content with investigations of a more statistical nature.

In the course of time the problem has been attacked by many different investigators. We shall here mention the important researches made by G. Fayet and H. N. Russell.

Fayet in the Bulletin Astronomique (1911) investigated the

situation of the minimum distances of the short-periodic comets known at the time from the orbit of Jupiter. Making use of amongst others the so-called Tisserand criterion, he found that a number of comets form a group of common origin. RUSSELL in a paper in The Astronomical Journal (1920) studied the minimum distances of the short-periodic comets then known from the orbits of the major planets, and came to the conclusion that Jupiter in this problem plays an absolutely dominating role among the planets. Saturn does not seem to be of much importance. The importance of Uranus seemed to be small, and that of Neptune negligible.

After the publication of FAYET's and RUSSELL's results the material of cometary orbits has considerably increased.

In Tables I and II we have compiled the material now available. Table I gives the orbits for all comets that have been observed in more than one apparition, while Table II contains the orbits of short-periodic comets that have not been rediscovered (the orbits of which are, however, on the whole to be considered as sufficiently reliable). In Table II we have, however, restricted the material to orbits with aphelion distances smaller than 35.0. The various columns in the tables give: the number, designation of the object, the perihelion time T, the longitude of the perihelion π, the longitude of the node Ω, the eccentricity e, the perihelion distance q, the inclination relative to the ecliptic i, the longitude of the perihelion reckoned from the node ω, the aphelion distance Q, and the period in years P. The table is arranged according to increasing period. In Table II we have not indicated the limit between the Jupiter group and the next group, as this limit is rather ill-defined. In our reasoning, as given below, we have identified the inclination relative to the ecliptic with the inclination relative to the orbit of the planet, an approximation that is of no importance to the reasoning. Similarly we have not reduced the elements to a common equinox. This is without any consequence whatever in our statistical discussion based on the elements i and ω. I am much indebted to Mr. K. A. THERNÖE M.Sc. and to Mr. P. NAUR for their valuable assistance in compiling the two tables.

It would undoubtedly be interesting to repeat the investigations

of FAYET and RUSSELL on the basis of the considerably greater material now available. We shall not, however, enter into this problem but restrict ourselves to a discussion from another point of view of the material contained in Tables I and II.

It has always been considered a fact that a small inclination (i) is favourable in as far as capture is concerned, and also that direct motion is more favourable than retrograde, as it makes it possible for the comet to move for a longer interval of time in the neighbourhood of the planet[1]. Statistical investigations of the orbits indeed indicate that small inclinations dominate, and that retrograde motion for short-periodic comets is very rare and does not occur at all in the Jupiter group. It is not, of course, excluded that a comet with large inclination (up to 180°) is captured in an exceptional case when the point of intersection with the ecliptic (the planetary orbit) so to speak accidentally falls *very* close to a point of the planetary orbit, but this is a question of extraordinary cases. There is another point that deserves more consideration.

It is a condition for referring a comet for instance to the Jupiter-group that the aphelion of the comet is at a distance from the sun about equal to the semi-major axis of the orbit of Jupiter (the range of the distances has proved to be rather wide, incidentally). This, however, is not sufficient. It is also required that the line of apsides of the comet lies in, or near the plane of the ecliptic (the planetary orbit). This condition is satisfied if the inclination is small, but it may also be satisfied if i is large, provided that the orbital element ω is equal to, or nearly equal to 0° or 180°.

Already TISSERAND in his Traité de Mécanique Céleste (Tome IV, p. 206, 1896) has remarked that the short-periodic comets

[1] This remark seems to give the explanation of a fact that would otherwise seem difficult to understand: Why do all these comets of the Jupiter group obtain their aphelia in the neighbourhood of the planet's position at the time of capture, i. e. why have they there a motion at a right angle (approximately) to the radius vector from the sun? Could we not imagine that the motion of a comet could cross the orbit of the planet at a wide angle? Of course there are many cases, where a comet crosses the planet's path at a wide angle, but then there will normally be no capture, because the planet and the comet then move in the neighbourhood of each other for a very short time only. Normally we get a capture only if the comet for a relatively long time moves near the planet. In other words: capturing requires normally a motion at a right angle (approximately) to the radius vector from the sun, and then there will be an aphelion (or a perihelion, cf. p. 9).

then known showed a certain regularity with regard to the orbital element ω. We have thought that an investigation based on all the material now available would be of a certain interest. A study of our two tables now leads to the following result. In the column i we have typographically indicated small values, and similarly we have in the column ω indicated values of ω that do not deviate from 0° or 180° by more than a small angle, in both cases up

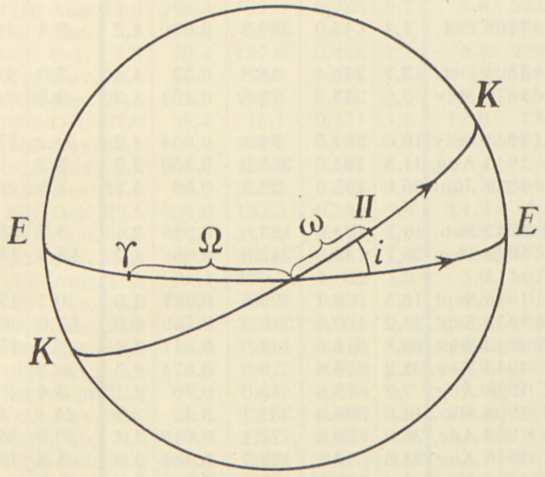

The Celestial Sphere from the Outside.

EE = the projection of the ecliptic on the celestial sphere. KK = the projection of a cometary orbit on the celestial sphere. γ = the vernal equinox. Ω = the longitude of the node. i = the inclination of the cometary orbit relative to the ecliptic. Π = the projection of the perihelion on the celestial sphere. ω = the arc from the ascending node to the perihelion.

to 16° by bold letters, up to 22° by italics. We now see how the conditions i small and ω close to 0° or 180°, separately or together, characterize the situation. We do not now consider the Saturn-, Uranus-, and Neptune-groups—we shall treat them on another occasion—we restrict ourselves to the Jupiter group, and we see that we have here a powerful statistical confirmation of the capture theory, not only with regard to the comets that have been observed in more than one apparition, *but also regarding the comets that have not been rediscovered after the apparition of discovery.*

Table I: Short-Periodic Comets Observed in more than one Apparition.

No.	Comet	T	π	Ω	e	q	i	ω	Q	P in years	No.
1	Encke	1937 Dec. 27.2	159°.6	334°.7	0.846	0.3	**12°.5**	**184°.9**	4.1	3.3	1
2	Grigg-Skjellerup[1] ..	1942 May 23.2	211.8	215.4	0.704	0.9	*17.6*	**356.4**	4.9	4.9	2
3	Tempel 2[1]	1946 July 2.3	310.3	119.4	0.54	1.4	**12.4**	**190.9**	4.7	5.3	3
4	Neujmin 2 ...	1927 Jan. 16.2	161.4	327.7	0.565	1.3	**10.6**	**193.7**	4.8	5.4	4
5	Brorson 1	1879 April 1.0	116.2	101.3	0.810	0.6	29.4	**14.9**	5.6	5.5	5
6	Tempel 3-L. Swift	1908 Oct. 1.4	44.0	290.3	0.62	1.2	**5.4**	113.7	5.2	5.7	6
7	de Vico-E. Swift	1894 Oct. 12.7	345.4	48.8	0.57	1.4	**3.0**	296.6	5.1	5.9	7
8	Tempel 1.....	1879 May 7.6	238.3	78.8	0.463	1.8	**9.8**	*159.5*	4.8	6.0	8
9	Pons-Winnecke[1] ..	1945 July 10.6	264.5	94.4	0.654	1.2	*21.7*	**170.1**	5.6	6.1	9
10	Kopff[1]	1945 Aug. 11.3	284.6	253.0	0.556	1.5	**7.2**	31.5	5.3	6.2	10
11	Forbes	1929 June 26.0	285.0	25.5	0.56	1.5	**4.6**	259.5	5.3	6.4	11
12	Schwassmann-Wachmann 2	1942 Feb. 14.3	124.0	126.0	0.385	2.1	**3.7**	**358.0**	4.8	6.5	12
13	Perrine 1.....	1922 Dec. 25.7	49.6	242.3	0.66	1.2	**15.7**	**167.3**	5.8	6.6	13
14	Giacobini-Zinner[1]	1946 Sept. 18.5	8.1	196.3	0.717	1.0	30.7	**171.9**	6.0	6.6	14
15	Biela	1852 Sept. 24.2	109.2	245.9	0.756	0.9	**12.6**	223.3	6.2	6.6	15
16	d'Arrest.....	1943 Sept. 23.8	318.0	143.6	0.611	1.4	*18.0*	**174.4**	5.7	6.7	16
17	Daniel	1943 Nov. 22.2	76.6	70.5	0.574	1.5	*19.9*	**6.1**	5.7	6.8	17
18	Finlay	1926 Aug. 7.2	5.9	45.3	0.70	1.1	**3.4**	320.6	6.2	6.9	18
19	Holmes	1906 Mar. 14.6	346.0	331.7	0.42	2.1	*20.8*	**14.3**	5.1	6.9	19
20	Borelly	1932 Aug. 26.3	69.6	77.1	0.617	1.4	30.5	**352.5**	5.8	6.9	20
21	Brooks 2[1]	1946 Aug. 25.8	13.3	177.7	0.484	1.9	**5.5**	**195.6**	5.4	7.0	21
22	Reinmuth	1935 May 1.4	133.8	125.0	0.504	1.9	**8.1**	8.8	5.7	7.2	22
23	Faye	1940 April 23.0	46.7	206.4	0.566	1.6	**10.6**	*200.3*	5.9	7.4	23
24	Whipple	1941 Jan. 13.3	19.0	188.8	0.349	2.5	**10.2**	**190.2**	5.2	7.5	24
25	Oterma 3[2]....	1942 Sept. 13.7	153.9	154.9	0.143	3.4	**4.0**	**359.0**	4.6	8.0	25
26	Schaumasse ..	1943 Nov. 4.5	137.7	86.7	0.705	1.2	**12.0**	51.0	6.8	8.2	26
27	Wolf 1.....	1942 June 7.6	5.3	204.3	0.405	2.4	27.3	*161.0*	5.8	8.3	27
28	Comas Solá ..	1944 April 11.6	104.6	65.7	0.576	1.8	**13.7**	38.9	6.6	8.5	28
29	Gale	1938 June 18.5	276.4	67.3	0.761	1.2	**11.7**	209.1	8.7	11.0	29
30	Tuttle 1	1939 Nov. 10.1	116.8	269.8	0.821	1.0	54.7	207.0	10.3	13.6	30
31	Schwassmann-Wachmann 1	1941 Sept. 1.2	323.4	323.0	0.142	**5.5**[3]	**9.4**	**0.4**	7.3	16.3	31
32	Neujmin 1 ...	1931 May 7.4	334.3	347.3	0.775	1.5	**15.2**	347.0	12.0	17.7	32
33	Pons-Forbes ..	1928 Nov. 5.0	86.0	250.1	0.93	0.7	28.9	**195.9**	18.0	27.9	33
34	Stephan-Oterma	1942 Dec. 18.9	76.7	78.6	0.858	1.6	*17.9*	**358.1**	17.9	37.8	34
35	Westphal.....	1913 Nov. 26.8	43.9	346.8	0.92	1.3	40.9	57.1	30.0	61.7	35
36	Brorson 2-Metcalf	1919 Oct. 17.4	80.3	310.8	0.97	0.5	*19.2*	129.5	33.2	69.1	36
37	Pons-Brooks ..	1884 Jan. 26.2	93.3	254.1	0.955	0.8	74.0	*199.2*	33.7	71.6	37
38	Olbers	1884 Oct. 9.0	149.8	84.5	0.931	1.2	44.6	65.3	33.6	72.7	38
39	Halley	1910 April 20.2	169.0	57.3	0.97	0.6	*162.2*	111.7	35.3	76.0	39
40	Herschel-Rigollet.....	1939 Aug. 9.5	24.4	355.1	0.974	0.7	64.2	29.3	57.2	150.7	40

[1] The list of short-periodic comets observed in more than one apparition was compiled in the autumn of 1944 for the "Festskrift" for Prof. N. E. Nörlund. Six of the comets in this list have been rediscovered at a later date. References for Comet Grigg-Skjellerup: U. A. I. Circ. 1080; for Comet Tempel 2: H. A. C. 745 and U. A. I. Circ. 1040; for Comet Pons-Winnecke: U. A. I. Circ. 998 and 1005; for Comet Kopff: U. A. I. Circ. 1019; for Comet Giacobini-Zinner: U. A. I. 755; for Comet Brooks 2: U. A. I. Circ. 1057.

[2] Comet Oterma 3 has been moved from Table II to Table I.

[3] Cf. p. 10.

Table II: Short-Periodic Comets Observed in one Apparition only (Aphelion distance < 35,0).

No.	Comet	T	π	Ω	e	q	i	ω	Q	P in years	No.
1	1766 II	1766 April 28.2	252°.0	71°.6	0.834	0.4	7°.8	180°.4	4.5	3.9	1
2	1819 IV.....	1819 Nov. 20.8	67.5	77.4	0.699	0.9	**9.1**	**350.1**	5.0	5.1	2
3	1678[1]	1678 Aug. 18.8	322.8	163.3	0.627	1.1	**2.9**	*159.5*	4.9	5.2	3
4	1930 VI.....	1930 June 14.2	269.1	76.8	0.666	1.0	*17.3*	**192.3**	5.0	5.3	4
5	1884 II	1884 Aug. 17.0	306.1	5.1	0.584	1.3	**5.5**	301.0	4.9	5.4	5
6	1743 I	1743 Jan. 8.7	93.3	86.9	0.721	0.9	**1.9**	**6.4**	5.3	5.4	6
7	1941 e	1941 July 21.2	298.8	229.6	0.579	1.3	**3.2**	69.2	4.9	5.4	7
8	1770 I	1770 Aug. 14.0	356.3	132.0	0.786	0.7	**1.6**	224.3	5.6	5.5	8
9	1886 IV.....	1886 June 7.2	230.3	53.5	0.579	1.3	**12.7**	**176.8**	5.0	5.6	9
10	1940 a[2]	1939 Oct. 3.5	70.4	137.6	0.448	1.7	**4.8**	292.8	5.1	5.6	10
11	1783.....	1783 Nov. 20.4	50.3	55.7	0.552	1.5	45.1	**354.6**	5.1	5.9	11
12	Giacobini[3]....	1928 Mar. 26.8	182.0	196.8	0.71	1.0	**1.4**	**345.2**	5.9	6.4	12
13	1890 VII.....	1890 Oct. 27.0	58.4	45.1	0.471	1.8	**12.8**	**13.3**	5.1	6.4	13
14	1900 III	1900 Nov. 28.5	7.8	196.7	0.733	0.9	29.8	**171.1**	6.1	6.5	14
15	1858 III	1858 May 3.5	200.8	175.1	0.674	1.1	*19.5*	25.7	5.9	6.6	15
16	1892 V.....	1892 Dec. 11.0	16.3	206.4	0.594	1.4	31.3	**169.9**	5.6	6.6	16
17	1896 V.....	1896 Oct. 28.5	334.0	193.5	0.589	1.5	**11.4**	140.5	5.6	6.6	17
18	1918 III	1918 Sept. 30.7	37.4	117.9	0.468	1.9	**5.6**	259.5	5.2	6.7	18
19	1916 I	1928 Oct. 22.4	103.8	108.3	0.487	1.8	*20.7*	**355.5**	5.3	6.8	19
20	1895 II	1895 Aug. 21.3	338.1	170.3	0.652	1.3	**3.0**	**167.8**	6.2	7.2	20
21	1894 I	1894 Feb. 9.9	130.6	84.4	0.697	1.1	**5.5**	46.2	6.4	7.4	21
22	1925 I	1925 Jan. 24.0	84.6	260.5	0.374	2.4	23.1	**184.1**	5.3	7.5	22
23	1906 VI.....	1906 Oct. 10.3	34.6	194.6	0.584	1.6	**14.6**	*200.0*	6.2	7.8	23
24	1936 IV.....	1936 Oct. 3.4	1.5	164.2	0.650	1.5	**13.3**	*197.3*	6.9	8.5	24
25	1881 V.....	1881 Sept. 13.8	18.4	65.9	0.828	0.7	**6.9**	312.5	7.7	8.7	25
26	1889 VI.....	1889 Nov. 30.1	40.2	330.4	0.685	1.4	**10.3**	69.8	7.2	8.9	26
27	1939 IV.....	1939 Feb. 9.0	179.9	135.5	0.624	1.8	**11.1**	44.4	7.6	10.1	27
28	1929 III	1929 June 28.2	298.7	158.2	0.585	2.0	**3.7**	140.5	7.8	10.9	28
29	1846 VI.....	1846 June 1.6	240.0	260.4	0.729	1.5	30.7	*339.6*	9.7	13.4	29
30	1944 c	1944 June 17.5	279.4	22.3	0.781	1.3	*18.6*	257.1	10.4	14.0	30
31	1585.....	1585 Oct. 8.5	9.9	38.0	0.826	1.1	**5.4**	331.9	11.4	15.5	31
32	1916 III	1916 June 14	319	224	0.93	0.5	103	95	12.4	16.4	32
33	1866 I	1866 Jan. 11.6	42.4	231.4	0.905	1.0	*162.7*	**171.0**	19.7	33.2	33
34	1863 V.....	1863 Dec. 27.1	59.3	305.0	0.946	0.8	63.6	114.3	27.8	53.2	34
35	1873 VII.....	1873 Dec. 2.5	85.9	250.0	0.949	0.7	29.2	**195.9**	28.1	54.8	35
36	1931 III	1931 June 10.8	150.4	191.6	0.935	1.0	42.5	318.8	30.6	62.9	36
37	1827 II	1827 Jan. 7.7	337.0	317.7	0.949	0.8	136.4	*19.3*	31.1	63.8	37
38	1883 II	1883 Dec. 25.6	41.9	264.3	0.981	0.3	114.7	137.6	31.9	64.6	38

[1] Possibly identical with No.7 in Table I (cf. LEVERRIER, Astr.Nachrichten 26, p.382-384).
[2] This comet was overlooked in the list of 1944.
[3] Very uncertain elements.

We have assumed—as is indicated by the statistics—that the aphelion of the captured comet is, within certain limits, situated close to the orbit of the planet (cf. the footnote on p. 6). Why the aphelion? Is it not possible that the result of the capture were that the perihelion of the comet came to be situated close to the planetary orbit? Capture results because the comet at a

certain time moves very close to the planet. When the planet has loosened its grip, the comet quickly glides into a practically unperturbed two-body motion relative to the sun.

If the comet through the capture has obtained a motion that makes it approach the sun, the aphelion of the new orbit will be in the neighbourhood of the point where the planet was situated in its orbit during the capture. Apparently this is the normal, and until recently it was the only case represented in our tables. The aphelion of the new cometary orbit is close to the planetary orbit, and its perihelion is situated on the other side of the sun. If, however, the comet through the capture has obtained an orbit in which it recedes from the sun, the perihelion of the new cometary orbit will be close to the planetary orbit, and the aphelion will be located on the opposite side of the sun. *A priori* this case would appear to be as probable as the other. A case of perihelion in the neighbourhood of the orbit of Jupiter now actually exists in comet Schwassmann-Wachmann 1 (No. 31 in Table I). The explanation of the fact that this case appears as an exception in the existing material instead of occurring quite often is probably the simple one that a comet having its perihelion close to the orbit of Jupiter during its entire motion will stay at a great distance from the earth, and therefore will be visible from the earth only in the case of abnormally great brightness. We must imagine that captured comets exist with all values of q from 0 up to the radius of the orbit of Jupiter (approximately) and such with values of Q from the value of the radius of the orbit of Jupiter (approximately) up to very high values, but the majority of them will never be discovered.

The problem of capture of comets contains many other questions of interest. Some of them we shall treat elsewhere.

Bibliography.

G. Fayet, Criterium de Tisserand pour les comètes à courte période (Bull. Astr. 1911).

H. N. Russell, On the Origin of Periodic Comets (The Astron. Journal 1920).

S. Oppenheim, Kometen (Enzyklopädie der Matematischen Wissenschaften, 1923).

A. Kopff, Die kurzperiodischen Kometen (Handbuch der Astrophysik Bd. IV, 1929).

Indleveret til Selskabet den 29. Marts 1947.
Færdig fra Trykkeriet den 15. December 1947.

DET KGL. DANSKE VIDENSKABERNES SELSKAB
MATEMATISK-FYSISKE MEDDELELSER, BIND XXIV, NR. 6

REACTIONS OF THE FURAN NUCLEUS; 2.5-DIALKOXY-2.5-DIHYDROFURANS AND 2.5-DIACETOXY-2.5-DIHYDROFURAN

BY

N. CLAUSON-KAAS

KØBENHAVN
I KOMMISSION HOS EJNAR MUNKSGAARD
1947

Printed in Denmark.
Bianco Lunos Bogtrykkeri

I. Introduction.

It has recently[1] been proved that MARQUIS' nitroacetin,[2] the compound prepared by nitration of furan with nitric acid in acetic anhydride, is a 1.4-addition product of furan. The radicals added are the nitro and the acetic acid group, presumably formed by cleavage of a mixed anhydride of nitric and acetic acid.

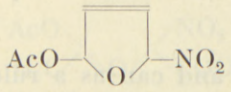

Nitroacetin.

The theory of 1.4-addition has proved extremely useful to explain the structure of compounds obtained from oxidation of furans. Already before THIELE's exposition (1899), the hypothesis was employed by HILL[3] in his classic investigations in the furan series. Later it has been repeatedly discussed, especially by GILMAN, JOHNSON, LUTZ, WRIGHT, MILAS, and their co-workers. However, other reaction mechanisms are often suggested and among chemists working on this subject there still seems to be some disagreement as to the reactive properties of furan and its derivatives.

In the author's opinion, our present knowledge of the chemistry of the furans warrants the view that the initial reaction between the furan nucleus and such oxidizing reagents as usually add to aliphatic double bonds, is always one of two. First, the reagent may add in 1.4-position to the double bonds; this is by far the commonest way of action, and no other diene system exhibits so marked a tendency towards 1.4-addition as the furan nucleus. Secondly, in some cases a β-substituted furan may be formed by what is usually called direct substitution. It shall be stressed that it is apparently an inherent property of the furan nucleus to react with oxidizing reagents

exclusively as described. So far no experimental evidence which demonstrates a 1.2-addition, a direct α-substitution, or any alternative mode of action has been given.

In Part II the different aspects of 1.4-addition are discussed. β-substitution will not be considered in this communication.

II. 1.4-Addition.

1.4-addition leads to the formation of a 2.5-dihydrofuran (I). The stability of such compounds depends largely upon the nature

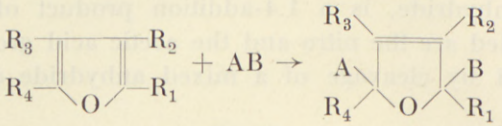

I

of the radicals added, and can as a rule be deduced from the structural formula. In general the dihydrofurans in question are very reactive at ordinary temperatures and only a small number have actually been isolated in a pure state.[2, 4-6] They decompose into smaller molecules or react with the reagent or the solvent. Many different ways of further reaction are possible and by selecting the proper experimental conditions, simple furans may be used for the synthesis of several compounds which are otherwise difficult of accession or not accessible at all. To exemplify this, a number of typical reactions will be cited below.

(a) 1.4-elimination; formation of an α-substitution product. KLOPP and WRIGHT[7] have shown that furan and bromocyanogen yield a mixture of 2-furonitrile and 2-bromofuran. It is evident, as pointed out by these authors, that 1.4-elimination of hydrogen bromide and hydrogen cyanide from the preliminarily formed 1.4-addition product has occurred.

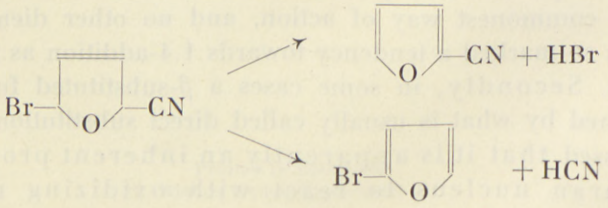

Often only one of the two possible ways of 1.4-elimination takes place; so the nitroacetates, formed by nitration of furans with MARQUIS' reagent,[2] only yield acetic acid and an α-nitrofuran when heated alone or with pyridine. No α-acetoxyfurans are obtained.

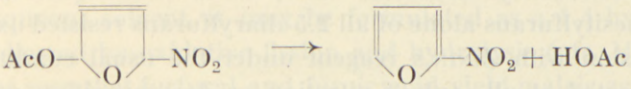

In some cases replaceable groups, such as carboxylic or sulphonic acid groups, are split off before 1.4-elimination (see FREURE and JOHNSON[5]). E. g. 2-methyl-5-furoic acid among other products yields 2-methyl-5-nitrofuran by nitration in acetic anhydride (RINKES[8]).

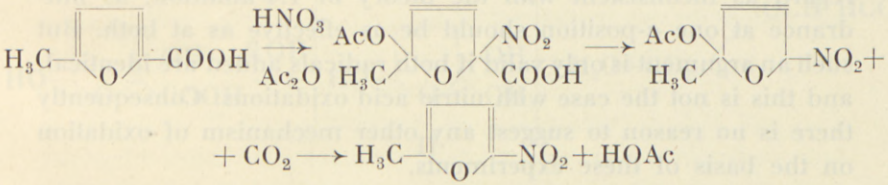

(b) Formation of unsaturated 1.4-dicarbonyl compounds. When the addition reactions are performed in acetic acid or in an aqueous solvent, unsaturated 1.4-dicarbonyl compounds may come into existence. In order to obtain good yields, the reaction must usually proceed at low temperature. Already ZININ[9] prepared 1.2.3.4-tetraphenyl-2-butene-1.4-dione by oxidation of tetraphenylfuran with nitric acid in glacial acetic acid. The method has later been employed by LUTZ and coworkers in numerous oxidation experiments on 2.5-diarylfurans. The reaction may be formulated as a 1.4-addition of the nitro and the acetic acid group, followed by hydrolysis or acetolysis to the dicarbonyl compound (see LUTZ et. al.[10, 11]).

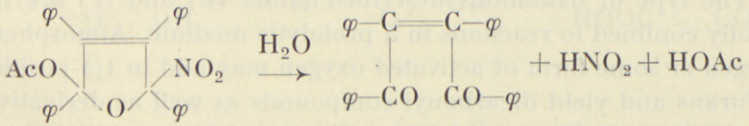

As in most 1.4-oxidations in a protolytic medium, where the addition product is not isolated, nothing is known with certainty

about the nature of the radicals actually added or about the way in which the dihydrofurans are transformed into carbonyl compounds, but it is evident that the reaction proceeds through a 1.4-addition.

In consistency with this view, LUTZ found (see 11) that 2.5-dimesitylfurans alone of all 2.5-diarylfurans resisted oxydative ring fission with ZININ's reagent under the usual conditions. If they reacted at all, only β-nitration or decomposition occurred. The failure to furnish unsaturated 1.4-diketones is readily understandable, if one assumes that the mesityl groups offer hindrance to addition at the α-carbons.

Later LUTZ and BOYER[12] found that α-mesitylfurans with only one mesityl group are easily oxidized to 1.4-diketones. This they regard as inconsistent with the theory of 1.4-addition, as hindrance at one α-position should be as effective as at both. But such an argument is only valid if both radicals added are identical, and this is not the case with nitric acid oxidations. Consequently there is no reason to suggest any other mechanism of oxidation on the basis of these experiments.

Furans with free α-positions may under carefully controlled conditions give $\alpha.\beta$-unsaturated aldehydes. Thus furan itself, when hydroxylated with hydrogen peroxide in aqueous methanol in the presence of osmiumtetroxide, yields malealdehyde.[13]

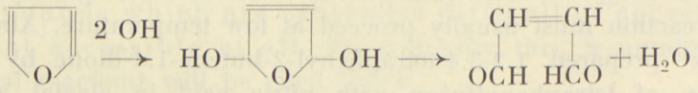

In such reactions the aldehyde groups may be oxidized further by the reagent to carboxylic acid groups; but some of the unsaturated aldehydes are so unstable, that polymerization or oxidation of other parts of the molecule occurs before the comparatively stable aldehyde groups are attacked.

The type of oxidations described under (b) and (c) are not wholly confined to reactions in a protolytic medium. Atmospheric oxygen or some form of activated oxygen may add in 1.4-position to furans and yield dicarbonyl compounds as well as derivatives of maleic acid. MILAS and WALSH[14] were able to oxidize furan, furfural, furfuryl alcohol, and furoic acid in vapour phase with oxygen and a catalyst to maleic acid; and SCHENK[15] oxidized

2.5-dimethylfuran with atmospheric oxygen to 1.2-diacetylethylene.

(c) Oxidative elimination of α-substituents. This is a very common reaction, which has often been observed, e. g. when furfural or furoic acid are oxidized. If oxidation takes place in an aqueous solvent, it may be formulated as a 1.4-hydroxylation followed by oxidative fission and hydrolysis (cfr. MILAS[16]). It will be seen that furfural and furoic acid yield maleic acid alde-

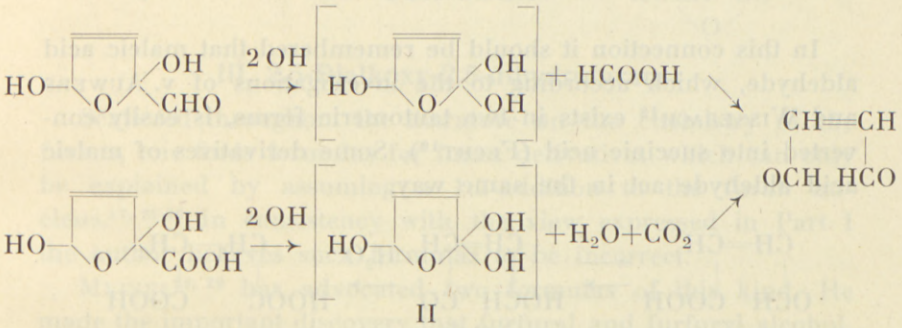

II

hyde together with formic acid and carbondioxide, respectively. The maleic acid aldehyde, which has been isolated repeatedly, is easily oxidized to maleic acid, and the numerous preparations of maleic and fumaric acid from the common furans belong to this category of reaction.

In one case, viz. when furfural was oxidized in water with CARO's acid at about 20—35° C. (CROSS, BEVAN, BRIGGS[17]), a considerable amount of succinic acid was obtained. This may be explained by assuming a 1.4-elimination of water from the intermediate compound II.

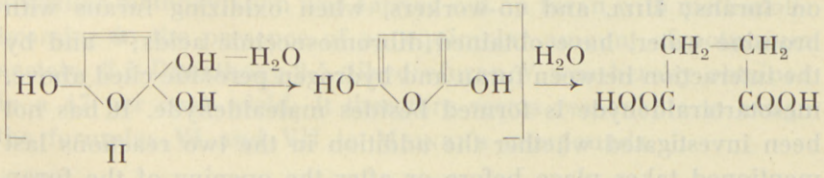

II

Another compound isolated from the reaction mixture was the barium salt of a dicarboxylic acid $C_5H_6O_5$. This acid is probably α-ketoglutaric acid formed by a similar process.

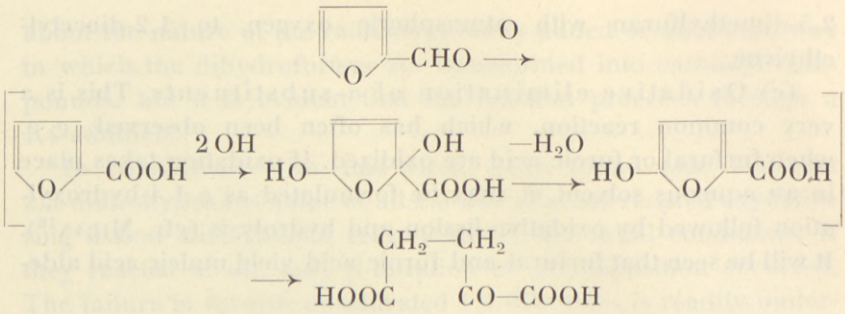

In this connection it should be remembered that maleic acid aldehyde, which according to the investigations of v. AUWERS and WISSEBACH[18] exists in two tautomeric forms, is easily converted into succinic acid (FECHT[19]). Some derivatives of maleic acid aldehyde act in the same way.

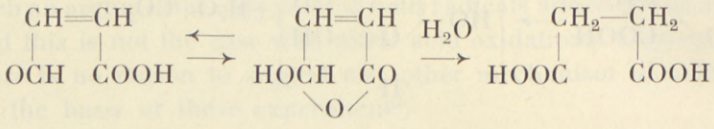

Possibly the above formulations involving a 1.4-elimination of water give no correct picture of what actually happens during the formation of the saturated acids, but all three reactions undoubtedly express the same tendency of similar dihydrofurans to rearrange in a similar manner.

(d) Reactions with the 3.4-double bond. In advance one would expect that reactions between the reagent and the 3.4-double bond of the dihydrofuran would frequently take place. Such reactions have also been observed. Tetrahalotetrahydrofurans may be isolated as the result of the action of halogens on furans; HILL and co-workers, when oxidizing furans with bromine water, have obtained dibromosuccinic acids;[20] and by the interaction between furan and hydrogen peroxide cited above, mesotartaraldehyde is formed besides malealdehyde. It has not been investigated whether the addition in the two reactions last mentioned takes place before or after the opening of the furan ring.

However, reactions of this type are rare because the double bond in the dihydrofurans or their products of hydrolysis is

rather inert. As by other double bonds, which are inert towards addition reagents, substitution of the adjacent hydrogen atoms may take place instead of addition. A typical example is the well-known oxidation of furfural or furoic acid to mucobromic or mucochloric acid with warm bromine, respectively chlorine water.[21]

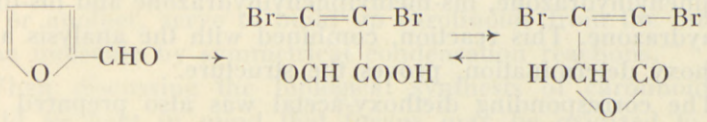

III. 2.5-Dialkoxy-2.5-dihydrofurans.

Scattered throughout the literature on the chemistry of the furans, one finds formulas for furan derivatives which can only be explained by assuming a 1.2-addition to the furan nucleus.[17, 22-28] In consistency with the view expressed in Part I the author believes such formulas to be incorrect.

MEINEL[28, 29] has advocated two formulas of this kind. He made the important discovery that furfural and furfuryl alcohol, when treated in methanolic solution with bromine or with compounds containing active bromine, e. g. N-bromophthalimide, add two methoxy groups. The aldehyde group of furfural is at the same time acetalized. MEINEL assigned the formulas III and IV to the addition products.

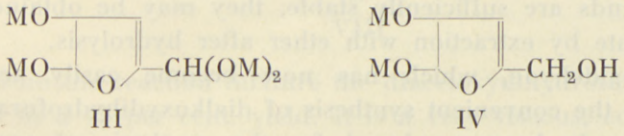

III IV

The experiments of MEINEL have not been repeated here, but a similar methoxylation was carried out on furan with methanolic bromine in the presence of an equimolar amount of potassium acetate. 2.5-Dimethoxy-2.5-dihydrofuran V was hereby obtained in a 47 per cent. yield. It therefore seems reasonable to assign the formulas VI and VII to MEINEL's compounds.

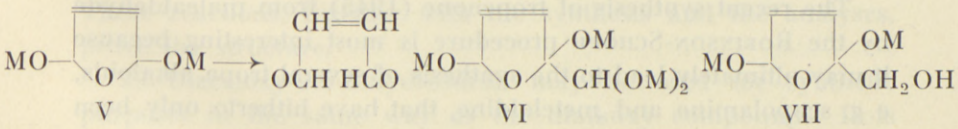

V VI VII

Dimethoxydihydrofuran is a cyclic acetal of malealdehyde. It has an odour similar to that of malealdehyde tetraethylacetal, prepared earlier by WOHL and MYLO,[30] and exhibits similar properties. It may be distilled in vacuum and is stable at ordinary temperature. It is rather soluble in water. In acid solution it is rapidly hydrolized to malealdehyde, which was identified as bis-phenylhydrazone, bis-methylphenylhydrazone and bis-diphenylhydrazone. This reaction, combined with the analysis and a methoxy determination, proves the structure.

The corresponding diethoxy-acetal was also prepared from furan and a solution of bromine in ethanol (yield 56 per cent.); the structure was proved in the same way as described for the dimethyl-acetal. The higher yield of the ethyl derivative is probably mainly due to its lesser solubility in water.

It is evident that the alkoxylation method is of general applicability in the furan series. The method makes it possible to synthesize stable acetals of labile unsaturated 1.4-dicarbonyl compounds, many of which, as pointed out in Part II, are of importance for synthetic purposes. It will as a rule be most convenient to prepare the ethyl acetals, which are easier to extract with ether than the methyl derivatives. In water or an aqueous solvent the acetals will react in the way of free carbonyl compounds when traces of acids are present. If the carbonyl compounds are sufficiently stable, they may be obtained in a pure state by extraction with ether after hydrolysis.

Malealdehyde, which has now become easily accessible through the convenient synthesis of dialkoxydihydrofurans, has so far only been employed for the synthesis of pyridazine (MARQUIS,[2] WOHL and BERNREUTHER[31]), of succinaldehyde and some of its derivatives (KEIMATSU and YOKOTA,[32] WOHL and BERNREUTHER[31]) and of tropenone (PREOBRAZHENSKIJ, RUBTSOV, DANKOVA, and PAVLOV[33]). However, this reactive dialdehyde will surely find a wider range of application when sufficient quantities are at hand.

The recent synthesis of tropenone (1945) from malealdehyde by the ROBINSON-SCHÖPF procedure is most interesting because it may ultimately lead to the synthesis of several tropa alkaloids, e. g. scopolamine and meteloidine, that have hitherto only been

isolated from natural sources. The Russian authors seem to be working along this line. Unfortunately only an abstract of their paper has been available.

If malealdehyde yields tropenone in the ROBINSON-SCHÖPF procedure, it should also be capable of participating in condensation reactions of similar types. It may therefore, in one way or another, serve to build up carotinoids from the middle of the molecule by symmetrical condensation reactions.

When discussing the biological synthesis of carotinoids it should be kept in mind that furans may be oxidized to unsaturated 1.4-dicarbonyl compounds under biological conditions, e. g. with atmospheric oxygen (CIAMICIAN and SILBER,[34] MILAS and MCALEVY,[35] SCHENK,[15] SCHERING A.-G.,[36] and DUNLOP, STOUT, and SWADESH[37]).

IV. 2.5-Diacetoxy-2.5-dihydrofuran.

In view of the stability of the dialkoxydihydrofurans it was highly probable that 2.5-diacetoxy-2.5-dihydrofuran (VIII) also would be a stable derivative of malealdehyde. In order to prepare this compound furan was treated with lead tetraacetate in acetic

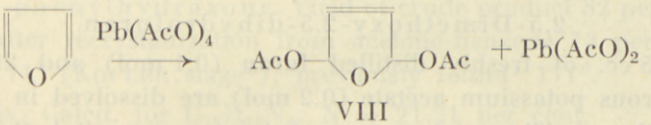

VIII

acid. From the reaction mixture the diacetoxydihydrofuran was isolated in a 45 per cent. yield. It is a very viscous, colourless oil boiling at about 130° C. in vacuum. The analysis and a molecular weight determination in benzene gave the correct values. Although almost insoluble in water, this mixed acetal-acetate is very easily hydrolyzed. The malealdehyde and the acetic acid formed by hydrolysis were identified as bis-phenylhydrazone and S-benzyl thiuronium salt, respectively. The acetic acid was further determined quantitatively by titration. These reactions, together with the synthesis and the analyses, prove the structure.

2.5-Diacetoxy-2.5-dihydrofuran may be used for synthetic purposes in the same way as the dialkoxy compounds. It is

possible that it will in some cases prove superior to the latter because it is easier to saponify in alkaline solution.

V. Summary.

The view is advanced, that reactions between the furan nucleus and what may be termed oxidizing double bond reagents only can be initiated by a β-substitution or a 1.4-addition. This mode of action seems to be an inherent property of the furan nucleus. The latter reaction is by far the most common and its different aspects are discussed.

In consistency with the conception of 1.4-addition, cyclic acetals of malealdehyde are obtained by alkoxylation of furan. The general applicability of this method for the synthesis of acetals of unsaturated 1.4-dicarbonyl compounds is suggested.

Another derivative of malealdehyde, viz. 2.5-diacetoxy-2.5-dihydrofuran, was obtained in a similar way by 1.4-addition of two acetoxy groups to furan. The acetoxylation was performed with lead tetraacetate.

VI. Experimental Part.

2.5-Dimethoxy-2.5-dihydrofuran.

7.25 cc. of freshly distilled furan (0.1 mol) and 20 g. of anhydrous potassium acetate (0.2 mol) are dissolved in 130 cc. of methanol. The mixture is cooled in an ice-salt bath and a solution of 5 cc. of bromine (0.1 mol) in 100 cc. of methanol is added under efficient stirring. The temperature must be kept below —7° C. After all the bromine has been added (20—30 min.) stirring is continued for 5 minutes. Then the reaction mixture is poured into 300 cc. of a cooled saturated solution of calcium chloride. The acetal is extracted with 400 cc. of ether and the etheral layer shaken with 50 cc. of a saturated solution of potassium carbonate and dried over 20 + 50 g. of solid potassium carbonate. The ether is removed on the steam bath through an ordinary VIGREUX column and the residue distilled in vacuum. Distillation begins at 48°/8 mm. and the fraction boiling at 48—53° was collected. A small amount (1.3 g.) of a higher boiling residue remained in the flask. The distillate consisted of pure

dimethoxydihydrofuran and boiled sharply at 47°/8 mm. when redistilled.

Yield 6.1 g. = 47 per cent.

Analysis: Calcd. for $C_6H_{10}O_3$: C = 55.36 per cent., H = 7.76 per cent., CH_3O = 47.7 per cent.
found : C = 55.56 per cent., H = 7.73 per cent., CH_3O = 45.7 per cent.

The acetal is a colourless, stable liquid. It smells like other lower acetals and exhibits similar chemical properties.

Bis-hydrazones of malealdehyde.

About 150 mg. of the acetal were boiled with 3 cc. of centinormal sulphuric acid for 45 seconds. After cooling, a solution of the corresponding hydrazine in diluted acetic acid (10 cc.) was added. The hydrazones precipitated immediately. The mixture was allowed to stand for some hours, then the precipitate was filtered off, washed thoroughly with water and dried in vacuum over calcium chloride. The crude products were recrystallized once and then proved to be identical with authentic specimens prepared from malealdehyde tetraethylacetal.[1]

Bis-phenylhydrazone. Yield of crude product 82 per cent. Yield after recrystallization from acetone-benzene 73 per cent. M. p. 171° (KOFLER stage*); previously found[1] 171°.

Analysis: Calcd. for $C_{16}H_{16}N_4$: N = 21.21 per cent.
found : N = 21.13 per cent.

Bis-methylphenylhydrazone. Yield of crude product 98 per cent. Yield after recrystallization from acetone-benzene 67 per cent. M. p. 176° (KOFLER); previously found[1] 176°.

Analysis: Calcd. for $C_{18}H_{20}N_4$: N = 19.18 per cent.
found : N = 19.14 per cent.

Bis-diphenylhydrazone. Yield of crude product 82 per cent. Yield after recrystallization from acetone-methanol 60 per cent. M. p. 180° (KOFLER); previously found[1] 177°.

Analysis: Calcd. for $C_{28}H_{24}N_4$: N = 13.46 per cent.
found : N = 13.68 per cent.

* All melting points are corrected.

2.5-Diethoxy-2.5-dihydrofuran.

This acetal was prepared in the same way as the methyl derivative, using ethanol instead of methanol. The etheral extract of the acetal contained a comparatively large amount of ethanol, which was removed by distillation through a small WIDMER column at ordinary pressure. An equal volume of ether was added to the residue and a crystalline precipitate filtered off. The acetal, when distilled in vacuum, boiled at 65—70°/10 mm. The first drops of the distillate had a strong yellow colour, due to some free malealdehyde. This could be removed by heating the distillate for some time on the steam bath. The malealdehyde was hereby destroyed and a colourless product obtained on redistillation.

Analysis: Calcd. for $C_8H_{14}O_3$: C = 60.76 per cent., H = 8.89 per cent., C_2H_5O = 56.9 per cent.
found : C = 60.30 per cent., H = 8.66 per cent., C_2H_5O = 54.9 per cent.

The acetal was hydrolyzed as described above and the bisphenylhydrazone of malealdehyde prepared. Yield of crude product 78 per cent. Yield after recrystallization 55 per cent. M. p. 167° (KOFLER).

Analysis: Calcd. for $C_{16}H_{16}N_4$: N = 21.21 per cent.
found : N = 21.27 per cent.

2.5-Diacetoxy-2.5-dihydrofuran.

Preparation. 3.4 g. of freshly distilled furan (0.05 mol), 22.2 g. of lead tetraacetate (0.05 mol) and 100 cc. of perfectly dry glacial acetic acid were placed in a 250 cc. round-bottomed flask fitted with a reflux condenser. The flask is heated over a flame under frequent shaking until the temperature of the mixture is about 100°. By this time all lead tetraacetate has dissolved. The temperature is kept at 90—100° for some minutes; then the flask is cooled with water. If crystals of lead tetraacetate appear on cooling, the reaction is not yet complete and heating must be repeated.

The acetic acid is evaporated under reduced pressure in a water bath. 100 cc. of water containing cracked ice and 200 cc. of ether is added, the mixture shaken vigorously and the aqueous

layer separated. The etheral layer is dried with sodium sulphate and calcium chloride and the ether removed at ordinary pressure. The residue is distilled in vacuum. After a fore-run af acetic acid, a small amount of free malealdehyde distils at 50—60°. Distillation of the diacetoxydihydrofuran begins at 129°/10 mm. The first drops of the distillate are yellow, the main portion is colourless. Distillation is interrupted when the distillate begins to turn yellow again due to destruction of the residue. The temperature is now about 135°. Yield 4.2 g. = 45 per cent. Redistillation yields 3.9 g. of a slightly yellow product boiling at 128—129°/10 mm. Very viscous oil, almost insoluble in water.

Analysis: Calcd. for $C_8H_{10}O_5$: C = 51.60 per cent., H = 5.42 per cent.
found : C = 52.01 per cent., H = 5.43 per cent.

Molecular weight determination. The freezing point depression of a benzene solution was measured. Calcd. M = 186, found M = 188.

Hydrolysis; identification of malealdehyde. Hydrolysis and preparation of the bis-phenylhydrazone of malealdehyde was performed as described for the dialkoxy compounds. Yield of crude product 68 per cent. Yield after recrystallization 58 per cent. M. p. 168—169° (KOFLER).

Analysis: Calcd. for $C_{16}H_{16}N_4$: N = 21.21 per cent.
found : N = 21.33 per cent.

Hydrolysis; titration of acetic acid. About 200 mg. were heated with 5 cc. of 0.02 normal hydrochloric acid to 100° for some minutes and the acetic acid formed by hydrolysis titrated with decinormal barium hydroxide. Found 98.5 per cent. of the theoretical amount.

Hydrolysis; identification of acetic acid. 186 mg. were boiled for one minute with 2 cc. of decinormal sulphuric acid. 3.1 cc. of normal sodium hydroxide were added and boiling continued for some minutes. Then 0.5 cc. of normal sulphuric acid and a solution of 420 mg. of S-benzyl thiuronium chloride

in 2 cc. of water was added and the mixture left in an ice bath for 10 minutes. The precipitate formed was filtered off, washed with 5 cc. of alcohol and dried in vacuum over calcium chloride. Yield 327 mg. = 72 per cent. Yield after recrystallization from 2 cc. of alcohol 180 mg. = 40 per cent. M. p. 132—133° (in a tube). Mixed melting point with an authentic specimen of S-benzyl thiuronium acetate 133°. (DONLEAVY[38] 134°; VEIBEL and LILLELUND[39] 135—136°).

Analysis: Calcd. for $C_{10}H_{14}O_2N_2S$: N = 12.39 per cent.
found : N = 12.32 per cent.

VII. Acknowledgements.

The analyses have been performed in a most careful way by my colleague Mr. O. ROSENLUND-HANSEN.

During the investigation I have received financial aid from the TUBORG FOUNDATION, Copenhagen.

I am grateful to the director of the Chemical Laboratory of the University of Copenhagen, Prof. Dr. A. LANGSETH, and to my former teacher Dr. K. A. JENSEN for their kind interest in my work. Very much was done to secure me the best possible conditions to carry out these experiments.

Copenhagen, February 1947.
Universitetets kemiske Laboratorium.

VIII. References.

(1) Clauson-Kaas a. J. Fakstorp, Acta chem. Scand. **1**, 210 (1947).
(2) R. Marquis, Ann. Chimie (8) **4**, 196 (1905).
(3) H. B. Hill a. R. W. Cornelison, Amer. Chem. J. **16**, 188 (1894).
(4) H. Gilman a. G. F. Wright, J. Amer. Chem. Soc. **52**, 2550 (1930).
(5) B. T. Freure a. J. R. Johnson, J. Amer. Chem. Soc. **53**, 1142 (1931).
(6) Probably the addition products isolated by H. B. Hill a. G. T. Hartshorn, Ber. dtsch. chem. Ges. **18**, 448 (1885); C. Moureu, Dufraisse a. J. R. Johnson, Ann. Chimie (10) **7**, 8 (1927); H. Gilman a. G. F. Wright, J. Amer. Chem. Soc. **52**, 3349 (1930); Scheibler, Jeschke a. Beiser (loc. cit. 26) and Rinkes (loc. cit. 8) are also 2.5-dihydrofurans, although this has not been claimed by these authors.
(7) A. H. Klopp a. G. F. Wright, J. Org. Chemistry **4**, 142 (1939).
(8) I. J. Rinkes, Recueil Trav. chim. Pays-Bas **49**, 1118 (1930).
(9) N. Zinin, J. prakt. Chem. (1) **101**, 160 (1867).
(10) R. E. Lutz a. F. N. Wilder, J. Amer. Chem. Soc. **56**, 978 (1934).
(11) R. E. Lutz a. C. J. Kibler, J. Amer. Chem. Soc. **62**, 1520 (1940).
(12) R. E. Lutz a. W. P. Boyer, J. Amer. Chem. Soc. **63**, 3189 (1941).
(13) N. Clauson-Kaas a. J. Fakstorp, Acta chem. Scand. **1**, 216 (1947).
(14) N. A. Milas a. W. L. Walsh, J. Amer. Chem. Soc. **57**, 1389 (1935).
(15) G. Schenk, Naturwiss. **31**, 387 (1943), Ber. dtsch. chem. Ges. **77**, 661 (1944).
(16) N. A. Milas, J. Amer. Chem. Soc. **49**, 2005 (1927).
(17) C. F. Cross, E. J. Bevan a. J. F. Briggs, Ber. dtsch. chem. Ges. **33**, 3132 (1900).
(18) K. v. Auwers a. H. Wissebach, Ber. dtsch. chem. Ges. **56**, 731 (1923).
(19) H. Fecht, Ber. dtsch. chem. Ges. **38**, 1272 (1905).
(20) See e. g. H. B. Hill, Ber. dtsch. chem. Ges. **16**, 1130 (1883).
(21) See H. Simonis, Ber. dtsch. chem. Ges. **32**, 2084 (1899).
(22) J. Böeseken, C. O. G. Vermij, H. Bunge a. C. van Meeuwen, Recueil Trav. chim. Pays-Bas **50**, 1023 (1931).
(23) C. F. Cross, E. J. Bevan a. T. Heiberg, J. chem. Soc. **75**, 747 (1899).

(24) E. E. Hughes a. S. F. Acree, J. Res. Nat. Bur. Standards **24**, 175 (1940).
(25) N. A. Milas a. A. McAlevy, J. Amer. Chem. Soc. **56**, 1221 (1934).
(26) H. Scheibler, J. Jeschke a. W. Beiser, J. prakt. Chem. **137**, 322 (1933).
(27) H. H. Hodgson a. R. R. Davies, J. chem. Soc. 1939, 806.
(28) K. Meinel, Liebigs Ann. d. Chem. **516**, 231 (1935).
(29) K. Meinel, Liebigs Ann. d. Chem. **510**, 129 (1934).
(30) A. Wohl a. B. Mylo, Ber. dtsch. chem. Ges. **45**, 322, 1746 (1912).
(31) A. Wohl a. A. Bernreuther, Liebigs Ann. d. Chem. **481**, 1 (1930).
(32) S. Keimatsu a. K. Yokota, J. Pharmac. Soc. Japan Nr. **542**, 41 (1927); Chem. Z. 1927 II, 237.
(33) N. A. Preobrazhenskij, I. A. Rubtsov, I. F. Dankova a. V. A. Pavlov, J. gen. Chem. (USSR) **15**, 958 (1945); C. A. **40**, 6488 (1946).
(34) G. Ciamician a. P. Silber, Ber. dtsch. chem. Ges. **46**, 1558 (1913).
(35) N. A. Milas a. A. McAlevy, J. Amer. Chem. Soc. **56**, 1219 (1934).
(36) Schering A.-G. Belg. 446, 142, July 31, 1942. C. A. 39, 1106 (1945).
(37) A. P. Dunlop, P. R. Stout a. S. Swadesh, Ind. Eng. Chem. Ind. Ed. **38**, 705 (1946).
(38) J. J. Donleavy, J. Amer. Chem. Soc. **58**, 1004 (1936).
(39) S. Veibel a. H. Lillelund, Bull. Soc. chim. France, Mém. (5) **5**, 1153 (1938).

Indleveret til Selskabet den 19. Februar 1947.
Færdig fra Trykkeriet den 21. Oktober 1947.

DET KGL. DANSKE VIDENSKABERNES SELSKAB
MATEMATISK-FYSISKE MEDDELELSER, BIND XXIV, NR. 7

A SPECIAL CASE OF VELOCITY FOCUSING IN A MAGNETIC DEFLECTING FIELD

BY

JØRGEN KOCH

KØBENHAVN
I KOMMISSION HOS EJNAR MUNKSGAARD
1948

CONTENTS

Printed in Denmark
Bianco Lunos Bogtrykkeri

I. Introduction.

The production of ion beams of high degree of homogeneity with respect to mass and energy is of increasing importance for a number of experimental investigations. In connection with experiments made with the mass spectrograph of the Institute for Theoretical Physics of the University of Copenhagen[1, 2] a very simple method has been worked out by which it is possible to meet rather strict demands for homogeneity, even though the d. c. high voltage used for accelerating the ions is not very constant[3]. This is of particular importance when very high voltages are used, for in this case a smoothing of the voltage ripple and other fluctuations may be inconvenient or impossible to carry out satisfactorily.

An essential feature of the proposed method is the application of a particular form of velocity focusing which even under the conditions mentioned makes it possible to focus the ions on a collecting cylinder or target placed behind the wedge-shaped magnetic field that is used to resolve the beam. To indicate the experimental conditions under which this method was applied[3] it should be pointed out that the mass spectrograph used here works with a very narrow beam produced by ions from a low voltage ion source. This beam is accelerated and collimated by means of a system of electrostatic lenses which makes use of high voltages. The relative energy spread of the ions is very slight, since the ions leave the ion source with very small energies. The magnetic deflecting field is kept constant by means of a large storage battery.

In the following a detailed account will be given of the general principles of the method of focusing, which has so far been only briefly described (loc. cit.). The treatment of the problem by means of geometrical optics shows that a focusing can be carried out for all kinds of charged particles traversing

an arbitrarily extended homogeneous wedge-shaped magnetic field. The calculations show certain features of the passage of charged particles through magnetic fields which may be useful in the construction of types of apparatus other than the one mentioned here.

II. General Description of the Method of Focusing.

Let us consider a narrow beam of ions of uniform mass and energy coming from the ion source I (fig. 1) and moving in parallel paths towards R, where the beam enters a homogeneous wedge-shaped magnetic field AOB with central angle ϑ. In the magnetic field the ions will be deflected in circular paths around the apex O with a radius

$$r = H^{-1}\sqrt{2\,VM/e}, \tag{1}$$

where V is the accelerating potential, e/M is the specific charge of the particles, and H is the magnetic field strength. At R' the ions continue their paths along a straight line.

Now, if the accelerating potential V is not constant, but changes as a function of time, so that $\Delta V = \Delta V(t)$, the radius of curvature of the ion paths will change correspondingly and the ion beam will strike the plane $n' - n''$ at various places. On a fluorescent screen placed there, slow variations of ΔV may be observed as oscillations about a central position, while rapid variations manifest themselves in an increase of the natural line breadth. If the beam contains several ion species differing slightly in mass, the beam at $n' - n''$ will be resolved into several components lying close together, provided that both the inherent line breadth and the oscillations of the beams are small compared with the mass dispersion.

To compensate for these oscillations it is possible, as will be proved below, to let the ion beam pass between the electrodes of a parallel plate condenser, placed at G, one plate of which (a) is grounded while the other (b) is supplied with a voltage E which is proportional to the fluctuations ΔV of the acceleration potential from its average value:

$$E = E_0 \Delta V, \quad \Delta V \ll V. \tag{2}$$

The proportionality factor E_0 takes account of the extent to

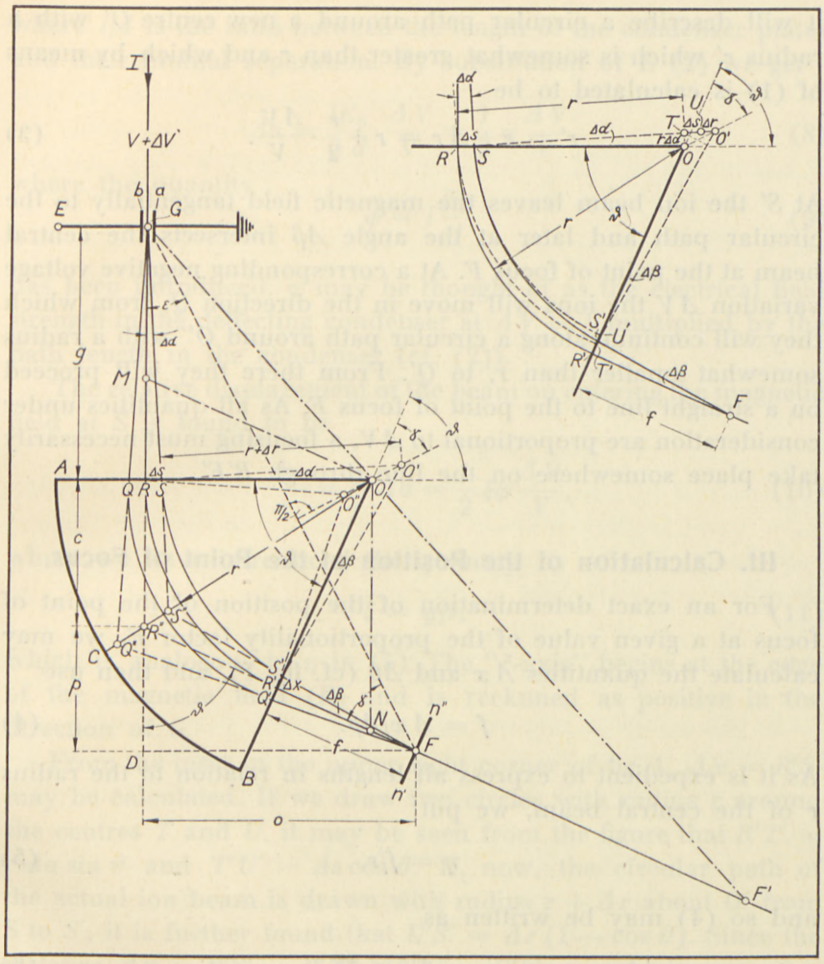

Fig. 1. Graphical construction for the computation of the point of focus F indicating the characteristic features of the construction of the ion paths by means of geometrical optics as discussed in section V.

which the deflecting voltage on the condenser must depend on the voltage variations ΔV. To show qualitatively that the intended focusing is obtained by this means, let us first assume that ΔV is positive. The ion beam then will suffer a slight angular deflection $\Delta\alpha = \text{const.} \times \Delta V$ in the direction of the plate a, so that it will appear to have been emitted from a virtual source G in the middle of the condenser. Entering the magnetic field at S

it will describe a circular path around a new centre O' with a radius r' which is somewhat greater than r and which by means of (1) is calculated to be

$$r' = r + \Delta r = r + \frac{r}{2} \cdot \frac{\Delta V}{V}. \tag{3}$$

At S' the ion beam leaves the magnetic field tangentially to the circular path and later at the angle $\Delta\beta$ intersects the central beam at the point of focus F. At a corresponding negative voltage variation ΔV the ions will move in the direction Q, from which they will continue along a circular path around O'' with a radius somewhat smaller than r, to Q'. From there they will proceed on a straight line to the point of focus F. As all quantities under consideration are proportional to ΔV, a focusing must necessarily take place somewhere on the line through $R'F'$.

III. Calculation of the Position of the Point of Focus.

For an exact determination of the position of the point of focus at a given value of the proportionality factor E_0 we may calculate the quantities Δx and $\Delta\beta$ (cf. fig. 1), and then use

$$f = \Delta x/\Delta\beta. \tag{4}$$

As it is expedient to express all lengths in relation to the radius r of the central beam, we put

$$\eta = f/r, \tag{5}$$

and so (4) may be written as

$$\eta = \Delta x/r\,\Delta\beta. \tag{6}$$

The "η-axis" introduced here begins at R' and is reckoned as positive in the direction of F.

For the calculation of (6) we shall first determine the angular deflection in the plate condenser, the field of which is assumed to be homogeneous*. In the case of small deflections we obtain the well-known expression

$$\Delta\alpha = \frac{lE}{2\,dV}, \quad (E \ll V), \tag{7}$$

* The effects of stray fields are not considered and only first order terms are retained in the calculations.

where l/d is the ratio between the length of the condenser plates and their mutual separation. By substitution of E (2) we get

$$\Delta\alpha = \frac{lE_0}{2\,d} \cdot \frac{\Delta V}{V} = \frac{1}{2}\varphi\frac{\Delta V}{V}, \tag{8}$$

where the quantity

$$\varphi = l\frac{E_0}{d} \tag{9}$$

has been introduced. φ may be thought of as the electrical field strength in the deflecting condenser at $\Delta V = 1$ multiplied by the path length in the condenser (cf. (2)).

The relative displacement of the beam on entering the magnetic field at S is found to be

$$\frac{\Delta s}{r} = \frac{g}{r}\Delta\alpha = \frac{1}{2}\xi\varphi\frac{\Delta V}{V}, \tag{10}$$

where we have introduced the quantity

$$\xi = g/r, \tag{11}$$

which is analogous to η in (5). The "ξ-axis" begins at the edge of the magnetic field (R) and is reckoned as positive in the direction of G.

From the inset in the upper right corner of fig. 1, $\Delta x = R'S'$ may be calculated. If we draw two circles with radius r around the centres T and U, it may be seen from the figure that $R'T' = r\,\Delta\alpha\sin\vartheta$ and $T'U' = \Delta s\cos\vartheta$. If, now, the circular path of the actual ion beam is drawn with radius $r + \Delta r$ about O' from S to S', it is further found that $U'S' = \Delta r\,(1 - \cos\vartheta)$. Since the distance $\Delta x = R'S' = R'T' + T'U' - U'S'$, we obtain

$$\frac{\Delta x}{r} = \Delta\alpha\sin\vartheta + \frac{\Delta s}{r}\cos\vartheta - \frac{\Delta r}{r}(1 - \cos\vartheta). \tag{12}$$

Substituting $\Delta\alpha$ (8), $\Delta s/r$ (10), and $\Delta r/r$ (3), we obtain

$$\frac{\Delta x}{r} = \frac{1}{2}(\varphi\sin\vartheta + \xi\varphi\cos\vartheta + \cos\vartheta - 1)\frac{\Delta V}{V}. \tag{13}$$

From the inset in fig. 1 it is found correspondingly that

$$\Delta\beta = [\sin\vartheta\,(\Delta s + \Delta r) - r\,\Delta\alpha\cos\vartheta]/r, \tag{14}$$

from which, with the same substitutions as used above, we obtain

$$\Delta\beta = \frac{1}{2}(\xi\varphi \sin\vartheta + \sin\vartheta - \varphi\cos\vartheta)\frac{\Delta V}{V}. \qquad (15)$$

Substituting (13) and (15) in (6), we finally find an expression for the relative position of the point of focus

$$\eta = \frac{\varphi\sin\vartheta + \xi\varphi\cos\vartheta + \cos\vartheta - 1}{\xi\varphi\sin\vartheta + \sin\vartheta - \varphi\cos\vartheta}. \qquad (16)$$

From this it appears that a focusing on the positive η-axis may take place at suitable values of φ, ξ and ϑ.

IV. The Proportionality Factor E_0.

In order to apply this method in practice we must calculate $E_0 = \varphi \cdot d/l$ for the values of η, ξ and ϑ given by the experimental conditions. For the discussion of the conditions of focusing we therefore solve (16) for φ, obtaining

$$\varphi = \frac{1 + \eta\sin\vartheta - \cos\vartheta}{(1 - \eta\xi)\sin\vartheta + (\eta + \xi)\cos\vartheta}. \qquad (17)$$

It should be remarked here that if, for the calculation of φ, the relative distances from F and G, respectively, to the intersection R'' of the η- and ξ-axes are used instead of η and ξ, viz.

$$\left.\begin{aligned} \eta' &= f/r + c/r = \eta + \operatorname{tg}\vartheta/2 \text{ and} \\ \xi' &= g/r + c/r = \xi + \operatorname{tg}\vartheta/2, \end{aligned}\right\} \qquad (18)$$

we obtain

$$\varphi = \frac{\eta'\sin\vartheta}{\eta' + \xi' - \eta'\xi'\sin\vartheta}. \qquad (19)$$

The reason why this expression is of a somewhat simpler form than (17) is that the bisector OC may be viewed as the principal plane of the cylindrical lens, since beams leading from G to F are apparently deflected there once (cf. section V, 1). In what follows the expression (17) for φ will, however, be used, as this offers the best possibility for carrying through a discussion of the conditions of focusing.

A general mathematical analysis of the function φ (17) gives the following result. If we present φ as a function of η with ξ

as parameter at a fixed value of ϑ, we get a set of equilateral hyperbolas which are symmetrical with respect to a pair of axes rotated by $\pi/4$ from the η, φ-system and having their centres at the points

$$\eta_c = \frac{\xi \cos\vartheta + \sin\vartheta}{\xi \sin\vartheta - \cos\vartheta}; \quad \varphi_c = -\frac{\sin\vartheta}{\xi \sin\vartheta - \cos\vartheta}. \tag{20}$$

The centres of the hyperbolas for various values of ξ lie on the straight line

$$\varphi_c(\eta_c) = -\sin^2\vartheta\,(\eta_c - \operatorname{ctg}\vartheta). \tag{21}$$

It is further characteristic that the hyperbolas for all values of ξ pass through the two points X and Y with coordinates

$$\eta_X = \operatorname{ctg}\vartheta; \quad \varphi_X = \sin\vartheta, \tag{22}$$

$$\eta_Y = (\cos\vartheta - 1)/\sin\vartheta; \quad \varphi_Y = 0. \tag{23}$$

A degenerate case arises when $\xi = \operatorname{ctg}\vartheta$. The function $\varphi(\eta)$ is then of the form

$$\varphi(\eta) = \sin^2\vartheta\left(\eta - \frac{\cos\vartheta - 1}{\sin\vartheta}\right), \tag{24}$$

i. e. φ is linearly dependent on η. Finally it should be stated that the function $\varphi(\eta)$ has a singularity ($\varphi = \pm\infty$) when the denominator in formula (17) vanishes, i. e. when

$$(1 - \eta\xi)\sin\vartheta + (\eta + \xi)\cos\vartheta = 0. \tag{25}$$

In connection with the physical problem discussed here only the course of $\varphi(\eta)$ at positive values of η and ξ is of interest. The reader is referred to section VI, where $\varphi(\eta)$ is represented graphically for $\vartheta = \pi/3$, $\pi/2$, π and $3\pi/2$. The connection between the above mentioned properties of the function $\varphi(\eta)$ ((22)—(25)) and the geometrical treatment of the problem of focusing will be discussed in detail in section V.

V. Characteristic Features of the Construction of the Ion Paths by Means of Geometrical Optics.

In what follows attention will be called to some characteristic features of the construction of the ion paths by means of

geometrical optics which are convenient to use in the graphical treatment of the focusing method mentioned here and are furthermore of particular importance in its practical application.

(1) As appears from fig. 1, the η and ξ-axes intersect at the point R'' on the bisector OC of the wedge-shaped field so that the deflection of the central beam is seen to be ϑ. As mentioned above (p. 8), the bisector OC, however, may generally be considered as a principal plane of the prism, all ion beams here apparently being subjected to one single deflection. This result appears by putting

$$(g + c)\, \Delta\alpha = (f + c)\, \Delta\beta, \tag{26}$$

from which follows

$$(\xi + \operatorname{tg} \vartheta/2)\, \Delta\alpha = (\eta + \operatorname{tg} \vartheta/2)\, \Delta\beta. \tag{27}$$

Substituting here (8) and (15), and replacing $\vartheta/2$ by ϑ we obtain an expression for φ that is in accordance with the expression (17). The centres O' and O'' of the circular paths SS' and QQ' are found by making the perpendiculars to the beams at the points S, S' and Q, Q' intersect.

(2) It is now to be demonstrated that (a) the centres O, O' and O'' of the circular arcs RR', SS' and QQ', respectively, lie on a straight line, and (b) the line through O, O', and O'' is perpendicular to the connecting line GF.

(a) From the inset in the upper right corner of fig. 1 it is found that

$$\operatorname{tg} (\vartheta - \gamma) = \frac{r\, \Delta\alpha}{\Delta s + \Delta r} \tag{28}$$

which, after substitution of $\Delta\alpha$ (8), Δs (10) and Δr (3) may be transformed into

$$\operatorname{tg} (\vartheta - \gamma) = \frac{\varphi}{\xi\varphi + 1}. \tag{29}$$

As this expression is independent of ΔV the centres O, O', and O'' must lie on a straight line.

(b) On the basis of the above assertion, we have $\sphericalangle GFR'' = \gamma$ and consequently $\varepsilon = \sphericalangle R''GF = \vartheta - \gamma$. From the right triangle

FDG we get

$$\operatorname{tg} \varepsilon = \frac{o}{g + c + p}. \tag{30}$$

Substituting here

$$\left.\begin{aligned} o/r &= (\eta + \operatorname{tg} \vartheta/2) \sin \vartheta, \\ p/r &= (\eta + \operatorname{tg} \vartheta/2) \cos \vartheta, \\ c/r &= \operatorname{tg} \vartheta/2 \end{aligned}\right\} \tag{31}$$

and then putting (29) = (30), we get

$$\frac{\varphi}{\xi\varphi + 1} = \frac{\sin \vartheta \, (\eta + \operatorname{tg} \vartheta/2)}{\xi + \operatorname{tg} \vartheta/2 + \cos \vartheta \, (\eta + \operatorname{tg} \vartheta/2)}, \tag{32}$$

which again leads to an expression for φ corresponding to (17). Thus it is proved that the straight line through the centres O, O' and O'' is perpendicular to the line GF. The application of this fact is particularly suitable for use in the geometrical construction of the ion paths.

(3) A focusing at the point F' (cf. fig. 1), which is lying on the straight line through the point of divergence G and the apex O cannot take place. This means

$$\operatorname{tg} \varepsilon = r/g = 1/\xi. \tag{33}$$

Using the formulas (30) and (31), this leads to

$$\cos \vartheta \, (\eta + \operatorname{tg} \vartheta/2) + \operatorname{tg} \vartheta/2 + \xi - \xi \sin \vartheta \, (\eta + \operatorname{tg} \vartheta/2) = 0. \tag{34}$$

By the substitution of ϑ for $\vartheta/2$ (34) may be transformed to

$$(1 + \cos \vartheta)(\sin \vartheta - \eta\xi \sin \vartheta + \eta \cos \vartheta + \xi \cos \vartheta) = 0. \tag{35}$$

This formula can only be satisfied for all values of ϑ if the expression in the parenthesis on the right is equal to zero, which, however, according to (25) corresponds to $\varphi = \pm\infty$. Hence we cannot obtain a focusing at the point F' or its immediate proximity, as the voltage variations of the deflecting condenser must be small compared with the acceleration potential (cf. (7)). We shall discuss in section VII, in connection with the graphical representations of φ in figs. 3—6, how close it is practically possible to approach the point F'.

Finally, attention should be called to the fact that the point F' is also of particular importance in the general theory of the passage of ion beams through a wedge-shaped magnetic field. R. HERZOG[4], N. F. BARBER[5] and W. E. STEPHENS[6] have independently shown that a slightly divergent bundle of charged particles with uniform energy coming from G will be focused at F' (direction focusing). It is generally said that F' is the image of G and the formula (25) gives the conditions that the image be formed.

(4) If the deflecting condenser (G) is placed at M, the intersection of the ξ-axis and the perpendicular to BO at O, then φ is linearly dependent on η. For under the conditions mentioned we have $\sphericalangle RMO = \vartheta$ and $\xi = g/r = \operatorname{ctg}\vartheta$ and the formula for $\varphi(\eta)$ then has the form (24) in accordance with the above insertion.

(5) If the beams are to be focused at N, the intersection of the η-axis and the perpendicular to AO at O, the deflecting condenser may be placed anywhere on the ξ-axis, and φ will have the same value for all positions. For under the conditions mentioned we have $\sphericalangle ONR' = \vartheta$ and $\eta = f/r = \operatorname{ctg}\vartheta$, which according to (22) corresponds to $\varphi = \sin\vartheta$ for all values of ξ.

It should be added that the point N is further characterised by being the one focus (in the ordinary optical sense) of the magnetic prism, since a parallel bundle of charged particles coming from I in the direction of R will just be focused here[4, 5, 6]. This form of focusing is closely connected with the peculiarity mentioned just above, which perhaps appears most clearly from a drawing of the ion paths at various values of ξ.*

(6) The derivation of the formula (17) for φ and the detailed discussion of the conditions of focusing have so far been carried out in connection with fig. 1, where an angle of deflection $\vartheta < \pi/2$ is chosen. By means of the above subsections (1)–(5) it is, however, easy to evaluate conditions in the case of an arbitrary angle.

Thus in fig. 2 an angle ϑ which is between π and $3\pi/2$ has been chosen as an example. The general features of the geometrical construction are easily recognized; in the case of $\vartheta > \pi$ there

* Instead of characterizing the position of the focus N by $\eta = \operatorname{ctg}\vartheta$ one often, as mentioned on p. 8, uses its relative distance from the principal plane OC of the prism, which is easily calculated to be $\eta' = 1/\sin\vartheta$. – The fact that the point M is the second focus of the prism is closely connected with the consideration mentioned in subsection (4) above.

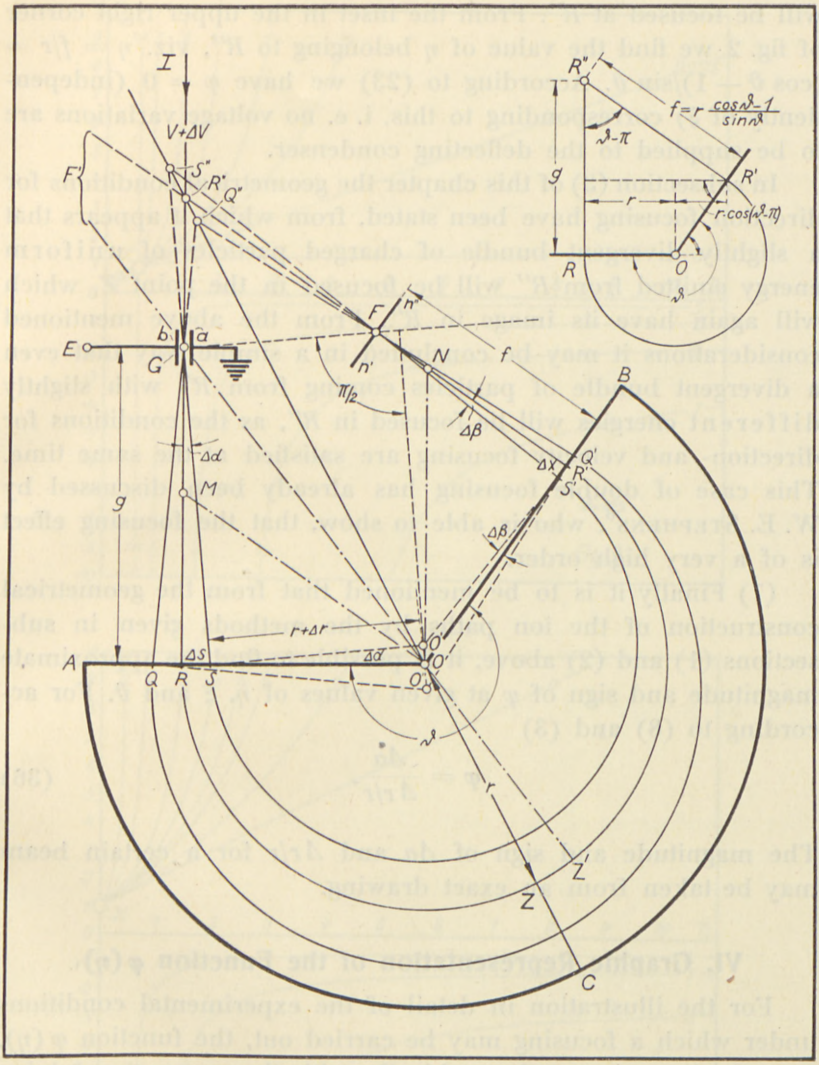

Fig. 2. Graphical construction of the point of focus at a central angle ϑ between π and $3\pi/2$.

is, however, an additional feature which should be mentioned. If the point of focus F coincides with R'', which is the intersection of the η- and ξ-axes, the magnetic field will itself have a velocity focusing effect, i. e. an ion beam coming from I with the energies $V + \Delta V(t)$ without any influence from a deflecting condenser

will be focused at R''. From the inset in the upper right corner of fig. 2 we find the value of η belonging to R'', viz. $\eta = f/r = (\cos\vartheta - 1)/\sin\vartheta$. According to (23) we have $\varphi = 0$ (independently of ξ) corresponding to this, i. e. no voltage variations are to be supplied to the deflecting condenser.

In subsection (3) of this chapter the geometrical conditions for direction focusing have been stated, from which it appears that a slightly divergent bundle of charged particles of uniform energy emitted from R'' will be focused in the point Z, which will again have its image in R''. From the above mentioned considerations it may be concluded in a simple way that even a divergent bundle of particles coming from R'' with slightly different energies will be focused in R'', as the conditions for direction- and velocity focusing are satisfied at the same time. This case of double focusing has already been discussed by W. E. STEPHENS[6], who is able to show, that the focusing effect is of a very high order.

(7) Finally it is to be mentioned that from the geometrical construction of the ion paths by the methods given in subsections (1) and (2) above, it is possible to find the approximate magnitude and sign of φ at given values of η, ξ and ϑ. For according to (8) and (3)

$$\varphi = \frac{\Delta\alpha}{\Delta r/r}. \tag{36}$$

The magnitude and sign of $\Delta\alpha$ and $\Delta r/r$ for a certain beam may be taken from an exact drawing.

VI. Graphic Representation of the Function $\varphi(\eta)$.

For the illustration in detail of the experimental conditions under which a focusing may be carried out, the function $\varphi(\eta)$, $(\eta > 0)$, is represented graphically with the parameter ξ lying between 0 and $+\infty$ for $\vartheta = \pi/3$, $\pi/2$, π and $3\pi/2$ (figs. 3—6). The general form of the curves, which was discussed in section IV, will be recognized.

Fig. 3. For $\vartheta = \pi/3$ the formula for $\varphi(\eta)$ has the following form:

$$\varphi(\eta) = \frac{0{,}500 + 0{,}866\,\eta}{0{,}866\,(1 - \eta\xi) + 0{,}500\,(\eta + \xi)}. \tag{37}$$

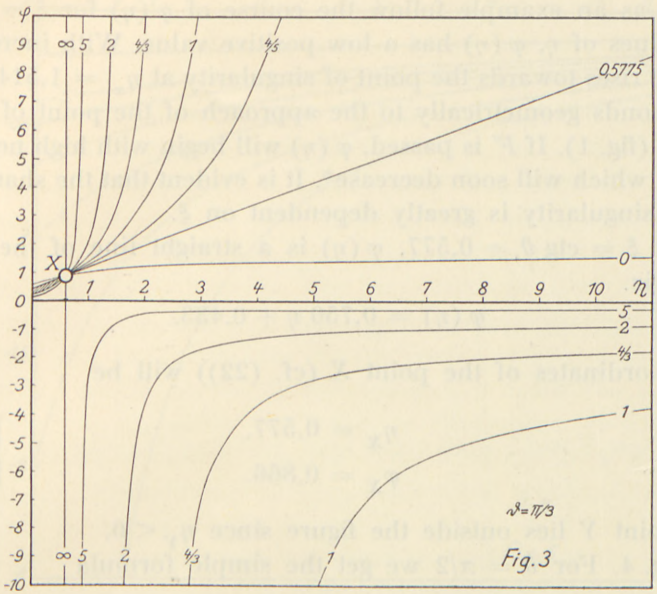

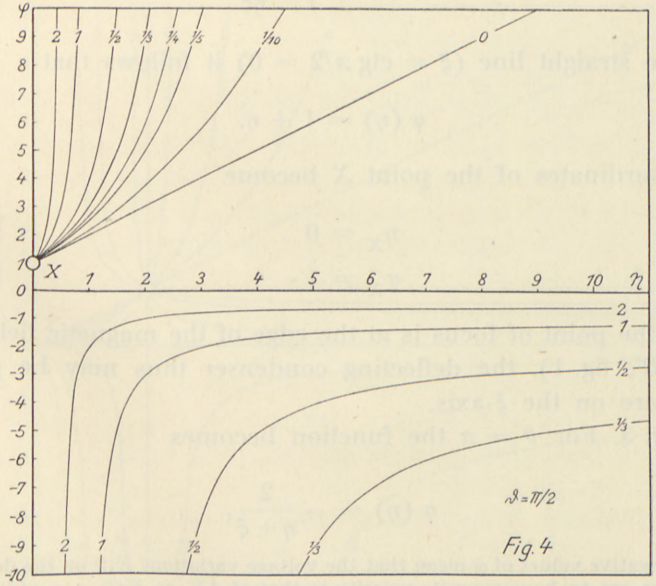

Figs. 3 and 4. Graphical representation of $\varphi(\eta)$. The numbers shown on the curves are values of the parameter ξ. The values of ϑ are $\pi/3$ and $\pi/2$ in the respective figures.

Let us as an example follow the course of $\varphi(\eta)$ for $\xi = 2$. At low values of η, $\varphi(\eta)$ has a low positive value. With increasing η, $\varphi(\eta)$ rises towards the point of singularity at $\eta_\infty = 1{,}514$. This corresponds geometrically to the approach of the point of focus F to F' (fig. 1). If F' is passed, $\varphi(\eta)$ will begin with high negative values, which will soon decrease*. It is evident that the sharpness of the singularity is greatly dependent on ξ.

For $\xi = \operatorname{ctg}\vartheta = 0{,}577$, $\varphi(\eta)$ is a straight line of the form (24), viz.

$$\varphi(\eta) = 0{,}750\,\eta + 0{,}433. \tag{38}$$

The coordinates of the point X (cf. (22)) will be

$$\left.\begin{aligned} \eta_X &= 0{,}577, \\ \varphi_X &= 0{,}866. \end{aligned}\right\} \tag{39}$$

The point Y lies outside the figure since $\eta_Y < 0$.

Fig. 4. For $\vartheta = \pi/2$ we get the simple formula

$$\varphi(\eta) = \frac{1+\eta}{1-\eta\xi}. \tag{40}$$

For the straight line ($\xi = \operatorname{ctg}\pi/2 = 0$) it follows that

$$\varphi(\eta) = 1 + \eta. \tag{41}$$

The coordinates of the point X become

$$\left.\begin{aligned} \eta_X &= 0 \\ \varphi_X &= 1 \end{aligned}\right\} \tag{42}$$

When the point of focus is at the edge of the magnetic field (the point R', fig. 1), the deflecting condenser thus may be placed anywhere on the ξ-axis.

Fig. 5. For $\vartheta = \pi$ the function becomes

$$\varphi(\eta) = -\frac{2}{\eta+\xi}. \tag{43}$$

* Negative values of φ mean that the voltage variations $E(t)$ on the deflecting condenser are to have opposite polarity to that of ΔV, as $E(t) = \varphi \cdot (d/l) \cdot \Delta V(t)$. If the d. c. linear amplifier[3] supplies voltage variations of the same sign as ΔV, it is only necessary to interchange the terminals to the condenser plates a and b (cf. fig. 1).

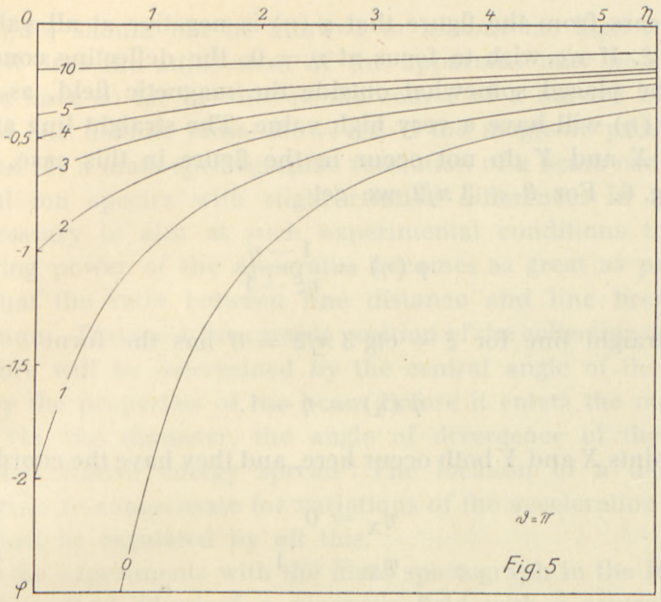

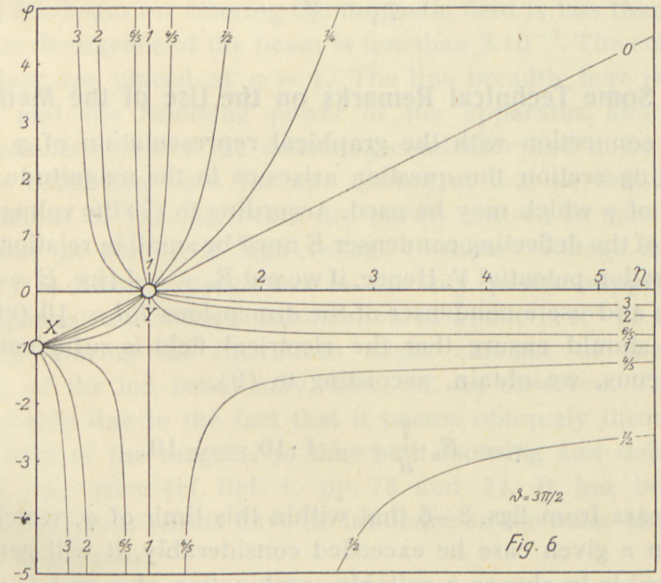

Figs. 5 and 6. Graphical representation of $\varphi(\eta)$. The parameter ϑ has the values π and $3\pi/2$ in the respective figures.

It appears from the figure that $\varphi(\eta)$ is negative at all values of η and ξ. If we wish to focus at $\eta = 0$, the deflecting condenser must be placed somewhat outside the magnetic field, as otherwise $\varphi(\eta)$ will have a very high value. The straight line and the points X and Y do not occur in the figure in this case.

Fig. 6. For $\vartheta = 3\pi/2$ we get

$$\varphi(\eta) = \frac{1-\eta}{\eta\xi - 1}. \tag{44}$$

The straight line for $\xi = \operatorname{ctg} 3\pi/2 = 0$ has the form

$$\varphi(\eta) = \eta - 1. \tag{45}$$

The points X and Y both occur here, and they have the coordinates

$$\left.\begin{aligned} \eta_X &= 0 \\ \varphi_X &= -1 \end{aligned}\right\} \tag{46}$$

$$\left.\begin{aligned} \eta_Y &= 1 \\ \varphi_Y &= 0 \end{aligned}\right\} \tag{47}$$

VII. Some Technical Remarks on the Use of the Method.

In connection with the graphical representation of φ in the preceding section the question arises as to the magnitude of the values of φ which may be used. According to (7) the voltage variations of the deflecting condenser E must be small in relation to the acceleration potential V. Hence, if we put $E_0 = \pm 1$ (i.e. $E = \pm \Delta V$; cf. (2)) and use a condenser of the dimensions $l/d = 10$ (cf. (7)), which should ensure that the electrical field is sufficiently homogeneous, we obtain, according to (9),

$$\varphi = E_0 \cdot \frac{l}{d} = \pm 1 \cdot 10 = \pm 10. \tag{48}$$

It appears from figs. 3—6 that within this limit of φ, which may even in a given case be exceeded considerably, it will generally be possible to choose a suitable combination of η and ξ, so that a focusing may be effected. It should, however, be taken into consideration that the slope of the curve at the operating point

$d\varphi(\eta)/d\eta$ should not be allowed to assume too high a value, for if it does the adjustment of the apparatus may be critical.

We have so far considered the course of a narrow beam of ions of one definite mass. However, if the magnetic prism is to be used for a mass-spectographic resolution of a beam containing several ion species with slight relative differences in mass it is necessary to aim at such experimental conditions that the resolving power of the apparatus becomes as great as possible, i. e. that the ratio between line distance and line breadth is maximum. The most favourable position of the collecting cylinder therefore will be determined by the central angle of the prism and by the properties of the beam before it enters the magnetic field, viz. the diameter, the angle of divergence of the beam and the relative energy spread[2]. The location of a deflecting condenser to compensate for variations of the acceleration potential must be regulated by all this.

In the experiments with the mass spectograph in the Institute for Theoretical Physics[2] a magnetic field with a central angle of $\vartheta = \pi/2$ and a mean radius of $r = 80$ cm is used. The diameter of the ion beam on entering the magnetic field is less than 1 cm, and the divergence of the beam is less than 2.10^{-3}. The collecting cylinders are placed at $\eta = 1$. The line breadth here is about 3 mm and the resolving power of the apparatus about 300. For reasons of space the deflecting condenser had to be placed at $\xi = 0.38$. The ratio l/d was chosen at 3.2, so that $E_0 \approx 1$. Oscillations of the ion beam are hardly noticed in spite of the fact that the source of high voltage (ordinary voltage doubling circuit) is directly connected to the city power supply. This corresponds to a voltage stabilization of about $1:10^4$ (7 volts at 70.000). During the operations slight changes of the cross section of the ion beam may, however, be observed. They are presumably due to the fact that it passes obliquely through the stray field of the magnet, so that both focusing and defocusing effects may arise (cf. Ref. 1, pp. 73 and 7). It has been observed that these effects have no influence on the mass-dispersion of the apparatus.

A diagram of an arrangement by means of which it is possible in a simple way to produce voltage variations proportional to ΔV has already been published[3]. Perhaps it should be

added that the d. c. linear amplifier consists of two stages with a total amplification of about 1,400. In the first stage is used an *AF* 7-valve, while in the second stage a transmitting valve is applied corresponding to the Philips type *PC* 1,5/100, which is fed from a 2,000 volt d. c. tension engine. The d. c. anode tension of the latter valve is 1,000 volts (corresponding to $\Delta V = 0$), which in the present arrangement is compensated for by means of a small rectifier instead of batteries. The voltage variation on the deflecting condenser is a linear function of the input voltage within the region $\pm$ 800 volts. The various parts of the apparatus are well screened in order to avoid disturbances from the outside.

In certain experiments, i. e. those of nuclear physics, it is of great importance that the accelerated ions always strike the target or collecting cylinder with uniform energy. This may be accomplished by insulating these electrodes and supplying them with voltage variations of the magnitude $E' = \Delta V$, since the difference in voltage between the ion source and the electrodes is in this case always V.[3] This method of compensation for the ripple and other fluctuations of the voltage may be useful even without magnetic analysis of the beam. By means of the focusing method proposed here it is, however, possible to make the ion beam pass through a magnetic deflecting field first, and thus to select one definite kind of ions for further experiments. The electrical circuits will become particularly simple if the experimental conditions for focusing are chosen so that $E = \Delta V$ ($E_0 = 1$), as in this case it is possible to connect the deflecting condenser directly to the target.

VIII. Summary.

In the mass-spectrographic analysis of a narrow beam of ions, uniform with respect to energy, by means of a homogeneous wedge-shaped magnetic field even small variations of the accelerating potential of the ions ΔV will have a very disturbing effect, as the ion beam at the collecting cylinder will fluctuate. This movement may be compensated for by making the ion beam, before it enters the magnetic field, pass through a de-

flecting condenser, one plate of which is grounded, while the other is supplied with a voltage proportional to ΔV. The magnitude of the proportionality factor E_0 is mainly determined by the central angle of the wedge-shaped field and by the position of the condenser and the collecting cylinder. The construction of the ion paths by means of geometrical optics shows certain very characteristic features, the discussion of which is closely connected with the general theory of the passage of charged particles through a magnetic prism. To facilitate the use of the method in practice a number of graphic representations are given, from which it is possible to read the magnitude of the proportionality factor E_0 for given experimental conditions. Finally, various technical questions related to the practical application of the method are discussed.

IX. Acknowledgments.

The present paper has been prepared in connection with the experiments made with the mass spectrograph of the Institute for Theoretical Physics. The author wants to offer his best thanks to the director of the Institute, Professor NIELS BOHR, for his constant interest in the present investigations. Further I want to offer my thanks to Mr. AAGE BOHR, M. Sc., for various discussions on the general theory of the passage of charged particles through magnetic fields, and to Mr. P. KRISTENSEN, B. Sc., for assisting in the mathematical analysis of the function φ. Finally I offer my thanks to Mr. E. DISSING SØRENSEN, C. E., for his cooperation in the technical construction and testing of the apparatus.

X. References.

1) J. KOCH, Diss. Copenhagen (Publ. by Thaning og Appel, 1942).
2) J. KOCH and B. BENDT-NIELSEN, D. Kgl. Danske Vidensk. Selskab, Mat.-fys. Medd. **21**, 8 (1944).
3) J. KOCH, Phys. Rev. **69**, 238 (1946).
4) R. HERZOG, Zs. Phys. **89**, 447 (1934).
5) N. F. BARBER, Proc. Leeds Phil. Soc. **2**, 427 (1933).
6) W. E. STEPHENS, Phys. Rev. **45**, 513 (1934).
7) C. REUTERSWÄRD, Arch. f. Mat., Astron. och Fysik **30**, 7 (1944).

Indleveret til Selskabet den 19. Marts 1947.
Færdig fra Trykkeriet den 4. Februar 1948.

DET KGL. DANSKE VIDENSKABERNES SELSKAB
MATEMATISK-FYSISKE MEDDELELSER, BIND XXIV, Nr. 8

SOME NOTES ON HEAT-TRANSFER BY RADIATION

BY

H. HØJGAARD JENSEN

KØBENHAVN
I KOMMISSION HOS EJNAR MUNKSGAARD
1948

Printed in Denmark
Bianco Lunos Bogtrykkeri

The following is a discussion of the heat transfer caused by radiation between two bodies of different temperatures, one of them entirely surrounding the other.

In the first part of the article we make some simplifying assumptions often allowed for technical surfaces (later on we are going to discuss the significance of the most important among them):

(1) The temperature-radiation obeys the cosine emission law.
(2) The surfaces of the bodies are reflecting according to the cosine law of reflection (completely diffuse reflection). The bodies are opaque.
(3) The reflectivity is independent of temperature and wavelength. According to Kirchhoff's law this means that the emitted temperature-radiation obeys Stefan-Boltzmann's law.
(4) The inner surface is everywhere convex and the outer one is everywhere concave.
(5) The temperature is constant on each body.

The energy emitted in unit of time from the inner body is $A_1 c_1 T_1^4$, where A_1 is the area of the surface, c_1 the "radiation-constant" and T_1 the absolute temperature of the body. If the surroundings are non-reflecting (absolutely black) the energy received and absorbed by the inner body in unit of time will be $A_1 c_1 T_2^4$, where T_2 is the absolute temperature of the surroundings. Hence, the net loss of energy from the inner body will be

$$H = A_1 c_1 (T_1^4 - T_2^4). \tag{1}$$

This formula is often used in practical calculations. It is only valid if the radiation emitted from the inner body and reabsorbed after reflection from the surroundings can be neglected.

If the reflected radiation is not vanishingly small, the loss of energy is less than given by (1). CHRISTIANSEN[1] arrived at the following formula:

$$H = \frac{A_1 c_1 (T_1^4 - T_2^4)}{1 + c_1 \left(\frac{1}{c_2} - \frac{1}{c_0}\right) \frac{A_1}{A_2}}. \qquad (2)$$

Index 2 refers to the outer surface; c_0 is the radiation-constant for a black body (Stefan's constant).

CLAUSING[2] and SAUNDERS[3] have shown, that (2) is not always correct; H also to some extent depends on the form and mutual position of the two surfaces. SAUNDERS has shown how to make corrections for this dependence if the reflectivity is so small that it is sufficient to take into account only one reflection.

We shall give equations determining H, show in which cases (2) is correct, and find an approximate solution in the general case.

The integral equations of the problem.

We choose two points x_1 and x_2 on the inner and outer surface, respectively (cf. fig. 1), so that x_1 can be seen from x_2 and vice versa. That part of the outer surface which can be seen from x_1 is denoted by A_2', while A_2'' means that part which cannot be seen from x_2. A_1' denotes that part of the inner surface, which can be seen from x_2. By $\varphi(x_1 x_2)$ we denote the function $\frac{\cos i_1 \cdot \cos i_2}{\pi r^2}$, where i_1 and i_2 are the angles shown in fig. 1, while r is the distance between the points x_1 and x_2. It is equal to the fraction of the radiation from the vicinity of x_1, which goes directly to unit of area around the point x_2 or vice versa. The corresponding function for radiation between two points x_2 and x_2' of the outer surface is denoted by $\varphi(x_2 x_2')$.

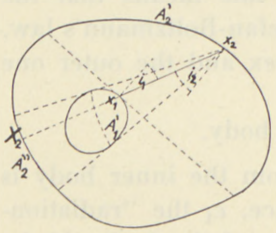

Fig. 1.

The resulting radiation (both emitted and reflected) in unit of time from unit of area near a point x is called $I(x)$.

[1] C. CHRISTIANSEN: Ann. d. Phys. u. Chem., Vol. 19, p. 267, 1883.
[2] CLAUSING: Revue d'Optique, Vol. 10, p. 353, 1931.
[3] SAUNDERS: Proc. of the Phys. Soc., Vol. 41, p. 569, 1929.

We now express that this resulting radiation is the sum of the emitted and the reflected radiation.

This leads to the following two integral equations:

$$I_1(x_1) = c_1 T_1^4 + \left(1 - \frac{c_1}{c_0}\right) \cdot \int_{A_2'} I_2(x_2)\, \varphi(x_1 x_2)\, dx_2 \tag{3}$$

$$I_2(x_2) = c_2 T_2^4 + \left(1 - \frac{c_2}{c_0}\right) \cdot \left\{ \int_{A_1'} I_1(x_1)\, \varphi(x_1 x_2)\, dx_1 + \int_{A_2 - A_2''} I_2(x_2')\, \varphi(x_2 x_2')\, dx_2' \right\}, \tag{4}$$

where as before index 1 refers to the inner, index 2 to the outer surface; dx_1, dx_2, and dx_2' denote surface elements. We have made use of Kirchhoff's law, according to which the reflectivity of a surface with the radiation-constant c is $1 - \frac{c}{c_0}$. The absorptivity is $\frac{c}{c_0}$.

Let X_2 denote the point where a straight line from x_2 to x_1 intersects the outer surface again (cf. fig. 1). It is then easily seen, that (4) can be rewritten as

$$I_2(x_2) = c_2 T_2^4 + \left(1 - \frac{c_2}{c_0}\right) \cdot \left\{ \int_{A_1'} (I_1(x_1) - I_2(X_2)) \cdot \varphi(x_1 x_2)\, dx_1 + \int_{A_2} I_2(x_2')\, \varphi(x_2 x_2')\, dx_2' \right\}. \tag{4 a}$$

The net energy-loss from the inner body is the difference between emitted radiation and absorbed radiation:

$$H = A_1 c_1 T_1^4 - \frac{c_1}{c_0} \cdot \int_{A_1} dx_1 \int_{A_2'} I_2(x_2)\, \varphi(x_1 x_2)\, dx_2 . \tag{5}$$

The equations (3), (4a), and (5) determine H, when the geometry of the system is known. They cannot often be solved exactly.

We first want to emphasise that Christiansen's formula (2) is valid, if the function

$$\varphi(x_2) = \int_{A_1'} \varphi(x_1 x_2)\, dx_1 \tag{6}$$

(i. e. the fraction of the radiation from the vicinity of x_2 which goes directly to the inner body) is independent of x_2. In that case $\varphi(x_2)$ can easily be found: From the definition (6) it follows that

$$\int_{A_2} \varphi(x_2)\, dx_2 = \int_{A_2} dx_2 \int_{A_1'} \varphi(x_1 x_2)\, dx_1 = \int_{A_1} dx_1 \int_{A_2'} \varphi(x_1 x_2)\, dx_2 = A_1, \quad (7)$$

so that if $\varphi(x_2)$ is constant, it must be equal to $\frac{A_1}{A_2}$.

In general $\frac{A_1}{A_2}$ is the mean value of $\varphi(x_2)$ over the outer surface.

When $\varphi(x_2) = \frac{A_1}{A_2}$, it is seen that (3) and (4 a) are satisfied by constant values of $I_1(x_1)$ and $I_2(x_2)$. Solving for I_1 and I_2 and inserting in (5), we get Christiansen's formula (2).

Some very simple forms and symmetrical arrangements of the two bodies give a constant value of $\varphi(x_2)$, e.g. two concentric spheres, two coaxial cylinders, or a sphere with a thin disk covering the equatorial plane (see below). In these cases Christiansen's formula (2) is valid, but if $\varphi(x_2)$, and consequently $I_1(x_1)$ and $I_2(x_2)$, vary, this formula is no longer correct. A simple example that can be solved exactly, will show this: Let the outer surface be a sphere and the inner body a hemisphere with slightly smaller radius (cf. fig. 2). Formula (2) then is valid for the radiation from the hemispherical surface and the plane surface separately (cf. p. 12). This means that H is a sum of two expressions of the form (2) with $\frac{A_1}{A_2}$ in the denominator replaced by 1 and $\frac{1}{2}$, respectively. This sum, however, is different from what is obtained by using formula (2) for the radiation from the total inner surface (putting $\frac{A_1}{A_2} = \frac{3}{4}$ in the denominator). One often gets a better approximation than (2) by separating the radiation in two or more parts of the form (2) as in this instance, e. g. when dealing with a flat radiator placed near a wall. On page 13 one more example is given, where such a separation is exact.

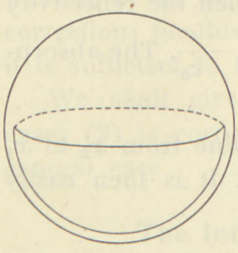

Fig. 2.

Approximate solution of the integral equations.

We shall now show how to find approximate solutions of the equations (3), (4a), and (5) in the general case.

The crudest approximation—formula (1)—is obtained by dis-

regarding the integral $\int_{A_1'} \cdots dx_1$ in (4a); this integral represents the influence of the inner body on the radiation from the outer surface. By doing so one gets the solution (black-body radiation):

$$I_2(x_2) = c_0 T_2^4; \tag{8}$$

which inserted in (3) gives

$$I_1(x_1) = c_1(T_1^4 - T_2^4) + c_0 T_2^4. \tag{9}$$

(5) then leads to the "zeroth" approximation (1).

These expressions for I_2 and I_1 are now inserted in the integral in (4 a) which was first disregarded. In the other terms of the equations (3), (4a), and (5) we put

$$I_1(x_1) = c_1(T_1^4 - T_2^4) + c_0 T_2^4 + f(x_1) \tag{10}$$

$$I_2(x_2) = c_0 T_2^4 + g(x_2). \tag{11}$$

We then get the following equations, where we have introduced the function $\varphi(x_2)$ defined by (6):

$$f(x_1) = \left(1 - \frac{c_1}{c_0}\right) \cdot \int_{A_2'} g(x_2)\, \varphi(x_1 x_2)\, dx_2 \tag{12}$$

$$g(x_2) = \left(1 - \frac{c_2}{c_0}\right) \cdot \left\{ c_1(T_1^4 - T_2^4) \cdot \varphi(x_2) + \int_{A_2} g(x_2')\, \varphi(x_2 x_2')\, dx_2' \right\} \tag{13}$$

$$H = A_1 c_1 (T_1^4 - T_2^4) - \frac{c_1}{c_0} \cdot \int_{A_2} g(x_2)\, \varphi(x_2)\, dx_2. \tag{14}$$

These equations can be solved without further approximations if the outer surface is a sphere. If it has the radius R, it is seen that

$$\varphi(x_2 x_2') = \frac{\cos i_2 \cdot \cos i_2'}{\pi \cdot r^2} = \frac{1}{4\pi R^2} = \frac{1}{A_2}, \tag{15}$$

because $\cos i_2 = \cos i_2' = \frac{r}{2R}$. The last term in equation (13) therefore is a constant so that

$$g(x_2) = \left(1 - \frac{c_2}{c_0}\right) \cdot c_1(T_1^4 - T_2^4) \cdot \{\varphi(x_2) + \text{const.}\}, \tag{16}$$

where the constant is found by inserting (16) into (13). Making use of (7) it is seen that the constant is equal to

$$\frac{c_0}{c_2} \cdot \left(1 - \frac{c_2}{c_0}\right) \cdot \frac{A_1}{A_2}. \tag{16 a}$$

H is then determined by means of (14). We denote mean values over the outer surface by a bar, e. g.

$$\overline{\varphi^2} = \frac{1}{A_2} \cdot \int_{A_2} [\varphi(x_2)]^2 dx_2 \text{ and } \bar{\varphi} = \frac{1}{A_2} \cdot \int_{A_2} \varphi(x_2)\, dx_2 = \frac{A_1}{A_2}$$

according to (7).

The resulting expression for H is

$$H = A_1 c_1 (T_1^4 - T_2^4) \cdot \left\{1 - \frac{A_1}{A_2} \cdot c_1 \cdot \left(\frac{1}{c_2} - \frac{1}{c_0}\right) \cdot \left(1 + \frac{c_2}{c_0} \cdot \frac{\overline{\varphi^2} - (\bar{\varphi})^2}{(\bar{\varphi})^2}\right)\right\}. \tag{17}$$

This may be considered as the first two terms of an expansion of H in powers of $\frac{A_1}{A_2}$. We know that Christiansen's formula (2) is correct when φ is constant, i. e. $\overline{\varphi^2} = (\bar{\varphi})^2$. We therefore obtain a better result if we transform the expansion (17) into an expression in which the denominator is expanded in powers of $\frac{A_1}{A_2}$ instead of the nominator. In this way we get from (17)

$$H = \frac{A_1 c_1 (T_1^4 - T_2^4)}{1 + c_1 \left(\frac{1}{c_2} - \frac{1}{c_0}\right) \cdot \frac{A_1}{A_2} \cdot \left(1 + \frac{c_2}{c_0} \cdot \frac{\overline{\varphi^2} - (\bar{\varphi})^2}{(\bar{\varphi})^2}\right)}. \tag{18}$$

It is of course possible to proceed along these lines and first get the term of order $\left(\frac{A_1}{A_2}\right)^2$ by introducing the now determined first order expressions for $I_2(x_2)$ and $I_1(x_1)$ into the integral $\int_{A_1} \cdots dx_1$, in (4 a). In the case of a surrounding sphere this—second—approximation can also be expressed in terms of simple mean values. Usually, however, (18) will be quite a sufficient approximation.

If the outer surface is not a sphere (18) will no longer be a consequent expansion until the first power of $\frac{A_1}{A_2}$ because (16) is not an exact solution of (13). In order to solve equation (13) in this case we make use of the following result from the theory of integral equations[1]:

[1] See, e. g., COURANT and HILBERT: *Methoden der mathematischen Physik*, Vol. 1.

The integral equation

$$g(x_2) = a\varphi(x_2) + b \cdot \int_{A_2} g(x_2')\, \varphi(x_2 x_2')\, dx_2', \tag{19}$$

where a and b are constant and the "kernel" $\varphi(x_2 x_2')$ is symmetrical in x_2 and x_2' (as in our case) has the solution

$$g(x_2) = a\left\{\varphi(x_2) + b \cdot \int_{A_2} \sum_{i=0}^{N} \frac{h_i(x_2) \cdot h_i(x_2')}{\lambda_i - b} \cdot \varphi(x_2')\, dx_2'\right\}. \tag{20}$$

In this expression $h_i(x_2)$ and λ_i (where i covers 0 to N) are the $N+1$ independent eigenfunctions and corresponding eigenvalues of the kernel $\varphi(x_2 x_2')$; they are defined by the statement that they satisfy the homogeneous integral equation:

$$h_i(x_2) = \lambda_i \cdot \int_{A_2} h_i(x_2')\, \varphi(x_2 x_2')\, dx_2'; \tag{21}$$

furthermore the eigenfunctions must be normalised and orthogonal, i. e.:

$$\int_{A_2} h_i(x_2) \cdot h_k(x_2)\, dx_2 = \begin{cases} 0, \text{ if } i \neq k \\ 1, \text{ if } i = k \end{cases}. \tag{22}$$

In our case $\int_{A_2} \varphi(x_2 x_2')\, dx_2' = 1$; it then follows from (21) that there is always a constant eigenfunction $h_0(x_2)$; owing to the normalisation it must have the value $\frac{1}{\sqrt{A_2}}$. The corresponding eigenvalue is $\lambda_0 = 1$ according to (21). In the solution (20) we treat this eigenfunction separately.

From (13), (19), (20), and (14) we get an expression for H similar to (17). Transforming to a form similar to (18), we finally get

$$H = \frac{A_1 c_1 (T_1^4 - T_2^4)}{1 + c_1\left(\frac{1}{c_2} - \frac{1}{c_0}\right) \cdot \frac{A_1}{A_2}\left(1 + \frac{c_2}{c_0} \cdot k\right)} \tag{23}$$

with

$$k = \frac{\overline{\varphi^2} - (\overline{\varphi})^2}{(\overline{\varphi})^2} + \left(1 - \frac{c_2}{c_0}\right) \cdot \frac{A_2}{(\overline{\varphi})^2} \cdot \sum_{i=1}^{N} \frac{(\overline{h_i \varphi})^2}{\lambda_i - \left(1 - \frac{c_2}{c_0}\right)}. \tag{24}$$

Generally the eigenfunctions cannot be found explicitly. However, it will often be a sufficiently good approximation to neglect the eigenfunctions of higher order than the zeroth, because they have zeropoints and consequently give smaller contributions to k than the zeroth. Below we shall treat an example where these contributions can be evaluated. If the eigenfunctions of higher order are neglected, (23) and (18) are identical.

Examples.

Two spheres.

We consider two spheres, one inside the other, with radii R and r and placed excentrically with a distance c between the centres (cf. fig. 3). We evaluate the function $\varphi(x_2)$ by means of the following quite general rule: The cone made up by the tangents from x_2 to the inner surface cuts a sphere with radius 1 and centre in x_2 in a certain closed curve; this curve is projected on the tangential plane of the outer surface in x_2; the area enclosed by the projection is $\pi \cdot \varphi(x_2)$. In the case of two spheres the projected curve is an ellipse, the area of which can easily be found by simple geometry. For a point x_2 on the outer sphere with a distance y from the centre of the inner sphere we find (for notation cf. fig. 3):

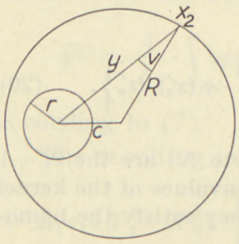

Fig. 3.

$$\varphi(x_2) = \varphi(y) = \frac{r^2}{y^2} \cdot \cos v = \frac{r^2}{y^2} \cdot \frac{R^2 + y^2 - c^2}{2\,Ry}. \qquad (25)$$

Integration then leads to

$$k = \frac{\overline{\varphi^2} - (\overline{\varphi})^2}{(\overline{\varphi})^2} = \frac{-1 + 7\left(\frac{c}{R}\right)^2 - 4\left(\frac{c}{R}\right)^4}{4\left(1 - \left(\frac{c}{R}\right)^2\right)^2} + \frac{1}{8 \cdot \frac{c}{R}} \cdot \log_e \frac{1 + \frac{c}{R}}{1 - \frac{c}{R}}; \qquad (26)$$

k is zero when $c = 0$; it is always positive and increases monotonously until $c = R - r$ (the spheres touch each other). The value of k for $c = R - r$—denoted by $k_{\max}$—is given below for some values of $\frac{R}{r}$:

$\frac{R}{r}$	8	4	2	1
$k_{\max}$	10	2.5	0.5	0

When $c \neq 0$, (18) leads to a smaller loss of energy than Christiansen's formula (2). A few examples will show the order

of magnitude of the difference. We take $\frac{R}{r} = 4$; the difference between (2) and (18), when the spheres touch each other, is then

$$6.4\ \% \text{ if } \frac{c_1}{c_0} = 1 \quad \frac{c_2}{c_0} = 0.5$$

$$3.7\ \% \text{ if } \frac{c_1}{c_0} = 1 \quad \frac{c_2}{c_0} = 0.75$$

$$2.8\ \% \text{ if } \frac{c_1}{c_0} = 0.75 \quad \frac{c_2}{c_0} = 0.75.$$

In the same three cases the differences between the values given by the uncorrected formula (1) and Christiansen's formula (2) are 5.9 per cent., 2.0 per cent., and 1.5 per cent., respectively.

(All numbers are given in per cent. of the uncorrected expression (1).)

Plane disk inside sphere.

We shall evaluate $k = \frac{\overline{\varphi^2} - (\overline{\varphi})^2}{(\overline{\varphi})^2}$ for a number of different positions and magnitudes of a plane disk inside a sphere in order to be able to estimate k for any position and magnitude of the disk.

In the first case (cf. fig. 4) the disk is circular and placed with its centre in the centre of the sphere.

It can be proved—by integration—that for a point x_2 with polar distance ϑ:

$$\left.\begin{aligned} \varphi(x_2) = \varphi(\vartheta) &= \frac{r^2}{\varrho_1 \varrho_2} \cdot \cos\vartheta = \\ &= \frac{r^2 \cos\vartheta}{\sqrt{R^4 + r^4 + 2\,r^2 R^2 \cos 2\vartheta}} \end{aligned}\right\} \quad (27)$$

(for notation cf. fig. 4).

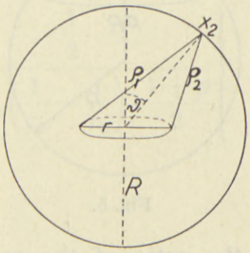

Fig. 4.

This leads to

$$k = \frac{R^2 - r^2}{r^2} \cdot \left(1 - \frac{R}{2\,r} \operatorname{arctg} \frac{2\,rR}{R^2 - r^2}\right); \quad (28)$$

k decreases from $\frac{1}{3}$ to 0 when r increases from 0 to R. The decrease is slow when r is small.

Next we consider a—not necessarily circular—disk which is

so small, that its magnitude only plays a minor role in determining k. (In the case above this corresponds to r being so small that k is not far from $\frac{1}{3}$). The disk is situated so that the straight line from the centre of the sphere to it is $p \cdot R$ in length, and the angle between this line and the direction perpendicular to the disk is u. It may then be shown that

$$k = k_1 \cos^2 u + k_2 \sin^2 u, \tag{29}$$

where k_1 and k_2 are the values of k in the two cases where the plate is respectively perpendicular to and parallel with the line to the centre of the sphere. The values of k_1 and k_2 are found by integration:

$$k_1 = \frac{4}{3(1-p^2)^2} - 1 \tag{30}$$

$$k_2 = \frac{1}{4p} \cdot \log_e \frac{1+p}{1-p} + \frac{5-3p^2}{6(1-p^2)^2} - 1. \tag{31}$$

Finally we consider a disk covering a parallel circle, the centre of which has a distance $p \cdot R$ from the centre of the sphere (fig. 5).

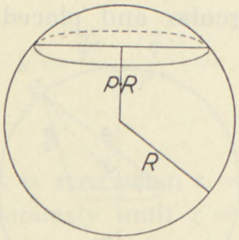

Fig. 5.

For a point x_2 on the smaller of the two spherical caps we have:

$$\left.\begin{aligned} \varphi(x_2) &= \int_{\text{disk}} \varphi(x_2 x_1)\, dx_1 = \int_{\text{big spherical cap}} \varphi(x_2 x_2')\, dx_2' \\ &= \frac{1}{4\pi R^2} \int_{\text{big spherical cap}} dx_2' = \frac{1+p}{2}. \end{aligned}\right\} \tag{32}$$

In the same way it is seen that $\varphi(x_2)$ is constant on the big spherical cap and equals the ratio of the area of the small spherical cap to the area of the whole sphere, i.e. $\frac{1-p}{2}$. Consequently we find

$$k = \frac{p^2}{1-p^2}. \tag{33}$$

By means of the results from the special cases treated above the value of k may be estimated in most cases without further integration. As an example we consider a circular disk per-

pendicular to the line from its centre to the centre of the sphere at a distance of $\frac{3}{4}R$ from the centre of the sphere $\left(p = \frac{3}{4}\right)$. If the disk is small, $k \simeq 6$ according to (30), while $k = 1.3$ for the corresponding parallel circle. For values of its radius between zero and the radius of the parallel circle $\left(\frac{\sqrt{7}}{4}R\right)$ we may estimate k from the way in which it is known to vary with radius in the first special case above (formula 28). If the radius is $\frac{1}{4}R$ we find $k \simeq 5$. The difference between the values of H given by (2) and (18), respectively, is—for the three sets of values of $\frac{c_1}{c_0}$ and $\frac{c_2}{c_0}$ used on page 11—: 7 per cent., 4 per cent. and 3 per cent., while the correction in Christiansen's formula ((1)—(2)) amounts to 3 per cent., 1 per cent. and 0.8 per cent. in the corresponding cases.

In the case of a parallel circle in a sphere treated above, H can be calculated exactly as a sum of two terms, each of the form (2), because $\varphi(x_2)$ is constant on each of the two spherical caps. We will therefore use this case for an estimation of the magnitude of the error made, when formula (18) is used:

The exact value of H is:

$$H = A_1 c_1 (T_1^4 - T_2^4) \cdot \left\{ \frac{\frac{1}{2}}{1 + c_1 \left(\frac{1}{c_2} - \frac{1}{c_0}\right) \cdot \frac{1-p}{2}} + \frac{\frac{1}{2}}{1 + c_1 \left(\frac{1}{c_2} - \frac{1}{c_0}\right) \cdot \frac{1+p}{2}} \right\}. \quad (34)$$

The approximation (18) leads to

$$H = A_1 c_1 (T_1^4 - T_2^4) \cdot \frac{1}{1 + c_1 \left(\frac{1}{c_2} - \frac{1}{c_0}\right) \cdot \frac{1-p^2}{2} \left(1 + \frac{c_2}{c_0} \cdot \frac{p^2}{1-p^2}\right)}. \quad (35)$$

Christiansen's formula (2) gives

$$H = A_1 c_1 (T_1^4 - T_2^4) \cdot \frac{1}{1 + c_1 \left(\frac{1}{c_2} - \frac{1}{c_0}\right) \cdot \frac{1-p^2}{2}}. \quad (36)$$

With the usual three sets of values of $\frac{c_1}{c_0}$ and $\frac{c_2}{c_0}$ (page 11) we find in this special case:

The error in the formula (1) is approximately 30 per cent., 14 per cent. and 11 per cent.
— — - Christiansen's formula (2) is approximately 17 p^2 per cent., 11 p^2 per cent. and 9 p^2 per cent.
— — - the formula (18) is approximately 4 p^2 per cent., 1.3 p^2 per cent. and 1.4 p^2 per cent.

(All numbers in percentages of the simple expression (1).)

Two infinite circular cylinders.

In this case the formulae (23) and (24) ought to be used. We introduce ordinary cylindrical coordinates θ and z for points on the outer cylinder. $g(x_2)$ is independent of z. Consequently the last term in equation (13) can at once be integrated with respect to z'. The result is:

$$g(\theta) = \left(1 - \frac{c_2}{c_0}\right) \cdot \left\{ c_1 (T_1^4 - T_2^4)\, \varphi(\theta) + \int_0^{2\pi} g(\theta') \cdot \frac{1}{4} \cdot \left| \sin \frac{\theta' - \theta}{2} \right| d\theta' \right\}. \quad (37)$$

The corresponding homogeneous integral equation is

$$\begin{aligned} h(\theta) &= \lambda \cdot \int_0^{2\pi} h(\theta') \cdot \frac{1}{4} \cdot \left| \sin \frac{\theta' - \theta}{2} \right| d\theta' \\ &= \lambda \cdot \left\{ - \int_0^{\theta} h(\theta') \cdot \frac{1}{4} \sin \frac{\theta' - \theta}{2}\, d\theta' + \int_{\theta}^{2\pi} h(\theta') \cdot \frac{1}{4} \sin \frac{\theta' - \theta}{2}\, d\theta' \right\}. \end{aligned} \quad (38)$$

Differentiation of this equation with respect to θ shows that the eigenfunction $h(\theta)$ must satisfy the differential equation

$$\frac{d^2 h}{d\theta^2} = \frac{1}{4} (\lambda - 1) \cdot h, \quad (39)$$

the solutions of which are $\begin{matrix} \sin \\ \cos \end{matrix} \left\{ \frac{\sqrt{1-\lambda}}{2} \cdot \theta \right\}$.
They must be periodic with period 2π, whence it follows that $\frac{\sqrt{1-\lambda}}{2}$ must be an integer. If we normalise the eigenfunctions according to the rule:

$$\int_0^{2\pi} [h(\theta)]^2 d\theta = 1, \quad (40)$$

we get the following series of independent eigenfunctions:

$$h_p(\theta) = \frac{1}{\sqrt{\pi}} \cdot \begin{Bmatrix} \cos p\theta \\ \sin p\theta \end{Bmatrix} \quad (p = 1, 2, \cdots) \tag{41}$$

with the corresponding eigenvalues

$$\lambda_p = 1 - 4p^2. \qquad (p = 1, 2, \cdots). \tag{42}$$

Besides these, we have the constant eigenfunction

$$h_0 = \frac{1}{\sqrt{2\pi}} \text{ with } \lambda_0 = 1. \tag{43}$$

Inserting these eigenfunctions and eigenvalues in (24) and the resulting k in (23), we find H. (It should be noted that the methods of normalisation used here and on page 9 are different, because A_2 now is infinite). If the zero-plane for θ is taken to be the plane through the axes of the cylinders, $\overline{\sin p\theta \cdot \varphi(\theta)} = 0$ (odd function of θ). Denoting the radii of the inner and outer cylinder by r and R, respectively, we find that the energy loss per unit of length from the inner cylinder is

$$H = \frac{2\pi r c_1 (T_1^4 - T_2^4)}{1 + c_1 \left(\frac{1}{c_2} - \frac{1}{c_0}\right) \cdot \frac{r}{R} \cdot \left(1 + \frac{c_2}{c_0} \cdot k\right)} \tag{44}$$

with

$$k = \frac{\overline{\varphi^2} - (\bar{\varphi})^2}{(\bar{\varphi})^2} - \left(1 - \frac{c_2}{c_0}\right) \cdot \sum_{p=1}^{\infty} \frac{2}{4p^2 - \frac{c_2}{c_0}} \left(\frac{\overline{\varphi \cos p\theta}}{\bar{\varphi}}\right)^2. \tag{45}$$

The distance between the axes of the cylinders we denote by c. The function $\varphi(x_2) = \varphi(\theta)$ may be determined by the method used on page 10 through a rather simple geometrical consideration. With x denoting the distance from the point θ to the axis of the inner cylinder we get:

$$\varphi(\theta) = \frac{r}{2R} \cdot \frac{R^2 + x^2 - c^2}{x^2}. \tag{46}$$

From this we get by integration

$$\frac{\overline{\varphi^2} - (\bar{\varphi})^2}{(\bar{\varphi})^2} = \frac{c^2}{2(R^2 - c^2)}. \tag{47}$$

The terms in the sum in (45) can be evaluated by integration (most easily by contour integration). We find:

$$\left(\frac{\overline{\varphi \cos p\theta}}{\bar{\varphi}}\right)^2 = \frac{1}{4}\left(\frac{c^2}{R^2}\right)^p. \tag{48}$$

When (47) and (48) are inserted in (45) we get

$$k = \frac{c^2}{2\,(R^2 - c^2)} - \frac{1}{2} \sum_{p=1}^{\infty} \frac{1 - \frac{c_2}{c_0}}{4\,p^2 - \frac{c_2}{c_0}} \cdot \left(\frac{c^2}{R^2}\right)^p. \qquad (49)$$

It is seen that the terms from the higher eigenfunctions decrease rapidly with increasing order. Even the contribution from the second term in (49) may generally be neglected. If e. g. $\frac{c_2}{c_0} = 0.75$, the ratio between the first and second term in (49) will be $13\,\frac{R^2}{R^2 - c^2}$, which is more than 13.

This result gives some justification for totally neglecting contributions from the other eigenfunctions than the zeroth, i. e. for using formula (18) even in cases where the outer surface is not a sphere.

We again calculate the difference between the values of H given by (1) and (2) and by (2) and (18) for the usual three sets of values of $\frac{c_1}{c_0}$ and $\frac{c_2}{c_0}$ (page 11). We choose as an example $r = \frac{1}{8}R$ and $c = R - r$ (the cylinders touch). By using formula (18) we neglect other terms in (49) than the first. (The contribution from the second is in this case 3—2 per cent. of the first). The result is that the difference between Christiansen's formula (2) and our formula (18) is 7.4 per cent., 4.5 per cent. and 3.5 per cent., respectively, while the corresponding differences between (1) and (2) are 11 per cent, 4 per cent. and 3 per cent.

The examples treated above show that in case of a very unsymmetrical position of the inner body with respect to the outer one, it is often so that very little is obtained by applying Christiansen's formula in calculating the heat transfer, because the error made may be just as large or larger than the correction which the formula gives compared with the simple expression $c_1 A_1 (T_1^4 - T_2^4)$. We must conclude that if we aim at such an accuracy that it is necessary to apply a corrected formula instead of (1), then (18) must be used in case of unsymmetrical position of the inner body. This is also practically possible, because the order of magnitude of the correction factor $\frac{\overline{\varphi^2} - (\overline{\varphi})^2}{(\overline{\varphi})^2}$ can often be estimated by simple geometrical or graphical methods.

Discussion of the assumptions made on page 3.

Equations analogous to (3), (4a), and (5) can easily be obtained in the most general case. The surface in the vicinity of

a point x has the absolute temperature T and a reflectivity denoted by $(i\alpha\,|\,r(\lambda Tx)\,|\,i'\alpha')$ and defined in the following way:

We consider monochromatic radiation of wavelength λ, which is falling on a surface element dA. The direction of the incoming ray will be characterized by the angles i (angle of incidence) and α (azimuth) as shown on fig. 6. Of this radiation a certain fraction will be reflected so that it leaves the surface within a solid angle $d\omega'$, the principal direction of which is characterized by i' and α' (cf. fig. 6). If the reflection is completely diffuse the reflected radiation is distributed according to the cosine law, i. e. the said fraction will be proportional to $\cos i'$ and independent of i, α, and α'. In general we therefore denote the fraction reflected to $d\omega'$ by

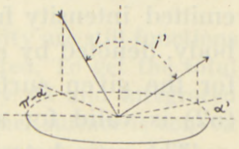

Fig. 6.

$$\frac{1}{\pi}\cdot(i\alpha\,|\,r(\lambda Tx)\,|\,i'\alpha')\cdot\cos i'\,d\omega'. \tag{50}$$

The notation $r(\lambda Tx)$ is chosen in order to show that the reflectivity in general will depend on wavelength, temperature, and constitution of the surface as well as on the angles. The factor $\frac{1}{\pi}$ is introduced for convenience.

The intensity of the emitted radiation (emitted radiation from unit of apparent area into unit of solid angle) in an arbitrary direction can be calculated by means of Kirchhoff's law, if the reflectivity is known:

We shall write down an equation expressing that the resulting intensity of radiation in a closed cavity, the walls of which all have the same temperature T, must everywhere be equal to the intensity of radiation from a black body $K_0(\lambda T)$. The resulting intensity from a point x in the direction $(i\alpha)$ is the sum of the emitted intensity $K_T(\lambda Tx, i\alpha)$ and the reflected intensity, an expression for which can be written down by means of (50); the equation is:

$$K_0(\lambda T) = K_T(\lambda Tx, i\alpha) + K_0(\lambda T)\cdot\frac{1}{\pi}\cdot\int_{\text{solid angle } 2\pi}(i'\alpha'\,|\,r(\lambda Tx)\,|\,i\alpha)\cos i'\,d\omega' \tag{51}$$

or

$$e(\lambda Tx, ia) \equiv \frac{K_T(\lambda Tx, ia)}{K_0(\lambda T)} = 1 - \frac{1}{\pi} \cdot \int_{\text{solid angle } 2\pi} (i'a' \,|\, r(\lambda Tx) \,|\, ia) \cos i' d\omega'. \quad (52)$$

The black body intensity $K_0(\lambda T)$ is given by Planck's radiation formula (it is independent of the angles). The ratio between the emitted intensity from the surface in question and from a black body, denoted by $e(\lambda Tx, ia)$ in (52), will be called the emissivity for the given surface, wavelength, temperature, and direction. (52) is valid for all wavelengths.

The ratio between the total hemispherical radiation of wavelength λ emitted from unit of area of the surface in question and from unit of area of a black body is:

$$E(\lambda Tx) = \frac{1}{\pi} \int_{\text{solid angle } 2\pi} e(\lambda Tx, ia) \cos i \, d\omega. \quad (53)$$

(For the so called "grey" surfaces treated above we have the equalities:

$$e(\lambda Tx, ia) = E(\lambda Tx) = \frac{c}{c_0}\Big).$$

We further define the absorptivity $a(\lambda Tx, ia)$, i. e. the fraction absorbed of radiation coming in from the direction (ia):

$$a(\lambda Tx, ia) = 1 - \frac{1}{\pi} \int_{\text{solid angle } 2\pi} (ia \,|\, r(\lambda Tx) \,|\, i'a') \cos i' d\omega'. \quad (54)^1$$

We now get the equations analogous to (3) and (4a) by expressing that the resulting intensity of radiation $K(iax)$ emerging from the point x on one of the surfaces in the direction (ia) is the sum of the emitted and reflected intensities:

$$K_1(i_1 a_1 x_1) = K_{T_1}(i_1 a_1) + \int_{A_2'} (i_1' a_1' \,|\, r_1 \,|\, i_1 a_1) K_2(i_2 a_2 x_2) \cdot \varphi(x_1 x_2) \, dx_2. \quad (55)$$

$$\left.\begin{aligned} K_2(i_2 a_2 x_2) = K_{T_2}(i_2 a_2) + \int_{A_1'} (i_2' a_2' \,|\, r_2 \,|\, i_2 a_2) \cdot \left[K_1(i_1 a_1 x_1) - K_2(i_2'' a_2'' X_2)\right] \cdot \\ \cdot \varphi(x_1 x_2) \, dx_1 + \int_{A_2} (i_2' a_2' \,|\, r_2 \,|\, i_2 a_2) \cdot K_2(i_2'' a_2'' x_2') \, \varphi(x_2 x_2') \, dx_2'. \end{aligned}\right\} \quad (56)$$

[1] If the so called Helmholtz's reciprocity law (H. v. Helmholtz: *Theoretische Physik*, Vol. 6, p. 161, 1903) is valid, we have: $(ia \,|\, r \,|\, i'a') = (i'a' \,|\, r \,|\, ia)$, and consequently $e \equiv a$.

The heat transfer from the inner body is in analogy with (5) (for monochromatic radiation):

$$H = A_1\pi \cdot E_1 \cdot K_0(T_1) - \pi \cdot \int_{A_1} dx_1 \int_{A_2'} K_2(i_2 a_2 x_2) \cdot a_1(i_1 a_1) \cdot \varphi(x_1 x_2)\, dx_2 . \quad (57)$$

(The emitted intensity of radiation and the reflectivity are still functions of $(\lambda T x)$, although these variables have been omitted. To get the total radiation the equation (57) must be multiplied by $d\lambda$ and integrated over all wavelengths. It is still assumed that the inner surface is convex and the outer one concave, and that both bodies are opaque; furthermore the inner body must have the same temperature and emissivity everywhere if (57) is to be correct. Apart from this the equations are quite general.)

Of course the equations can only be solved exactly in special cases, of which we are going to consider some in what follows, in order to exemplify the applicability of the method of integral equations.

(a) Non-validity of Stefan-Boltzmann's law.

If the reflectivity depends on wavelength and temperature, but not on angles and position (x), the assumptions (3) on page 3 are not valid, but the rest is. In this case all the calculations in the first part of this paper hold true for the heat transfer caused by radiation in a narrow interval $d\lambda$ of wavelength (monochromatic radiation). (Fluorescence, etc., must of course be excluded.) The total heat transfer is then obtained by integration over all wavelengths. The formula analogous to (18) now is

$$H = \int_0^\infty d\lambda \cdot \left\{ \frac{\pi \cdot A_1 \cdot E_1(\lambda T_1)\,[K_0(\lambda T_1) - K_0(\lambda T_2)]}{1 + \frac{E_1(\lambda T_1)}{E_2(\lambda T_2)} \cdot (1 - E_2(\lambda T_2)) \cdot \frac{A_1}{A_2} \cdot \left(1 + E_2(\lambda T_2) \cdot \frac{\overline{\varphi^2} - (\overline{\varphi})^2}{(\overline{\varphi})^2}\right)} \right\} . \quad (58)$$

The ratios $\frac{c_1}{c_0}$ and $\frac{c_2}{c_0}$ from the case of "grey" bodies have been replaced by $E_1(\lambda T_1)$ and $E_2(\lambda T_2)$, while $c_0 T^4$ has been replaced by $\pi K_0(\lambda T)$.

(b) Non-validity of the cosine law for the inner surface.

The inner surface is now assumed to reflect in an arbitrary way, while the outer one still has a reflectivity that is independent

of the angles (completely diffuse reflection). It is then easy to show from (55), (56), and (57), in a way similar to that which led to formula (18) or (58), that formulae analogous to (18) or (58) hold, but the term $\frac{\overline{\varphi^2}-(\overline{\varphi})^2}{(\overline{\varphi})^2}$ must be replaced by

$$k' = \frac{\overline{\psi\psi'}-(\overline{\psi})^2}{(\overline{\psi})^2}, \tag{59}$$

where

$$\psi(x_2) = \int_{A_1'} \frac{e_1(\lambda T_1 i_1 a_1)}{E_1(\lambda T_1)} \cdot \varphi(x_1 x_2)\, dx_1 \tag{60}$$

and

$$\psi'(x_2) = \int_{A_1'} \frac{a_1(\lambda T_1 i_1 a_1)}{E_1(\lambda T_1)} \cdot \varphi(x_1 x_2)\, dx_1\,; \tag{61}$$[1]

ψ and ψ' are straightforward generalisations of the function $\varphi(x_2)$ for emission and reflection, respectively. The definitions (52), (53), and (54) together with the definition of $\varphi(x_1 x_2)$ show that

$$\overline{\psi(x_2)} = \overline{\psi'(x_2)} = \overline{\varphi(x_2)} = \frac{A_1}{A_2}. \tag{62}$$

It is worth noticing that Christiansen's formula (2), perhaps modified in order to take into account a possible dependence of the reflectivity on wavelength and temperature, still holds for concentric spheres and coaxial cylinders, in which cases $\psi(x_2)$ and $\psi'(x_2)$ are constant. But $\psi(x_2)$ and $\psi'(x_2)$ are not necessarily constant in all cases where $\varphi(x_2)$ is so. They are not so, e. g., in the case treated on page 6 and 12, where the outer surface is a sphere and the inner body a disk covering the equatorial plane. In such cases Christiansen's formula therefore is only correct, if the inner body radiates according to the cosine law.

(c) Non-validity of the cosine law for the reflection from the outer surface.

The case which gives the largest deviation from the uncorrected formula (1) is the following: The system consists of two concentric spheres or coaxial cylinders of which the outer is reflecting specularly, Every ray which, coming from the inner

[1] If Helmholtz's reciprocity-law holds, then $\psi(x_2) \equiv \psi'(x_2)$.

surface, is reflected on the outer one, will then hit the inner surface again. If especially the reflectivities are independent of wavelength and temperature, and the absorptivities are independent of the angles, the reduction in loss of energy due to reflection must therefore be the same as if the inner body was closely surrounded by the outer one. We then get in place of (2)

$$H = \frac{A_1 \cdot c_1 \cdot (T_1^4 - T_2^4)}{1 + c_1 \left(\frac{1}{c_2} - \frac{1}{c_0} \right)}. \tag{63}$$

This formula is also due to Christiansen (footnote on page 4). It can easily be generalised to the case of wavelength- and temperature-dependent reflectivities.

As mentioned above, (63) is valid for concentric spheres and coaxial cylinders. But as soon as the spheres or cylinders are placed a little excentrically, or deformed somehow, the fraction of the reflected radiation that reenters on the inner surface will decrease considerably, and the loss of energy increases. It is worth noticing that the loss of energy in case of specular reflection is the smallest possible in the concentric position, while it is largest in this position if the reflection is diffuse. The formulae (2) and (63) give the maximum and minimum values of the loss of energy, while excentric position or unsymmetric form gives formulae like (18) lying between (2) and (63).

It will often be a good approximation to assume that the outer surface is reflecting a certain fraction s of the reflected radiation completely diffusely, while the rest — $(1 - s)$ — is reflected specularly. Furthermore we assume that s and the total reflectivity is independent of the angle of incidence. The heat transfer between concentric spheres or coaxial cylinders can then easily be calculated. Either (55), (56), and (57) may be used (for the outer surface we may put $(i\alpha \,|\, r_2 \,|\, i'\alpha') = \left(1 - \frac{c_2}{c_0}\right) \cdot \left\{ s + \frac{\pi \cdot (1-s)}{\sin i \cdot \cos i} \cdot \delta(i - i') \cdot \delta(\alpha - (\alpha' + \pi)) \right\}$, where $\delta(x - x')$ is Dirac's δ-function), or we may at once write down analogous equations for the total resulting radiation from the two surfaces. We only give the result in case the radiation constants are independent of wavelength and temperature and the absorptivity of the inner surface is independent of the angles:

$$H = A_1 c_1 (T_1^4 - T_2^4) \cdot \frac{s + (1-s) \cdot \frac{c_2}{c_0}}{s\left[1 + c_1\left(\frac{1}{c_2} - \frac{1}{c_0}\right) \cdot \frac{A_1}{A_2}\right] + (1-s) \cdot \frac{c_2}{c_0} \cdot \left[1 + c_1\left(\frac{1}{c_2} - \frac{1}{c_0}\right)\right]} \quad (64)$$

This shows that the heat transfer is nearer to the value for diffuse reflection, i. e. larger, than that obtained by simply adding expressions of the form (2) and (63) in the ratio s: $(1-s)$.

It has not been found possible to obtain a general formula in case of angle-dependent reflectivity of the outer surface.

(d) The temperature and emissivity of the outer body varies over the surface. Resulting radiation field within a closed cavity.

Let all assumptions made on page 3 be correct, except that T_2 and c_2 are functions of x_2.

We only treat the case of a very small inner body $\left(\frac{A_1}{A_2} \simeq 0\right)$ corresponding to the "zeroth" approximation (1). Consequently we must solve the equation for $I_2(x_2)$ without contributions from an inner body. For convenience we omit the index 2 in I_2, x_2, c_2, etc.:

$$I(x) = c(x) \cdot T(x)^4 + \left(1 - \frac{c(x)}{c_0}\right) \cdot \int_A I(x') \cdot \varphi(xx')\, dx' . \quad (65)$$

This equation is a straightforward generalisation of (4a) or specialisation of (56). If T is a constant, it has of course the solution $I(x) = c_0 T^4$ irrespective of the values of $c(x)$ and the form of the enclosure (black body radiation). In general, however, it can only be solved numerically, e. g. by replacing it by a number of linear equations corresponding to the required accuracy. If the cavity is a sphere, it can be solved exactly, for in this case we have $\varphi(xx') = \frac{1}{A}$, so that (65) takes the form

$$I(x) = c(x) \cdot T(x)^4 + \left(1 - \frac{c(x)}{c_0}\right) \cdot \bar{I} \quad (66)$$

where $\overline{I} = \frac{1}{A}\int_A I(x')\,dx'$ is the mean value of $I(x)$ over the surface. Taking mean values of the terms in (66), we get

$$\overline{I} = \overline{cT^4} + \left(1 - \frac{\overline{c}}{c_0}\right) \cdot \overline{I}, \tag{67}$$

whence

$$\overline{I} = c_0 \cdot \frac{\overline{cT^4}}{\overline{c}}, \tag{68}$$

which inserted in (66) leads to

$$I(x) = c_0 \cdot \frac{\overline{cT^4}}{\overline{c}} + c(x) \cdot \left[T(x)^4 - \frac{\overline{cT^4}}{\overline{c}}\right]. \tag{69}$$

From this result the heat exchange with a small body with uniform temperature T_1 and radiation constant c_1 can be calculated when the contributions from this body to the radiation field can be neglected $\left(\frac{A_1}{A_2} \simeq 0\right)$. By means of (69) and (5) page 5 we get instead of (1):

$$\left.\begin{aligned} H &= A_1 c_1 \left[T_1^4 - \frac{1}{c_0} \cdot \frac{\overline{I(x) \cdot \varphi(x)}}{\overline{\varphi(x)}}\right] = \\ &= A_1 \cdot c_1 \cdot \left[T_1^4 - \frac{\overline{cT^4}}{\overline{c}} - \frac{1}{c_0}\frac{\overline{cT^4\varphi}}{\overline{\varphi}} + \frac{1}{c_0} \cdot \frac{\overline{cT^4}}{\overline{c}} \cdot \frac{\overline{c\varphi}}{\overline{\varphi}}\right]. \end{aligned}\right\} \tag{70}$$

We may define a "resulting radiation temperature" T_0 of the sphere with respect to the small inner body as the uniform temperature which the sphere ought to have if it were black and were to exchange the same amount of heat as (70) with the inner body, i. e. we put

$$H_1 = A_1 c_1 (T_1^4 - T_0^4), \tag{71}$$

whence

$$T_0^4 = \frac{1}{c_0} \cdot \frac{\overline{I\varphi}}{\overline{\varphi}} = \frac{\overline{cT^4}}{\overline{c}} + \frac{1}{c_0} \cdot \frac{\overline{cT^4\varphi}}{\overline{\varphi}} - \frac{1}{c_0} \cdot \frac{\overline{cT^4}}{\overline{c}} \cdot \frac{\overline{c\varphi}}{\overline{\varphi}}. \tag{72}$$

This is strictly correct for a sphere and will probably be a good approximation in many other cases. If the temperature does not vary too much, it may be a sufficient approximation to use the temperatures in °C in (72) instead of the fourth powers of the absolute temperatures.

(e) Cavities in a surface.

A cavity the walls of which have a certain emissivity, may be replaced by a surface covering the cavity, but with another emissivity, which generally will vary over the surface and depend on the direction of emission. The method of integral equations can also be used to find this apparent emissivity.

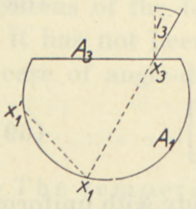

Fig. 7.

We assume that the walls of the cavity are reflecting diffusely and independently of wavelength, temperature, and direction. The radiation constant is c_1 and the uniform temperature T_1; the emitted intensity of radiation is then $\frac{1}{\pi} c_1 T_1^4$ in all directions. We are going to find the resulting radiation intensity $K_3(x_3 i_3 a_3)$ in an arbitrary point x_3 on the replacing surface A_3 and in an arbitrary direction (i_3, a_3) (cf. fig. 7). First, we have that the intensity sought for is equal to the resulting intensity from the corresponding point x_1 (cf. fig. 7):

$$K_3(x_3 i_3 a_3) = K_1(x_1) \tag{73}$$

$K_1(x_1)$ is independent of direction owing to the completely diffuse reflection and may be found from an integral equation expressing it as a sum of emitted and reflected radiation as usual:

$$K_1(x_1) = \frac{1}{\pi} c_1 T_1^4 + \left(1 - \frac{c_1}{c_0}\right) \cdot \int_{A_1} K_1(x_1') \cdot \varphi(x_1 x_1')\, dx_1' . \tag{74}$$

It is seen that only if the function

$$\varphi(x_1) = \int_{A_1} \varphi(x_1 x_1')\, dx_1' = 1 - \int_{A_3} \varphi(x_1 x_3)\, dx_3 \tag{75}$$

is independent of x_1, we find a constant value of $K_1(x_1)$, and only in this case, therefore, K_3 is independent of x_3 and the direction $(i_3 a_3)$.

If $\varphi(x_1)$ is constant, the value of it may be found, because

$$\int_{A_1} dx_1 \int_{A_3} \varphi(x_1 x_3)\, dx_3 = \int_{A_3} dx_3 \int_{A_1} \varphi(x_1 x_3)\, dx_1 = A_3 . \tag{76}$$

From this and (75) it follows that

$$\varphi(x_1) = 1 - \frac{A_3}{A_1}. \tag{77}$$

(In (76) it is assumed, that A_3 is plane.)
With this value of $\varphi(x_1)$, K_3 may be found from (73) and (74):

$$K_3 = K_1 = \frac{\frac{1}{\pi} \cdot c_1 \cdot T_1^4}{1 - \left(1 - \frac{c_1}{c_0}\right)\left(1 - \frac{A_3}{A_1}\right)}. \tag{78}$$

We define the apparent radiation constant c_3 by putting

$$K_3 = \frac{1}{\pi} c_3 T_1^4. \tag{79}$$

(79) and (78) then lead to

$$\frac{1}{c_3} = \frac{1}{c_1} \cdot \frac{A_3}{A_1} + \frac{1}{c_0}\left(1 - \frac{A_3}{A_1}\right). \tag{80}$$

It is seen that $c_3 \to c_0$, if $\frac{A_3}{A_1} \to 0$, as it must, because we then get an artificial "black body".

If $\varphi(x_1)$ is not constant, (74) may be solved numerically or by iteration. $\varphi(x_1)$ is constant, if the cavity is a spherical cap (cf. page 12). If the distance from the centre of the sphere with radius R to the plane A_3 is $p \cdot R$ (p positive to the interior of the cavity), we get $\frac{A_3}{A_1} = \frac{1+p}{2}$, whence

$$\frac{1}{c_3} = \frac{1}{c_1} \cdot \frac{1+p}{2} + \frac{1}{c_0} \cdot \frac{1-p}{2} \qquad (-1 < p < 1). \tag{81}$$

The results and methods used in this section and section *d* may be useful in estimating the deviations of the radiation from a cavity from black body radiation.

Summary. The net loss of energy suffered by a radiating body entirely surrounded by another body of different temperature is investigated with special respect to its dependence on the form and mutual position of the bodies. Integral equations are given which determine the heat transfer ((3), (4a), and (5) for

"grey" radiation, and (55), (56), and (57) in the general case). The equations for "grey" radiation are solved approximately and a formula for the heat transfer is given — (18) — and applied to several examples. The radiation between surfaces which are not grey is treated in some special cases. On page 22 (section *d*) the case of variation in temperature on the outer body is treated, and formulae for the radiation field inside a sphere and for the heat exchange with a small body inside a sphere are obtained (formulae (69) — (72)). Finally, in section (*e*), page 24, equations determining the apparent emissivity of a cavity are obtained and solved for a cavity shaped as a spherical cap.

The methods and results may be of some interest in the heating technique, the illumination technique, and optical pyrometry.

The author wants to express his thanks to Professor T. Bjerge, Professor F. Becker, and cand. polyt. V. Korsgaard for helpful suggestions and discussions.

Danmarks tekniske Højskoles fysiske Samling.

Indleveret til Selskabet den 3. Februar 1947.
Færdig fra Trykkeriet den 4. Februar 1948.

DET KGL. DANSKE VIDENSKABERNES SELSKAB
MATEMATISK-FYSISKE MEDDELELSER, BIND XXIV, NR. 9

SPECTROSCOPY AND THERMODYNAMICS

I.
MOMENTS OF INERTIA OF METHYL BROMIDE

II.
EQUILIBRIUM CONSTANTS OF THE REACTION
$CH_3Br + HCl \rightleftarrows CH_3Cl + HBr$
MOMENTS OF INERTIA OF METHYL BROMIDE

BY

B. BAK

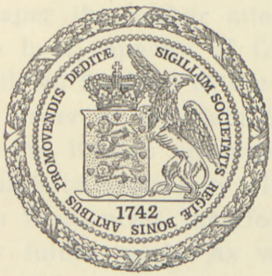

KØBENHAVN
I KOMMISSION HOS EJNAR MUNKSGAARD
1948

CONTENTS

Page

I.

II.

Printed in Denmark.
Bianco Lunos Bogtrykkeri.

I. MOMENTS OF INERTIA OF METHYL BROMIDE

I. Introduction.

In recent years, the application of quantum mechanics to chemical questions has proved especially fruitful in the treatment of problems which hitherto could only be dealt with correctly from a purely thermodynamical point of view, such as the determination of standard entropies, chemical affinities, etc. As quantum mechanics mainly work with symbols to be experimentally determined by means of spectroscopical methods, a near relationship between spectroscopy and thermodynamics has been established.

A survey of the work accomplished within this common field of spectroscopy and thermodynamics up to 1936 was given by KASSEL.[1] It is a striking fact that most of the compounds investigated are simple inorganic molecules, and the development of the last ten years has hardly altered the situation. This is due partly to the restrictions laid upon the experimentator when working with unstable organic molecules, partly, as will be pointed out later, to theoretical difficulties arising when the more complex organic molecules are treated.

In the present paper the author attempts to combine the determination of the heat capacity of CH_3Br, carried out by EGAN and KEMP,[2] with an analysis of the optical spectra of the same compound. In order to ascertain the correctness of the vibrational analysis, the Raman spectrum of CH_3Br was reinvestigated. Our result is in conformity with the results obtained earlier. The vibration frequencies, therefore, can only be unessentially changed by future work. As will be shown in the present paper, the combination of thermodynamical and spectroscopical data leads to definite values of the moments of inertia of CH_3Br.

[1] KASSEL, Chem. Rev. **18**, 277 (1936).
[2] EGAN and KEMP, J. Am. Chem. Soc. **60**, 2097 (1938).

II. Entropy in Terms of Spectroscopically Determinable Quantities.

The fundamental equations were coherently published by GIAUQUE.[1] The general expression for the absolute entropy of one mole of an *ideal gas*, S°, is:

$$S^\circ = S^\circ_{trans} + R\left(\ln Z + T\frac{d\ln Z}{dT}\right). \qquad (I)$$

Here, R is the gas constant, T the absolute temperature, and S°_{trans} the translational entropy.[2] Z is the so-called 'state sum'. For an ideal gas the individual molecule has a well-defined ground state, a first excited level, etc., unquantized translational energy being neglected. The separation of the translational energy from the quantized vibrational-rotational energy is correct for the ideal gas state because, in the field-free space, the part of the Schroedinger equation dealing with the translational movement of the molecule, factors out.[3] In Table I a survey of present circumstances is taken.

Table 1.

State	Energy minus translational energy	A priori probality of state	Number of molecules in state
Ground State	ε'	p_0	Ap_0
1. excited level.....	$\varepsilon'_0 + \varepsilon_1$	p_1	$Ap_1 e^{\frac{-\varepsilon_1}{kT}}$
2. excited level.....	$\varepsilon'_0 + \varepsilon_2$	p_2	$Ap_2 e^{\frac{-\varepsilon_2}{kT}}$
. . ..	.	.	.
i. excited level	$\varepsilon'_0 + \varepsilon_i$	p_i	$Ap_i e^{\frac{-\varepsilon_i}{kT}}$
. . ..	.	.	.

If the total number of molecules is denoted by N, we obtain:

$$N = A\left(p_0 + \sum_{i=1}^{\infty} p_i e^{\frac{-\varepsilon_i}{kT}}\right). \qquad Z = p_0 + \sum_{i=1}^{\infty} p_i e^{\frac{-\varepsilon_i}{kT}}.$$

[1] GIAUQUE, J. Am. Chem. Soc. **52**, 4808 (1930).

[2] The subscript zero applies to the ideal state throughout this and the following paper.

[3] KASSEL, Chem. Rev. **18**, 279 (1936).

Within this field most rules are conveniently formulated by means of Z, as for example in (I). It should, however, be kept in mind that the state sum is sometimes defined as $Z = \sum_{i=0}^{\infty} p_i e^{\frac{-(\varepsilon_i + \varepsilon_0')}{kT}}$, where ε_0 is zero. This is done e. g. in the important paper by GORDON and BARNES.[1] As is seen from the papers cited,

$$Z \text{ (Giauque)} = e^{\frac{\varepsilon_0'}{kT}} Z \text{ (Gordon and Barnes)}.$$

However, Giauque's definition seems to be more commonly used.

For the ideal gas state

$$S^\circ_{trans} = \frac{3}{2} R \ln M + \frac{5}{2} R \ln T - R \ln P + \frac{5}{2} R + C + R \ln R'.$$

Here, M is the molecular weight proportional to oxygen, P the pressure in atmospheres, R′ the gas constant in ccm atmospheres per degree and $C = R \ln \cdot \frac{(2\pi k)^{3/2}}{h^3 N^{5/2}}$, where k is Boltzmann's constant, h Planck's constant and N is Avogadro's number. Thus, for one mole of an ideal gas

$$\left.\begin{aligned} S^\circ = \frac{3}{2} R \ln M + \frac{5}{2} R \ln T - R \ln P + \frac{5}{2} R + C + R \ln R' + \\ + R \left(\ln Z + T \frac{d \ln Z}{dT} \right). \end{aligned}\right\} \quad \text{(II)}$$

Let us now try to find the special form for (II) in the case of CH_3Br by following the approximations step by step.

As a first approximation let us assume that no molecules are in a state of electronic excitation. This is practically true for most molecules up to ca. 1500°, because the available kinetic energy per degree of freedom at 0° C is ~ 100 cm^{-1} while the electronic excitation energy is 10000—100000 cm^{-1}.

Furthermore, in the case of CH_3Br, p_0, the a priori probability of the electronic ground level, is 1. Hence

[1] GORDON and BARNES, J. Chem. Phys. 1, 298 (1933).

$$Z = 1 + \sum_{i=1}^{\infty} p_i e^{\frac{-\varepsilon_i}{kT}},$$

where ε now simply means the height of one of the vibrational-rotational levels above the ground level. By defining $\varepsilon_0 = 0$ we may write:

$$Z = \sum_{i=0}^{\infty} p_i e^{\frac{-\varepsilon_i}{kT}},$$

where p_0 is equal to 1.

Generally, the vibrational and rotational energies of a molecule vary almost independently of each other. However, special interest will be paid to the case where they are completely independent. The correctness of this assumption will be discussed later. The assumption means that each ε_i can be written as $\varepsilon_n\,(\text{vib}) + \varepsilon_j\,(\text{rot})$, defining $\varepsilon_0\,(\text{vib}) = \varepsilon_0\,(\text{rot}) = 0$. To every fixed value of $\varepsilon_n\,(\text{vib})$ belongs the same series of rotational levels $\varepsilon_0\,(\text{rot})$, $\varepsilon_1\,(\text{rot})$, $\varepsilon_2\,(\text{rot})\cdots$, superposed on the vibrational level. Simultaneously, p can be written as $p_n\,(\text{vib})\cdot p_j\,(\text{rot})$, because of the independence of the a priori probabilities of the vibrational and the rotational states. As $p_0\,(\text{vib}) = p_0\,(\text{rot}) = 1$ we get:

$$Z = \sum_{i=0}^{\infty} p_i e^{\frac{-\varepsilon_i}{kT}} = \sum_{n=0}^{\infty} \sum_{j=0}^{\infty} p_n\,(\text{vib})\, p_j\,(\text{rot})\, e^{\frac{-\varepsilon_n(\text{vib}) - \varepsilon_j(\text{rot})}{kT}} =$$

$$= \sum_{n=0}^{\infty} p_n\,(\text{vib})\, e^{\frac{-\varepsilon_n(\text{vib})}{kT}} \sum_{j=0}^{\infty} p_j\,(\text{rot})\, e^{\frac{-\varepsilon_j(\text{rot})}{kT}} = Z_{\text{vib}} \cdot Z_{\text{rot}}.$$

The entropy expression (I), therefore, is changed into

$$S^\circ = S^\circ_{\text{trans}} + S^\circ_{\text{vib}} + S^\circ_{\text{rot}}. \qquad \text{(III)}$$

a. Calculation of the vibrational entropy.

Here the simplifying assumption will be made that the molecules of the system perform harmonic vibrations. For a diatomic molecule, with only one vibration frequency, the vibrational energy diagram is considered to consist of a series

of equidistant levels instead of the actually occurring converging ones.

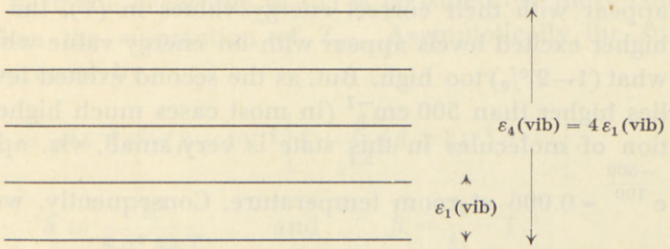

Fig. 1.

Fig. 1 is the energy diagram for a harmonic oscillator with one degree of freedom. $\varepsilon_i(\text{vib}) = i \cdot \varepsilon_1(\text{vib})$. The a priori probability of each level is 1. Therefore

$$Z\,(\text{vib., diatomic molecule}) = \sum_{i=0}^{\infty} e^{\frac{-\varepsilon_i(\text{vib})}{kT}} = \frac{1}{1 - e^{\frac{-\varepsilon_1(\text{vib})}{kT}}}.$$

If, moreover, we imagine a molecule with two vibrational degrees of freedom, an energy pattern like that shown in fig. 1 (but with a different distance between adjacent levels) must be superposed on each of the levels of fig. 1. Thus, when calculating Z_{vib}, the situation is completely analogous to that described earlier, which permitted the rotational state sum Z_{rot} to be factored out from the combined $Z_{rot+vib}$: each vibrational level is superposed with the same series of other vibrational levels. Consequently, in the case of two vibrational degrees of freedom, Z_{vib} consists of two factors, each of the form stated for the diatomic molecule. Generally, for a molecule with n atoms, possessing $3n-6$ vibrational degrees of freedom, corresponding to $3n-6$ fundamental frequencies ν_f, where $h\nu_f = \varepsilon_f$, we get:

$$Z_{vib} = \prod_{1}^{3n-6} \frac{1}{1 - e^{\frac{-\varepsilon_f}{kT}}} \qquad (1)$$

If ν_f is a double degenerate frequency, e. g. $\nu_f = \nu_{f+1}$, the same factor appears twice in (1); if ν_f is threefold degenerate, the same factor appears three times, etc.

The approximation made by assuming harmonic vibrations is mostly very good. The ground level and the first excited level appear with their correct energy values in (1), the second and higher excited levels appear with an energy value which is somewhat (1—2 %) too high. But, as the second excited level generally lies higher than 500 cm^{-1} (in most cases much higher), the fraction of molecules in this state is very small, viz. approximately $e^{\frac{-500}{100}} \sim 0.006$ at room temperature. Consequently, we may write

$$S^{\circ}_{vib} = R \sum_{f=1}^{f=3n-6} \left(\frac{\frac{\varepsilon_f}{kT}}{e^{\frac{\varepsilon_f}{kT}} - 1} - \ln\left(1 - e^{\frac{-\varepsilon_f}{kT}}\right) \right).$$

$\frac{\frac{\varepsilon_f}{kT}}{e^{\frac{\varepsilon_f}{kT}} - 1} - \ln\left(1 - e^{-\frac{\varepsilon_f}{kT}}\right)$ is often abbreviated as $S_{Ein}(\nu_f, T)$.

We then obtain:

$$S^{\circ}_{vib} = R \sum_{f=1}^{f=3n-6} S_{Ein}(\nu_f, T).$$

b. Calculation of the rotational entropy.

$$Z_{rot} = \sum_{j=0}^{\infty} p_j(rot)\, e^{\frac{-\varepsilon_j(rot)}{kT}}$$

A common expression valid for all types of molecules; e. g. at room temperature, cannot be given. For small molecules a direct summation generally pays (H_2, HF). For larger molecules, such as CH_3Br, approximate formulas have been developed. CH_3Br has two different principal moments of inertia, A and C. If C be the moment of inertia around the C-Br axis,

$$\varepsilon_j(rot) = \frac{h^2}{8\pi^2 A}\left[k(k+1) + n^2\left(\frac{A}{C} - 1\right)\right] \qquad |n| \leq k.$$

k and n are the integral quantum numbers. For a state with quantum numbers n, k the a priori weight is $2k+1$. The summation to be made according to (2) is considerably more complicated than the summation of Z_{vib}. Asymptotically the sum can be expressed by

$$Z = \pi^{\frac{1}{2}}\delta^{-\frac{3}{2}} e^{\delta/4}(\beta+1)^{-\frac{1}{2}}\left[1+\frac{\beta}{12}(\beta+1)^{-1}\delta\cdots\right],$$

where $\delta = \dfrac{h^2}{8\pi^2 AkT}$ and $\beta = \dfrac{A}{C} - 1$.[1]

In the case of CH_3Br the expression in the square brackets in good approximation is equal to 1. As $A \sim 10^{-38}$ gcm² we get $\delta \sim \dfrac{40\cdot 10^{-54}}{8\cdot 10\cdot 10^{-38}\cdot 1.4\cdot 10^{-16}\cdot T} \sim \dfrac{1}{2.8\,T}$. $A/C \sim 15$. Thus $\beta \sim 14$ and $\dfrac{\beta}{12}(\beta+1)^{-1}\delta \sim \dfrac{1}{40\,T}$. At 100° K this is less than 0.001 and can safely be neglected.

$e^{\delta/4} \sim e^{\frac{1}{11\,T}}$. At 100° K this is approximately 0.001. Consequently, in good approximation we have

$$Z_{rot} = \pi^{\frac{1}{2}}\delta^{-\frac{3}{2}}(\beta+1)^{-\frac{1}{2}} \quad \text{and} \quad S^\circ_{rot} = R\ln\cdot\left[\frac{8\pi^{\frac{7}{3}}A^{\frac{2}{3}}C^{\frac{1}{3}}kTe}{h^2}\right]^{\frac{3}{2}}.$$

Finally,

$$S^\circ = S^\circ_{trans} + S^\circ_{vib} + S^\circ_{rot} = R\left[\frac{3}{2}\ln M + \frac{5}{2}\ln T - \ln P + \frac{5}{2} + \right.$$

$$\left. + \frac{C}{R} + \ln R' + \sum_{f=1}^{3n-6} S_{Ein}(\nu_f, T) + \ln\left(\frac{8\pi^{\frac{7}{3}}A^{\frac{2}{3}}C^{\frac{1}{3}}kTe}{h^2}\right)^{\frac{3}{2}}\right].$$

Looking more closely into the matter and taking into consideration the possible presence of spin isomers, optical isomers, and a possible multiplicity of the electronic ground state differing from unity, we find:

[1] KASSEL, loc. cit.

$$S^\circ = R\left[\frac{3}{2}\ln M + \frac{5}{2}\ln T - \ln P + \frac{5}{2} + \frac{C}{R} + \ln R' + \right.$$
$$\left. + \sum_{f=1}^{f=3n-6} S_{Ein}(\nu_f, T) + \ln\left(\frac{8\pi^{\frac{7}{3}} A^{\frac{2}{3}} C^{\frac{1}{3}} kTe}{h^2}\right)^{\frac{3}{2}} \frac{p_e p_n I}{\sigma}\right]. \qquad \text{(IV)}$$

Here, p_e is the a priori probability of the electronic ground state (= 1 for CH_3Br), p_n is the number of nuclear spin isomers, I is the number of optical isomers (= 1 for CH_3Br), and σ is the 'symmetry number', equal to the number of permutations of identical atoms in a single molecule which could be carried out by rotating the molecule (= 3 for CH_3Br). The number p_n is unknown for the molecule in question, which means that the absolute entropy given by (IV) cannot be calculated. However, most entropy determinations are carried through at temperatures between a few degrees above the absolute zero and room temperature. As in all cases the calorimetric effect of the presence of spin isomers is detectable only in the immediate neighbourhood of 0° K, this means that such effects are not included in the experimentally determined entropy values. These experimental values may, therefore, be put equal to S, calculated from (IV), putting $p_n = 1$.

In this connexion it is worth mentioning that in the calculation of equilibrium constants for chemical reactions above 100° K all nuclear spin effects can be ignored[1].

Defining $A' = A \cdot 10^{38}$ and $C' = C \cdot 10^{38}$, and using the usual numerical values for the natural constants, we get the formula:

$$S^\circ = R\left[2.307 + 4\ln T + \frac{3}{2}\ln M + 1/2\ln A'^2 C' + \right.$$
$$\left. + \ln\frac{p_e n_n I}{\sigma} + \sum_{f=1}^{f=3n-6} S_{Ein}(\nu_f, T)\right], \qquad \text{(V)}$$

valid for the entropy of one mole in the ideal gas state at a pressure of one atmosphere.

[1] Gibson and Heitler, Z. Phys. **49**, 465 (1928).

III. Moments of Inertia of Methyl Bromide.

a. Application of the calorimetric data of Egan and Kemp.

Egan and Kemp (loc. cit.) determined the entropy of CH_3Br-gas in the ideal state at 1 atm. and 276°.66 K (the boiling point) to 57.86 cal. deg.$^{-1}$ mol.$^{-1}$. They estimated the values of A′ and C′, using the data of Levy and Brockway[1] for the C-Br distance (1.91 ± 0.06 Å) and taking C-H equal to 1.09 Å and < H-C-H = 111°. These values correspond to $A = 85.3\ 10^{-40}$ gcm^2 and $C = 5.36\ 10^{-40}$ gcm^2. Inserting A and C into (V) together with the known vibration frequencies, T, M, and σ (= 3), they calculated the entropy per mole CH_3Br in the ideal gas state at 276°.66 K to 57.99 cal. deg.$^{-1}$. Thus, good agreement between the calculated and the experimentally determined entropy was found.

In the present paper, however, we wish to reverse matters, e. g. exactly to determine the contribution of Egan and Kemp's calorimetric data to our knowledge of the dimensions of the CH_3Br-molecule. As is seen from (V), the calorimetric data determine the product $A'^2 C'$. By combining the value found with spectroscopic results, the best possible values for the moments of inertia of CH_3Br are obtained. These figures will be applied in a paper to be published later.

From (V) we obtain:

$$1/2 \ln A'^2 C' = \frac{57.86}{R} + \ln 3 - \left(2.307 + 4 \ln T + \frac{3}{2} \ln M + \right.$$

$$\left. + \sum_{f=1}^{3n-6}{}' S_{Ein}(\nu_f, T) \right).$$

The uncertainty of the value 57.86 is ± 0.1, all other figures are known to be practically exact. This means that

$$A^2 \cdot C = 33400\ 10^{-120} g^3 cm^6 \pm 10\ \%. \qquad (V')$$

[1] J. Am. Chem. Soc. **59**, 1662 (1937).

b. Application of the structure of infrared bands.

In 1928, BENNETT and MAYER have studied the infrared absorption spectrum of gaseous CH_3Br.[1] Parallel bands ($\parallel$) were found at 610, 1305 and 2972 cm^{-1}, perpendicular bands ($\perp$) at 956.9, 1450.5 and 3061.5 cm^{-1}. A study of the structure of these bands gives us some information on the size of the molecule.

From the structure of the $\parallel$ bands the absorption maxima of the P- and R-branches could be determined. The distance between the absorption maxima of a single band is called the doublet separation and is denoted by $\delta\nu$. GERHARD and DENNISON[2] have demonstrated that

$$\delta\nu = \frac{S}{\pi}\sqrt{\frac{kT}{A}} \qquad \log_{10} S = \frac{0.721}{\left(\frac{A}{C}+3\right)^{1.13}}. \qquad \text{(VI)}$$

$\delta\nu$ is ~ 25 cm^{-1} and could only be measured with an accuracy of ~ 2—3 cm^{-1}.

Therefore the average of the following results is taken.

Doublet separation cm^{-1}.

BENNET and MAYER[3]	25	23	23
MOORHEAD[4]	26	25	24
SLEATOR[5]		26	
BARKER and NIELSEN[6]		27.5	

As an average value is used $\delta\nu = 25.0$ $cm^{-1} \pm 1.0$.

The $\perp$ bands show a rotational fine structure which was resolved by BENNETT and MAYER (loc. cit.). The fine structure is found to be more complicated than usual since the $\perp$ vibrational levels are double-degenerate; this means that an interaction between rotational and vibrational movements takes place, disturb-

[1] Phys. Rev. **32**, 888 (1928).
[2] GERHARD and DENNISON, Phys. Rev. **43**, 197 (1933).
[3] BENNETT and MEYER, loc. cit.
[4] MOORHEAD, Phys. Rev. **39**, 788 (1932).
[5] SLEATOR, Phys. Rev. **38**, 147 (1932).
[6] BARKER and NIELSEN, Phys. Rev. **46**, 970 (1934).

ing the usual regularity of the bands. However, DENNISON and JOHNSTON[1] assuming harmonic vibrations, showed that

$$\sum_1^3 \Delta\nu = \frac{h}{4\pi^2}\left(\frac{3}{C} - \frac{7}{2A}\right), \qquad \text{(VII)}$$

where $\Delta\nu$ is the average line spacing within one of the $\perp$ bands, and $\sum_1^3 \Delta\nu$ is the sum of the average values of all three $\perp$ bands. (VII) mainly determines C, because $A \sim 15\ C$. For a given A, DENNISON and JOHNSTON (loc. cit.) estimated that C may be found with an error of about 5 %.

c. Numerical calculations.

From (VII) it is seen that only a rough knowledge of A is necessary to obtain a good value of C. Using $A = 85 \cdot 10^{-40}$ gcm^2 in accordance with EGAN and KEMP, we obtain

$$C = 5.42\ 10^{-40}\ \text{gcm}^2 \pm 5\ \%.$$

An error of 10 % in the value assumed for A, only changes C by 1 %. The calculation is carried through on the basis of $\sum_1^3 \Delta\nu = 28.32\ \text{cm}^{-1}$ from the paper of BENNETT and MAYER (loc. cit.).

Now, by inserting $C = 5.42\ 10^{-40}$ in (V′) and (VI) we get two values of A. Substituting C in (V′) and allowing for an error of 5 % in C and 10 % in the calorimetric A^2C-value we find

$$A = 78 \cdot 10^{-40}\ \text{gcm}^2 \pm 8\ \%.$$

Inserting $C = 5.42 \cdot 10^{-40}$ in (VI), it is seen at once that, as $A/C \sim 15$, $S \sim 1.065$. If C changes by 5 %, S becomes 1.070, *viz.* a change in C within the experimentally permissible limits is of negligible effect on S. Thus, the error of A simply is about twice the error of $\delta\nu$. Consequently we get:

$$A = 82 \cdot 10^{-40}\ \text{gcm}^2 \pm 10\ \%.$$

[1] DENNISON and JOHNSTON, Phys. Rev. **48**, 868 (1935).

According to the above-mentioned results the value of A, equally well consistent with calorimetric and with spectroscopic data, is then

$$A = 80 \cdot 10^{-40} \text{ gcm}^2 \pm 6\ \%.$$

In the calculation of $A = 82 \cdot 10^{-40}$ gcm^2 by means of (VI) and (VII) due regard was paid to the interdependence of rotational and vibrational energies. In using (VII) and (V′) which leads to $A = 78 \cdot 10^{-40}$ gcm^2, this interdependence is partly ignored. The fact that almost the same values of A are obtained supports the view that the approximation made in formulating (V) is rather good.

VI. Summary.

(1) The expression for the entropy of 1 mole of CH_3Br in the ideal gas state is considered and the derivation from more general expressions is discussed.

(2) The calorimetric data given by Egan and Kemp are applied to find the product A^2C. The infrared measurements of Bennett and Meyer are used to calculate the value of C. Combining calorimetric and spectroscopic data $A = 78 \cdot 10^{-40}$ gcm^2 (± 8 per cent) and $C = 5.42 \cdot 10^{-40}$ gcm^2 (± 5 per cent) is obtained.

Infrared measurements by Bennett and Meyer, Moorhead, Sleator, Barker and Nielsen permit the calculation of $A = 82 \cdot 10^{-40}$ gcm^2 (± 10 per cent) on a purely spectroscopical basis.

(3) A value for A, equally well consistent with spectroscopical and heat capacity measurements, is $80 \cdot 10^{-40}$ gcm^2.

Universitetets kemiske Laboratorium.
Copenhagen.

II. EQUILIBRIUM CONSTANTS OF THE REACTION $CH_3Br + HCl \rightleftarrows CH_3Cl + HBr$ MOMENTS OF INERTIA OF METHYL BROMIDE

I. Introduction.

In a previous paper by the present author[1] the formula

$$S^\circ = R\left[2.307 + 4\ln T + \frac{3}{2}\ln M + \frac{1}{2}\ln A'^2C' + \ln\frac{P_e P_n I}{\sigma} + \sum_{f=1}^{3n-6} S_{Ein}(\nu_f, T)\right] \quad (I)$$

was shown to be valid in a large temperature interval (100°—1000° K) for the entropy of one mole of CH_3Br-gas in the ideal state at 1 atm. It was demonstrated how the measurements of heat capacity by EGAN and KEMP[2] can be used for finding the product A'^2C'. In the present paper it is shown how A' can be determined by measuring another thermodynamical quantity, *viz.* the equilibrium constant of the reaction

$$CH_3Br + HCl \rightleftarrows CH_3Cl + HBr$$

at various temperatures, the final calculation of A' being based upon the equilibrium constants of the above reaction and spectroscopical data available in the literature.

For the most convenient formulation of the problem (I) is combined with the general thermodynamical relation

$$G = E - TS + pV, \quad (1)$$

where the thermodynamical potential G, is defined as a function of the internal energy E, the absolute temperature T, the entropy

[1] D. Kgl. Danske Vidensk. Selskab, Mat.-fys. Medd. XXIV, 9. Here cited as (S-TI).

[2] J. Am. Chem. Soc. **60**, 2097 (1938).

S, the pressure p, and the volume V. As only ideal gases are considered $pV = RT$. Furthermore, $E^\circ = E_0^\circ + \frac{3}{2}RT + RT^2\frac{d\ln \cdot Z}{dT}$, where E_0° is the internal energy at the absolute zero, $\frac{3}{2}RT$ is the translational energy, and the last term is the energy due to all other degrees of freedom (electronic, vibrational, etc.). This equation is easy to derive by means of Table I, (S-TI). Substituting for E° in (1) we get

$$G^\circ = E_0^\circ + \frac{5}{2}RT - TS^\circ + RT^2\frac{d\ln Z}{dT}. \qquad (2)$$

As already shown (S-TI), Z can be written as $Z_{vib} \cdot Z_{rot}$, which means that

$$\frac{d\ln Z}{dT} = \frac{d\ln Z_{vib}}{dT} + \frac{d\ln Z_{rot}}{dT}.$$

But

$$RT^2\frac{d\ln Z_{vib}}{dT} = RT\sum_{f=1}^{3n-6}\frac{\frac{\varepsilon_f}{kT}}{e^{\frac{\varepsilon_f}{kT}}-1} \quad \text{and} \quad RT^2\frac{d\ln Z_{rot}}{dT} = \frac{3}{2}RT.$$

Substituting for Z in (2) we get

$$\frac{G^\circ - E_0^\circ}{T} = R\left[4 - \frac{S^\circ}{R} + \sum_{f=1}^{3n-6}\frac{\frac{\varepsilon_f}{kT}}{e^{\frac{\varepsilon_f}{kT}}-1}\right]. \qquad (3)$$

Introducing the value of S given by (I) we derive

$$\left.\begin{aligned}\frac{G^\circ - E_0^\circ}{T} = R\Bigg[1.694 - 4\ln T - \frac{3}{2}\ln M - \frac{1}{2}\ln A'^2C' + \\ + \ln 3 + \sum_{f=1}^{3n-6}\ln\left(1 - e^{\frac{-\varepsilon_f}{kT}}\right)\Bigg].\end{aligned}\right\} \qquad (4)$$

Now, we want to form $\Delta\frac{G^\circ - E_0^\circ}{T}$ for the reaction $CH_3Br + HCl = CH_3Cl + HBr$. The part of the function originating from the conversion of CH_3Br into CH_3Cl is easily seen to be

$$R\left[\frac{3}{2}\ln\frac{M(CH_3Br)}{M(CH_3Cl)}+\ln\frac{A'(CH_3Br)}{A'(CH_3Cl)}+\right.$$
$$\left.+\sum_{f=1}^{3n-6}{}_{(CH_3Cl)}\ln\left(1-e^{\frac{-\varepsilon_f}{kT}}\right)-\sum_{f=1}^{3n-6}{}_{(CH_3Br)}\ln\left(1-e^{\frac{-\varepsilon_f}{kT}}\right)\right]. \quad (5)$$

Here, $M(CH_3Y)$ is the molecular weight of the molecule CH_3Y, and $A'(CH_3Y)$ is $10^{38}\times$ the moment of inertia of the molecule with respect to an axis perpendicular to the C—Y bond through the centre of gravity. The term

$$\ln\cdot\frac{C'(CH_3Br)}{C'(CH_3Cl)}$$

has been put equal to zero. Experimentally $C'(CH_3Br)$ was found to be 0.0542, viz. the same as for CH_4.[1] Using the same experimental method, $C'(CH_3Cl)$ is found to be 0.0544. However, both values have an uncertainty of 5 per cent, but the deviations from $C'(CH_4)$ must have the same sign and be very nearly equal. Thus $C'(CH_3Br) = C'(CH_3Cl)$.

The part of the function $\Delta\frac{G^\circ-E_0^\circ}{T}$ originating from the conversion of HCl into HBr is found from tables available in the literature.[2] In Table I values of $-\frac{G^\circ-E_0^\circ}{T}$ for HBr and HCl are given.

Table I.

Values of $-\frac{G^\circ-E_0^\circ}{T}$ for HBr and HCl.

(cal. deg.$^{-1}$ mole^{-1})

Abs. temp....	250	300	400	500	600	700	800	900	1000
HBr	39.330	40.594	42.589	44.139	45.409	46.487	47.426	48.259	49.019
HCl.....	36.487	37.778	39.771	41.321	42.588	43.663	44.597	45.425	46.171
Difference ...	2.843	2.816	2.818	2.818	2.821	2.824	2.829	2.834	2.839

[1] S-T I, p. 9—10.

[2] Gordon and Barnes, Journ. Chem. Phys. (1), 692 (1933); Giauque, J. Am. Chem. Soc. **54**, 1731 (1932).

The equilibrium in question was studied in the temperature interval 350° K—600° K. Table I shows that in this interval $\Delta \frac{G^\circ - E_0^\circ}{T}$ originating from HCl → HBr can with good approximation be put equal to -2.819 cal. deg.$^{-1}$ mole^{-1}.

Consequently we get for the reaction $CH_3Br + HCl \rightarrow CH_3Cl + HBr$

$$\left.\begin{aligned}\Delta \frac{G^\circ - E_0^\circ}{T} = R\left[\frac{3}{2}\ln\frac{M(CH_3Br)}{M(CH_3Cl)} + \ln\frac{A'(CH_3Br)}{A'(CH_3Cl)} + \right.\\ \left. + \sum_{f=1}^{3n-6}\ln\left(1-e^{\frac{-\varepsilon_f}{kT}}\right)_{(CH_3Cl)} - \sum_{f=1}^{3n-6}\ln\left(1-e^{\frac{-\varepsilon_f}{kT}}\right)_{(CH_3Br)} - \frac{2.819}{R}\right].\end{aligned}\right\} \quad (6)$$

The general relation between the ΔG of a given reaction and the equilibrium constant for the corresponding equilibrium is

$$\Delta G = -RT\ln k,$$

where k or k (T), as it will often be written, is the thermodynamic equilibrium constant. Combining this relation with (6) we get

$$\left.\begin{aligned}k(T) = \left(\frac{M(CH_3Cl)}{M(CH_3Br)}\right)^{3/2}\frac{A'(CH_3Cl)}{A'(CH_3Br)}\frac{\prod_{f=1}^{3n-6}\left(1-e^{\frac{-\varepsilon_f}{kT}}\right)_{CH_3Br}}{\prod_{f=1}^{3n-6}\left(1-e^{\frac{-\varepsilon_f}{kT}}\right)_{CH_3Cl}} e^{\frac{2.819}{R}-\frac{\Delta E_0^\circ}{RT}}.\end{aligned}\right\} \quad (7)$$

If the equilibrium constants at two different temperatures are known, the knowledge of the quantity ΔE_0° is unnecessary for our purpose (8):

$$\left.\begin{aligned}\frac{k(T_1)^{\frac{T_1}{T_1-T_2}}}{k(T_2)^{\frac{T_2}{T_1-T_2}}} = e^{\frac{2.819}{R}}\left(\frac{M(CH_3Cl)}{M(CH_3Br)}\right)^{3/2}\frac{A'(CH_3Cl)}{A'(CH_3Br)}\cdot\\ \cdot\left[\frac{\prod_{f=1}^{3n-6}\left(1-e^{\frac{-\varepsilon_f}{kT_1}}\right)_{CH_3Br}}{\prod_{f=1}^{3n-6}\left(1-e^{\frac{-\varepsilon_f}{kT_1}}\right)_{CH_3Cl}}\right]^{\frac{T_1}{T_1-T_2}}\left[\frac{\prod_{f=1}^{3n-6}\left(1-e^{\frac{-\varepsilon_f}{kT_2}}\right)_{CH_3Cl}}{\prod_{f=1}^{3n-6}\left(1-e^{\frac{-\varepsilon_f}{kT_2}}\right)_{CH_3Br}}\right]^{\frac{T_2}{T_1-T_2}}\end{aligned}\right\} \quad (8)$$

Thus, by means of equilibrium data and spectroscopical data the ratio

$$\frac{A'(CH_3Cl)}{A'(CH_3Br)}$$

can be calculated. From the fairly accurate value of $A'(CH_3Cl)$, known from work in the infrared by NIELSEN,[1] $A'(CH_3Br)$ can be calculated.[2]

II. Experimental Determination of the Equilibrium Constant at Different Temperatures.

a. Preparation of CH_3Br.

Commercial bromine was freed from chlorine by being kept 24 hours in contact with an aqueous solution of KBr under shaking at intervals. Subsequently the bromine was distilled off and reduced to HBr by means of SO_2 in the usual way, a constantly boiling hydrobromic acid being prepared. By heating the hydrobromic acid to 70° C and adding methyl alcohol a gentle evolution of gaseous CH_3Br is obtained. The gas is fractionated through a column, jacketed with water, at 5° C, led through 3 wash-bottles with water and 3 with concentrated sulphuric acid and is finally condensed. Its purity was checked by its Raman spectrum. Since the spectrum showed no lines originating from water, methyl alcohol, dimethyl ether, methyl chloride, or any other compound, the sample contains no water or methyl alcohol, such substances being very easily detectable in the Raman spectrum. Dimethyl ether and methyl chloride must be present in amounts of less than c. $\frac{1}{2}$ per cent and, actually, the way of preparing the sample makes it highly probable that it is even less. Unfortunately the constancy of the melting point and the course of the premelting curve could not be studied.

The CH_3Br was kept in a glass vessel, M (fig. 1), surrounded by ice. Prior to each experiment c. 1 g was distilled from M to T_1 (or T_2), which was placed in liquid air. Then a high vacuum was established and the CH_3Br was twice sublimated from T_1 to T_2, and vice-versa. At the end of each sublimation the last one-tenth was pumped off. This treatment ensures the presence

[1] NIELSEN, Phys. Rev. **56**, 847 (1939).
[2] Compare, however, the note added in proof.

of an air-free sample, which was afterwards allowed to distil into that part of the apparatus (A), where the amount of CH_3Br was determined.

b. Preparation of HCl.

While a suitable amount of CH_3Br was prepared for a whole series of experiments, HCl was produced for each single determination of the equilibrium. Conc. hydrochloric acid (0.5—0.7 cc) was added to 400 cc conc. H_2SO_4[1] in a carfully evacuated flask through a separatory funnel, the tube of which was led to the bottom of the sulphuric acid (H, fig. 1). When the stopcock of the separatory funnel is cautiously opened the hydrochloric acid distils to the bottom of the conc. sulphuric acid, and a stream of dry HCl is obtained. The gas is condensed in T_1 or T_2. Before using it in the experiment it is subjected to the same treatment as CH_3Br (sublimation *in vacuo*). In this way an air- and water-free sample of HCl was prepared as will be seen from experiments referred to under d.

The pink, crystalline modification of HCl, noticed by Grey and Burt[2] and by Giauque and Wiebe[3] was again observed.

c. Determination of the amount of CH_3Br used in the experiments.

From the evacuated tube T_1 (or T_2) CH_3Br was distilled into an evacuated 1 l-bulb A, placed in a thermostat. After 2 hours the pressure of the gas was read off by means of the mercury manometer P. A Dewar vessel with liquid air was put around the evacuated tube B until all CH_3Br was condensed. Now, in a series of preliminary experiments, the tube B was carefully sealed off, washed outside with ethyl alcohol and dried *in vacuo* over P_2O_5. The weight of the tube was determined on the analytical balance. Subsequently, the tube was broken by being scratched cautiously and heated in a little (2 mm) flame. In this way, a tube can be opened with practically no loss of solid material, as blanks have shown. The tube was again dried *in vacuo* and weighed. Its volume was determined by its water content being weighed.

[1] This amount suffices for abt. 20 preparations of 0.01 mole dry HCl.
[2] Journ. Chem. Soc. Lond., 1669 (1909).
[3] Journ. Am. Chem. Soc. **50**, 101 (1928).

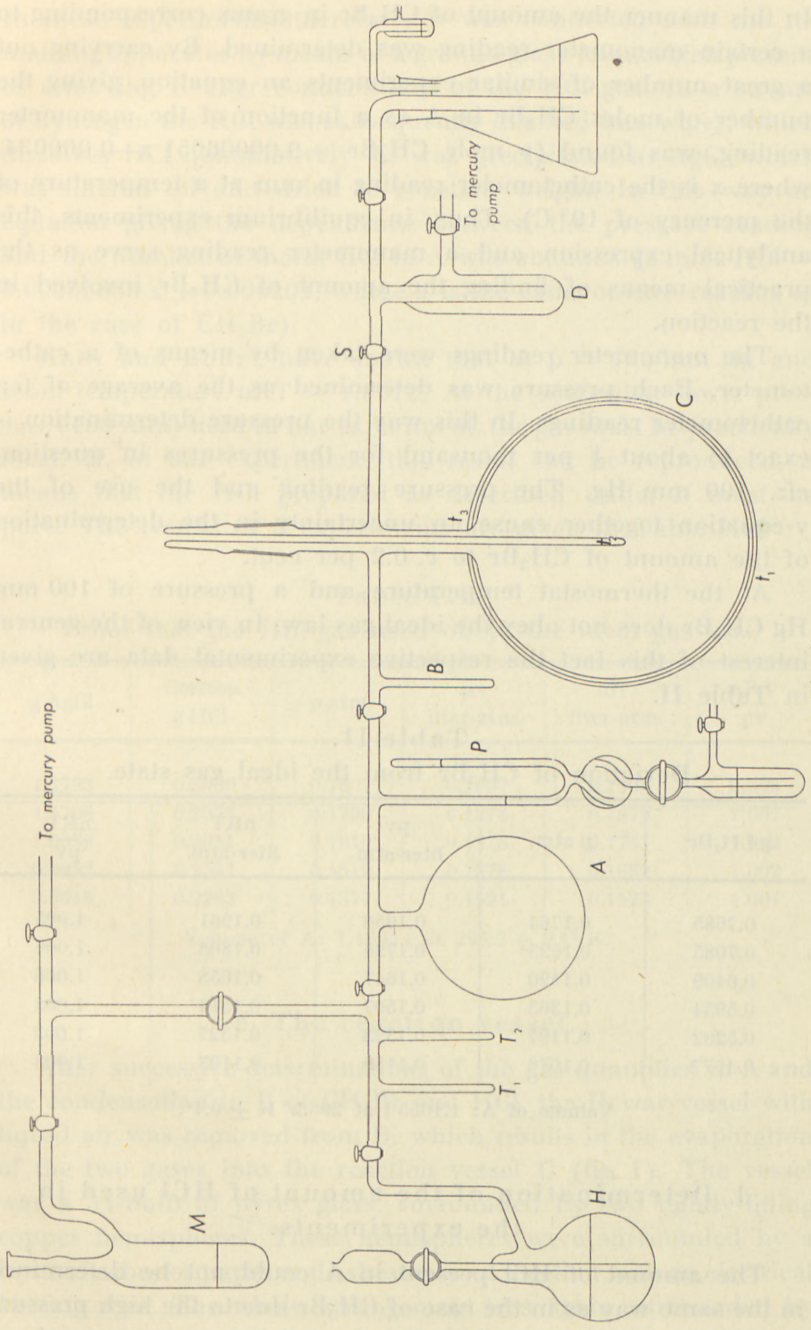

Fig. 1.

In this manner the amount of CH_3Br in grams corresponding to a certain manometer reading was determined. By carrying out a great number of similar experiments an equation, giving the number of moles CH_3Br in A as a function of the manometer reading, was found (y mole CH_3Br = 0.00006051 x—0.000034, where x is the cathetometer reading in mm at a temperature of the mercury of 19° C). Thus, in equilibrium experiments, this analytical expression and a manometer reading serve as the practical means of finding the amount of CH_3Br involved in the reaction.

The manometer readings were taken by means of a cathetometer. Each pressure was determined as the average of ten cathetometer readings. In this way the pressure determination is exact to about ½ per thousand for the pressures in question, *viz.* 100 mm Hg. The pressure reading and the use of the y-equation together cause an uncertainty in the determination of the amount of CH_3Br to c. 0.2 per cent.

At the thermostat temperature and a pressure of 100 mm Hg CH_3Br does not obey the ideal gas law. In view of the general interest of this fact the respective experimental data are given in Table II.

Table II.

Deviation of CH_3Br from the ideal gas state.

g CH_3Br	p atm.	pv liter-atm.	nRT liter-atm.	$\frac{nRT}{pv}$
0.7685	0,1764	0.1950	0.1961	1.005
0.7085	0.1625	0.1796	0.1808	1.006
0.6499	0.1490	0.1647	0.1658	1.006
0.5934	0.1363	0.1507	0.1514	1.005
0.5202	0.1197	0.1323	0.1327	1.003
0.4677	0.1076	0.1189	0.1193	1.003

Volume of A: 1.1055 l at 295.2° K ± 0.1°.

d. Determination of the amount of HCl used in the experiments.

The amount of HCl present in A could not be determined in the same way as in the case of CH_3Br due to the high pressure developing in the ampulla when heated to room temperature.

In these experiments, therefore, B was connected with the remaining apparatus by means of a ground glass joint, which permits of removing B after condensation of the HCl gas. In a stream of hydrogen the HCl was subsequently distilled into water, which dissolves HCl quantitatively. Cl was precipitated as AgCl, which was filtered off and dried to constant weight. In this way an equation giving the dependence between the pressure reading and the number of moles HCl in A was obtained (z mole HCl = 0.00005883 x + 0.000101, where x is the cathetometer reading as in the case of CH_3Br).

GREY and BURT[1] have shown that at p = 180 mm Hg and room temperature nRT = 1.0012. At the somewhat lower pressure (100 mm) used in our experiment, the gas must be practically ideal. If, in our experiment, this result can be reproduced, it means that the HCl prepared as described under b must be pure. The results of 5 experiments are given in Table III.

Table III.

Proof that the HCl-gas used obeys the ideal gas law.

g AgCl	Corresp. g HCl	p atm.	pv liter-atm.	nRT liter-atm.	$\frac{nRT}{pv}$
1.1793	0.3000	0.1807	0.1997	0.1993	0.998
1.1706	0.2978	0.1790	0.1978	0.1979	1.001
1.0539	0.2681	0.1610	0.1778	0.1781	1.002
0.9952	0.2531	0.1519	0.1678	0.1682	1.002
0.9015	0.2293	0.1377	0.1521	0.1523	1.001

Volume of A: 1.1055 l at 295.2 ± 0.1° K.

e. The reaction vessel.

After successive determinations of the gas quantities in A and the condensation in B of CH_3Br and HCl, the Dewar vessel with liquid air was removed from B, which results in the evaporation of the two gases into the reaction vessel C (fig. 1). The vessel was a 3 l-bulb of pyrex glass, surrounded by two tightly-fitting copper hemispheres. These hemispheres were surrounded by a layer of asbestos paper and asbestos wool together with an electrical heating wire. The whole arrangement was again surrounded by

[1] Journ. Chem. Soc. Lond., 1669 (1909).

a big tin container, filled with kieselguhr. Copper-constantan thermocouples were placed at t_1, t_2, and t_3. In this way it was possible to maintain temperatures deviating less than 2°, t_2 generally being very nearly the mean of t_1 and t_3. No thermo-regulator was necessary for keeping the temperature constant within 1° during an experiment. By varying the heating current any desired temperature between 20° C and 450° C could be obtained.

The thermocouples were calibrated in the vapors of boiling benzene, water, toluene, bromobenzene, naphtalene, benzophenon and mercury. At 350° C the reading is accurate to 0.5°, at 100° C it is accurate to 0.2°.

f. Analytical determination of the position of the equilibrium.

After equilibrium had been established in C, the equilibrium mixture was frozen down into the carefully evacuated trap D, surrounded by liquid air. After 2 hours the stopcock S was closed. By means of a stream of hydrogen the reaction mixture was passed through 75 cc water in an 300 cc Erlenmeyer flask. HBr and HCl are dissolved quantitatively in water. Most of the CH_3Br and CH_3Cl is passing, as blanks have shown, the rest is removed by continued bubbling-through of hydrogen for 2 hours. In a special experiment it was shown, moreover, that neither CH_3Br nor CH_3Cl hydrolyse under the present circumstances.

The amount of acid was determined by titration with 0.5 n NaOH. Blank experiments with HCl alone prove that the quantity of acid found by means of this titration is in excellent agreement with the amount calculated by means of the equation mentioned under d.

Using the mass-law of action for the equilibrium we obtain:

$$CH_3Br + HCl \rightleftarrows CH_3Cl + HBr$$

Number of moles before reaction:	mc	c	o	o
Number of moles in the equilibrium:	$c(m-\alpha)$	$c(1-\alpha)$	$c\alpha$	$c\alpha$

$$k = \frac{\alpha^2}{(m-\alpha)(1-\alpha)}.$$

m is the known ratio between the number of moles CH_3Br and HCl before the reaction. If the ratio between HBr and HCl in the equilibrium is f, a is given by $f = \frac{1-a}{a}$. Consequently a determination of the ratio between $\overline{Br}$ and $\overline{Cl}$ in the aqueous solution of HBr + HCl must be made.

This special problem has been studied by several authors. (See e. g. GMELIN, Handb. der anorg. Chem.). I have checked a series of these methods. The method described by LANG[1] (oxidation of HBr by $KMnO_4$ in the presence of HCN and H_3PO_4, reduction of surplus $KMnO_4$ by $FeSO_4$, addition of KJ and titration with $Na_2S_2O_3$) was found to be of suitable accuracy and convenience. By this method the contents of $\overline{Br}$ can be determined almost independently of the contents of $\overline{Cl}$. In the present experiments we are interested in determining $\overline{Br}$ in the presence of 3—5 times as much $\overline{Cl}$. Table IV gives the results of using Lang's method on weighed quantities of KBr and KCl.

Table IV.

g KBr	Equiv. $\overline{Br}$.	g KCl	Equiv. $\overline{Cl}$.	$\frac{\overline{Br}}{\overline{Cl}}$	Equiv. $\overline{Br}$. found.	Error
0.2029	0.001704	0.5025	0.006740	0.252	0.001721	1.0 %
0.1943	0.001632	0.5047	0.006769	0.241	0.001649	1.0 %
0.1460	0.001226	0.5103	0.006844	0.179	0.001239	1.1 %
0.1277	0.001073	0.4973	0.006670	0.161	0.001085	1.2 %

Lang's method thus gives reproduceable, although not quite correct values for the $\overline{Br}$ contents. In practice, the thiosulphate solution used was adjusted to solutions of KBr + KCl, almost like those to be analyzed. In this way the amount of $\overline{Br}$ can be found with an accuracy of about 0.3 per cent.

The inaccuracy in the determination of m and f is seen to cause an inaccuracy of k of about 1.5—2 per cent, as verified by equilibrium experiments.

g. The determination of the equilibrium constant at 606° K in the absence of a catalyst.

As seen from the preceding sections, the equilibrium was studied by mixing known amounts of CH_3Br and HCl in 'C' and

[1] Zeitsch. f. anorg. u. allg. Chemie **144**, 75 (1925).

heating the mixture. As preliminary experiments show, the exchange of Br and Cl starts at 250—300° C in the absence of a catalyst. At 330—340° C, equilibrium is established within 40—50 hours. Some experiments aiming at a faster establishment of the equilibrium were carried out at higher temperatures. At 390° C the following observations were made: After 40 hours the reaction mixture was led to the trap D. The condensation, being complete in corresponding experiments at 330° C, now was incomplete. At the same time the number of equivalents of acid, present in D after the reaction, exceeded the number present before the reaction. Thus, some 'side reaction' must take place, because all the reaction partners of the equilibrium $CH_3Br + HCl \rightleftarrows CH_3Cl + HBr$, are condensable and the number of equivalents of acid is constant. In fact, the only compound which could not be condensed in liquid air and which could be formed from the reaction partners, is hydrogen. When, in a following experiment, HCl was omitted, the contents of 'C' were likewise not completely condensable in D after 24 hours, a considerable amount of HBr (c. 0.1 mole per cent) being simultaneously formed. This indicates that the 'side reaction' probably is

$$2\,CH_3Br \rightarrow H_2 + \begin{matrix} CH_2Br \\ | \\ CH_2Br \end{matrix}$$

HBr being produced by subsequent reactions such as

$$\begin{matrix} CH_2Br \\ | \\ CH_2Br \end{matrix} \rightarrow HBr + \begin{matrix} CHBr \\ \| \\ CH_2 \end{matrix} \qquad \text{or} \qquad \begin{matrix} CH_2Br \\ | \\ CH_2Br \end{matrix} + H_2 \rightarrow \begin{matrix} CH_3 \\ | \\ CH_2Br \end{matrix} + HBr\,.$$

At 330° C, however, the condensation in D was complete and no extra equivalents of acid were formed. To ensure that no secondary reactions take place in experiments at this temperature, an experiment with 0.01 mole CH_3Br alone was run for 10 days at 330° C. The subsequent condensation in D was complete and no HBr was formed. In a similar experiment with 0.05 mole CH_3Br the condensate in D was distilled into a Raman tube and the Raman spectrum was photographed. The spectrum showed no signs of other lines than those corresponding to CH_3Br. If e. g.

CH_2BrCH_2Br had been present it would have been particularly easy to detect because of the isolated Raman line of the C—C bond.

Consequently it was decided to carry out a series of determinations of the equilibrium constant at some temperature between 330 and 340° C. The results are given in table V.

Table V.

Equilibrium constant determinations at 606° K.

Exp. Nr.	Duration. (hours)	Equiv. CH_3Br. before exper.	Equiv. HCl before exper.	m	Equiv. HCl + HBr aft. exp.	Equiv. HBr after exper.	f	a	$\frac{a^2}{(m-a)(1-a)}$
1	22 hours	0.007891	0.007986	0.9882	0.007996	0.001975	0.3280	0.2470	0.1093
2	46 —	0.007786	0.006162	1.2635	0.006162	0.001845	0.4274	0.2994	0.1327
3	64 —	0.007121	0.007146	0.9965	0.007131	0.001916	0.3674	0.2687	0.1356
4	93 —	0.007125	0.007381	0.9653	0.007377	0.001947	0.3586	0.2639	0.1349
5	112 —	0.007200	0.007007	1.0275	0.006982	0.001896	0.3728	0.2716	0.1340
6	141 —	0.006522	0.008077	0.8074	0.008087	0.001951	0.3180	0.2413	0.1355
7	72 —	0.007863	0.007767	1.0123	0.007767	0.002096	0.3696	0.2698	0.1342
8	72 —	0.007797	0.006774	1.1510	0.006781	0.001965	0.4080	0.2898	0.1373
9	67 —	0.006704	0.007587	0.8836	0.007578	0.001918	0.3389	0.2531	0.1360
10	63 —	0.007791	0.006341	1.2286	0.006334	0.001890	0.4253	0.2984	0.1364

Mean of experiments 2—10: 0.1352. Result: $0.1352 \pm 0.0008 = k$.

In connexion with Table V the use of the mass-law of action may be discussed. The law is only fulfilled for ideal gases. At higher temperatures and lower pressure, the actual gases can be considered ideal with better and better approximation. As HCl and HBr are already ideal at p = 150 mm Hg and room temperature they are even more so at the pressure of the experiment (50—100 mm Hg) and the temperatures 80°—340° C. Table II shows that at room temperature CH_3Br deviates a little from ideality. The same is probably the case with CH_3Cl. At the higher temperatures of the experiments the deviations from ideality are minor. Thus, the ratio between the activities of CH_3Br and CH_3Cl as a good approximation must be equal to the ratio between the concentrations. The application of the mass-law of action must be permissible.

h. Determinations of the equilibrium constant at 357° K in the presence of a catalyst.

For the determination of the equilibrium at a temperature as far as possible from 606° K a suitable catalyst was looked for. The first attempt with granulated active carbon turned out to be successful. The catalyst was suspended in a glass spiral in the centre of C (fig. 1). In the presence of this catalyst it is possible to study the equilibrium even at 80° C.

The first experiment with the catalyst was made at the same temperature as the experiments without a catalyst, 606° K. The experiment lasted for 24 hours. After that time the condensation in the trap D was incomplete and the number of equivalents of acid had increased. Thus, some side reaction is catalyzed, too. In the following experiment at the same temperature, which was interrupted after one hour, the condensation in D was nearly complete and the number of equivalents of acid had only increased by 0.5 per cent. When calculating the equilibrium constant on the assumption that no side reaction had taken place k was found to be 0.1300. Without a catalyst k = 0.1352. In broad outline these experiments indicate that active carbon is an excellent catalyst for the reaction we want to study. Since, however, also the side reactions are catalyzed it is impossible to study the equilibrium with and without a catalyst at the same temperature.

Next the highest possible temperature at which the side reactions are negligible was looked for. In experiments at 533° K and 497° K, excess equivalents of acid were formed in the course of 40 hours. At 458° K no excess equivalents of acid were produced during 40 hours. At 419° K the same result was found. Thus experiments with the catalyst at temperatures lower than about 450° K (177° C) can be performed without the complications originating from the side reactions.

Finally the lowest possible temperature at which the equilibrium can conveniently be studied was sought for. At 357° K (84° C) equilibrium is established in the course of 30—40 hours. As this is a suitable period, the experiments of Table VI were carried out at that temperature.

Table VI.
Determination of the equilibrium constant at 357°K.

Exp. no.	Duration. (hours)	Equiv. CH_3Br before exper.	Equiv. HCl before exper.	m	Equiv. HBr + HCl after exp.	Equiv. HBr after exp.	f	α	$\frac{\alpha^2}{(1-\alpha)(1-\alpha)}$
1	20	0.006335	0.006678	0.9486	0.006647	0.001003	0.1777	0.1509	0.03366
2	39	0.006730	0.006376	1.0555	0.006376	0.001027	0.1920	0.1611	0.03459
3	45	0.007021	0.006696	1.0485	0.006685	0.001070	0.1906	0.1601	0.03435
4	42	0.006264	0.007147	0.8888	0.007126	0.001035	0.1728	0.1473	0.03431
5	64	0.006270	0.006782	0.9245	0.006775	0.001021	0.1774	0.1507	0.34560
6	40	0.007167	0.006516	1.1000	0.006510	0.001070	0.1967	0.1644	0.03457
7	40	0.006724	0.007328	0.9230	0.007325	0.001101	0.1769	0.1503	0.03441
8	40	0.006247	0.006649	0.9395	0.006623	0.000998	0.1774	0.1507	0.03390
9	43	0.006635	0.007017	0.9455	0.007025	0.001063	0.1783	0.1513	0.03396

Mean number of experiments 2—9: 0.03433. Result: $k = 0.03433 \pm 0.00014$.

III. Calculation of Spectroscopically and Thermodynamically Important Quantities.

a. Calculation of the greatest moment of inertia of CH_3Br.

Formula (8) shows that sufficient data are now available to calculate A′ (CH_3Br), the greatest moment of inertia of CH_3Br. Putting $T_1 = 606° K \pm 1.0°$, $T_2 = 357° K \pm 0.5°$ and A′ (CH_3Cl) $= 0.579$[1] and using the vibration data of BENNETT and MAYER[2] we obtain

$$A'(CH_3Br) = 0.782 \text{ gcm}^2 \pm 4 \text{ per cent.}$$

As $A'(CH_3Br) = A(CH_3Br) \cdot 10^{38}$, where $A(CH_3Br)$ is the true moment of inertia, we get

$$75 \cdot 10^{-40} \text{ gcm}^2 < A(CH_3Br) < 81 \cdot 10^{-40} \text{ gcm}^2.$$

This value is in excellent agreement with values found by previous authors (S-TI, p. 13).

[1] NIELSEN, Phys. Rev. **56**, 847 (1939). Compare the note added in proof.
[2] BENNETT and MAYER, Phys. Rev. **32**, 888 (1928)

The limits given for the value of A (CH_3Br) were calculated on the assumption that the sources of experimental error are exclusively to be found in the temperature measurements and the analytical determination of the equilibrium. To check the correctness of this we may determine the equilibrium at a third temperature, as different as possible from 357° K and 606° K. On page 28 it was mentioned that the equilibrium in question can be established at 458° K in the presence of the catalyst without side reactions. A temperature of 443° K (170° C) was chosen for the experiment. Two determinations were made.

Determination of the equilibrium at 443° K.

1. experiment. Duration 36 hours ..... $k = 0.06610$
2. experiment. — 67 — ..... $k = 0.06643$

Mean number: $k = 0.06636 \pm 0.00100$

Now, calculating A (CH_3Br) by means of the results at 606° K and 443° K we obtain

$$A\,(CH_3Br) = 70 \cdot 10^{-40}\ gcm^2 \pm 8 \text{ per cent.}$$

The agreement between the two values found by the present 'equilibrium method' is not quite so satisfactory as was expected. This might mean that some systematic error was neglected. As no such error seems to have occurred in the experimental determination of the equilibrium constants it seems natural to reconsider the theoretical basis. In the derivation of equation (I) the simplifying, partly uncontrollable assumption was made that the interaction between the rotational and vibrational movements of the molecule can be neglected. For the methyl halides it is known with certainty that such interaction occurs. Unfortunately it is very difficult, if not impossible at present, to see to what extent such interaction will influence equations (I) and (8).

Paying due regard to both determinations of A (CH_3Br) made in this paper, we get:

$$A\,(CH_3Br) = 76.5 \cdot 10^{-40}\ gcm^2 \pm 4 \text{ per cent.}$$

Even if a systematic error of 5 per cent is taken into account the value found by the present 'equilibrium method' is of the

same accuracy as the values hitherto determined by spectroscopical or physico-chemical methods.

Spectroscopical methods	$82 \cdot 10^{-40}$ gcm^2	$\pm$ 10	per cent.
Heat capacity measurements ...	$78 \cdot 10^{-40}$ —	$\pm$ 8	—
'Equilibrium method'	$76.5 \cdot 10^{-40}$ —	$\pm$ 4	—

The value, equally well conceivable with spectroscopical heat capacity and equilibrium measurements, is:

$$A\,(CH_3Br) = 77.5 \cdot 10^{-40} \pm 4 \text{ per cent.}$$

b. Calculation of ΔE_0° and the heat of reaction different temperatures.[1]

From (7) it follows that

$$e^{\frac{\Delta E_0^\circ}{RT}} = e^{\frac{2.819}{R}} \left(\frac{M\,(CH_3Cl)}{M\,(CH_3Br)} \right)^{3/2} \frac{A'\,(CH_3Cl)}{A'\,(CH_3Br)} \frac{\prod_{f=1}^{3n-6} \left(1 - e^{\frac{-\varepsilon_f}{kT}}\right)_{CH_3Br}}{\prod_{f=1}^{3n-6} \left(1 - e^{\frac{-\varepsilon_f}{kT}}\right)_{CH_3Cl}} k\,(T)^{-1}. \quad (9)$$

As all the quantities of the right-hand side are known, we can calculate:

$$\Delta E_0^\circ = 2500 \text{ gcalmole}^{-1} \pm 75.$$

The enthalpy H, the thermodynamical potential G, the entropy S, and the temperature T are connected by the relation:

$$H = G + TS.$$

Taking the value of G from (3) we get:

$$H^\circ = E_0^\circ + RT \left(4 + \sum_{f=1}^{3n-6} \frac{\frac{\varepsilon_f}{kT}}{e^{\frac{\varepsilon_f}{kT}} - 1} \right).$$

[1] In the newest American literature ΔH_0° is were commonly used for ΔE_0°.

We now want to calculate ΔH° for the reaction $CH_3Br + HCl \rightarrow CH_3Cl + HBr$. The fraction of ΔH° originating from $CH_3Br \rightarrow CH_3Cl$ is easily seen to be:

$$\Delta H^\circ(CH_3Br \rightarrow CH_3Cl) = \Delta E_0^\circ(CH_3Br \rightarrow CH_3Cl) + \\ + RT\left(\sum_{f=1}^{3n-6}{}_{(CH_3Cl)} \frac{\frac{\varepsilon_f}{kT}}{e^{\frac{\varepsilon_f}{kT}}-1} - \sum_{f=1}^{3n-6}{}_{(CH_3Br)} \frac{\frac{\varepsilon_f}{kT}}{e^{\frac{\varepsilon_f}{kT}}-1}\right).$$

For the hydrogen halides tables of $\frac{G^\circ - E_0^\circ}{T}$ are available.[1] Denoting this function by B we can write $G = E_0 + BT$ and

$$H = E_0 + BT + TS.$$

Thus,

$$\Delta H^\circ(HCl \rightarrow HBr) = \Delta E_0^\circ(HCl \rightarrow HBr) + T\Delta B^\circ(HCl \rightarrow HBr) + \\ + T\Delta S^\circ(HCl \rightarrow HBr)^2$$

and

$$\Delta H^\circ(CH_3Br + HCl \rightarrow CH_3Cl + HBr) = \Delta E_0^\circ(CH_3Br + HCl \rightarrow CH_3Br + HBr) + \\ + RT\left(\sum_{f=1}^{3n-6}{}_{CH_3Cl} \frac{\frac{\varepsilon_f}{kT}}{e^{\frac{\varepsilon_f}{kT}}-1} - \sum_{f=1}^{3n-6}{}_{CH_3Br} \frac{\frac{\varepsilon_f}{kT}}{e^{\frac{\varepsilon_f}{kT}}-1}\right) + \\ + T\Delta B^\circ(HCl \rightarrow HBr) + T\Delta S^\circ(HCl \rightarrow HBr).$$

By insertion of numerical values we get:

T°K	T°C	gcal mole^{-1}
0	−273	2500
298	25	2450
606	333	2340

[1] Gordon and Barnes, Journ. Chem. Phys. (1), 692 (1933); Giauque, Journ. Am. Chem. Soc. **54**, 1731 (1932).

[2] Values of S for HCl and HBr in the papers of Gordon and Giauque.

The change in the evolution of heat at a change in temperature of about 300° is of the same order of magnitude as the experimental error.

The evolution of heat at the present reaction can be calculated in advance by using the data available from the literature.[1]

$$CH_3Br + HCl \rightarrow CH_3Cl + HBr$$

Heat of formation, kcal mole^{-1}	8.5	22.06	20.1	8.65

Consequently

$$\Delta Q^\circ = -\Delta H^\circ = (20.1 + 8.65) - (8.5 + 22.06) = -1.81 \text{ kcal.}$$

In this paper it is found that

$$\Delta Q^\circ = -2.45 \text{ kcal.}$$

The values of the heat of formation of HCl and HBr undoubtedly are correct, as they are based on consistent thermochemical and spectroscopical data. The data for the heat of formation of CH_3Br and CH_3Cl are mainly due to THOMSEN.[2] From Thomsen's book and from a paper by BERTHELOT[3] it is evident that the determination of the heat of combustion of the methyl halides meets with considerable difficulties. It seems safe to conclude that one or both of Thomsen's values of the heat of formation of CH_3Br and CH_3Cl are incorrect.

IV. Summary.

(1) A relation between the equilibrium constants at two different temperatures of the reaction $CH_3Br + HCl \rightleftarrows CH_3Cl + HBr$ and spectroscopically determinable quantities has been derived.

[1] Revised and edited by BICHOWSKY and ROSSINI, Thermochemistry of Chemical Substances, New York 1936.

[2] THOMSEN, Thermochemische Untersuchungen IV, 86 and 116 (1886).

[3] BERTHELOT, Ann. de Chemie et de Physique (V), **23**, 214 (1881).

(2) An experimental determination of the equilibrium constants at various temperatures was carried through. The reaction vessel was a 3-l Pyrex bulb. At 606° K k = 0.1352 ± 0.0008 was found in the absence of a catalyst. At 357° K k = 0.03433 ± 0.00014 was found. At 443° K k = 0.06636 ± 0.00100 was found. The two last-mentioned determinations were carried through in the presence of an active carbon catalyst.

(3) The results obtained permit of calculating the greatest moment of inertia of CH_3Br, A (CH_3Br) = $76.5 \cdot 10^{-40}$ gcm^2 ± 4 per cent. The result is in good agreement with the values found by means of infrared spectroscopy ($82 \cdot 10^{-40}$ ± 10 per cent) and by heat capacity measurements ($78 \cdot 10^{-40}$ ± 8 per cent). At present A (CH_3Br) = $77.5 \cdot 10^{-40}$ gcm^2 is considered the best value. It is accurate to 4 per cent.

(4) Furthermore, ΔE_0° for the reaction $CH_3Br + HCl \rightarrow CH_3Cl + HBr$ was found to be 2500 gcal mole^{-1} ± 75. The heat of the reaction at various temperatures was calculated. The value found is inconsistent with the value which can be calculated from existing thermochemical data. It is concluded that Thomsen's values for the heat of formation of CH_3Br and CH_3Cl must be incorrect.

The author wants to thank Professor Langseth for helpful discussions on the subject.

Note added in proof: In a 'letter' to Phys. Rev. 72, 344, (1947) Gordy, Simmons and Smith have reported the results of microwave experiments with CH_3Cl and CH_3Br. For CH_3Cl^{35} A is found to be $63.1 \cdot 10^{-40}$ gcm^2, for CH_3Cl^{37} A = $64.0 \cdot 10^{-40}$ e. g. the 'weighed' average for ordinary methyl chloride is $63.4 \cdot 10^{-40}$. A serious discrepancy thus exists between this result and Nielsen's value A = $57.9 \cdot 10^{-40}$ used in this work. The discrepancy is hardly explanable by experimental uncertainty. If the microwave results are confirmed by future experiments the results of the present paper are changed as follows:

pag. 29: A (CH_3Br) = $85.6 \cdot 10^{-40}$ gcm^2 ± 4 per cent.

This is in fine agreement with the microwave result by GORDY et. al. who found $A(CH_3Br) = 87.5 \cdot 10^{-40}$ by direct measurement

pag. 31: $\Delta E_0^\circ = \Delta H_0^\circ = 2464$ gcal $mol^{-1} \pm 75$.
pag. 32: $\Delta H^\circ (298^\circ K) = 2414$ gcal $mole^{-1}$.
pag. 33: $\Delta Q^\circ (298^\circ K) = -24.1$ kcal $mole^{-1}$.

Universitetets kemiske Laboratorium.
Copenhagen.

Indleveret til Selskabet den 6. August 1946.
Færdig fra Trykkeriet den 11. Februar 1948.

DET KGL. DANSKE VIDENSKABERNES SELSKAB
MATEMATISK-FYSISKE MEDDELELSER, BIND XXIV, NR. 10

GEOMETRY OF THE MOLECULES METHYL CHLORIDE AND METHYL BROMIDE

BY

B. BAK

KØBENHAVN
I KOMMISSION HOS EJNAR MUNKSGAARD
1947

Printed in Denmark.
Bianco Lunos Bogtrykkeri

1. Introduction.

The determination of the exact geometrical shape of the methyl halides is of more general interest. It has long been realized that numerous chemical problems which hitherto could only be treated empirically or half-empirically, as e. g. the Walden inversion, should be studied by means of the methods of quantum mechanics. A first step which should enable us to perform such calculations is, of course, the study of the geometrical configuration of the molecule.

In organic-chemical problems we often meet with the question to what extent the substitution of one or more hydrogen atoms by so-called "electro-negative" atoms or groups, such as the halogens, will alter the original stereochemistry of the compound. In this respect the simplest cases are the methyl halides, and conditions are most favourable in the case of CH_3Cl and CH_3Br. Here, comparatively exact spectroscopical and interferometrical data are available which, in connection with thermodynamical data, offer the best possible information on the geometrical properties of the molecules.

PENNEY[1] has given a quantum mechanical treatment of the bond energies and the valency angles of the methyl halides. The treatment, of course, is only approximative. To quote PENNEY, the result is that "if some or all of the hydrogen atoms in methane are replaced by other mono-valent groups, the resulting deviations from the tetrahedral angle are remarkably small, and can hardly exceed a few degrees". Beside this theoretical treatment, a contribution based upon spectroscopical results was later given by SUTHERLAND[2]. However, since the paper of SUTHERLAND was

[1] PENNEY, Trans. Far. Soc. **31**, 734 (1935).

[2] SUTHERLAND, ibid. **34**, 325 (1938).

published, many new important spectroscopical and thermodynamical data have been found which make a new treatment interesting.

2. Relations Between the Intramolecular Distances and Angles in the Methyl Halides and the Two Principal Moments of Inertia. Numerical Calculations.

In Fig. 1, X is the halogen atom, C the carbon atom, and H a hydrogen atom. T is the center of gravity, d is the distance C—H, and a the distance C—X. The supplementary angle to

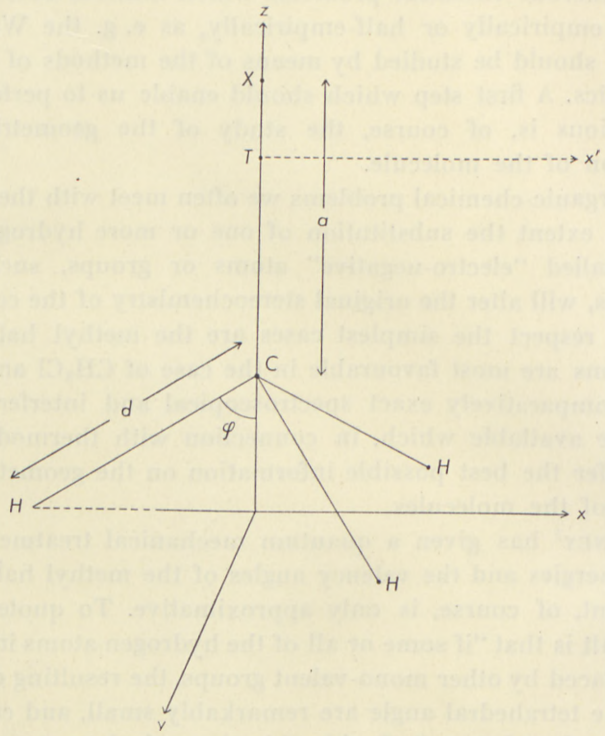

Fig. 1.

H—C—X is denoted by φ. I_C is the moment of inertia around the z-axis and I_A the corresponding quantity around the x'-axis. Then, the following relations hold:

$$I_C = 3\, m_H\, d^2 \sin^2 \varphi. \qquad (1)$$

$$I_A - \frac{1}{2} I_C = a^2 \frac{m_X\, m_C}{m_{CH_3X}} + 3\,(a + d\cos\varphi)^2 \frac{m_H\, m_X}{m_{CH_3X}} + 3\, d^2 \cos^2\varphi \frac{m_C m_H}{m_{CH_3X}}. \qquad (2)$$

Here, m_H is the mass of the hydrogen atom, etc.

The quantities to be determined are a, d and φ. a, the distance between the carbon and the halogen atom, has been determined by electron scattering experiments.

	a Å.	
CH_3Cl	1.77 ± 0.02	SUTTON and BROCKWAY[1].
CH_3Br	1.91 ± 0.06	LEWY and BROCKWAY[2].

It is to be expected that these values are rather reliable since in the electronic scattering experiments the molecule practically acts as if it was diatomic owing to the small scattering effect of the hydrogen atoms. Thus, the additional knowledge of I_A and I_C will enable us to calculate d and φ by means of (1) and (2).

Our present knowledge of I_A and I_C for *CH_3Cl* is mainly based upon a work of NIELSEN[3] and papers by BENNETT and MAYER[4] and JOHNSTON and DENNISON[5]. Studying the fine structure of the infrared band at 1355 cm^{-1} NIELSEN was able to show that $I_A = 57.9\ 10^{-40}$ gcm^2. Utilizing the measurements of BENNETT and MAYER, JOHNSTON and DENNISON could show that $I_C = 5.44\ 10^{-40}$ gcm^2. NIELSEN's value of I_A is probably exact within 1—2 per cent*, while I_C is uncertain to 5 per cent.

The present values of I_A and I_C for *CH_3Br* were communicated and discussed by the author in a previous paper[6]. $I_C = 5.37\ 10^{-40}$ $gcm^2 \pm 5$ per cent and $I_A = 77.5\ 10^{-40}$ $gcm^2 \pm 4$ per cent, values which are equally well consistent with spectroscopical[7], heat capacity[8], and equilibrium[9] data.

[1] Journ. Am. Chem. Soc. **57**, 473 (1935).
[2] Ibid. **59**, 1662 (1937).
[3] NIELSEN, Phys. Rev. **56**, 847 (1939).
[4] BENNETT and MAYER, Phys. Rev. **32**, 888 (1928).
[5] JOHNSTON and DENNISON, Phys. Rev. **48**, 868 (1935).
[6] B. BAK, D. Kgl. Danske Vidensk. Selskab, Mat.-fys. Medd. XXIV, 9 (1948).
[7] BENNETT and MAYER, loc. cit.
[8] EGAN and KEMP, Journ. Am. Chem. Soc. **60**, 2097 (1938).
[9] B. BAK, loc. cit.

* Compare, however, the note added in proof.

	$I_A \cdot 10^{40}$	$I_C \cdot 10^{40}$
CH_3Cl	57.9	5.44
CH_3Br	77.5	5.37

By means of these values the following figures for d and φ are calculated:

	$I_A\,10^{40}$	a Å	$I_C\,10^{40}$	φ	d Å
CH_3Cl	57.9	1.77	5.44	87°	1.05
CH_3Br	77.5	1.91	5.37	90°	1.04
Tetrahedral angle:				70°	
C—H distance in CH_4:					1.09

The figures given here are, of course, not exact, as the experimental data on which they are based have a given uncertainty. Considering equation (2) we see that the least possible value of φ is obtained by using the highest possible value of I_A and, at the same time, minimum values of a and I_C. When carrying through the calculations as above we find:

	$I_A\,10^{40}$	a Å	$I_C\,10^{40}$	φ	d Å
CH_3Cl	59.0	1.75	5.17	78°	1.04
CH_3Br	80.5	1.85	5.11	69°	1.08
Tetrahedral angle:				70°	
C—H distance in CH_4					1.09

In the case of CH_3Cl it seems firmly established that φ deviates considerably from the tetrahedral angle. For CH_3Br it is necessary to assume a maximum deviation from the experimental average in order to get a model with $\varphi = 70°$. It seems thus unevitable to draw the conclusion that the methyl group of CH_3Cl and CH_3Br is far more "flat" than that of CH_4, in contrast to the result obtained by PENNEY.

Note added in proof: In a letter to Phys. Rev. 72, 344 (1947) GORDY, SIMMONS and SMITH have reported $I_A(CH_3Cl^{35}) = 63.1 \cdot 10^{-40}$ gcm^2 and $I_A(CH_3Br) = 87.5 \cdot 10^{-40}$ gcm^2. A serious discrepancy thus exists between this microwave value and $I_A(CH_3Cl) = 57.9 \cdot 10^{-40}$ gcm^2 given by NIELSEN (loc. cit.), which is hardly explanable by experimental uncertainty. Should the values found

by means of the new microwave technique be confirmed by future experiments, they will mean a confirmation of PENNEY's viewpoint:

	$I_A\,10^{40}$	a Å	$I_C\,10^{40}$	φ	d Å
CH_3Cl	63.1	1.77	5.44	69°	1.10
CH_3Br	87.5	1.91	5.37	67°	1.12
Tetrahedral angle:				70°	
C—H distance in CH_4					1.09

Universitetets kemiske Laboratorium.
Copenhagen.

Indleveret til Trykkeriet d. 6. August 1946.
Færdig fra Trykkeriet d. 31. December 1947.

DET KGL. DANSKE VIDENSKABERNES SELSKAB
MATEMATISK-FYSISKE MEDDELELSER, BIND XXIV, NR. 11

ON A GENERALIZATION OF KRONECKER'S THEOREM

BY

HANS TORNEHAVE

KØBENHAVN
I KOMMISSION HOS EJNAR MUNKSGAARD
1948

Printed in Denmark
Bianco Lunos Bogtrykkeri

INTRODUCTION

The following well-known theorem by KRONECKER

Theorem 1. *If m real numbers $\lambda_1, \cdots, \lambda_m$ do not satisfy any relation*

$$r_1\lambda_1 + \cdots + r_m\lambda_m = 0,$$

where $r_1, \cdots, r_m$ are rational numbers and at least one r_ν is $\neq 0$, then there exists to any given real numbers $v_1, \cdots, v_m$ and any positive ε a number t satisfying

$$|\lambda_\nu t - v_\nu| \leq \varepsilon \pmod{2\pi}, \quad \nu = 1, \cdots, m,$$

is equivalent to the following

Theorem 2. *If $h_\nu(t) = e^{i\lambda_\nu t}$; $\nu = 1, \cdots, m$ are pure oscillations, whose frequencies $\frac{\lambda_\nu}{2\pi}$; $\nu = 1, \cdots, m$ do not satisfy any relation*

$$r_1\frac{\lambda_1}{2\pi} + \cdots + r_m\frac{\lambda_m}{2\pi} = 0,$$

where $r_1, \cdots, r_m$ are rational numbers and at least one r_ν is $\neq 0$, then there exists to any given real numbers $v_1, \cdots, v_m$ and any positive ε a number t satisfying

$$|h_\nu(t) - e^{iv_\nu}| \leq \varepsilon; \quad \nu = 1, \cdots, m. \tag{1}$$

If the numbers $\lambda_1, \cdots, \lambda_m$ satisfy the condition of Theorem 1, they are called *rationally independent.* Theorem 1 states that the straight line $x_\nu = \lambda_\nu t$; $\nu = 1, \cdots, m$, where $\lambda_1, \cdots, \lambda_m$ are rationally independent, is mod. 2π everywhere dense in the m-dimensional space.

In this paper we shall consider *phase-modulated oscillations*, i. e. functions

$$H(t) = e^{i(ct + g(t))},$$

where c is a real constant and $g(t)$ a real-valued function, almost periodic in the sense of BOHR. Its frequency (in mean) is determined by the constant c, which is called the *mean motion* of $H(t)$. We shall prove in this paper that Theorem 2 is valid also for phase-modulated oscillations, i. e. we shall prove the following

Theorem 3. *Let $H_1(t), \cdots, H_m(t)$ be phase-modulated oscillations with rationally independent mean motions. To any given real numbers $v_1, \cdots, v_m$ and any positive ε there exists a number t, satisfying*

$$|H_\nu(t) - e^{iv_\nu}| \leq \varepsilon; \quad \nu = 1, \cdots, m.$$

Apparently we lose nothing by this generalization although Theorem 3 is evidently much more far-reaching than Theorem 2. However, it is well-known that BOHL has proved that the set of numbers t satisfying (1) is relatively dense and WEYL has proved that the set of numbers t satisfying (1) has the relative measure $\left(\frac{2 \arcsin \frac{\varepsilon}{2}}{\pi}\right)^m$ on the t-axis. It will be proved that BOHL's result is valid also in the general case, but we lose WEYL's result. This is, in fact, not valid for the single oscillation $H(t) = e^{i(t+\sin t)}$, if we take $v = 0$ and $\varepsilon < 2$.

Theorem 3 states that the curve $x_\nu = c_\nu t + g_\nu(t)$; $\nu = 1, \cdots, m$, where $c_1, \cdots, c_m$ are rationally independent, is mod 2π everywhere dense in the m-dimensional space.

The result is brought in closer connection with the theory of almost periodic functions by the following theorem by H. BOHR[1].

Theorem 4. *A complex-valued almost periodic function $f(t)$; $-\infty < t < \infty$, satisfying $|f(t)| \geq k > 0$, can be written*

$$f(t) = r(t) \cdot H(t),$$

where $r(t)$ is a positive almost periodic function and $H(t)$ is a phase-modulated oscillation.

The mean motion of $H(t)$ is also called the *mean motion* of $f(t)$. If $f(t)$ is almost periodic and a and b are complex con-

[1] H. BOHR: Kleinere Beiträge zur Theorie der fastperiodischen Funktionen, I. Det Kgl. Danske Videnskabernes Selskab. Math.-fys. Meddelelser, X, 10 (1930). Über fastperiodische ebene Bewegungen. Comment. math. helv. 4 (1932).

stants such that $f(t)-a$ and $f(t)-b$ satisfy the condition of Theorem 4, the mean motions of these functions have a rational ratio. This was first proved by JESSEN[1] and later JESSEN and FENCHEL[2] found a more general theorem concerning almost periodic movements on closed or plane surfaces. In this paper we shall deduce some generalizations of JESSEN's original theorem in another direction. For the present we observe that JESSEN's theorem is a corollary of Theorem 3. In fact, JESSEN's theorem may be expressed as the following

Theorem 5. *If two almost periodic functions $f_1(t)$ and $f_2(t)$, which do not come arbitrarily near to zero, satisfy a linear relation*

$$\alpha_1 f_1(t) + \alpha_2 f_2(t) = \alpha_3, \tag{2}$$

where α_1, α_2 and α_3 are complex constants $\neq 0$, the mean motions c_1 and c_2 of $f_1(t)$ and $f_2(t)$ are rationally dependent.

In fact, if c_1 and c_2 were rationally independent, there would according to Theorem 3 exist a number t such that the complex numbers $\alpha_1 f_1(t)$, $\alpha_2 f_2(t)$ and $-\alpha_3$ would have nearly equal arguments and that would render the relation (2) impossible.

We shall prove that Theorem 5 is valid for an arbitrary number of almost periodic functions satisfying a similar condition. If, on the other hand, we restrict the number of functions to three, we may replace the linear relation (2) by a homogeneous quadratic equation, and the theorem is still true.

§ 1. Some Preliminary Remarks.

For the convenience of the reader we shall first mention some results concerning periodic and limit periodic functions of a denumerable set of variables, which we shall use in the sequel. We shall permanently use the vector notations $\boldsymbol{x} = (x_1, x_2, \cdots)$. For two vectors $\boldsymbol{x} = (x_1, x_2, \cdots)$ and $\boldsymbol{y} = (y_1, y_2, \cdots)$ and two numbers k and l we define the linear combination

$$k\boldsymbol{x} + l\boldsymbol{y} = (kx_1 + ly_1, kx_2 + ly_2, \cdots),$$

[1] B. JESSEN: Über die Säkularkonstanten einer fastperiodischen Funktion. Math. Ann. 111 (1935).

[2] W. FENCHEL und B. JESSEN: Über fastperiodische Bewegungen in ebenen Bereichen und auf Flächen. Kgl. Danske Videnskabernes Selskab. Math.-fys. Meddelelser XIII, 6 (1935).

and if one of the vectors $\boldsymbol{x}$ and $\boldsymbol{y}$ has only a finite number of coordinates $\neq 0$, we have the inner product

$$\boldsymbol{x}\boldsymbol{y} = x_1 y_1 + x_2 y_2 + \cdots .$$

A sequence $\boldsymbol{x}_\nu = (x_{\nu 1}, x_{\nu 2}, \cdots)$; $\nu = 1, 2, \cdots$ of vectors is said to converge towards a vector $\boldsymbol{x}_0 = (x_{01}, x_{02}, \cdots)$ if $x_{\nu\mu} \to x_{0\mu}$ for $\mu = 1, 2, \cdots$ and $\nu \to \infty$. A function $F(\boldsymbol{x})$ is called continuous for $\boldsymbol{x} = \boldsymbol{x}_0$ if $F(\boldsymbol{x}_\nu) \to F(\boldsymbol{x}_0)$, when $\boldsymbol{x}_\nu$ runs through a sequence of vectors belonging to the domain where $F(\boldsymbol{x})$ is defined, and converging towards $\boldsymbol{x}_0$. A function is continuous in a domain (i. e. continuous in every point of this domain) if it can be approximated uniformly with any given accuracy by a continuous function depending only on a finite number of variables. In what follows the domain in question is the real infinite-dimensional space. A function $F(\boldsymbol{x}) = F(x_1, x_2, \cdots)$ is called limit periodic with the limit period 2π, if it can be approximated uniformly in the whole space by a continuous function depending only on a finite number of variables and periodic in each of these with a period that is an integral multiple of 2π. Hence a limit periodic function is continuous. The function $F(\boldsymbol{x})$ can be approximated uniformly in the whole space with any given accuracy by an exponential polynomial

$$P(\boldsymbol{x}) = \sum\nolimits^{*} a_{\boldsymbol{r}} e^{i\boldsymbol{r}\boldsymbol{x}}$$

where $\boldsymbol{r}$ runs through a finite set of vectors with rational coordinates, among which only a finite number are $\neq 0$[1].

The numbers $\lambda_1, \cdots, \lambda_m$ are called *rationally independent* if a relation

$$r_1\lambda_1 + \cdots + r_m\lambda_m = 0$$

with rational $r_1, \cdots, r_m$ is possible only when $r_1 = \cdots = r_m = 0$. The numbers $\lambda_1, \lambda_2, \cdots$ are rationally independent if $\lambda_1, \cdots, \lambda_m$ are rationally independent for all values of m.

In the sequel we shall give a very brief account of some principal theorems concerning almost periodic functions[2]. We shall start with two preliminary definitions:

[1] A detailed discussion of the properties of limit periodic functions is given by H. Bohr: Zur Theorie der fastperiodischen Funktionen II. Acta math. **46** (1925).

[2] For detailed proofs, cf. H. Bohr: Fastperiodische Funktionen, Berlin 1932.

A set of real numbers is called *relatively dense* if there exists a number l such that any interval of length l contains at least one number of the set.

A number τ is called a *translation number* of a function $f(t), -\infty < t < \infty$ corresponding to $\varepsilon > 0$, if

$$|f(t+\tau) - f(t)| \leq \varepsilon$$

for $-\infty < t < \infty$.

A function $f(t)$ is called *almost periodic* if it has the following property

(i) The set of translation numbers of $f(t)$ corresponding to any $\varepsilon > 0$ is relatively dense.

It is a main result of the theory of almost periodic functions that any of the following two properties is equivalent to the preceding one:

(ii) To any $\varepsilon > 0$ exists an exponential polynomial

$$\sum\nolimits^{*} a_\lambda e^{i\lambda t},$$

where λ runs through a finite set of real numbers, approximating $f(t)$ everywhere with the accuracy ε.

(iii) There exist a series of linearly independent real numbers $\beta_1, \beta_2, \cdots$ and a function $F(x)$ with the limit period 2π such that

$$f(t) = F(\beta t) = F(\beta_1 t, \beta_2 t, \cdots).$$

The function $F(x)$ is called a spatial extension (or *the* spatial extension, although $F(x)$ is not uniquely determined) of $f(t)$.

The equivalence of the two latter properties is rather easily proved and it is also rather simple to prove that they imply the property (i), but it is much more difficult to prove that (i) implies (ii) or (iii). This is the main theorem in the theory of almost periodic functions. In the sequel we shall almost exclusively use the property (iii). From the theory of almost periodic functions we also have

Theorem 6. *The set of values assumed by the spatial extension of an almost periodic function $f(t)$ is a subset of the closure of the set of values assumed by $f(t)$.*

Theorem 7. *The set of common translation numbers of a finite number of almost periodic functions corresponding to an arbitrary* $\varepsilon > 0$ *is relatively dense.*

Sum and product of a finite number of almost periodic functions are almost periodic, and if $g(t)$ is almost periodic the function $e^{ig(t)}$ is also almost periodic.

It is important that the numbers $\beta_1, \beta_2, \cdots$ in (iii) can be chosen in a great variety of manners. E. g. any set $\gamma_1, \gamma_2, \cdots$ of linearly independent numbers such that any β_γ can be written as a linear combination with rational coefficient of a finite number of the γ 's. From this follows further

Theorem 8. *To a sequence* $f_1(t), f_2(t), \cdots$ *of almost periodic functions exist a sequence* $\beta_1, \beta_2, \cdots$ *of rationally independent real numbers and a sequence* $F_1(x), F_2(x), \cdots$ *of limit periodic functions such that*

$$f_\nu(t) = F_\nu(\beta t); \ \nu = 1, 2, \cdots,$$

and the sequence $\beta_1, \beta_2, \cdots$ *can be chosen such that it contains any given sequence of rationally independent numbers as a subsequence.*

From the theory of almost periodic functions follows further

Theorem 9. *If a denumerable set* $f_1(t), f_2(t), \cdots$ *of almost periodic functions satisfy an equation*

$$\Phi(f_1(t), f_2(t), \cdots) = 0,$$

where $\Phi(u_1, u_2, \cdots)$ *is continuous when* u_ν *for* $\nu = 1, 2, \cdots$ *belongs to the closure of the set of values assumed by* $f_\nu(t)$, *the spatial extensions* $F_1(x), F_2(x), \cdots$ *satisfy the equation*

$$\Phi(F_1(x), F_2(x), \cdots) = 0.$$

Theorem 10. *If* $G(x)$ *has the limit period* 2π, *and* $(r_1, r_2, \cdots)$ *is a vector with rational coordinates, of which only a finite number are* $\neq 0$, *the function*

$$e^{i(r_1 x_1 + r_2 x_2 + \cdots + G(x))}$$

has the limit period 2π.

If $g(t)$ is almost periodic and c is an arbitrary real number, the function

$$e^{i(ct+g(t))}$$

is almost periodic.

§ 2. The Mean Motions of Limit Periodic and Almost Periodic Functions.

A continuous argument of a continuous function $P(\boldsymbol{x}) = P(x_1, \cdots, x_m)$ with the period 2π in each variable and not assuming the value 0 can evidently be written

$$\arg P(\boldsymbol{x}) = \boldsymbol{p}\boldsymbol{x} + Q(\boldsymbol{x}) = p_1 x_1 + \cdots + p_m x_m + Q(\boldsymbol{x}),$$

where $p_1, \cdots, p_m$ are integers and $Q(\boldsymbol{x})$ is continuous and has the period 2π. For a limit periodic function we have

Theorem 11. *If $F(\boldsymbol{x}) = F(x_1, x_2, \cdots)$ has the limit period 2π and satisfies $|F(\boldsymbol{x})| \geqq k > 0$, a continuous argument of $F(\boldsymbol{x})$ can be written*

$$\arg F(\boldsymbol{x}) = r_1 x_1 + r_2 x_2 + \cdots + G(\boldsymbol{x}) = \boldsymbol{r}\boldsymbol{x} + G(\boldsymbol{x}),$$

where $r_1, r_2, \cdots$ are rational numbers, of which only a finite number are $\neq 0$, and $G(\boldsymbol{x})$ has the limit period 2π.

The vector $\boldsymbol{r}$ is called the mean motion vector of $F(\boldsymbol{x})$.

For the proof[1] we consider a sequence $P_1(\boldsymbol{x}), P_2(\boldsymbol{x}), \cdots$ of continuous functions with the following properties: (i) Each function depends only on a finite number of variables and has a period that is an integral multiple of 2π. (ii) The functions $P_\nu(\boldsymbol{x})$ converge uniformly towards $F(\boldsymbol{x})$ and satisfy

$$|F(\boldsymbol{x}) - P_\nu(\boldsymbol{x})| \leqq \frac{k}{2}; \quad \nu = 1, 2, \cdots.$$

We can choose continuous arguments such that

$$|\arg F(\boldsymbol{x}) - \arg P_\nu(\boldsymbol{x})| < \frac{\pi}{2}; \quad \nu = 1, 2, \cdots \tag{3}$$

and we have for any integer ν

[1] The following proof is very similar to a proof of Theorem 4 given by B. JESSEN *loc. cit.*

$$\arg P_\nu(\boldsymbol{x}) = r_1 x_1 + r_2 x_2 + \cdots + Q_\nu(\boldsymbol{x}),$$

where $r_1, r_2, \cdots$ are rational numbers, of which only a finite number are $\neq 0$, and $Q_\nu(\boldsymbol{x})$ is a continuous function depending on a finite number of variables and having a period that is an integral multiple of 2π. From this and (3) follows

$$\arg F(\boldsymbol{x}) = r_1 x_1 + r_2 x_2 + \cdots + G(\boldsymbol{x}),$$

where $G(\boldsymbol{x})$ is continuous and bounded. But it also follows that the numbers $r_1, r_2, \cdots$ do not depend on ν. Hence it follows that $Q_\nu(\boldsymbol{x})$ converges towards $G(\boldsymbol{x})$, which implies that $G(\boldsymbol{x})$ has the limit period 2π.

Concerning almost periodic functions we have

Theorem 12. *Let $f(t)$ denote an almost periodic function and $F(\boldsymbol{x})$ its spatial extension such that*

$$f(t) = F(\beta_1 t, \beta_2 t, \cdots),$$

where $\beta_1, \beta_2, \cdots$ are rationally independent real numbers. If $f(t)$ satisfies the condition $|f(t)| \geq k > 0$, continuous arguments of $F(\boldsymbol{x})$ and $f(t)$ can be written

$$\arg F(\boldsymbol{x}) = r_1 x_1 + r_2 x_2 + \cdots + G(\boldsymbol{x})$$

and

$$\arg f(t) = ct + g(t),$$

where

$$c = r_1 \beta_1 + r_2 \beta_2 + \cdots$$

and

$$g(t) = G(\beta_1 t, \beta_2 t, \cdots),$$

i. e. $g(t)$ *is almost periodic.*

The constant c is called the mean motion of $f(t)$.

The theorem is an immediate consequence of Theorems 6 and 11. It contains Theorem 4 as a special case.

§ 3. An Auxiliary Theorem on Convergence in an Infinite-Dimensional Space.

A denumerable set $\boldsymbol{a}_\mu = (a_{\mu 1}, a_{\mu 2}, \cdots)$; $\mu = 1, 2, \cdots$ of infinite-dimensional vectors, each with only a finite number of

its coordinates $\neq 0$, is called a complete set of linearly independent vectors if every vector with only a finite number of its coordinates $\neq 0$ in one and only one way can be written as a linear combination of a finite number of the vectors $\boldsymbol{a}_\mu$. This will be the case if and only if any finite number of the vectors $\boldsymbol{a}_\mu$ are linearly independent and each of the unit vectors $\boldsymbol{e}_1 = (1,0,0,\cdots)$, $\boldsymbol{e}_2 = (0,1,0,\cdots)$, $\cdots$ can be written as a linear combination of a finite number of the vectors $\boldsymbol{a}_\mu$.

For the proof of a generalization of Theorem 3 to a denumertable set of phase-modulated oscillations we shall need the following theorem.

Theorem 13. *Let $\boldsymbol{a}_1, \boldsymbol{a}_2, \cdots$ be a complete set of linearly independent vectors, each with only a finite number of its coordinates $\neq 0$, and let $K_1, K_2, \cdots$ be a sequence of positive numbers. Any sequence $\boldsymbol{x}_\nu = (x_{\nu 1}, x_{\nu 2}, \cdots)$; $\nu = 1,2,\cdots$ of vectors satisfying*

$$(4)\quad \begin{cases} |\boldsymbol{a}_\mu \boldsymbol{x}_\nu| = |a_{\mu 1}x_{\nu 1} + a_{\mu 2}x_{\nu 2} + \cdots| \leqq K_\mu; \ \mu = 1,2,\cdots,\nu; \\ \nu = 1,2,\cdots \end{cases}$$

possesses a convergent subsequence.

In fact, for each n we have a representation

$$\boldsymbol{e}_n = \alpha_{n1}\boldsymbol{a}_1 + \cdots + \alpha_{nN_n}\boldsymbol{a}_{N_n},$$

which implies that

$$(5)\qquad x_{\nu n} = \boldsymbol{e}_n \boldsymbol{x}_\nu = \alpha_{n1}\boldsymbol{a}_1\boldsymbol{x}_\nu + \cdots + \alpha_{nN_n}\boldsymbol{a}_{N_n}\boldsymbol{x}_\nu$$

and from (4) and (5) follows that

$$|x_{\nu n}| \leqq |\alpha_{n1}||\boldsymbol{a}_1\boldsymbol{x}_\nu| + \cdots + |\alpha_{nN_n}||\boldsymbol{a}_{N_n}\boldsymbol{x}_\nu| \leqq |\alpha_{n1}|K_1 + \cdots + |\alpha_{nN_n}|K_{N_n};\ \nu = n, n+1, \cdots$$

or

$$|x_{\nu n}| \leqq K_n^*;\ n = 1,2,\cdots;\ \nu = 1,2,\cdots,$$

and it follows by the usual diagonal method that the sequence has a convergent subsequence.

It is easily proved that any sequence of vectors $\boldsymbol{a}_1, \boldsymbol{a}_2, \cdots$, each with only a finite number of its coordinates $\neq 0$, and of

which any finite number are linearly independent, can be enlarged to a complete set of linearly independent vectors, e. g. by adding to the sequence a conveniently chosen subsequence of the sequence of unit vectors.

§ 4. An Auxiliary Theorem from the Topology.

The greater part of our theory will be founded on the following topological theorem, which is an immediate consequence of the theory of the Kronecker index of a surface [1].

Theorem 14. *Let* $\mathfrak{y} = \mathfrak{f}(\mathfrak{x})$ *or* $y_1 = f_1(\mathfrak{x}), \cdots, y_m = f_m(\mathfrak{x})$ *be a continuous vector function in m-dimensional space. If there exists a constant K such that* $|f_\nu(\mathfrak{x})| \leq K$ *for* $\nu = 1, \cdots, m$ *and all vectors* $\mathfrak{x}$, *the vector function* $\mathfrak{y} = \mathfrak{x} + f(\mathfrak{x})$ *maps the total m-dimensional space on itself.*

Generally, of course, the mapping is not a one-to-one-correspondence. For the infinite-dimensional space we shall prove the somewhat more general theorem:

Theorem 15. *Let* $\mathfrak{a}_1, \mathfrak{a}_2, \cdots$ *denote a complete set of linearly independent real vectors,* $K_1, K_2, \cdots$ *positive numbers and* $Q_1(\mathfrak{x}), Q_2(\mathfrak{x}), \cdots$ *continuous real functions satisfying* $|Q_\nu(\mathfrak{x})| \leq K_\nu$; $\nu = 1, 2, \cdots$. *To arbitrary real numbers* $y_1, y_2, \cdots$ *exists a corresponding vector* $\mathfrak{x}$ *satisfying*

$$\mathfrak{a}_\nu \mathfrak{x} + Q_\nu(\mathfrak{x}) = y_\nu; \quad \nu = 1, 2, \cdots. \tag{6}$$

At first we shall restrict our considerations to the equations

$$\mathfrak{a}_\nu \mathfrak{x} + Q_\nu(\mathfrak{x}) = y_\nu; \quad \nu = 1, \cdots, m.$$

It is easily proved that these equations possess a solution. In fact we can enlarge the system so that we obtain a new system

$$\mathfrak{b}_\nu \mathfrak{x} + R_\nu(\mathfrak{x}) = y_\nu; \quad \nu = 1, \cdots, N,$$

where $\mathfrak{b}_1, \cdots, \mathfrak{b}_N$ are linearly independent N-dimensional vectors such that for $\nu = 1, \cdots, m$ the coordinates of $\mathfrak{b}_\nu$ are identical

[1] Cf. e. g. J. Tannery: Introduction à la théorie des fonctions d'une variable, 2. éd., vol. 2, Paris 1910. Note de M. J. Hadamard.

with the N first coordinates of $\boldsymbol{a}_\nu$ including all that are different from zero. If we introduce $z_\nu = \boldsymbol{b}_\nu \boldsymbol{x}$; $\nu = 1, \cdots, N$ as new variables, we obtain a new system of equations satisfying the conditions of Theorem 14 and the assertion follows. We choose zero for the coordinates $x_{N+1}, x_{N+2}, \cdots$.

The solution $\boldsymbol{x}_m$ found in this manner satisfies

$$|\boldsymbol{a}_\nu \boldsymbol{x}_m| = |y_\nu - Q_\nu(\boldsymbol{x})| \leqq |y_\nu| + K_\nu$$

and from Theorem 13 follows that some subsequence of the sequence of vectors $\boldsymbol{x}_m$ converges towards a limit vector $\boldsymbol{x}$, which evidently satisfies all the equations (6).

§ 5. The Main Theorems.

From Theorems 11 and 15 follows immediately

Theorem 16. *Let $F_\nu(\boldsymbol{x}) = F_\nu(x_1, x_2, \cdots)$; $\nu = 1, 2, \cdots$ be a sequence of functions with the limit period 2π and satisfying $|F_\nu(\boldsymbol{x})| \geqq k_\nu > 0$ for all vectors $\boldsymbol{x}$. If the mean motion vectors corresponding to any finite number of the functions $F_\nu(\boldsymbol{x})$ are linearly independent and $v_1, v_2, \cdots$ are arbitrary real numbers, there exists a vector $\boldsymbol{x}$ such that*

$$\arg F_\nu(\boldsymbol{x}) = v_\nu; \quad \nu = 1, 2, \cdots.$$

In fact, if the set of mean motion vectors is not a complete set of linearly independent real vectors, we can make it complete by enlarging the system of functions $F_\nu(\boldsymbol{x})$.

For a finite set of almost periodic functions we have

Theorem 17. *If $c_1, \cdots, c_n$ are rationally independent real numbers and $g_1(t), \cdots, g_n(t)$ are arbitrary almost periodic functions, there exists to any given real numbers $v_1, \cdots, v_n$ and any positive ε a number t satisfying*

$$|c_\nu t + g_\nu(t) - v_\nu| \leqq \varepsilon \pmod{2\pi}; \quad \nu = 1, \cdots, n, \tag{7}$$

i. e. *the curve $x_\nu = c_\nu t + g_\nu(t)$; $\nu = 1, \cdots, n$ is* mod. 2π *everywhere dense in the n-dimensional space.*

According to Theorem 8 we choose a sequence $\beta_1, \beta_2, \cdots$ of rationally independent real numbers, where $\beta_1 = c_1, \cdots, \beta_n = c_n$, such that

$$c_\nu t + g_\nu(t) = \beta_\nu t + G_\nu(\boldsymbol{\beta} t); \ \nu = 1, \cdots, n,$$

where the functions $G_\nu(\boldsymbol{x})$; $\nu = 1, \cdots, n$ have the limit period 2π. It follows from Theorem 14 that there exists a vector $\boldsymbol{x}^* = (x_1^*, \cdots, x_n^*, 0, \cdots)$, satisfying

$$x_\nu^* + G_\nu(\boldsymbol{x}^*) = v_\nu.$$

We can further choose continuous periodic functions $Q_1(\boldsymbol{x})$, $\cdots, Q_n(\boldsymbol{x})$ each depending only on a finite number of variables, such that

$$|G_\nu(\boldsymbol{x}) - Q_\nu(\boldsymbol{x})| \leq \frac{\varepsilon}{3}; \ \nu = 1, \cdots, n$$

for all vectors $\boldsymbol{x}$. From Kronecker's theorem follows the existence of a number t satisfying

$$|Q_\nu(\boldsymbol{x}^*) - Q_\nu(\boldsymbol{\beta} t)| \leq \frac{\varepsilon}{6}; \ \nu = 1, \cdots, n$$

and

$$|x_\nu^* - \beta_\nu t| \leq \frac{\varepsilon}{6} \ (\text{mod. } 2\pi); \ \nu = 1, \cdots, n.$$

Hence

$$\begin{aligned} |c_\nu t + g_\nu(t) - v_\nu| &= |\beta_\nu t + G_\nu(\boldsymbol{\beta} t) - v_\nu| \leq |G_\nu(\boldsymbol{\beta} t) - Q_\nu(\boldsymbol{\beta} t)| + \\ &+ |\beta_\nu t - x_\nu^*| + |Q_\nu(\boldsymbol{\beta} t) - Q_\nu(\boldsymbol{x}^*)| + |Q_\nu(\boldsymbol{x}^*) - G_\nu(\boldsymbol{x}^*)| + \\ &+ |x_\nu^* + G_\nu(\boldsymbol{x}^*) - v_\nu| \leq \frac{\varepsilon}{3} + \frac{\varepsilon}{6} + \frac{\varepsilon}{6} + \frac{\varepsilon}{3} + 0 = \varepsilon \ (\text{mod. } 2\pi), \end{aligned}$$

which proves the theorem.

Theorem 3, announced in the introduction, is evidently equivalent with Theorem 17. We observe that the theorem is not valid for a denumerable set of almost periodic functions. E. g. the pure oscillations $e^{i\beta_1 t}, e^{i\beta_2 t}, \cdots$, where the numbers $\beta_1, \beta_2, \cdots$ are rationally independent and converge towards zero, will never simultaneously obtain values near -1.

We shall further prove the following generalization of the Kronecker-Bohl theorem.

Theorem 18. *The set of numbers satisfying* (7) *is relatively dense.*

In fact, if we choose the real number t_0 satisfying

$$|c_\nu t_0 + g_\nu(t_0) - v_\nu| \leqq \frac{\varepsilon}{2} (\text{mod. } 2\pi); \quad \nu = 1, \cdots, n,$$

any number $t_0 + \tau$, where τ is a common translation number of the almost periodic functions

$$e^{i(c_\nu t + g_\nu(t) - v_\nu)}$$

corresponding to $2 \sin \frac{\varepsilon}{4}$, satisfies (7). Hence the theorem follows from Theorem 7.

§ 6. On Limit Periodic and Almost Periodic Functions Satisfying Linear Relations.

From Theorem 15 follows

Theorem 19. *If a sequence of functions* $F_\nu(\boldsymbol{x}) = F_\nu(x_1, x_2, \cdots)$ *with the limit period* 2π *and with the property* $|F_\nu(\boldsymbol{x})| \geq k_\nu > 0$; $\nu = 1, 2, \cdots$ *for all* $\boldsymbol{x}$ *satisfies a linear relation*

$$\alpha_1 F_1(\boldsymbol{x}) + \alpha_2 F_2(\boldsymbol{x}) + \cdots = 0, \tag{8}$$

where $\alpha_1, \alpha_2, \cdots$ *are complex constants that are* $\neq 0$, *and the series on the left converges for all real vectors* $\boldsymbol{x}$, *the mean motion vectors* $\boldsymbol{r}_1, \boldsymbol{r}_2, \cdots$ *are linearly dependent, i. e. the set of mean motion vectors has a finite subset of vectors that are linearly dependent. This is still true even if the condition* $|F_\nu(\boldsymbol{x})| \geq k_\nu > 0$ *is satisfied for only one value of* ν, *if for every* ν *we have a representation*

$$F_\nu(\boldsymbol{x}) = |F_\nu(\boldsymbol{x})| \, e^{i(\boldsymbol{r}_\nu \boldsymbol{x} + G_\nu(\boldsymbol{x}))}$$

where $G_\nu(\boldsymbol{x})$ *is continuous and bounded and* $\boldsymbol{r}_\nu$ *is a vector with rational coordinates, of which only a finite number are* $\neq 0$.

In fact, if the vectors $\boldsymbol{r}_\nu$ were linearly independent, according to Theorem 15 there would exist a vector $\boldsymbol{x}^*$ satisfying

$$\boldsymbol{r}_\nu \boldsymbol{x}^* + G_\nu(\boldsymbol{x}^*) + \arg \alpha_\nu = 0; \quad \nu = 1, 2, \cdots,$$

and for $x = x^*$ the left side of (8) would be positive and the relation would not be satisfied.

Theorem 20. *Let $f_1(t), f_2(t), \cdots$ be a sequence of almost periodic functions satisfying $|f_\nu(t)| \geq k_\nu > 0$; $\nu = 1, 2, \cdots$ and let K_ν denote the upper bound of $|f_\nu(t)|$; $\nu = 1, 2, \cdots$. If $\alpha_1, \alpha_2, \cdots$ are complex numbers different from zero such that $\sum_{\nu=0}^{\infty} |\alpha_\nu| K_\nu$ is convergent and if we have*

$$\alpha_1 f_1(t) + \alpha_2 f_2(t) + \cdots = 0, \tag{9}$$

the mean motions $c_1, c_2, \cdots$ of $f_1(t), f_2(t), \cdots$ are rationally dependent.

From Theorem 9 follows that the relation (9) implies an analogous relation between the spatial extensions and the theorem therefore follows immediately from Theorems 19 and 12.

We shall prove some stronger theorems concerning finite sets of almost periodic functions satisfying linear relations. For the sake of brevity a function $r(t)\, e^{i(ct+g(t))}$, where $g(t)$ is a real almost periodic function and $r(t)$ is a real, non-negative function, will be called a *modulated oscillation*. It will further be called *normal* if the set of zeros of $r(t)$ contains no intervals.

Theorem 21. *If a finite set of modulated oscillations $f_\nu(t) = r_\nu(t)\, e^{i(c_\nu t + g_\nu(t))}$; $\nu = 1, \cdots, n$ satisfy a linear relation*

$$\alpha_1 f_1(t) + \cdots + \alpha_n f_n(t) + \beta = 0, \tag{10}$$

where $\alpha_1, \cdots, \alpha_n$, and β are arbitrary complex numbers $\neq 0$, the mean motions $c_1, \cdots, c_n$ are rationally dependent.

If the numbers $c_1, \cdots, c_n$ were rationally independent, it would follow from Theorem 17 that the inequalities

$$|c_\nu t + g_\nu(t) + \arg \alpha_\nu - \arg \beta| \leq \frac{\pi}{2} \pmod{2\pi}; \quad \nu = 1, \cdots, n$$

were satisfied for some value of t in contradiction to the relation (10).

We notice that Theorem 21 is a generalization of theorem 5, mentioned in the introduction. In the case where $\beta = 0$, we have

Theorem 22. *If a finite set of modulated oscillations* $f_\nu(t) = r_\nu(t)\, e^{i(c_\nu t + g_\nu(t))}$; $\nu = 1, \cdots, n$, *of which at least one is normal, satisfy a relation*

$$\alpha_1 f_1(t) + \cdots + \alpha_n f_n(t) = 0, \tag{11}$$

where $\alpha_1, \cdots, \alpha_n$ *are arbitrary complex numbers that are* $\neq 0$, *the mean motions* $c_1, \cdots, c_n$ *satisfy a linear relation*

$$r_1 c_1 + \cdots + r_n c_n = 0,$$

where $r_1, \cdots, r_n$ *are rational numbers satisfying*

$$r_1 + \cdots + r_n = 0,$$

and not all zeros.

We choose a real number c that cannot be written $c = r_1 c_1 + \cdots + r_n c_n$ with rational $r_1, \cdots, r_n$. If the real numbers $c + c_1, \cdots, c + c_n$ were rationally independent, it would follow from Theorem 17 and the continuity of $g_1(t), \cdots, g_n(t)$ that the inequalities

$$|(c + c_\nu)\, t + g_\nu(t) + \arg \alpha_\nu| \leqq \frac{\pi}{4} \pmod{2\pi}; \quad \nu = 1, \cdots, n$$

were satisfied for all values of t belonging to some interval $t_1 \leqq t \leqq t_2$. One of the oscillations, say $f_\mu(t)$, is normal, and hence the interval $t_1 \leqq t \leqq t_2$ contains a point t^*, where $r_\mu(t^*) > 0$. From this would follow that the term $\alpha_\mu f_\mu(t^*)\, e^{ict}$ had a positive real part and none of the terms $\alpha_\nu f_\nu(t^*)\, e^{ict}$ had negative real parts, and the relation (11) could not be satisfied for $t = t^*$. We have thus proved the existence of a relation

$$r_1(c + c_1) + \cdots + r_n(c + c_n) = 0, \tag{12}$$

where $r_1, \cdots, r_n$ are rational and not all zero. As c cannot be written as a linear combination of $c_1, \cdots, c_n$ with rational coefficients the relation (12) implies the following two relations

$$r_1 + \cdots + r_n = 0$$

$$r_1 c_1 + \cdots + r_n c_n = 0,$$

which proves the theorem.

As a very special case of Theorem 21 we have the following theorem, which is a slight generalization of Jessen's original theorem mentioned in the introduction.

Theorem 23. *Let $f(t)$ be an almost periodic function. We consider all complex numbers a, for which we have a representation*

$$f(t)-a=|f(t)-a|\,e^{i(ct+g(t))},$$

where $g(t)$ is an almost periodic function. The values c corresponding to all possible values of a are rational multiples of one real number.

§ 7. On Almost Periodic Functions Satisfying Quadratic Relations.

Theorem 24. *Let $f_1(t)$, $f_2(t)$, and $f_3(t)$ be three almost periodic functions satisfying $|f_\nu(t)|\geqq k>0$; $\nu=1,2,3$, and let c_1, c_2, and c_3 denote their mean motions. If we have a relation*

$$a_1f_1(t)^2+a_2f_2(t)^2+a_3f_3(t)^2+b_1f_2(t)f_3(t)+b_2f_3(t)f_1(t)+\\+b_3f_1(t)f_2(t)+k=0,$$

where at least one of the complex numbers $a_1, a_2, a_3, b_1, b_2, b_3$, and k is $\neq 0$, we have a relation

$$r_1c_1+r_2c_2+r_3c_3=0,$$

where r_1, r_2, and r_3 are rational numbers of which at least one is $\neq 0$.

From Theorem 9 follows that the spatial extensions $F_1(\mathfrak{x})$, $F_2(\mathfrak{x})$, and $F_3(\mathfrak{x})$ satisfy the equation

$$(13)\qquad a_1z_1^2+a_2z_2^2+a_3z_3^2+b_1z_2z_3+b_2z_3z_1+b_3z_1z_2+k=0$$

and if c_1, c_2, c_3 were rationally independent it would follow from Theorems 12 and 16 that the equation (13) would possess solutions z_1, z_2, z_3 with any given set of arguments $\varphi_1, \varphi_2, \varphi_3$. Hence it is sufficient to prove the existence of a set of numbers $\varphi_1, \varphi_2, \varphi_3$ such that the equation

$$a_1 r_1^2 e^{2i\varphi_1} + a_2 r_2^2 e^{2i\varphi_2} + a_3 r_3^2 e^{2i\varphi_3} + b_1 r_2 r_3 e^{i(\varphi_2+\varphi_3)} + b_2 r_3 r_1 e^{i(\varphi_3+\varphi_1)} + \\ + b_3 r_1 r_2 e^{i(\varphi_1+\varphi_2)} + k = 0$$

is not satisfied for any positive values of r_1, r_2, r_3. Without restricting the generality we may suppose that $k \geqq 0$ (if not, we multiply the equation by a convenient factor $e^{i\varphi}$).

Let us first suppose that at most one of the numbers b_1, b_2, b_3 is zero. In this case it is sufficient to determine $\varphi_1, \varphi_2, \varphi_3$ such that

$$|2\varphi_\nu + \operatorname{Arg} a_\nu| \leqq \frac{\pi}{2} \quad (\text{mod. } 2\pi);\ \nu = 1,2,3$$

$$|\varphi_2 + \varphi_3 + \operatorname{Arg} b_1| \leqq \frac{\pi}{2} \quad (\text{mod. } 2\pi)$$

$$|\varphi_3 + \varphi_1 + \operatorname{Arg} b_2| \leqq \frac{\pi}{2} \quad (\text{mod. } 2\pi)$$

$$|\varphi_1 + \varphi_2 + \operatorname{Arg} b_3| \leqq \frac{\pi}{2} \quad (\text{mod. } 2\pi),$$

where the sign $<$ holds in at least two of the three last inequalities (If a coefficient is zero, its argument is in this connection defined as zero). If we put

$$\psi_\nu = \varphi_\nu + \frac{1}{2} \operatorname{Arg} a_\nu;\ \nu = 1,2,3, \tag{14}$$

we obtain a new set of equations

$$|\psi_\nu| \leqq \frac{\pi}{4} \quad (\text{mod. } \pi);\ \nu = 1,2,3 \tag{15}$$

$$\begin{cases} |\psi_2 + \psi_3 - \alpha_1| \leqq \frac{\pi}{2} \quad (\text{mod. } 2\pi) \\ |\psi_3 + \psi_1 - \alpha_2| \leqq \frac{\pi}{2} \quad (\text{mod. } 2\pi) \\ |\psi_1 + \psi_2 - \alpha_3| \leqq \frac{\pi}{2} \quad (\text{mod. } 2\pi), \end{cases} \tag{16}$$

and to prove our theorem we shall find solutions to this system such that the sign $<$ holds in two of the last three inequalities.

If at least two of the numbers $\alpha_1, \alpha_2, \alpha_3$, say α_1 and α_2, are neither 0 nor π (mod. 2π), we have

$$\left|\varepsilon_1 \frac{\pi}{2} - \alpha_1\right| < \frac{\pi}{2} \quad (\text{mod. } 2\pi)$$

$$\left|\varepsilon_2 \frac{\pi}{2} - \alpha_2\right| < \frac{\pi}{2} \quad (\text{mod. } 2\pi)$$

$$\left|\varepsilon_3 \frac{\pi}{2} - \alpha_3\right| \leqq \frac{\pi}{2} \quad (\text{mod. } 2\pi)$$

when $\varepsilon_1, \varepsilon_2, \varepsilon_3$ are chosen conveniently as 1 or -1. If we choose ψ_1, ψ_2, ψ_3 such that

$$(17) \quad \begin{cases} \psi_2 + \psi_3 = \varepsilon_1 \dfrac{\pi}{2} \\ \psi_3 + \psi_1 = \varepsilon_2 \dfrac{\pi}{2} \\ \psi_1 + \psi_2 = \varepsilon_3 \dfrac{\pi}{2}, \end{cases}$$

the inequalities (16) are satisfied and the sign $<$ holds in at least two of them. But from the equations (17) results

$$\psi_1 + \psi_2 + \psi_3 = \pm \frac{\pi}{4} \text{ or } \pm \frac{3\pi}{4},$$

and it follows that ψ_1, ψ_2, and ψ_3 have also values $\pm \frac{\pi}{4}$ or $\pm \frac{3\pi}{4}$, which proves that the inequalities (15) are satisfied.

If at least two of the numbers $\alpha_1, \alpha_2, \alpha_3$, say α_1 and α_2, are 0 or π (mod. 2π), we choose $\varepsilon_3 = \pm 1$ such that $\left|\varepsilon_3 \frac{\pi}{2} - \alpha_3\right| \leqq \frac{\pi}{2}$ (mod. 2π), and it is sufficient to choose ψ_1, ψ_2, ψ_3 as solutions of the equations

$$\begin{aligned} \psi_2 + \psi_3 &= \alpha_1 \\ \psi_3 + \psi_1 &= \alpha_2 \\ \psi_1 + \psi_2 &= \varepsilon_3 \frac{\pi}{2}. \end{aligned}$$

Finally we consider the case, where at least two of the numbers b_1, b_2, and b_3, say b_1 and b_2, are zero. It is then sufficient to determine ψ_1, ψ_2, and ψ_3 such that

$$|2\varphi_1 + \operatorname{Arg} a_1| < \frac{\pi}{2} \quad (\text{mod. } 2\pi)$$

$$|2\varphi_2 + \operatorname{Arg} a_2| < \frac{\pi}{2} \quad (\text{mod. } 2\pi)$$

$$|2\varphi_3 + \operatorname{Arg} a_3| < \frac{\pi}{2} \quad (\text{mod. } 2\pi)$$

$$|\varphi_1 + \varphi_2 \operatorname{Arg} b_3| < \frac{\pi}{2} \quad (\text{mod. } 2\pi).$$

As φ_3 occurs in only one inequality, it is sufficient to consider φ_1 and φ_2. If we use (14) once more, we obtain the inequalities

$$|\psi_2| < \frac{\pi}{4} \quad (\text{mod. } \pi)$$

$$|\psi_2| < \frac{\pi}{4} \quad (\text{mod. } \pi)$$

$$|\psi_1 + \psi_2 + \alpha| < \frac{\pi}{2} \quad (\text{mod. } 2\pi),$$

which have solutions. In fact, any angle between $-\frac{\pi}{2}$ and $\frac{\pi}{2}$ can be written as $\psi_1 + \psi_2$, where $|\psi_1| < \frac{\pi}{4}$ and $|\psi_2| < \frac{\pi}{4}$, and any angle between $\frac{\pi}{2}$ and $\frac{3\pi}{2}$ can be written $\psi_1 + \psi_2$ with $|\psi_1| < \frac{\pi}{4}$, and $\frac{3\pi}{4} < \psi_2 < \frac{5\pi}{4}$. This proves the theorem.

Theorem 25. *If the constant k vanishes, the numbers r_1, r_2, and r_3 can be chosen such that*

$$r_1 + r_2 + r_3 = 0.$$

We choose a real number c that cannot be written $r_1 c_1 + r_2 c_2 + r_3 c_3$, and Theorem 25 follows, when Theorem 24 is applied to the functions $f_1(t)\, e^{ict}$, $f_2(t)\, e^{ict}$, $f_3(t)\, e^{ict}$.

Indleveret til Selskabet den 9. Maj 1947.
Færdig fra Trykkeriet den 11. Maj 1948.

DET KGL. DANSKE VIDENSKABERNES SELSKAB
MATEMATISK-FYSISKE MEDDELELSER, BIND XXIV, NR. 12

INFINITE SYSTEMS OF LINEAR CONGRUENCES WITH INFINITELY MANY VARIABLES

BY

HARALD BOHR AND ERLING FØLNER

KØBENHAVN
I KOMMISSION HOS EJNAR MUNKSGAARD
1948

TABLE OF CONTENTS

Printed in Denmark
Bianco Lunos Bogtrykkeri

§ 1. Introduction.

In the present paper we shall investigate a general problem concerning an arbitrary enumerable system of linear congruences with an enumerable number of variables

$$(1)\qquad \begin{aligned} &a_{11}x_1 + a_{12}x_2 + \cdots + a_{1n_1}x_{n_1} \equiv \theta_1 \pmod 1 \\ &a_{21}x_1 + a_{22}x_2 + \cdots + a_{2n_2}x_{n_2} \equiv \theta_2 \pmod 1 \\ &\cdots\cdots\cdots\cdots\cdots\cdots\cdots\cdots \end{aligned}$$

where every congruence only contains a finite number of variables and the a's and the θ's are arbitrary (real) numbers.

By the consideration of certain classifications of the almost periodic functions one of the authors[1] met with a problem concerning a system of congruences of the above form but in the special case where all the a's were *rational* numbers. The problem was to give a convenient necessary and sufficient condition on the system of linear forms

$$(2)\qquad \begin{aligned} &a_{11}x_1 + a_{12}x_2 + \cdots + a_{1n_1}x_{n_1} \\ &a_{21}x_1 + a_{22}x_2 + \cdots + a_{2n_2}x_{n_2} \\ &\cdots\cdots\cdots\cdots\cdots\cdots\cdots \end{aligned}$$

in order that it possesses the following property: For every choice of the numbers $\theta_1, \theta_2, \cdots$ for which any finite subsystem of the system of congruences (1) has a solution[2]—or, what amounts to the same, for which for any N the system of the N first of

1) H. Bohr: Unendlich viele lineare Kongruenzen mit unendlich vielen Unbekannten. Kgl. Danske Videnskabernes Selskab. Math.-fys. Meddelelser, Bind VII, 1925. In the following this paper is cited by (I). We do not, however, assume the reader to be acquainted with (I).

2) It will be convenient to interpret, not only a solution of the whole system (1), but also a solution of a finite subsystem of (1) as a point $(x_1, x_2, \cdots)$ in the infinite-dimensional space, although for a subsystem only a finite number of the variables really enters in the congruences in question (and the rest of the variables therefore can be chosen quite arbitrarily).

the congruences (1) has a solution—there shall exist a solution of the whole system (1).

If instead of the congruences (1) we consider the corresponding system of equations (now without limitation to rational coefficients) there exists no analogous problem. In fact, it follows from a general investigation of Toeplitz on such systems of equations that for an arbitrary given system the existence of a solution of any finite subsystem always will involve the existence of a solution of the whole system of equations. A direct proof of this special theorem can be found in the paper (I).

That the analogous theorem really is not true for congruences (not even if we restrict ourselves to rational coefficients) can be seen from the following simple example where, moreover, only a single variable x_1 explicitly enters (all the other variables $x_2, x_3, \cdots$ having the coefficients 0).

Example 1. We consider the system of congruences

$$\frac{1}{3}x_1 \equiv \theta_1 \pmod 1$$

$$\frac{1}{9}x_1 \equiv \theta_2 \pmod 1$$

$$\cdots\cdots\cdots\cdots$$

$$\frac{1}{3^n}x_1 \equiv \theta_n \pmod 1$$

$$\cdots\cdots\cdots\cdots$$

for $\theta_1 = \theta_2 = \cdots = \frac{1}{2}$. The solutions of the n^{th} congruence are all points $(x_1, x_2, \cdots)$ where $x_2, x_3, \cdots$ are arbitrary numbers and x_1 is a number from the "lattice" $x_1 \equiv \frac{3^n}{2} \pmod{3^n}$. These solutions are also solutions of the $(n-1)^{\text{th}}$ congruence, for if $x_1 \equiv \frac{3^n}{2} \pmod{3^n}$ then also $x_1 \equiv \frac{3^n}{2} \pmod{3^{n-1}}$, i. e. $x_1 \equiv \frac{3^{n-1}}{2} \pmod{3^{n-1}}$, since $\frac{3^n}{2} = \frac{3^{n-1}}{2} + 3^{n-1}$. Hence for every N the N first congruences have solutions, viz. all the solutions $x_1 \equiv \frac{3^N}{2} \pmod{3^N}$ of the N^{th} congruence. But nevertheless, there is no solution of the whole system of congruences, for if $(x_1, x_2, \cdots)$ is a solution of the N^{th} congruence then $|x_1| \geqq \frac{3^N}{2}$ which $\to \infty$ for $N \to \infty$.

For a given system of linear forms (2) we shall denote by π_1 the set of points $(\theta_1, \theta_2, \cdots)$ for which the corresponding infinite

system (1) has a solution, and by π_2 the set of points $(\theta_1, \theta_2, \cdots)$ for which any finite subsystem of (1) has a solution. It is plain that $\pi_1 \subseteqq \pi_2$ and that both sets contain the point $(0, 0, \cdots)$.

The previous, in (I) treated, problem was to indicate a necessary and sufficient condition that a given system of linear forms (2) with rational coefficients have $\pi_1 = \pi_2$. Before stating the result we shall have to mention the notion of a *substitution* in an enumerable number of variables. A substitution is a linear transformation of the form

$$
\begin{aligned}
y_1 &= a_{11}x_1 + a_{12}x_2 + \cdots + a_{1p_1}x_{p_1} \\
y_2 &= a_{21}x_1 + a_{22}x_2 + \cdots + a_{2p_2}x_{p_2} \qquad (3) \\
&\cdots\cdots\cdots\cdots\cdots\cdots\cdots
\end{aligned}
$$

which establishes a one-to-one mapping of the whole infinite-dimensional space on the *whole* infinite-dimensional space. As shown in (I) (cp. also § 4 of the present paper) a necessary and sufficient condition that the transformation (3) be a substitution is that no linear dependance exists amongst (any finite number of) the linear forms on the right-hand side of (3) and that each of the variables x_m can be "isolated", i. e. written as a linear combination of a finite number of the linear forms. In particular, any substitution has an "inverse substitution"

$$
\begin{aligned}
x_1 &= \beta_{11}y_1 + \beta_{12}y_2 + \cdots + \beta_{1q_1}y_{q_1} \\
x_2 &= \beta_{21}y_1 + \beta_{22}y_2 + \cdots + \beta_{2q_2}y_{q_2} \\
&\cdots\cdots\cdots\cdots\cdots\cdots\cdots
\end{aligned}
$$

If a substitution is applied to a linear form we get a new linear form. The importance of substitutions in our problem is plain because a substitution applied to a system of linear forms will not change any of the sets π_1 and π_2 simply because two linear forms which correspond by the substitution will take the same value for corresponding values of the variables.

The solution of the former problem can now be stated as follows. *A necessary and sufficient condition that a system of linear forms with rational coefficients have $\pi_1 = \pi_2$ is that the system by a substitution can be transfered into an integral system, i. e. a system with mere integral coefficients.*

We remark, for orientation, that the *sufficiency* of the condition is easy to prove. In fact, on account of the invariance of the sets π_1 and π_2 by a substitution (applied to the linear forms) we need only show that every integral system (2) has $\pi_1 = \pi_2$. Denoting by $(\theta_1, \theta_2, \cdots)$ an arbitrary point from π_2 we shall show that it also lies in π_1. Let $P_N = (\xi_1^{(N)}, \xi_2^{(N)}, \cdots)$ be a solution of the N first congruences (1), $N = 1, 2, \cdots$. Since all a's are integral we can assume all ξ's reduced modulo 1 to lie in the interval $0 \leqq \xi < 1$. Hence we can choose a subsequence P_{N_p}, $p = 1, 2, \cdots$, of the sequence P_N, such that every coordinate sequence $\xi_i^{(N_p)}$ (i fixed) converges towards a number ξ_i for $p \to \infty$. The "limit-point" $(\xi_1, \xi_2, \cdots)$ will then be a solution of all the congruences (1), for if N_0 is an arbitrary positive integral number then $(\xi_1, \xi_2, \cdots)$ from continuity reasons will satisfy the N_0^{th} congruence because this congruence only contains a finite number of variables and the point $(\xi_1^{(N_p)}, \xi_2^{(N_p)}, \cdots)$ for every $p \geqq N_0$ is a solution of the congruence.—The real problem in (I) was to show the necessity of the condition, i. e. that amongst the rational systems there are no other systems than those mentioned above which have $\pi_1 = \pi_2$.

In the present paper we shall treat the corresponding problem for congruences with *arbitrary* coefficients. Also in this general case the systems with $\pi_1 = \pi_2$ can be characterized as systems which by substitutions can be transfered into systems of a certain simple type, denoted by S, which obviously has $\pi_1 = \pi_2$ and whose algebraic structure can be accounted for.

By *a system of linear forms of the type S* we shall understand a system where certain of the variables (finite or infinite in number) have mere integral coefficients while each of the other variables (finite or infinite in number) necessarily becomes 0 if for a sufficiently large N (i. e. for $N \geqq N_0$ where N_0 depends on the variable) one solves the N first "zero-congruences" corresponding to the linear forms, i. e. the congruences (1) with $\theta_1 = \theta_2 = \cdots = 0$.

Our purpose is to prove the following

Main Theorem[1]. *A necessary and sufficient condition that a*

1) Incidentally, our proof of the main theorem in reality yields a stronger form of this theorem than the one indicated here. For the formulation of the theorem in the stronger form we refer to § 5.

system of linear forms have $\pi_1 = \pi_2$ is that the system by a substitution can be transfered into a system of the type S.

Also in this case it is easy to prove that the condition is *sufficient*. We only have to show that every system of the type S has $\pi_1 = \pi_2$. Denoting by $(\theta_1, \theta_2, \cdots)$ an arbitrary point from π_2 we shall show that it also belongs to π_1. Let $P_N = (\xi_1^{(N)}, \xi_2^{(N)}, \cdots)$ be a solution of the N first congruences (1). We may assume those coordinates which in all congruences have integral coefficients reduced modulo 1 to lie in the interval $0 \leqq \xi < 1$. Everyone of the remaining coordinates $\xi_i^{(N)}$ will possess a constant value ξ_i for $N \geqq N_0$ where $N_0 = N_0(i)$ is determined such that every solution $(x_1, x_2, \cdots)$ of the N_0 first zero-congruences will have $x_i = 0$; for as the two points $(\xi_1^{(N_0)}, \xi_2^{(N_0)}, \cdots)$ and $(\xi_1^{(N)}, \xi_2^{(N)}, \cdots)$ are both solutions of the N_0 first congruences (1) their difference $(\xi_1^{(N)} - \xi_1^{(N_0)}, \xi_2^{(N)} - \xi_2^{(N_0)}, \cdots)$ will be a solution of the N_0 first zero-congruences and hence $\xi_i^{(N)} - \xi_i^{(N_0)} = 0$, i. e. $\xi_i^{(N)} = \xi_i^{(N_0)} = \xi_i$ for $N \geqq N_0$. We now extract a subsequence from our sequence of points $P_N = (\xi_1^{(N)}, \xi_2^{(N)}, \cdots)$ such that any coordinate sequence $\xi_i^{(N)}$ (i fixed) which does not end in being a constant will converge towards a number ξ_i; this can be done since they are all lying in the interval $0 \leqq \xi < 1$. The limit point $(\xi_1, \xi_2, \cdots)$ will obviously (for continuity reasons) be a solution of all the congruences (1) and hence the point $(\theta_1, \theta_2, \cdots)$ will lie in π_1.

That the main theorem above contains the main theorem in (I) can be seen in the following way. Since every integral system is also a system of the type S the "trivial" part of the main theorem in (I) (concerning the sufficiency of the condition) is contained in the trivial part of the general main theorem. To show that the non-trivial part of the general main theorem involves the non-trivial part of the main theorem in (I) requires a little consideration. We are to show that any rational system (2) with $\pi_1 = \pi_2$ can be transfered into an integral system. The general main theorem only states that it can be transfered into a system of the type S. By using, however, that the system is rational we can easily prove that the resulting system of the type S always must be integral. Otherwise, in fact, there would exist in this system a variable y_m which for N sufficiently large necessarily becomes 0 by solution of the N first zero-congruences. The

solutions of the N first zero-congruences in the original system would therefore satisfy an equation $a_{m1}x_1 + \cdots + a_{mp_m}x_{p_m} = 0$ whose left-hand side is that linear form which in the substitution used is put equal to y_m. Denoting, however, by G a common denominator of all the coefficients in the N first linear forms in the original system, obviously all points $(h_1G, h_2G, \cdots)$ where h_1, h_2, $\cdots$ are arbitrary integers will be solutions of the corresponding zero-congruences, and these points cannot possibly all satisfy the equation $a_{m1}x_1 + \cdots + a_{mp_m}x_{p_m} = 0$ (whose coefficients are not all 0). Hence our assumption has led to a contradiction.

That the proof of the general main theorem cannot follow quite the same line as the proof in the rational case given in (I) is due to the fact that certain finite-dimensional sets which enter in the investigation (see § 2), and which in (I) without real limitation could be supposed to be lattices, in the present case are modules of a more general kind. If, however, closures are taken of the sets in question these closures will get properties analogous to the sets in (I). But in order to obtain the substitution which transfers a given system of linear forms with $\pi_1 = \pi_2$ into a system of the special type S we should still as in (I) have to consider the mentioned sets themselves and not their closures. Now, however, from the properties of the closures it would be possible to get at analogous properties for the sets themselves which would allow the seeking out of the substitution wanted. This would be a similar, though more complicated line to that followed in (I) and until recently our intension had been to use this arrangement. Then, however, B. Jessen asked us whether in the infinite-dimensional space in question a structural theorem existed for closed modules analogous to that holding for such modules in a finite-dimensional space. That this is really the case we could answer affirmatively by help of our main theorem. Later on we found a more direct proof of this structural theorem for closed modules in the infinite-dimensional space by using the dual connection between our space and another infinite-dimensional space, a connection which in case of the finite-dimensional space was introduced by M. Riesz. Now, conversely, it turned out that a more perspicious proof of the main theorem could be obtained by first establishing the structural theorem for closed

modules and then applying it to our problem. In fact, by applying this structural theorem to the closed module Γ formed by the set of all solutions of the zero-congruences corresponding to the given system of linear forms we could directly obtain the desired substitution, i. e. the substitution which takes our system (1) into a system of the type S and thus avoiding all difficulties arising from the consideration of the above mentioned non-closed modules.

In the present paper we have prefered to give the proof in this latter arrangement.

§ 2. Some important sets.

Already by the definition of a system of linear forms of the type S we had to consider the corresponding zero-congruences. In our treatment of the arbitrary system of congruences (1) the corresponding system of zero-congruences

$$
\begin{aligned}
&a_{11}x_1 + a_{12}x_2 + \cdots + a_{1n_1}x_{n_1} \equiv 0 \pmod 1 \\
&a_{21}x_1 + a_{22}x_2 + \cdots + a_{2n_2}x_{n_2} \equiv 0 \pmod 1 \\
&\cdots\cdots\cdots\cdots\cdots\cdots\cdots\cdots
\end{aligned} \tag{4}
$$

will play an important role. In connection with the zero-congruences (4) we introduce the following notations.

$$
\left\{
\begin{array}{ll}
\Gamma & : \text{The set of solutions of the zero-congruences (4).} \\
\Gamma_m & : \text{The projection of } \Gamma \text{ on the } x_1 \cdots x_m\text{-space.} \\
H_m & : \text{The closure of } \Gamma_m. \\
\Lambda^{(N)} & : \text{The set of solutions of the } N \text{ first zero-congruences in (4).} \\
\Lambda_m^{(N)} & : \text{The projection of } \Lambda^{(N)} \text{ on the } x_1 \cdots x_m\text{-space.} \\
H_m^{(N)} & : \text{The closure of } \Lambda_m^{(N)}.
\end{array}
\right. \tag{5}
$$

Here Γ and $\Lambda^{(N)}$ are point sets in the infinite-dimensional space while the four other sets (with lower index m) are point sets in the m-dimensional $x_1 \cdots x_m$-space. Γ_m and $\Lambda_m^{(N)}$ are obviously (vector-) modules and hence H_m and $H_m^{(N)}$ are closed modules. Further, for $m_1 < m$, the module Γ_{m_1} is the projection of Γ_m on the $x_1 \cdots x_{m_1}$-space, and similarly $\Lambda_{m_1}^{(N)}$ is the projection of $\Lambda_m^{(N)}$.

As well-known the closed modules in the $x_1 \cdots x_m$-space have an especially simple structure. Let H be an arbitrary closed module in the m-dimensional space. Then it is possible to find a system of *linearly independent* vectors $F_1, \cdots, F_p, V_1, \cdots, V_q$ $(p + q \leqq m)$ such that H consists of all vectors (points) of the form

$$P = \xi_1 F_1 + \xi_2 F_2 + \cdots + \xi_p F_p + h_1 V_1 + \cdots + h_q V_q$$

where the ξ's are arbitrary numbers and the h's are arbitrary integers. Conversely, each such point set is a closed module. We shall say that the vectors $F_1, \cdots, F_p$ and $V_1, \cdots, V_q$ (together) generate H with respectively arbitrary and integral coefficients.

If H does not contain any vector space (with exception of the space 0 consisting only of the origin) there can be no F-vectors and H is a *lattice*. The parallelotope determined by the vectors $V_1, \cdots, V_q$ is then called a *fundamental parallelotope* of the lattice.

The general closed module H can be called a *lattice cylinder* erected on the lattice generated by the vectors $V_1, \cdots, V_q$ (integral coefficients) with the space determined by the vectors $F_1, \cdots, F_p$ as space of generatrix directions. Concerning the freedom by which one can choose a generating system of linearly independent vectors for a closed module in the m-dimensional space we state the following well-known

Theorem. *If H is a closed module and T an arbitrary (vector-) space both lying in the m-dimensional space we can determine a system of linearly independent vectors which generates H (with arbitrary, respectively integral coefficients) by determining first in an arbitrary manner such a generating system of the closed submodule $H \cap T$*[1]*, and next supplementing these vectors with certain other vectors (if necessary).*

Let us consider the sets (5) for a numerically given system of zero-congruences.

Example 2. Let the system of zero-congruences be

$$\begin{aligned} x_1 - x_2 &\equiv 0 \pmod 1 \\ \sqrt{2}\, x_2 &\equiv 0 \pmod 1 \\ \frac{1}{2}(x_1 - x_2) &\equiv 0 \pmod 1 \\ \frac{1}{2}\sqrt{2}\, x_2 &\equiv 0 \pmod 1 \end{aligned}$$

1) $H \cap T$ denotes the common part of H and T.

$$\frac{1}{4}(x_1 - x_2) \equiv 0 \pmod 1$$

$$\frac{1}{4}\sqrt{2}x_2 \equiv 0 \pmod 1$$

. . . . . .

Only the two variables x_1 and x_2 occur in these congruences. Hence for $m \geq 2$ the set $A_m^{(N)}$ consists of all points $(x_1, \cdots, x_m)$ whose projections on the x_1x_2-plane lie in $A_2^{(N)}$, just as $A^{(N)}$ consists of all points $(x_1, x_2, \cdots)$ whose projections on the x_1x_2-plane lie in $A_2^{(N)}$. The set $A_2^{(1)}$ is the closed module in the x_1x_2-plane determined by $x_1 - x_2 \equiv 0 \pmod 1$ (it may for instance be generated by $F_1 = (1, 1)$ and $V_1 = (1, 0)$). The sets $A_2^{(2)} \supset A_2^{(3)} \supset \cdots$ form a strictly decreasing sequence of lattices in the x_1x_2-plane; for instance $A_2^{(2)}$ is the lattice generated by the vectors $V_1 = (1, 0)$ and $V_2 = \left(\frac{1}{\sqrt{2}}, \frac{1}{\sqrt{2}}\right)$, and more generally $A_2^{(2n)}$ is the lattice generated by the vectors $V_1 = (2^{n-1}, 0)$ and $V_2 = \left(\frac{2^{n-1}}{\sqrt{2}}, \frac{2^{n-1}}{\sqrt{2}}\right)$. As to the projections on the x_1-axis we see that $A_1^{(1)}$ is the whole x_1-axis while $A_1^{(2)} \supset A_1^{(3)} \supset \cdots$ is a strictly decreasing sequence of non-closed modules which are all lying everywhere dense on the x_1-axis. All these modules can be generated by a finite number of vectors, though of course not by linearly independent vectors; for instance $A_1^{(2)}$ is generated by the vectors $V_1 = 1$ and $V_2 = \frac{1}{\sqrt{2}}$ and more generally $A_1^{(2n)}$ is generated by the vectors $V_1 = 2^{n-1}$ and $V_2 = \frac{2^{n-1}}{\sqrt{2}}$.[1] Since the sets $A_1^{(n)}$ are everywhere dense on the x_1-axis it follows that their closures $H_1^{(n)}$ are all equal to the whole x_1-axis. Finally we see that $\Gamma = \{(0, 0, x_3, x_4, \cdots)\}$ where $x_3, x_4, \cdots$ are arbitrary numbers so that the sets Γ_1 and Γ_2 consist only of the origin.

In the rational case the knowledge of Γ is sufficient to decide whether $\pi_1 = \pi_2$ or not. In fact, by help of the main theorem in the rational case we can easily show that a necessary and sufficient condition that $\pi_1 = \pi_2$ is that Γ by a substitution can be transfered into a set which contains the "unit lattice" in the infinite-dimensional space, i. e. the set $\{(h_1, h_2, \cdots)\}$ where the h's are arbitrary integers. This can be seen in the following way.

1) It can easily be seen that for any m and N the set $A_m^{(N)}$ also in the case of an *arbitrary* system of linear forms may be generated by a *finite* number of (generally non-independent) vectors with arbitrary, respectively integral coefficients. In fact if $M > m$ denotes a positive integer so large that no variable with larger index than M really occurs (i. e. has a coefficient different from 0) in any of the N first linear forms we see that $A_M^{(N)}$ is a closed module in the $x_1 \cdots x_M$-space and that $A_m^{(N)}$ is its projection on the $x_1 \cdots x_m$-space. The projection of a system of (linearly independent) generators of the closed module $A_M^{(N)}$ will therefore be a system of (in general linearly dependent) generators of $A_m^{(N)}$.

(i). If Γ by a substitution can be transfered into a set which contains the unit lattice, then the linear forms by the substitution must be transfered into linear forms whose corresponding zero-congruences amongst their solutions have all points $(h_1, h_2, \cdots)$. If this is used for the points $(1, 0, 0, \cdots)$, $(0, 1, 0, 0, \cdots)$, $\cdots$ it follows that the coefficients of x_1, the coefficients of x_2, $\cdots$ are all integral. Hence, on account of the main theorem, $\pi_1 = \pi_2$.

(ii). If $\pi_1 = \pi_2$, the linear forms can, on account of the main theorem, be transfered into an integral system. The corresponding system of zero-congruences of this integral system is obviously satisfied by all points from the unit lattice. Hence, by the substitution, Γ is transfered into a set which contains the unit lattice.

In the general case where the coefficients are arbitrary numbers the knowledge of Γ is not sufficient to decide whether $\pi_1 = \pi_2$. In fact we can easily indicate two systems of linear forms which have the same Γ but such that $\pi_1 \neq \pi_2$ for the one system and $\pi_1 = \pi_2$ for the other. This we do in the following example.

Example 3. We consider the two systems of linear forms

$$\begin{array}{ll} \frac{1}{3}x_1 & x_1 \\ \frac{1}{9}x_1 & \sqrt{2}x_1 \\ \frac{1}{27}x_1 & 0x_1 \\ \cdot & \cdot \\ \cdot & \cdot \\ \cdot & \cdot \\ \frac{1}{3^n}x_1 & 0x_1 \\ \cdot & \cdot \\ \cdot & \cdot \\ \cdot & \cdot \end{array}$$

where the first system is the same as that used in example 1, § 1. In both systems only the one variable x_1 really occurs. It is clear that the two systems have the same Γ, namely the set $\{(0, x_2, x_3, \cdots)\}$ where $x_2, x_3, \ldots$ are arbitrary numbers. The first system, however, has $\pi_1 \neq \pi_2$— in fact we proved in example 1 that the point $\left(\frac{1}{2}, \frac{1}{2}, \cdots\right)$ was lying in π_2 but not in π_1—while the second system obviously has $\pi_1 = \pi_2$ since in reality it only contains a finite number (namely 2) of linear forms.

While, thus, a consideration of Γ alone cannot decide whether $\pi_1 = \pi_2$ we shall see in the following paragraph that the knowledge of the sets $H_m^{(N)}$ is sufficient for that purpose.

§ 3. The sets $H_m^{(N)}$, H_m and the condition $\pi_1 = \pi_2$.

In this paragraph we shall indicate as a statement on the sets $H_m^{(N)}$ a necessary and sufficient condition for the validity of $\pi_1 = \pi_2$. Moreover, in the case $\pi_1 = \pi_2$ we shall find a connection between the sets $H_m^{(N)}$ and H_m.

Theorem. *A necessary and sufficient condition that* $\pi_1 = \pi_2$ *is that for every* $m = 1, 2, \cdots$ *the sequence of m-dimensional sets*

$$H_m^{(1)} \supseteq H_m^{(2)} \supseteq H_m^{(3)} \supseteq \cdots$$

is constant from a certain step (depending on m).

Additional Theorem. *If* $H_m^{(1)} \supseteq H_m^{(2)} \supseteq H_m^{(3)} \supseteq \cdots$ *for every m is constant from a certain step (and hence* $\pi_1 = \pi_2$*) this constant set is just the set* H_m.

We remark that if for a given m the sequence

$$H_m^{(1)} \supseteq H_m^{(2)} \supseteq H_m^{(3)} \supseteq \cdots$$

is constant ($= \Phi_m$) from a certain step N_0 then for every $m_1 < m$ the sequence

$$H_{m_1}^{(1)} \supseteq H_{m_1}^{(2)} \supseteq H_{m_1}^{(3)} \supseteq \cdots$$

will also—at the latest from the same step—be constant (= the closure of the projection of Φ_m on the $x_1 \cdots x_{m_1}$-space); for two sets (viz. Φ_m and $A_m^{(N)}$ for $N \geqq N_0$) in the $x_1 \cdots x_m$-space with identical closures (viz. Φ_m) are projected into two sets in the $x_1 \cdots x_{m_1}$-space with identical closures, because the condition that two sets have identical closures is that every point in each of the sets can be approximated by points in the other and this property obviously is preserved by projection.

We divide the theorem above, together with its addition, in a theorem A for the sufficiency and the addition and a theorem B for the necessity.

Theorem A. *If for every m the sequence*

$$H_m^{(1)} \supseteq H_m^{(2)} \supseteq H_m^{(3)} \supseteq \cdots$$

is constant from a certain step, then $\pi_1 = \pi_2$ *and the constant set is equal to* H_m.

Proof. We first show that $\pi_1 = \pi_2$. Denoting by $(\theta_1, \theta_2, \cdots)$ an arbitrary point from π_2 we are to show that it also lies in π_1, i. e. that there exists a solution $Y = (y_1, y_2, \cdots)$ of all the congruences (1). Let

$$H_m^{(1)} \supseteq H_m^{(2)} \supseteq H_m^{(3)} \supseteq \cdots \supseteq H_m^{(N)} \supseteq \cdots$$

be constant for $N \geqq N_m$ where the integral sequence N_m moreover is chosen to be strictly increasing (and hence $\to \infty$).

We take our starting-point in an arbitrary positive integer M[1] and in an arbitrary chosen solution $Y^{(M)} = (y_1^{(M)}, y_2^{(M)}, \cdots)$ of the N_M first congruences (1). Next we choose a solution $X^{(M+1)} = (x_1^{(M+1)}, x_2^{(M+1)}, \cdots)$ of the N_{M+1} first congruences. This solution can be altered by an arbitrary point $Z^{(M+1)}$ from $\Lambda^{(N_{M+1})}$, i. e. for any point $Z^{(M+1)}$ from $\Lambda^{(N_{M+1})}$ (and no other points) the point $X^{(M+1)} + Z^{(M+1)}$ is again a solution of the N_{M+1} first congruences; this is true since $\Lambda^{(N_{M+1})}$ is the set of solutions of the N_{M+1} first zero-congruences (4). *Hence we can alter the solution* $X^{(M+1)} = (x_1^{(M+1)}, x_2^{(M+1)}, \cdots)$ *such that the projected point* $(x_1^{(M+1)}, \cdots, x_M^{(M+1)})$ *is altered by an arbitrary point from* $\Lambda_M^{(N_{M+1})}$ when only the other coordinates of $X^{(M+1)}$ are altered in a suitable manner. Our wish is now that the altered point $X^{(M+1)} + Z^{(M+1)}$ shall lie "near to" $Y^{(M)}$. Since $N_{M+1} > N_M$ the point $X^{(M+1)}$ is as $Y^{(M)}$ a solution of the N_M first congruences and hence their difference $Y^{(M)} - X^{(M+1)}$ is lying in $\Lambda^{(N_M)}$. The difference of the projected points $(y_1^{(M)}, \cdots, y_M^{(M)}) - (x_1^{(M+1)}, \cdots, x_M^{(M+1)})$ will therefore lie in $\Lambda_M^{(N_M)}$ and hence a fortiori in $H_M^{(N_M)}$ *and hence also in* $H_M^{(N_{M+1})}$. Since, as mentioned above, the solution $X^{(M+1)}$ of the N_{M+1} first congruences can be altered to another solution $Y^{(M+1)} = (y_1^{(M+1)}, y_2^{(M+1)}, \cdots)$ of these congruences such that the difference $(y_1^{(M+1)}, \cdots, y_M^{(M+1)}) - (x_1^{(M+1)}, \cdots, x_M^{(M+1)})$ becomes an arbitrarily chosen point of $\Lambda_M^{(N_{M+1})}$ and since the previous difference $(y_1^{(M)}, \cdots, y_M^{(M)}) - (x_1^{(M+1)}, \cdots, x_M^{(M+1)})$ is lying in the closure $H_M^{(N_{M+1})}$ of the set $\Lambda_M^{(N_{M+1})}$ it is clear that to every $\varepsilon_M > 0$ we can choose our solution $Y^{(M+1)}$ such that the first of the two M-dimensional point-differences ε_M-approximates the latter, i. e. such that

1) For the proof of $\pi_1 = \pi_2$ we could choose $M = 1$. When M is chosen arbitrarily it is in view of the proof of the additional theorem.

$$\left|(y_1^{(M+1)} - x_1^{(M+1)}) - (y_1^{(M)} - x_1^{(M+1)})\right| = \left|y_1^{(M+1)} - y_1^{(M)}\right| < \varepsilon_M$$

. . . . . .

$$\left|(y_M^{(M+1)} - x_M^{(M+1)}) - (y_M^{(M)} - x_M^{(M+1)})\right| = \left|y_M^{(M+1)} - y_M^{(M)}\right| < \varepsilon_M.$$

Next, let $X^{(M+2)} = (x_1^{(M+2)}, x_2^{(M+2)}, \cdots)$ be a solution of the N_{M+2} first congruences (1). This solution can be altered by an arbitrary point from $\Lambda^{(N_{M+2})}$ and hence $X^{(M+2)}$ can be altered such that the projected point $(x_1^{(M+2)}, \cdots, x_{M+1}^{(M+2)})$ is altered by an arbitrary point from $\Lambda_{M+1}^{(N_{M+2})}$ when only the other coordinates of $X^{(M+2)}$ are altered in a suitable manner. Our wish is that the altered point shall lie "near to" $Y^{(M+1)}$. Since $N_{M+2} > N_{M+1}$ the point $X^{(M+2)}$ is as $Y^{(M+1)}$ a solution of the N_{M+1} first congruences. The difference $(y_1^{(M+1)}, \cdots, y_{M+1}^{(M+1)}) - (x_1^{(M+2)}, \cdots, x_{M+1}^{(M+2)})$ is therefore lying in $\Lambda_{M+1}^{(N_{M+1})}$ and hence a fortiori in $H_{M+1}^{(N_{M+1})}$ *and hence also in* $H_{M+1}^{(N_{M+2})}$. Since, as mentioned above, the solution $X^{(M+2)}$ of the N_{M+2} first congruences can be altered to another solution $Y^{(M+2)} = (y_1^{(M+2)}, y_2^{(M+2)}, \cdots)$ of these congruences such that the difference $(y_1^{(M+2)}, \cdots, y_{M+1}^{(M+2)}) - (x_1^{(M+2)}, \cdots, x_{M+1}^{(M+2)})$ becomes an arbitrarily chosen point of $\Lambda_{M+1}^{(N_{M+2})}$ and since the previous difference $(y_1^{(M+1)}, \cdots, y_{M+1}^{(M+1)}) - (x_1^{(M+2)}, \cdots, x_{M+1}^{(M+2)})$ is lying in the closure $H_{M+1}^{(N_{M+2})}$ of the set $\Lambda_{M+1}^{(N_{M+2})}$ it is clear that to every $\varepsilon_{M+1} > 0$ we can choose the solution $Y^{(M+2)}$ such that the first of the two $(M+1)$-dimensional point-differences ε_{M+1}-approximates the latter, i. e. such that

$$\left|(y_1^{(M+2)} - x_1^{(M+2)}) - (y_1^{(M+1)} - x_1^{(M+2)})\right| = \left|y_1^{(M+2)} - y_1^{(M+1)}\right| < \varepsilon_{M+1}$$

. . . . . .

$$\left|(y_{M+1}^{(M+2)} - x_{M+1}^{(M+2)}) - (y_{M+1}^{(M+1)} - x_{M+1}^{(M+2)})\right| = \left|y_{M+1}^{(M+2)} - y_{M+1}^{(M+1)}\right| < \varepsilon_{M+1}.$$

In general, i. e. for an arbitrary $n \geq M+1$, let the point $X^{(n)} = (x_1^{(n)}, x_2^{(n)}, \cdots)$ be a solution of the N_n first congruences (1). This solution can be altered by an arbitrary point from $\Lambda^{(N_n)}$ and hence $X^{(n)}$ can be altered such that the projected point $(x_1^{(n)}, \cdots, x_{n-1}^{(n)})$ is altered by an arbitrary point from $\Lambda_{n-1}^{(N_n)}$ when only the other coordinates of $X^{(N)}$ are altered in a suitable manner. Our wish is that the altered point shall lie "near to" $Y^{(n-1)}$. Since $N_n > N_{n-1}$ the point $X^{(n)}$ is as $Y^{(n-1)}$ a solution

of the N_{n-1} first congruences. The difference $(y_1^{(n-1)}, \cdots, y_{n-1}^{(n-1)}) - (x_1^{(n)}, \cdots, x_{n-1}^{(n)})$ is therefore lying in $A_{n-1}^{(N_{n-1})}$ and hence a fortiori in $H_{n-1}^{(N_{n-1})}$ *and hence also in* $H_{n-1}^{(N_n)}$. Since, as mentioned above, the solution $X^{(n)}$ of the N_n first congruences can be altered to another solution $Y^{(n)} = (y_1^{(n)}, y_2^{(n)}, \cdots)$ of these congruences such that the difference $(y_1^{(n)}, \cdots, y_{n-1}^{(n)}) - (x_1^{(n)}, \cdots, x_{n-1}^{(n)})$ becomes an arbitrarily chosen point of $A_{n-1}^{(N_n)}$ and since the previous difference $(y_1^{(n-1)}, \cdots, y_{n-1}^{(n-1)}) - (x_1^{(n)}, \cdots, x_{n-1}^{(n)})$ is lying in the closure $H_{n-1}^{(N_n)}$ of the set $A_{n-1}^{(N_n)}$ it is clear that to every $\varepsilon_{n-1} > 0$ we can choose the point $Y^{(n)}$ such that the first of the two $(n-1)$-dimensional point-differences ε_{n-1}-approximates the other, i. e. such that

$$\left|(y_1^{(n)} - x_1^{(n)}) - (y_1^{(n-1)} - x_1^{(n)})\right| = \left|y_1^{(n)} - y_1^{(n-1)}\right| < \varepsilon_{n-1}$$

. . . . . .

$$\left|(y_{n-1}^{(n)} - x_{n-1}^{(n)}) - (y_{n-1}^{(n-1)} - x_{n-1}^{(n)})\right| = \left|y_{n-1}^{(n)} - y_{n-1}^{(n-1)}\right| < \varepsilon_{n-1}.$$

- -

Choosing our ε's such that $\sum_M^\infty \varepsilon_r$ is convergent we consider the sequence

$$\begin{aligned} Y^{(M)} &= (y_1^{(M)}, y_2^{(M)}, \cdots) \\ Y^{(M+1)} &= (y_1^{(M+1)}, y_2^{(M+1)}, \cdots) \\ Y^{(M+2)} &= (y_1^{(M+2)}, y_2^{(M+2)}, \cdots) \\ &\cdots\cdots\cdots\cdots \end{aligned}$$

The M first coordinate sequences $y_\nu^{(M)}, y_\nu^{(M+1)}, y_\nu^{(M+2)}, \cdots (\nu = 1, 2, \cdots, M)$ satisfy

$$\left|y_\nu^{(p)} - y_\nu^{(q)}\right| \leqq \sum_q^\infty \varepsilon_r \quad \text{for} \quad p > q \geqq M$$

while each of the following coordinate sequences $y_n^{(M)}, y_n^{(M+1)}, y_n^{(M+2)}, \cdots (n \geqq M+1)$ satisfy

$$\left|y_n^{(p)} - y_n^{(q)}\right| \leqq \sum_q^\infty \varepsilon_r \quad \text{for} \quad p > q \geqq n.$$

Hence, in particular, all the coordinate sequences converge towards respective numbers $y_1, y_2, \cdots$. The limit point

$$Y = (y_1, y_2, \cdots)$$

will then be a solution of all the congruences (1). In fact, to see that Y is a solution of the N^{th} congruence we observe that $Y^{(n)} = (y_1^{(n)}, y_2^{(n)}, \cdots)$ from a certain step is a solution of this congruence. Since only a finite number of variables really occurs in the congruence the statement follows from continuity reasons. Thus $(\theta_1, \theta_2, \cdots)$ is lying in π_1 and hence $\pi_1 = \pi_2$. Out of regard to the following we observe that the M first coordinates $y_1, \cdots, y_M$ of Y satisfy the inequalities

$$\begin{aligned} |y_1 - y_1^{(M)}| &\leqq \sum_M^\infty \varepsilon_r \\ &\cdots\cdots\cdots\cdots \\ |y_M - y_M^{(M)}| &\leqq \sum_M^\infty \varepsilon_r. \end{aligned} \tag{6}$$

Now, to conclude the proof of theorem A, we have to show that the constant final set $H_M^{(N_M)}$ in the sequence

$$H_M^{(1)} \supseteq H_M^{(2)} \supseteq H_M^{(3)} \supseteq \cdots$$

for every $M = 1, 2, \cdots$ is equal to H_M. Since $\Gamma_M \subseteq \Lambda_M^{(N_M)}$, it is plain that $H_M \subseteq H_M^{(N_M)}$. In order to show that, conversely, $H_M^{(N_M)} \subseteq H_M$ for an arbitrarily given M we use the proof above in the case $\theta_1 = \theta_2 = \cdots = 0$ with our present M as the M in the proof. The previous point $Y^{(M)} = (y_1^{(M)}, y_2^{(M)}, \cdots)$ is then an arbitrary point from $\Lambda^{(N_M)}$ and the projected point $(y_1^{(M)}, \cdots, y_M^{(M)})$ is therefore *an arbitrary point from* $\Lambda_M^{(N_M)}$. We are to show that $(y_1^{(M)}, \cdots, y_M^{(M)})$ can be approximated by points from Γ_M. But this is an immediate consequence of the fact that (in the present case $\theta_1 = \theta_2 = \cdots = 0$) the point Y constructed in the proof above is lying in Γ and that its M first coordinates satisfy the inequalities (6) where $\sum_M^\infty \varepsilon_r$ can be chosen arbitrarily small.

Theorem B. *If* $\pi_1 = \pi_2$ *the sequence*

$$H_m^{(1)} \supseteq H_m^{(2)} \supseteq H_m^{(3)} \supseteq \cdots$$

will for every m *be constant from a certain step.*

Proof. Indirectly, we assume that there exists an m_0 for which $H_{m_0}^{(1)} \supseteq H_{m_0}^{(2)} \supseteq H_{m_0}^{(3)} \supseteq \cdots$ is not constant from a certain step and

are to show that $\pi_1 \neq \pi_2$, i. e. that there exists a $(\theta_1, \theta_2, \cdots)$ which belongs to π_2 but not to π_1. We first consider the geometric appearance of the sequence of modules $H_{m_0}^{(n)}$ $(n = 1, 2, \cdots)$. This sequence is an essentially decreasing[1] sequence of lattice cylinders (see § 2). It is therefore plain that from a certain step $n \geqq N_0$ the least space (vector space) which contains $H_{m_0}^{(n)}$, and the space of generatrix directions of the cylinder $H_{m_0}^{(n)}$, will be constant spaces R_p and R_{p_1} of dimensions (say) p and p_1. Furthermore from this step the lattice base G_n of $H_{m_0}^{(n)}$ can be chosen in such a way that the least space which contains G_n is *a fixed space* R_q (dimension q with $p = p_1 + q$). The lattices G_n form from this step an essentially decreasing sequence in their common least space R_q. Therefore the q-dimensional content of the fundamental parallelotope of G_n ("fundamental content G_n") is an essentially increasing sequence which $\to \infty$ (since the fundamental content is at least doubled by the transition from one lattice to the next every time the lattices are different).

By $K(\varrho)$ we denote the open sphere in R_q with radius ϱ and center O as also the q-dimensional content of this sphere. By $C(\varrho)$ we denote the corresponding sphere cylinder in R_p with the sphere $K(\varrho)$ as base and the space of generatrix directions R_{p_1}. We also consider spheres in R_q whose centers are not lying in O and the corresponding sphere cylinders in R_q. In the following we denote for abbreviation sphere cylinders with base-sphere in R_q and space of generatrix directions R_{p_1} as "sphere cylinders" without further specification. By the sphere cylinder around the point P in R_p with radius ϱ we understand the sphere cylinder corresponding to the sphere with radius ϱ and center in the projection of P on R_q in the direction of R_{p_1}.

We first determine a sequence of strictly increasing positive numbers $N_1, N_2, \cdots, N_\nu, \cdots$ and the corresponding positive numbers $\varrho_1, \varrho_2, \cdots, \varrho_\nu, \cdots$ by the following procedure.

1°. Let $N_1 \geqq N_0$ be chosen such that the fundamental content G_{N_1} is larger than the sphere content $K(1)$. Then the sphere $K(1)$ cannot contain a complete system of representatives in R_q modulo G_{N_1} and hence the sphere cylinder $C(1)$ cannot contain a complete

1) An essentially decreasing sequence of sets is here and in the following a sequence where every element is contained in the preceding and which is not constant from a certain step. The expression, an essentially increasing sequence of numbers, used below, has an analogous meaning.

system of representatives in R_p modulo $H_{m_0}^{(N_1)}$. To this N_1 we choose the positive number ϱ_1 so large that every sphere in R_q with radius ϱ_1 contains a complete system of representatives in R_q modulo G_{N_1} and hence also a complete system of representatives in R_p modulo $H_{m_0}^{(N_1)}$. In particular, everyone of our sphere cylinders in R_p with radius ϱ_1 will contain a complete system of representatives in R_p modulo $H_{m_0}^{(N_1)}$.

2°. Next we determine $N_2 > N_1$ such that the fundamental content G_{N_2} is larger than $K(\varrho_1 + 2)$. Then the sphere cylinder $C(\varrho_1 + 2)$ cannot contain a complete system of representatives in R_p modulo $H_{m_0}^{(N_2)}$. To this N_2 we determine the positive number ϱ_2 so large that everyone of our sphere cylinders in R_p with radius ϱ_2 contains a complete system of representatives in R_p modulo $H_{m_0}^{(N_2)}$.

ν°. After having determined $N_{\nu-1}$ and $\varrho_{\nu-1}$ we determine $N_\nu > N_{\nu-1}$ such that the fundamental content G_{N_ν} is larger than $K(\varrho_{\nu-1} + \nu)$. Then the sphere cylinder $C(\varrho_{\nu-1} + \nu)$ cannot contain a complete system of representatives in R_p modulo $H_{m_0}^{(N_\nu)}$. To this N_ν we determine the positive number ϱ_ν so large that everyone of our sphere cylinders in R_p with radius ϱ_ν contains a complete system of representatives in R_p modulo $H_{m_0}^{(N_\nu)}$.

After having determined N_ν and ϱ_ν ($\nu = 1, 2, \cdots$) we now pass to the direct searching of a point $(\theta_1, \theta_2, \cdots)$ which belongs to the set π_2 but not to the set π_1. The idea in this (successive) determination modulo 1 of the numbers $\theta_1, \theta_2, \cdots$, the kernel of which can be found in example 1, § 1, is that we try to see that the set of projections $(x_1, \cdots, x_{m_0})$ on the $x_1 \cdots x_{m_0}$-space of all solutions $(x_1, x_2, \cdots)$ of the N first congruences (1) will lie farther and farther away from O for increasing values of N. More precisely, we will see that the set of projections for $N = N_\nu$ will lie in R_p and outside $C(\nu)$.

1st step. We first choose an arbitrary point $P^{(1)} = (x_1^{(1)}, x_2^{(1)}, \cdots)$ in the infinite-dimensional space which only satisfies the condition that the projected point $P_{m_0}^{(1)} = (x_1^{(1)}, \cdots, x_{m_0}^{(1)})$ is lying in R_p and has no equivalent point modulo $H_{m_0}^{(N_1)}$ lying in $C(1)$.

Such a point exists on account of 1° since $C(1)$ does not contain a complete system of representatives in R_p modulo $H_{m_0}^{(N_1)}$. We substitute $(x_1, x_2, \cdots) = (x_1^{(1)}, x_2^{(1)}, \cdots)$ in the N_1 first linear forms (2). The numbers thus determined (but only considered modulo 1) shall be our numbers $\theta_1, \theta_2, \cdots, \theta_{N_1}$. We observe that the total set of solutions of the N_1 first congruences (1) (with the θ's just chosen) is the set $P^{(1)} + \Lambda^{(N_1)}$ because $\Lambda^{(N_1)}$ is the set of solutions of the N_1 first zero-congruences. From the choice of $P^{(1)}$ it follows that the projection of this set $P^{(1)} + \Lambda^{(N_1)}$ on the $x_1 \cdots x_{m_0}$-space—i. e. the set $P_{m_0}^{(1)} + \Lambda_{m_0}^{(N_1)}$ which consists of all points equivalent to $P_{m_0}^{(1)}$ modulo $\Lambda_{m_0}^{(N_1)}$—is lying in R_p and outside $C(1)$.

2nd step. Next we choose (which is possible from the choice of N_2) a point $D_{m_0}^{(2)} = (d_1^{(2)}, \cdots, d_{m_0}^{(2)})$ in R_p which has no equivalent point modulo $H_{m_0}^{(N_2)}$ in $C(\varrho_1 + 2)$. The sphere cylinder in R_p around $D_{m_0}^{(2)}$ with radius ϱ_1 contains (on account of the choice of ϱ_1) a point equivalent to $P_{m_0}^{(1)}$ modulo $H_{m_0}^{(N_1)}$. Since $\Lambda_{m_0}^{(N_1)}$ is lying everywhere dense in $H_{m_0}^{(N_1)}$ this cylinder also contains a point $P_{m_0}^{(2)} = (x_1^{(2)}, \cdots, x_{m_0}^{(2)})$ equivalent to $P_{m_0}^{(1)}$ modulo $\Lambda_{m_0}^{(N_1)}$. We can therefore choose a point $P^{(2)} = (x_1^{(2)}, x_2^{(2)}, \cdots)$ whose projection on the $x_1 \cdots x_{m_0}$-space is $P_{m_0}^{(2)}$ and which is equivalent to $P^{(1)}$ modulo $\Lambda^{(N_1)}$. In particular $P^{(2)}$ is a solution of the N_1 first congruences (1). We now substitute $(x_1, x_2, \cdots) = (x_1^{(2)}, x_2^{(2)}, \cdots)$ in the N_2 first linear forms (2) and denote the numbers thus determined (modulo 1) by $\theta_1, \cdots, \theta_{N_2}$. The N_1 first of these numbers coincide with the numbers $\theta_1, \cdots, \theta_{N_1}$ determined by the first step, since $P^{(2)}$ satisfies the N_1 first congruences (formed with these θ's). We now consider the set of solutions $(x_1, x_2, \cdots)$ of the N_2 first (with the above θ's formed) congruences (1), i. e. the set $P^{(2)} + \Lambda^{(N_2)}$. Then the projection of this set on the $x_1 \cdots x_{m_0}$-space—i. e. the set $P_{m_0}^{(2)} + \Lambda_{m_0}^{(N_2)}$ which consists of all points equivalent to $P_{m_0}^{(2)}$ modulo $\Lambda_{m_0}^{(N_2)}$—is lying in R_p and outside $C(2)$; that the set is lying in R_p is plain, and the second statement follows from the fact that $P_{m_0}^{(2)}$ is lying in a sphere cylinder around $D_{m_0}^{(2)}$ with radius ϱ_1 where $D_{m_0}^{(2)}$ has no equivalent point in $C(\varrho_1 + 2)$ modulo $H_{m_0}^{(N_2)}$ and hence a fortiori no equivalent point modulo $\Lambda_{m_0}^{(N_2)}$.

ν^{th} *step.* We choose (which is possible from the choice of N_ν) a point $D_{m_0}^{(\nu)} = (d_1^{(\nu)}, \cdots, d_{m_0}^{(\nu)})$ in R_p which has no equivalent point modulo $H_{m_0}^{(N_\nu)}$ in $C(\varrho_{\nu-1} + \nu)$. The sphere cylinder in R_p around $D_{m_0}^{(\nu)}$ with radius $\varrho_{\nu-1}$ contains (on account of the choice of $\varrho_{\nu-1}$) a point equivalent to $P_{m_0}^{(\nu-1)}$ modulo $H_{m_0}^{(N_\nu-1)}$ and hence also a point $P_{m_0}^{(\nu)} = (x_1^{(\nu)}, \cdots, x_{m_0}^{(\nu)})$ equivalent to $P_{m_0}^{(\nu-1)}$ modulo $A_{m_0}^{(N_\nu-1)}$. We can therefore choose a point $P^{(\nu)} = (x_1^{(\nu)}, x_2^{(\nu)}, \cdots)$ whose projection on the $x_1 \cdots x_{m_0}$-space is $P_{m_0}^{(\nu)}$ and which is equivalent to $P^{(\nu-1)}$ modulo $A^{(N_\nu-1)}$. In particular $P^{(\nu)}$ is a solution of the $N_{\nu-1}$ first congruences (1). We now substitute $(x_1, x_2, \cdots) = (x_1^{(\nu)}, x_2^{(\nu)}, \cdots)$ in the N_ν first linear forms (2) and denote the numbers thus determined (modulo 1) by $\theta_1, \cdots, \theta_{N_\nu}$. The $N_{\nu-1}$ first of these numbers coincide with the numbers $\theta_1, \cdots, \theta_{N_{\nu-1}}$ determined by the $(\nu-1)^{\text{th}}$ step. We consider the set of solutions $(x_1, x_2, \cdots)$ of the N_ν first (with the above θ's formed) congruences (1). Then the projection of this set on the $x_1 \cdots x_{m_0}$-space—i. e. the set $P_{m_0}^{(\nu)} + A_{m_0}^{(N_\nu)}$ which consists of all points equivalent to $P_{m_0}^{(\nu)}$ modulo $A_{m_0}^{(N_\nu)}$—lies in R_p and outside $C(\nu)$; that the set is lying in R_p is plain, and the second statement follows from the fact that $P_{m_0}^{(\nu)}$ is lying in a sphere cylinder around $D_{m_0}^{(\nu)}$ with radius $\varrho_{\nu-1}$ where $D_{m_0}^{(\nu)}$ has no equivalent point in $C(\varrho_{\nu-1} + \nu)$ modulo $H_{m_0}^{(N_\nu)}$ and hence a fortiori no equivalent point modulo $A_{m_0}^{(N_\nu)}$.

In this manner we have got a point $(\theta_1, \theta_2, \cdots)$ with the desired properties. In fact, the point is belonging to π_2 since for every ν the N_ν first (with these θ's formed) congruences (1) have a solution $P^{(\nu)} = (x_1^{(\nu)}, x_2^{(\nu)}, \cdots)$, and here $N_\nu \to \infty$ for $\nu \to \infty$. On the other hand the point $(\theta_1, \theta_2, \cdots)$ does not belong to π_1, i. e. there is no solution of the whole system of congruences (1); for every solution of the N_ν first congruences has a projection on the $x_1 \cdots x_{m_0}$-space which lies in R_p and outside $C(\nu)$.

Remark. The theorems of this paragraph connect the condition $\pi_1 = \pi_2$ with the closures $H_m^{(N)}$ and H_m of the modules $A_m^{(N)}$ and Γ_m. We shall mention that analogous theorems hold for the sets $A_m^{(N)}$ and Γ_m themselves, viz.

Theorem. *A necessary and sufficient condition that* $\pi_1 = \pi_2$ *is that for every* $m = 1, 2, \cdots$ *the sequence*

$$\Lambda_m^{(1)} \supseteq \Lambda_m^{(2)} \supseteq \Lambda_m^{(3)} \supseteq \cdots$$

is constant from a certain step (depending on m).

Additional Theorem. *If* $\Lambda_m^{(1)} \supseteq \Lambda_m^{(2)} \supseteq \Lambda_m^{(3)} \supseteq \cdots$ *for every m is constant from a certain step this constant set is just the set* Γ_m.

If these theorems, as their analogues for the closures, are divided in a theorem A for the sufficiency and the addition and a theorem B for the necessity, the theorem A is even simpler to prove than the previous theorem A. Theorem B, however, lies deeper than its analogue. We can obtain the new theorem B from the old one by the following

Theorem. *For an arbitrary system of linear forms* (1) *(with* $\pi_1 = \pi_2$ *or* $\pi_1 \neq \pi_2$*) there exists to every positive integer m an integer* $M \geq m$ *and a positive integer N such that the sequence* $\Lambda_m^{(N)} \supseteq \Lambda_m^{(N+1)} \supseteq \Lambda_m^{(N+2)} \supseteq \cdots$ *is the projection on the* $x_1 \cdots x_m$*-space of the sequence* $H_M^{(N)} \supseteq H_M^{(N+1)} \supseteq H_M^{(N+2)} \supseteq \cdots$.

We omit, however, the proofs of these theorems which are unnecessary for the proof of our main theorem in its present framing (cp. p. 8-9).

§ 4. The structure of closed modules in the infinite-dimensional space.

In this paragraph we shall study the closed modules in our infinite-dimensional space—which from now on is denoted by R^∞—where the underlying convergence notion, occasionally used in the previous paragraphs, is that of convergence in each of the coordinates. As we shall see the closed modules in the space R^∞ possess quite a similar structure as that of the closed modules in the usual m-dimensional space R_m (see § 2).

In order to prove the structure theorem in R^∞ we shall use the analogous structure theorem in R_m, $m = 1, 2, \cdots$. The transition from the finite-dimensional case is, however, not a trivial one. We shal have to put in an intermediate space R_∞ between the finite-dimensional spaces R_m and the space R^∞. The space R_∞ is as R^∞ an infinite-dimensional space, but while a point $X = (x_1, x_2, \cdots)$ in R^∞ may have quite arbitrary coor-

dinates, a point $A = (a_1, a_2, \circ\circ\circ)$[1] in R_∞ always has coordinates which from a certain step (depending on the point) are 0, i. e. $a_n = 0$ for $n \geqq N = N(A)$.

Between the spaces R_∞ and R^∞ there exists, when a convergence notion in R_∞ is suitably chosen, a *duality*. Once established this duality permits us to get at the structure theorem for closed modules in R^∞ from an analogous structure theorem for closed modules in R_∞. Now, as mentioned, the space R_∞ is lying nearer to the finite-dimensional spaces R_m than does R^∞, in fact it can be exhausted by the $a_1 a_2 \cdots a_m$-space for $m \to \infty$. This is the reason why, as we shall see, the structure theorem in R_∞ can easily be obtained from the finite-dimensional case.

The duality, mentioned above, between R_∞ and R^∞ is analogous to a duality considered by M. Riesz between two m-dimensional spaces $R_m = \{(a_1, \cdots, a_m)\}$ and $R_m = \{(x_1, \cdots, x_m)\}$.

If M is an arbitrary module in R_m Riesz considers the point set in (the other space) R_m consisting of all points $A = (a_1, \cdots, a_m)$ from this latter R_m for which

$$A \cdot X = a_1 x_1 + a_2 x_2 + \cdots + a_m x_m \equiv 0 \pmod 1$$

for every point $X = (x_1, x_2, \cdots, x_m)$ from M. This point set is a closed module in R_m and is called the *dual* module of M. We denote it by M'. If we repeat the operation of passing to the dual module we get a closed module $M'' = (M')'$ in (the original space) R_m. The relation between M and M'' appears from the following important theorem.

Riesz's Theorem. *If M is an arbitrary module in R_m the dual module M'' of its dual module M' is the closure $\overline{M}$ of M, i. e.*

$$M'' = \overline{M}.$$

For a closed module H in R_m we get in particular $H'' = H$.

We now pass to the establishment of the duality between R_∞ and R^∞, or rather that side of the duality which will be needed in the following. A full account of the duality can be found in another paper[2] where the topic of this paragraph is discussed in more detail.

1) For points in R_∞ we use the notation $(a_1, a_2, \circ\circ\circ)$ in order to make apparent that their coordinates are all zero from a certain step.

2) H. Bohr and E. Følner: On a structure theorem for closed modules in an infinite-dimensional space, to appear elsewhere.

Let T be an arbitrary linear transformation in R_∞ and let the fundamental points $(1, 0, 0, \circ\circ\circ)$, $(0, 1, 0, \circ\circ\circ)$, $\cdots$ by the transformation be taken into the points

$$T\{(1, 0, 0, \circ\circ\circ)\} = S_1 = (t_{11}, t_{21}, \circ\circ\circ)$$
$$T\{(0, 1, 0, \circ\circ\circ)\} = S_2 = (t_{12}, t_{22}, \circ\circ\circ)$$
$$\cdots\cdots\cdots\cdots\cdots\cdots\cdots\cdots$$

from R_∞. The arbitrary point $A = (a_1, a_2, \circ\circ\circ)$ from R_∞ will then be carried into the point

$$B = T(A) = a_1 S_1 + a_2 S_2 + \circ\circ\circ.$$

Introducing the matrix $T = \{t_{rs}\}$ the linear transformation may be written $B = TA$. In the following we denote a linear transformation in R_∞ and the corresponding (uniquely determined) matrix by the same letter T.

Conversely, each such matrix equation

$$\begin{Bmatrix} b_1 \\ b_2 \\ \circ \\ \circ \\ \circ \end{Bmatrix} = \begin{Bmatrix} t_{11} t_{12} \cdots \\ t_{21} t_{22} \cdots \\ \circ\ \circ \\ \circ\ \circ \\ \circ\ \circ \end{Bmatrix} \begin{Bmatrix} a_1 \\ a_2 \\ \circ \\ \circ \\ \circ \end{Bmatrix}$$

where the column vectors are arbitrary points from R_∞ is a linear transformation in R_∞.

We now define the scalar product between two points $A = (a_1, a_2, \circ\circ\circ)$ and $X = (x_1, x_2, \cdots)$ from R_∞ and R^∞, respectively. We put

$$A \cdot X = X \cdot A = a_1 x_1 + a_2 x_2 + \circ\circ\circ.$$

In matrix notation the scalar product is expressed by A^*X or X^*A[1] when we agree on considering the points as column vectors (for convenience we usually write them horizontally).

For a given linear transformation T in R_∞ and two variable points X and Y from R^∞ we now set up the condition

(7) $\qquad A \cdot X = T(A) \cdot Y$ for every A from R_∞.

1) The star denotes the operation of transposing a matrix.

We shall show that this condition on X and Y is equivalent to a linear transformation in R^∞ (expressed by linear expressions as (3), § 1) of Y into X (and thus, in particular, that to any given Y there exists one and only one X satisfying (7)).

In matrix notation the condition runs as follows

$$A^*X = (TA)^*Y \quad \text{or} \quad A^*X = A^*T^*Y.$$

Putting successively $A^* = (1, 0, 0, \circ\circ\circ)$, $(0, 1, 0, \circ\circ\circ)$, $\cdots$ in this relation we get

$$X = T^*Y \tag{8}$$

and conversely the former condition follows from (8) by left-multiplying it with A^*.

Putting (8) into (7) and changing Y to X we get the relation

$$A \cdot T^*(X) = T(A) \cdot X \text{ for every } A \text{ from } R_\infty \text{ and every } X \text{ from } R^\infty. \tag{9}$$

We now define a *substitution in* R_∞ as a linear, one-to-one transformation of R_∞ onto R_∞.

If T is a substitution the condition (7) is equivalent to the condition

$$A \cdot Y = T^{-1}(A) \cdot X \text{ for every } A \text{ from } R_\infty, \tag{10}$$

in fact we have only substituted $T^{-1}(A)$ for A and interchanged the two sides of the equation (7). Here T^{-1} denotes the inverse substitution of T. Since (7) is equivalent to (8) we see that (10) is equivalent to

$$Y = (T^{-1})^*X. \tag{11}$$

Hence also the relations (8) and (11) are equivalent which shows that T^* is a one-to-one transformation of R^∞ onto R^∞ and therefore what we have called a substitution in R^∞ (see § 1). Putting $T' = (T^*)^{-1}$ and replacing X by $T'(X)$ in (9) we obtain the following

Theorem 1. *If T is a substitution in R_∞ then T^* is a substitution in R^∞ and there exists a uniquely determined substitution T' in R^∞ such that*

(12) $A \cdot X = T(A) \cdot T'(X)$ *for every* A *from* R_∞ *and every* X *from* R^∞,

viz. the substitution $T' = (T^*)^{-1} = (T^{-1})^*$.

We call T' the *dual substitution* of T.

In order to speak of *closed* modules in R_∞ and R^∞ we must know the underlying convergence notion of the two spaces. We have already mentioned that in R^∞ our convergence notion is that of convergence in every coordinate. In order to define a suitable convergence notion in R_∞ we first observe that our convergence notion in R^∞ may also be stated as follows:

A sequence $X^{(n)}$ *converges towards* X *if and only if*

$$A \cdot X^{(n)} \to A \cdot X \text{ for every } A \text{ from } R_\infty.$$

In fact, since a point A from R_∞ only contains a finite number of non-zero coordinates the former condition involves the latter, and conversely, the former condition is obtained from the latter by putting successively $A = (1, 0, 0, \circ\circ\circ), (0, 1, 0, \circ\circ\circ), \cdots$.

In the new form the notion of convergence in R^∞ has a dual notion of convergence in R_∞:

A sequence $A^{(n)}$ *of points from* R_∞ *is said to converge towards a point* A *from* R_∞ *if and only if*

$$X \cdot A^{(n)} \to X \cdot A \text{ for every } X \text{ from } R^\infty.$$

This is going to be our convergence notion in R_∞.[1)]

Remark. Our substitutions in R^∞ are obviously *bicontinuous*. In order to show that our substitutions in R_∞ are also bicontinuous we remark that on account of (9) every linear transformation T in R_∞ is continuous; in fact, when $A^{(n)} \to A$ we get from (9)

$$X \cdot T(A^{(n)}) = T^*(X) \cdot A^{(n)} \to T^*(X) \cdot A = X \cdot T(A)$$

for every X from R^∞ which shows that $T(A^{(n)}) \to T(A)$. It can

1) In the following we shall only use the definition of convergence in R_∞ in the above form; we may, however, mention that this definition, as easily seen, is equivalent to the following (more direct) one: Convergence of a sequence in R_∞ means convergence in every coordinate and moreover the existence of a p only depending on the sequence, such that all points of the sequence have 0 on the coordinate places with higher number than p

easily be shown that our substitutions in R^∞ or R_∞ are just the linear, one-to-one, bicontinuous transformations of the space onto itself (in the case of R_∞ nothing is left to prove).

For an arbitrary closed module H in R_∞ we consider the point set H' in R^∞ which consists of all points X for which

$$A \cdot X \equiv 0 \pmod 1 \text{ for every } A \text{ from } H.$$

Obviously the set H' is a module. Furthermore H' is closed, for if $X^{(n)} \to X$ in R^∞ and all $X^{(n)}$ are lying in H', then for every A from H we have $0 \equiv A \cdot X^{(n)} \to A \cdot X$ so that $A \cdot X \equiv 0$. We call the closed module H' the *dual module* of the closed module H. The following simple theorem indicates the connection between the two notions, dual module and dual substitution.

Theorem 2. *If we subject a closed module H in R_∞ to a substitution T and subject the dual module H' in R^∞ to the dual substitution T' then the resulting module $T'(H')$ in the latter case is the dual module of the resulting module $T(H)$ in the former case, i. e.*

$$T'(H') = (T(H))'.$$

This is an immediate consequence of the relation (12) when we only observe that $T(A)$ runs through $T(H)$ and $T'(X)$ runs through $T'(H')$ when A runs through H and X through H'.

We have defined above the dual module of a closed module from R_∞. Analogously, we define the dual module H' of a closed module H from R^∞ as the point set (eo ipso closed module) consisting of the points A from R_∞ for which

$$X \cdot A \equiv 0 \pmod 1 \text{ for every } X \text{ from } H.$$

Then we have the following important

Theorem 3. *For an arbitrary closed module H in R^∞ the dual module H'' of its dual module H' is the module itself, i. e.*

$$H'' = H.$$

Obviously $H'' \supseteq H$. Thus we only have to prove that $H'' \subseteq H$. Let then $Y = (y_1, y_2, \cdots)$ be an arbitrary point from H''. In order to show that Y is lying in H, let m be an arbitrary positive

integer. We consider the points $(a_1, a_2, \cdots, a_m, 0, 0, \circ\circ\circ) = (a_1, a_2, \cdots, a_m)$ from the common part L of H' and the $a_1 a_2 \cdots a_m$-space. Then for every point in L we have

$$(13) \qquad (y_1, y_2, \cdots, y_m) \cdot (a_1, a_2, \cdots, a_m) \equiv 0 \pmod 1.$$

Next, let M denote the projection of H on the $x_1 x_2 \cdots x_m$-space (i. e. the set of points $(x_1, x_2, \cdots, x_m)$ arising from the points $(x_1, x_2, \cdots)$ of H by cancelling all coordinates with indices $> m$). M is again a module, but not necessarily a closed module. Plainly, $L = M'$ and thus on account of (13) the point $(y_1, y_2, \cdots, y_m)$ belongs to M''. Now, according to Riesz's theorem

$$M'' = \bar{M}$$

and hence $(y_1, y_2, \cdots, y_m)$ can be approximated by points $(x_1, x_2, \cdots, x_m)$ from M. Since m is arbitrary it follows that $Y = (y_1, y_2, \cdots)$ can be approximated by points $(x_1, x_2, \cdots)$ from H, i. e. Y must lie in $\bar{H} = H$, q. e. d.

We shall now prove the following structure theorem for closed modules in R_∞.

Structure Theorem R_∞. *A closed module H in the infinite-dimensional space R_∞ is a point set E which by a substitution can be transfered into a point set of a special form, in the following denoted by S_∞, namely a point set $\{(a_1, a_2, \circ\circ\circ)\}$ of the following structure: The indices $1, 2, \cdots, n, \cdots$ can be divided into three fixed classes $\{n_r\}$, $\{n_s\}$, $\{n_t\}$ depending only on the point set, such that the coordinates a_{n_r} independently run through all numbers, and the coordinates a_{n_s} independently run through all integers, while all the remaining coordinates a_{n_t} are constantly zero. Only, of course, the simultaneous variation of the a_{n_r} and the a_{n_s} in the set is limited by the obvious demand that $(a_1, a_2, \circ\circ\circ)$ always shall lie in R_∞, i. e. have 0 from a certain coordinate place (depending on the point). Conversely, each such point set E is a closed module.*

The latter part of the theorem follows immediately from the remark on p. 26.

In order to prove the first (and real) part of the theorem, let H_m denote the common part of H and the $x_1 \cdots x_m$-space. Then, obviously, H_m is in the usual sense a closed module in

the $a_1 \cdots a_m$-space. Furthermore, H_m is the common part of H_{m+1} and the $a_1 \cdots a_m$-space. Hence it follows from the theorem on p. 10, for $m = 1, 2, \cdots$, that we can generate successively the closed modules $H_1, H_2, \cdots$ by linearly independent vectors with arbitrary and integral coefficients in such a way that the generating vectors of H_{m+1} are the generating vectors of H_m with the same types of coefficients, in connection with other vectors (if necessary). In this way we get a sequence of linearly independent vectors $G_1, G_2, \cdots$ which provided with suitable types of coefficients (integral or arbitrary) will generate H (generation of course in the sense that for each vector of H only a finite number of generators is used). With arbitrary coefficients the vectors spann a subspace $R(H)$ of R_∞. Let R_1 denote the common part of $R(H)$ and the x_1-axis. If the space R_1 is not the whole x_1-axis, but only the 0-vector we place a non-zero vector on the x_1-axis. Then this vector together with $R(H)$ will spann a space $R^{(1)}$ which contains the x_1-axis. If $R(H)$ itself contains the x_1-axis we put $R^{(1)} = R(H)$. Next, let R_2 denote the common part of $R^{(1)}$ and the x_1x_2-plane. If the space R_2 is not the whole x_1x_2-plane, but only the x_1-axis we place a vector in the x_1x_2-plane outside the x_1-axis. Then this vector together with $R^{(1)}$ will spann a space $R^{(2)}$ which contains the x_1x_2-plane. If $R^{(1)}$ itself contains the x_1x_2-plane we put $R^{(2)} = R^{(1)}$. In this way we continue. If the vectors thus found in some way or other are put into a sequence with the vectors $G_1, G_2, \cdots$ we get a sequence of linearly independent vectors $U_1, U_2, \cdots$ which provided with suitable types of coefficients (zero, integral or arbitrary) will generate H and with mere arbitrary coefficients the whole space R_∞. The linear independence of $U_1, U_2, \cdots$ secures that each point in R_∞ has only one representation by this generation. Hence

$$B = a_1U_1 + a_2U_2 + \circ\circ\circ$$

is a substitution in R_∞ of $A = (a_1, a_2, \circ\circ\circ)$ into B. It takes the fundamental vectors $(1, 0, 0, \circ\circ\circ)$, $(0, 1, 0, \circ\circ\circ)$, $\cdots$ into the vectors $U_1, U_2, \cdots$. Therefore the inverse substitution, which takes $U_1, U_2, \cdots$ into the fundamental vectors, will take the closed module H into a set $\{(a_1, a_2, \circ\circ\circ)\}$ determined by $a_i = 0$ for certain i, a_i arbitrary integral for certain i, and

a_i arbitrary for the remaining i. This proves structure theorem R_∞.

By help of structure theorem R_∞ and the duality between R_∞ and R^∞ we shall now obtain the main result of this paragraph, viz.

Structure Theorem R^∞. *A closed module in the infinite-dimensional space R^∞ is a point set E which by a substitution can be transfered into a point set of a special form, denoted by S^∞, namely a point set $\{(x_1, x_2, \cdots)\}$ of the following structure: The indices $1, 2, \cdots, n, \cdots$ can be divided into three fixed classes $\{n_r\}, \{n_s\}, \{n_t\}$ which depend only on the point set, such that the coordinates x_{n_r} independently run through all numbers, and the coordinates x_{n_s} independently run through all integers, while all the remaining coordinates x_{n_t} are constantly zero. Conversely, each such point set E is a closed module.*

Again, the latter part of the theorem follows immediately from the remark on p. 26.

In order to obtain a proof of the first (and real) part of the theorem by help of the corresponding theorem in R_∞ let us first show that the dual module of a closed module of the special form S_∞ is a closed module of the special form S^∞. More precisely we shall prove

Theorem 4. *For a closed module H in R_∞ of the special form S_∞, explicitly $\{(a_1, a_2, \circ\circ\circ)\}$ with the coordinates a_{n_r} arbitrary, the coordinates a_{n_s} integral, and the coordinates a_{n_t} zero, the dual module H' in R^∞ is of the special form S^∞, and more precisely the dual module is $\{(x_1, x_2, \cdots)\}$ where the x_{n_r} are zero, the x_{n_s} integral, and the x_{n_t} arbitrary.*

We first observe that obviously all points X of the form mentioned are lying in H'. Conversely, we have to show that all points in H' have the form mentioned. Since the points X in H' have to fulfill

$$(\circ\circ\circ\ \xi_{n_r}\ \circ\circ\circ)\cdot X \equiv 0 \pmod 1 \text{ for all values } \xi_{n_r}$$

it follows that the n_r^{th} coordinate of X must be zero, and since

$$\underset{1\,2\cdots n_s\cdots}{(\circ\circ\circ\ 1\ \circ\circ\circ)}\cdot X \equiv 0 \pmod 1$$

it follows that the n_s^{th} coordinate of X must be integral. This proves theorem 4.

We have now got all means necessary to prove structure theorem R^∞. Let first H be an arbitrary closed module in R_∞. Then on account of structure theorem R_∞ there exists a substitution T in R_∞ such that $T(H)$ has the special form S_∞. The dual module H' of H is a closed module in R^∞. We shall show that H' by a substitution can be taken into a closed module of the special form S^∞. In fact, the dual substitution T' of T has this property, for it follows from theorem 2 that $T'(H') = (T(H))'$ and from theorem 4 that $(T(H))'$, as the dual module of a closed module of the special form S_∞, is itself a closed module of the special form S^∞. Hence we see that every closed module in R^∞ which is the dual module of a closed module in R_∞ by a substitution can be taken into a set of the form S^∞. In order to complete the proof of structure theorem R^∞ we therefore only have to show that *every* closed module H in R^∞ can be written in the form K' where K is a closed module in R_∞. This, however, is a consequence of theorem 3 which tells that $H = H''$ so that for K we may use H'.

§ 5. Proof of the main theorem.

Already in § 1 we have formulated the main theorem and proved the simple "half" of it, namely that a sufficient condition that a system of linear forms (2) have $\pi_1 = \pi_2$ is that the system by a substitution can be taken into a system of the type S. We shall now show that this condition is also necessary, i. e. that every system of linear forms which has $\pi_1 = \pi_2$ by a substitution can be taken into a system of the type S.

For a system of congruences (1) the set Γ of solutions of the corresponding zero congruences is obviously always (i. e. whether $\pi_1 = \pi_2$ or not) a closed module in R^∞. Hence the structure theorem R^∞ from § 4 states that there exists a substitution T which takes Γ into a point set of the form S^∞, corresponding (say) to the classes $\{n_r\}, \{n_s\}, \{n_t\}$. By this substitution T the system of linear forms will be taken into a system where the coefficient columns corresponding to the variables x_{n_r} are zero

columns while the coefficient columns corresponding to the variables x_{n_s} are integral columns. This is seen by putting $(\circ\circ\circ\ \xi_{n_r}\ \circ\circ\circ)$ with arbitrary ξ_{n_r}, respectively $(\circ\circ\circ\ \underset{12\ldots n_s\ldots}{1}\ \circ\circ\circ)$ into the zero-congruences. Conversely, a coefficient column of zero's corresponds to a variable x_{n_r} and an integral coefficient column which is not a zero column to a variable x_{n_s}.

Now, we shall show that if $\pi_1 = \pi_2$ for the original system, and hence also for the transformed system, the latter of these systems will be of the type S.

Obviously it makes no real difference if all the coefficient columns corresponding to the variables x_{n_r} are removed together with their respective variables. For since all these columns consist of zero's this removal will neither change the property of having or not having $\pi_1 = \pi_2$, nor the property of being or not being a system of the type S.

We shall use theorem A and B from § 3 on the system after the removal. Since $\pi_1 = \pi_2$ the modules $H_m^{(N)}$ of this system will for each m be constant from a certain step $N \geqq N_0 = N_0(m)$ and equal to the modul H_m. Since Γ_m is a module of the form $\{(x_1, x_2, \cdots, x_m)\}$ where the indices $1, 2, \cdots, m$ can be divided into two classes $\{n_s\}$ and $\{n_t\}$ such that the coordinates x_{n_s} are integral and the coordinates x_{n_t} are zero, Γ_m is in particular a closed modul so that $H_m = \Gamma_m = \{(x_1, x_2, \cdots, x_m)\} = \{(\text{integral, zero})\}$. Hence from the step N_0 also $H_m^{(N)} = \{(\text{integral, zero})\}$. Finally, using that $A_m^{(N)} \subseteq H_m^{(N)}$ we find the following property of our new system: Each of the variables x_{n_t} becomes zero if one solve the N first zero-congruences for sufficiently large N (depending on the variable). Hence the system is of the type S. *This proves the main theorem.* Furthermore we see that each of the variables x_{n_s} becomes integral if one solve the N first zero-congruences for sufficiently large N (depending on the variable). The same of course is also true for the system before the removal of the variables x_{n_r} with mere zero coefficients.— This proves the following

Stronger form of the main theorem. *A necessary (and sufficient) condition that a system of linear forms have $\pi_1 = \pi_2$ is that the linear forms by a substitution can be transfered into a system which is of the type S and moreover possesses the property*

that each of the variables belonging to the integral columns necessarily becomes integral if one solve the N first zero-congruences, corresponding to the linear forms, for sufficiently large N (depending on the variable).

Remark. A (necessary and) sufficient condition that a system of linear forms of the type S have the additional property mentioned in the theorem above is that the variables mentioned necessarily become integral if one solve the system of *all* the zero-congruences corresponding to the linear forms.

In fact, to prove this, we may use theorem A and B from § 3 in a similar way as above.

§ 6. A remark on the algebraic structure of a system of the special type *S*.

The notion of a system of linear forms of the type S was defined in § 1 as a system of linear forms where certain variables had mere integral coefficients while each of the other variables necessarily became 0 by solution of a suitable finite selection of the zero-congruences corresponding to the linear forms.

The question, therefore, naturally arises how a finite system of zero-congruences (in a finite number of variables) can force one of the variables to be zero. In this final paragraph we treat this problem by giving *a necessary and sufficient condition that a system of linear zero-congruences in* $x_1, \cdots, x_n$

$$\begin{aligned} a_{11}x_1 + a_{12}x_2 + \cdots + a_{1n}x_n &\equiv 0 \pmod 1 \\ a_{21}x_1 + a_{22}x_2 + \cdots + a_{2n}x_n &\equiv 0 \pmod 1 \\ \cdots\cdots\cdots\cdots\cdots\cdots\cdots\cdots\cdots\cdots & \\ a_{m1}x_1 + a_{m2}x_2 + \cdots + a_{mn}x_n &\equiv 0 \pmod 1 \end{aligned}$$

will involve $x_1 = 0$.

Let in the corresponding matrix

$$\begin{Bmatrix} a_{11}a_{12}\cdots a_{1n} \\ a_{21}a_{22}\cdots a_{2n} \\ \cdots\cdots\cdots\cdots \\ a_{m1}a_{m2}\cdots a_{mn} \end{Bmatrix}$$

the system of row vectors $R_1, R_2, \cdots, R_m$ have the maximal rank ϱ. Then we can find ϱ linearly independent vectors amongst these row vectors. Let it be, for instance, $R_1, R_2, \cdots, R_\varrho$. Then numbers α exist such that

$$\begin{aligned} R_{\varrho+1} &= \alpha_{11}R_1 + \alpha_{12}R_2 + \cdots + \alpha_{1\varrho}R_\varrho \\ R_{\varrho+2} &= \alpha_{21}R_1 + \alpha_{22}R_2 + \cdots + \alpha_{2\varrho}R_\varrho \\ &\cdots\cdots\cdots\cdots\cdots\cdots\cdots \\ R_m &= \alpha_{m-\varrho,1}R_1 + \alpha_{m-\varrho,2}R_2 + \cdots + \alpha_{m-\varrho,\varrho}R_\varrho . \end{aligned}$$

The column vectors in the abridged matrix

$$\begin{Bmatrix} a_{11} \cdots a_{1n} \\ \cdots\cdots\cdots \\ a_{\varrho 1} \cdots a_{\varrho n} \end{Bmatrix}$$

are denoted by $S_1, \cdots, S_n$. They have the maximal rank ϱ. The column vectors in the matrix

$$\begin{Bmatrix} a_{11} \cdots\cdots\cdots a_{1\varrho} \\ \cdots\cdots\cdots\cdots\cdots \\ a_{m-\varrho,1} \cdots a_{m-\varrho,\varrho} \end{Bmatrix}$$

are denoted by $\mathfrak{S}_1, \cdots, \mathfrak{S}_\varrho$.

Instead of the congruences we can equally well consider the equations

$$\begin{aligned} a_{11}x_1 &+ \cdots + a_{1n}x_n &&= h_1 \\ a_{21}x_1 &+ \cdots + a_{2n}x_n &&= h_2 \\ &\cdots\cdots\cdots\cdots\cdots\cdots\cdots \\ a_{\varrho 1}x_1 &+ \cdots + a_{\varrho n}x_n &&= h_\varrho \\ a_{\varrho+1,1}x_1 &+ \cdots + a_{\varrho+1,n}x_n &&= h_{\varrho+1} \\ &\cdots\cdots\cdots\cdots\cdots\cdots\cdots \\ a_{m1}x_1 &+ \cdots + a_{mn}x_n &&= h_m \end{aligned} \tag{14}$$

where the h's are new integral variables. This system of equations can be solved for a given choice of $h_1, \cdots, h_\varrho$ if and only if

$$h_1\mathfrak{S}_1 + h_2\mathfrak{S}_2 + \cdots + h_\varrho\mathfrak{S}_\varrho \equiv 0 \pmod 1)^{1};$$

1) Here, by $A \equiv 0 \pmod 1$ we mean that A is an integral vector.

for the ϱ first equations can always be solved and they involve the validity of the others if the condition above is satisfied, while otherwise at least one equation is not satisfied. In particular, the condition is satisfied if $h_1 = h_2 = \cdots = h_\varrho = 0$.

If the vectors $S_2, \cdots, S_n$ have the maximal rank ϱ we can choose x_1 arbitrarily by the solution of the ϱ first equations with $h_1 = \cdots = h_\varrho = 0$. If our congruences have no solutions with $x_1 \neq 0$ it follows that $S_2, \cdots, S_n$ must have the maximal rank $\varrho - 1$. Let this necessary condition be satisfied. The integral solutions $(h_1, h_2, \cdots, h_\varrho)$ of

$$h_1\mathfrak{S}_1 + h_2\mathfrak{S}_2 + \cdots + h_\varrho\mathfrak{S}_\varrho \equiv 0 \pmod 1$$

form a lattice. Then obviously a necessary and sufficient condition that every solution of the equations (14) has $x_1 = 0$ is that the lattice $\{(h_1, h_2, \cdots, h_\varrho)\}$ is contained in the space spanned by $S_2, \cdots, S_n$. Hence we have the result:

A necessary and sufficient condition that the congruences involve $x_1 = 0$ *is that* $S_2, \cdots, S_n$ *have the maximal rank* $\varrho - 1$ *and that the lattice* $\{(h_1, h_2, \cdots, h_\varrho)\}$ *of integral solutions* $(h_1, h_2, \cdots, h_\varrho)$ *of*

$$h_1\mathfrak{S}_1 + h_2\mathfrak{S}_2 + \cdots + h_\varrho\mathfrak{S}_\varrho \equiv 0 \pmod 1$$

is contained in the space spanned by $S_2, \cdots, S_n$.

Indleveret til Selskabet d. 31. Oktober 1947.
Færdig fra Trykkeriet d. 12. Juli 1948.

DET KGL. DANSKE VIDENSKABERNES SELSKAB
MATEMATISK-FYSISKE MEDDELELSER, BIND XXIV, NR. 13

THE SOLUBILITY OF CARBON MONOXIDE IN SOME LOWER MONOVALENT ALCOHOLS

BY

J. CHR. GJALDBÄK

KØBENHAVN
I KOMMISSION HOS EJNAR MUNKSGAARD
1948

Printed in Denmark.
Bianco Lunos Bogtrykkeri.

In an earlier paper (1) on the reaction velocity in the process between carbon monoxide and methyl- and ethyl alcoholate dissolved in the corresponding alcohols the solubility of carbon monoxide in these alcohols entered into the calculation of the velocity constant. A final calculation of the experiments was impossible owing to the lack of data on the solubility of carbon monoxide between 20° and 50°. The present paper deals with this solubility in methyl-, ethyl-, normal propyl- and isopropyl alcohol as well as in normal butyl- and isobutyl alcohol at the temperatures in question.

The solubility of carbon monoxide in methyl- and ethyl alcohol has previously been investigated by CARIUS (2), JUST (3) and SKIRROW (4), and a review of the results is given in Table 1. But the literature, as far as the author is aware, does not contain any data on the solubility of carbon monoxide in the propyl- and butyl alcohols. The solubilities recorded in Table 1 are expressed by means of Ostwald's absorption coefficient, i. e. the ratio between the concentration of the gas in the saturated solution and the concentration of the gas in the gas phase. CARIUS expresses the solubility of carbon monoxide in ethyl alcohol by means of Bunsen's absorption coefficient as 0.204 from 0° to 25°; this is in the table converted according to Ostwald's absorption coefficient.

Table 1.

Solubility (l = Ostwald's absorption coefficient) of carbon monoxide in alcohols.

	CH_3OH		C_2H_5OH	
	20°	25°	20°	25°
Carius, 1855.....			0.219	0.223
Just, 1901	0.1830	0.1955	0.1901	0.1921
Skirrow, 1902		0.196		0.192

Apparatus.

The solubility determinations described in the present paper were carried out in an apparatus which in principle is first described by ESTREICHER (5) and later improved by LANNUNG (6), whose paper on the subject contains a sketch and a detailed description. The particular advantage of the apparatus is that the experimental space is shut off by mercury, so that neither gas nor solvent during the experiment comes into contact with stopcocks and stopcock grease. During the experiment the apparatus was constantly shaken in an air thermostat the temperature of which between 20° and 50° could be kept constant with an accuracy of about 0.05°.

The procedure followed in the solubility determinations is described in detail by LANNUNG in the paper cited. In principle it is as follows: After the apparatus is completely filled with mercury a suitable volume of alcohol (about 20 ml) is sucked in and freed from air by keeping the apparatus evacuated for about 12 hours with repeated suction and shaking, whereupon the alcohol is confined between two mercury surfaces. Next about 6 ml of carbon monoxide is sucked into another part of the apparatus where it likewise is confined between mercury surfaces. The apparatus is now placed in the thermostat at 20° and the volume and pressure of the carbon monoxide read after temperature adjustment. Then the carbon monoxide is brought into contact with the alcohol by the separating string of mercury being allowed to drop down into the alcohol. The shaking is started and continued until the manometer reading shows no change for at least half an hour. Then the equilibrium adjustment is carried out at different temperatures. Finally the volume of liquid is determined by weighing the amount of mercury that can be drawn to a calibration mark. The volume of the manometer tube of the apparatus and the volume between the various marks are determined by weighing with mercury.

Materials.

Methyl-, ethyl-, and normal propyl alcohol were dehydrated in an apparatus made completely of glass, magnesium being used

according to H. Lund and J. Bjerrum (7). It was attempted to dehydrate isopropyl alcohol by the same method, but magnesium could not be made to react with this alcohol. The dehydration of isopropyl alcohol, normal butyl- and isobutyl alcohol was accomplished by slow distillation in a wire-gauze column (8) with 50 plates. Table 2 presents a summary of the boiling points

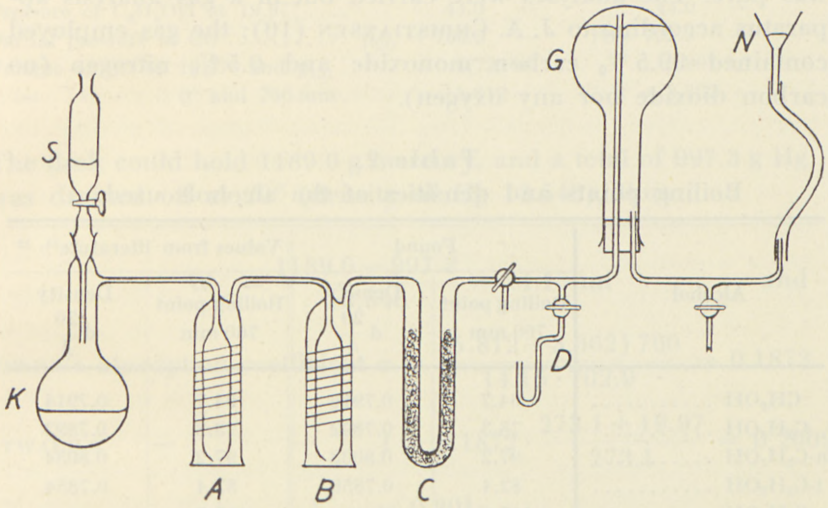

Fig. 1. S: Formic acid. K: Sulphuric acid. A: Sodium hydroxide solution. B: Sulphuric acid. C: Cotton-wool filter. G: Gasometer with mercury. N: Levelling container.

and densities found, the last two columns giving the corresponding constants from the literature. The boiling points were determined by distillation of 20 ml of alcohol in a boiling point apparatus described by H. Baggesgaard Rasmussen and F. Reimers (9). Calibrated thermometers were placed so that the whole mercury column was in alcohol vapour. The boiling points are converted to 760 mm pressure. The densities were determined at 20.°00 ± 0.02° in a 50 ml pycnometer with two graduated capillary tubes provided with ground-glass caps. In the calculation of the density correction is made for the buoyancy of the air.

Carbon monoxide was prepared in an apparatus like the one sketched in Fig. 1. From the separating funnel (S) anhydrous formic acid dripped into concentrated sulphuric acid in the flask (K). The carbon monoxide was led through glass spiral washing

bottles containing sodium hydroxide solution (A) and concentrated sulphuric acid (B) and a cotton-wool filter (C) into a 500 ml Berzelius gasometer (G) with levelling container (N). The carbon monoxide production was made very slow so that the washing could be effective. The gasometer was filled and emptied until sampling (stopcock D) showed that the carbon monoxide was pure. The analyses were carried out in a gas analysis apparatus according to J. A. CHRISTIANSEN (10); the gas employed contained 99.5 % carbon monoxide and 0.5 % nitrogen (no carbon dioxide nor any oxygen).

Table 2.
Boiling points and densities of the alcohols used.

Alcohol	Found		Values from literature[11, 12]	
	Boiling point 760 mm	Density $d\frac{20}{4}$	Boiling point 760 mm	Density $d\frac{20}{4}$
CH_3OH	64.7	0.7916	64.7	0.7914
C_2H_5OH	78.3	0.7892	78.3	0.7893
n-C_3H_7OH	97.2	0.8038	97.2	0.8034
i-C_3H_7OH	82.4	0.7859	82.4	0.7854
n-C_4H_9OH	117.8		117.7	
i-C_4H_9OH	107.9		107.9	

Experimental results.

The densities and vapour pressures used in the calculations are given in Table 3. The solubilities are expressed by Ostwald's absorption coefficient (l) and calculated from

$$l = \frac{(W - w) \cdot 760 \cdot T}{W_L \cdot P \cdot 273.1},$$

where W is the volume (0°, 760 mm) of the gas introduced, w the volume (0°, 760 mm) of the gas that remains after the absorption. W_L is the volume of the alcohol and P the partial pressure of the carbon monoxide, both at the prevailing absolute temperature T. The following survey shows an example of the calculation of the solubility

of carbon monoxide in ethyl alcohol:

	Before the absorption	After the absorption
Temperature t° C	19.97°	19.97°
$1 + \frac{t}{273.1}$	1.0732	1.0732
Total pressure in the container ...	749.3 mm Hg	746.9 mm Hg
Pressure of C_2H_5OH at 19.97°	44.0 —	44.0 —
Partial pressure of CO ..... p_{CO} =	705.3 —	P = 702.9 —
Volume of CO at 19.97° and p_{CO} .	6.721 ml	3.901 ml
— - - - 0° and 760 mm .	5.812 -	w = 3.362 -

The flask could hold 1189.0 g mercury, and a total of 997.3 g Hg was drained off at 20° (density of Hg 13.546), thus

$$W_L = \frac{1189.0 - 997.3}{13.546} = 14.15 \text{ ml} \qquad \text{and}$$

BUNSEN's absorption coefficient $\alpha = \frac{(5.812 - 3.362)\,760}{14.15 \cdot 702.9} = 0.1872$

OSTWALD's — — $l = 0.1872 \cdot \frac{273.1 + 19.97}{273.1} = 0.2009.$

$$l_{20.0°} = 0.201.$$

Table 3.

Values of densities and vapour pressures of the alcohols used in the calculations.

	Temp.	CH_3OH	C_2H_5OH	n-C_3H_7OH	i-C_3H_7OH	n-C_4H_9OH	i-C_4H_9OH
Density $d\frac{t}{4}$	20.0	0.7915	0.7894	0.8035	0.7851	0.8098	0.8018
	30.0	0.7825	0.7810	0.7960	0.7769	0.8026	0.7941
	40.0	0.7740	0.7722	0.7875	0.7686	0.7954	0.7864
	50.0	0.7650	0.7633	0.7785	0.7603	0.7882	0.7785
	Lit.	(13)	(13)	(13)	(12)	(12)	(12)
Vapor pressure mm Hg	20.0	95.1	44.0	14.5	32.4	4.39	8.6
	30.0	160.3	78.1	27.6	59.1	9.52	17.0
	40.0	260.4	133.4	50.2	105.6	18.6	31.6
	50.0	409.4	219.8	87.2	176.8	33.7	56.2
	Lit.	(13)	(13)	(12)	(14)	(12)	(15)

In the numerical treatment of the experiments at other temperatures consideration was given to the various alcohol vapour pressures and to the coefficients of expansion of the alcohols, the mercury and the glass. The alcohol vapour pressures were not corrected for the reduction which is attributable to the dissolved carbon monoxide, nor was the volume of the alcohols corrected for changes due to evaporation or to carbon monoxide dissolved. The three last mentioned corrections are small in proportion to the experimental errors.

Tables 4—9 show the solubilities found. Values in the same vertical column originate from the same charge of alcohol and carbon monoxide. The experiments with methyl alcohol (Table 4) were difficult to reproduce, undoubtedly because of the very high vapour pressure. At 20° l was found to be 0.224, thus a value about 23 % higher than that found by JUST (Table 1). An experiment with methyl alcohol to which had been added 1 % of water gave at 20° l = 0.220. When the carbon monoxide pressure was varied the following values were found for the solubility in anhydrous methyl alcohol at 20°: 538 mm (0.227), 680 mm (0.224), 754 mm (0.224), thus the same within the experimental accuracy. The difference between JUST's results and those of the present investigation may perhaps be explained by the circumstance that different values of the vapour pressure of methyl alcohol have been used. JUST found that the solubility between 20° and 25° rises 0.0021 per degree, while the present experiments give a rise of 0.0008 per degree. A comparison of JUST's temperature coefficient with the temperature coefficient for the solubility of carbon monoxide in the other alcohols (Table 10) shows JUST's coefficient to be incredibly high.

For the solubility of carbon monoxide in ethyl alcohol (Table 5) l was found to be 0.200 at 20°, thus a value lying between those found by CARIUS and JUST (Table 1). The experiments reported under "Apparatus A" were carried out in an apparatus having a flask volume of about 300 ml. About one year later (a new dehydrated alcohol and a newly prepared carbon monoxide being used) experiments were made in "Apparatus B", with a flask volume of about 90 ml. Since only less than 20 ml of alcohol can be introduced because of the high solubility, and the rest of the flask is filled with mercury, Apparatus B makes the method so much more rapid and more satisfactory in producing tem-

perature equilibrium. As Table 5 shows, the two apparatuses gave the same value for the solubilities. In the case of the other alcohols only Apparatus B has been used. Ethyl alcohol with 1 % of water gave $l = 0.190$ at 20°. From CARIUS' results one arrives at a temperature coefficient of 0.0007. JUST's results give no reliable temperature coefficient (0.0004) since the deviations of the solubilities found are so small. The present experiments show an increase in solubility of 0.00053 per degree, which is of the same order of magnitude as for the rest of the alcohols investigated.

Table 10 presents a survey of the solubilities found, interpolated to the temperatures 20°, 35° and 50°, as well as the corresponding temperature coefficients.

Table 4.
Solubility in methyl alcohol.

t	l	l	l
19.9	0.226		
20.0			0.222
20.1		0.224	
29.0	0.225		
34.2		0.236	
35.2			0.228
39.5	0.233		
48.8	0.241		
49.8			0.250

Table 5.
Solubility in ethyl alcohol.

Apparatus A			Apparatus B		
t	l	l	t	l	l
20.0	0.200	0.200	20.0.....	0.201	
35.1		0.206	20.3.....		0.203
40.0	0.210		20.7.....	0.201*	
40.6		0.208	28.9.....	0.204	
50.2	0.215		29.8.....		0.206
			33.7.....	0.208*	
			37.9.....	0.211	
			38.8.....		0.211
			47.9.....	0.214	
			50.2.....		0.217

* The equilibrium entered from higher to lower temperature.

Table 6.
Solubility in normal propyl alcohol.

t	l	l
20.0	0.177	0.177
34.8	0.182	
35.0		0.182
50.0	0.191	0.188

Table 7.
Solubility in isopropyl alcohol.

t	l
20.0	0.190
20.0	0.190
35.1	0.196
51.2	0.207

Table 8.
Solubility in normal butyl alcohol.

t	l	l
19.8.....		0.165
19.9.....	0.164	0.164
20.0.....		0.164
20.0.....		0.165
35.1.....	0.168	
35.7.....		0.170
35.7.....		0.169
49.8.....	0.173	
49.9.....		0.173

Table 9.
Solubility in isobutyl alcohol.

t	l	l
20.0.....	0.174	0.173
35.0.....	0.180	0.181
49.8.....		0.185
50.0.....	0.186	

Table 10.
Solubility (l) of carbon monoxide in the alcohols.

Temp.	20°.0	35°.0	50°.0	$\frac{dl}{dt}$ (20°—50°)
CH_3OH	0.224	0.230	0.248	0.0008
C_2H_5OH	0.200	0.207	0.216	0.00053
n-C_3H_7OH	0.177	0.182	0.189	0.00040
i-C_3H_7OH	0.190	0.196	0.206	0.00053
n-C_4H_9OH	0.164	0.169	0.173	0.00030
i-C_4H_9OH	0.174	0.180	0.186	0.00040

Discussion.

Fig. 2 shows corresponding values of $\frac{1}{T} \cdot 10^5$ (abscissae) and log l (ordinates). The degrees centigrade corresponding to the reciprocal absolute temperature are plotted on the upper hori-

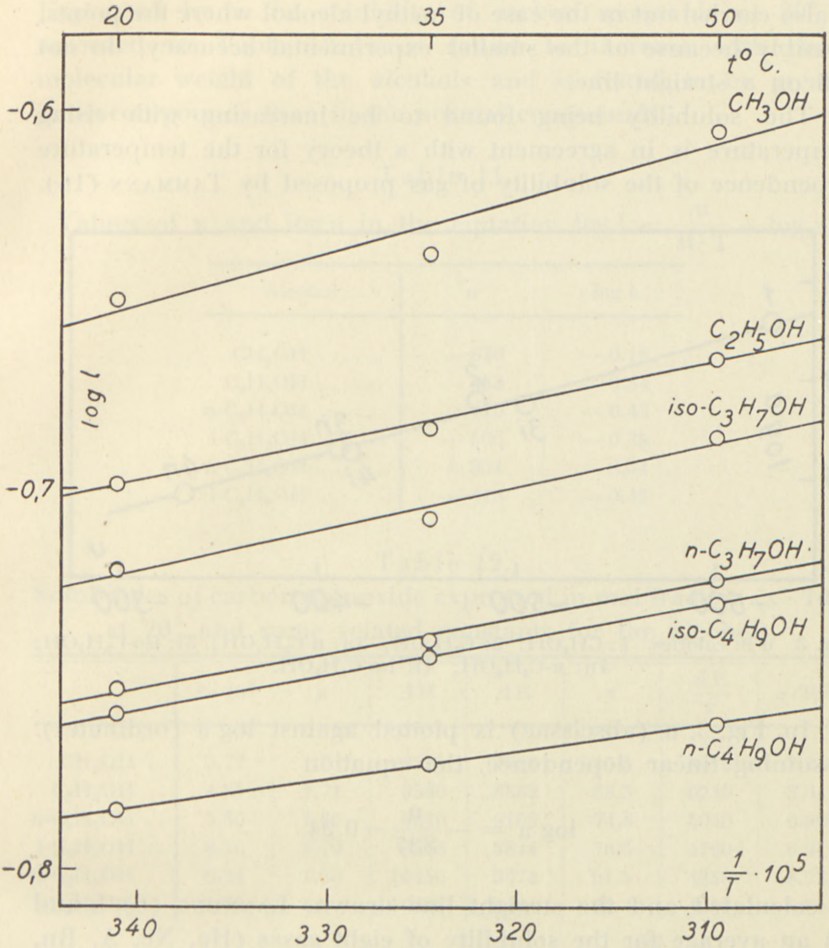

Fig. 2. Solubility-temperature curves.

zontal axis. Integration of the equation for the temperature dependence of the solubility, $\frac{d \ln l}{dT} = -\frac{u}{RT^2}$, where u is the heat of solution, gives, for constant u:

$$\ln l = \frac{u}{1.986 \cdot T} + \ln a, \text{ or } \log l = \frac{u}{4.57 \cdot T} + \log a.$$

The constants u and log a in the last equation are calculated by means of the method of least squares, Table 11. The calculation

is also carried out in the case of methyl alcohol where the points, possibly because of the smaller experimental accuracy, do not fall on a straight line.

The solubility being found to be increasing with rising temperature is in agreement with a theory for the temperature dependence of the solubility of gas proposed by TAMMANN (16).

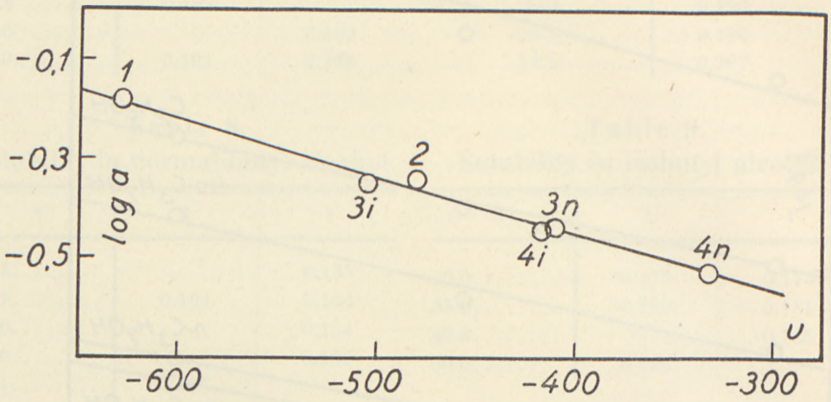

Fig. 3. u in calories. 1: CH_3OH; 2: C_2H_5OH; 3n: n-C_3H_7OH; 3i: iso-C_3H_7OH; 4n: n-C_4H_9OH; 4i: iso-C_4H_9OH.

In Fig. 3, u (abscissae) is plotted against log a (ordinates). Assuming linear dependence, the equation

$$\log a = -\frac{u}{837} - 0.94$$

is calculated and the straight line drawn. LANNUNG (6) found on an average for the solubility of eight gases (He, Ne, A, Rn, H_2, CO, CO_2) in methyl alcohol, ethyl alcohol, acetone, cyclohexane and cyclohexanol the equation:

$$\log a = -\frac{u}{3000} - 0.3.$$

When comparing the solubility of gases in different liquids it is the most reasonable to express the solubility in mol fraction (x) which for sparingly soluble gases can be calculated from

$$x = \frac{l \cdot 273.1 \cdot \text{molecular weight}_{\text{alcohol}} \cdot 10^{-3}}{T \cdot 22.4 \cdot d_{T\,(\text{alcohol})}}.$$

Expressed by x the solubility of carbon monoxide at 20° is recorded in Table 12. x is found to increase with rising molecular weight of the alcohols and is found to be greater in isocompounds than in the normal compounds.

Table 11.

Values of u and log a in the equation $\log l = \frac{u}{R \cdot T} + \log a$.

Alcohol	u	log a
CH_3OH	— 630	— 0.18
C_2H_5OH	— 483	— 0.34
n-C_3H_7OH	— 410	— 0.45
i-C_3H_7OH	— 506	— 0.35
n-C_4H_9OH	— 334	— 0.54
i-C_4H_9OH	— 419	— 0.45

Table 12.

Solubilities of carbon monoxide expressed in mol fraction ($x \cdot 10^4$) at 20° and some related constants for the alcohols.

	$x \cdot 10^4$	μ	ΔH	ΔE	v	$\frac{\Delta E}{v}$	$\alpha \cdot 10^{24}$
CH_3OH ..	3.77	1.6	8520	7850	40.5	8010	3.24
C_2H_5OH ..	4.85	1.71	9580	8882	58.3	6240	5.04
n-C_3H_7OH ..	5.50	1.66	9840	9105	74.8	5040	6.90
i-C_3H_7OH ..	6.10	1.70	9550	8844	76.5	4790	6.91
n-C_4H_9OH ..	6.24	1.66	10450	9674	91.5	4380	8.72
i-C_4H_9OH ..	6.69	1.8	10220	9464	92.4	4250	8.74

μ: Dipole moment in Debye; ΔH: Heat of vaporization in $\frac{cal}{mol}$; ΔE: Energy of vaporization in $\frac{cal}{mol}$ ($= \Delta H - RT$); v: Molecular volume in ml; $\frac{\Delta E}{v}$: "Internal pressure" in atm.; α: Polarizability calculated from molecular refractivity (R), $\alpha = \frac{3R}{4\pi N}$. Values from Intern. Crit. Tables and Landolt-Börnstein's Tables.

Table 12 moreover records the dipole moments (μ), heats of vaporization (ΔH), molecular volumes (v), and polarizabilities (α) of the alcohols. Moreover, $\frac{\Delta E}{v}$ has been calculated (see the table), presumably giving quite valuable information regarding the relative internal pressures in the alcohols which are almost

Table 13.

Solubility of different gases in the alcohols expressed in mol fraction ($x \cdot 10^4$) at 20°. Ar at 0°.

	He[6]	Ne[6]	Ar[18]	Rn[20]	H_2[3]	N_2[3]	O_2[21]	CO	CO_2	N_2O[22]
"Ideal"*		1.7	21	710**		10	16	11	178	202
CH_3OH ...	0.57	0.78	4.8	94	1.5	2.3	3.1	3.77	60[22]	53
C_2H_5OH ...	0.73	1.05	6.5	170	2.1	3.4	3.7	4.85	69[22]	72
n-C_3H_7OH ...			7.3	266				5.50	77[3]	
i-C_3H_7OH ...				215				6.10		
n-C_4H_9OH ...			8.6	338				6.24		
i-C_4H_9OH ...			9.4	308				6.69	75[3]	

* Calculated by HILDEBRAND (17).** Calculated by the author.

identical in polarity. Carbon monoxide belongs to the non-polar gases (dipole moment 0.12 Debye (11)). The fact that the solubility is found to increase with decreasing internal pressure is in agreement with a long series of earlier observations (see, for example, a review of the solubility of non-polar gases in different liquids, on p. 134 of HILDEBRAND's monograph (17)). The fact that the solubility varies in the same manner as the polarizability is in agreement with a series of observations by SISSKIND and KASARNOWSKY (18).

DOLEZALEK (19) has shown that for a number of liquid mixtures of two non-electrolytes, A and B, (e. g. benzene and ethylene chloride) one finds for the whole range of concentration that

$$p = p_0 \cdot x,$$

where p is the partial pressure of A (B), p_0 the vapour pressure of pure A (B) and x the concentration of A (B) calculated as mol fraction. If one of the components is associated (e. g. CCl_4 in benzene), or the components enter into additive combination with each other (e. g. acetone and chloroform), this circumstance must be taken into account in the calculation of x. On the basis of the following considerations, DOLEZALEK has proposed a method for calculating the ideal solubility of gases in liquids: A liquid which is saturated by a gas of the partial pressure p can be imagined to be formed by mixing into the liquid so much "liquid gas" that the mixture has a partial pressure of the gas

of the magnitude p. The solubility of the gas given at a partial pressure of one atmosphere then is

$$\text{solubility} = x = \frac{1}{p_0}.$$

where p_0 is the vapour pressure of the gas in liquid form at the temperature considered.

Most of the gases for which solubility measurements are available have critical temperatures considerably below the temperature at which the solubility determinations have been carried out. HILDEBRAND (17) has, however, for a number of gases calculated theoretical solubilities according to the above equation by extrapolating available vapour pressure measurements of the condensed gases to 20°. Some of the results of these calculations are reproduced in Table 13. The solubility of radium emanation has by the present author been calculated on the basis of vapour pressure measurements by GRAY and RAMSAY (23), by interpolating to a vapour pressure at 20° of 14.1 atmospheres, whence $x = \frac{1}{14.1} = 0.0710$. This calculation of solubilities is thus very approximate, but nevertheless gives a fair orientation regarding the relative magnitude of these quantities. This "ideal solubility", x, is independent of the solvent. In practice the solubilities are most generally found to depend on the solvent, and as a rule to be between one and ten times as small as the "ideal" one, though for the solubility in water one as a rule finds that it is about one hundred times smaller.

Table 13 surveys the solubility of different one-, two-, and three-atomic gases in six alcohols. The values are inter- or extrapolated to 20° and converted into mol fraction.

The present investigations have been carried out in the Department of Inorganic Chemistry, the Danish School of Pharmacy. The author wishes to thank the Head of the Department, Professor CARL FAURHOLT, for permission to do this work and for the excellent working conditions which were available. He is moreover indebted to Professor NIELS BJERRUM for the loan of the apparatus in which the solubility determinations were made, and to the Carlsberg Foundation for financial support in the purchase of a gas analysis apparatus.

Summary.

The solubility of carbon monoxide between the temperatures 20° and 50° is determined in methyl-, ethyl-, normal propyl-, isopropyl-, normal butyl-, and isobutyl alcohol. The results are expressed by means of Ostwald's solubility coefficient (l) and recorded in Table 10, where also dl/dt is calculated. A graphical presentation of the measurements is given in Fig. 2. Within the experimental accuracy the points found lie on a straight line for the equation of which ($\log l = \frac{u}{R \cdot T} + \log a$) the constants u and log a are calculated in Table 11.

Table 12 gives the solubility expressed in mol fraction ($x \cdot 10^4$). This table also includes a calculation of the ratio between the energy of vaporization and the molecular volume for each alcohol, $\frac{\Delta E}{v}$, which for the alcohols almost identical in polarity furnishes information regarding the relative internal pressure. It will be seen that the solubility of carbon monoxide increases with falling internal pressure for the alcohols, which rule is in agreement with that governing the solubility of other gases in various solvents.

Literature.

(1) J. A. Christiansen og J. C. Gjaldbäk. Det Kgl. Danske Vidensk. Selskab. Mat.-fys. Medd. **XX**, Nr. 3 (1942).
(2) L. Carius. Lieb. Ann. der Chem. **94**, 129 (1855).
(3) G. Just. Z. physik. Chem. **37**, 342 (1901).
(4) F. W. Skirrow. Z. physik. Chem. **41**, 139 (1902).
(5) T. Estreicher. Z. physik. Chem. **31**, 176 (1899).
(6) A. Lannung. J. Amer. Chem. Soc. **52**, 68 (1930).
(7) H. Lund u. J. Bjerrum. Ber. chem. Ges. **64**, 210 (1931).
(8) A. Klit. Fraktioneret Destillation. København. (1943).
(9) H. Baggesgaard Rasmussen og F. Reimers. Dansk Tidsskrift f. Farmaci. **16**, 161 (1942).
(10) J. A. Christiansen. Kemisk Maanedsblad. **9**, 133 (1942).
(11) Landolt-Börnstein. Physikalisch-chemische Tabellen.
(12) Intern. Crit. Tables.
(13) S. Young. Dublin Proc. a. Trans. **12**, (2), 374 (1910).
(14) G. S. Parks a. B. Barton. J. Amer. Chem. Soc. **50**, 25 (1928).
(15) G. C. Schmidt. Z. physik. Chem. **8**, 628 (1891).
(16) G. Tammann. Z. anorg. allgem. Chem. **158**, 17 (1926).
(17) J. H. Hildebrand. Solubility of Non-Electrolytes. New York. (1936).
(18) B. Sisskind u. I. Kasarnowsky. Z. anorg. allgem. Chem. **200**, 279 (1931); **214**, 385 (1933).
(19) F. Dolezalek. Z. physik. Chem. **64**, 727 (1908); **71**, 191 (1910).
(20) G. Hofbauer. Sitzungsber. d. Wiener Akad. **123**, (2 a), 2001 (1914).
(21) F. Fischer u. G. Pfleiderer. Z. anorg. allgem. Chem. **124**, 61 (1922).
(22) W. Kunerth. Phys. Rev. **19**, 512 (1922).
(23) R. W. Gray a. W. Ramsay. J. Chem. Soc. **95**, 1073 (1909).

Indleveret til Selskabet den 24. September 1947.
Færdig fra Trykkeriet den 13. April 1948.

DET KGL. DANSKE VIDENSKABERNES SELSKAB
MATEMATISK-FYSISKE MEDDELELSER, BIND XXIV, NR. 14

THE INACTIVATION VELOCITY OF PENICILLIN G BY ACIDS AS A FUNCTION OF THE SALT CONCENTRATION

BY

ROLF BRODERSEN

KØBENHAVN
I KOMMISSION HOS EJNAR MUNKSGAARD
1948

Printed in Denmark.
Bianco Lunos Bogtrykkeri

In previous publications (BRODERSEN, 1 and 2, 1947) the rate of inactivation of G-penicillin was examined with regard to its dependence on the hydrogen ion concentration and the temperature. The present investigation deals with the variation of the inactivation velocity with the salt concentration.

I. The Mechanism of the Salt Effect.

According to the previously propounded theory of the mechanism of the reaction the course of the inactivation is represented by the following diagram:

$$\begin{array}{lll} & Pn^-H^+ \rightarrow P' & I \\ & \downarrow\uparrow & \\ Pn^- + H^+ \rightleftarrows & HPn \rightarrow P' & II \\ & + & \\ & H & \\ & \downarrow\uparrow & \\ & HPnH^+ \rightarrow P' & III \end{array}$$

The irreversible reactions denoted by single arrows are assumed to be velocity determining, while the protolytic equilibrium reactions denoted by the double arrows are assumed to proceed at such high velocities that equilibrium is established momentarily. In case of great hydrogen ion concentrations reaction III will become dominating. It is not possible on the basis of any previous investigations to ascertain whether reaction I or reaction II is dominating in case of small hydrogen ion concentrations.

We shall return to this question later on. Meanwhile we shall, however, omit consideration of the possibility of reaction I and at the same time assume that the concentration of $Pn^- H^+$ is small when compared to the concentration of HPn.

If h_0 denotes the velocity of reaction II, and if the other designations are the same as those used previously, the velocities of reactions II and III respectively will be:

$$h_0 = k_0 c_0; \qquad h_+ = k_+ c_+ . \tag{1}$$

The total velocity will be equal to the sum of these two figures.

$$h = h_0 + h_+ = k_0 c_0 + k_+ c_+ . \tag{2}$$

For the equilibriums of the reaction scheme we have:

$$f_{H^+} \frac{f_-}{f_0} c_{H^+} \frac{c_-}{c_0} = K_{(0)} \tag{3}$$

$$f_{H^+} \frac{f_0}{f_+} c_{H^+} \frac{c_0}{c_+} = K_{(+)} \tag{4}$$

where f denotes the activity coefficients, while $K_{(0)}$ and $K_{(+)}$ are the thermo-dynamic dissociation constants which are independent of the salt concentration.

For stoichiometric reasons we have

$$c = c_0 + c_- + c_+ . \tag{5}$$

As c_+ is small compared to c, we have with approximation:

$$c = c_0 + c_- . \tag{6}$$

From this we can find c_- and substitute in (3), so that we have:

$$c_0 = \frac{f_{H^+} \frac{f_-}{f_0} c}{K_0 + f_{H^+} \frac{f_-}{f_0} c_{H^+}} c_{H^+} \tag{7}$$

c_+ may now be found by substituting (7) in (4)

$$c_+ = \frac{(f_{H^+})^2 \frac{f_-}{f_+} c}{K_{(+)}\left(K_{(0)} + f_{H^+}\frac{f_-}{f_0} c_{H^+}\right)} (c_{H^+})^2 \qquad (8)$$

(7) and (8) are substituted in (2), and the velocity constant of the whole reaction is found to be:

$$k = \frac{h}{c} = \left(k_0 + \frac{k_+ f_0}{K_{(+)} f_+} f_{H^+} c_{H^+}\right) \frac{c_{H^+}}{\frac{f_0}{f_- f_{H^+}} K_{(0)} + c_{H^+}}. \qquad (9)$$

It is possible to calculate the salt effect from this equation if the variation with the salt concentration of the quantities on the right side of the equation is known.

If in stead of assuming reaction II to take place, we consider the inactivation to proceed according to reaction I, i. e. through the ampho-ion Pn^-H^+, we find by a deduction analogous to the one particularized above, the following equation:

$$k = \frac{h}{c} = \left(\frac{k_\pm}{K_{(\pm)}} \cdot \frac{f_0}{f_\pm} K_{(0)} + \frac{k_+}{K_{(+)}} \cdot \frac{f_0}{f_+} f_{H^+} c_{H^+}\right) \frac{c_{H^+}}{\frac{f_0}{f_- f_{H^+}} K_{(0)} + c_{H^+}}. \qquad (10)$$

II. The Salt Effect in Case of Small Salt Concentrations.

Theory.

In the equations (9) and (10) k_0, k_+, and $k_\pm$ denote the velocity constants for the velocity determining reactions. Such reactions must be supposed to be brought about by collisions between water molecules and penicillin molecules.

As the water molecules are without electric charge the velocity of the reaction will be independent of the salt concentration at small values of the ionic strength (Brønsted (1924) and Christiansen (1924)), for which reason k_0, k_+, and $k_\pm$ may here be considered to be constant. The values of these quantities at an ionic strength of 0 we shall denote $k_{(0)}$, $k_{(+)}$, and $k_{(\pm)}$. It appears from Kirkwood's equation (1924) for the activity coef-

ficient of an ion with both positive and negative charges that the activity of an ion in a diluted salt solution is approximately constant even if an equally large number of positive and negative charges are added to the charge of the ion. The activity coefficient is thus chiefly determined by the surplus number of positive and negative charges so that it is possible to consider $f_0 = f_{\pm}$.

As $K_{(0)}$ and $K_{(\pm)}$ are independent of the salt concentration, it is seen that for diluted solutions the salt effect on the inactivation of penicillin must be found to be the same whether we use equation (9) or equation (10). We shall in the following discussion apply equation (10).

We have hitherto assumed that at hydrogen ion concentrations about 10^{-7} m penicillin exists as a monovalent, negative ion, Pn^-, which in acid solution combines with a hydrogen ion and forms the uncharged penicillin molecule HPn. For the purpose of the previous investigations which dealt with the rate of inactivation at constant salt concentration it is, however, of no importance whether HPn is assumed to be without charge or having a positive or negative charge or charges, as long as Pn^- is considered to have one negative charge more than HPn. The results will be independent of these assumptions, and it is therefore also impossible to draw any conclusions from these experiments with regard to the total charge of penicillin.

It is quite otherwise when the investigation deals with the effect of the salt concentration on the reaction. In this case the magnitude of the total charge will be of decisive importance as the calculated salt effect will vary according to the assumed number of charges of HPn.

In sufficiently diluted solutions it is possible to calculate the salt effect on the velocity of the reaction corresponding to different charges of HPn in the following manner.

If f_n denotes the activity coefficient of an ion of the valency n, we have:

$$f_0 = f_{\pm}; \qquad f_{H^+} = f_1. \tag{11}$$

If the valency of HPn is referred to as z, we have:

$$f_+ = f_{z+1}; \qquad f_- = f_{z-1}. \tag{12}$$

f_0 in (10) is substituted by f_z

$$k = \left(\frac{k_{(\pm)}}{K_{(\pm)}} K_{(0)} + \frac{k_{(+)}}{K_{(+)}} \cdot \frac{f_z}{f_{z+1}} f_1 c_{H^+} \right) \frac{c_{H^+}}{\frac{f_z}{f_{z-1} f_1} K_{(0)} + c_{H^+}} . \quad (13)$$

If we now substitute $f_n = f_1^{(n^2)}$, we have:

$$k = \left(\frac{k_{(\pm)}}{K_{(\pm)}} K_{(0)} + \frac{k_{(+)}}{K_{(+)}} f_1^{-2z} c_{H^+} \right) \frac{c_{H^+}}{f_1^{2z-2} K_{(0)} + c_{H^+}} . \quad (14)$$

f_1 can be calculated from Poisson-Boltzmann's equation

$$- \log f_z = \frac{z^2 A \sqrt{J}}{(DT)^{\frac{3}{2}}} \quad (15)$$

where $A = 1.82$ and $D = 76$ at 30°C, which for $z = 1$ gives

$$- \log f_1 = 0.52 \sqrt{J} \quad (16)$$

where J is the total ionic strength of the solution.

Equations (14) and (16) make it possible to calculate the dependence of the rate of inactivation on the salt concentration for different values of z if the hydrogen ion concentrations and the other quantities of equation (14) are known.

Experiments and Calculation.

The velocity constants of the inactivation of penicillin G were determined at 30° C at different concentrations of sodium chloride, the measurements being performed according to previously described methods.

Three series of experiments were carried out—at the hydrogen ion concentrations 0.024, 0.0024 and 0.0004 m respectively. Diluted hydrochloric acid was used as buffer medium during the first two series of experiments and diluted acetic acid during the last one. Ordinary glycine and acetate buffers, the buffering capacity of which is greater, were not convenient as the experiments were to be carried out at low values of the ionic strength. The hydrogen ion concentrations of the solutions used could be

reproduced with an accuracy of 0.01—0.02 p_H-units and did not change measurably during the reaction.

In diluted hydrochloric acid solutions the hydrogen ion concentrations were observed to remain unchanged when penicillin had been added and to be independent of addition of salt. This was verified by electrometric measurement by means of a glass electrode, the solutions being compared to hydrochloric acid solutions of known concentrations with the same sodium chloride concentrations.

During the third series of experiments, which was performed in 0.0095 m acetic acid, it was observed that the hydrogen ion concentration decreased somewhat when penicillin was added, and it is likewise necessary here to allow for the fact that dissociation equilibrium of acetic acid is sensitive to salt. The hydrogen ion concentration must therefore be determined for each salt concentration during these experiments. This may be done by calculation or experimentally by comparison with hydrochloric acid—sodium chloride solutions. As it is impossible, however, to use the experimental method at very small ionic strengths the hydrogen ion concentration has been determined at various larger salt concentrations both by calculation and experimentally. The calculated figures have been found to conform accurately to the experimentally determined results, and all other hydrogen ion concentrations have subsequently been determined by calculation in the following manner.

By addition of penicillin, which in all the experiments dealt with here was used in an initial concentration of 10^{-5} m, a reduction of the hydrogen ion concentration is caused which, on the basis of the law af mass action, may be calculated to correspond to a consumption of about $17 \cdot 10^{-5}$ m hydrogen ion. This consumption is constant at different salt concentrations and may be imagined to be caused by the fact that the penicillin employed contains a little bicarbonate. The law of mass action for acetic acid

$$K_{(EH)} = \frac{f_{H^+} f_{E^-}}{f_{EH}} \cdot \frac{c_{H^+} c_{E^-}}{c_{EH}} \qquad (17)$$

may now be used for calculating the hydrogen ion concentration as we have

$$c_{E^-} + c_{EH} = 0.0095; \qquad c_{E^-} - c_{H^+} = 0.00017$$

$K_{(EH)} = 1.750 \cdot 10^{-5}$ at 30° C. (see HARNED & OWEN, 1934), when, as above, we substitute

$$f_{EH} = 1; \qquad f_{E^-} = f_{H^+} = f_1$$

where f_1 is calculated from (16).

The quantities $\frac{k_{(+)}}{K_{(+)}}$, $\frac{k_{(\pm)}}{K_{(\pm)}}$, and $K_{(0)}$ may be found in the following way:

The velocity constant k was determined for an ionic strength of 0 in the three experimental series by extrapolation.

The following values were found:

c_{H^+}	= 0.024	0.0024	0.00031	
k	= 0.16	0.028	0.0065	for J = 0.

By substituting these three pairs of figures in (10) we get three equations in which the three quantities which we are trying to determine are the only unknown quantities as all the activity

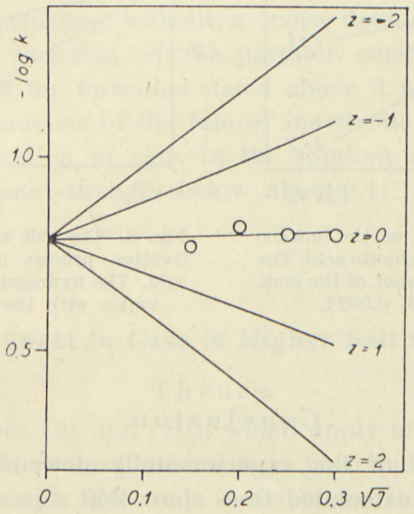

Fig. 1. The salt effect on the inactivation process in hydrochloric acid. The abscissa is the square root of the ionic strength. $c_{H^+} = 0.024$.

coefficients are unity. These three equations can be solved by trial and error, whereby we obtain:

$$\frac{k_{(+)}}{K_{(+)}} = 6.0 \qquad \frac{k_{(\pm)}}{K_{(\pm)}} = 25.3 \qquad K_{(0)} = 0.00100 \qquad (18)$$

It is now possible by means of equations (14) and (16) to calculate the relationship between the velocity constant and the ionic strength for different charges of the molecule HPn. The results appear from figs. 1—3 in which the fully drawn curves represent these relations. The points marked with circles represent the values determined experimentally.

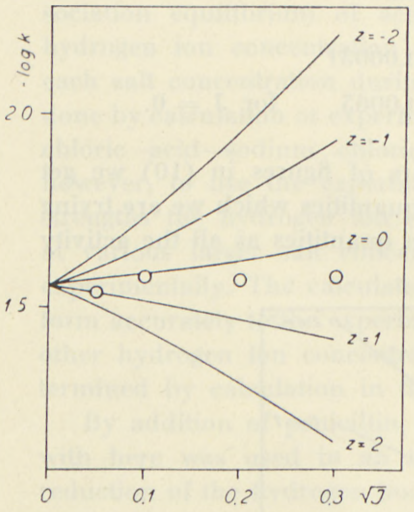

Fig. 2. The salt effect on the inactivation process in hydrochloric acid. The abscissa is the square root of the ionic strength. $C_{H+} = 0.0024$.

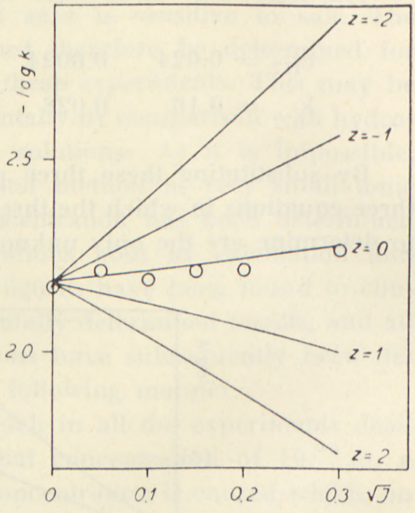

Fig. 3. The salt effect on the inactivation process in 0.0095 m acetic acid. The hydrogen ion concentration varies with the ionic strength.

Conclusion.

The positions of the experimentally determined points as compared to the calculated lines show that z is equal to 0, i. e. that at hydrogen ion concentrations about 10^{-5} the G-penicillin preferably occurs as a single ion with one negative charge, which

in a solution of higher acidity equilibrates a molecule without any charge.

In fig. 2 it is, however, impossible to distinguish with certainty between the two possibilities $z = 0$ and $z = 1$. The mean error of the experimental determination of log k in these experiments amounts to 0.02—0.03, so that only the point representing $J = 0.3$ can be said to show a greater deviation from the line $z = 0$ than may be explained by accidental variations. The theory on which the calculation of the curves is based is, however, not so accurate for this ionic strength that any importance can be attached to the deviation.

This result with regard to the charge of the penicillin molecule is in conformity with the results which we should have expected to obtain according to the structural formula for penicillin propounded by British and American scientists (Committee on Medical Research and the Medical Research Council, 1945).

The partition coefficient of penicillin in water and ether is about unity for c_{H^+} = about 10^{-4}, decreases at higher hydrogen ion concentrations and increases at lower hydrogen ion concentrations. From this one might be tempted to conclude that penicillin carries the number of charges indicated by the above experiments on the salt effect. It is, however, impossible to draw any definite conclusions without a more detailed knowledge of the numerical variation of the partition coefficient.

By means of the formulae stated above it is possible to calculate the dependence of the rate of inactivation of G-penicillin on the concentration of salts in the solution corresponding to values of the ionic strength below about 0.1.

III. The Salt Effect in Case of Higher Salt Concentrations.

Theory.

The equations (9) and (10), which apply to each of the two possible inactivation mechanisms, have been deduced irrespective of the ionic strength. We may therefor use these equations as a basis for the calculation of the effect of salt in solutions of higher concentrations as well. In the following we shall

discuss the possibility of an approximate calculation of the quantities in question at higher salt concentrations.

Suppose the ion PnH^+ is activated by collision with water molecules whereby a complex is formed which may either be subjected to an irreversible decomposition or return to the original condition: a positive penicillin ion and a water molecule.

$$PnH^+ + H_2O \rightleftarrows Pn^*H^+H_2O \rightarrow Pn'. \tag{19}$$

If we further suppose the irreversible action to proceed slowly when compared to the reversible action so that the complex is in equilibrium with penicillin ion and water, we have:

$$\frac{c_+ c_{H_2O}}{c_+^*} \cdot \frac{f_+ f_{H_2O}}{f_+^*} = K. \tag{20}$$

As the velocity of the irreversible conversion of the buffer complex is equal to the velocity at which PnH^+ is consumed, we have:

$$c_+ k_+ = c_+^* k_+^* \tag{21}$$

where k_+^* represents the probability of the irreversible transformation of a molecule $Pn^*H^+H_2O$ within unit of time. We will assume that this quantity is independent of the salt concentration. It is difficult to obtain any idea as to the accuracy of this assumption. It is based on the hypothesis that a substance the molecules of which are transformed spontaneously through an irreversible reaction will exhibit a velocity of reaction independent of the salt concentration.

In equation (20) we shall further substitute

$$f_+ = f_+^* \tag{22}$$

the buffer complex and the penicillin ion having the same charge and almost the same molecular weight, since the difference is merely the relatively small water molecule.

By now applying equations (20) any (21) at the salt concentration 0 and at some other salt concentration, we get

$$k_+ = k_{(+)} \frac{f_{H_2O} c_{H_2O}}{c_{(H_2O)}} \tag{23}$$

where $k_{(+)}$ is k_+ for a salt concentration of 0 and $c_{(H_2O)}$ is the concentration of water for a salt concentration of 0. The fraction in equation (23) is very nearly equal to the ratio of the water vapour pressure of the salt solution to that of pure water at the same temperature. For a 4-molar sodium chloride solution this ratio is 0.87. If we make the further approximation of assuming this fraction to be unity, we have

$$k_+ = k_{(+)} \qquad (24)$$

which means that the velocity constant of the irreversible transformation of the positive penicillin ion is independent of the salt concentration.

The investigations performed by HAMMET & MARTIN (1934) with regard to the influence of the potassium chloride concentration on the hydrolysis of ethyl acetate by means of hydrochloric acid support the view that the approximation represented by the assumptions made here is not more rough than warranted by the purpose.

By a quite analogous deduction we obtain

$$k_0 = k_{(0)} \qquad \text{and} \qquad k_\pm = k_{(\pm)} \qquad (25)$$

We shall now consider the dependence on the salt concentration of the activity coefficients of the equations (9) and (10). $\frac{f_0 f_{H^+}}{f_+}$ can only with a rough approximation be considered to be constantly independent of the salt concentration. As this quantity, however, only occurs in the second term of the parenthesis of (9) and (10), which in case of the hydrogen ion concentrations used here only amounts to about one tenth of the sum of the two terms, we shall consider it to be unity for all salt concentrations.

LARSSON & ADELL (1931) have determined the dependence on the salt concentration of the activity factor $\frac{f_- f_{H^+}}{f_0}$ for 24 different acids which, as regards charge, are of the same type as acetic acid. On the basis of these measurements in connection with the determinations performed for α-dinitro phenol by HALBAN & KORTÜM (1934), HARNED & OWEN (1943) propounded the

rule that the variation of the activity factor with the ionic strength is approximately independent of the acid used, consequently the activity factor for an acid at a certain salt concentration may be taken to be the same as that of another acid for which this quantity has been determined at the salt concentration in question. Moreover the activity factor is, according to HARNED & OWEN, equal to $f_{H^+} f_{Cl^-}$, a quantity for which they give numerical values in a number of excellent tables. However, the law only applies when the neutral salt added is the same. If f. inst. potassium chloride is used in stead of sodium chloride, the value of the activity factor will change. We shall consider this law to hold also with regard to penicillin. The approximation thus made should, according to the statements by LARSSON & ADELL and HARNED & OWEN, cause an error in log k which is smaller than 0.1.

Finally we shall consider the calculation of $f_{\pm}/f_0$.

KIRKWOOD (1934) has devised a formula for the calculation of the activity coefficient $f_{\pm}$ of ampho-ions. The formula holds on the following conditions:

1) The ampho-ions must be spherical.

2) The concentration of the ampho-ions must be so small that the inter-ionic forces between these ions may be neglected.

3) The dipole moment of the ampho-ions must be very large compared to that of the solution.

4) No deviations, except of electric nature, from the laws applying to diluted solutions must occur.

5) Corrections of the type stated by GRONWALL-LA MER (GRONWALL-LA MER & SANDVED (1928)) originating from non-linear terms of the Poisson-Boltzmann equation must be small.

Out of these conditions only those listed under 2) and 3) can be assumed to be fulfilled in this case. To overcome this difficulty the following consideration is set forth:

Let us consider the above-mentioned rule propounded by HARNED & OWEN:

$$\frac{f_- f_{H^+}}{f_0} = \text{constant} \qquad (26)$$

which holds only in case the composition of the salt used is the same, but which applies irrespective of the acid employed. If

we consider f_{H^+} in this equation to be independent of the acid used, we have

$$f_- = f_0 \cdot \text{constant} \qquad (27)$$

i. e. the activity coefficient of any monovalent anion may be considered to be a product of two factors: the activity coefficient of the corresponding uncharged molecule and a constant which is independent of the nature of the anion, but dependent on the salt employed in the solution. This constant may be said to represent the share contributed by the negative charge to the activity coefficient of the ion.

An analogous relation may also be deduced for monovalent positive ions. HAMMET & MARTIN (1934) have shown that the reaction velocity of the hydrolysis of ethyl acetate with acids varies as the equilibrium concentration of a positively charged indicator of the type ammonia-ammonium ion, irrespectively of the nature and concentration of the salt added. The hydrolysis of ethyl acetate is assumed to proceed via the formation of a monovalent cation consisting of an ethyl acetate molecule and a hydrogen ion. If we assume the velocity to be proportional to the concentration of this cation, it will be seen that the dissociation equilibrium of the esters as well as of the indicators employed must be independent of the latter, which means that a relation analogous to equation (26) will apply, hence

$$f_+ = f_0 \cdot \text{constant.} \qquad (28)$$

On the basis of the equations (27) and (28) it would now be natural analogically to conclude that

$$f_\pm = f_0 \cdot \text{constant.} \qquad (29)$$

The constant of this equation represents the effect of the charges upon the activity coefficient, and it is seen to be equal to $f_\pm$ if we assume f_0 to be unity, i. e. if we neglect non-electrical contributions towards the activity coefficient. With a certain approximation we should be able to assume that it is this electrical contribution which we obtain from Kirkwood's formula, for which reason we shall replace $f_\pm$ by $f_\pm/f_0$ in this formula, the more so as the latter quantity forms part of equation (10).

These considerations cannot, of course, lay claim to any exact validity. As, however, exact methods for the calculation of the activity coefficient are lacking, it is the author's intention to attempt to use the results obtained according to the described method, and by comparison with experimentally determined values form an idea of the reliability of the procedure.

Kirkwood's formula is as follows:

$$-\frac{D}{D_0}\ln f = -\frac{Q_0}{2DkT}\cdot\frac{\varkappa}{1+\varkappa a} - \frac{\varkappa^2}{2DkT}\sum_{n=1}^{\infty}\frac{(2n-1)\,Q_n}{(2n-1)(n+1)^2 a^{2n-1}}\cdot \frac{K_{n-1}(\varkappa a)}{K_{n+1}(\varkappa a)+\dfrac{n\,b^{2n+1}\varkappa^2 K_{n-1}(\varkappa a)}{(n+1)(2n-1)(2n+1)\,a^{2n-1}}}. \tag{30}$$

Q_n is found from the equation:

$$Q_n = \sum_{k=1}^{M}\sum_{l=1}^{M} e_k e_l r_k^n r_e^n P_n\ (\cos v_{kl}) \tag{31}$$

P_n being the ordinary Legendre functions which for low values of n have the following configurations:

$$\begin{aligned} P_0(x) &= 1,\\ P_1(x) &= x.\\ P_2(x) &= \frac{3x^2-1}{2}\\ P_3(x) &= \frac{5x^3-3x}{2}\\ P_4(x) &= \frac{1}{8}(35x^4-30x^2+3)\\ P_5(x) &= \frac{1}{8}(63x^5-70x^3+15x) \end{aligned} \tag{32}$$

v_{kl} is the angle between the distances represented by r_k and r_e from the centre of the molecule to the charges e_k and e_l. M is the total number of charges.

In (30) we further have

$$\varkappa^2 = \frac{8\pi N \varepsilon^2 J}{1000\, DkT} \qquad \text{where}$$

N is Avogadro's number, $6.06 \cdot 10^{23}$
ε is the charge of the electron, $4.774 \cdot 10^{-10}$ E.S.U.
k is Boltzmann's constant, $1.375 \cdot 10^{-16}$
J is the ionic strength of the solution.

The functions $K_n(x)$ can be found from

$$K_n(x) = \sum_{s=0}^{n} \frac{2^s n!\,(2n-s)!}{s!\,(2n)!\,(n-s)!} x^s. \qquad (33)$$

D is the dielectric constant of the solution.
D_0 is the dielectric constant of the solvent.
b is the radius of the molecule with the activity coefficient f.
a is the sum of b and the mean value of the radii of the ions of the salt solution.

It is improbable that the penicillin molecule is spherical. The value chosen for b must consequently to a certain extent be based on an estimate. If a spatial model of the molecule of G-penicillin is drawn, it will be seen that the sphere which approximates the penicillin molecule most closely has a radius of 4.7 Å. On the basis of the figure 0.268 cm²/24 hours at 10° C for the diffusion constant of penicillin determined by KLENOW (1947), b is calculated from Riecke's equation to be 4.7 Å and from Stoke's equation to be 5.2 Å (BRODERSEN & KLENOW, 1947). The specific gravity of the molecule is in this case taken to be 1.3. From the formula for G-penicillin advanced by British and American scientists a molecular weight of 334 is obtained. On this basis b is calculated to be 4.7 Å for this molecular specific gravity.

We shall consider the figure 4.7 Å to be the most probable value for b.

From roentgeno-crystallographic data the mean radius of the sodium and the chloride ion is calculated to be 1.0 Å. HARNED & OWEN are of the opinion that at the moment of collision the distance between the centre of the sodium or chloride ion and

the surface of the other ion is greater than 1 Å. According to measurements performed by GRONWALL, LA MER & SANDVED (1928) this distance is about 2 Å. According to HARNED & OWEN the difference between these values is due to hydration of the ions. KIRKWOOD, whose investigations are of a more recent date than those performed by GRONWALL, LA MER & SANDVED, is of the opinion that the figure 1 Å should be used. With regard to KIRKWOOD's own experiments the best conformity between the figures for the activity coefficient of glycine obtained by calculation from the formula and those determined experimentally is obtained at a value of 0.7 Å, although the figure 1.0 Å also gives fairly good conformity. GRONWALL, LA MER & SANDVED's figures are determined by means of conductivity measurements, and it therefore seems desirable, to use the figures found by these authors, when the purpose is to calculate the conductivity. In our case, where the purpose is to calculate an activity coefficient by means of Kirkwood's formula, it appears natural to use a value which has proved statisfactory in connection with this formula. Here we shall therefore consider the "effective mean radius" of the sodium and chloride ion to be 1.0 Å. This figure is thus, to a certain extent, empirically determined. By choosing this value instead of 0.7 Å we have avoided an inconsistency with the crystallographic figures. a is thus 5.7 Å.

We shall assume the distance between the charges of the penicillin ampho-ion to be the same as the distance between the charges in an α-amino, since the configuration of the part of the molecule to which the charges are attached is the same in both cases. WYMAN (1934) has determined the dipole moment of α-amino acids to be 20×10^{-18} E.S.U. From this we find $R = 4.2$ Å.

With regard to r, the distance from the centre of the molecule to the charges, we shall take it to equal b, assuming the charges to be located on the surface of the molecule.

Moreover we shall assume that D equals D_0, irrespective of the salt concentration.

We are now able to calculate $f_\pm/f_0$. From the quantities in formulae (9) and (10) we have as yet no knowledge of the hydrogen ion concentration. Like some of the experiments on

the effect of small salt concentrations dealt with in the preceding section, these experiments were performed in a 0.0095 m acetic acid, the hydrogen ion concentration of which is dependent on the salt concentration. The calculation of the interdependence in the case of small salt concentrations has been dealt with in the section in question. The formulae set forth may, by approximation, be extended to solutions of a somewhat higher concentration by subjecting the activity coefficient to a treatment analogous to that described above. The hydrogen ion concentrations calculated in this manner are found in table 1.

Results.

The values of the velocity constant for different concentrations of sodium chloride determined by means of formulae (9) and (10) are to be found in table 1. These two relations are represented by curves in fig. 4 in which the experimental results are plotted.

With regard to experimental method reference should be made to the section on weak salt solutions. The measurements dealt with here are a direct continuation of the experimental series performed for low concentrations.

Table 1.

(Referring to fig. 4).

J	c_{H^+} calculated	$\frac{f_\pm}{f_0}$ from Kirkwood's formula (30)	$-\log k$ from eq. (9)	$-\log k$ from eq. (10)
0.00	0.0003204	1.00	2.18	2.18
0.01	0.0003608	0.98	2.21	2.20
0.02	0.0003755	0.97	2.22	2.20
0.03	0.0003857	0.96	2.22	2.20
0.06	0.0004060	0.93	2.23	2.20
0.11	0.0004170	0.89	2.25	2.20
0.21	0.0004489	0.82	2.25	2.17
0.51	0.0004626	0.67	2.26	2.10
1.01	0.0004466	0.52	2.26	1.99
2.01	0.0003766	0.38	2.22	1.82
3.01	0.0003003	0.29	2.17	1.65

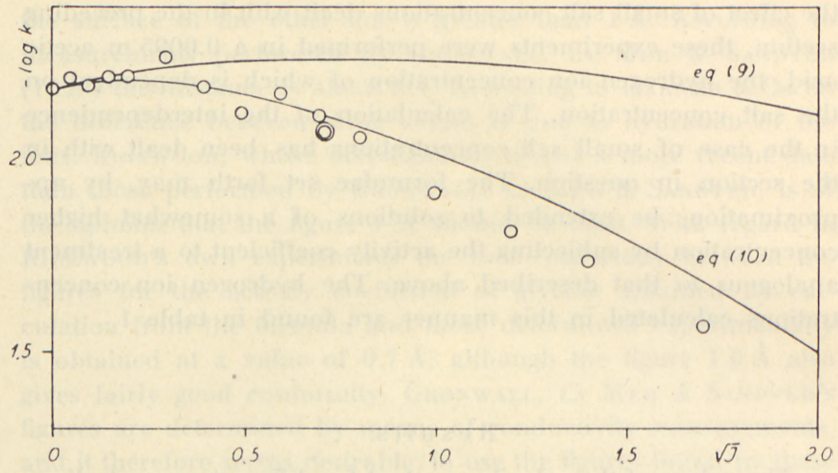

Fig. 4. The salt effect on the inactivation process in 0.0095 m acetic acid at greater salt concentrations. The curves are plotted from the equations (9) and (10), the first of which is based on the assumption that the molecule HPn is labile, and the second on the assumption that PN^-H^+ is labile. The point ◎ represents has been determined as the mean value of a great number of determinations.

It will be seen that there are considerable discrepancies between the experimentally determined figures and those calculated from formula (9), while the conformity with the course calculated according to (10) is quite good. As appears from the manner in which these two equations were deduced formula (9) is based on the condition that a penicillin molecule without charge is unstable, due to the prescence of a hydrogen atom in the carboxyl group. Formula (10) is on the other hand based on the assumption that it is only possible to inactivate the uncharged penicillin molecule by converting it into an ampho-ion, the instability being caused by the combination of a hydrogen ion and the nitrogen of the amido group. The question is now whether it is warrantable, on the basis of these calculations and experiments, to accept as correct the theory on which (10) is based.

The inaccuracy of the calculation performed with equation (9) as a basis is essentially due to the inaccuracy attached to 1) the assumption that k_0 is constant, 2) the calculation of $f_0/f\_f_{H^+}$, and finally, 3) the calculation of c_{H^+}, hence the second term of the parenthesis, at the hydrogen ion concentrations dealt with here, is rather small compared to k_0. It is possible to obtain

an idea of the variation of k_0 with the salt concentration by considering the dependence of the rate of transformation of another uncharged molecule on the salt concentration. HARNED & PFANSTIEL (1922) have examined the dependence of the hydrolysis of ethyl acetate by 0.1 m hydrochloric acid on the concentration of potassium chloride, which was added in amounts varying from 0 to 3 m. They found a variation in log k of 0.02. Apart from this investigation the literature seems to present no examples of determinations of this type of dependence which appear reliable enough to warrant an application in this connection.

According to the statements in the theoretical section on the calculation of $f_0/f\_f_{H^+}$ the error to which this calculation is subject cannot be supposed to cause en error greater than 0.1 in log k. As the calculation of the hydrogen ion concentration is based on the same theoretical suppositions as the calculation of the activity coefficient, the error originating from this calculation may be supposed to be of the same order of magnitude. As, however, the conformity between calculated and experimentally determined hydrogen ion concentrations is even better than might have been expected on this basis, the error is probably even smaller.

It is thus on the whole not very probable that the error to which the calculation of log k from equation (9) is subject is more than 0.4, if the hypothesis with regard to the mechanism of reaction on which (9) is based is correct. As the deviation determined experimentally in some cases is as great as 0.7, it may be said that most probably the assumptions on which formula (9) is based are incorrect.

If we now consider the calculations based on equation (10), it will at once be seen that the difference between the experimentally determined and the calculated values is smaller than the expected maximum error. This good conformity must, however, to some extent be ascribed to incidental circumstances, as the conditions on which the application of Kirkwood's equation is based are not completely fulfilled, and some of the assumptions we have made in order to be able to calculate the individual basic constants are rather uncertain. The conformity found shows, however, that the deviation from the course calculated according to equation (9) as regards direction and order of magnitude

corresponds to the deviation which should be expected to occur if the instability of penicillin is assumed to be due to the taking up of a hydrogen ion at the nitrogen atom in the four-membered ring.

It is thus highly probable that the factor which decides whether a penicillin molecule is stable or unstable in a slightly acid solution is the existence of a hydrogen ion linked to the above mentioned nitrogen atom, while the degree of dissociation of the carboxyl group only influences to a certain extent the velocity at which the inactivation takes place (BRODERSEN, 1947). This theory becomes even more probable when one considers that the inactivation must be assumed to consist in an opening of the four-membered ring and that inactivation in strongly acid solution, as shown in the above quoted work, is due to the taking up of a hydrogen ion at this point of the molecule.

Summary.

I. The result of the calculation of the salt effect on the inactivation of G penicillin in acid solution is dependent on the electric charge of the penicillin molecule and on whether we assume the inactivation in slightly acid solution to be due to the taking up of a hydrogen ion at the nitrogen atom in the four-membered ring or to the taking up of a hydrogen ion in the COO-group.

The location of the hydrogen ion is of no importance in weak salt solutions.

II. A formula (14) from which the salt effect may be calculated at small ionic strengths is deduced. This equation contains the electric charge of the acid penicillin molecule.

From this formula the salt effect on the inactivation in 0.029 and 0.0024 m hydrochloric acid and in 0.0095 m acetic acid to which sodium chloride is added is calculated for different values of the electric charge. In the case of the last mentioned solution allowance is made for the fact that the hydrogen ion concentration varies with the ionic strength.

By comparison with the experimentally determined salt effect it appears that the acid penicillin molecule is uncharged, while

the penicillin ion present in a neutral solution has a single negative charge.

III. An attempt is made to calculate the salt effect at high ionic strengths on the basis of the two theories on the reaction mechanism indicated above. To be able to carry out these calculations it is necessary to make a fairly large number of simplifying assumptions, which, of course, renders the results less reliable. A comparison with the experimentally determined figures shows, however, good conformity with the calculation method which is based on the assumption that the instability is due to the fact that a hydrogen ion has been taken up at the nitrogen atom in the four-membered ring.

An estimate of the errors to which the calculations are subject is shown to confirm this theory about the reaction mechanism, a theory which is also supported by previous investigations.

The expenses of the experiments dealt with in this paper have been covered by grants from "Medicinalfabrikantforeningen". The penicillin used was kindly placed at my disposal by Professor K. A. Jensen, M. D. Helge Brodersen, cand. act. performed the calculations. I am indebted to the late Professor J. N. Brønsted, Ph. D. and Professor J. A. Christiansen, Ph. D. for instructive conversations during the work.

From the Department of General Pathology, University of Copenhagen.
(Professor K. A. Jensen, M. D.).

References.

1) Brodersen, R.: 1. Trans. Farad. Soc. 1947. **43**, 351.
2) — : 2. Acta chem. 1947, **1**, 403.
3) Brodersen, R. & H. Klenow: D. Kgl. Danske Vidensk. Selskab, Biol. Medd. XX Nr. 7.
4) Brønsted, J. N.: J. phys. Chem. 1924, **28**, 579. (Z. physik. Chemie, 1922, **102**, 169; 1925, **115**, 337).
5) Christiansen, J. A.: Z. physik. Chemie, 1924, **113**, 35.
6) Committee on Medical Research and the Medical Research Council, Nature, 1945, **156**, 766.
7) Gronwall, T. H., V. K. la Mer & K. Sandved: Physik. Z., 1928, **29**, 358.
8) Halban, H. v. & G. Kortüm: Z. physik. Chemie, 1934, **A 170**, 351.
9) Hammet, L. P. & A. P. Martin: J. Am. chem. Soc., 1934, **56**, 827 and 830.
10) Harned, H. S. & B. B. Owen: "The Physical Chemistry of Electrolytic Solutions", New York, 1943.
11) Harned, H. S. & R. Pfanstiel: J. Am. chem. Soc. 1922, **44**, 2193.
12) Kirkwood, J. G.: J. Chem. Phys., 1934, **2**, 351.
13) Klenow, H.: Acta chem. Scand. 1947, **1**, 328.
14) Larsson, E. & B. Adell: Z. physik. Chem., 1931, **A 157**, 342 and 1931, **A 156**, 381.
15) Wyman, J.: J. Am. chem. Soc., 1934, **56**, 536.

Indleveret til Selskabet den 29. November 1947.
Færdig fra Trykkeriet den 18. Juni 1948.

DET KGL. DANSKE VIDENSKABERNES SELSKAB
MATEMATISK-FYSISKE MEDDELELSER, BIND XXIV, NR. 15

KINETICAL INVESTIGATIONS INTO ENCYMATIC INACTIVATION OF PENICILLIN G

BY

ROLF BRODERSEN

KØBENHAVN
I KOMMISSION HOS EJNAR MUNKSGAARD
1948

Printed in Denmark
Bianco Lunos Bogtrykkeri

Under the action of the enzyme penicillinase penicillins are converted into biologically inactive substances, the amide bond in the four ring presumably being opened on hydrolysis. In a previous paper (BRODERSEN 1947 a), it has been shown that, in all probability, different penicillinases of bacterial origin exist, since marked differences seem to prevail, on the one hand, between an enzyme studied by WOODRUFF and FOSTER (1945) and prepared from a grampositive, spore-forming air bacterium and, on the other hand, an enzyme which is produced by a gram-negative coli-like bacterium. The present work deals with the course of penicillin inactivation by the latter enzyme.

The investigations communicated in the above cited paper show that we here meet with a substance having the properties typical of enzymes. It has, however, not been demonstrated whether the accelerating effect of this substance on the inactivation of penicillin is due to catalysis or possibly is an ordinary stoichiometric reaction. In the latter case, the ratio between the quantity of the inactivator consumed and the quantity of penicillin inactivated is independent of the experimental conditions.

We shall, therefore, first investigate whether penicillinase has a catalytic effect.

Technique.

Penicillinase was applied in form of a culture filtrate of the previously described coli-like bacterium (BRODERSEN 1947 b). The cultivation procedure is described in the same paper.

The culture filtrate was adjusted to pH 6.7 and an equal volume of phosphate buffer (Sørensen) of the same pH was added. In the different experiments, to 5 ml of this mixture a small volume of a rather concentrated penicillin solution was added. In this

way, the hydrogen ion concentration and the salt concentration were the same in all experiments.

If not otherwise stated, the experimental temperature was 30° C. The temperature of the solution was adjusted prior to the addition of penicillin.

From the reaction mixture samples were drawn at intervals. In these samples, the inactivation process was interrupted by treatment with alcohol at room temperature for 10 minutes, as described earlier. Subsequently, the mixture was diluted to an alcohol content of c. 10 vol %. This alcohol concentration is without detectable influence on the penicillin determinations.

After end experiment, the penicillin activities were measured in the thus treated samples by means of the agar cup method. Generally, each sample was measured in one cup, only. In order nevertheless to obtain a reliable determination of the course of the curve, a considerable number of samples were drawn in each experiment. It might possibly appear more natural to confine oneself to a smaller number of samples and, instead, to determine each of them more accurately in different cups. However, the above procedure was preferred, because the relative change of the penicillin concentration frequently increases markedly towards the end of the experiment; thus, it was necessary to draw samples at rather short intervals in order to ensure a point in the last part of the curve.

Demonstration of the Catalytic Effect of Penicillinase.

Fig. 6 shows the course of the inactivation of pure penicillin-G-sodium salt "Glaxo" (in the following denoted as "preparation A"). The three curves correspond to three different initial concentrations. If the curves are displaced in such a way that the points with the same penicillin concentration fall on the same ordinate (Fig. 1), it appears that the curves are congruent. This means that for any penicillin concentration the reaction velocity is independent of the quantity of penicillin inactivated before the respective time. Disregarding the shape of the curves, this can be explained in two ways:

(1) Penicillin reacts stoichiometrically with a substance the molar concentration of which is high compared with even the highest penicillin concentration applied.

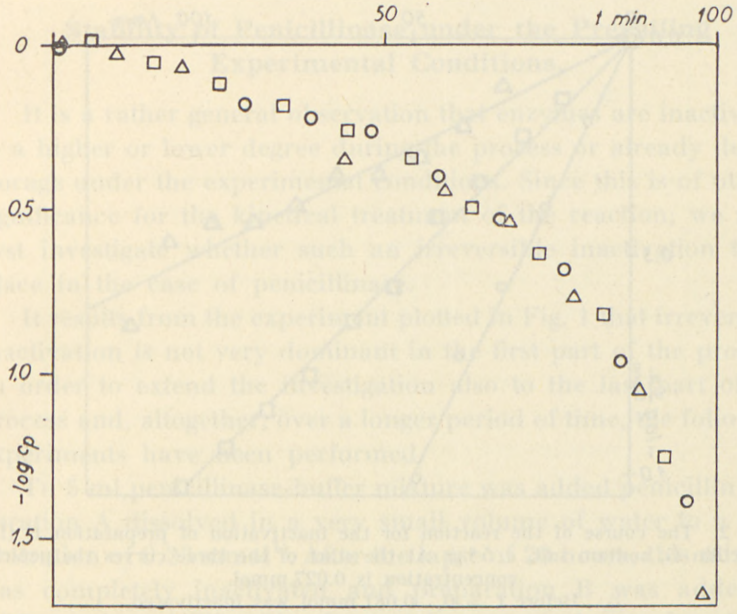

Fig. 1. The course of the reaction for the inactivation of preparation A (penicillin G "Glaxo"). At the start of the three curves the penicillin concentration is 0.208 mml.

○ Before t = 0, 0.408 mmol was inactivated.
□ — t = 0, 0.208 — — — .
△ — t = 0, 0 — — — .

(2) Penicillinase is a catalyst which does not change its catalytic activity during the process.

In the first case, we would expect to find a first-order reaction (pseudomonomolecular process). The curves obtained correspond approximately to a reaction of zero order, which is frequently found in enzymatic processes. This is in favour of the assumption that penicillinase is a catalyst.

Fig. 2 exhibits curves obtained in almost the same way as those represented in Fig. 1, however with another penicillin preparation (B) containing but c. 5 % sodium salt of penicillin G and, besides, biologically inactive substances. The inactivation of this preparation is a first-order reaction in accordance with assumption (1). On the basis of this assumption it seems, however, impossible to explain why the process occurs the slowlier, the higher the initial penicillin concentration. This observation

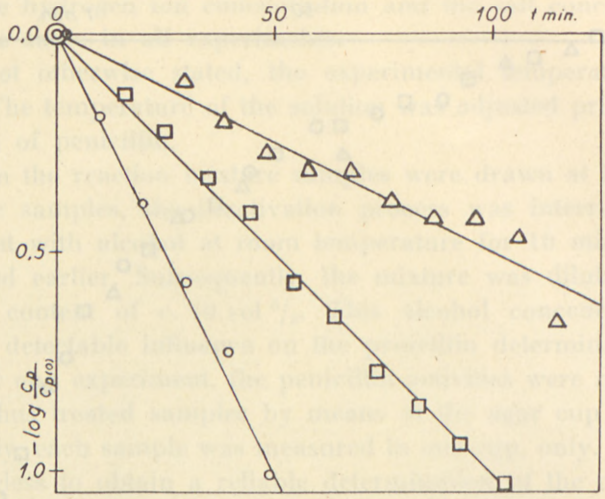

Fig. 2. The course of the reaction for the inactivation of preparation B (Leo-penicillin G, sodium salt, c. 5 %). At the start of the three curves the penicillin concentration is 0.027 mmol.

△ Before t = 0, 0.081 mmol was inactivated.
□ — t = 0, 0.027 — — — .
○ — t = 0, 0 — — — .

may, however, be explained when assuming the penicillinase to be a catalyst which is competitively inhibited by a substance present in the penicillin preparation. The impeding substance must then be present in a concentration so high that the amount of penicillinase bound to penicillin at any time is small as compared with the amount bound to the impeding substance. In this case, the slopes of the straight lines of Fig. 2 should be inversely proportional to the added quantity of the penicillin preparation. This condition is fulfilled in good approximation.

A closer derivation of the theory concerning the course of the process will be given below. Here it may only be stated that the curves considered are in good agreement with the assumption that the inactivated substance is a catalyst; on the other hand, they cannot be explained if it is assumed that the inactivation is a stoichiometric reaction between penicillin and another substance.

Stability of Penicillinase under the Prevailing Experimental Conditions.

It is a rather general observation that enzymes are inactivated to a higher or lower degree during the process or already during storage under the experimental conditions. Since this is of utmost significance for the kinetical treatment of the reaction, we shall first investigate whether such an irreversible inactivation takes place in the case of penicillinase.

It results from the experiment plotted in Fig. 1 that irreversible inactivation is not very dominant in the first part of the process. In order to extend the investigation also to the last part of the process and, altogether, over a longer period of time, the following experiments have been performed.

To 5 ml penicillinase-buffer mixture was added penicillin preparation A dissolved in a very small volume of water to a concentration of 0.23 mmol[1]. After the lapse of 20 hours, this mixture was completely inactivated and preparation B was added to 0.27 mmol penicillin. Simultaneously, a control experiment was started in the following way: to another 5 ml penicillinase-buffer mixture the same amount of preparation B was added. The course of the reactions in these two glasses was studied and compared.

If, under these conditions, the penicillinase is stable for 20 hours, we should expect to find the same course of reaction in both glasses, while the process in the control experiment should occur more rapidly if a partially irreversible inactivation of the enzyme takes place.

For the last part of the experiment, preparation A could also have been used. However, it is possible that, during inactivation of the portion of preparation A added first, a small amount of competitively inhibiting substance was formed which, in view of the measuring uncertainty, did not manifest itself in the experiment shown in Fig. 1. A closer examination of the uncertainty shows that this could be the cause of an erroneous result of the experiment. If, on the other hand, preparation B is used, containing large amounts of competitively inhibiting substances, the

1) Here, the penicillin concentrations are expressed in millimol per litre (mmol), since this proved to be more rational in chemical work than OU/ml. (1 OU/ml = 0.001795 mmol).

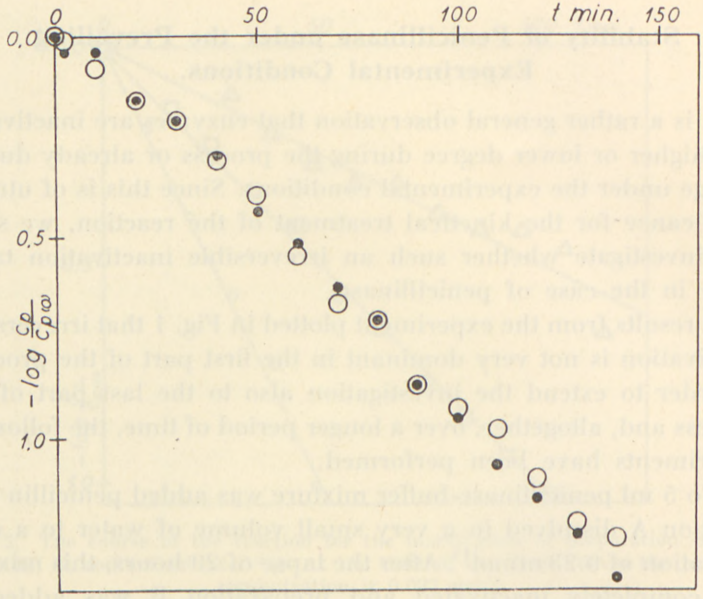

Fig. 3. The course of the reaction for the inactivation of preparation B after the same quantity of enzyme had inactivated a certain quantity of preparation A.
○ Before t = 0, 0.233 mmol of preparation A was inactivated.
● — t = 0, 0 — - — - — — .

effect of the inhibiting substance possibly formed in the first phase of the experiment will not be detectable.

The results of the measurements are shown in Fig. 3. The difference between the two curves appears to be very slight. Therefore, we shall in the following assume that penicillinase is stable throughout the experiment.

The Course of the Inactivation Process.

Theory.

On the basis of the orientating investigations outlined in the preceding section, we shall now deduce a formula for the course of the reaction with time and, then, compare this formula with the curves found experimentally.

In agreement with MICHAËLIS and MENTEN's theory (1913), we assume that the first step of the process is the formation of

an enzyme- and penicillin complex. This complex is subsequently converted and finally split into enzyme and reaction product.

$$P + E \rightleftarrows PE \rightarrow P'E \rightleftarrows P' + E \qquad (1)$$

The equilibrium reactions symbolized by double arrows are assumed to occur with velocities very high as compared with the velocity of the irreversible process which, thus, determines the rate of the reaction. If the equilibrium written on the right side is not completely displaced towards the right side, the reaction product exerts a competitive inhibition.

Moreover, we must reckon with the presence of one or several other competitively inhibiting substances which compete with penicillin in reversibly combining with the enzyme, whereby the reaction velocity is decreased. A_1 denotes such a substance in the penicillin preparation, A_2 one in the enzyme preparation.

$$\left.\begin{aligned} A_1 + E &\rightleftarrows A_1E \\ A_2 + E &\rightleftarrows A_2E \end{aligned}\right| \qquad (2)$$

Assuming that the molar concentration of the enzyme is small as compared with the concentrations of P, P', A_1, and A_2, the mass action terms corresponding to these equilibria can be written

$$K_P = \frac{c_P c_E}{c_{PE}} \qquad (3)$$

$$K_{P'} = \frac{c_{P'} c_E}{c_{P'E}} \qquad (4)$$

$$\left.\begin{aligned} K_{A_1} &= \frac{c_{A_1} c_E}{c_{A_1E}} \\ K_{A_2} &= \frac{c_{A_2} c_E}{c_{A_2E}} \end{aligned}\right| \qquad (5)$$

For stoichiometric reasons, we obtain

$$c_{P'} + c_P = c_{P(0)}. \qquad (6)$$

The total concentration of free and reversibly bound enzymes is

$$C_E = c_E + c_{PE} + c_{P'E}. \tag{7}$$

Finally, we assume that the reaction velocity at any time is proportional to the concentration of the enzyme-penicillin complex

$$-\frac{dc_P}{dt} = k_{PE} c_{PE}. \tag{8}$$

After eliminating from equations (3)—(7) c_E, c_{PE}, $c_{P'E}$, c_{A_1E}, and c_{A_2E} we obtain

$$-\frac{dc_P}{dt}\left[1 + \frac{K_P}{c_P} + \frac{K_P}{K_{P'}}\left(\frac{c_{P(0)}}{c_P} - 1\right) + \frac{K_P}{c_P}\left(\frac{c_{A_1}}{K_{A_1}} + \frac{c_{A_2}}{K_{A_2}}\right)\right] = C_E k_{PE}. \tag{9}$$

For $t = 0$, we have $c_P = c_{P(0)}$, and by integration we obtain

$$\left.\begin{aligned} &c_{P(0)}\left(1 - \frac{c_P}{c_{P(0)}}\right)\left(1 - \frac{K_P}{K_{P'}}\right) + \\ &+ K_P\left(1 + \frac{c_{P(0)}}{K_{P'}} + \frac{c_{A_1}}{K_{A_1}} + \frac{c_{A_2}}{K_{A_2}}\right)\left(-\ln \frac{c_P}{c_{P(0)}}\right) = C_E k_{PE} t. \end{aligned}\right\} \tag{10}$$

This equation describes the relation between the time t and the penicillin concentration c_P.

The Course of the Reaction as a Function af the Enzyme Concentration.

Equation (10) shows that, as it is generally the case, inverse proportionality between the time and the total enzyme concentration must be expected if the other quantities in the formula are constant. In the following, this relation will be checked experimentally.

To this purpose, the enzyme concentration should be varied without simultaneously changing the salt concentration or the concentrations of inhibiting substances possibly present in the penicillinase solution. This is not feasible by changing the amount of culture filtrate in the reaction mixture, since the composition of the culture filtrate with respect to inhibiting substances, and partly also with respect to salts, is unknown. The most correct way of solving this problem would be to prepare the pure enzyme.

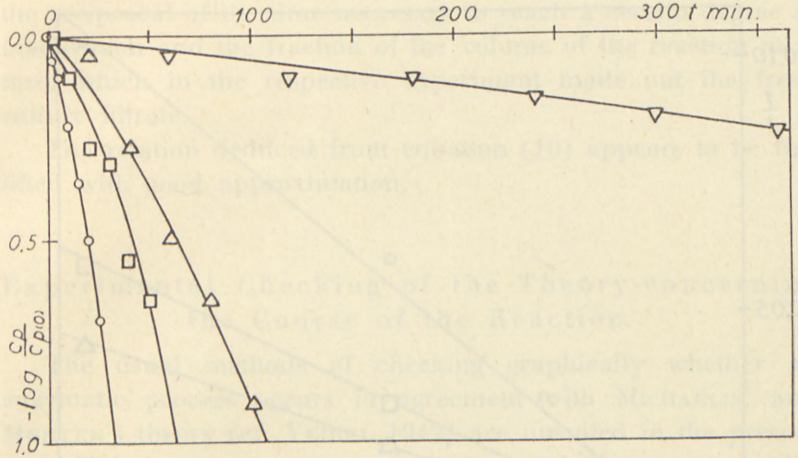

Fig. 4. The course of the reaction as a function of the enzyme concentration (penicillin G "Glaxo". $c_{P(0)} = 0.059$ mmol).

○ 2 ml culture filtrate + 0 ml boiled do. + 2 ml. buffer + 0.01 ml. penicillin solution.
□ 1 ml — — + 1 ml boiled do. + 2 ml. buffer + 0.01 ml. penicillin solution.
△ 0.5 ml — — + 1.5 ml boiled do. + 2 ml. buffer + 0.01 ml. penicillin solution.
▽ 0 ml — — + 2 ml boiled do. + 2 ml. buffer + 0.01 ml. penicillin solution.

However, numerous attempts at a purification failed. Therefore, the following procedure had to be used. The culture filtrate was boiled so that the enzyme was destroyed. The solutions used for the experiments were then made up of different quantities of fresh and of boiled culture filtrate in such a way that the sum was kept constant. In order to obtain complete destruction of the enzyme, it was found necessary, however, to boil the filtrate for more than 20 minutes. During this procedure, a precipitate was formed in the solution. As it was unknown whether the removal of the substance forming this precipitate would affect the process, it was preferred to boil the culture filtrate for one minute, only, and to refrain from a complete destruction of the enzyme.

The enzyme concentration in the fresh culture filtrate will be denoted by c_{E_1} and the volume applied by V_{E_1}. The corresponding quantities for the boiled enzyme solution will be denoted by c_{E_2} and V_{E_2}, and the total volume of the reaction mixture we

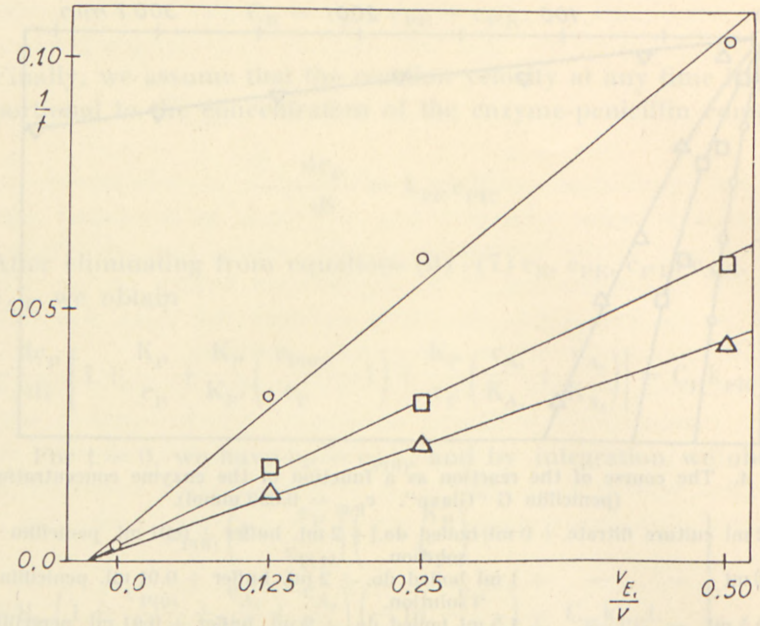

Fig. 5. Velocity variation as a function of the enzyme concentration. Abscissa: the fraction of the total volume of the reaction mixture made out by the non-boiled culture filtrate. Ordinate: reciprocal time elapsing to reach the following degrees of inactivation:

○ — $\log c_P/c_{P(0)} = 0.20$ mmol.
□ — $\log c_P/c_{P(0)} = 0.40$ — .
△ — $\log c_P/c_{P(0)} = 0.60$ — .

shall call V. For the sake of simplicity, equation (10) will be written

$$C_E k_{PE} t = f(c_P) \tag{11}$$

from which we obtain

$$\frac{1}{t} = \frac{k_{PE}}{f_{(c_P)}}(c_{E_1} - c_{E_2})\frac{V_{E_1}}{V} + c_{E_2}\frac{(V_{E_1} + V_{E_2})}{V}. \tag{12}$$

The reciprocal of the time necessary to obtain a certain degree of inactivation for constant $c_{p(o)}$, c_{A_1} etc. will be a linear function of the fraction of the total volume of the reaction mixture which is made out of the fresh culture filtrate. For different degrees of inactivation different slopes are obtained, but all lines should intersect the axis of abscissae at the same point.

The curves obtained for different enzyme concentrations are to be seen in Fig. 4. Fig. 5 illustrates the interdependence between

the reciprocal of the time necessary to reach a certain degree of inactivation and the fraction of the volume of the reaction mixture, which in the respective experiment made out the fresh culture filtrate.

The relation deduced from equation (10) appears to be fulfilled with good approximation.

Experimental Checking of the Theory concerning the Course of the Reaction.

The usual methods of checking graphically whether an enzymatic process occurs in agreement with MICHAËLIS' and MENTEN's theory (cf. VEIBEL 1942) are unsuited in the present case. This is a consequence of the poor relative accuracy with which the penicillin concentrations can be measured. On the other hand, penicillin can be determined in much lower concentrations than most other substances, a fact which should be utilized here. This may be done by the procedure described in the following.

Equation (10) can be transformed into

$$t = c_{P(0)} \left\{ \frac{\left(1 - \frac{c_P}{c_{P(0)}}\right)\left(1 - \frac{K_P}{K_{P'}}\right) + \left(-\ln \frac{c_P}{c_{P(0)}}\right)\left(\frac{K_P}{K_{P'}} + \frac{K_P}{K_{A_1}} \cdot \frac{c_{A_1}}{c_{P(0)}}\right)}{C_E k_{PE}} + \right. \\ \left. + \frac{\left(-\ln \frac{c_P}{c_{P(0)}}\right) K_P \left(1 + \frac{c_{A_2}}{K_{A_2}}\right)}{C_E k_{PE}} \right\} \quad (13)$$

Here, $c_{A_1}/c_{P(0)}$ is constant for one and the same penicillin preparation, and c_{A_2} is constant for one and the same enzyme preparation.

It is obvious that the time necessary to reach a certain degree of inactivation must be expected to be linearly dependent on the initial concentration of penicillin at a constant concentration of the enzyme.

Figs. 6 and 7 show the results of two series of experiments performed with the above discussed preparations A and B, respectively. For each preparation, the course of inactivation was

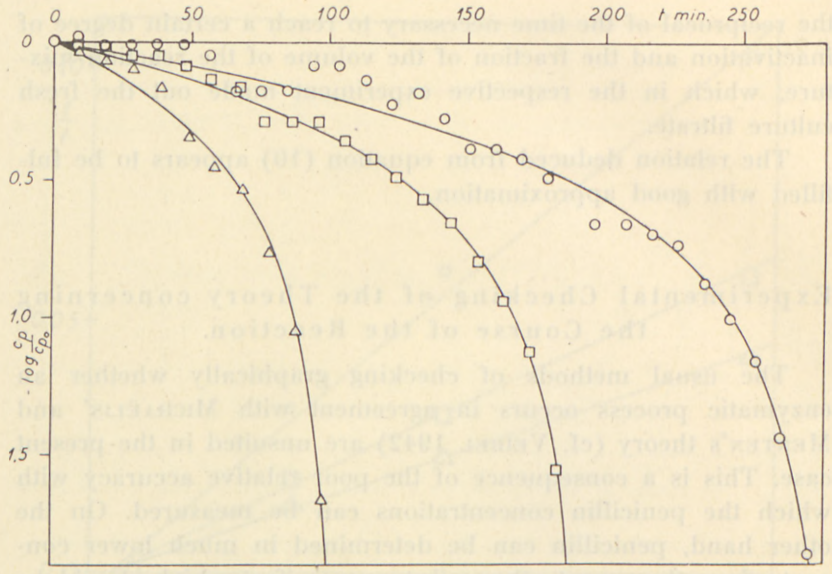

Fig. 6. The course of the enzymatic inactivation of pure penicillin G "Glaxo" (preparation A) at different initial concentrations of penicillin.
○ $c_{P(0)} = 0.625$ mmol.
□ $c_{P(0)} = 0.423$ — .
△ $c_{P(0)} = 0.217$ — .
The drawn curves are calculated.

determined with three different initial concentrations. Owing to the addition of different volumes of penicillin solution, the enzyme concentration is different from experiment to experiment. However, these differences are rather small, since the volume of the penicillin solution added never exceeded 6 % of the total volume. Correction was made for the presumable influence of the slight difference in enzyme concentration on the rate of the process by means of the formula deduced above. To this purpose, the times of the determinations are calculated in such a way that the points inserted refer to the enzyme concentration in the solution prior to the addition of penicillin. In both experimental series given here the same enzyme preparation was used. Thus, C_E can be regarded as constant.

The times found for certain constant degrees of inactivation as a function of the initial concentration are shown in Fig. 8. (The times inserted were found by interpolation between the

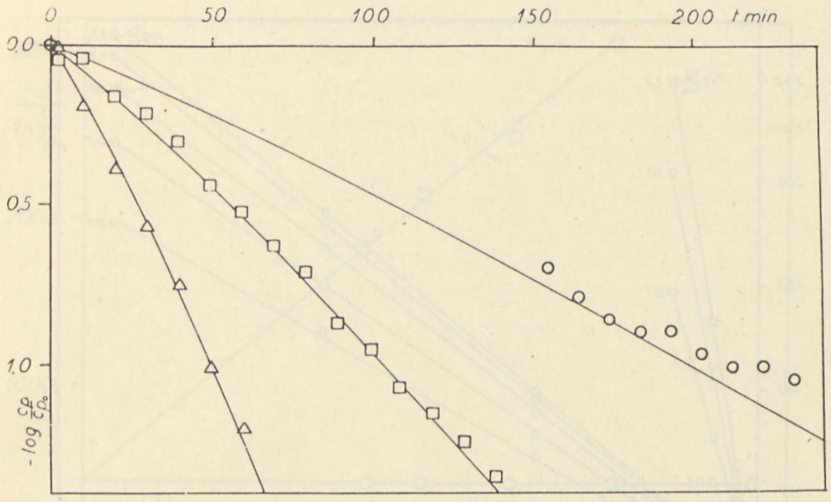

Fig. 7. The course of the enzymatic inactivation of a c. 5 % preparation of penicillin G (preparation B) at different initial concentrations of penicillin.
○ $c_{P(0)} = 0.0830$ mmol.
□ $c_{P(0)} = 0.0423$ — .
△ $c_{P(0)} = 0.0194$ — .
The drawn curves are calculated.

experimental points and not by reading from the curves; these curves are calculated and can first be drawn later.) Fig. 8 shows a linear interdependency between the time and the initial concentration, which is in agreement with equation (13). The lines are drawn in such a way that the parts between the origin and the points of intersection with the axis of ordinates are proportional to $-\ln c_P/c_{P(0)}$, which should be the case according to (13). The experimental uncertainty is too great as to permit a confirmation of the proportionality on the basis of these experiments. This support can, however, be obtained from a third series of experiments which will be discussed later.

Now, we shall investigate whether the slopes of the lines in Fig. 8 are in agreement with equation (13) which will be written as follows:

$$t = a c_{P(0)} + q \tag{14}$$

$$a = \frac{\left(1 - \frac{c_P}{c_{P(0)}}\right)\left(1 - \frac{K_P}{K_{P'}}\right) + \left(-\ln \frac{c_P}{c_{P(0)}}\right)\left(\frac{K_P}{K_{P'}} + \frac{K_P}{K_{A_1}} \cdot \frac{c_{A_1}}{c_{P(0)}}\right)}{C_E k_{PE}} \tag{15}$$

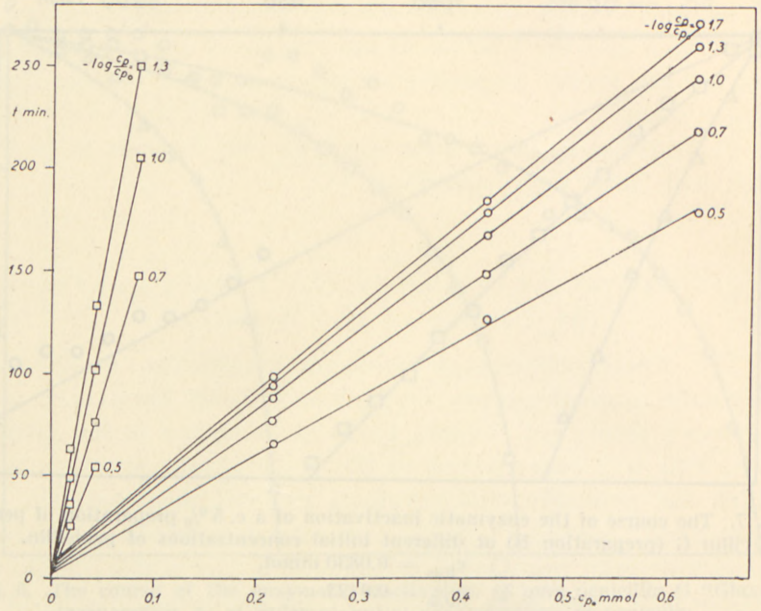

Fig. 8. The time elapsing to reach the given degrees of inactivation is seen to be linearly dependent on the initial concentration.
○ preparation A.
□ preparation B.

$$q = \frac{\left(-\ln \frac{c_P}{c_{P(0)}}\right) K_P \left(1 + \frac{c_{A_2}}{K_{A_2}}\right)}{C_E k_{PE}}. \qquad (16)$$

In Fig. 9, the ordinate $\alpha/(1 - c_P/c_{P(0)})$ is plotted against a function of the degree of inactivation. For the series with preparation A, this figure appears to be approximately independent of the degree of inactivation; the deviations found correspond to the experimental uncertainty. Thus, in this series of experiments, α is proportional to $1 - c_P/c_{P(0)}$. According to equation (15) this means that the second term in the numerator can be put equal to zero. Thus, we obtain

$$\frac{K_P}{K_{P'}} + \frac{K_P}{K_{A_1}} \cdot \frac{c_{A_1}}{c_{P(0)}} \approx 0. \qquad (17)$$

Since both terms are positive it is seen that, in practice, each of them can be put equal to zero.

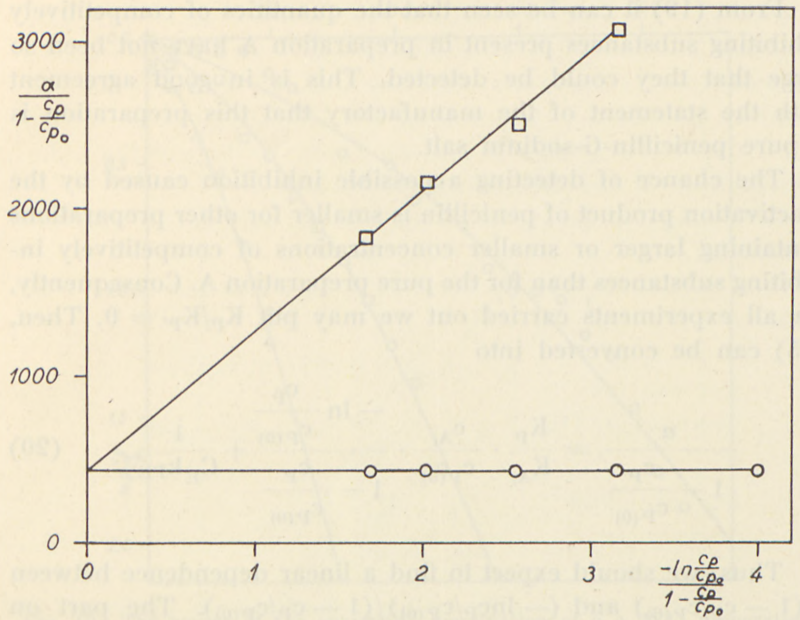

Fig. 9. Checking of formula (20).
○ preparation A.
□ preparation B.

$$\frac{K_P}{K_{P'}} \approx 0, \tag{18}$$

$$\frac{K_P}{K_{A_1}} \cdot \frac{c_{A_1}}{c_{P(0)}} \approx 0. \tag{19}$$

This does not mean, however, that K_P is very small as compared with $K_{P'}$, but only that the ratio between the two quantities is so small that, in these experiments, no inhibition of the enzyme caused by the inactivation product of penicillin can be detected. The experimental conditions can, of course, be changed in such a way that a more accurate investigation of a possible inhibition becomes feasible; it appears from equation (15) that the investigations should be extended to higher degrees of inactivation, which involves the use of larger amounts of penicillin. Such experiments could not be performed with the quantity of penicillin at our disposal.

From (19) it can be seen that the quantities of competitively inhibiting substances present in preparation A have not been so large that they could be detected. This is in good agreement with the statement of the manufactory that this preparation is a pure penicillin-G-sodium salt.

The chance of detecting a possible inhibition caused by the inactivation product of penicillin is smaller for other preparations containing larger or smaller concentrations of competitively inhibiting substances than for the pure preparation A. Consequently, for all experiments carried out we may put $K_P/K_{P'} = 0$. Then, (15) can be converted into

$$\frac{a}{1-\frac{c_P}{c_{P(0)}}} = \frac{K_P}{K_{A_1}} \cdot \frac{c_{A_1}}{c_{P(0)}} \cdot \frac{-\ln \frac{c_P}{c_{P(0)}}}{1-\frac{c_P}{c_{P(0)}}} + \frac{1}{C_E k_{PE}}. \qquad (20)$$

Thus, we should expect to find a linear dependence between $a/(1 - c_P/c_{P(0)})$ and $(-\ln c_P/c_{P(0)})/(1 - c_P/c_{P(0)})$. The part on the axis of ordinates gives the reciprocal of $C_E k_{PE}$, a figure which must be expected to be constant for one and the same enzyme preparation independent of the concentration of inhibiting substances in the penicillin preparation.

From Fig. 9 this is seen to be fulfilled for both preparations A and B.

From Figs. 8 and 9, we find

For enzyme preparation I:

$$\begin{cases} C_E k_{PE} = 0.00233 \text{ mmol/min.} \\ K_P\left(1 + \frac{c_{A_2}}{K_{A_2}}\right) = 0.004 \text{ mmol.} \end{cases}$$

For penicillin preparation A:

$$\frac{K_P}{K_{A_1}} \cdot \frac{c_{A_1}}{c_{P(0)}} \sim 0.$$

For penicillin preparation B:

$$\frac{K_P}{K_{A_1}} \cdot \frac{c_{A_1}}{c_{P(0)}} = 1.96.$$

The curves drawn in Figs. 7 and 6 are calculated from these figures by means of equation (13). There is very good agreement between these curves and the points found experimentally.

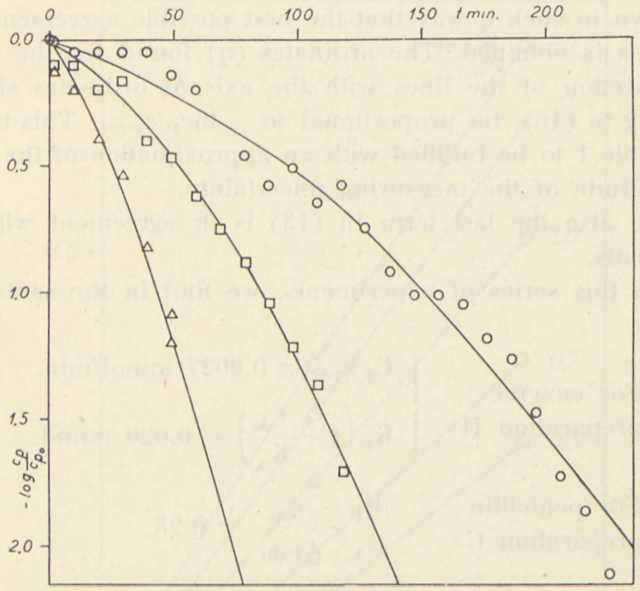

Fig. 10. The course of the enzymatic inactivation of a c. 25 % preparation of penicillin G (preparation C), employing an enzyme preparation (II) different from those applied until now.

○ $c_{P(0)} = 0.235$ mmol.
□ $c_{P(0)} = 0.1190$ — .
△ $c_{P(0)} = 0.0470$ — .

As mentioned above, it is still left to investigate whether the form of the last term in equation (13) can be verified experimentally. In both series of experiments performed up to the present, the numerical values of this term are too small as to make these experiments suitable for such an investigation.

Higher values of the last term in equation (13) were found when another enzyme preparation was applied which was prepared in the same way as the preparation discussed above, but from another charge. Fig. 10 illustrates the course of inactivation of an American commercial preparation of penicillin-G-sodium salt (preparation C, presumably c. 25 %) found when applying this last mentioned enzyme preparation. In Fig. 11 are plotted the times necessary to reach certain degrees of inactivation as a function of the initial concentration of the penicillin. Also here, the linear relation is seen to be valid. The lines in the figure

are drawn in such a way that the best possible agreement with the points is obtained. The ordinates (q) found for the points of intersection of the lines with the axis of ordinates should, according to (16), be proportional to $-\ln c_P/c_{P(0)}$. This is seen from Table 1 to be fulfilled with an approximation of the order of magnitude of the measuring uncertainty.

Thus, also the last term in (13) is in agreement with the experiments.

From this series of experiments, we find in the same way as above

For enzyme preparation II

$$\begin{cases} C_E k_{PE} = 0.0027 \text{ mmol/min.} \\ K_P\left(1 + \dfrac{c_{A_2}}{K_{A_2}}\right) = 0.020 \text{ mmol.} \end{cases}$$

For penicillin preparation C

$$\frac{K_P}{K_{A_1}} \cdot \frac{c_{A_1}}{c_{P(0)}} = 0.28.$$

The curves drawn in Fig. 10 are calculated on the basis of these figures.

As compared with the penicillin content, the content of competitively inhibiting substances in preparation C is seen to be smaller than in preparation B, which is in good agreement with the high purity of preparation C.

For the enzyme preparation II, the quantity $K_P(1 + c_{A_2}/K_{A_2})$ is five times as large as for the enzyme preparation I. It appears improbable that the two values of K_P should be so different. Both preparations are prepared from one and the same strain of bacteria and under approximately the same cultivation conditions; therefore, it can scarcely be assumed that we here have to do with two chemically different enzymes. Hydrogen ion- and salt concentrations have also been approximately equal in both preparations. For an explanation of the experimental results it is, thus, necessary to assume that the divergency is due to different values of c_{A_2}.

Herewith, the presence of a competitively inhibiting substance in the enzyme solutions is made probable.

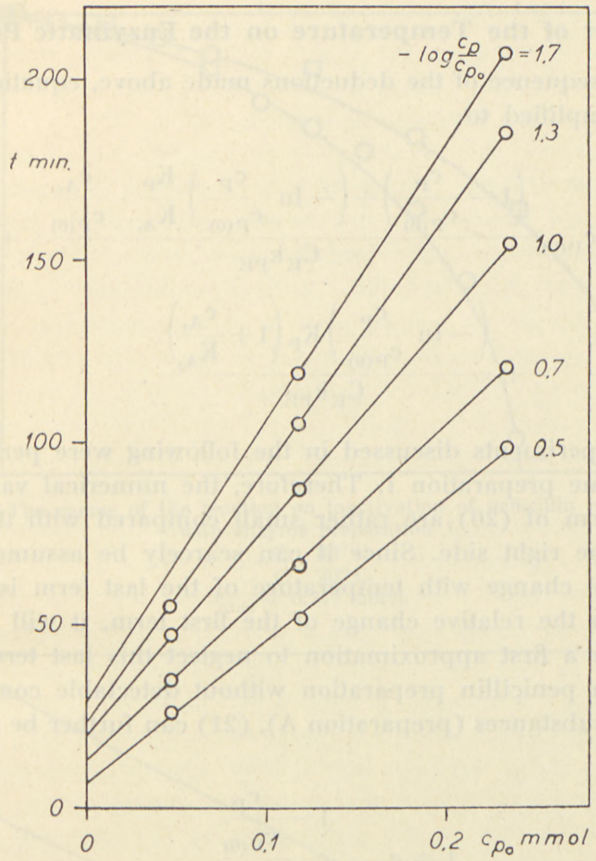

Fig. 11. The time elapsing to reach the given degrees of inactivation in Fig. 10. Here, the lines are seen to intersect the axis of ordinates at a higher point than in Fig. 8. This can be explained by assuming that the enzyme preparation (II) used contains a competitively inhibiting substance in higher concentration than does the enzyme preparation I.

Table 1 (cf. Fig. 11).

$-\log \frac{c_P}{c_{P(0)}}$	q	$\frac{q}{-\ln \frac{c_P}{c_{P(0)}}}$
1.7	30	7.2
1.3	24	8.0
1.0	20	8.5
0.7	13	8
0.5	7	6

The Effect of the Temperature on the Enzymatic Process.

In consequence of the deductions made above, equation (13) can be simplified to

$$t = c_{P(0)} \left\{ \frac{\left(1 - \frac{c_P}{c_{P(0)}}\right) + \left(-\ln \frac{c_P}{c_{P(0)}}\right) \frac{K_P}{K_{A_1}} \cdot \frac{c_{A_1}}{c_{P(0)}}}{C_E k_{PE}} + \right. \\ \left. + \frac{\left(-\ln \frac{c_P}{c_{P(0)}}\right) K_P \left(1 + \frac{c_{A_2}}{K_{A_2}}\right)}{C_E k_{PE}} \right\} \quad (21)$$

The experiments discussed in the following were performed with enzyme preparation I. Therefore, the numerical values of the last term of (20) are rather small compared with the first term on the right side. Since it can scarcely be assumed that the relative change with temperature of the last term is much larger than the relative change of the first term, it will be admissible in a first approximation to neglect this last term.

Using a penicillin preparation without detectable content of inhibiting substances (preparation A), (21) can further be simplified to

$$t = c_{P(0)} \frac{1 - \frac{c_P}{c_{P(0)}}}{C_E k_{PE}} . \quad (22)$$

Here, only k_{PE} is dependent on temperature. According to this equation, we should expect to find the course of the reaction to change with temperature in such a way that t for constant $c_P/c_{P(0)}$ is changed at a given change in temperature by a constant factor, independent of the degree of inactivation.

In the experiment shown in Fig. 12 this condition appears to be fulfilled in good approximation. Thus, the change in the course of the reaction with temperature can be characterized only by the change of the time elapsing until a given degree of inactivation is reached.

It becomes clear from the course of the curves that the most accurate expression for the temperature dependence is obtained

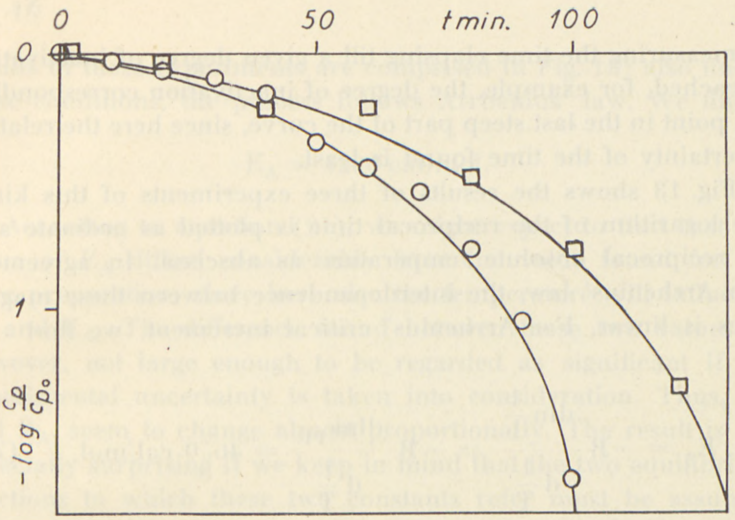

Fig. 12. The course of the reaction on inactivation of penicillin preparation A with enzyme preparation I.
○ 30° C.
□ 20° C.
$c_{P(0)} = 0.217$ mmol.

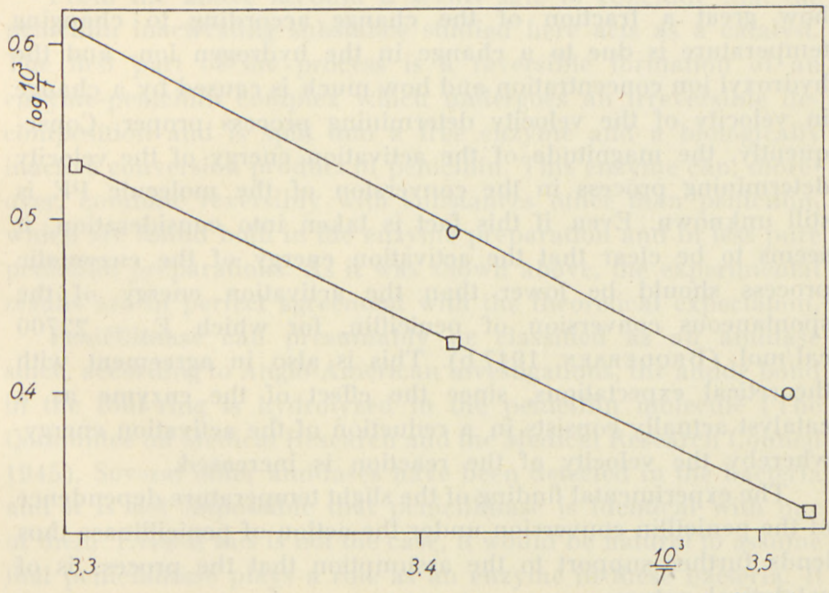

Fig. 13. The logarithm of the velocity of the enzymatic process (ordinate) as a function of the reciprocal of the absolute temperature (abscissa).
○ preparation A.
□ preparation B.

by measuring the time elapsing till a given degree of inactivation is reached, for example, the degree of inactivation corresponding to a point in the last steep part of the curve, since here the relative uncertainty of the time found is least.

Fig. 13 shows the results of three experiments of this kind. The logarithm of the reciprocal time is plotted as ordinate and the reciprocal absolute temperature as abscissa. In agreement with Arrhenius' law, the interdependence between these magnitudes is linear. For Arrhenius' critical increment, we find

$$E_A = -R \frac{d\ln \frac{1}{t}}{d\frac{1}{T}} = -R \frac{d\ln k_{PE}}{d\frac{1}{T}} = 4070 \text{ cal/mol.} \qquad (23)$$

This figure holds for the buffer and for the hydrogen ion concentration (phosphate + c. $^1/_2$ m NaCl, $c_{H^+} = 10^{-6.7}$) applied here. In other buffers other numerical values are to be expected.

From these experiments, no conclusions can be drawn as to how great a fraction of the change according to changing temperature is due to a change in the hydrogen ion- and the hydroxyl ion concentration and how much is caused by a change in velocity of the velocity determining process proper. Consequently, the magnitude of the activation energy of the velocity determining process in the conversion of the molecule PE is still unknown. Even if this fact is taken into consideration, it seems to be clear that the activation energy of the enzymatic process should be lower than the activation energy of the spontaneous conversion of penicillin, for which $E_A = 22700$ cal/mol (Brodersen 1947 b). This is also in agreement with theoretical expectations, since the effect of the enzyme as a catalyst actually consists in a reduction of the activation energy, whereby the velocity of the reaction is increased.

The experimental finding of the slight temperature dependence of the penicillin conversion under the action of penicillinase thus lends further support to the assumption that the process is of catalytical nature.

Finally, experiments were performed on the temperature coefficient of the inactivation of the impure preparation B. The

results of these experiments are comprised in Fig. 13; also under these conditions, the process follows Arrhenius' law. We find

$$E_A = 4200 \text{ cal/mol.}$$

According to equation (21), we might expect to find that the value of E_A differs considerably from the value found for the pure preparation, since here also the temperature will influence K_P and K_{A_1}. The difference found between these two values is, however, not large enough to be regarded as significant if the experimental uncertainty is taken into consideration. Thus, K_P and K_{A_1} seem to change almost proportionally. The result is not especially surprising if we keep in mind that the two equilibrium reactions to which these two constants refer must be assumed to be chemically related.

Discussion.

From the above account it seems safe to conclude that the penicillin inactivating substance studied here acts as a catalyst. The first part of the process is a reversible formation of an enzyme-penicillin complex which undergoes an irreversible decomposition and is split into a free enzyme and a biologically inactive conversion product of penicillin. This enzyme can, moreover, combine reversibly with substances other than penicillin, which are found both in the enzyme preparation and in less pure penicillin preparations. As it was shown above, the experimental results are in perfect agreement with the theoretical expectation.

Penicillinase can presumably be classified as an amidase since, according to Anglo-American investigations, the amide bond in the four ring is hydrolyzed in the penicillin molecule (The Committee on Medical Research and the Medical Research Council 1945). Several other amidases have been detected in the bacteria and it is not impossible that penicillinase is identical with one of them. Even if this is not the case, it would be natural to assume that penicillinase plays a role as an enzyme in these bacteria. It is rather improbable that strains of bacteria which have never been exposed to penicillin should contain an enzyme the only function of which is to inactivate penicillin. This other process

which is catalyzed by penicillinase in the bacteria will be inhibited in the presence of penicillin, since part of the penicillinase will be bound to penicillin and, thus, be ineffective in the other process. In this connection, we remember TURNER's et al. (1943) statement that penicillin inhibits the splitting of urea with urease which also is an amidase.

Now, it may be assumed that the inhibiting effect of penicillin on the growth of the bacteria is a blocking of an amidase necessary for the normal growth of the bacteria. If this holds, it should also be expected that the substances competitively inhibiting penicillinase detected above should have the same bacteriological effect as has penicillin. This is not the case and, therefore, the explanation of the mode of action of penicillin should possibly be searched in other fields. On the basis of the above discussion it will, however, appear appropriate in future investigations into the action of penicillin to pay special attention to the amidases of the bacteria.

Summary.

The course of reaction for the enzymatic inactivation of some penicillin G preparations is investigated as a function of penicillin- and enzyme concentration and temperature.

It is shown that the penicillinase acts as a catalyst.

The enzyme is shown to be stable during the process at 30°C and pH 6.7.

A relation is deduced for the course of the reaction as a function of the concentrations of penicillinase, penicillin, and competitively inhibiting substances, applying MICHAËLIS and MENTEN's theory.

Good agreement is prevailing between this relation and the experimental curves, if it is taken into consideration that both the less pure penicillin preparations and the enzyme preparations contain competitively inhibiting substances.

The temperature dependence is shown to be in agreement with expectations.

The expenses in connection with the experiments discussed in this paper were defrayed by Medicinalfabrikantforeningen. The penicillin employed was kindly put at my disposal by Professor K. A. Jensen (M.D.) and by Løvens kemiske Fabrik. Cand. act. Helge Brodersen was very helpful in the calculation work.

From the Department of General Pathology, University of Copenhagen.
(Professor K. A. Jensen, M. D.).

References.

Brodersen, R., Acta pathol. et microbiol. 1947a, *24*, 383.
— R., Acta chem. 1947b, *1*, 403.
Committee on Medical Research and the Medical Research Council. Nature 1945, **156**, 766.
Michaëlis, L. and Menten, M. L., Biochem. Z. 1913, **49**, 333.
Turner, J. C., Heath, F. K. and Magasanik, B., Nature 1943, **152**, 326.
Veibel, S., Ingeniøren 1942, Nr. 11. K. 9—14.
Woodruff, H. B. and Foster, J. F., J. Bact. 1945, **49**, 7.

Indleveret til Selskabet den 20. September 1947.
Færdig fra Trykkeriet den 9. Juni 1948.

DET KGL. DANSKE VIDENSKABERNES SELSKAB
MATEMATISK-FYSISKE MEDDELELSER, BIND XXIV, NR. 16

ON THE SYSTEMATIC CHANGES OF THE ECCENTRICITIES OF NEARLY PARABOLIC ORBITS

BY

ERIK SINDING

KØBENHAVN
I KOMMISSION HOS EJNAR MUNKSGAARD
1948

Printed in Denmark
Bianco Lunos Bogtrykkeri

It is well known that investigations of comets moving in nearly parabolic orbits have shown that the majority of the original orbits were certainly elliptical, and that no certain case of an originally hyperbolic orbit exists. The results of the investigations were based on calculations of planetary perturbations of the nearly parabolic orbits during the time of the passage of the comet from outer space through the inner parts of the solar system. The available material consists partly in approximate calculations by G. FAYET[1] for about 150 comets, partly in rigorous calculations carried out by a number of investigators according to the principles developed by E. STRÖMGREN[2].

In the great majority of cases the eccentricity of the original orbit is smaller than the osculating eccentricity in the part of the orbit where the comet is observed. This tendency is very marked, and clearly shown both by the rigorous and the approximate calculations. However, since FAYET's work can only be regarded as an approximation of statistical value, we shall here restrict ourselves to a consideration of the results of the rigorous calculations.

GEELMUYDEN-STRÖMGREN, *Lærebog i Astronomi*, 2. Udg., Oslo 1945, on p. 285 contains a list of 21 rigorous calculations of the eccentricities of original cometary orbits. From this list we have taken the data given below and added a column giving the value of $\Delta\left(\frac{1}{a}\right)$, i. e. original $\frac{1}{a}$ — osculating $\frac{1}{a}$ in the observable part of the orbit, a being the semi-major axis.

The osculating $\frac{1}{a}$ is the reciprocal of the value of a found by a definitive orbit determination. The original $\frac{1}{a}$-values given

[1] G. FAYET, *Recherches concernant les excentricités des comètes*, Paris 1906.
[2] E. STRÖMGREN, *Über den Ursprung der Kometen*, Copenhagen 1914.

were found through numerical calculations of the perturbations by Jupiter and Saturn (in some cases by other planets, too) which covered a period extending so far back in time that the further perturbations were negligible. The original $\frac{1}{a}$-values refer to the motion of the comet with regard to the centre of gravity of the sun, Jupiter, and Saturn.

No.	Comet	Osculating $\frac{1}{a}$	Original $\frac{1}{a}$	$\Delta\left(\frac{1}{a}\right)$
1...	1853 III	−0.0008193	+0.0000829	+0.0009022
2...	1863 VI	−0.0004949	+0.0000166	+0.0005115
3...	1882 II	+0.0118963	+0.0121488	+0.0002525
4...	1886 I	−0.0006944	−0.0000071	+0.0006873
5...	1886 II	−0.0004770	+0.0003166	+0.0007936
6...	1886 IX	−0.0005765	+0.0000630	+0.0006395
7...	1889 I	−0.0006915	+0.000042	+0.0007335
8...	1890 II	−0.0002151	+0.0000718	+0.0002869
9...	1897 I	−0.0008722	+0.0000396	+0.0009118
10...	1898 VII	−0.0006074	−0.0000157	+0.0005917
11...	1902 III	+0.0000810	+0.0000054	−0.0000756
12...	1904 I	−0.0005040	+0.0002165	+0.0007205
13...	1905 VI	−0.0001424	+0.0006210	+0.0007634
14...	1907 I	−0.0004991	+0.0000252	+0.0005243
15...	1910 I	+0.0002143	(+0.0033021)	(+0.0030878)
16...	1914 V	−0.0001465	+0.0000119	+0.0001584
17...	1922 II	−0.0003806	+0.0000038	+0.0003844
18...	1925 I	−0.0005665	+0.0000540	+0.0006205
19...	1925 VII	−0.0002730	+0.0001150	+0.0003880
20...	1932 VI	−0.0005948	+0.0000441	+0.0006389
21...	1936 I	−0.000487	+0.000205	+0.000692

It appears from the table that for 20 out of 21 comets the orbits have shifted in the elliptical direction, when going back in time, i. e. $\Delta\left(\frac{1}{a}\right)$ is positive, while there is a slight shift in the hyperbolic direction for one comet. The order of magnitude of $\Delta\left(\frac{1}{a}\right)$ is $+0.0005$. Comet 1910 I is apparently an exception. An examination of the data given for this comet,[1] however, shows that the investigation contains an error in the derivation of the

[1] K. Lous, *Die ursprüngliche Bahn des Kometen 1910 I* (A. N. **220**, 167, Kiel 1924).

elements for 1904, January 24. The correct value of $\frac{1}{a}$ is $+0.0006921$. Hence, $\Delta\left(\frac{1}{a}\right) = +0.0004778$, a result which is in good agreement with the other values of $\Delta\left(\frac{1}{a}\right)$.

The mean value of the values of $\Delta\left(\frac{1}{a}\right)$ now becomes $\Delta\left(\frac{1}{a}\right)_m = +0.000552$. Examination of the distribution of the $\Delta\left(\frac{1}{a}\right)$ around the mean value shows that this may be characterized as random, as the material is small (cf. Fig. 1).

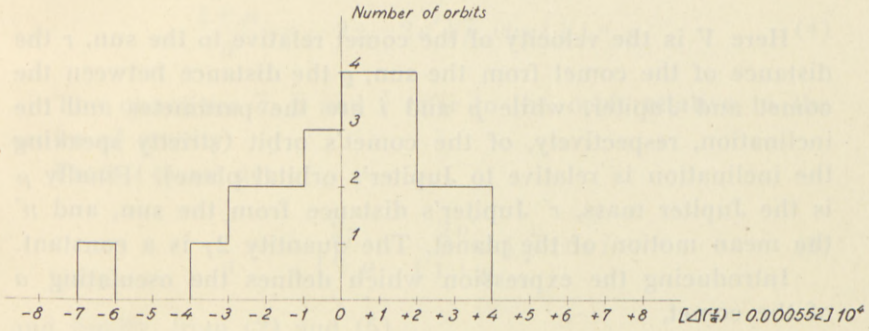

Fig. 1.

From the distribution it is found that the standard error of $\Delta\left(\frac{1}{a}\right)_m$ is ± 0.000055, thus

$$\Delta\left(\frac{1}{a}\right)_m = +0.000552 \pm 0.000055.$$

The prediction for an individual comet is

$$\Delta\left(\frac{1}{a}\right) = +0.00055 \pm 0.00025.$$

In what follows we shall attempt to show how the systematic change in the eccentricity may be understood on the basis of certain simplifying assumptions.

We consider a simplified system consisting of the sun, Jupiter and the comet. We assume that Jupiter is moving in a

circular orbit with the sun at the centre. In this case a Jacobian integral is valid for the system.

The integral in question has been derived by H. SEELIGER.[1] SEELIGER considered the motion relative to the sun (not relative to the centre of gravity of the sun and Jupiter). Putting $k = 1$ (which corresponds to the adoption of a unit of time equal to about 58 days), we find

$$V^2 = 2\gamma + \frac{2}{r} + \frac{2\mu}{\varrho} + 2n'\sqrt{p}\cos i - \frac{\mu}{r'^3}(r^2 - \varrho^2). \qquad (1)$$

Here V is the velocity of the comet relative to the sun, r the distance of the comet from the sun, ϱ the distance between the comet and Jupiter, while p and i are the parameter and the inclination, respectively, of the comet's orbit (strictly speaking the inclination is relative to Jupiter's orbital plane). Finally μ is the Jupiter mass, r' Jupiter's distance from the sun, and n' the mean motion of the planet. The quantity 2γ is a constant.

Introducing the expression which defines the osculating a of the comet,

$$V^2 = \frac{2}{r} - \frac{1}{a},$$

we get

$$\frac{1}{a} = -2\gamma - \frac{2\mu}{\varrho} - 2n'\sqrt{p}\cos i + \frac{\mu}{r'^3}(r^2 - \varrho^2). \qquad (2)$$

Usually the Jacobian integral is written in terms of the motion relative to the centre of gravity of the system. In this case we get the following equation:

$$\overline{V}^2 = \frac{2}{r} + \frac{2\mu}{\varrho} + 2n'\left(\bar{x}\frac{d\bar{y}}{dt} - \bar{y}\frac{d\bar{x}}{dt}\right) - C. \qquad (3)$$

Here $\overline{V}$ is the velocity of the comet relative to the centre of gravity, r and ϱ as before denote the distances sun—comet and Jupiter—comet, while μ and n' are the mass and the mean motion of Jupiter. The quantities $\bar{x}$ and $\bar{y}$ are the co-ordinates of the comet relative to the centre of gravity, and C is a

[1] H. SEELIGER, *Notiz über einen Tisserand'schen Satz* (A. N. 124, 209, Kiel 1890).

new constant. The latter constant is practically equal to -2γ, however, and for our purposes we may put $C = -2\gamma$.

If we consider the motion of the comet at a great distance from the sun, and using

$$\overline{V}^2 = (1+\mu)\left(\frac{2}{r} - \frac{1}{\bar{a}}\right),$$

where we have put r equal to ϱ equal to the distance of the comet from the centre of gravity, we find

$$\frac{1+\mu}{\bar{a}} = -2\gamma - 2n'\sqrt{\bar{p}}\,\cos\bar{i}\,\sqrt{1+\mu}. \tag{4}$$

The quantities $\bar{a}$, $\bar{p}$ and $\bar{i}$ refer to the orbit relative to the centre of gravity.

From (4) we get

$$\frac{1}{\bar{a}} = -\frac{2\gamma}{1+\mu} - \frac{2n'}{\sqrt{1+\mu}}\sqrt{\bar{p}}\,\cos\bar{i} \tag{5}$$

and finally, from (2) and (5),

$$\left.\begin{aligned} \Delta\left(\frac{1}{a}\right) = \frac{1}{\bar{a}} - \frac{1}{a} = \frac{2\mu}{\varrho} - \frac{\mu}{r'^3}(r^2-\varrho^2) + \\ + \frac{\mu}{1+\mu}2\gamma - \left(\frac{2n'}{\sqrt{1+\mu}}\sqrt{\bar{p}}\,\cos\bar{i} - 2n'\sqrt{p}\,\cos i\right). \end{aligned}\right\} \tag{6}$$

Here ϱ and r denote the distances from the comet to Jupiter and the sun, respectively, at the epoch of osculation of the definitive orbit in question. If we wish to study the average value of $\Delta\left(\frac{1}{a}\right)$, it is only necessary to take account of the terms in (6) which are systematic in character. This leads to

$$\Delta\left(\frac{1}{a}\right)_m = \frac{2\mu}{\varrho} - \frac{\mu}{r'^3}(r^2-\varrho^2). \tag{7}$$

Introducing an average value of ϱ equal to $r' = 5.203$, and putting $r = 1$ and $\mu = \frac{1}{1047}$, we find

$$\Delta\left(\frac{1}{a}\right)_m = +0.000544,$$

in good agreement with the value obtained from the material of rigorous calculations.

These considerations show that the phenomenon that nearly parabolic orbits change systematically in the elliptical direction when epochs further and further back in time are considered, is connected with the fact that the sun and Jupiter act as one combined mass when the comets are at a great distance from the sun, and that the influence of Jupiter dominates over that of the other planets.

In conclusion it may be noted that the above considerations of course apply also to the case of the change of a nearly parabolic orbit throughout the time interval following the perihelion passage.

Indleveret til Selskabet den 18. Juni 1947.
Færdig fra Trykkeriet den 13. April 1948.

DET KGL. DANSKE VIDENSKABERNES SELSKAB
MATEMATISK-FYSISKE MEDDELELSER, BIND XXIV, NR. 17

ON SOME APPROXIMATIVE DIRICHLET-POLYNOMIALS IN THE THEORY OF THE ZETA-FUNCTION OF RIEMANN

BY

PAUL TURÁN

KØBENHAVN
I KOMMISSION HOS EJNAR MUNKSGAARD
1948

Printed in Denmark
Bianco Lunos Bogtrykkeri

1. The zeta-function of Riemann is defined in the complex $s = \sigma + it$ plane for the half-plane $\sigma > 1$ by

$$\zeta(s) = \frac{1}{1^s} + \frac{1}{2^s} + \cdots + \frac{1}{n^s} + \cdots . \tag{1.1}$$

Here is valid also the product-representation of Euler

$$\zeta(s) = \prod_p \frac{1}{1 - \frac{1}{p^s}},$$

where p runs through the consecutive primes. From this representation it follows clearly that

$$\zeta(s) \neq 0 \qquad \text{for } \sigma > 1 . \tag{1.2}$$

As is well-known, the function $\zeta(s)$ is regular in the whole plane except at $s = 1$, where there is a pole of the first order. It is also well-known that the distribution of its roots is of fundamental importance in the theory of numbers. We know from the functional equation

$$\pi^{-\frac{s}{2}} \Gamma\left(\frac{s}{2}\right) \zeta(s) = \pi^{-\frac{1-s}{2}} \Gamma\left(\frac{1-s}{2}\right) \zeta(1-s) \tag{1.3}$$

that in the half-plane $\sigma < 0$ the only zeros are $s = -2, -4, -6, \ldots$ and that there are an infinite number of roots $\varrho = \sigma_\varrho + i t_\varrho$, the so called "non trivial roots", such that

$$0 < \sigma_\varrho < 1 . \tag{1.4}$$

The famous hypothesis of Riemann, unproved so far, states that

these all lie on the line $\sigma = \frac{1}{2}$. Using the fact obvious from the functional-equation (1.3) that they are symmetrical with respect to $s = \frac{1}{2}$ we can express the content of this hypothesis in the form that

$$\zeta(s) \neq 0 \quad \text{for} \quad \sigma > \frac{1}{2}. \tag{1.5}$$

No one has yet been able to prove even the existence of a ϑ with $\frac{1}{2} \leq \vartheta < 1$ such that

$$\zeta(s) \neq 0 \quad \text{for} \quad \sigma > \vartheta. \tag{1.6}$$

2. Next we consider the partial-sums

$$U_n(s) = \frac{1}{1^s} + \frac{1}{2^s} + \cdots + \frac{1}{n^s} \tag{2.1}$$

of the series (1.1). They obviously converge to $\zeta(s)$ for $\sigma > 1$. We ask whether these partial-sums share with $\zeta(s)$ the property of being non-vanishing in the half-plane $\sigma > 1$. We have found the somewhat striking

Theorem I. If there is an n_0 such that for $n > n_0$ the partial-sums $U_n(s)$ do not vanish in the half-plane $\sigma > 1$, then Riemann's conjecture (1.5) is true.[1)]

More generally

Theorem II. If there are positive numbers n_0 and K such that for $n > n_0$ the partial-sum $U_n(s)$ does not vanish in the half-plane

$$\sigma \geq 1 + \frac{K}{\sqrt{n}}, \tag{2.2}$$

then Riemann's hypothesis (1.5) is true.[2)]

Still more generally

Theorem III. If there are positive numbers n_0, K and ϑ satisfying

1) This elegant form of the theorem is due to Prof. B. Jessen; my original form was more awkward.

2) This theorem is due to my pupil Mr. P. Ungár who observed that the method of proof of theorem I furnishes at the same time the proof of theorem II.

$$\frac{1}{2} \leqq \vartheta < 1 \tag{2.3}$$

such that for $n > n_0$ the sum $U_n(s)$ does not vanish in the half-plane

$$\sigma \geqq 1 + \frac{K}{n^{1-\vartheta}}, \tag{2.4}$$

then $\zeta(s) \neq 0$ in the half-plane $\sigma > \vartheta$.

A further not uninteresting generalisation is given by

Theorem IV. If there are positive n_0, K, K_1 and ϑ satisfying (2.3) such that for $n > n_0$ the polynomial $U_n(s)$ omits in the half-plane (2.4) a real value c_n with[1]

$$-\frac{K_1}{n^{1-\vartheta}} \leqq c_n \leqq \frac{K_1}{n^{1-\vartheta}},$$

then $\zeta(s) \neq 0$ for $\sigma > \vartheta$.

3. All these theorems admit a further generalisation which asserts that these theorems remain true even if there is an infinity of exceptional n's provided that there are "not too many". We state explicitly only the analogue of theorem II.

Theorem V. If there is a positive K such that—denoting by $a(x)$ the number of n-values not exceeding x for which $U_n(s)$ has zeros in the half-plane $\sigma \geqq 1 + \frac{K}{\sqrt{n}}$—we have

$$\lim_{x \to \infty} \frac{a(x)}{\log x} = 0, \tag{3.1}$$

then Riemann's hypothesis (1.5) is true.

Such connection between Riemann's hypothesis and the roots of the partial-sums seems not to have been observed so far. The very interesting question whether, supposing Riemann's hypothesis to be true, we can deduce consequences on the roots of the sections, remains open.

On the basis of theorem III we have an interesting situation for the roots of the partial-sums $U_n(s)$. If Riemann's hypothesis

[1] The stronger statement that the omitted value c_n must satisfy only $|c_n| \leqq K_1 n^{\vartheta - 1}$ we cannot prove.

(1.5) is not true, or more exactly $\sup \sigma_\varrho = \Theta > \frac{1}{2}$, then there is an infinity of n's such that $U_n(s)$ vanishes in the half-plane $\sigma > 1$ and even in the half-plane $\sigma > 1 + n^{\Theta-1-\varepsilon}$, where ε is an arbitrarily small preassigned number. But if Riemann's hypothesis (1.5) is true, then, curiously, the method fails and nothing can be said about the roots of $U_n(s)$ this way.

4. What can actually be said about the roots of $U_n(s)$? According to a theorem of K. Knopp[1] every point of the line $\sigma = 1$ is a condensation-point for the zeros of $U_n(s)$. But in an interesting way this condensation happens at least for $|t| \geqq \tau_0$, where τ_0 is a sufficiently large numerical constant[2] only from the left.

More exactly we can prove

Theorem VI. There exist numerical τ_0 and K_2 such that $U_n(s)$ does not vanish for

$$\tau_0 \leqq |t| \leqq e^{K_2 \log n \log\log n}, \qquad \sigma \geqq 1, \qquad n > n_0. \tag{4.1}$$

Further $U_n(s)$ does not vanish in the half-plane

$$\sigma \geqq 1 + 2\frac{\log\log n}{\log n}, \qquad n > n_0. \tag{4.2}$$

In the estimation (4.1) of the domain of non-vanishing we could replace $\log n \log\log n$ by $\log^k n$ with a suitable $k > 1$, using estimations of Vinogradoff instead of estimations of Weyl.

The first part of theorem VI shows the indicated behaviour of the roots of $U_n(s)$; but to prove only this for all sufficiently large t we could use a more elementary reasoning. We write $U_n(s)$ in the form

$$U_n(s) = \zeta(s) - r_n(s), \qquad r_n(s) = \sum_{\nu > n} \nu^{-s}. \tag{4.3}$$

In what follows we denote by $K_3, \ldots$ positive quantities, whose dependence upon eventual parameters will be indicated explicitly; if no such dependence is mentioned they denote numerical constants. If

1) See the paper of R. Jentzsch: Untersuchungen zur Theorie der Folgen analytischer Functionen. Acta Math. 41 (1918), p. 219—251, in particular p. 236.

2) This probably also holds with $\tau_0 = 0$.

$$1 < \sigma \leqq 2, \qquad |t| \geqq 4, \tag{4.4}$$

then

$$\left|(\nu+1)^{1-s} - \nu^{1-s} - \frac{1-s}{\nu^s}\right| \leqq \left|\left(1+\frac{1}{\nu}\right)^{1-s} - 1 - \frac{1-s}{\nu}\right| < \frac{K_3 t^2}{\nu^2},$$

and summing over $\nu > n$

$$|r_n(s)| < 2\frac{n^{1-\sigma}}{|t|} + \frac{2K_3|t|}{n}.$$

This is true for any s in the domain (4.4) and obviously for $\sigma \geqq 1$, $|t| \geqq 4$; hence for $n \geqq t^2$

$$|r_n(s)| \leqq \frac{K_4}{|t|}. \tag{4.5}$$

Since for a suitable positive K_5 we have[1] for $\sigma \geqq 1$, $|t| \geqq 4$

$$\frac{1}{|\zeta(s)|} < K_5 \log|t|, \tag{4.6}$$

it follows from this, (4.5) and (4.3), that for $\sigma \geqq 1$, $|t| \geqq K_6$, $n \geqq t^2$

$$\left|U_n(s)\right| > \frac{1}{K_5 \log|t|} - \frac{K_4}{|t|} > 0. \qquad \textit{Q. e. d.}$$

We do not know so far of a single $U_n(s)$ vanishing in the half-plane $\sigma > 1$. Beyond the obvious fact that $U_n(s) \neq 0$ there for $n \leqq 3$, we know only from a remark of Prof. B. Jessen that $U_4(s)$ as well as $U_5(s)$ does not vanish in the half-plane $\sigma \geqq 1$. For the set of values of $U_4(s)$ coincides "essentially" with that of the function

$$g_4(\varphi, \psi, \sigma) = 1 + \frac{1}{2^\sigma} e^{i\varphi} + \frac{1}{3^\sigma} e^{i\psi} + \frac{1}{4^\sigma} e^{2i\varphi}$$

and

$$\Re g_4(\varphi, \psi, \sigma) = 1 + \frac{1}{2^\sigma}\cos\varphi + \frac{1}{3^\sigma}\cos\psi + \frac{1}{4^\sigma}\cos 2\varphi,$$

so that for fixed $\sigma = \sigma_0 \geqq 1$

1) T. H. Gronwall: Sur la fonction $\zeta(s)$ de Riemann au voisinage de $\sigma = 1$. Rend. Circ. Mat. di Pal. T. XXXV, 1913, p. 95—102.

$$\Re g_4(\varphi, \psi, \sigma_0) \geqq 1 - \frac{1}{3^{\sigma_0}} + \min_{\varphi} \left(\frac{1}{2^{\sigma_0}} \cos\varphi + \frac{1}{4^{\sigma_0}} \cos 2\varphi \right) =$$

$$= 1 - \frac{1}{3^{\sigma_0}} - \frac{1}{8} - \frac{1}{4^{\sigma_0}}$$

and for $\sigma \geqq 1$

$$\Re U_4(s) \geqq \frac{7}{24}.$$

Similarly we have

$$\Re U_5(s) \geqq \frac{7}{24} - \frac{1}{5} = \frac{11}{120}.$$

5. We can prove all the corresponding theorems on replacing $U_n(s)$ with the Cesaro-means[1] of the series (1.1)

$$C_n(s) = \sum_{\nu \leqq n}{}' \frac{n-\nu+1}{n+1} \cdot \nu^{-s}. \tag{5.1}$$

To see what alterations are necessary in the proofs we shall treat explicitly only

Theorem VII. If there exist positive K and n_0 so that the polynomial $C_n(s)$ does not vanish in the half-plane

$$\sigma \geqq 1 + \frac{K}{\sqrt{n}},$$

then Riemann's hypothesis (1.5) is true.

Though the numerical evidences that the polynomials $C_n(s)$ do not vanish in the half-plane $\sigma \geqq 1$ are more numerous (e. g. the non-vanishing of $C_6(s)$ in this half-plane follows quite trivially), we cannot enlarge the domain of non-vanishing (4.1) of theorem VI for the Cesaro-means. For the Riesz-means

$$R_n(s) = \sum_{\nu \leqq n}{}' \left(1 - \frac{\log \nu}{\log n}\right) \nu^{-s},$$

for which the analogous theorems would have a somewhat enhanced interest because of the fact that they converge to $\zeta(s)$ in the closed half-plane $\sigma \geqq 1$, our method fails in principle.

1) Analogous theorems hold for Cesaro-means of higher order.

6. Another interesting series for the zeta-function is

$$\frac{1}{1^s}-\frac{1}{2^s}+\frac{1}{3^s}-\cdots+\frac{(-1)^{n+1}}{n^s}+\cdots, \tag{6.1}$$

which represents in the half-plane $\sigma > 0$ the function

$$\left(1-\frac{2}{2^s}\right)\zeta(s). \tag{6.2}$$

This function vanishes in the half-plane $\sigma > 0$ at the points $s = \varrho$ as well as at

$$s = w_k = 1+\frac{2k\pi i}{\log 2} \tag{6.3}$$

$$k = \pm 1, \pm 2, \cdots.$$

Hence from the well-known theorem of Hurwitz it follows that the partial-sums

$$V_n(s) = \sum_{m\leq n}(-1)^{m+1}m^{-s} \tag{6.4}$$

have roots "near" to w_k if n is sufficiently large, and we prove that these occur infinitely often in the half-plane $\sigma > 1$. Hence the analogue of theorem I is meaningless; but the analogues of theorems II, III, IV and V are true. We shall prove only

Theorem VIII. If there exist positive n_0 and K such that for $n > n_0$ the partial-sums $V_n(s)$ do not vanish in the half-plane $\sigma \geqq 1+\frac{K}{\sqrt{n}}$, then Riemann's conjecture (1.5) is true,

and

Theorem IX. There is an infinity of values of n for which $V_n(s)$ vanishes in the half-plane $\sigma > 1$.

This will follow from the fact that those roots of $V_{2n}(s)$ which converge for a fixed k to w_k may be expressed asymptotically as

$$w_k+\frac{1}{4\log 2\cdot\zeta(w_k)}\cdot n^{-1+\frac{2k\pi i}{\log 2}}.$$

7. Returning to the partial-sums $U_n(s)$ we have mentioned the fact that every point of the line $\sigma = 1$ is a clustering point of the zeros of the polynomials $U_n(s)$. Are these all the clustering points? The answer, as we can prove easily, is affirmative. For

$$(\nu+1)^{1-s}-\nu^{1-s}-(1-s)\,\nu^{-s} = \nu^{1-s}\left(\left(1+\frac{1}{\nu}\right)^{1-s}-1-\frac{1-s}{\nu}\right) =$$

$$= \nu^{1-s}\int_0^{1/\nu}(1-s)(-s)(1+r)^{-s-1}\left(\frac{1}{\nu}-r\right)dr$$

and summing over ν

$$\left.\begin{aligned}|(n+1)^{1-s}-1-(1-s)\,U_n(s)| &\leqq |s||s-1|\sum_{1\leqq\nu\leqq n}\nu^{1-\sigma}\frac{1}{\nu^2}\max_{0\leqq y\leqq\frac{1}{\nu}}(1+y)^{-\sigma-1}\leqq\\ &\leqq |s||s-1|\sum_{\nu=1}^{\infty}\nu^{-1-\sigma}.\end{aligned}\right\}\quad(7.1)$$

If a point $s^* = \sigma^* + it^*$ in the strip $\varepsilon \leqq \sigma \leqq 1-\varepsilon\left(0<\varepsilon<\frac{1}{4}\right)$ could be an accumulation-point for the zeros of $U_n(s)$ then we have for an infinity of values of n that $U_n(s)$ vanishes in the domain

$$\frac{\varepsilon}{2}\leqq\sigma\leqq 1-\frac{\varepsilon}{2}, \qquad |t|\leqq(t^*+1). \tag{7.2}$$

But from (7.1) it follows that in the domain (7.2)

$$|(n+1)^{1-s}-1-(1-s)\,U_n(s)|\leqq\frac{4|s||s-1|}{\varepsilon}$$

$$|1-s||U_n(s)|\geqq(n+1)^{\frac{\varepsilon}{2}}-\frac{4|s||s-1|}{\varepsilon}-1>0$$

if $n > n_2 = n_2(t^*, \varepsilon)$, which is a contradiction. For the half-plane $\sigma < \varepsilon$ the proof runs similarly. Analogous statements hold for the Cesaro-means $C_n(s)$ and the Riesz-means $R_n(s)$. Similarly we can show that the complete set of accumulation points of zeros of $V_n(s)$ consists of the points of the line $\sigma = 0$, the non trivial roots ϱ of the zeta-function and the points w_k of (6.3).

8. These results suggest interesting further questions. Let there be given the series

$$a_1 e^{-\lambda_1 s} + a_2 e^{-\lambda_2 s} + \cdots + a_n e^{-\lambda_n s} + \cdots, \qquad 0 \leqq \lambda_1 < \lambda_2 < \cdots \to \infty, \quad (8.1)$$

which is convergent for $\sigma > 0$. We denote by H the clustering set of the zeros of its partial-sums. Is it always true that H consists of the zeros in $\sigma > 0$ of the function $f(s)$ defined by the series (8.1) and of the points of the line $\sigma = 0$? We can show that the set H can consist of the whole half-plane $\sigma \leqq 0$; by this we give the answer to a question raised by L. Fejér. Let $r_1, r_2, \cdots$ be the set of all positive rational numbers, arranged in such a way that every fixed one occurs infinitely often; we consider the product

$$g(s) = \prod_{\nu=1}^{\infty} \left[1 - (e^{-s-r_\nu})^{2^\nu}\right]. \quad (8.2)$$

Since the product

$$\prod_{\nu=1}^{\infty} \left[1 + e^{-2^\nu \sigma}\right]$$

is convergent for $\sigma > 0$ the product (8.2) can be expressed in the form (8.1) convergent for $\sigma > 0$. We observe that because of the rapid growth of the numbers 2^ν every partial-product is at the same time a partial-sum; hence all the numbers

$$s = -r_\nu + \frac{2\,l\pi i}{2^\nu} \qquad \begin{matrix} l = 0, \pm 1, \pm 2, \cdots \\ \nu = 1, 2, \cdots \end{matrix}$$

are roots of certain partial-sums. Since every fixed r_μ occurs infinitely often, every point of the line $\sigma = -r_\mu$ is a clustering point of such roots and so are all points of the half-plane[1] $\sigma \leqq 0$.

Somewhat more peculiar is the behaviour of the zeros of the sections of the series

$$1 + e^{-(s+10)} + e^{-2s} + e^{-3(s+10)} + \cdots + e^{-2ns} + e^{-(2n+1)(s+10)} + \cdots,$$

as P. Erdös remarked. As is easily shown, the set H consists

1) Putting $e^{-s} = z$, we obtain a power series, regular for $|z| < 1$ with the property, that the roots of the partial-sums cluster to every point in $|z| \geqq 1$.

in this case of the lines $\sigma = 0$ and $\sigma = -10$. Probably one can prescribe in the half-plane $\sigma < 0$ the cluster set H of a Dirichlet-series regular in $\sigma > 0$.

9. The theorems I—V raise the question whether the zeros of the partial-sums of a series (8.1) convergent for $\sigma > 0$ can cluster to the points of the line $\sigma = 0$ only from the left side. That this is, indeed, possible is shown for example by series of the type

$$\sum_{\nu=1}^{\infty} a_\nu e^{-\nu s}, \tag{9.1}$$

where the a_ν's are positive and tend monotonously to 0 in such a manner that the line of convergence is the line $\sigma = 0$. That all the roots of all partial-sums of the series (9.1) lie in the half-plane $\sigma < 0$, follows from the theorem of Eneström-Kakeya. If the coefficients are chosen positive and increasing, then all the roots of all partial-sums lie in the half-plane $\sigma > 0$. For the sake of completeness we mention that the function

$$_1(s) = \prod_{\nu=1}^{\infty} \left[1 - \left(e^{-s-l_\nu}\right)^{2^\nu}\right],$$

where the sequence $l_\nu \to 0$ and contains an infinite number of both positive and negative terms, has an expansion of the form (8.1) (even (9.1)) with the property, that every point of the line $\sigma = 0$ is a condensation-point of zeros from the left half-plane and at the same time a condensation-point of zeros from the right half-plane.

10. Of course a direct approach to the investigation of the roots of partial-sums or arithmetical means in the half-plane $\sigma > 1$ seems to be very difficult; the stress of this paper is laid upon the connection between these questions and Riemann's hypothesis. In any case the results raise the question how the roots of the function given by a Dirichlet-series can influence the roots of its partial-sums or suitable means. In this direction no results are known so far which hold for the means of finite index. If the function is given by a Taylor-series the situation changes. If e. g.

$$f(s) = \sum_{\nu=0}^{\infty} a_\nu s^\nu$$

is an integral function of order 1, whose roots lie in the half-plane $\sigma < 0$, then all roots of all "Jensen-means" of $f(s)$

$$J_n(f) = a_0 + a_1 s + a_2\left(1-\frac{1}{n}\right)s^2 + a_3\left(1-\frac{1}{n}\right)\left(1-\frac{2}{n}\right)s^3 + \cdots +$$

$$+ a_n\left(1-\frac{1}{n}\right)\left(1-\frac{2}{n}\right)\cdots\left(1-\frac{n-1}{n}\right)s^n$$

lie in the half-plane $\sigma \leqq 0$. The proof is very easy and runs on known lines.

I wish to thank Mrs. Helen K. Nickerson for linguistic assistance in the preparation of the manuscript.

11. Now we pass on to the proof of theorems I—IV. Obviously it is sufficient to prove theorem IV. We base the proof on an important theorem of H. Bohr[1], combining it with a classical reasoning of Landau[2]. First we recall that given a sequence

$$\lambda_1 < \lambda_2 < \cdots < \lambda_n < \cdots \to \infty, \tag{11.1}$$

we call the sequence B of linearly independent numbers

$$\beta_1, \beta_2, \ldots \tag{11.2}$$

a basis of (11.1), if

$$\lambda_n = r_{n_1}\beta_1 + r_{n_2}\beta_2 + \cdots + r_{n_{q_n}}\beta_{q_n}$$

with rational r_{n_ν}'s. If $f(s)$ is defined in the half-plane $\sigma > A$ by the absolutely convergent series

$$f(s) = \sum_{\nu=1}^{\infty} a_\nu e^{-\lambda_\nu s}, \tag{11.3}$$

1) H. Bohr, Zur Theorie der allgemeinen Dirichletschen Reihen. Math. Ann. B 79, 1919, p. 136—156. See in particular Satz. 4.

2) E. Landau: Über einen Satz von Tschebischeff. Math. Ann. 61, 1905, p. 527—550. The whole method of **14.** is due to him. He proved moreover that the integral (14.2) converges for $\sigma > \gamma$, but we do not use this fact.

Bohr calls every function

$$g(s) = \sum_{\nu=1}^{\infty} b_\nu e^{-\lambda_\nu s}$$

equivalent to $f(s)$, if for suitable $\varphi_1, \varphi_2, \cdots$ and $n = 1, 2, \cdots$

$$b_n = a_n e^{-i(r_{n_1}\varphi_1 + r_{n_2}\varphi_2 + \cdots + r_{n_{q_n}}\varphi_{q_n})} \tag{11.4}$$

Obviously $g(s)$ is also absolutely convergent for $\sigma > A$. Now the above-mentioned theorem of Bohr asserts that the sets of values assumed by $f(s)$ and $g(s)$ resp. in the half-plane $\sigma > A$ are identical.

We may apply this theorem to $f(s) = U_n(s)$ with

$$B \equiv (\log 2, \log 3, \cdots, \log p, \cdots), \quad \varphi_\nu = \pi \quad (\nu = 1, 2, \cdots). \tag{11.5}$$

If $\nu = p_1^{\alpha_1} p_2^{\alpha_2} \cdots p_r^{\alpha_r}$, then

$$\log \nu = \sum_{j=1}^{r} \alpha_j \log p_j;$$

hence

$$b_\nu = \exp\left(-i\pi \sum_{j=1}^{r} \alpha_j\right) = \lambda(\nu),$$

where, as usual, $\lambda(\nu)$ denotes Liouville's number theoretic function. Hence the set of values assumed by $U_n(s)$ in the half-plane

$$\sigma > 1 + Kn^{\vartheta-1} \tag{11.6}$$

is identical with that assumed here by the polynomial

$$W_n(s) = \sum_{\nu \leq n} \frac{\lambda(\nu)}{\nu^s}. \tag{11.7}$$

If $U_n(s)$ does not assume the value c_n in the half-plane (11.6) the same holds for $W_n(s)$. But then the function

$$W_n(s) - c_n, \tag{11.8}$$

which is real on the real axis and is positive at infinity, if $n > n_1$, where

$$K_1 n_1^{\vartheta-1} < 1, \tag{11.9}$$

is necessarily positive on the whole positive axis in the half-plane (11.6) and in particular non negative for $s = 1 + Kn^{\vartheta-1}$. This gives that if

$$n > K_7 = \max(n_0, n_1),$$

$$\sum_{\nu \leqq n}' \frac{\lambda(\nu)}{\nu^{1+Kn^{\vartheta-1}}} \geqq c_n. \tag{11.10}$$

12. Using the restrictions on c_n, we may write (11.10) for $n > K_7$ in the form

$$\sum_{\nu \leqq n}' \lambda(\nu)\, \nu^{-1-Kn^{\vartheta-1}} \geqq -K_1 n^{\vartheta-1}. \tag{12.1}$$

Since

$$\left| e^{-Kn^{\vartheta-1}\log\nu} - 1 + Kn^{\vartheta-1}\log\nu \right| < \frac{1}{2} \cdot \frac{K^2}{n^{2(1-\vartheta)}} \log^2\nu,$$

the error made in replacing the left hand member of (12.1) by

$$\sum_{\nu \leqq n}' \frac{\lambda(\nu)}{\nu} - Kn^{\vartheta-1} \sum_{\nu \leqq n}' \frac{\lambda(\nu)\log\nu}{\nu}$$

is in absolute value

$$\leqq \frac{K^2}{2n^{2(1-\vartheta)}} \sum_{\nu \leqq n}' \frac{\log^2\nu}{\nu} < \frac{K^2}{6n^{2(1-\vartheta)}} \log^3 n < \frac{K^2}{6} n^{\vartheta-1}$$

if $n > n_2 = K_8(\vartheta)$. Hence for $n > \max(K_7, K_8(\vartheta))$

$$\sum_{\nu \leqq n}' \frac{\lambda(\nu)}{\nu} > Kn^{\vartheta-1} \sum_{\nu \leqq n}' \frac{\lambda(\nu)\log\nu}{\nu} - \left(K_1 + \frac{K^2}{6}\right) n^{\vartheta-1}. \tag{12.2}$$

Now since for $\sigma > 0$

$$\sum_{\nu=1}^{\infty}{}' \frac{\lambda(\nu)\log\nu}{\nu} \cdot \frac{1}{\nu^s} = \frac{\zeta(2s+2)\,\zeta'(s+1) - 2\,\zeta(s+1)\,\zeta'(2s+2)}{\zeta(s+1)^2},$$

the usual method of complex integration shows that

$$\sum_{\nu}{}' \frac{\lambda(\nu)\log\nu}{\nu}$$

is convergent and that its sum is $-\frac{\pi^2}{6}$. Therefore for $n > K_9$ we have $\sum_{\nu \leqq n}{}' \frac{\lambda(\nu)\log\nu}{\nu} \geqq -2$ and for $n > \max(K_7, K_8(\vartheta), K_9) = K_{10}(\vartheta)$

$$L(n) \equiv \sum_{\nu \leqq n}{}' \frac{\lambda(\nu)}{\nu} > -\left(2 + K_1 + \frac{K^2}{6}\right) n^{\vartheta-1} = -K_{11}\, n^{\vartheta-1}. \quad (12.3)$$

13. The inequality (12.3) can be written in the form

$$L(n) + K_{11}\, n^{\vartheta-1} > 0 \quad (13.1)$$

for integral $n > K_{10}(\vartheta)$. Now we consider for a continuously varying $x \geqq K_{10}(\vartheta)$ the function

$$L(x) + 2K_{11}\, x^{\vartheta-1},$$

and we assert that this is positive for all $x \geqq K_{10}(\vartheta)$. We consider the x-values belonging to the interval $m \leqq x < m+1$, m an integer and $\geqq K_{10}(\vartheta)$. For $x = m$ our assertion is evident. To estimate this function for other x-values we remark that $L(x)$ being a step-function is constant for $m \leqq x < m+1$ and hence

$$\begin{aligned} L(x) + 2K_{11}\, x^{\vartheta-1} &= L(m) + K_{11}\, m^{\vartheta-1} + K_{11}\left(2x^{\vartheta-1} - m^{\vartheta-1}\right) \geqq \\ &\geqq \left(L(m) + K_{11}\, m^{\vartheta-1}\right) + K_{11}\left(2(m+1)^{\vartheta-1} - m^{\vartheta-1}\right) \geqq \\ &\geqq K_{11}(m+1)^{\vartheta-1}\left(2 - \left(1 + \frac{1}{m}\right)^{1-\vartheta}\right) \geqq 0. \end{aligned}$$

14. Now for $\sigma > 0$ we have

$$\sum_{\nu=1}^{\infty}{}' \frac{\lambda(\nu)}{\nu} \cdot \frac{1}{\nu^s} = \frac{\zeta(2s+2)}{\zeta(s+1)} = s\int_1^{\infty} \frac{L(x)}{x^{s+1}}\, dx,$$

$$s\int_0^{\infty} \frac{x^{\vartheta-1}}{x^{s+1}}\, dx = \frac{s}{s+1-\vartheta};$$

therefore for $\sigma > 0$

$$\int_1^\infty \frac{L(x) + 2K_{11} x^{\vartheta-1}}{x^{s+1}} dx = \frac{\zeta(2s+2)}{s\zeta(s+1)} + \frac{2K_{11}}{s+1-\vartheta};$$

or for $\sigma > 1$

$$\int_1^\infty \frac{L(x) + 2K_{11} x^{\vartheta-1}}{x^{s}} dx = \frac{\zeta(2s)}{(s-1)\zeta(s)} + \frac{2K_{11}}{s-\vartheta}. \qquad (14.1)$$

From **13.** it follows that the numerator of the integrand is positive for all sufficiently large x's; hence we may apply the following theorem of Landau[1]: if a function $\varphi(s)$ is defined for $\sigma > 1$ as

$$\varphi(s) = \int_1^\infty \frac{A(x)}{x^s} dx, \qquad (14.2)$$

where $A(x)$ does not change sign for $x > x_0$ and $\varphi(s)$ is regular on the real axis for $s > \gamma\ (< 1)$, then $\varphi(s)$ is regular in the entire half-plane $\sigma > \gamma$.

Hence we have only to consider the singularities of the right of (14.1) on the real axis. The first term is regular for $s > \frac{1}{2}$, the second for $s > \vartheta$, hence their sum is regular for $s > \vartheta$. Then Landau's theorem applied to (14.1) shows that the function on the right is regular in the half-plane $\sigma > \vartheta$. But then $\zeta(s)$ cannot vanish in this half-plane and theorem IV is proved.

The basis of the proof is the observation that for given arbitrarily small positive ε and η we can find $\tau_1 = \tau_1(\varepsilon, \eta)$ such that for $\sigma > 1 + \eta$ we have

$$\left| \zeta(s + i\tau_1) - \frac{\zeta(2s)}{\zeta(s)} \right| \leqq \varepsilon.$$

15. The proof of theorem V runs on the same line but instead of Landau's theorem we use the following theorem of Pólya.[2] Considering functions of type (14.2) let

1) See above p. 13, note 2.

2) G. Pólya: Über das Vorzeichen des Restgliedes im Primzahl-Satz. Gött. Nachr. 1930, p. 19—27. A special case of his theorem is given here in a slightly altered form.

$$1 = x_0 < x_1 < x_2 < \cdots < x_n < \cdots \tag{15.1}$$

be a sequence[1] which does not cluster to any finite positive value and with the property

$$(-1)^\nu A(x) \geqq 0 \qquad \text{for} \qquad x_\nu \leqq x < x_{\nu+1}. \tag{15.2}$$

The values x_ν are called sign-changing values. If $B(x)$ is defined by

$$B(\omega) = \sum_{\substack{\nu \\ x_\nu \leqq \omega}} 1 \tag{15.3}$$

he assumes that $A(x)$ has "not too many" sign-changing values, or more exactly

$$\overline{\lim_{\omega \to \infty}} \frac{B(\omega)}{\log \omega} = 0. \tag{15.4}$$

Then Pólya's theorem asserts that if Θ is the exact regularity-abscissa of $\varphi(s)$ and $\varphi(s)$ is meromorphic in a half-plane $\sigma > \Theta - b$ $(b > 0)$, then the statement of Landau's theorem holds i. e. the point $s = \Theta$ is a singular point of $\varphi(s)$. Applying this theorem to the function on the right in (14.1) we see that the condition of meromorphism is fulfilled. If we can deduce from (3.1) that the number of the sign-changing places of $L(x) + 2K_{11}x^{\vartheta-1}$ satisfies (15.4) the proof of theorem V will be completed.

We consider first the integral x-values. If n is a value sufficiently large such that $U_n(s) \neq 0$ for $\sigma \geqq 1 + \frac{K}{\sqrt{n}}$ — or briefly if n is a "good" value—the reasoning of **11.** and **12.** gives that $L(n) + K_{11}n^{\vartheta-1} > 0$. Then the reasoning of **13.** shows that for good n's

$$L(x) + 2K_{11}x^{\vartheta-1} > 0 \qquad n \leqq x < n+1. \tag{15.5}$$

If n is not a good value—or let us rather call it a "bad" value —then $L(n) + K_{11}n^{\vartheta-1}$ may be positive; and in this case (15.5) is true again. Finally if n is a bad value for which $L(n) + K_{11}n^{\vartheta-1}$ is $\leqq 0$, then since both of the functions[2]

$$L(x) + K_{11}x^{\vartheta-1}, \qquad L(x) + 2K_{11}x^{\vartheta-1}$$

1) This can consist of a finite number of terms or even of the single term x_0.
2) Using the fact that $L(x)$ is constant there, being a step-function.

are monotonously decreasing for $n \leqq x < n+1$, the second of them is either positive throughout $n \leqq x < n+1$ or negative throughout or finally positive for $x = n$ and decreasingly negative for $x \to (n+1)$ from the left. Hence the number of sign-changes $\leqq \omega$ for $L(x) + 2K_{11}x^{\vartheta-1}$ cannot surpass three times the number of bad n's $\leqq \omega$; but then using (3.1) we see that Pólya's further condition (15.4) is fulfilled, indeed.

We can easily show that if Riemann's hypothesis (1.5) is not true, then the partial-sums $U_n(s)$ vanish infinitely often in the half-plane $\sigma > 1$ or more generally for every positive ε and for an infinity of n's $U_n(s)$ vanishes in the half-plane

$$\sigma > 1 + \frac{1}{n^{1-\Theta+\varepsilon}},$$

where $\sup \sigma_\varrho = \Theta > \frac{1}{2}$. For if we have an ε_1 with $\Theta - \varepsilon_1 > \frac{1}{2}$ such that $U_n(s) \neq 0$ in the half-plane

$$\sigma > 1 + \frac{1}{n^{1-\Theta+\varepsilon_1}}$$

for all sufficiently large n, then from theorem III we could conclude that $\zeta(s) \neq 0$ in the half-plane $\sigma > \Theta - \varepsilon_1$, a contradiction. This reasoning fails completely if $\Theta = \frac{1}{2}$; the identity (14.1) valid for $\sigma > 1$

$$\int_1^\infty \frac{L(x) + 2K_{11}x^{-\frac{1}{2}}}{x^s}\,dx = \frac{(2s-1)\zeta(2s)}{2(s-1)\zeta(s)} \cdot \frac{1}{s-\frac{1}{2}} + \frac{2K_{11}}{s-\frac{1}{2}},$$

whose right-side is continuable over the whole plane and behaves asymptotically[1] if $s \to \frac{1}{2} + 0$ as

$$\frac{1}{s-\frac{1}{2}}\left(2K_{11} - \frac{1}{\zeta\left(\frac{1}{2}\right)}\right) = \left(2K_{11} + \frac{1}{\left|\zeta\left(\frac{1}{2}\right)\right|}\right)\frac{1}{s-\frac{1}{2}},$$

shows that the point $s = \frac{1}{2}$ is certainly a singular point.

1) We use the fact—which plays here a decisive role—that $\zeta\left(\frac{1}{2}\right)$ is negative.

16. Now we turn to the proof of theorem VI. The second part is only mentioned for the sake of completeness; for in the half-plane

$$\sigma \geqq 1+2\frac{\log\log n}{\log n}$$

$$|U_n(s)| = |\zeta(s)-r_n(s)| \geqq |\zeta(s)|-|r_n(s)| \geqq \prod \frac{1}{1+\frac{1}{p^\sigma}} -$$

$$-\sum_{\nu>n}\nu^{-\sigma} = \frac{\zeta(2\sigma)}{\zeta(\sigma)} - \frac{n^{1-\sigma}}{\sigma-1} > K_{12}\cdot(\sigma-1) - \frac{1}{(\sigma-1)\log^2 n} >$$

$$> \frac{K_{12}}{(\sigma-1)\log^2 n}\left(4(\log\log n)^2 - \frac{1}{K_{12}}\right) > 0$$

for $n > n_0$.

For the proof of (4.1) we use an inequality of Weyl[1] according to which for $\sigma > 0, r$ an integer, $t > 3$, $N \leqq N' < 2N$ we have

$$\left|\sum_{\nu=N}^{N'} \frac{1}{(\nu+1)^s}\right| < 2^{17}\log^{2^{1-r}} t \cdot$$

$$\cdot\left\{N^{1-2^{1-r}-\sigma} t^{\frac{1}{(r+1)2^{r-1}}} + N^{1-\sigma} t^{-\frac{1}{(r+1)2^{r-1}}} \log^{\frac{r-1}{2^{r-1}}} N\right\}.$$

For $\sigma \geqq 1$ we have

$$\left.\begin{aligned}\left|\sum_{\nu=N}^{N'} \frac{1}{(\nu+1)^s}\right| &< 2^{17}\log^{2^{1-r}} t \cdot \\ \cdot\left\{N^{-2^{1-r}} t^{\frac{1}{(r+1)2^{r-1}}} + t^{-\frac{1}{(r+1)2^{r-1}}} \log^{\frac{r-1}{2^{r-1}}} N\right\}&.\end{aligned}\right\} \quad (16.1)$$

To estimate $r_n(s)$ for $\sigma > 1$ and $n > t^2$ we start from

$$\left|(\nu+1)^{1-s} - \nu^{1-s} - \frac{1-s}{\nu^s}\right| < \frac{K_3 t^2}{\nu^2}, \qquad t \geqq 4;$$

1) See Landau: Vorl. über Zahlenth. II. Theorem 389.

summing over ν

$$|r_n(s)| = \left|\sum_{\nu>n}{}' \nu^{-s}\right| \leqq \frac{K_4}{t}. \tag{16.2}$$

Obviously the same estimation holds for $\sigma \geqq 1$ as we have seen in (4.5).

For $\sqrt{t} \leqq n \leqq t^2$ we have

$$|r_n(s)| < \left|\sum_{n<\nu\leqq t^2}{}' \nu^{-s}\right| + \frac{K_4}{t} \equiv |S_1| + \frac{K_4}{t}. \tag{16.3}$$

To estimate $|S_1|$ we split it into $O(\log t)$ sums of the form (16.1); applying (16.1) to each of them with

$$r = 2, \qquad \sqrt{t} \leqq N \leqq t^2,$$

we obtain that for $t > K_{13}$ each such sum is in absolute value

$$< K_{14}\sqrt{\log t}\left\{t^{-\frac{1}{12}} + t^{-\frac{1}{6}}\sqrt{\log t}\right\} < \frac{K_{15}}{\log^3 t},$$

i. e. $|S_1| < \frac{K_{16}}{\log^2 t}$, and from (16.3) for $t > K_{13}$ we have

$$|r_n(s)| < \frac{K_{17}}{\log^2 t}. \tag{16.4}$$

As appears from (16.2) and (16.4) this estimation is valid for all $n \geqq \sqrt{t}$.

Now we suppose only

$$n > t^{\frac{1}{\log\log t}}. \tag{16.5}$$

Then using (16.4) we have

$$\left.\begin{aligned} |r_n(s)| \leqq \left|\sum_{n<\nu\leqq\sqrt{t}}{}' \nu^{-s}\right| + \left|\sum_{\nu>\sqrt{t}}{}' \nu^{-s}\right| < \frac{K_{17}}{\log^2 t} + \left|\sum_{n<\nu\leqq\sqrt{t}}{}' \nu^{-s}\right| = \\ = \frac{K_{17}}{\log^2 t} + |S_2|. \end{aligned}\right\} \tag{16.6}$$

Because of (16.5) we can split S_2 into $O(\log\log t)$ sums of the form

$$S_2^{(k)} = \sum_{t^{\frac{2}{k+2}} < \nu \leqq t^{\frac{2}{k+1}}} \nu^{-s}, \qquad 3 \leqq k \leqq 2\log\log t. \tag{16.7}$$

$S_2^{(k)}$ can be split into $O(\log t)$ sums of the form (16.1); applying (16.1) to them with

$$r = k, \qquad t^{\frac{2}{k+2}} \leqq N \leqq t^{\frac{2}{k+1}}$$

we obtain that they are in absolute value

$$< K_{18}\log^{2^{1-k}} t \left\{ t^{-\frac{2}{k+2}\cdot\frac{1}{2^{k-1}} + \frac{1}{(k+1)2^{k-1}}} + t^{-\frac{1}{(k+1)2^{k-2}}} \log^{\frac{k-1}{2^{k-1}}} t \right\} < K_{19}\log^{-4} t,$$

and hence

$$|S_2| < \frac{K_{19}}{\log^2 t}.$$

Thus for $t > K_{20}$, $n > t^{\frac{1}{\log\log t}}$, $\sigma \geqq 1$

$$|r_n(s)| < \frac{K_{20}}{\log^2 t}. \tag{16.8}$$

The inequality $n > t^{\frac{1}{\log\log t}}$ can obviously be written in the form

$$|t| \leqq e^{K_{21}\log n \log\log n}.$$

Finally using Gronwall's inequality (4.6) we obtain for $\sigma \geqq 1$, $t > K_{22}$

$$|U_n(s)| \geqq |\zeta(s)| - |r_n(s)| > \frac{1}{K_5\log t} - \frac{K_{20}}{\log^2 t} > 0. \qquad \textit{Q. e. d.}$$

17. Next we sketch the proof of theorem VII. A reasoning similar to that of **11.** shows that from our hypothesis it follows that for $n > K_{23}$

$$\sum_{\nu=1}^{n}{}^{\urcorner}(n-\nu+1)\frac{\lambda(\nu)}{\nu^{1+Kn^{-\frac{1}{2}}}} \geqq 0,$$

and by an argument similar to that of **12.** we obtain for these n's

$$C(n) \equiv \sum_{\nu \leqq n}{}^{\urcorner}(n-\nu+1)\frac{\lambda(\nu)}{\nu} \geqq -K_{24}\sqrt{n}$$

and

$$C(x)+2K_{24}\sqrt{x} \geqq 0 \qquad \text{for } x > K_{25}. \tag{17.1}$$

Next we have to find the analogue of formula (14.1). Generally if for $\sigma > 0$

$$f(s) = \sum_{\nu=1}^{\infty}{}^{\urcorner}\frac{d_\nu}{\nu^s}, \qquad \sum_{\nu \leqq n}{}^{\urcorner} d_\nu = D_n,$$

$$\sum_{n \leqq m}{}^{\urcorner} D_n = \sum_{\nu \leqq m}{}^{\urcorner}(m-\nu+1)\,d_\nu = S_m,$$

then

$$\left.\begin{aligned}
f(s) &= \sum_{\nu=1}^{\infty}{}^{\urcorner} D_\nu\left(\nu^{-s}-(\nu+1)^{-s}\right) = \\
&= \sum_{\nu=1}^{\infty}{}^{\urcorner} S_\nu\left(\nu^{-s}-2(\nu+1)^{-s}+(\nu+2)^{-s}\right) = \\
&= \sum_{\nu=1}^{\infty}{}^{\urcorner} S_\nu\left\{ s\int_{\nu}^{\nu+1} x^{-s-1}\,dx - s\int_{\nu+1}^{\nu+2} x^{-s-1}\,dx \right\} = \\
&= s\sum_{\nu=1}^{\infty}{}^{\urcorner} S_\nu \int_{\nu}^{\nu+1}\left(x^{-s-1}-(x+1)^{-s-1}\right)dx = \\
&= s\int_{1}^{\infty} S(x)\left(x^{-s-1}-(x+1)^{-s-1}\right)dx = \\
&= s(s+1)\int_{1}^{\infty} S(x)\left(\int_{0}^{1}(x+y)^{-s-2}\,dy\right)dx.
\end{aligned}\right\} \tag{17.2}$$

Hence for $\sigma > 0$

$$\frac{\zeta(2s+2)}{\zeta(s+1)} = s(s+1)\int_1^\infty C(x)\left(\int_0^1 (x+y)^{-s-2}\,dy\right)dx. \qquad (17.3)$$

Let

$$J \equiv s(s+1)\int_1^\infty \sqrt{x}\left(\int_0^1 (x+y)^{-s-2}\,dy\right)dx =$$

$$= s(s+1)\int_1^\infty x^{-s-\frac{3}{2}}\left(\int_0^1 \left(1+\frac{y}{x}\right)^{-s-2} dy\right)dx.$$

But then

$$\frac{J - \dfrac{s(s+1)}{s+\dfrac{1}{2}}}{s(s+1)(s+2)} = \frac{J - s(s+1)\displaystyle\int_1^\infty x^{-s-\frac{3}{2}}\,dx}{s(s+1)(s+2)} =$$

$$= -\int_1^\infty x^{-s-\frac{3}{2}}\int_0^1 dy\left(\int_1^{1+\frac{y}{x}} \zeta^{-s-3}\,d\zeta\right)dx,$$

and since for $\sigma > -\dfrac{3}{2}$ the last expression is in absolute value

$$< \frac{1}{2}\int_1^\infty x^{-\sigma-\frac{5}{2}}\,dx$$

it represents a function $\vartheta(s)$ regular and bounded in every half-plane $\sigma \geqq -\dfrac{3}{2} + \varepsilon$. Hence for $\sigma > 0$

$$\left.\begin{aligned} s(s+1)\int_1^\infty \sqrt{x}\left(\int_0^1 (x+y)^{-s-2}\,dy\right)dx \;&= \\ = \frac{s(s+1)}{s+\frac{1}{2}} + s(s+1)(s+2)\,\vartheta(s)& \end{aligned}\right\} \qquad (17.4)$$

and from (17.3) and (17.4)

$$s(s+1)\int_1^\infty \left(C(x)+2K_{24}\sqrt{x}\right)\left(\int_0^1 (x+y)^{-s-2}\,dy\right)dx =$$

$$= \frac{\zeta(2s+2)}{\zeta(s+1)} + 2K_{24}\frac{s(s+1)}{s+\frac{1}{2}} + 2K_{24}s(s+1)(s+2)\vartheta(s),$$

or for $\sigma > 1$

$$\left.\begin{aligned} &\int_1^\infty \left(C(x)+2K_{24}\sqrt{x}\right)\left(\int_0^1 (x+y)^{-s-1}\,dy\right)dx = \\ &= \frac{\zeta(2s)}{(s-1)\zeta(s)}\cdot\frac{1}{s} + \frac{2K_{24}}{s-\frac{1}{2}} + 2K_{24}(s+1)\vartheta(s-1). \end{aligned}\right\} \quad (17.5)$$

This is the required analogue of (17.1). Now Landau's theorem cannot be applied directly; but we can apply his method. Suppose we have proved the following Lemma. If

$$\varphi_1(s) = \int_1^\infty E(x)\left(\int_0^1 (x+y)^{-s-1}\,dy\right)dx \quad (17.6)$$

is convergent in the half-plane $\sigma > 1$ with $E(x)$ non negative for all sufficiently large x and is regular on the real axis for $s > \gamma\ (< 1)$, then $\varphi_1(s)$ is also regular in the whole half-plane $\sigma > \gamma$.

Then (17.1) and the representation (17.5) give that the requirements of the lemma are satisfied with $\gamma = \frac{1}{2}$; hence $(s-1)\zeta(s) \neq 0$ in the half-plane $\sigma > \frac{1}{2}$ and theorem VII is proved.

Now we prove the lemma following Landau's paradigma; we prove more, viz. that the representation (17.6) is convergent for $\sigma > \gamma$. Suppose the representation were convergent on the real axis only for $s > \delta$ where $\gamma < \delta \leqq 1$. Then $\varphi_1(s)$ is obviously absolutely convergent in the half-plane $\sigma > \delta$ and regular here. Hence the Taylor-expansion around $s_1 = 2$ is convergent at least in the circle $|s - s_1| < 2 - \delta$; since according to our hypothesis $\varphi_1(s)$ is also regular for $s = \delta$ the radius of the circle of convergence is greater than $2 - \delta$ and hence there is a $\delta_1 < \delta$ such that the Taylor-series is convergent at $s = \delta_1$. But this Taylor-series is

$$\varphi_1(\delta_1) = \sum_{\nu=0}^{\infty}{}' \frac{(-\delta_1+2)^\nu}{\nu!} \int_1^\infty E(x) \left(\int_0^1 (x+y)^{-3} \log^\nu (x+y)\, dy \right) dx;$$

since the integrand and all terms are positive we can interchange the summation and integration and hence

$$\varphi_1(\delta_1) = \int_1^\infty E(x) \left(\int_0^1 (x+y)^{-\delta_1-1}\, dy \right) dx,$$

i. e. the integral is convergent for $s = \delta_1 < \delta$, a contradiction. Hence the lemma is proved and the proof of theorem VII is completed.

18. Now we sketch the proof of theorem VIII. The arguments of **11.** and **12.** show that for $n > K_{25}$

$$\sum_{\nu \leqq n}{}' (-1)^{\nu+1} \lambda(\nu)\, \nu^{-1-Kn^{-\frac{1}{2}}} \geqq 0;$$

for these n's

$$L_1(n) \equiv \sum_{\nu \leqq n}{}' (-1)^{\nu+1} \frac{\lambda(\nu)}{\nu} > -K_{26}\, n^{-\frac{1}{2}}$$

and for $x > K_{27}$

$$L_1(x) + 2\, K_{26}\, x^{-\frac{1}{2}} > 0. \tag{18.1}$$

Next we must find the generating functions of $\sum{}' (-1)^{\nu+1} \frac{\lambda(\nu)}{\nu^s}$.

We assert that for $\sigma > 1$

$$g(s) = \sum_{\nu=1}^{\infty}{}' (-1)^{\nu+1} \frac{\lambda(\nu)}{\nu^s} = \left(1 + \frac{2}{2^s}\right) \frac{\zeta(2s)}{\zeta(s)}. \tag{18.2}$$

For

$$g(s) = 2 \sum_{\nu \text{ odd}}{}' \frac{\lambda(\nu)}{\nu^s} - \sum_{\nu=1}^{\infty}{}' \frac{\lambda(\nu)}{\nu^s} = 2 \prod_{p>2} \frac{1}{1+\frac{1}{p^s}} - \frac{\zeta(2s)}{\zeta(s)} =$$

$$= \left\{ 2\left(1 + \frac{1}{2^s}\right) - 1 \right\} \frac{\zeta(2s)}{\zeta(s)} = \left(1 + \frac{2}{2^s}\right) \frac{\zeta(2s)}{\zeta(s)}.$$

Hence for $\sigma > 0$

$$s\int_1^\infty \frac{L_1(x)}{x^{s+1}}\,dx = \left(1+\frac{2}{2^{s+1}}\right)\frac{\zeta(2s+2)}{\zeta(s+1)}$$

$$\int_1^\infty \frac{L_1(x)+2K_{26}x^{-\frac{1}{2}}}{x^{s+1}}\,dx = \left(1+\frac{2}{2^{s+1}}\right)\frac{\zeta(2s+2)}{s\zeta(s+1)}+\frac{2K_{26}}{s+\frac{1}{2}},$$

or for $\sigma > 1$

$$\int_1^\infty \frac{L_1(x)+2K_{26}x^{-\frac{1}{2}}}{x^{s}}\,dx = \left(1+\frac{2}{2^{s}}\right)\frac{\zeta(2s)}{(s-1)\zeta(s)}+\frac{2K_{26}}{s-\frac{1}{2}}.$$

Now the remainder of the proof is similar to that of theorem IV.

19. Finally we show that for an infinity of n's the partial-sums[1]

$$V_{2n}(s) = \sum_{\nu\leqq 2n}{}^{7}(-1)^{\nu+1}\nu^{-s}$$

vanish in the half-plane $\sigma > 1$. For this purpose we consider the values $V_{2n}(w_k)$, k fixed and $w_k = 1+\frac{2k\pi i}{\log 2} \equiv 1+iv_k$.

20. First we show that

$$\left|V_{2n}(w_k)+\frac{1}{4}(n+1)^{-1+iv_k}\right| < \frac{(2+|v_k|)^2}{n^2}. \qquad (20.1)$$

Starting from the identity

$$\left(1-\frac{2}{2^s}\right)U_n(s) = V_{2n}(s)-2^{1-s}\left(\frac{1}{(n+1)^s}+\cdots+\frac{1}{(2n)^s}\right)$$

we obtain, on setting $s = w_k$,

$$V_{2n}(w_k) = \frac{1}{(n+1)^{w_k}}+\frac{1}{(n+2)^{w_k}}+\cdots+\frac{1}{(2n)^{w_k}}. \qquad (20.2)$$

1) The restriction to even indices is only for the sake of convenience.

Now we have

$$\left(1+\frac{1}{\nu}\right)^{iv_k}-1-\binom{iv_k}{1}\frac{1}{\nu}-\binom{iv_k}{2}\frac{1}{\nu^2}=3\binom{iv_k}{3}\int_0^{1/\nu}\left(\frac{1}{\nu}-y\right)^2(1+y)^{iv_k-3}\,dy;$$

hence

$$\left|(\nu+1)^{iv_k}-\nu^{ia_k}-\binom{iv_k}{1}\nu^{-1+iv_k}-\binom{iv_k}{2}\nu^{-2+iv_k}\right|<|v_k|\frac{(2+|v_k|)^2}{6}\cdot\frac{1}{\nu^3}.$$

Putting $\nu=(n+1),(n+2),\cdots 2n$ and summing we obtain

$$\left.\begin{aligned}\left|(2n+1)^{iv_k}-(n+1)^{iv_k}-\binom{iv_k}{1}\sum_{\nu=n+1}^{2n}\nu^{-1+iv_k}-\binom{iv_k}{2}\sum_{\nu=n+1}^{2n}\nu^{-2+iv_k}\right|<\\ <|v_k|\frac{(2+|v_k|)^2}{12}\cdot\frac{1}{n^2}.\end{aligned}\right\}\quad(20.3)$$

The first two bracketed terms can be written in the form

$$\left.\begin{aligned}&\left((2n+1)^{iv_k}-(2n+2)^{iv_k}\right)+\left((2n+2)^{iv_k}-(n+1)^{iv_k}\right)=\\ &=-(2n+1)^{iv_k}\left(\left(1+\frac{1}{2n+1}\right)^{iv_k}-1\right)+(n+1)^{iv_k}\left(2^{iv_k}-1\right)=\\ &=-(2n+1)^{iv_k}\left(\left(1+\frac{1}{2n+1}\right)^{iv_k}-1\right);\end{aligned}\right\}\quad(20.4)$$

hence from (20.2), (20.3) and (20.4)

$$\left.\begin{aligned}\left|-(2n+1)^{iv_k}\left(\left(1+\frac{1}{2n+1}\right)^{iv_k}-1\right)-iv_k\,V_{2n}(w_k)-\binom{iv_k}{2}\sum_{\nu=n+1}^{2n}\nu^{-2+iv_k}\right|<\\ <|v_k|\frac{(2+|v_k|)^2}{12}\cdot\frac{1}{n^2}.\end{aligned}\right\}\quad(20.5)$$

Now

$$\left(1+\frac{1}{2n+1}\right)^{iv_k}-1-\frac{iv_k}{2n+1}=\int_0^{\frac{1}{2n+1}}\left(\frac{1}{2n+1}-y\right)(1+y)^{iv_k-2}\,dy\,(iv_k)\,(iv_k-1),$$

$$\left|\left(1+\frac{1}{2n+1}\right)^{iv_k}-1-\frac{iv_k}{2n+1}\right|<\frac{1}{2}\frac{|v_k|(1+|v_k|)}{(2n+1)^2};$$

hence from (20.5)

$$\left|-iv_k(2n+1)^{-1+iv_k}-iv_k V_{2n}(w_k)-\binom{iv_k}{2}\sum_{\nu=n+1}^{2n}{}'\nu^{-2+iv_k}\right|<$$

$$<|v_k|\frac{(2+|v_k|)^2}{12}\cdot\frac{1}{n^2}+\frac{1}{8}\frac{|v_k|(1+|v_k|)}{n^2}<\frac{|v_k|(2+|v_k|)^2}{4}\cdot\frac{1}{n^2}$$

or

$$\left|V_{2n}(w_k)+(2n+1)^{-1+iv_k}-\frac{1-iv_k}{2}\sum_{\nu=n+1}^{2n}{}'\nu^{-2+iv_k}\right|<\frac{(2+|v_k|)^2}{4}\cdot\frac{1}{n^2}. \quad (20.6)$$

Further

$$\left(1+\frac{1}{\nu}\right)^{-1+iv_k}-1-(-1+iv_k)\frac{1}{\nu}=$$

$$=\int_0^{1/\nu}\left(\frac{1}{\nu}-y\right)(1+y)^{-3+iv_k}dy\,(-1+iv_k)(-2+iv_k)$$

$$\left|(\nu+1)^{-1+iv_k}-\nu^{-1+iv_k}+(1-iv_k)\nu^{-2+iv_k}\right|<\frac{1}{\nu^3}\cdot\frac{1}{2}(2+|v_k|)^2;$$

a summation over $\nu=(n+1),\cdots,2n$ gives

$$\left|-\frac{(2n+1)^{-1+iv_k}}{2}+\frac{(n+1)^{-1+iv_k}}{2}-\frac{1-iv_k}{2}\sum_{\nu=n+1}^{2n}{}'\nu^{-2+iv_k}\right|<\frac{(2+|v_k|)^2}{4}\cdot\frac{1}{n^2}.$$

Putting this into (20.6) we obtain

$$\left|V_{2n}(w_k)+\left(\frac{3}{2}(2n+1)^{-1+iv_k}-\frac{1}{2}(n+1)^{-1+iv_k}\right)\right|<\frac{1}{2}\frac{(2+|v_k|)^2}{n^2}. \quad (20.7)$$

If we use the transformation (20.4) again the sum of the two bracketed terms is

$$\left.\begin{aligned}&\frac{3}{2}\left((2n+1)^{-1+iv_k}-(2n+2)^{-1+iv_k}\right)+\\&+\left(\frac{3}{2}\cdot 2^{-1+iv_k}-\frac{1}{2}\right)(n+1)^{-1+iv_k}=\frac{1}{4}(n+1)^{-1+iv_k}-\\&-\frac{3}{2}(2n+1)^{-1+iv_k}\left(\left(1+\frac{1}{2n+1}\right)^{-1+iv_k}-1\right).\end{aligned}\right\}\quad(20.8)$$

Since the second term of the right-hand member of (20.8) is in absolute value

$$<\frac{3}{2}\cdot\frac{1}{2n+1}(1+|v_k|)\frac{1}{2n+1}<\frac{3}{8}\frac{(2+|v_k|)^2}{n^2}$$

we obtain from (20.7) and (20.8)

$$\left|V_{2n}(w_k)+\frac{1}{4}(n+1)^{-1+iv_k}\right|<\frac{(2+|v_k|)^2}{n^2},\qquad(20.9)$$

i. e. (20.1) is proved.

Now we consider $V'_{2n}(w_k)$. Obviously

$$V'_{2n}(w_k)=\left(\left(1-\frac{2}{2^s}\right)\zeta(s)\right)'_{s=w_k}+\sum_{\nu>2n}'\frac{(-1)^{\nu+1}\log\nu}{\nu^{w_k}}.\qquad(21.1)$$

The first term is obviously

$$\log 2\cdot\zeta(w_k).\qquad(21.2)$$

To estimate the second term of (21.1) we observe that

$$\left|\frac{\log(2l+1)}{(2l+1)^{w_k}}-\frac{\log(2l+2)}{(2l+2)^{w_k}}\right|\leq\frac{1}{2l+1}\log\frac{2l+2}{1l+1}+$$

$$+\log(2l+2)\left|(2l+1)^{-w_k}-(2l+2)^{-w_k}\right|<\frac{(2+|v_k|)\log(2l+2)}{(2l+1)^2};$$

hence for $n>10$ the second term of (21.1) is in absolute value

$$<(2+|v_k|)\sum_{\nu>n}'\frac{\log(2\nu+2)}{(2\nu+1)^2}<(2+|v_k|)\frac{\log n}{n}.$$

From this (21.2) and (21.1) we obtain

$$|V'_{2n}(w_k) - \log 2 \cdot \zeta(w_k)| < (2 + |w_k|) \frac{\log n}{n}. \tag{21.3}$$

Now we consider the expression

$$F_{2n}(s) = V_{2n}(w_k) + V'_{2n}(w_k)(s - w_k), \tag{21.4}$$

which is linear and has its zero at

$$w'_{kn} = w_k - \frac{V_{2n}(w_k)}{V'_{2n}(w_k)};$$

using (20.1) and (21.3) we get

$$w'_{kn} = w_k + \frac{1}{4 \log 2 \cdot \zeta(w_k)} (n+1)^{-1+iv_k} + \Theta_3 K_{27}(k) \frac{\log n}{n^2}. \tag{21.5}$$

$$|\Theta_3| \leqq 1.$$

22. We show that for fixed k and $n \to \infty$

$$w^*_{kn} = w_k + \frac{1}{4 \log 2 \cdot \zeta(w_k)} (n+1)^{-1+iv_k} \tag{22.1}$$

is the asymptotical expression of that root of $V_{2n}(s)$ which $\to w_k$ if $n \to \infty$. To show this we consider the circle

$$|s - w'_{kn}| = K_{27}(k) \frac{\log^2 n}{n^2}; \tag{22.2}$$

(21.5) and (22.1) show that w^*_{kn} lies in this circle. We have

$$V_{2n}(s) = F_{2n}(s) + \sum_{j=2}^{\infty} \frac{1}{j!} V^{(j)}_{2n}(w_k)(s - w_k)^j. \tag{22.3}$$

For $F_{2n}(s)$ we have identically

$$F_{2n}(s) = V'_{2n}(w_k)(s - w'_{kn}),$$

so that on the whole circumference of the circle (22.2), if n is sufficiently large,

$$|F_{2n}(s)| > \frac{1}{2}|\zeta(w_k)|\frac{K_{27}(k)\log^2 n}{n^2} = K_{28}(k)\frac{\log^2 n}{n^2}. \quad (22.4)$$

Since on the circle $|s-w_k| \leqq \frac{1}{2}$

$$|V_{2n}(s)| \leqq K_{29}(k)$$

independently of n we have from Cauchy's estimation of coefficients

$$\left|\frac{V_{2n}^{(j)}(w_k)}{j!}\right| < K_{29}(k)\,2^j$$

and on the circle (22.2)

$$|s-w_k| \leqq |s-w'_{kn}| + |w'_{kn}-w_k| \leqq K_{27}(k)\frac{\log^2 n}{n^2} + \\ + \frac{K_{30}(k)}{n} + K_{27}(k)\frac{\log n}{n^2} < K_{31}(k)\frac{1}{n};$$

hence on the circle (22.2) the second term of (22.3) is in absolute value

$$< \sum_{j=2}^{\infty} K_{29}(k)\left(\frac{2\,K_{31}(k)}{n}\right)^j < K_{32}(k)\frac{1}{n^2}. \quad (22.5)$$

From (22.4) and (22.3) we obtain for $n > K_{33}(k)$ on the circumference of (22.2)

$$|F_{2n}(s)| > K_{28}(k)\frac{\log^2 n}{n^2} > \frac{K_{32}(k)}{n^2} > \left|\sum_{j=2}^{\infty}\frac{1}{j!}V_{2n}^{(j)}(w_k)(s-w_k)^j\right|;$$

hence it follows from Rouché's theorem that the circle (22.2) contains as many zeros of $V_{2n}(s)$ as of $F_{2n}(s)$, i. e. exactly one. But this circle is contained in the circle

$$|s-w^*_{kn}| < |s-w'_{kn}| + |w'_{kn}-w^*_{kn}| < 2\,K_{27}\frac{\log^2 n}{n^2}. \quad (22.6)$$

23. To prove finally that for an infinity of n's the polynomials $V_{2n}(s)$ vanish in the half-plane $\sigma > 1$ we have only to observe that for fixed k

$$v_k \log(n+1) - v_k \log n \to 0.$$

Then for an infinity of n's we have

$$\Re w_{kn}^* > 1 + \frac{1}{5 \log 2 \left| \zeta w_k) \right|} \cdot \frac{1}{n+1};$$

hence from (22.6) the real part of the corresponding root of $V_{2k}(s)$ is

$$> 1 + \frac{1}{5 \log 2 \left| \zeta(w_k) \right|} \cdot \frac{1}{n+1} - \frac{2 K_{27}(k) \log^2 n}{n^2} > 1,$$

if n is sufficiently large.

We remark finally that for fixed k and $n \to \infty$ these roots in the half-plane $\sigma > 1$ lie in half-planes of the form

$$1 + \frac{K_{33}(k)}{n},$$

i. e. their location does not refute the hypothesis of theorem VIII. It would be interesting to study these roots if k is not fixed.

It is perhaps of some interest to note that for fixed k the behaviour of the corresponding roots of the Riesz-means is different. Denoting by w_{kn}'' that root of the n^{th} Riesz-mean of the series (6.1) which for $n \to \infty$ tends to w_k, we have

$$\left| w_{kn}'' - w_k + \frac{1}{\log n} \right| < \frac{K_{34}(k)}{\log^2 n}.$$

Hence these roots converge to w_k from the left in a particularly simple way. Thus there is some chance that the behaviour of the roots of the Riesz-means is more regular.

Added in proof.

24. An easy modification of the proofs gives also a more general theorem from which I mention only two special cases.

Theorem X. If for a modulus k there is a character $\chi(n)$

such that the partial-sums of the corresponding L-function of Dirichlet

$$L(s, \chi) = \sum_{n=1}^{\infty} \frac{\chi(n)}{n^s} \tag{24.1}$$

do not wanish in the half-plane $\sigma > 1$, then Riemann's hypothesis (1.5) is true.

I cannot prove that this property of the partial-sums of (24.1) implies the non-vanishing of $L(s, \chi)$ itself.

Of course theorem X admits all refinements similarly as theorems II–V refine theorem I.

The interest of theorem X compared to theorem VIII lies obviously in the fact that the function $L(s, \chi)$ has no roots on the line $\sigma = 1$, in contrast to $\left(1 - \frac{2}{2^s}\right)\zeta(s)$.

Theorem XI. If for real sequence $\beta_1, \beta_2, \ldots$ the partial-sums of the series

$$f_\beta(s) = \prod_{\nu=1}^{\infty} \frac{1}{1 - \frac{e^{i\beta_\nu}}{p_\nu^s}} = \sum_{n=1}^{\infty} \frac{d_n}{n^s} \tag{24.2}$$

do not vanish in the half-plane $\sigma > 1$, then Riemann's hypothesis (1.5) is true.

Prof. Jessen[1] proved that for "almost all" β-sequences the functions $f_\beta(s)$ do not vanish in the half-plane $\sigma > \frac{1}{2}$. To obtain an explicit $f_\beta(s)$ which has this property, we may choose according to a remark of Prof. A. Selberg

$$e^{i\beta_\nu} = (-1)^\nu,$$

where $p_1 = 2$, $p_2 = 3$, ... denote the increasingly ordered sequence of primes.

Theorem XI admits the same refinements as theorem X.

25. We proved implicitly that if the partial-sums

1) B. Jessen: Some analytical problems relating to probability. Journ. of Math. and Physics. Mass. Inst. Techn. vol. XIV (1935), p. 24—27.

$$L(n) = \sum_{\nu \leq n} \frac{\lambda(\nu)}{\nu} \tag{25.1}$$

are of one sign for all sufficiently large n's or are for these n's

$$> -K_{11}\, n^{\vartheta - 1}, \tag{25.2}$$

then the hypothesis (1.6) is true. Pólya[1] remarked, that if

$$L_1(n) = \sum_{\nu \leq n} \lambda(\nu) \tag{25.3}$$

is non-positive for all sufficiently large n's, then Riemann's hypothesis (1.5) is true; with the same reasoning he could prove that from the inequality

$$L_1(n) < K_{35}\, n^{\vartheta}, \tag{25.4}$$

valid for all sufficiently large n's, the conjecture (1.6) follows. It seems to me that the condition (25.2) is somewhat less deep than (25.4), i. e. one can deduce (25.2) from (25.4). If we replace, however, (25.2) and (25.4) by twosided inequalities, the corresponding statement follows by partial summation.

Pólya showed by computation the validity of (25.3) for $2 \leq n \leq 1500$; this has been extended by H. Gupta[2] up to 20,000. The young danish mathematicians Erik Eilertsen, Poul Kristensen, Aage Petersen, Niels Ove Roy Poulsen, and Aage Winther calculated the values of $L(n)$ for $n \leq 1000$. They found all of them to be positive; for $L(1000)$ they found the value

$$L(1000) = 0{,}028970560\,.$$

It is remarkable that in this range the minimal value is attained at $n = 293$ and that

$$L(293) = 0{,}005102273,$$

a much smaller value than $L(1000)$.

1) G. Pólya: Verschiedene Bemerkungen zur Zahlentheorie. Jahresb. der deutsch. Math. Ver. 28 (1919), p. 31—40.

2) H. Gupta: On a table of values of $L_1(n)$. Proc. Indian Acad. Sci. Sect. A. vol. 12 (1940), p. 407—409.

26. I conclude with two remarks. As Paul Erdös remarked, he can prove that to any given closed set H in the domain $|z| \geq 1$ which contains the circumference of the unit-circle one can give a power-series, convergent in $|z| < 1$, such that the roots of its partial-sums cluster in $|z| \geq 1$ to the points of H and only to those.

As Prof. Sherwood Sherman remarked, my statement on p. 13 about the Jensen-means is true only if we suppose in addition of the roots of the function $f(s)$, that the sum of their reciprocal values is convergent.

Indleveret til Selskabet den 31. Oktober 1947.
Færdig fra Trykkeriet den 9. September 1948.

DET KGL. DANSKE VIDENSKABERNES SELSKAB
MATEMATISK-FYSISKE MEDDELELSER, BIND XXIV, NR. 18

THE MOTION OF COMET OLBERS 1815–1956

BY

HANS Q. RASMUSEN

KØBENHAVN
I KOMMISSION HOS EJNAR MUNKSGAARD
1948

Printed in Denmark
Bianco Lunos Bogtrykkeri

Periodic Comet Olbers belongs to a group which comprises in addition the comets Westphal, Brorsen II-Metcalf, Pons-Brooks, and Halley. It was discovered 1815 March 6 by Olbers, then a doctor and amateur astronomer in Bremen. The comet was visible in telescopes during a period of 29 weeks, and was observed 346 times, the last observation being by Gauss with a 10-foot telescope of the Göttingen Observatory on August 25. After that day the comet disappeared in the twilight of the evening sky. The closest approach to the earth occured on May 26, the smallest distance being 1.37 astronomical units. Bessel in his paper[1] states that the comet was at that time just visible to the naked eye, so that it may be assumed that the magnitude was then 5^m—6^m. In the paper mentioned Bessel has published orbital elements of the comet and the perturbations of the orbit during the interval until the next transit of perihelion which according to these calculations was to take place 1887 February 9.

As Bessel, however, had not made use of all the observations in his determination of the elements, Ginzel in 1881 made a new calculation[2] using all available observations, revised positions of the comparison stars and improved values of the solar co-ordinates (Le Verrier). The following elements resulted:

A

T	= 1815 April 26.030146 m. B. T.	
Ω	= 62°51′22″75	Equatorial Elements Equinox 1815.0
i	= 51 29 34 01	
π	= 158 46 36 75	
$\log q$	= 0.08379982	
e	= 0.93114958	
U	= 73.9333	

[1] F. W. Bessel: Abhandlung der Königlichen Akademie der Wissenschaften in Berlin 1812—13. Page 119.

[2] F. K. Ginzel: Neue Untersuchungen über die Bahn des Olberschen Cometen und seine Wiederkehr. Haarlem, De Erven Loosjes 1881.

Ginzel further computed the perturbations of the comet from 1815 to 1887. His predicted time of the next perihelion passage was 1887 December 17.

The comet was rediscovered by Brooks on 1887 August 25 and could be observed during an interval of 45 weeks until 1888 July 5 when it was observed by Barnard with the 90-cm refractor of the Lick Observatory. Altogether the comet was now observed 326 times. The perihelion passage took place on 1887 October 8. The closest approach to the earth occurred practically at the same time, the minimum distance being 1.88 A. U. The magnitude was then about 9^m.

In a following paper Ginzel continued his investigation of the orbit, and in 1893 he published definitive elements computed from the observations 1887—1888[1]:

B

T =	1887 October 8.516025 m. B. T.	
Ω =	63°43′51″95	Equatorial Elements
i =	51 10 30 63	Equinox 1890.0
π =	159 38 6 58	
$\log q$ =	0.0788620	
e =	0.9311297	

In the same paper Ginzel published perturbations from 1815 to 1887 without obtaining satisfactory agreement between observation and calculation, however, and the work was not completed.

Rather than continuing Ginzel's calculations I decided to solve the problem in a different manner, taking for a model Cowell's and Crommelin's calculation of the motion of Halley's comet from 1759 to 1910[2]. I set myself the following task:

I. The elements of 1887 have to be corrected until they give a satisfactory agreement between observation and calculation in 1887—88 as well as in 1815, when the perturbations of all the major planets during the time interval in question are taken into account.

[1] F. K. Ginzel: Veröffentlichungen des Rechen-Instituts der Königlichen Sternwarte zu Berlin Nr. 3.

[2] P. H. Cowell and A. C. D. Crommelin: Essay on the Return of Halleys Comet. Publication der Astronomischen Gesellschaft No. 23 1910 Greenwich Observations 1910.

II. On the basis of the corrected elements thus obtained the motion should be followed up to the time of the next perihelion passage, account being again taken of the perturbations of all the major planets, and an ephemeris calculated for the coming apparition.

The method I have used in the calculation of the motion of the comet is that of numerical integration of rectangular equatorial co-ordinates.

The integration can be carried out in various ways. Thus, Cowell and Crommelin made use of the following relations

$$x_0^{II} = f_0 + \frac{1}{12} f_0^{II} - \frac{1}{240} f_0^{IV} + \cdots \quad \left(f_0 = w^2 \frac{d^2x}{dt^2}\right)$$

$$x_{+1} = 2x_0 - x_{-1} + x_0^{II}.$$

In Noumerov's method a table of σ is employed, where

$$\sigma\left(1 - \frac{\sigma}{12}\right)^2 = \frac{w^2 k^2}{r^3}.$$

The aim is similar in both methods, namely, to eliminate extrapolation as far as possible, and thus to make it possible to use a greater interval of integration. Both methods have certain drawbacks, however. Thus, in Noumerov's method the table of σ is calculated with the value of the Gaussian constant corresponding to the solar mass equal to 1, so that it cannot be used directly when it is desired to take account of the influence of the inner planets by the substitution of $k^2(1+m)$ for k^2.

I have preferred to make use of the classical method of numerical integration

$$x_0 = {}^{II}f_0 + \frac{1}{12} f_0 - \frac{1}{240} f_0^{II} + \cdots \quad \left(f_0 = w^2 \frac{d^2x}{dt^2}\right).$$

in which the second and the following terms are extrapolated. After a rigorous calculation of $\frac{d^2x_0}{dt^2}$, the calculation then proceeds one interval by

$$\cdots\cdots {}^{II}f_{+1} = 2\,{}^{II}f_0 - {}^{II}f_{-1} + f_0.$$

This is the method of integration that has been used in the extensive calculations of orbits in the three-body problem that have been carried out at the Copenhagen Observatory for half a century under the direction of Thiele, Burrau, and E. Strömgren. In this connection a paper[1] by E. Strömgren (1900) on the applicability of the method to problems of celestial mechanics should be mentioned.

In the calculation of the perturbations it is necessary to know the rectangular co-ordinates of the major planets during the time interval of two revolutions of the comet. For Jupiter, Saturn, Uranus, and Neptune the co-ordinates and the attractions on the sun are given for the time interval 1900 to 1960 in Nautical Almanac Office Publications[2]. For Venus, the earth, and Mars similar tables are available, but only from 1920 to 1960. For the time interval 1815 to 1900 I have myself calculated the co-ordinates for Jupiter, Saturn[3], Uranus, and Neptune[4], and for 1887 also those of Venus, the earth, and Mars. The perturbations by Mercury have been taken into account approximately only, by the use of the combined mass of the sun and Mercury, equal to 1.00000014, and the corresponding value of the Gaussian constant $k^2 = 0.000295\,912250$.

The perturbations and attractions on the sun by Venus, the earth, and Mars have only been taken into account in the time interval from 1887 January 8 to 1888 September 19 as well as from 1955 August 21 to 1956 July 6. Outside these intervals the distance of the comet from the sun is so great that the procedure of adding the masses of the four inner planets to that of the sun and using the corresponding Gaussian constant $k^2 = 0.000295\,913969$ gives quite sufficient accuracy, and of course it is very much simpler.

[1] E. Strömgren: Über Mekanische Integration und deren Verwendung für numerische Rechnungen auf dem Gebiete des Drei-Körper-Problemes. Meddelanden från Lunds Astronomiska Observatorium Nr. 13.

[2] H. M. Nautical Almanac Office: Planetary Co-ordinates for the Years 1800—1940 and 1940—1960.

[3] H. Q. Rasmusen: Äquatoreale Jupiter- und Saturn-Koordinaten für den Zeitraum 1800—1900. Astronomische Nachrichten Nr. 6172.
Publikationer og mindre Meddelelser fra Københavns Observatorium Nr. 107.

[4] H. Q. Rasmusen: Äquatoreale Uranus- und Neptun-Koordinaten für den Zeitraum 1800—1903. Astronomische Nachrichten 269, 3.
Publikationer og mindre Meddelelser fra Københavns Observatorium Nr. 121.

The method just indicated does not take account of the attractions of the four inner planets on the sun. These attractions change so rapidly with time that already with an interval of 20 days the higher differences of the attractions would vary irregularly if the attractions in question were included in the calculations, and it would become impossible to use the regularity of the higher differences as a check on the numerical calculations. The reason is, of course, the relatively short periods of the inner planets.

A more rigorous method for the calculation of the motion would be the use of an interval that was never greater than 10 days. This, however, would be an immense task. There are also other ways in which the difficulty might be overcome. It is possible, for instance, to carry out the integration in a co-ordinate system the origin of which coincides with the centre of gravity of the sun and the four inner planets, or that of the sun and all the major planets. When the calculation is started, all co-ordinates and velocities are reduced to this co-ordinate system with the aid of simple formulae, and the attractions of the planets on the sun do not enter into the calculation any more. When the integration has been completed the co-ordinates and velocities are reduced back to the standard co-ordinate system with the sun in the origin. Cowell and Crommelin made use of this method in their calculations of the motion of Halley's comet. The method has the drawback, however, that the co-ordinates of Jupiter, Saturn, Uranus, and Neptune, and also that of the sun, have to be reduced to the centre of gravity. In the present investigation the co-ordinate system with the sun at the origin has been used throughout. The perturbations by Jupiter, Saturn, Uranus, and Neptune have been taken into account rigorously throughout the whole time interval. The attraction of Mercury on the sun has been omitted. The attractions of Venus, the earth, and Mars on the sun and on the comet have been calculated rigorously for those time intervals around the perihelions in 1887 and 1956 where the interval of integration was 5 or 10 days, i. e. for that part of the orbit for which the distance of the comet from the sun is smaller than about 4 A. U. Throughout the rest of the orbit the modified Gaussian constant was used while the attractions of the four inner planets on the sun were ignored. It is advisable to make the change-over at a time of a superior con-

junction of Venus and the sun, since the attractions of Venus and the earth on the sun then cancel approximately, so that the differences run rather smoothly in spite of the change-over.

For 1815 no account was taken of Venus, the earth, and Mars, since the effects would be without any consequence, because the integration terminates here.

The mass of Pluto is assumed to be between 0.5 and 1 in units of the earth's mass. The attraction of Pluto on the sun must therefore be less than $2 \cdot 10^{-8}$ for an interval of 160 days. The influence on the comet is of the same order of magnitude, as the distance between Pluto and the comet is quite large all the time. Thus the eighth decimal of the calculation is influenced. Since, however, the mass of Pluto is so uncertain, I decided not to take account of this planet, as I feared that the accuracy of the calculation might hereby actually be diminished.

For the same reason I have made no attempt to take account of the attractions of the asteroids. In examining the motion of the comet in the neighbourhood of the asteroid ring it is noted that the cometary orbit passes through the ecliptic at a distance of 1.5 A. U. from the sun, and that the angle of the orbit with the ecliptic at this point is rather large, since the inclination is 44°, and the angle between the node and the perihelion 65°. Therefore the duration of the passage of the comet through the asteroid region is relatively short. Since the majority of the asteroids have distances of 2—3 A. U. from the sun, and since the total mass is very small and evenly distributed around the sun, the attractions on the sun can be neglected.

However, the total attraction of the asteroids on the comet in the outer part of its orbit might be of some influence. According to an investigation by G. Stracke[1] the total mass of the asteroids up to 1024 is 1:864 of the earth's mass, or 1:285 000 000 in units of the solar mass (upper limit). The sum of the masses of the sun and the asteroids being 1.0000 000035, the period

$$P = \frac{2\pi}{\mu} = \frac{2\pi}{k} a^{3/2}$$

is increased by 0.000 00013 years, or 4 seconds (upper limit).

[1] G. Stracke: Die kleine Planeten. Ergebnisse der exakten Naturwissenschaften. Band 4.

From the available observations of Comet Olbers the following normal places have been derived[1]. The times have been reduced to Greenwich Mean Time, reduced from noon before 1925.0, from midnight (Universal Time) after 1925.0. All the observations have been reduced to the equinox 1950.0, and this equinox has been used throughout in the present investigation.

Normal Places.

				α	δ
1	1815	Mar.	16.96279	54°52′ 2″.1	+ 37°50′16″.6
2			30.96279	61 56 46 .7	44 50 7 .3
3		Apr.	9.96279	69 2 35 .8	49 44 6 .0
4			21.96279	80 46 45 .4	55 11 2 .7
5		May	4.96279	98 56 10 .8	59 41 17 .5
6			15.96279	118 55 58 .3	61 10 30 .0
7			28.96279	144 5 16 .3	58 50 17 .2
8		Jun.	9.96279	163 38 40 .2	52 56 17 .1
9			23.96279	180 21 2 .7	43 23 33 .5
10		Jul.	5.96279	190 49 6 .0	34 31 55 .9
11			29.96279	206 1 52 .7	18 22 20 .1
12		Aug.	24.96279	218 32 35 .7	5 7 57 .2
13	1887		31.96279	136 25 45 .0	29 41 0 .9
14		Sep.	16.96279	155 9 46 .9	29 37 17 .2
15			27.96279	168 44 1 .7	28 9 50 .2
16		Oct.	20.96279	195 48 39 .2	21 39 44 .0
17		Nov.	12.96279	218 7 24 .6	13 9 51 .7
18		Dec.	2.96279	233 28 35 .7	6 31 23 .1
19			22.96279	245 53 30 .4	+ 1 21 40 .8
20	1888	Jan.	15.96279	257 45 22 .2	— 2 59 9 .1
21		Feb.	15.96279	268 49 15 .0	6 31 29 .3
22		Mar.	21.96279	275 12 40 .3	9 20 31 .6
23		Apr.	5.96279	275 37 47 .7	10 37 7 .5
24		Jun.	26.96279	257 11 54 .6	— 20 10 49 .1

The normal places given by Ginzel are called by him mean places. In the notation now used they are "apparent place minus

[1] F. K. Ginzel: Neue Untersuchungen über die Bahn des Olberschen Cometen und seine Wiederkehr. Haarlem, .De Erven Loosjes 1881. Page 6.
F. K. Ginzel: Veröffentlichungen des Rechen-Instituts der Königlichen Sternwarte zu Berlin Nr. 3. Page 28.

the (f, g, G)-terms", or the equivalent, namely, "mean place plus the (i, h, H)-terms". The aberration times have been applied to the times of observation. Thus the comparison between observation and calculation is made by computing the position with the aid of cometary and solar co-ordinates corresponding to the time given, namely, time of observation minus aberration time.

The following solar co-ordinates for the normal places are according to the tables of Le Verrier:

Solar co-ordinates.

	X	Y	Z
1	+ 0.995088	— 0.033410	— 0.014474
2	+ 0.978752	+ 0.186905	+ 0.081156
3	+ 0.932278	+ 0.338478	+ 0.146943
4	+ 0.840568	+ 0.506847	+ 0.220027
5	+ 0.701922	+ 0.665241	+ 0.288769
6	+ 0.557592	+ 0.774354	+ 0.336131
7	+ 0.362786	+ 0.868615	+ 0.377035
8	+ 0.167256	+ 0.918930	+ 0.398872
9	— 0.068786	+ 0.930393	+ 0.403837
10	— 0.268641	+ 0.899554	+ 0.390448
11	— 0.628043	+ 0.731380	+ 0.317439
12	— 0.901775	+ 0.417743	+ 0.181295
13	— 0.945095	+ 0.323472	+ 0.140327
14	— 1.000929	+ 0.078756	+ 0.034157
15	— 0.996184	— 0.094017	— 0.040803
16	— 0.873319	— 0.437242	— 0.189708
17	— 0.613577	— 0.711710	— 0.308783
18	— 0.306337	— 0.859162	— 0.372755
19	+ 0.038354	— 0.901508	— 0.391123
20	+ 0.441924	— 0.806338	— 0.349826
21	+ 0.839372	— 0.478609	— 0.207636
22	+ 0.995681	+ 0.050295	+ 0.021834
23	+ 0.952783	+ 0.283153	+ 0.122859
24	— 0.124248	+ 0.925714	+ 0.401619

The elements B which form the starting point of my investigation are somewhat uncertain with regard to the semi-major axis a, and hence with regard to the period. In order to determine

better values of a and P it is necessary to calculate the perturbed motion back to 1815 and to compare with the observations of that year.

We reduce elements B to the normal equinox 1950.0 and to Greenwich Mean Time. Thus we get:

Epoch 1887 Oct. 5.5. G. M. T.

$$B_{\mathrm{I}} \begin{cases} T = 1887\ \text{Oct.}\ 8.478815 \\ \omega = 96^\circ\ 5'31''.45 \\ \Omega = 64\ 22\ 51\ .68 \\ i = 50\ 52\ 29\ .13 \\ e = 0.9311297 \\ a = 17.411250 \end{cases} \left.\begin{matrix} \\ \\ \\ \end{matrix}\right\} \text{Equator } 1950.0$$

and the corresponding equatorial constants:

$$\begin{aligned} P_x &= -0.611656063 & Q_x &= -0.369558583 \\ P_y &= +0.175608284 & Q_y &= -0.925552969 \\ P_z &= +0.771387446 & Q_z &= -0.082329548 \end{aligned}$$

For practical reasons the date of osculation has been changed from 1887 October 8.5 to 1887 October 5.5. This is permissible, since the elements have to be improved anyway, and since the corrections to be expected are much larger than the small differences thus introduced. We now calculate the co-ordinates and velocities for 1887 October 5.5.

Co-ordinates and velocities.

$$\begin{aligned} x &= -0.70886407 & 10\frac{dx}{dt} &= -0.084359783 \\ y &= +0.27058629 & 10\frac{dy}{dt} &= -0.200820211 \\ z &= +0.92963296 & 10\frac{dz}{dt} &= -0.013234677 \end{aligned}$$

With these values the numerical integration is started. The time interval 1887—1815 is covered by 250 integration intervals of 10, 20, 50, 100, 200, 100, 50, and 25 days, respectively. The

co-ordinates are given in Table I. Finally the following osculating elements are deduced from the co-ordinates and velocities for 1815 June 25.5.

Epoch 1815 Jun. 25.5. G. M. T.

$$A_{\mathrm{I}}\left\{\begin{array}{rl} T = & 1815\ \text{Jan.}\ 20.8646 \\ \omega = & 96^\circ 18' 35''.80 \\ \Omega = & 64\ 18\ 43\ .34 \\ i = & 50\ 49\ 53\ .33 \\ e = & 0.9317807 \\ a = & 17.76309 \end{array}\right.\quad \left.\begin{array}{l}\\ \\ \\ \\ \\ \\ \end{array}\right\}\ \text{Equator 1950.0}$$

These elements give only a bad fit with the observations of 1815. The principal reason for the discrepancy is the error of the computed perihelion time. According to the elements A, calculated from the observations of 1815, the perihelion passage took place 1815 April 25.9929. This is $95^{\mathrm{d}}.1283$ later than the perihelion time computed by carrying back the elements B_{I}. Therefore, a correction of the perihelion time of the elements A_{I} equal to $+95^{\mathrm{d}}.1283$ is required. Introducing this, the difference between observation and calculation is reduced to a few minutes of arc. It is clear that the principal source of the error of the elements A_{I} is the error of the semi-major axis of the elements B_{I}, this quantity being slightly too large. We therefore correct the element a of B_{I} by -0.041640, a correction calculated so as to give a change in the period equal to $-95^{\mathrm{d}}.1283$, corresponding to the determined error of the perihelion time in 1815. Next the corrections to the other elements were found from Ginzel's equations of condition[1] through a process of introducing $da = -0.041640$ as a known quantity and eliminating dq.

From

$$q = a\,(1 - e)$$

one finds

$$\frac{dq}{q} = \frac{da}{a} - \frac{de}{1-e},$$

[1] F. K. Ginzel: Veröffentlichungen der Rechen-Instituts der Königlichen Sternwarte zu Berlin Nr. 3, page 31. Here is a misprint in equation VII. Instead of 9.9633 read 9.6633. Moreover Ginzel has made a miscalculation in this section; on the seventh line from the bottom of page 32. $dT = +0.005355$ ought to be $dT = +0.002684$. This error appears in the elements on page 33 Instead of $T =$ October 8.516025 read 8.513354. The error recurs in the present investigation in the elements B^{I}, but the following correction of the elements makes it disappear.

hence

$$d \log_{10} q = 0.434294 \frac{\frac{1}{a}(1-e)\, da - de}{1-e}.$$

Solving the reduced equations of condition by the method of least squares we get the following corrections to the elements B_{I}:

$$\begin{aligned} dT &= -0^{\mathrm{d}}.00288 \\ d\omega &= -4''.481 \\ d\Omega &= +0''.455 \\ di &= +0''.843 \\ de &= -0.0001646 \\ da &= -0.041640 \end{aligned}$$

Applying these corrections to the elements B_{I}, we get the following system of elements:

Epoch 1887 Oct. 5.5. G. M. T.

B_{II}

T =	1887 Oct. 8.47594	
ω =	96° 5′26″.97	Equator 1950.0
Ω =	64 22 52.14	Equator 1950.0
i =	50 52 29.97	Equator 1950.0
e =	0.9309651	
a =	17.369610	

$$\begin{aligned} P_x &= -0.611645591 & Q_x &= -0.369570105 \\ P_y &= +0.175625663 & Q_y &= -0.925549834 \\ P_z &= +0.771391793 & Q_z &= -0.082313064 \end{aligned}$$

As a check we compare these elements with the observations from 1887—88. In order to be able to do so we must know the perturbations from the date of osculation 1887 October 5.5 up to the times of the normal places. These perturbations are given in Ginzel's paper. Since, however, the elements had been changed appreciably, I decided to recalculate the perturbations with the aid of the elements B_{II}. In these calculations I used Encke's method. In this way the following perturbations, interpolated to the times of the normal places, are obtained.

1887—88	ξ	η	ζ	Pa	$P\delta$
13	0	0	— 9	0″.0	—0″.1
14	0	0	— 3	0.0	0.0
15	0	0	0	0.0	0.0
16	— 1	— 2	— 3	0.0	0.0
17	— 4	— 12	— 22	+ 0.1	—0.2
18	— 10	— 33	— 53	+ 0.1	—0.5
19	— 20	— 69	— 106	+ 0.1	—1.0
20	— 46	— 139	— 197	— 0.1	—1.6
21	— 122	— 282	— 365	— 1.0	—2.7
22	— 314	— 536	— 640	— 3.9	—4.8
23	— 448	— 684	— 788	— 5.6	—6.0
24	—2119	—2142	—2023	—13.6	—8.2

It is now possible to compare elements B_{II} with the observations. The following result is obtained:

1887—88	$\Delta a \cos\delta$	$\Delta\delta$
13	— 1″.4	+ 0″.5
14	+ 0.7	+ 0.8
15	+ 0.4	— 1.4
16	+ 1.4	— 1.2
17	+ 3.8	— 0.6
18	— 0.4	— 1.9
19	— 0.9	— 2.3
20	— 5.4	— 1.8
21	— 5.5	— 0.1
22	— 6.2	+ 5.6
23	—11.5	+ 0.9
24	+ 1.7	+10.6

The agreement is as good as could be expected. Therefore, it now only remains to obtain a confirmation of the adopted value of the period by a comparison with the observations in 1815. Since the difference between the elements B_I and B_{II} is rather large, however, the perturbations calculated with B_I cannot be regarded as sufficiently accurate. It is therefore neces-

sary to repeat the whole calculation of the motion 1887—1815, using now the elements B_{II}. The integration is started with the following co-ordinates and velocities:

$$x = -0.70887065 \qquad 10\frac{dx}{dt} = -0.08435565$$

$$y = +0.27054523 \qquad 10\frac{dy}{dt} = -0.20081286$$

$$z = +0.92962634 \qquad 10\frac{dz}{dt} = -0.01323487$$

The time interval is covered by 290 intervals of 10, 20, 50, 100, 200, 100, 50, 25, and $12^1/_2$ days (Table II).

The following osculating elements are derived for 1815 June 25.5:

Epoch 1815 June 25.5. G. M. T.

A_{II}

T =	1815 May 1.1170	
ω =	96°21′ 4″.00	Equator 1950.0
Ω =	64 18 47 .15	
i =	50 49 14 .82	
e =	0.9317235	
a =	17.76603	

These leave the following residuals observation minus calculation

1815	$\Delta\alpha$	$\Delta\delta$
1	−0° 1′19″.3	+3° 0′32″.4
2	+0 16 5 .3	+3 11 41 .9
3	+0 43 10 .4	+3 17 50 .7
4	+1 45 5 .6	+3 19 32 .5
5	+3 44 50 .6	+3 3 25 .7
6	+5 50 23 .8	+2 22 29 .4
7	+7 6 21 .5	+1 1 17 .2
8	+6 27 7 .0	−0 14 58 .3
9	+4 55 38 .0	−1 14 20 .1
10	+3 47 11 .7	−1 37 48 .3
11	+2 19 32 .9	−1 39 1 .9
12	+1 29 43 .2	−1 16 49 .9

The discrepancies are still too large, but it is possible to reduce them to the magnitude of the uncertainty of the observations, $\pm 15''$, by a change of perihelion time in the elements A_{II} to 1815 April 26.0000. It must therefore be assumed that the remaining error of the period of the elements B_{II} is $5^d.1170$. This corresponds to a correction in a equal to $+0.002241$, so that the correct value of a in 1887 should be 17.371851.

The reason why the first improvement of the elements did not lead to the correct result is that the perturbations of the first integration 1887—1815 are somewhat in error due to the errors of the elements upon which that integration was based. In particular the relatively large change in a has resulted in rather large changes in the perturbations.

We now repeat the process of improvement of the elements, assuming a correction $da = -0.039399$ of the elements B_I corresponding to a change of the period of $90^d.0142$. For the other elements the changes will not differ very much from those resulting from the first improvement process. I have, therefore, simply used the former corrections reduced in the ratio of the two corrections of the perihelion time 90.0142:95.1283, instead of repeating the solution of the reduced equations of condition by the method of least squares. The new corrections are:

$$\begin{aligned} dT &= -0^d.00272 \\ d\omega &= -4''.240 \\ d\Omega &= +0''.431 \\ di &= +0''.798 \\ de &= -0.0001557 \\ da &= -0.039399 \end{aligned}$$

Applying these corrections to the elements B_I we finally get the following elements:

Epoch 1887 Oct. 5.5. G. M. T.

B_{III}

T =	1887 Oct. 8.47609	
ω =	96° 5′27″.21	Equator 1950.0
Ω =	64 22 52.11	
i =	50 52 29.93	
e =	0.9309740	
a =	17.371851	

$$\begin{aligned} P_x &= -0.611646134 & Q_x &= -0.369569514 \\ P_y &= +0.175624739 & Q_y &= -0.925549992 \\ P_z &= +0.771391572 & Q_z &= -0.082313951 \end{aligned}$$

A useful summary of the perturbations and their changes with the assumed elements is obtained by subtracting elements B_{I} from A_{I}, and B_{II} from A_{II}. The perturbation in perihelion time, however, is obtained by subtracting $(T_{1887} - 360 : \mu_{1887})$ from the value of T_{1815} which is obtained as the osculating T corresponding to the co-ordinates and velocities for 1815 June 15.5. For the two orbits we thus get the following two sets of perturbations, and the differences between the two sets:

	Orbit I	Orbit II	II — I
PT =	+ 22.$^{\mathrm{d}}$1318	+ 17.$^{\mathrm{d}}$0148	— 5.$^{\mathrm{d}}$1170
$P\omega$ =	+ 13′ 4″.35	+ 15′37″.03	+ 2′32″.68
$P\Omega$ =	— 4 8.34	— 4 4.99	+ 3.35
Pi =	— 2 35.80	— 3 15.15	— 39.35
Pe =	+ 0.0006510	+ 0.0007584	+ 0.0001074
Pa =	+ 0.35184	+ 0.39642	+ 0.04458

The differences are not particularly great, and it may therefore be assumed that the perturbations obtained through the second integration are close to the true values. Applying these perturbations to the elements B_{III} we obtain the following elements A_{III} valid for 1815 June 25.5

Epoch 1815 June 25.5. G. M. T.

$$A_{\mathrm{III}} \begin{cases} T = 1815 \text{ April } 25.9999 \\ \omega = 96°21′\ 4″.24 \\ \Omega = 64\ 18\ 47.12 \\ i = 50\ 49\ 14.78 \\ e = 0.9317324 \\ a = 17.76827 \end{cases} \left.\begin{matrix} \\ \\ \\ \end{matrix}\right\} \text{Equator } 1950.0$$

The perihelion time, however, has been calculated as follows:

$$T_{1815} = T_{1887} - \frac{360}{\mu_{1887}} + PT.$$

Comparison with elements A (cf. p. 3) shows that this perihelion time is close to the true value.

According to Bessel and Ginzel the perturbations in α and δ within the time interval of observations in 1815 are of the order

of magnitude of 1″. Therefore they could safely be neglected. Comparisons of the elements A_{III} with the observations of 1815 and the elements B_{III} with the observations of 1887—88 give the following result:

1815	$\Delta\alpha \cos\delta$	$\Delta\delta$	1887-88	$\Delta\alpha \cos\delta$	$\Delta\delta$
1.....	— 22″.5	— 7″.5	13.....	— 1″.0	+ 0″.5
2.....	— 11.4	+ 3.6	14.....	+ 1.3	+ 0.8
3.....	— 10.2	+ 5.5	15.....	+ 0.4	— 1.6
4.....	— 10.5	+ 4.1	16.....	+ 2.8	— 1.4
5.....	— 5.0	+ 0.2	17.....	+ 3.6	— 0.5
6.....	+ 0.1	+ 14.9	18.....	— 0.3	— 1.9
7.....	+ 5.8	+ 1.0	19.....	— 0.7	— 2.4
8.....	+ 1.6	— 1.3	20.....	— 5.4	— 1.8
9.....	— 9.1	— 3.2	21.....	— 5.2	— 0.1
10.....	+ 6.9	— 4.5	22.....	— 5.9	+ 5.6
11.....	+ 12.0	— 29.7	23.....	— 11.0	+ 0.7
12.....	+ 15.2	— 12.0	24.....	+ 1.9	+ 10.2

The agreement can now be considered as rather satisfactory when the inaccuracy of the old observations is kept in mind. A third integration based on elements B_{III} would undoubtedly yield practically correct values of the perturbations 1887—1815 and possibly lead to a still better agreement with the observations in 1815.

However, I have come to the conclusion that it should not be necessary to carry out this third integration. It is estimated that the uncertainty of the period of the elements B_{III} is less than 12 hours.

Reducing now the equatorial elements B_{III} to ecliptic elements we find:

Epoch 1887 Oct. 5.5. G. M. T.

$$B_{III\,a}\begin{cases} T = 1887\ \text{Oct.}\ 8.47609 \\ \omega = 65°20'47''.11 \\ \Omega = 85\ 22\ 6.89 \\ i = 44\ 34\ 16.75 \\ e = 0.9309740 \\ a = 17.371851 \\ P = 72^{y}.4051 \end{cases} \left.\begin{matrix} \\ \\ \\ \\ \\ \\ \end{matrix}\right\} \begin{matrix} \text{Ecliptic} \\ 1950.0 \end{matrix}$$

II

Elements B_{III} (B_{IIIa}) now form the basis of a calculation of the motion of the comet from 1887 to the next perihelion passage. As before we calculate co-ordinates and velocities for the epoch of osculation 1887 October 5.5.

$$x = -0.70887009 \qquad 5\frac{dx}{dt} = -0.04217794$$

$$y = +0.27054729 \qquad 5\frac{dy}{dt} = -0.10040665$$

$$z = +0.92962642 \qquad 5\frac{dz}{dt} = -0.00661743$$

The intervals are now chosen so as to correspond to those used in the Nautical Almanac Tables of Planetary Co-ordinates 1900—1960. The numerical integration is started with an interval of integration equal to 5 days. The interval is then successively changed to 10, 20, 40, 80, 160, 80, 40, 20, and 10 days. The time interval 1887—1956 is covered by 325 intervals. Table III gives the co-ordinates of the comet x, y, z, the attractions of the planets on the comet

$$\sum' X' = \sum 10^9 w^2 k^2 m_1 \frac{x - x_1}{\Delta^3}$$

$$\sum' Y' = \sum 10^9 w^2 k^2 m_1 \frac{y - y_1}{\Delta^3}$$

$$\sum' Z' = \sum 10^9 w^2 k^2 m_1 \frac{z - z_1}{\Delta^3}$$

and the attractions of the planets on sun

$$\sum' X = \sum 10^9 w^2 k^2 m_1 \frac{x_1}{r_1^3}$$

$$\sum' Y = \sum 10^9 w^2 k^2 m_1 \frac{y_1}{r_1^3}$$

$$\sum' Z = \sum 10^9 w^2 k^2 m_1 \frac{z_1}{r_1^3}$$

As a result of the integration we obtain co-ordinates and velocities for 1956 June 16, and osculating elements corresponding to these values.

Epoch 1956 June 16.0. G. M. T. (U. T.)

$$C \begin{cases} T = 1956 \text{ June } 15.8673 \\ \omega = 64^\circ 38' 10''.21 \\ \Omega = 85\ 24\ 55\ .19 \\ i = 44\ 36\ 35\ .80 \\ e = 0.9303273 \\ a = 16.91523 \\ P = 69^y.5692 \end{cases} \quad \text{Ecliptic 1950.0}$$

$$P_x = -0.6069823 \qquad Q_x = -0.3762061$$
$$P_y = +0.1864259 \qquad Q_y = -0.9236804$$
$$P_z = +0.7725399 \qquad Q_z = -0.0726855$$

With the aid of the co-ordinates in Table III I have calculated a search ephemeris from 1955 August 1 to 1956 June 16 (Table IV). The ephemeris gives right ascension and declination for the equinox 1950.0 together with the heliocentric distance r and the geocentric distance Δ. It appears from the ephemeris that the comet will be somewhat more favourably placed for observation than in the previous apparition. Also the minimum geocentric distance is somewhat smaller than in 1887—88. Table V gives the precession from the equinox 1950.0 to 1955.0—1956.0 and the corrections of right ascension and declination for T one day later.

It appears from an inspection of elements B_{III} and the computed time of revolution 1815—1887 that the period of Comet Olbers is about 72.4 years. Accordingly one would expect the next passage of perihelion to take place in March 1960. It is, therefore, perhaps somewhat surprising to find from the integration that the comet will reach perihelion again already 1956 June 15, or nearly four years earlier than expected. The reason is that the comet during the years 1888—89 came relatively close to Jupiter. In January 1889 the distance was only 1.5 A. U. This approach to Jupiter reduced the velocity of the comet and thus lead to a diminution of the semi-major axis and the period.

On 1887 July 28 the comet passed Mars at a small distance,

not more than 0.08 A. U. The influence of this passage on the velocity of the comet was small, however, because of the small mass of the planet. The following table (Table VI) gives a summary of the distances between the comet and the major planets.

During the time interval 1815—1956 the osculating period of the comet changes appreciably. This is shown graphically in the accompanying figure. This figure clearly shows the great change

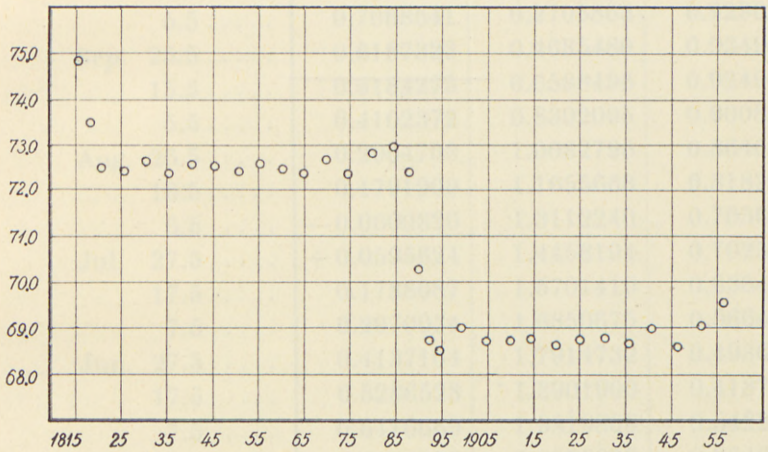

in the period that took place in connection with the approach to Jupiter in 1889.

Through the calculations described above the problems formulated on p. 4 have been solved. The observations during the coming apparition will indicate the magnitude of the remaining errors of the elements obtained.

In making the calculations 8 decimals have been retained in the summations and differences, and 9 decimals in the calculations of the perturbations. The tables given in this paper have been abridged to 7 decimals in the co-ordinates, since the accumulated effect of rounding-off errors leads to an uncertainty greater than one unit of the eighth decimal even in the orbit of the comet, while the corresponding error of the position in the orbit is still greater. The calculations have been checked by differencing whenever that was possible. All reductions as well as the calculations required for starting the integrations have

been checked independently. I gratefully acknowledge the help that JENS P. MÖLLER, M. Sc., and B. SVANHOF, M. Sc., have given me in making these checks. The entire first integration (I) was carried out by OLE HESSELBERG, M. Sc. I also gratefully acknowledge the great help the Carlsberg Foundation has rendered me in placing a calculating machine at my disposal.

Værslevgaarden, April 1947.

Indleveret til Selskabet den 27. Juni 1947.
Færdig fra Trykkeriet den 31. Juli 1948.

Table I.

G. M. T.			x	y	z
1887	Nov.	14.5	−0.9409739	−0.5340691	+0.7592007
		4.5	0.9028881	0.3373105	0.8215735
	Oct.	25.5	0.8516988	−0.1357067	0.8719958
		15.5	0.7869174	+0.0680232	0.9084808
		5.5	0.7088641	0.2705863	0.9296328
	Sep.	25.5	0.6187323	0.4685480	0.9349496
		15.5	0.5184275	0.6588496	0.9249171
		5.5	0.4102372	0.8392095	0.9008584
	Aug.	26.5	0.2964703	1.0082796	0.8646166
		16.5	0.1791900	1.1655668	0.8182165
		6.5	−0.0600826	1.3112240	0.7636092
	Jul.	27.5	+0.0595624	1.4458194	0.7025254
		17.5	0.1788087	1.5701419	0.6364235
		7.5	0.2970034	1.6850675	0.5664928
	Jun.	27.5	0.4137104	1.7914732	0.4936826
		17.5	0.5286528	1.8901900	0.4187419
		7.5	0.6416669	1.9819808	0.3422577
	May	28.5	0.7526682	2.0675329	0.2646890
		18.5	0.8616266	2.1474582	0.1863944
		8.5	0.9685494	2.2222983	0.1076539
	Apr.	28.5	1.0734681	2.2925315	+0.0286867
		18.5	1.1764303	2.3585794	−0.0503358
		8.5	1.2774933	2.4208141	0.1292793
	Mar.	29.5	1.3767197	2.4795643	0.2080387
		19.5	1.4741754	2.5351213	0.2865318
		9.5	1.5699261	2.5877436	0.3646945
	Feb.	27.5	1.6640377	2.6376612	0.4424771
		17.5	1.7565739	2.6850800	0.5198415
		7.5	1.8475968	2.7301835	0.5967584
	Jan.	28.5	1.9371658	2.7731371	0.6732060
		18.5	2.0253380	2.8140897	0.7491685
		8.5	2.1121685	2.8531776	0.8246336
1886	Dec.	19.5	2.2820044	2.9262255	0.9740484
		29.5	+2.4470561	+2.9931287	−1.1214235

Table I

G. M. T.	x	y	z
1886 Nov. 9.5	+ 2.6076667	+ 3.0545918	— 1.2667647
Oct. 20.5	2.7641444	3.1112069	1.4100989
Sep. 30.5	2.9167658	3.1634759	1.5514659
10.5	3.0657800	3.2118274	1.6909138
Aug. 21.5	3.2114114	3.2566306	1.8284952
1.5	3.3538630	3.2982049	1.9642651
Jul. 12.5	3.4933188	3.3368293	2.0982791
Jun. 22.5	3.6299459	3.3727480	2.2305928
2.5	3.7638967	3.4061765	2.3612603
May 13.5	3.8953104	3.4373056	2.4903345
Apr. 23.5	4.0243146	3.4663053	2.6178666
3.5	4.1510267	3.4933274	2.7439058
Mar. 14.5	4.2755544	3.5185080	2.8684992
Feb. 22.5	4.3979975	3.5419699	2.9916921
2.5	4.5184481	3.5638240	3.1135276
Jan. 13.5	4.6369917	3.5841709	3.2340472
1885 Dec. 24.5	4.7537078	3.6031020	3.3532901
4.5	4.8686702	3.6207007	3.4712939
Nov. 14.5	4.9819479	3.6370434	3.5880946
Oct. 25.5	5.0936054	3.6522000	3.7037262
5.5	5.2037029	3.6662349	3.8182216
Sep. 15.5	5.3122970	3.6792073	3.9316117
Aug. 26.5	5.4194407	3.6911719	4.0439265
6.5	5.5251841	3.7021794	4.1551942
Jul. 17.5	5.6295740	3.7122768	4.2654422
Jun. 27.5	5.7326550	3.7215075	4.3746964
7.5	5.8344688	3.7299122	4.4829817
May 18.5	5.9350550	3.7375286	4.5903218
Apr. 28.5	6.0344510	3.7443922	4.6967396
8.5	6.1326925	3.7505358	4.8022570
Mar. 19.5	6.2298132	3.7559904	4.9068949
Feb. 27.5	6.3258449	3.7607848	5.0106733
Jan. 8.5	6.5613569	3.7700579	5.2664846
1884 Nov. 19.5	+ 6.7906870	+ 3.7757540	— 5.5173251

Table I

G. M. T.	x	y	z
1884 Sep. 30.5 . . .	+ 7.0142238	+ 3.7782038	— 5.7034505
Aug. 11.5 . . .	7.2323146	3.7776948	6.0050940
Jun. 22.5 . . .	7.4452712	3.7744783	6.2424682
May 3.5 . . .	7.6533745	3.7687756	6.4757681
Mar. 14.5 . . .	7.8568791	3.7607822	6.7051732
Jan. 24.5 . . .	8.0560160	3.7506721	6.9308484
1883 Dec. 5.5 . . .	8.2509964	3.7386004	7.1529466
Oct. 16.5 . . .	8.4420134	3.7247064	7.3716093
Aug. 27.5 . . .	8.6292431	3.7091152	7.5869671
Jul. 8.5 . . .	8.8128494	3.6919402	7.7991428
May 19.5 . . .	8.9929823	3.6732841	8.0082500
Mar. 30.5 . . .	9.1697809	3.6532403	8.2143951
Feb. 8.5 . . .	9.3433739	3.6318940	8.4176775
1882 Dec. 20.5 . . .	9.5138811	3.6093233	8.6181905
Oct. 31.5 . . .	9.6814141	3.5856000	8.8160216
Sep. 11.5 . . .	9.8460767	3.5607901	9.0112532
Jul. 23.5 . . .	10.0079662	3.5349546	9.2039627
Jun. 3.5 . . .	10.1671736	3.5081499	9.3942231
Apr. 14.5 . . .	10.3237842	3.4804286	9.5821034
Feb. 23.5 . . .	10.4778782	3.4518393	9.7676689
Jan. 4.5 . . .	10.6295312	3.4224276	9.9509811
1881 Nov. 15.5 . . .	10.7788143	3.3922360	10.1320984
Aug. 7.5 . . .	11.0705362	3.3296704	10.4879673
Apr. 29.5 . . .	11.3535401	3.2644335	10.8356862
Jan. 19.5 . . .	11.6282729	3.1967839	11.1756263
1880 Oct. 11.5 . . .	11.8951396	3.1269528	11.5081250
Jul. 3.5 . . .	12.1545099	3.0551479	11.8334898
Mar. 25.5 . . .	12.4067229	2.9815566	12.1520024
1879 Dec. 16.5 . . .	12.6520917	2.9063488	12.4639213
Sep. 7.5 . . .	12.8909064	2.8296782	12.7694852
May 30.5 . . .	13.1234372	2.7516843	13.0689147
Feb. 19.5 . . .	13.3499364	2.6724934	13.3624152
1878 Nov. 11.5 . . .	13.5706406	2.5922199	13.6501777
Aug. 3.5 . . .	+ 13.7857715	+ 2.5109672	— 13.9323811

Table I

G. M. T.	x	y	z
1878 Apr. 25.5 . . .	+ 13.9955375	+ 2.4288286	— 14.2091930
Jan. 15.5 . . .	14.2001346	2.3458877	14.4807707
1877 Oct. 7.5 . . .	14.3997471	2.2622199	14.7472628
Jun. 29.5 . . .	14.5945485	2.1778927	15.0088096
Mar. 21.5 . . .	14.7847019	2.0929665	15.2655435
1876 Dec. 11.5 . . .	14.9703609	2.0074951	15.5175905
Sep. 2.5 . . .	15.1516698	1.9215268	15.7650697
May 25.5 . . .	15.3287645	1.8351045	16.0080947
Feb. 15.5 . . .	15.5017727	1.7482665	16.2467733
1875 Nov. 7.5 . . .	15.6708144	1.6610468	16.4812084
Jul. 30.5 . . .	15.8360024	1.5734758	16.7114980
Apr. 21.5 . . .	15.9974427	1.4855804	16.9377357
Jan. 11.5 . . .	16.1552350	1.3973845	17.1600110
1874 Oct. 3.5 . . .	16.3094727	1.3089094	17.3784093
Jun. 25.5 . . .	16.4602433	1.2201740	17.5930124
Mar. 17.5 . . .	16.6076290	1.1311950	17.8038984
1873 Aug. 29.5 . . .	16.8925475	0.9525643	18.2148159
Feb. 10.5 . . .	17.1647824	0.7731189	18.6117240
1872 Jul. 25.5 . . .	17.4248123	0.5929425	18.9951380
Jan. 7.5 . . .	17.6730457	0.4121096	19.3655290
1871 Jun. 21.5 . . .	17.9098265	0.2306950	19.7233252
1870 Dec. 3.5 . . .	18.1354416	+ 0.0487830	20.0689134
May 17.5 . . .	18.3501316	— 0.1335218	20.4026365
1869 Oct. 29.5 . . .	18.5541049	0.3160883	20.7247959
Apr. 12.5 . . .	18.7475571	0.4987527	21.0356524
1868 Sep. 24.5 . . .	18.9306884	0.6813245	21.3354307
Mar. 8.5 . . .	19.1037210	0.8635963	21.6243270
1867 Aug. 21.5 . . .	19.2669073	1.0453596	21.9025180
Feb. 2.5 . . .	19.4205300	1.2264219	22.1701704
1866 Jul. 17.5 . . .	19.5648930	1.4066199	22.4274474
1865 Dec. 29.5 . . .	19.7003101	1.5858270	22.6745132
Jun. 12.5 . . .	19.8270902	1.7639556	22.9115343
1864 Nov. 24.5 . . .	19.9455277	1.9409537	23.1386796
May 8.5 . . .	+ 20.0558940	— 2.1167996	— 23.3561179

Table I

G. M. T.	x	y	z
1863 Oct. 21.5 . . .	+ 20.1584335	— 2.2914966	— 23.5640168
Apr. 4.5 . . .	20.2533604	2.4650659	23.7625406
1862 Sep. 16.5 . . .	20.3408591	2.6375446	23.9518493
Feb. 28.5 . . .	20.4210816	2.8089776	24.1320972
1861 Aug. 12.5 . . .	20.4941485	2.9794165	24.3034319
Jan. 24.5 . . .	20.5601474	3.1489140	24.4659925
1860 Jul. 8.5 . . .	20.6191331	3.3175190	24.6199088
1859 Dec. 21.5 . . .	20.6711270	3.4852705	24.7652978
Jun. 4.5 . . .	20.7161201	3.6521905	24.9022624
1858 Nov. 16.5 . . .	20.7540762	3.8182754	25.0308873
Apr. 30.5 . . .	20.7849416	3.9834882	25.1512362
1857 Oct. 12.5 . . .	20.8086762	4.1477528	25.2633502
Mar. 26.5 . . .	20.8251759	4.3109544	25.3672481
1856 Sep. 7.5 . . .	20.8344781	4.4729446	25.4629304
Feb. 20.5 . . .	20.8365846	4.6335554	25.5503829
1855 Aug. 4.5 . . .	20.8315617	4.7926174	25.6295895
Jan. 16.5 . . .	20.8195147	4.9499750	25.7005353
1854 Jun. 30.5 . . .	20.8005795	5.1054993	25.7632127
1853 Dec. 12.5 . . .	20.7749073	5.2590947	25.8176248
May 26.5 . . .	20.7426508	5.4106990	25.8637853
1852 Nov. 7.5 . . .	20.7039536	5.5602801	25.9017150
Apr. 21.5 . . .	20.6589422	5.7078307	25.9314422
1851 Oct. 4.5 . . .	20.6077241	5.8533622	25.9529971
Mar. 18.5 . . .	20.5503805	5.9969001	25.9664123
1850 Aug. 30.5 . . .	20.4869704	6.1384787	25.9717189
Feb. 11.5 . . .	20.4175253	6.2781383	25.9689460
1849 Jul. 26.5 . . .	20.3420501	6.4159201	25.9581188
Jan. 7.5 . . .	20.2605228	6.5518625	25.9392565
1848 Jun. 21.5 . . .	20.1728922	6.6859964	25.9123707
1847 Dec. 4.5 . . .	20.0790788	6.8183380	25.8774619
May 18.5 . . .	19.9789772	6.9488821	25.8345173
1846 Oct. 30.5 . . .	19.8724608	7.0775935	25.7835063
Apr. 13.5 . . .	19.7593923	7.2044009	25.7243783
1845 Sep. 25.5 . . .	+ 19.6396368	— 7.3291870	— 25.6570607

Table I

G. M. T.	x	y	z
1845 Mar. 9.5 . . .	+ 19.5130788	— 7.4518020	— 25.5814602
1844 Aug. 21.5 . . .	19.3796370	7.5720605	25.4974669
Feb. 3.5 . . .	19.2392739	7.6897630	25.4049605
1843 Jul. 18.5 . . .	19.0919982	7.8047116	25.3038187
1842 Dec. 30.5 . . .	18.9378549	7.9167252	25.1939222
Jun. 13.5 . . .	18.7769153	8.0256519	25.0751605
1841 Nov. 25.5 . . .	18.6092601	8.1313705	24.9474317
May 9.5 . . .	18.4349676	8.2337907	24.8106418
1840 Oct. 21.5 . . .	18.2541021	8.3328478	24.6647024
Apr. 4.5 . . .	18.0667085	8.4284967	24.5095270
1839 Sep. 17.5 . . .	17.8728074	8.5207061	24.3450284
Mar. 1.5 . . .	17.6723936	8.6094534	24.1711160
1838 Aug. 13.5 . . .	17.4654335	8.6947189	23.9876936
Jan. 25.5 . . .	17.2518649	8.7764833	23.7946567
1837 Jul. 9.5 . . .	17.0315951	8.8547213	23.5918908
1836 Dec. 21.5 . . .	16.8044999	8.9293984	23.3792687
Jun. 4.5 . . .	16.5704219	9.0004635	23.1566469
1835 Nov. 17.5 . . .	16.3291718	9.0678428	22.9238628
May 1.5 . . .	16.0805302	9.1314298	22.6807295
1834 Oct. 13.5 . . .	15.8242539	9.1910776	22.4270321
Mar. 27.5 . . .	15.5600863	9.2465903	22.1625232
1833 Sep. 8.5 . . .	15.2877726	9.2977198	21.8869213
Feb. 20.5 . . .	15.0070746	9.3441687	21.5999105
1832 Aug. 4.5 . . .	14.7177844	9.3856001	21.3011452
Jan. 17.5 . . .	14.4197304	9.4216528	20.9902538
1831 Jul. 1.5 . . .	14.1127742	9.4519559	20.6668455
1830 Dec. 13.5 . . .	13.7967999	9.4761430	20.3305130
May 27.5 . . .	13.4716977	9.4938554	19.9808328
1829 Nov. 8.5 . . .	13.137350	9.504742	19.617363
Apr. 22.5 . . .	12.793614	9.508453	19.239636
1828 Oct. 4.5 . . .	12.440316	9.504631	18.847154
Mar. 18.5 . . .	12.077238	9.492896	18.439377
1827 Aug. 31.5 . . .	11.704114	9.472840	18.015714
Feb. 12.5 . . .	+ 11.320629	— 9.444008	— 17.575517

Table I

G. M. T.	x	y	z
1826 Jul. 27.5	+ 10.926404	— 9.405892	— 17.118066
Jan. 8.5	10.521001	9.357911	16.642557
1825 Jun. 22.5	10.103908	9.299392	16.148087
Mar. 14.5	9.890798	9.265942	15.893427
1824 Dec. 4.5	9.674538	9.229554	15.633635
Aug. 26.5	9.455041	9.190109	15.368560
May 18.5	9.232214	9.147477	15.098042
Feb. 8.5	9.005958	9.101514	14.821910
1823 Oct. 31.5	8.776167	9.052065	14.539977
Jul. 23.5	8.542728	8.998958	14.252047
Apr. 14.5	8.305523	8.942006	13.957904
Jan. 4.5	8.064424	8.881001	13.657316
1822 Sep. 26.5	7.819298	8.815714	13.350033
Jun. 18.5	7.570004	8.745894	13.035783
Mar. 10.5	7.316392	8.671261	12.714270
1821 Nov. 30.5	7.058306	8.591507	12.385170
Aug. 22.5	6.795580	8.506288	12.048132
May 14.5	6.528040	8.415224	11.702771
Feb. 3.5	6.255500	8.317888	11.348662
1820 Oct. 26.5	5.977763	8.213807	10.985338
Jul. 18.5	5.694620	8.102446	10.612282
Apr. 9.5	5.405845	7.983201	10.228922
1819 Dec. 31.5	5.111195	7.855388	9.834614
Sep. 22.5	4.810405	7.718223	9.428639
Jun. 14.5	4.503187	7.570801	9.010180
Mar. 6.5	4.189223	7.412067	8.578310
1818 Nov. 26.5	3.868163	7.240781	8.131964
Aug. 18.5	3.539619	7.055465	7.669909
May 10.5	3.203163	6.854332	7.190706
Jan. 30.5	2.858322	6.635194	6.692653
1817 Oct. 22.5	2.504583	6.395310	6.173716
Jul. 14.5	2.141397	6.131189	5.631426
Apr. 5.5	1.768208	5.838255	5.062725
1816 Dec. 26.5	+ 1.384504	— 5.510327	— 4.463763

Table I

G. M. T.	x	y	z
1816 Nov. 6.5	+ 1.188595	— 5.330667	— 4.151434
Sep. 17.5	0.989961	5.138741	3.829563
Jul. 29.5	0.788646	4.932815	3.497272
Jun. 9.5	0.584764	4.710724	3.153540
Apr. 20.5	0.378561	4.469716	2.797170
Mar. 26.5	0.274718	4.341038	2.613816
1.5	0.170488	4.206205	2.426759
Feb. 5.5	+ 0.065986	4.064576	2.235785
Jan. 11.5	— 0.038635	3.915404	2.040666
1815 Dec. 17.5	0.143167	3.757800	1.841160
Nov. 22.5	0.247332	3.590706	1.637012
Oct. 28.5	0.350745	3.412841	1.427965
3.5	0.452878	3.222642	1.213773
Sep. 8.5	0.552988	3.018174	0.994229
Aug. 14.5	0.650012	2.797014	0.769220
Jul. 20.5	0.742400	2.556088	0.538825
Jun. 25.5	0.827835	2.291464	0.303514
May 31.5	0.902764	1.998088	— 0.064532
6.5	— 0.961607	— 1.669587	+ 0.175342

Table II.

G. M. T.	x	y	z
1887 Nov. 14.5	— 0.9409622	— 0.5340770	+ 0.7591916
4.5	0.9028810	0.3373272	0.8215650
Oct. 25.5	0.8516964	— 0.1357319	0.8719880
15.5	0.7869196	+ 0.0679898	0.9084738
5.5	0.7088706	0.2705452	0.9296263
Sep. 25.5	0.6187428	0.4684999	0.9349430
15.5	0.5184413	0.6587947	0.9249100
5.5	0.4102535	0.8391482	0.9008499
Aug. 26.5	0.2964884	1.0082116	0.8646056
16.5	0.1792092	1.1654913	0.8182020
6.5	— 0.0601026	1.3111404	0.7635898
Jul. 27.5	+ 0.0595419	1.4457264	0.7025006
17.5	0.1787870	1.5700386	0.6363925
7.5	0.2969802	1.6849526	0.5664551
Jun. 27.5	0.4136858	1.7913454	0.4936378
17.5	0.5286264	1.8900484	0.4186896
7.5	0.6416383	1.9818243	0.3421979
May 28.5	0.7526370	2.0673604	0.2646216
18.5	0.8615925	2.1472689	0.1863194
8.5	0.9685118	2.2220914	0.1075714
Apr. 28.5	1.0734268	2.2923062	+ 0.0285967
18.5	1.1763847	2.3583350	— 0.0504330
8.5	1.2774430	2.4205500	0.1293837
Mar. 29.5	1.3766643	2.4792799	0.2081500
19.5	1.4741143	2.5348161	0.2866497
9.5	1.5698591	2.5874170	0.3648189
Feb. 27.5	1.6639642	2.6373129	0.4426078
17.5	1.7564937	2.6847094	0.5199782
7.5	1.8475094	2.7297903	0.5969008
Jan. 28.5	1.9370709	2.7727211	0.6733539
18.5	2.0252351	2.8136504	0.7493215
8.5	2.1120571	2.8527134	0.8247919
1886 Dec. 19.5	2.2818754	2.9257130	0.9742160
Nov. 29.5	+ 2.4469081	+ 2.9925669	— 1.1215993

Table II

G. M. T.	x	y	z
1886 Nov. 9.5	+ 2.6074984	+ 3.0539798	— 1.2669478
Oct. 20.5	2.7639546	3.1105440	1.4102882
Sep. 30.5	2.9165535	3.1627615	1.5516605
10.5	3.0655440	3.2110609	1.6911126
Aug. 21.5	3.2111508	3.2558115	1.8286974
1.5	3.3535769	3.2973328	1.9644698
Jul. 12.5	3.4930061	3.3359038	2.0984854
Jun. 22.5	3.6296057	3.3717687	2.2307998
2.5	3.7635282	3.4051431	2.3614672
May 13.5	3.8949128	3.4362179	2.4905405
Apr. 23.5	4.0238871	3.4651630	2.6180709
3.5	4.1505684	3.4921303	2.7441075
Mar. 14.5	4.2750647	3.5172559	2.8686977
Feb. 22.5	4.3974757	3.5406627	2.9918866
2.5	4.5178934	3.5624615	3.1137175
Jan. 13.5	4.6364035	3.5827529	3.2342316
1885 Dec. 24.5	4.7530854	3.6016284	3.3534684
4.5	4.8680130	3.6191714	3.4714655
Nov. 14.5	4.9812553	3.6354583	3.5882588
Oct. 25.5	5.0928768	3.6505591	3.7038824
5.5	5.2029377	3.6645381	3.8183690
Sep. 15.5	5.3114946	3.6774545	3.9317499
Aug. 26.5	5.4186007	3.6893631	4.0440547
6.5	5.5243058	3.7003145	4.1553120
Jul. 17.5	5.6286570	3.7103557	4.2655489
Jun. 27.5	5.7316986	3.7195303	4.3747914
7.5	5.8334726	3.7278788	4.4830644
May 18.5	5.9340185	3.7354391	4.5903918
Apr. 28.5	6.0333738	3.7422464	4.6967963
8.5	6.1315741	3.7483338	4.8022997
Mar. 19.5	6.2286530	3.7537321	4.9069232
Feb. 27.5	6.3246425	3.7584703	5.0106867
Jan. 8.5	6.5600469	3.7676026	5.2664583
1884 Nov. 19.5	+ 6.7892667	+ 3.7731582	— 5.5172560

Table II

G. M. T.	x	y	z
1884 Sep. 30.5 . . .	+ 7.0126908	+ 3.7754675	— 5.7633357
Aug. 11.5 . . .	7.2306664	3.7748182	6.0049304
Jun. 22.5 . . .	7.4435052	3.7714616	6.2422530
May 3.5 . . .	7.6514886	3.7656190	6.4754987
Mar. 14.5 . . .	7.8548708	3.7574859	6.7048466
Jan. 24.5 . . .	8.0538834	3.7472363	6.9304622
1883 Dec. 5.5 . . .	8.2487373	3.7350255	7.1524981
Oct. 16.5 . . .	8.4396253	3.7209926	7.3710958
Aug. 27.5 . . .	8.6267248	3.7052629	7.5863866
Jul. 8.5 . . .	8.8101985	3.6879497	7.7984926
May 19.5 . . .	8.9901969	3.6691557	8.0075278
Mar. 30.5 . . .	9.1668591	3.6489743	8.2135986
Feb. 8.5 . . .	9.3403139	3.6274909	8.4168044
1882 Dec. 20.5 . . .	9.5106811	3.6047834	8.6172385
Oct. 31.5 . . .	9.6780723	3.5809237	8.8149886
Sep. 11.5 . . .	9.8425915	3.5559777	9.0101369
Jul. 23.5 . . .	10.0043358	3.5300065	9.2027610
Jun. 3.5 . . .	10.1633963	3.5030666	9.3929340
Apr. 14.5 . . .	10.3198584	3.4752103	9.5807248
Feb. 23.5 . . .	10.4738024	3.4464865	9.7661987
Jan. 4.5 . . .	10.6253037	3.4169407	9.9494173
1881 Nov. 15.5 . . .	10.7744335	3.3866155	10.1304390
Aug. 7.5 . . .	11.0658444	3.3237838	10.4861108
Apr. 29.5 . . .	11.3485311	3.2582825	10.8336249
Jan. 19.5 . . .	11.6229409	3.1903702	11.1733526
1880 Oct. 11.5 . . .	11.8894789	3.1202781	11.5056316
Jul. 3.5 . . .	12.1485149	3.0482140	11.8307694
Mar. 25.5 . . .	12.4003882	2.9743653	12.1490478
1879 Dec. 16.5 . . .	12.6454117	2.8989018	12.4607254
Sep. 7.5 . . .	12.8838759	2.8219773	12.7660410
May 30.5 . . .	13.1160510	2.7437312	13.0652154
Feb. 19.5 . . .	13.3421894	2.6642901	13.3584540
1878 Nov. 11.5 . . .	13.5625277	2.5837681	13.6459480
Aug. 3.5 . . .	+ 13.7772876	+ 2.5022688	— 13.9278762

Table II

G. M. T.	x	y	z
1878 Apr. 25.5 . . .	+ 13.9866777	+ 2.4198854	— 14.2044062
Jan. 15.5 . . .	14.1908940	2.3367016	14.4756957
1877 Oct. 7.5 . . .	14.3901210	2.2527928	14.7418931
Jun. 29.5 . . .	14.5845320	2.1682265	15.0031387
Mar. 21.5 . . .	14.7742902	2.0830629	15.2595652
1876 Dec. 11.5 . . .	14.9595494	1.9973562	15.5112984
Sept. 2.5 . . .	15.1404538	1.9111545	15.7584575
May 25.5 . . .	15.3171393	1.8245006	16.0011562
Feb. 15.5 . . .	15.4897337	1.7374330	16.2395022
1875 Nov. 7.5 . . .	15.6583571	1.6499856	16.4735986
Jul. 30.5 . . .	15.8231222	1.5621888	16.7035433
Apr. 21.5 . . .	15.9841352	1.4740698	16.9294301
Jan. 11.5 . . .	16.1414956	1.3856521	17.1513482
1874 Oct. 3.5 . . .	16.2952968	1.2969572	17.3693832
Jun. 25.5 . . .	16.4456266	1.2080040	17.5836169
Mar. 17.5 . . .	16.5925670	1.1188093	17.7941275
1873 Aug. 29.5 . . .	16.8765816	0.9397532	18.2042760
Feb. 10.5 . . .	17.1478948	0.7598906	18.6003909
1872 Jul. 25.5 . . .	17.4069855	0.5793053	18.9829874
Jan. 7.5 . . .	17.6542621	0.3980720	19.3525368
1871 Jun. 21.5 . . .	17.8900686	0.2162654	19.7094674
1870 Dec. 3.5 . . .	18.1146919	+ 0.0339702	20.0541653
May 17.5 . . .	18.3283725	— 0.1487094	20.3869739
1869 Oct. 29.5 . . .	18.5313190	0.3316411	20.7081944
Apr. 12.5 . . .	18.7237264	0.5146619	21.0180873
1868 Sep. 24.5 . . .	18.9057953	0.6975808	21.3168773
Mar. 8.5 . . .	19.0777477	0.8801904	21.6047605
1867 Aug. 21.5 . . .	19.2398359	1.0622819	21.8819133
Feb. 2.5 . . .	19.3923425	1.2436625	22.1485021
1866 Jul. 17.5 . . .	19.5355715	1.4241688	22.4046896
1865 Dec. 29.5 . . .	19.6698361	1.6036743	22.6506405
Jun. 12.5 . . .	19.7954454	1.7820908	22.8865206
1864 Nov. 24.5 . . .	19.9126933	1.9593663	23.1124983
May 8.5 . . .	+ 20.0218514	— 2.1354787	— 23.3287424

Table II

G. M. T.	x	y	z
1863 Oct. 21.5 . . .	+ 20.1231635	— 2.3104310	— 23.5354199
Apr. 4.5 . . .	20.2168442	2.4842450	23.7326949
1862 Sep. 16.5 . . .	20.3030769	2.6569562	23.9207270
Feb. 28.5 . . .	20.3820139	2.8286103	24.0996701
1861 Aug. 12.5 . . .	20.4537753	2.9992582	24.2696713
Jan. 24.5 . . .	20.5184485	3.1689522	24.4308692
1860 Jul. 8.5 . . .	20.5760879	3.3377412	24.5833932
1859 Dec. 21.5 . . .	20.6267150	3.5056638	24.7273600
Jun. 4.5 . . .	20.6703200	3.6727415	24.8628717
1858 Nov. 16.5 . . .	20.7068665	3.8389704	24.9900124
Apr. 30.5 . . .	20.7363004	4.0043133	25.1088454
1857 Oct. 12.5 . . .	20.7585625	4.1686937	25.2194110
Mar. 26.5 . . .	20.7736050	4.3319960	25.3217274
1856 Sep. 7.5 . . .	20.7814081	4.4940718	25.4157940
Feb. 20.5 . . .	20.7819921	4.6547530	25.5015974
1855 Aug. 4.5 . . .	20.7754222	4.8138690	25.5791193
Jan. 16.5 . . .	20.7618043	4.9712639	25.6483441
1854 Jun. 30.5 . . .	20.7412734	5.1268085	25.7092638
1853 Dec. 12.5 . . .	20.7139799	5.2804065	25.7618806
May 26.5 . . .	20.6800761	5.4319954	25.8062070
1852 Nov. 7.5 . . .	20.6397048	5.5815424	25.8422632
Apr. 21.5 . . .	20.5929925	5.7290392	25.8700761
1851 Oct. 4.5 . . .	20.5400450	5.8744969	25.8896752
Mar. 18.5 . . .	20.4809447	6.0179403	25.9010919
1850 Aug. 30.5 . . .	20.4157478	6.1594030	25.9043560
Feb. 11.5 . . .	20.3444860	6.2989244	25.8994953
1849 Jul. 26.5 . . .	20.2671676	6.4365450	25.8865338
Jan. 7.5 . . .	20.1837576	6.5723023	25.8654896
1848 Jun. 21.5 . . .	20.0942156	6.7062261	25.8363723
1847 Dec. 4.5 . . .	19.9984575	6.8383320	25.7991813
May 18.5 . . .	19.8963768	6.9686135	25.7539019
1846 Oct. 30.5 . . .	19.7878461	7.0970344	25.7005020
Apr. 13.5 . . .	19.6727268	7.2235211	25.6389290
1845 Sep. 25.5 . . .	+ 19.5508830	— 7.3479586	— 25.5691086

Table II

G. M. T.	x	y	z
1845 Mar. 9.5 . . .	+ 19.4221979	— 7.4701922	— 25.4909454
1844 Aug. 21.5 . . .	19.2865889	7.5900364	25.4043273
Feb. 3.5 . . .	19.1440175	7.7072901	25.3091319
1843 Jul. 18.5 . . .	18.9944901	7.8217536	25.2052340
1842 Dec. 30.5 . . .	18.8380512	7.9332449	25.0925122
Jun. 13.5 . . .	18.6747700	8.0416095	24.9708531
1841 Nov. 25.5 . . .	18.5047257	8.1467247	24.8401518
May 9.5 . . .	18.3279944	8.2484976	24.7003114
1840 Oct. 21.5 . . .	18.1446389	8.3468617	24.5512400
Apr. 4.5 . . .	17.9547019	8.4417693	24.3928475
1839 Sep. 17.5 . . .	17.7582019	8.5331866	24.2250431
Mar. 1.5 . . .	17.5551311	8.6210879	24.0477317
1838 Aug. 13.5 . . .	17.3454537	8.7054510	23.8608129
Jan. 25.5 . . .	17.1291046	8.7862525	23.6641775
1837 Jul. 9.5 . . .	16.9059883	8.8634642	23.4577059
1836 Dec. 21.5 . . .	16.6759773	8.9370471	23.2412651
Jun. 4.5 . . .	16.4389112	9.0069462	23.0147060
1835 Nov. 17.5 . . .	16.1945969	9.0730826	22.7778590
May 1.5 . . .	15.9428111	9.1353452	22.5305306
1834 Oct. 13.5 . . .	15.6833063	9.1935810	22.2724980
Mar. 27.5 . . .	15.4158215	9.2475880	22.0035051
1833 Sep. 8.5 . . .	15.1400966	9.2971112	21.7232615
Feb. 20.5 . . .	14.8558881	9.3418455	21.4314414
1832 Aug. 4.5 . . .	14.5629823	9.3814457	21.1276877
Jan. 17.5 . . .	14.2612011	9.4155406	20.8116167
1831 Jul. 1.5 . . .	13.9503988	9.4437493	20.4828238
1830 Dec. 13.5 . . .	13.6304516	9.4656929	20.1408865
May 27.5 . . .	13.3012411	9.4809995	19.7853647
1829 Nov. 8.5 . . .	12.9626394	9.4893029	19.4157974
Apr. 22.5 . . .	12.6144942	9.4902360	19.0316966
1828 Oct. 4.5 . . .	12.2566183	9.4834201	18.6325391
Jun. 26.5 . . .	12.0739611	9.4769824	18.4271391
Mar. 18.5 . . .	11.8887811	9.4684545	18.2177584
1827 Dec. 9.5 . . .	+ 11.7010415	— 9.4577810	— 18.0043177

Table II

G. M. T.	x	y	z
1827 Aug. 31.5 . . .	+ 11.5107024	— 9.4449030	— 17.7867338
May 23.5 . . .	11.3177202	9.4297585	17.5649189
Feb. 12.5 . . .	11.1220472	9.4122816	17.3387806
1826 Nov. 4.5 . . .	10.9236323	9.3924019	17.1082213
Jul. 27.5 . . .	10.7224199	9.3700443	16.8731377
Apr. 18.5 . . .	10.5183500	9.3451281	16.6334206
Jan. 8.5 . . .	10.3113639	9.3175669	16.3889541
1825 Sep. 30.5 . . .	10.1013747	9.2872667	16.1396144
Jun. 22.5 . . .	9.8883255	9.2541270	15.8852709
Mar. 14.5 . . .	9.6721305	9.2180384	15.6257836
1824 Dec. 4.5 . . .	9.4527040	9.1788819	15.3610030
Aug. 26.5 . . .	9.2299544	9.1365282	15.0907695
May 18.5 . . .	9.0037838	9.0908361	14.8149115
Feb. 8.5 . . .	8.7740874	9.0416510	14.5332452
1823 Oct. 31.5 . . .	8.5407537	8.9888037	14.2455724
Jul. 23.5 . . .	8.3036640	8.9321080	13.9516794
Apr. 14.5 . . .	8.0626922	8.8713589	13.6513356
Jan. 4.5 . . .	7.8177041	8.8063303	13.3442909
1822 Sep. 26.5 . . .	7.5685581	8.7367725	13.0302739
Jun. 18.5 . . .	7.3151038	8.6624089	12.7089897
Mar. 10.5 . . .	7.0571824	8.5829325	12.3801165
1821 Nov. 30.5 . . .	6.7946260	8.4980028	12.0433028
Aug. 22.5 . . .	6.5272569	8.4072397	11.6981632
May 14.5 . . .	6.2548870	8.3102198	11.3442748
Feb. 3.5 . . .	5.9773160	8.2064678	10.9811702
1820 Oct. 26.5 . . .	5.6943305	8.0954496	10.6083330
Jul. 18.5 . . .	5.4057020	7.9765614	10.2251883
Apr. 9.5 . . .	5.1111841	7.8491166	9.8310942
1819 Dec. 31.5 . . .	4.8105101	7.7123290	9.4253292
Sep. 22.5 . . .	4.5033893	7.5652917	9.0070775
Aug. 3.5 . . .	4.3473133	7.4876057	8.7929838
Jun. 14.5 . . .	4.1895034	7.4069472	8.5754094
Apr. 25.5 . . .	4.0299156	7.3231544	8.3542173
Mar. 6.5 . . .	+ 3.8685017	— 7.2360513	— 8.1292582

Table II

G. M. T.	x	y	z
1819 Jan. 15.5	+ 3.705213	— 7.145444	— 7.900458
1818 Nov. 26.5	3.539998	7.051121	7.667388
Oct. 7.5	3.372799	6.952849	7.430117
Aug. 18.5	3.203561	6.850368	7.188354
Jun. 29.5	3.032222	6.743389	6.941880
May 10.5	2.858720	6.631594	6.690449
Mar. 21.5	2.682988	6.514618	6.433798
Jan. 30.5	2.504957	6.392057	6.171631
1817 Dec. 11.5	2.324559	6.263446	5.903625
Oct. 22.5	2.141719	6.128257	5.629420
Sep. 2.5	1.956370	5.985882	5.348614
Jul. 14.5	1.768442	5.835615	5.060755
May 25.5	1.577870	5.676628	4.765336
Apr. 5.5	1.384608	5.507944	4.461779
Feb. 14.5	1.188614	5.328394	4.149425
1816 Dec. 26.5	0.989883	5.136566	3.827514
Nov. 6.5	0.788458	4.930721	3.495170
Oct. 12.5	0.686766	4.821886	3.324772
Sep. 17.5	0.584454	4.708693	3.151370
Aug. 23.5	0.481554	4.590777	2.974808
Jul. 29.5	0.378115	4.467723	2.794919
4.5	0.274200	4.339056	2.611519
Jun. 9.5	0.169896	4.204222	2.424411
May 15.5	+ 0.065317	4.062586	2.233383
Apr. 20.5	— 0.039380	3.913393	2.038206
Mar. 26.5	0.143991	3.755757	1.838638
1.5	0.248234	3.588615	1.634424
Feb. 5.5	0.351722	3.410685	1.425308
Jan. 24.0	0.403026	3.317197	1.318833
11.5	0.453927	3.220398	1.211043
1815 Dec. 30.0	0.504325	3.120033	1.101914
17.5	0.554101	3.015816	0.991427
5.0	0.603108	2.907430	0.879570
Nov. 22.5	— 0.651175	— 2.794512	— 0.766345

Table II

G. M. T.	x	y	z
1815 Nov. 10.0	— 0.698090	— 2.676656	— 0.651769
Oct. 28.5	0.743595	2.553402	0.535883
16.0	0.787372	2.424229	0.418759
3.5	0.829030	2.288545	0.300518
Sep. 21.0	0.868081	2.145680	0.181343
8.5	0.903912	1.994880	0.061507
2.25	0.920387	1.916245	— 0.001462
Aug. 27.0	0.935754	1.835303	+ 0.058583
20.75	0.949884	1.751937	0.118551
14.5	0.962632	1.666026	0.178343
8.25	0.973838	1.577446	0.237849
2.0	0.983317	1.486074	0.296931
Jul. 26.75	0.990867	1.391788	0.355429
20.5	0.996260	1.294476	0.413150
14.25	0.999243	1.194036	0.469870
8.0	0.999539	1.090392	0.525323
1.75	0.996847	0.983491	0.579202
Jun. 25.5	0.990842	0.873329	0.631153
19.25	0.981185	0.759954	0.680775
13.0	— 0.967531	— 0.643490	+ 0.727618

Table III.

G. M. T.	x	y	z
1887 Sep. 25.5	— 0.6187421	+ 0.4685024	+ 0.9349430
30.5	0.6652102	0.3703056	0.9342568
Oct. 5.5	0.7088701	0.2705473	0.9296264
10.5	0.7494988	0.1696326	0.9210216
15.5	0.7869192	+ 0.0679914	0.9084740
20.5	0.8210074	— 0.0339390	0.8920789
25.5	0.8516961	0.1357308	0.8719887
30.5	0.8789738	0.2369816	0.8484049
Nov. 4.5	0.9028809	0.3373266	0.8215660
9.5	0.9235030	0.4364474	0.7917362
14.5	0.9409623	0.5340769	0.7591930
19.5	0.9554085	0.6299996	0.7242170
24.5	0.9670104	0.7240500	0.6870830
29.5	0.9759476	0.8161084	0.6480539
Dec. 4.5	0.9824041	0.9060954	0.6073758
9.5	0.9865629	0.9939660	0.5652756
14.5	0.9886023	1.0797039	0.5219594
19.5	0.9886929	1.1633159	0.4776129
24.5	0.9869958	1.2448267	0.4324015
29.5	0.9836619	1.3242751	0.3864717
1888 Jan. 3.5	0.9788309	1.4017100	0.3399526
8.5	0.9726320	1.4771876	0.2929574
13.5	0.9651834	1.5507689	0.2455847
18.5	0.9565936	1.6225179	0.1979207
23.5	0.9469615	1.6925001	0.1500402
28.5	0.9363770	1.7607812	0.1020080
Feb. 2.5	0.9249220	1.8274264	+ 0.0538802
12.5	0.8996919	1.9560640	— 0.0424748
22.5	0.8717892	2.0789032	0.1387115
Mar. 3.5	0.8416422	2.1964005	0.2345978
13.5	0.8096056	2.3089744	0.3299632
23.5	0.7759745	2.4170062	0.4246837
Apr. 2.5	0.7409948	2.5208413	0.5186702
12.5	— 0.7048727	— 2.6207916	— 0.6118603

Table III.

$\sum X'$	$\sum Y'$	$\sum Z'$	$\sum X$	$\sum Y$	$\sum Z$
— 135	— 128	— 90	+ 130	+ 128	+ 53
137	132	95	131	124	50
140	136	100	132	119	48
143	141	106	133	114	46
147	145	111	135	110	44
152	150	117	138	106	42
157	155	122	142	102	40
163	160	128	146	100	39
169	166	134	150	98	38
176	172	140	156	98	37
183	178	146	161	96	36
191	184	153	167	97	36
198	190	159	172	97	36
207	198	166	177	99	37
216	206	172	183	102	38
225	214	179	188	105	39
235	221	186	193	108	40
245	229	193	197	112	42
255	237	200	201	118	44
265	245	207	203	124	46
276	254	214	205	129	49
288	263	222	206	135	52
300	271	229	208	141	54
311	278	237	208	148	57
321	284	245	208	154	60
334	296	251	206	160	63
354	308	256	204	167	66
1532	1315	1081	788	710	286
1661	1404	1134	754	748	305
1800	1495	1183	711	776	319
1952	1590	1232	666	796	332
2116	1689	1278	619	808	338
2292	1790	1320	574	810	340
— 2482	— 1897	— 1359	+ 533	+ 805	+ 341

Table III

G. M. T.			x	y	z
1888	Apr.	22.5	— 0.6677816	— 2.7171392	— 0.7042119
	May	2.5	0.6298682	2.8101384	0.7956980
		12.5	0.5912568	2.9000193	0.8863030
		22.5	0.5520536	2.9869901	0.9760203
	Jun.	1.5	0.5123493	3.0712396	1.0648500
		11.5	0.4722218	3.1529393	1.1527968
		21.5	0.4317385	3.2322451	1.2398694
	Jul.	1.5	0.3909574	3.3092994	1.3260793
		11.5	0.3499292	3.3842323	1.4114397
		21.5	0.3086977	3.4571628	1.4959655
		31.5	0.2673015	3.5282003	1.5796722
	Aug.	10.5	0.2257742	3.5974453	1.6625764
		20.5	0.1841454	3.6649903	1.7446945
		30.5	0.1424411	3.7309209	1.8260434
	Sep.	9.5	0.1006845	3.7953162	1.9066398
		19.5	— 0.0588958	3.8582495	1.9865002
	Oct.	9.5	+ 0.0247075	3.9799973	2.1440783
		29.5	0.1082478	4.0966540	2.2989039
	Nov.	18.5	0.1916294	4.2086449	2.4510968
	Dec.	8.5	0.2747772	4.3163428	2.6007696
		28.5	0.3576326	4.4200732	2.7480279
1889	Jan.	17.5	0.4401504	4.5201246	2.8929706
	Feb.	6.5	0.5222966	4.6167527	3.0356908
		26.5	0.6040462	4.7101850	3.1762767
	Mar.	18.5	0.6853813	4.8006257	3.3148118
	Apr.	7.5	0.7662896	4.8882585	3.4513758
		27.5	0.8467626	4.9732497	3.5860446
	May	17.5	0.9267951	5.0557507	3.7188902
	Jun.	6.5	1.0063837	5.1358992	3.8499810
		26.5	1.0855269	5.2138218	3.9793818
	Jul.	16.5	1.1642241	5.2896342	4.1071534
	Aug.	5.5	1.2424740	5.3634433	4.2333536
		25.5	1.3202836	5.4353472	4.3580365
	Sep.	14.5	+ 1.3976490	— 5.5054368	— 4.4812533

Table III

$\sum X'$	$\sum Y'$	$\sum Z'$	$\sum X$	$\sum Y$	$\sum Z$
— 2686	— 2008	— 1392	+ 499	+ 793	+ 337
2902	2120	1417	471	775	329
3138	2240	1436	453	757	320
3390	2364	1445	443	737	310
3660	2492	1442	444	724	302
3949	2625	1426	449	713	295
4259	2764	1395	460	708	291
4590	2904	1345	473	711	291
4941	3045	1273	485	723	294
5314	3187	1177	495	744	300
5706	3328	1051	499	767	311
6116	3464	893	496	797	323
6542	3594	697	483	828	336
6981	3715	463	460	858	350
7427	3822	— 185	432	880	362
7877	3914	+ 147	395	901	372
35018	16141	3811	1428	3259	1362
38141	16099	7866	1327	3298	1382
40488	15413	12611	1224	3335	1400
41675	14000	17754	1121	3369	1418
41404	11883	22836	1016	3401	1433
39575	9220	27313	909	3430	1448
36376	6274	30715	801	3457	1462
32183	3354	32743	692	3480	1475
27504	— 719	33362	582	3501	1487
22801	+ 1465	32760	470	3520	1497
18430	3131	31238	357	3535	1507
14592	4306	29130	243	3548	1514
11358	5057	26719	127	3557	1522
8716	5474	24227	+ 12	3564	1527
6603	5641	21799	— 104	3568	1531
4943	5634	19520	222	3568	1534
3650	5510	17437	340	3565	1536
— 2640	+ 5309	+ 15561	— 459	+ 3559	+ 1535

Table III

G. M. T.	x	y	z
1889 Oct. 4.5	+ 1.4745745	— 5.5737964	— 4.6030521
24.5	1.5510628	5.6405040	4.7234785
Nov. 13.5	1.6271173	5.7056321	4.8425755
Dec. 3.5	1.7027414	5.7692483	4.9603835
23.5	1.7779388	5.8314155	5.0769410
1890 Jan. 12.5	1.8527134	5.8921927	5.1922846
Feb. 1.5	1.9270693	5.9516349	5.3064485
Mar. 13.5	2.0745422	6.0667178	5.5313674
Apr. 22.5	2.2203923	6.1770407	5.7519412
Jun. 1.5	2.3646550	6.2829374	5.9683910
Jul. 11.5	2.5073664	6.3847049	6.1809182
Aug. 20.5	2.6485621	6.4826092	6.3897068
Sep. 29.5	2.7882771	6.5768895	6.5949257
Nov. 8.5	2.9265460	6.6677617	6.7967302
Dec. 18.5	3.0634023	6.7554214	6.9952638
1891 Jan. 27.5	3.1988787	6.8400467	7.1906592
Mar. 8.5	3.3330068	6.9218000	7.3830394
Apr. 17.5	3.4658171	7.0008302	7.5725191
May 27.5	3.5973393	7.0772738	7.7592048
Jul. 6.5	3.7276019	7.1512566	7.9431964
Aug. 15.5	3.8566324	7.2228949	8.1245870
Sep. 24.5	3.9844575	7.2922962	8.3034642
Nov. 3.5	4.1111027	7.3595603	8.4799102
Dec. 13.5	4.2365928	7.4247799	8.6540022
1892 Jan. 22.5	4.3609517	7.4880415	8.8258131
Mar. 2.5	4.4842023	7.5494258	8.9954116
Apr. 11.5	4.6063670	7.6090082	9.1628628
May 21.5	4.7274673	7.6668594	9.3282281
Jun. 30.5	4.8475239	7.7230457	9.4915658
Sep. 18.5	5.0845859	7.8306692	9.8123768
Dec. 7.5	5.3177062	7.9323353	10.1257059
1893 Feb. 25.5	5.5470290	8.0284497	10.4319248
May 16.5	5.7726896	8.1193755	10.7313713
Aug. 4.5	+ 5.9948155	— 8.2054387	— 11.0243538

Table III.

$\sum X'$	$\sum Y'$	$\sum Z'$	$\sum X$	$\sum Y$	$\sum Z$
— 1889	+ 5067	+ 13892	— 577	+ 3550	+ 1535
1307	4801	12416	697	3538	1531
864	4530	11116	816	3522	1528
531	4260	9973	936	3503	1523
280	4000	8969	1054	3481	1515
— 94	3751	8087	1174	3455	1507
+ 43	3516	7311	1293	3425	1498
848	12365	24091	6120	13416	5892
1163	10899	20056	7057	13078	5769
1267	9642	16864	7979	12685	5622
1250	8567	14315	8881	12233	5449
1168	7645	12260	9758	11724	5251
1051	6854	10586	10607	11158	5029
919	6172	9213	11421	10537	4782
784	5582	8075	12198	9863	4511
652	5068	7125	12929	9136	4217
528	4620	6326	13611	8360	3899
412	4227	5650	14241	7535	3561
305	3880	5074	14812	6669	3202
208	3573	4580	15321	5763	2825
120	3301	4155	15762	4822	2431
+ 40	3058	3786	16134	3848	2021
— 31	2841	3465	16434	2847	1601
96	2646	3185	16656	1828	1166
154	2470	2938	16800	+ 792	725
206	2311	2721	16864	— 253	+ 278
252	2167	2529	16847	1302	— 173
294	2037	2358	16750	2348	626
1328	7670	8824	66279	13547	4299
1587	6836	7793	63881	21655	7839
1798	6133	6960	60256	29347	11233
1971	5535	6282	55495	36450	14399
2114	5023	5723	49726	42811	17272
— 2234	+ 4581	+ 5261	— 43103	— 48314	— 19797

Table III

G. M. T.	x	y	z
1893 Oct. 23.5 . . .	+ 6.2135272	— 8.2869328	— 11.3111546
1894 Jan. 11.5 . . .	6.4289384	8.3641232	11.5920329
Apr. 1.5 . . .	6.6411566	8.4372505	11.8672272
Jun. 20.5 . . .	6.8502837	8.5065332	12.1369577
Sep. 8.5 . . .	7.0564158	8.5721705	12.4014282
Nov. 27.5 . . .	7.2596440	8.6343442	12.6608272
1895 Feb. 15.5 . . .	7.4600545	8.6932207	12.9153303
May 6.5 . . .	7.6577286	8.7489526	13.1651007
Jul. 25.5 . . .	7.8527436	8.8016800	13.4102905
Oct. 13.5 . . .	8.0451721	8.8515319	13.6510418
1896 Jan. 1.5 . . .	8.2350828	8.8986274	13.8874878
Mar. 21.5 . . .	8.4225409	8.9430765	14.1197531
Jun. 9.5 . . .	8.6076075	8.9849810	14.3479548
Aug. 28.5 . . .	8.7903405	9.0244355	14.5722030
Nov. 16.5 . . .	8.9707947	9.0615277	14.7926013
1897 Feb. 4.5 . . .	9.1490214	9.0963394	15.0092475
Jul. 14.5 . . .	9.4989839	9.1594214	15.4316477
Dec. 21.5 . . .	9.8405841	9.2142343	15.8400841
1898 May 30.5 . . .	10.1741377	9.2612642	16.2351681
Nov. 6.5 . . .	10.4999237	9.3009416	16.6174517
1899 Apr. 15.5 . . .	10.8181884	9.3336506	16.9874357
Sep. 22.5 . . .	11.1291476	9.3597368	17.3455762
1900 Mar. 1.5 . . .	11.4329896	9.3795138	17.6922907
Aug. 8.5 . . .	11.7298774	9.3932696	18.0279634
1901 Jan. 15.5 . . .	12.0199513	9.4012721	18.3529499
Jun. 24.5 . . .	12.3033316	9.4037740	18.6675811
Dec. 1.5 . . .	12.5801215	9.4010176	18.9721674
1902 May 10.5 . . .	12.8504114	9.3932391	19.2670022
Oct. 17.5 . . .	13.1142832	9.3806717	19.5523645
1903 Mar. 26.5 . . .	13.3718156	9.3635477	19.8285214
Sep. 2.5 . . .	13.6230901	9.3420990	20.0957291
1904 Feb. 9.5 . . .	13.8681954	9.3165551	20.3542333
Jul. 18.5 . . .	14.1072320	9.2871400	20.6042682
Dec. 25.5 . . .	+ 14.3403142	— 9.2540671	— 20.8460553

Table III

$\sum X'$	$\sum Y'$	$\sum Z'$	$\sum X$	$\sum Y$	$\sum Z$
— 2334	+ 4196	+ 4875	— 35791	— 52865	— 21931
2420	3860	4552	27969	56404	23642
2495	3564	4281	19822	58905	24916
2560	3301	4052	11516	60371	25749
2619	3068	3860	— 3220	60831	26151
2672	2858	3697	+ 4925	60335	26137
2722	2670	3561	12793	58944	25733
2768	2500	3447	20273	56738	24970
2811	2343	3353	27282	53797	23878
2856	2205	3277	33750	50214	22499
2898	2076	3216	39631	46071	20863
2940	1957	3169	44883	41452	19010
2982	1847	3135	49487	36437	16969
3025	1747	3114	53429	31100	14775
3067	1652	3103	56709	25512	12456
12442	6259	12414	237289	78938	40155
12798	5627	12539	250349	— 31327	— 20027
13163	5077	12821	253209	+ 16839	+ 588
13532	4598	13259	246223	64202	21103
13890	4188	13853	229730	109537	40986
14214	3852	14600	204040	151630	59702
14469	3601	15492	169473	189169	76684
14604	3451	16504	126472	220675	91287
14557	3425	17579	75744	244466	102772
14264	3541	18623	+ 18463	258664	110302
13680	3802	19499	— 43515	261327	113000
12804	4183	20049	107461	250696	110042
11703	4623	20145	169685	225568	100823
10496	5040	19741	225663	185751	85151
9317	5357	18897	270445	132536	63458
8270	5532	17750	299359	+ 68955	36928
7405	5564	16459	308921	— 310	+ 7489
6726	5477	15155	297647	69454	— 22408
— 6212	+ 5307	+ 13922	—266512	—132487	— 50170

Table III

G. M. T.	x	y	z
1905 Jun. 3.5 . . .	+ 14.5675693	— 9.2175349	— 21.0798018
Nov. 10.5 . . .	14.7891352	9.1777220	21.3056995
1906 Apr. 19.5 . . .	15.0051558	9.1347847	21.5239237
Sep. 26.5 . . .	15.2157760	9.0888558	21.7346336
1907 Mar. 5.5 . . .	15.4211367	9.0400459	21.9379723
Aug. 12.5 . . .	15.6213704	8.9884450	22.1340688
1908 Jan. 19.5 . . .	15.8165989	8.9341258	22.3230391
Jun. 27.5 . . .	16.0069310	8.8771466	22.5049878
Dec. 4.5 . . .	16.1924619	8.8175542	22.6800098
1909 May 13.5 . . .	16.3732727	8.7553869	22.8481917
Oct. 20.5 . . .	16.5494311	8.6906764	23.0096127
1910 Mar. 29.5 . . .	16.7209916	8.6234496	23.1643460
Sep. 5.5 . . .	16.8879956	8.5537310	23.3124595
1911 Feb. 12.5 . . .	17.0504726	8.4815432	23.4540167
Jul. 22.5 . . .	17.2084403	8.4069091	23.5890774
Dec. 29.5 . . .	17.3619048	8.3298528	23.7176985
1912 Jun. 6.6 . . .	17.5108616	8.2504018	23.8399349
Nov. 13.5 . . .	17.6552962	8.1685882	23.9558403
1913 Apr. 22.5 . . .	17.7951853	8.0844511	24.0654683
Sep. 29.5 . . .	17.9304988	7.9980384	24.1688734
1914 Mar. 8.5 . . .	18.0612026	7.9094086	24.2661116
Aug. 15.5 . . .	18.1872619	7.8186324	24.3572425
1915 Jan. 22.5 . . .	18.3086460	7.7257923	24.4423275
Jul. 1.5 . . .	18.4253327	7.6309828	24.5214318
Dec. 8.5 . . .	18.5373134	7.5343063	24.5946218
1916 May 16.5 . . .	18.6445962	7.4358699	24.6619643
Oct. 23.5 . . .	18.7472078	7.3357789	24.7235234
1917 Apr. 1.5 . . .	18.8451924	7.2341318	24.7793585
Sep. 8.5 . . .	18.9386092	7.1310145	24.8295220
1918 Feb. 15.5 . . .	19.0275270	7.0264972	24.8740576
Jul. 25.5 . . .	19.1120194	6.9206325	24.9129993
1919 Jan. 1.5 . . .	19.1921587	6.8134556	24.9463720
Jun. 10.5 . . .	19.2680123	6.7049861	24.9741914
Nov. 17.5 . . .	+ 19.3396384	— 6.5952303	— 24.9964655

Table III.

$\sum X'$	$\sum Y'$	$\sum Z'$	$\sum X$	$\sum Y$	$\sum Z$
— 5834	+ 5085	+ 12805	—218812	—184249	— 73499
5562	4839	11817	159481	221209	90764
5376	4580	10960	94129	241817	101161
5257	4322	10223	— 28085	246363	104684
5193	4068	9597	+ 34240	236499	101933
5176	3819	9072	89643	214664	93881
5193	3580	8638	136104	183561	81635
5257	3345	8293	172591	145787	66284
5346	3118	8028	198735	103641	48808
5463	2898	7841	214614	59062	30042
5605	2686	7731	220505	— 13664	— 10684
5768	2481	7697	216761	+ 31192	+ 8674
5947	2287	7741	203717	74275	27491
6134	2106	7864	181690	114382	45246
6319	1945	8065	151006	150234	61383
6488	1811	8341	112101	180398	75271
6620	1718	8681	65657	203235	86193
6693	1679	9060	+ 12797	216932	93345
6684	1707	9440	— 44706	219598	95869
6576	1807	9770	104248	209500	92962
6365	1974	9989	162279	185412	84006
6070	2183	10045	214408	147067	68784
5724	2402	9913	255780	95617	47671
5369	2592	9604	281739	+ 33930	+ 21784
5043	2724	9161	288724	— 33465	— 7021
4774	2788	8646	275106	100864	36334
4563	2781	8101	241671	162280	63569
4417	2720	7585	191568	212473	86392
4326	2616	7111	129653	247768	103118
4282	2487	6703	— 61543	266462	112867
4277	2342	6360	+ 7332	268723	115586
4306	2189	6079	72429	256135	111836
4363	2032	5860	130395	231132	102584
— 4445	+ 1874	+ 5697	+179085	—196457	— 88949

Table III

G. M. T.	x	y	z
1920 Apr. 25.5 . . .	+ 19.4070847	— 6.4841837	— 25.0131955
Oct. 2.5 . . .	19.4703866	6.3718344	25.0243770
1921 Mar. 11.5 . . .	19.5295671	6.2581647	25.0300013
Aug. 18.5 . . .	19.5846365	6.1431538	25.0300559
1922 Jan. 25.5 . . .	19.6355932	6.0267796	25.0245255
Jul. 4.5 . . .	19.6824235	5.9090195	25.0133925
Dec. 11.5 . . .	19.7251019	5.7898527	24.9966378
1923 May 20.5 . . .	19.7635924	5.6692609	24.9742411
Oct. 27.5 . . .	19.7978472	5.5472296	24.9461813
1924 Apr. 4.5 . . .	19.8278089	5.4237499	24.9124376
Sep. 11.5 . . .	19.8534098	5.2988201	24.8729899
1925 Feb. 19.0 . . .	19.8745741	5.1724471	24.8278192
Jul. 29.0 . . .	19.8912186	5.0446490	24.7769093
1926 Jan. 5.0 . . .	19.9032561	4.9154562	24.7202467
Jun. 14.0 . . .	19.9105979	4.7849130	24.6578217
Nov. 21.0 . . .	19.9131590	4.6530782	24.5896287
1927 Apr. 30.0 . . .	19.9108620	4.5200235	24.5156657
Oct. 7.0 . . .	19.9036422	4.3858319	24.4359331
1928 Mar. 15.0 . . .	19.8914512	4.2505928	24.3504324
Aug. 22.0 . . .	19.8742585	4.1143967	24.2591632
1929 Jan. 29.0 . . .	19.8520508	3.9773291	24.1621210
Jul. 8.0 . . .	19.8248300	3.8394656	24.0592943
Dec. 15.0 . . .	19.7926073	3.7008677	23.9506628
1930 May 24.0 . . .	19.7553985	3.5615810	23.8361968
Oct. 31.0 . . .	19.7132179	3.4216350	23.7158562
1931 Apr. 9.0 . . .	19.6660739	3.2810447	23.5895914
Sep. 16.0 . . .	19.6139651	3.1398130	23.4573438
1932 Feb. 23.0 . . .	19.5568776	2.9979333	23.3190473
Aug. 1.0 . . .	19.4947848	2.8553924	23.1746283
1933 Jan. 8.0 . . .	19.4276452	2.7121731	23.0240079
Jun. 17.0 . . .	19.3554030	2.5682561	22.8671015
Nov. 24.0 . . .	19.2779883	2.4236219	22.7038198
1934 May 3.0 . . .	19.1953170	2.2782524	22.5340695
Oct. 10.0 . . .	+ 19.1072908	— 2.1321323	— 22.3577528

Table III

$\sum X'$	$\sum Y'$	$\sum Z'$	$\sum X$	$\sum Y$	$\sum Z$
— 4550	+ 1715	+ 5587	+ 217350	— 154779	— 72052
4678	1555	5528	244773	108490	52905
4827	1396	5517	261387	59623	32384
4997	1234	5557	267473	— 9878	— 11224
5186	1072	5649	263398	+ 39296	+ 9946
5393	908	5795	249543	86610	30560
5615	745	5999	226273	130821	50079
5846	586	6266	193962	170638	67939
6078	439	6598	153080	204627	83512
6299	314	6993	104320	231172	96088
6493	224	7443	+ 48785	248478	104872
6642	186	7928	— 11814	254667	109011
6726	215	8414	74953	247962	107688
6732	321	8854	137185	227065	100255
6658	499	9194	194196	191556	86429
6516	727	9387	241131	142371	66495
6333	970	9413	273231	82147	41461
6142	1189	9281	286692	+ 15214	+ 13098
5970	1352	9029	279554	— 52810	— 16235
5836	1444	8709	252247	115886	43937
5749	1464	8370	207616	168573	67603
5708	1422	8053	150368	206933	85430
5709	1331	7781	86101	228984	96427
5748	1206	7570	— 20338	234679	100443
5817	1057	7424	+ 42222	225477	97989
5913	895	7344	98088	203766	90002
6031	726	7328	144999	172301	77610
6170	554	7373	181743	133788	61945
6327	382	7474	207878	90653	44034
6503	213	7630	223447	— 44954	24766
6687	+ 58	7836	228748	+ 1605	— 4876
6907	— 117	8098	224173	47593	+ 15011
7137	277	8411	210111	91749	34345
— 7386	— 435	+ 8780	+ 186926	+ 132866	+ 52599

Table III

G. M. T.	x	y	z
1935 Mar. 19.0 . . .	+ 19.0137975	— 1.9852502	— 22.1747687
Aug. 26.0 . . .	18.9147111	1.8376004	21.9850124
1936 Feb. 2.0 . . .	18.8098916	1.6891840	21.7883760
Jul. 11.0 . . .	18.6991856	1.5400108	21.5847489
Dec. 18.0 . . .	18.5824269	1.3901015	21.3740180
1937 May 27.0 . . .	18.4594375	1.2394890	21.1560679
Nov. 3.0 . . .	18.3300300	1.0882214	20.9307819
1938 Apr. 12.0 . . .	18.1940098	0.9363623	20.6980417
Sep. 19.0 . . .	18.0511798	0.7839924	20.4577274
1939 Feb. 26.0 . . .	17.9013431	0.6312083	20.2097165
Aug. 5.0 . . .	17.7443085	0.4781212	19.9538828
1940 Jan. 12.0 . . .	17.5798924	0.3248518	19.6900933
Jun. 20.0 . . .	17.4079204	0.1715262	19.4182057
Nov. 27.0 . . .	17.2282259	— 0.0182704	19.1380645
1941 May 6.0 . . .	17.0406468	+ 0.1347956	18.8494974
Oct. 13.0 . . .	16.8450183	0.2875604	18.5523126
1942 Mar. 22.0 . . .	16.6411672	0.4399227	18.2462958
Aug. 29.0 . . .	16.4289041	0.5917917	17.9312089
1943 Feb. 5.0 . . .	16.2080169	0.7430840	17.6067891
Jul. 15.0 . . .	15.9782647	0.8937205	17.2727472
Dec. 22.0 . . .	15.7393733	1.0436228	16.9287670
1944 May 30.0 . . .	15.4910308	1.1927088	16.5745042
Nov. 6.0 . . .	15.2328837	1.3408887	16.2095839
1945 Apr. 15.0 . . .	14.9645328	1.4880609	15.8335991
Sep. 22.0 . . .	14.6855288	1.6341076	15.4461064
1946 Mar. 1.0 . . .	14.3953671	1.7788911	15.0466237
Aug. 8.0 . . .	14.0934819	1.9222477	14.6346240
Oct. 27.0 . . .	13.9379475	1.9933316	14.4237522
1947 Jan. 15.0 . . .	13.7792382	2.0639833	14.2095305
Apr. 5.0 . . .	13.6172623	2.1341724	13.9918778
Jun. 24.0 . . .	13.4519226	2.2038657	13.7707090
Sep. 12.0 . . .	13.2831160	2.2730272	13.5459346
Dec. 1.0 . . .	13.1107328	2.3416170	13.3174600
1948 Feb. 19.0 . . .	+ 12.9346567	+ 2.4095914	— 13.0851860

Table III.

$\sum X'$	$\sum Y'$	$\sum Z'$	$\sum X$	$\sum Y$	$\sum Z$
— 7653	— 590	+ 9211	+ 154983	+ 169693	+ 69225
7935	739	9710	114724	200829	83612
8226	874	10286	66802	224698	95069
8514	979	10942	+ 12262	239524	102808
8779	1032	11675	— 47252	243434	105982
8997	998	12463	109294	234645	103769
9141	841	13257	170499	211795	95498
9188	532	13981	226600	174373	80848
9132	— 69	14536	272746	123201	60054
8986	+ 513	14834	304111	+ 60785	34068
8787	1143	14826	316753	— 8627	+ 4618
8578	1737	14524	308517	79442	— 25950
8399	2227	13994	279645	145549	55010
8275	2576	13327	232843	201363	80098
8217	2778	12608	172766	242758	99328
8228	2846	11904	105051	267584	111646
8306	2803	11258	— 35306	275669	116838
8447	2671	10693	+ 31666	268397	115379
8649	2465	10219	92272	248106	108190
8907	2196	9834	144160	217533	96379
9235	1871	9550	186040	179358	81074
9623	1488	9357	217395	136013	63291
10086	1065	9255	238202	89541	43917
10626	+ 516	9253	248680	— 41648	23683
11254	— 97	9361	249160	+ 6234	— 3216
11984	821	9593	239954	52834	+ 16939
12830	1685	9976	221354	96931	36248
3326	545	2559	52154	29412	11354
3453	681	2637	48410	34312	13539
3589	831	2731	44118	38887	15599
3737	996	2842	39294	43089	17512
3895	1178	2974	33958	46864	19254
4065	1378	3130	28135	50156	20801
— 4247	— 1600	+ 3314	+ 21860	+ 52907	+ 22127

Table III

G. M. T.	x	y	z
1948 May 9.0 . . .	+ 12.7547637	+ 2.4769025	— 12.8490077
Jul. 28.0 . . .	12.5709220	2.5434975	12.6088140
Oct. 16.0 . . .	12.3829908	2.6093187	12.3644876
1949 Jan. 4.0 . . .	12.1908203	2.6743019	12.1159038
Mar. 25.0 . . .	11.9942502	2.7383767	11.8629303
Jun. 13.0 . . .	11.7931089	2.8014653	11.6054261
Sep. 1.0 . . .	11.5872129	2.8634817	11.3432409
Nov. 20.0 . . .	11.3763648	2.9243308	11.0762141
1950 Feb. 8.0 . . .	11.1603526	2.9839073	10.8041733
Apr. 29.0 . . .	10.9389478	3.0420941	10.5269335
Jul. 18.0 . . .	10.7119032	3.0987613	10.2442954
Oct. 6.0 . . .	10.4789514	3.1537643	9.9560435
Dec. 25.0 . . .	10.2398014	3.2069414	9.6619445
1951 Mar. 15.0 . . .	9.9941357	3.2581118	9.3617447
Jun. 3.0 . . .	9.7416068	3.3070724	9.0551674
Aug. 22.0 . . .	9.4818320	3.3535941	8.7419096
Nov. 10.0 . . .	9.2143885	3.3974172	8.4216386
1952 Jan. 29.0 . . .	8.9388062	3.4382461	8.0939874
Apr. 18.0 . . .	8.6545596	3.4757413	7.7585491
Jul. 7.0 . . .	8.3610573	3.5095110	7.4148710
Sep. 25.0 . . .	8.0576295	3.5390987	7.0624464
Nov. 4.0 . . .	7.9019588	3.5521603	6.8827789
Dec. 14.0 . . .	7.7435115	3.5639681	6.7007054
1953 Jan. 23.0 . . .	7.5821740	3.5744388	6.5161429
Mar. 4.0 . . .	7.4178236	3.5834822	6.3290027
Apr. 13.0 . . .	7.2503280	3.5909976	6.1391900
May 23.0 . . .	7.0795439	3.5968757	5.9466033
Jul. 2.0 . . .	6.9053157	3.6009945	5.7511334
Aug. 11.0 . . .	6.7274741	3.6032188	5.5526633
Sep. 20.0 . . .	6.5458340	3.6033978	5.3510667
Oct. 30.0 . . .	6.3601926	3.6013627	5.1462071
Dec. 9.0 . . .	6.1703270	3.5969237	4.9379371
1954 Jan. 18.0 . . .	5.9759911	3.5898662	4.7260964
Feb. 27.0 . . .	+ 5.7769121	+ 3.5799462	— 4.5105109

Table III

$\sum X'$	$\sum Y'$	$\sum Z'$	$\sum X$	$\sum Y$	$\sum Z$
— 4442	— 1843	+ 3532	+ 15173	+ 55056	+ 23205
4651	2110	3788	8132	56541	24007
4873	2401	4090	+ 802	57301	24506
5109	2717	4447	— 6736	57278	24674
5358	3056	4865	14384	56420	24486
5620	3415	5357	22031	54685	23922
5894	3788	5932	29551	52044	22967
6177	4166	6599	36802	48483	21612
6467	4534	7368	43636	44013	19855
6763	4875	8242	49895	38664	17709
7063	5165	9222	55420	32499	15195
7364	5377	10298	60061	25605	12346
7669	5480	11452	63678	18100	9211
7978	5448	12653	66156	10127	5847
8297	5261	13859	67404	+ 1852	+ 2325
8635	4911	15021	67365	— 6541	— 1280
9000	4402	16091	66024	14862	4886
9403	3758	17022	63405	22917	8408
9857	3015	17782	59571	30522	11766
10372	2216	18358	54622	37508	14886
10956	1405	18750	48689	43731	17702
2820	252	4720	11351	11629	4745
2905	156	4744	10482	12268	5040
2997	— 64	4758	9574	12846	5310
3094	+ 24	4765	8629	13362	5555
3197	107	4765	7655	13814	5773
3308	183	4760	6657	14202	5964
3426	254	4751	5640	14524	6127
3552	319	4737	4610	14781	6262
3687	377	4721	3572	14973	6370
3832	429	4704	2532	15102	6451
3988	474	4685	1494	15168	6505
4156	512	4665	— 464	15173	6532
— 4337	+ 546	+ 4647	+ 556	— 15119	— 6534

Table III

G. M. T.			x	y	z
1954	Apr.	8.0	+ 5.5727866	+ 3.5668850	— 4.2909908
	May	18.0	5.3632747	3.5503617	4.0673285
	Jun.	27.0	5.1479948	3.5300050	3.8392967
	Aug.	6.0	4.9265152	3.5053811	3.6066458
		26.0	4.8132996	3.4913128	3.4885033
	Sep.	15.0	4.6983446	3.4759794	3.3691008
	Oct.	5.0	4.5815777	3.4593017	3.2483995
		25.0	4.4629207	3.4411934	3.1263588
	Nov.	14.0	4.3422897	3.4215592	3.0029357
	Dec.	4.0	4.2195942	3.4002945	2.8780854
		24.0	4.0947363	3.3772834	2.7517606
1955	Jan.	13.0	3.9676101	3.3523974	2.6239119
	Feb.	2.0	3.8381003	3.3254936	2.4944873
		22.0	3.7060818	3.2964118	2.3634327
	Mar.	14.0	3.5714177	3.2649727	2.2306914
	Apr.	3.0	3.4339584	3.2309738	2.0962049
		23.0	3.2935396	3.1941858	1.9599124
	May	13.0	3.1499807	3.1543475	1.8217520
		23.0	3.0769597	3.1331926	1.7519518
	Jun.	2.0	3.0030819	3.1111595	1.6816611
		12.0	2.9283121	3.0882036	1.6108722
		22.0	2.8526225	3.0642770	1.5395774
	Jul.	2.0	2.7759819	3.0393278	1.4677694
		12.0	2.6983570	3.0132999	1.3954411
		22.0	2.6197127	2.9861327	1.3225857
	Aug.	1.0	2.5400122	2.9577604	1.2491971
		11.0	2.4592161	2.9281115	1.1752700
		21.0	2.3772833	2.8971078	1.1007996
		31.0	2.2941698	2.8646643	1.0257828
	Sep.	10.0	2.2098295	2.8306876	0.9502176
		20.0	2.1242134	2.7950754	0.8741042
		30.0	2.0372698	2.7577150	0.7974447
	Oct.	10.0	1.9489440	2.7184822	0.7202445
		20.0	+ 1.8591782	+ 2.6772394	— 0.6425127

Table III.

$\sum X'$	$\sum Y'$	$\sum Z'$	$\sum X$	$\sum Y$	$\sum Z$
— 4533	+ 572	+ 4628	+ 1561	— 15007	— 6510
4747	593	4610	2547	14841	6463
4980	607	4594	3511	14622	6392
5237	618	4578	4449	14353	6300
1344	155	1142	1226	3548	1561
1379	155	1141	1340	3509	1546
1418	155	1139	1450	3464	1530
1458	155	1137	1560	3418	1513
1500	155	1135	1667	3370	1495
1545	154	1133	1772	3318	1475
1593	153	1131	1874	3264	1454
1643	151	1129	1975	3207	1432
1696	149	1126	2073	3148	1409
1753	148	1124	2169	3087	1386
1814	146	1121	2262	3024	1361
1879	143	1117	2354	2959	1335
1948	141	1113	2442	2892	1308
2022	139	1108	2529	2823	1281
515	35	276	643	697	317
525	34	275	653	688	313
536	34	274	663	679	310
547	34	274	674	670	306
558	34	273	684	661	302
570	34	271	693	651	298
583	34	270	703	642	294
596	33	269	712	632	291
609	34	267	722	623	287
623	34	265	731	613	283
644	25	266	790	622	296
659	25	264	805	590	283
675	24	262	810	558	268
692	23	260	807	527	254
711	22	257	797	502	241
— 730	+ 22	+ 254	+ 781	— 482	— 231

Table III

G. M. T.	x	y	z
1955 Oct. 30.0	+ 1.7679119	+ 2.6338342	— 0.5642628
Nov. 9.0	1.6750812	2.5880967	0.4855142
19.0	1.5806196	2.5398373	0.4062937
29.0	1.4844579	2.4888439	0.3266373
Dec. 9.0	1.3865249	2.4348781	0.2465923
19.0	1.2867481	2.3776713	0.1662210
29.0	1.1850553	2.3169202	0.0856040
1956 Jan. 8.0	1.0813762	2.2522810	0.0048462
18.0	0.9756460	2.1833633	0.0759175
28.0	0.8678090	2.1097230	0.1565131
Feb. 7.0	0.7578261	2.0308546	0.2367157
17.0	0.6456832	1.9461828	0.3162357
27.0	0.5314055	1.8550549	0.3946976
Mar. 8.0	0.4150768	1.7567354	0.4716214
18.0	0.2968668	1.6504042	0.5463803
28.0	0.1770699	1.5351657	0.6181733
Apr. 7.0	+ 0.0561565	1.4100743	0.6859765
17.0	— 0.0651602	1.2741903	0.7484998
27.0	0.1858488	1.1266767	0.8041542
May 7.0	0.3044812	0.9669662	0.8510538
17.0	0.4191940	0.7949803	0.8870889
27.0	0.5277268	0.6113952	0.9101097
Jun. 6.0	0.6276002	0.4178552	0.9182371
16.0	0.7164452	0.2170093	0.9102480
26.0	0.7924125	0.0122626	0.8858968
Jul. 6.0	— 0.8544995	+ 0.1927283	— 0.8460121

Table III.

$\sum X'$	$\sum Y'$	$\sum Z'$	$\sum X$	$\sum Y$	$\sum Z$
— 750	+ 22	+ 252	+ 762	— 471	— 224
770	22	248	742	467	220
794	22	245	724	471	219
818	23	240	711	481	222
844	24	233	704	498	228
870	26	227	705	517	236
897	29	221	714	539	245
925	32	213	734	559	254
954	34	202	763	577	263
985	37	191	798	589	270
1018	41	179	844	593	274
1054	47	166	893	588	274
1092	54	150	944	572	270
1130	69	131	994	544	261
1166	90	112	1039	507	247
1199	116	92	1076	460	229
1229	145	71	1103	407	207
1257	177	49	1117	349	183
1279	214	27	1118	290	157
1296	253	+ 6	1106	234	132
1305	295	— 14	1082	182	108
1304	340	32	1047	139	87
1291	385	45	1005	105	72
1266	429	54	958	82	58
1232	469	56	909	72	51
— 1190	+ 504	— 52	+ 862	— 72	— 50

Table IV.

0^h G.M.T. (U.T.)	$\alpha_{1950.0}$	$\delta_{1950.0}$	r	Δ
1955 Aug. 1	$4^h10^m17^s$	— 12°36′.5	4.094	4.263
3	11 43	12 39.1	4.075	4.220
5	13 8	12 42.0	4.056	4.177
7	14 30	12 45.3	4.038	4.135
9	15 51	12 49.0	4.019	4.092
11	17 10	12 53.0	4.000	4.049
13	18 28	12 57.4	3.981	4.006
15	19 43	13 2.1	3.962	3.962
17	20 56	13 7.3	3.944	3.919
19	22 6	13 12.8	3.925	3.875
21	23 14	13 18.6	3.906	3.832
23	24 20	13 24.9	3.887	3.788
25	25 23	13 31.5	3.868	3.744
27	26 24	13 38.4	3.849	3.701
29	27 22	13 45.7	3.830	3.657
31	28 16	13 53.3	3.811	3.613
Sep. 2	29 8	14 1.3	3.792	3.570
4	29 56	14 9.6	3.773	3.526
6	30 41	14 18.2	3.753	3.483
8	31 23	14 27.0	3.734	3.439
10	32 1	14 36.2	3.715	3.396
12	32 36	14 45.7	3.696	3.354
14	33 6	14 55.5	3.676	3.311
16	33 33	15 5.5	3.657	3.269
18	33 55	15 15.8	3.637	3.226
20	34 13	15 26.3	3.618	3.184
22	34 26	15 36.9	3.598	3.143
24	34 35	15 47.8	3.579	3.101
26	34 40	15 58.8	3.559	3.060
28	34 39	16 10.1	3.540	3.019
30	34 33	16 21.4	3.520	2.979
Oct. 2	34 22	16 33.0	3.500	2.939
4	34 6	16 44.2	3.481	2.899
6	4 33 44	— 16 55.7	3.461	2.861

Table IV

0^h G. M. T. (U. T.)	$\alpha_{1950.0}$	$\delta_{1950.0}$	r	Δ
1955 Oct. 8.....	$4^h33^m17^s$	−17° 7′2	3.442	2.823
10.....	32 44	17 18.6	3.422	2.785
12.....	32 5	17 29.8	3.402	2.748
14.....	31 20	17 40.9	3.382	2.711
16.....	30 30	17 51.9	3.362	2.676
18.....	29 33	18 2.6	3.342	2.641
20.....	28 30	18 13.0	3.322	2.606
22.....	27 20	18 23.0	3.302	2.572
24.....	26 5	18 32.7	3.282	2.539
26.....	24 43	18 41.9	3.262	2.506
28.....	23 15	18 50.5	3.242	2.475
30.....	21 41	18 58.6	3.222	2.444
Nov. 1.....	20 0	19 6.0	3.202	2.414
3.....	18 14	19 12.7	3.182	2.385
5.....	16 22	19 18.5	3.161	2.357
7.....	14 24	19 23.5	3.141	2.330
9.....	12 20	19 27.6	3.121	2.304
11.....	10 11	19 30.7	3.101	2.279
13.....	7 57	19 32.7	3.080	2.255
15.....	5 39	19 33.5	3.060	2.232
17.....	3 16	19 33.2	3.039	2.210
19.....	4 0 49	19 31.6	3.019	2.189
21.....	3 58 18	19 28.7	2.998	2.169
23.....	55 44	19 24.4	2.978	2.150
25.....	53 8	19 18.7	2.957	2.132
27.....	50 29	19 11.5	2.937	2.115
29.....	47 49	19 2.9	2.916	2.099
Dec. 1.....	45 7	18 52.7	2.895	2.084
3.....	42 25	18 41.0	2.875	2.070
5.....	39 43	18 27.8	2.854	2.058
7.....	37 2	18 13.0	2.834	2.046
9.....	34 22	17 56.6	2.813	2.035
11.....	31 43	17 38.7	2.792	2.025
13.....	3 29 7	−17 19.2	2.771	2.017

Table IV

0^h G.M.T. (U.T.)	$\alpha_{1950.0}$	$\delta_{1950.0}$	r	Δ
1955 Dec. 15.....	$3^h26^m33^s$	— 16°58′.3	2.751	2.009
17.....	24 3	16 35.8	2.730	2.002
19.....	21 36	16 11.9	2.709	1.996
21.....	19 14	15 46.6	2.688	1.991
23.....	16 56	15 19.9	2.667	1.987
25.....	14 44	14 51.8	2.646	1.984
27.....	12 37	14 22.4	2.625	1.982
29.....	10 36	13 51.9	2.604	1.980
31.....	8 41	13 20.2	2.583	1.979
1956 Jan. 2.....	6 53	12 47.4	2.562	1.979
4.....	5 11	12 13.6	2.541	1.979
6.....	3 36	11 38.7	2.519	1.980
8.....	2 8	11 3.0	2.498	1.981
10.....	3 0 47	10 26.4	2.477	1.983
12.....	2 59 33	9 49.0	2.456	1.986
14.....	58 27	9 10.8	2.435	1.989
16.....	57 28	8 31.9	2.414	1.993
18.....	56 37	7 52.4	2.393	1.996
20.....	55 53	7 12.3	2.371	2.001
22.....	55 16	6 31.6	2.350	2.005
24.....	54 48	5 50.4	2.329	2.010
26.....	54 26	5 8.8	2.308	2.015
28.....	54 12	4 26.7	2.287	2.020
30.....	54 5	3 44.2	2.265	2.027
Feb. 1.....	54 6	3 1.3	2.244	2.033
3.....	54 13	2 18.2	2.223	2.039
5.....	54 28	1 34.7	2.202	2.045
7.....	54 50	0 50.9	2.180	2.049
9.....	55 19	— 0 6.9	2.159	2.055
11.....	55 54	+ 0 37.3	2.138	2.060
13.....	56 37	1 21.8	2.117	2.065
15.....	57 26	2 6.5	2.096	2.070
17.....	58 22	2 51.3	2.075	2.076
19.....	2 59 24	+ 3 36.3	2.054	2.081

Table IV

0^h G.M.T. (U.T.)	$\alpha_{1950.0}$	$\delta_{1950.0}$	r	Δ
1956 Feb. 21.....	$3^h\ 0^m33^s$	+ 4°21′.6	2.033	2.086
23.....	1 48	5 6.9	2.012	2.091
25.....	3 9	5 52.4	1.991	2.095
27.....	4 37	6 38.1	1.970	2.099
29.....	6 11	7 23.9	1.949	2.104
Mar. 2.....	7 51	8 9.8	1.928	2.108
4.....	9 38	8 55.8	1.907	2.112
6.....	11 30	9 41.9	1.886	2.115
8.....	13 29	10 28.2	1.866	2.118
10.....	15 34	11 14.6	1.845	2.121
12.....	17 44	12 1.1	1.825	2.123
14.....	20 1	12 47.8	1.804	2.125
16.....	22 24	13 34.5	1.784	2.127
18.....	24 53	14 21.4	1.764	2.128
20.....	27 29	15 8.4	1.744	2.129
22.....	30 10	15 55.4	1.724	2.130
24.....	32 58	16 42.6	1.704	2.130
26.....	35 52	17 29.8	1.684	2.129
28.....	38 53	18 17.2	1.664	2.129
30.....	42 0	19 4.7	1.645	2.128
Apr. 1.....	45 13	19 52.3	1.626	2.126
3.....	48 34	20 40.0	1.607	2.124
5.....	52 1	21 27.8	1.588	2.122
7.....	55 36	22 15.6	1.569	2.120
9.....	3 59 18	23 3.5	1.551	2.116
11.....	4 3 7	23 51.4	1.533	2.113
13.....	7 4	24 39.4	1.515	2.109
15.....	11 8	25 27.3	1.497	2.105
17.....	15 21	26 15.3	1.479	2.100
19.....	19 42	27 3.3	1.462	2.095
21.....	24 12	27 51.2	1.445	2.090
23.....	28 51	28 39.0	1.429	2.084
25.....	33 39	29 26.8	1.412	2.078
27.....	4 38 37	+ 30 14.4	1.397	2.071

Table IV

0^h G.M.T. (U.T.)	$\alpha_{1950.0}$	$\delta_{1950.0}$	r	Δ
1956 Apr. 29.....	$4^h43^m44^s$	+31° 1'.9	1.381	2.064
May 1.....	49 2	31 49.1	1.366	2.057
3.....	4 54 31	32 36.0	1.351	2.050
5.....	5 0 11	33 22.6	1.337	2.042
7.....	6 3	34 8.8	1.324	2.034
9.....	12 7	34 54.5	1.310	2.025
11.....	18 23	35 39.6	1.298	2.017
13.....	24 53	36 24.1	1.285	2.008
15.....	31 36	37 7.9	1.274	1.999
17.....	38 33	37 50.8	1.263	1.989
19.....	45 45	38 32.8	1.252	1.980
21.....	5 53 11	39 13.7	1.242	1.970
23.....	6 0 53	39 53.3	1.233	1.961
25.....	8 51	40 31.6	1.225	1.951
27.....	17 5	41 8.4	1.217	1.941
29.....	25 35	41 43.5	1.210	1.932
31.....	34 22	42 16.7	1.203	1.922
Jun. 2.....	43 26	42 47.9	1.197	1.912
4.....	6 52 46	43 16.8	1.192	1.903
6.....	7 2 22	43 43.3	1.188	1.893
8.....	12 15	44 7.1	1.185	1.884
10.....	22 23	44 28.1	1.182	1.875
12.....	32 46	44 46.0	1.180	1.866
14.....	43 23	45 0.7	1.179	1.858
16.....	7 54 12	+45 11.9	1.178	1.850

Table V.

0^h G.M.T. (U.T.)	Precession from 1950.0 to 1955.0 — 1956.0		Correction for T 1 day later	
1955 Aug. 1	+ 14.0	+ 0.77	— 19^s	— 4.7
11	14.0	0.72	21	4.9
21	13.9	0.68	23	5.2
31	13.9	0.65	25	5.5
Sep. 10	13.8	0.63	28	5.8
20	13.6	0.61	30	6.0
30	13.5	0.61	32	6.3
Oct. 10	13.4	0.62	35	6.4
20	13.3	0.65	37	6.7
30	13.3	0.69	39	6.8
Nov. 9	13.3	0.76	39	6.9
19	13.3	0.83	38	7.0
29	13.4	0.91	36	7.2
Dec. 9	13.6	0.99	33	7.5
19	13.9	1.06	29	8.0
29	14.2	1.13	24	8.8
1956 Jan. 8	17.3	1.40	20	9.7
18	17.7	1.44	16	10.8
28	18.0	1.45	14	11.8
Feb. 7	18.4	1.45	12	13.1
17	18.7	1.43	11	14.1
27	19.1	1.39	12	15.4
Mar. 8	19.5	1.33	13	16.5
18	20.0	1.26	16	17.9
28	20.6	1.16	20	19.1
Apr. 7	21.2	1.04	26	20.4
17	22.0	0.88	34	21.6
27	22.8	0.70	45	22.8
May 7	23.7	0.47	61	23.7
17	24.6	+ 0.19	82	23.9
27	25.4	— 0.15	110	23.0
Jun. 6	25.8	0.54	144	20.7
16	+ 25.5	— 0.96	— 178	— 16.3

Table VI.

Distances between the major planets and Comet Olbers	Jupiter	Saturn	Uranus	Neptun	Pluto	$a\sqrt{a}$
1815 Aug. 14.5 . . .	4.3	9.7	17.3	28.7	45.6	74.87
1818 Jan. 30.5 . . .	5.2	8.7	12.6	22.7	42.1	73.49
1820 Jul. 18.5 . . .	11.8	14.7	11.6	20.6	40.3	72.52
1825 Jun. 22.5 . . .	25.4	26.8	11.8	18.9	39.0	72.45
1830 May 27.5 . . .	22.1	33.6	14.2	18.6	39.4	72.65
1835 May 1.5 . . .	32.0	33.4	18.2	18.9	40.5	72.39
1840 Apr. 4.5 . . .	32.2	28.8	23.1	19.7	41.9	72.58
1845 Mar. 9.5 . . .	31.0	25.8	28.1	20.8	43.4	72.54
1850 Feb. 11.5 . . .	37.6	29.6	32.9	22.3	44.7	72.43
1855 Jan. 16.5 . . .	29.7	36.7	36.9	24.0	45.7	72.56
1859 Dec. 21.5 . . .	35.8	39.9	39.7	25.5	46.3	72.46
1864 Nov. 24.5 . . .	30.5	36.3	41.2	26.7	46.6	72.39
1869 Oct. 29.5 . . .	27.0	28.0	40.8	27.5	46.3	72.67
1874 Oct. 3.5 . . .	27.6	18.9	38.5	27.6	45.5	72.36
1879 Sep. 7.5 . . .	15.2	13.7	33.9	26.9	44.4	72.81
1884 Aug. 11.5 . . .	13.4	11.5	26.5	25.7	43.6	72.96
1888 Jan. 3.5 . . .	4.0	9.7	17.1	31.3	49.9	72.51
1888 Jul. 11.5 . . .	2.2	12.0	17.3	33.2	51.7	72.81
1889 Jan. 17.5 . . .	1.5	13.6	17.8	34.4	52.7	72.01
1889 Jul. 16.5 . . .	2.2	14.8	18.3	35.3	53.4	70.27
1890 Jan. 12.5 . . .	3.6	15.8	18.8	36.1	54.0	69.55
1894 Jun. 20.5 . . .	20.0	19.6	21.6	41.9	57.5	68.51
1899 Apr. 15.5 . . .	22.9	18.4	22.1	47.1	60.4	69.01
1904 Jul. 18.5 . . .	25.4	19.3	21.1	51.7	62.9	68.72
1909 Oct. 20.5 . . .	33.2	27.8	20.0	55.2	64.7	68.73
1914 Aug. 15.5 . . .	27.5	36.5	19.8	57.3	65.9	68.79
1919 Nov. 17.5 . . .	36.5	39.9	21.1	58.6	66.4	68.64
1925 Feb. 19.0 . . .	29.9	35.7	23.6	58.6	66.0	68.75
1930 May 24.0 . . .	33.4	27.7	26.4	57.5	64.8	68.77
1935 Aug. 26.0 . . .	29.9	22.6	28.8	55.2	62.5	68.67
1940 Nov. 27.0 . . .	24.7	24.4	29.9	51.7	58.9	68.99
1946 Mar. 1.0 . . .	24.5	26.3	29.0	47.0	53.8	68.60
1951 Jun. 3.0 . . .	10.7	21.7	25.0	40.9	46.2	69.08
1956 Jun. 16.0 . . .	4.6	10.1	17.7	30.0	33.8	69.57

DET KGL. DANSKE VIDENSKABERNES SELSKAB
MATEMATISK-FYSISKE MEDDELELSER, BIND XXIV, NR. 19

ATOMIC INTERACTION IN PENETRATION PHENOMENA

BY

AAGE BOHR

KØBENHAVN
I KOMMISSION HOS EJNAR MUNKSGAARD
1948

CONTENTS

Printed in Denmark
Bianco Lunos Bogtrykkeri

§ 1. Introduction.

The theory of the penetration of fast charged particles through matter was originally developed on the basis of an analysis of collisions between the moving particle and individual atoms[1]. In such a treatment, the influence of phase relations between the effects produced in the atoms along the path and, in particular, the resulting coupling between the different encounters is disregarded. This approximation will often be justified, but phenomena do exist for which such atomic interaction effects are of essential importance.

Thus, it was observed by ČERENKOV (1934) that very fast electrons, when passing through dense materials, give rise to a peculiar radiation the properties of which reveal that one has to do, not with independent emission processes by individual excited atoms, but with a radiation emitted coherently by larger portions of the substance. A theory of this phenomenon was developed by FRANK and TAMM (1937) and by TAMM (1939), who showed its immediate connection with the fact that the velocity of the electrons may exceed the rate of propagation of electromagnetic waves in the surrounding medium. Just on account of the interplay of the atoms, the phase velocity of such waves may indeed, over certain spectral regions, be smaller than the velocity of light in vacuo.

The problem of a possible influence of atomic interaction on the stopping and ionization of fast particles was raised by SWANN (1938), who pointed out that the polarization induced by the particle in the matter through which it passes will give rise to a certain screening effect which might, under circumstances,

1) A comprehensive treatment of this subject has recently been given by N. BOHR (1948) and, in the following, we shall often refer to this survey for fuller information regarding general aspects of penetration theory.

reduce the rate of energy loss. The question was treated in detail by FERMI (1939, 1940), who found that the phenomenon may be of great significance for very fast particles, but is in general negligible for non-relativistic velocities. Still, there are exceptions to this rule and, in particular, it has been shown by KRAMERS (1947) that the stopping power of metals is always essentially influenced by the polarization effect.

In the above-mentioned treatments, the matter penetrated is described, in a macroscopic way, as a continuum and since, moreover, on account of the dispersive properties of the medium, which are essential for the phenomena, the electromagnetic fields are resolved in harmonic components, the connection with the simple theory of atomic collisions is somewhat obscure. For this reason, we shall in the following attempt a treatment of the coupling between the encounters from a microscopic point of view so as to bring out as clearly as possible the relationship to ordinary penetration theory. Such an approach is also found to be well suited to obtain simple generalizations of FERMI's formulae.

As a preliminary, we shall in § 2 briefly discuss the arguments which justify a distinction between close and distant collisions of the particle with the atoms in the substance. The mutual interaction of the atoms is of significance only in the distant encounters, the treatment of which is especially simple, since the description may be based entirely on classical mechanical pictures. A few main principles from ordinary stopping theory, of use in the following, are reviewed in § 3, in particular with respect to the influence of the atomic binding forces which effectively limit the radius of action of the penetrating particle by giving the collisions beyond a certain distance an adiabatic character.

In § 4, it is shown how the atomic interaction, from the microscopic point of view, may be regarded as a further screening factor and, especially in the non-relativistic case, may be treated in close analogy to the effect of the atomic binding forces. Moreover, a treatment of the energy loss of the particle is given, in which the stopping power is described as a force with which the atoms in the medium act on the moving particle. The special case of materials containing free electrons is considered more

closely in § 5, where also the influence of damping effects is taken into account. For particle velocities close to that of light, the atomic interaction presents new aspects connected with the retardation of the forces. This problem is discussed in outline in § 6 with reference to corresponding modifications in the relativistic two-body problem considered in Appendix I, and a simple interpretation of the main results of FERMI is obtained.

The Čerenkov radiation and its relation to the stopping power is dealt with in § 7. From the microscopic point of view, the phenomenon simply implies that part of the energy which is intermediately transferred from the particle to the atomic electrons is subsequently emitted as coherent electromagnetic waves. In a macroscopic description, the energy loss of the particle falls naturally into two parts, the first of which is absorbed by the substance in the neighbourhood of the path, while the second is directly transmitted to larger distances in the form of radiation. The distinction leads to some general relations regarding the stopping power for relativistic and non-relativistic particle velocities. In this connection, it is shown in Appendix II how the stopping problem may be treated by the formalism of radiation theory well known from quantum electrodynamics.

While, in the first part of the paper, the atoms are treated as simple dispersion oscillators of a single frequency, more general atomic models are considered in § 8. In this case, exact calculations are rather complicated, but it is shown how the analysis in § 6 makes it possible to obtain a general survey of the phenomena and leads to simple approximate formulae. In § 9, an attempt is made to deduce comprehensive expressions for the influence of atomic interaction on the stopping power of heavy substances. Finally, some experimental data are discussed in § 10. Among the more important applications of the theory is the stopping power of metals and the stopping and ionization of very fast particles; there appears to be satisfactory agreement with the available empirical evidence.

§ 2. Separation between Close and Distant Collisions.

The collisions between a charged particle and an atom must, of course, in general be treated in configuration space by means of proper quantum-mechanical methods, but for a large variety of problems it is permissible to use a simplified procedure in which the particle is described as a centre of force moving along a well-defined path. This description was proved by MOTT (1931) to lead to the same atomic excitation probabilities as the more general treatment, in case of particles of mass large compared with that of the electron and energy great in comparison with the atomic binding energies. Actually, it is a sufficient condition for the adequacy of the procedure that the momentum of the incident particle be large compared with the momentum changes involved in the collision. In fact, the effect of the collision on the atom will, under such circumstances, be approximately independent of the inertial properties of the particle which, thus, acts as if it were infinitely heavy. The condition in question, which is essentially equivalent to the requirement that the wave-length of the particle be small compared with atomic dimensions, is also, from the possibility of representing the particle by a wave-packet, immediately seen to ensure the validity of the simple method.

As regards the problem of the mutual influence of the atoms in the stopping substance, the more violent collisions involving large momentum transfers may obviously be neglected and, in the present connection, we may thus treat the penetrating particle as moving along a fixed path. The atoms may then be specified by their distance from the path, the so-called impact parameter p; as we shall see later in this paragraph, the atomic interaction phenomena will be of importance only for $p \gg a_0$, where a_0 denotes the "radius" of the hydrogen atom, which is a suitable measure for atomic dimensions.

In such distant collisions, the effect of the impact on the atom will, in general[1], amount to only a small perturbation and. since

1) For very large values of the charge of the incident particle combined with a relatively small velocity, special considerations are necessary since then the condition $p \gg a_0$ may not be sufficient to justify a perturbation procedure. Although, in this case, one may proceed by much the same methods (cf. N. BOHR 1948, p. 84), we shall disregard such problems in the present connection, since they may be shown to be quite insignificant under circumstances where the atomic interaction phenomena are of importance.

moreover, for $p \gg a_0$, the perturbing field is approximately constant over atomic dimensions, the encounter may be treated by means of simple mechanical considerations. In fact, as is well known, e. g., from dispersion theory, the atom will behave, with respect to average energy absorption and with respect to the electromagnetic field it generates, like an ensemble of classical harmonic oscillators corresponding to the various excitation and ionization possibilities.

In order to justify that close collisions are disregarded, we have still to make an estimate of the order of magnitude of the distances at which the atomic interaction effects become significant. This interaction arises from the displacement of the atomic electrons during the collision, which turns the neutral atoms into dipoles, and it is evident that the ensuing force K acting on an atomic electron will be comparable with the dipole moment per unit volume, multiplied by the electronic charge $-e$. If $z_1 e$ and v denote the charge and velocity of the particle, and μ the electron mass, the displacement of the electrons during the collision will, for free electrons, be of the order of $z_1 e^2/\mu v^2$ (cf. (3.3)) and tend to be smaller if account is taken of the binding forces. We thus have

$$K \lesssim \frac{z_1 e^2}{\mu v^2} n e^2, \tag{2.1}$$

where n denotes the number of electrons per unit volume. Now, even in dense materials, n never exceeds a_0^{-3} and, introducing $\frac{e^2}{a_0} = \mu v_0^2$, where v_0 is the "velocity" of the electron in the hydrogen atom, it follows that K will be small compared with the direct force of the particle, $\frac{z_1 e^2}{p^2}$, at any rate if

$$p < a_0 \frac{v}{v_0}. \tag{2.2}$$

Thus, for v large compared with v_0, representing the order of magnitude of the "orbital velocity" of the most loosely bound electrons in atoms, it is seen that the polarization effect is of importance only for $p \gg a_0$. In this case we may, therefore, corresponding to the above argumentation, divide the collisions into

two groups with $p < q$ and $p > q$, respectively, where q is chosen in such a manner that, for the first group, the atomic interaction effect is negligible and ordinary penetration theory applies while, for the second group, we are dealing only with distant collisions, which can be treated by classical mechanical methods.

For particle velocities comparable with or smaller than v_0, the penetration phenomena change essentially in character (cf. N. Bohr 1948). In such problems, one need in first approximation consider only the influence of the particle on those atoms through which it actually passes, and the interaction effects will only constitute a minor correction, the taking into account of which would even be a rather spurious refinement due to the difficulties of an accurate treatment of the penetration problem for very slow particles. Throughout the following, we shall therefore confine ourselves to the case of $v \gg v_0$.

§ 3. Collisions between Particle and Single Atom.

Before turning to the problem of the mutual influence of the atoms in penetration phenomena, it will be convenient to review briefly some of the main aspects of a collision between a fast particle and an isolated atom. If, in the first instance, the atomic binding forces are disregarded, we have a pure two-body problem which, in case of distant collisions, is further simplified by the fact that the displacement of the electron during the actual encounter will be small compared with the impact parameter. Moreover, in such encounters, the momentum transfer is always small compared with μc, where c is the light velocity, and we may, therefore, neglect relativity effects as regards the electronic motion.

From symmetry reasons, it follows that the final velocity of the electron will be practically perpendicular to the path of the particle, and for the motion of the electron in this direction we thus have, by means of the well-known expression for the electric field surrounding a uniformly moving point charge,

$$\mu \ddot{\eta} = \frac{z_1 e^2 p \gamma}{(p^2 + \gamma^2 v^2 t^2)^{3/2}}, \tag{3.1}$$

where η is the displacement and where $\gamma = \left(1 - \frac{v^2}{c^2}\right)^{-1/2}$. By simple integrations, (3.1) gives

$$\dot{\eta} = \frac{z_1 e^2}{\mu p v}\left(1 + \frac{\gamma v t}{\sqrt{p^2 + \gamma^2 v^2 t^2}}\right) \tag{3.2}$$

and

$$\eta = \frac{z_1 e^2}{\gamma \mu v^2}\left(\sqrt{1 + \frac{\gamma^2 v^2 t^2}{p^2}} + \frac{\gamma v t}{p}\right). \tag{3.3}$$

As is seen from these expressions, the encounter may be approximately characterized by an effective "collision time" of the order of $p/\gamma v$, during which the acting force is comparable with $z_1 e^2 \gamma / p^2$.

From (3.2) we get in particular

$$T = \frac{1}{2}\mu(\dot{\eta})^2_{t\to\infty} = 2\frac{z_1^2 e^4}{\mu v^2}\frac{1}{p^2} \tag{3.4}$$

for the energy transferred to an electron in a free collision. Since the stopping power of a substance is proportional to the integral of $Tpdp$, expression (3.4) cannot, however, be applied for arbitrarily large values of p, and it is thus essential in penetration theory to take into account the factors which tend to restrain the electrons from moving freely. These factors, acting as a kind of screening, may be said to determine a "radius of action" of the particle, representing an upper limit $p_{\max}$, below which the simple expression (3.4) applies. At larger distances, the collisions acquire an increasingly adiabatic character due to the influence of the screening, and the energy transfer will be small compared to that of free encounters. For the energy loss of the particle per unit path, originating in collisions with atoms for which $p > q$, we have accordingly

$$S_q = n\int_q^{p_{\max}} T \cdot 2\pi p\, dp = B \log \frac{p_{\max}}{q}, \tag{3.5}$$

a relation which may be taken to define an effective value of $p_{\max}$. The abbreviation B is given by

$$B = 4\pi \frac{z_1^2 e^4}{\mu v^2} n. \tag{3.6}$$

In the following, a main problem will just be to examine the various screening factors and estimate the corresponding limits of free energy transfer.

In collisions between the particle and isolated atoms, the only screening effect arises from the influence of the atomic binding forces. As mentioned in § 2, we may account for the binding by treating the atom as an ensemble of oscillators of frequencies corresponding to the various transition possibilities. For simplicity, however, we shall in the first instance consider all oscillators to have the same cyclic frequency ω_a; in § 8, we shall return to the problem of more general atomic models.

Besides the force of the particle, there will thus be a binding force of magnitude $\mu\omega_a^2\eta$, acting on the electrons. Of course, the latter force will eventually, when the particle has passed, determine the state of motion of the electrons, but it will be negligible during the actual encounter and, therefore, of no influence on the energy transfer, provided only

$$\mu\omega_a^2\eta \ll \mu\ddot{\eta} \tag{3.7}$$

for $|t| \lesssim \frac{p}{\gamma v}$, or, according to (3.1) and (3.3), if

$$p \ll d_a = \frac{v}{\omega_a}\gamma. \tag{3.8}$$

The limiting distance d_a just corresponds to a collision time comparable with the proper period of the oscillators and it is, indeed, evident that, in case of shorter impulses, the energy balance is independent of the binding forces. For collisions of larger duration, however, these forces will essentially reduce the energy transfer. In fact, in the extreme case of $p \gg d_a$, the electron will with high approximation pass through a succession of equilibrium states and, finally, be left in its original position.

A more detailed calculation of the energy transfer to an electron bound in a quasi-elastic field of force leads (N. Bohr 1913, 1915) to the following expression for the stopping effect in distant collisions

$$S_q = B\left(\log\frac{k\gamma v}{q\omega_a} - \frac{1}{2}\frac{v^2}{c^2}\right), \tag{3.9}$$

where k is a numerical factor equal to 1.123. Formula (3.9) is seen to coincide with (3.5) for a value of $p_{\max}$ closely equal to d_a given by (3.8). It may be noted that, in the deduction of (3.9), it is assumed that q may be chosen small compared with d_a. For the treatment of the atomic interaction problems it is required (cf. § 2) that $q \gg a_0$, and the two conditions are thus compatible only for $d_a \gg a_0$. The problem of larger frequencies ω_a for which $d_a \gtrsim a_0$ may, however, be neglected in the present connection, since in that case the atomic binding forces produce a screening already at distances where the interaction effects are negligible.

§ 4. Atomic Interaction for Non-Relativistic Particle Velocities.

Turning now to the problem of the mutual interaction of the atoms in the stopping material, we shall see that this phenomenon may be characterized essentially as a further screening effect. In fact, when the electrons during the passage of the particle are displaced from their equilibrium positions, the medium is polarized and, hence, each atomic electron will be subjected to a restitutional force from the surrounding material.

It will be convenient first to confine ourselves to the more simple case of non-relativistic particle velocities, where the problem can be treated quite analogously to the influence of the internal atomic binding forces discussed in § 3. Introducing the field vectors $\boldsymbol{E}$ and $\boldsymbol{D}$, we note that, in the quasi-electrostatic approximation corresponding to $v \ll c$, we have rot $\boldsymbol{E} = 0$ and, therefore, also rot $\boldsymbol{D} = 0$, assuming the medium to be homogeneous and isotropic. This last relation will hold irrespective of the dispersion properties of the substance. Thus, $\boldsymbol{D}$ is determined from the same equations as, and must equal, the field surrounding the particle in vacuo. Now, the average electric field in the medium is given by $\boldsymbol{E} = \boldsymbol{D} - 4\pi \boldsymbol{P}$, where $\boldsymbol{P}$ is the dipole moment per unit volume and, consequently, the polarization produces a force on the electrons, equal to $4\pi e \boldsymbol{P}$.

Since $\boldsymbol{P}$ is given by $-ne\boldsymbol{\xi}$, where $\boldsymbol{\xi}$ is the electronic displacement vector and n is the density of electrons, the polarization

force is seen to be of the quasi-elastic type, corresponding to a cyclic frequency ν given by

$$\nu^2 = \frac{4\pi n e^2}{\mu} \tag{4.1}$$

and representing the frequency with which "free" electrons may oscillate in the medium. The influence of the atomic interaction forces on the motion of the electrons may, thus, be treated exactly like the effect of the atomic binding forces and will, in particular, imply a screening at a distance d_ν given by

$$d_\nu = \frac{v}{\nu} \tag{4.2}$$

in analogy to (3.8) for $\gamma = 1$.

It should be noted that the total force with which the medium acts on an electron may differ from $4\pi e \boldsymbol{P}$, corresponding to the well-known fact that the actual average field $\boldsymbol{F}$ to which the electrons are subjected will, in general, deviate from $\boldsymbol{E}$. In simple dielectrica like gases, where the neutral molecules may be regarded as independent entities, it may, thus, be shown that $\boldsymbol{F}$ equals $\boldsymbol{E} + \frac{4\pi}{3}\boldsymbol{P}$, and, also in denser materials, the same relation between $\boldsymbol{F}$ and $\boldsymbol{E}$ will hold in certain cases. Still, it is of particular interest for the following discussion to note that, if the electrons are not bound to certain fixed positions, but move all over space, as in metals or ionized materials, $\boldsymbol{F}$ and $\boldsymbol{E}$ will coincide (cf. DARWIN 1934). More generally, we may put $\boldsymbol{F} = \boldsymbol{E} + 4\pi a \boldsymbol{P}$, where a is a numerical constant characteristic of the structure of the substance. Since, however, the additional force $\boldsymbol{F} - \boldsymbol{E}$ may be ascribed to the effect of the atoms in the immediate neighbourhood of the electron considered, it will be convenient to include it in the atomic binding force $-\mu\omega_a^2\boldsymbol{\xi}$. If, thus, ω_a' represents the binding frequency of an isolated atom, we have,

$$\omega_a^2 = \omega_a'^2 - a\nu^2, \tag{4.3}$$

where ν is given by (4.1). As is well known from dispersion theory, ω_a will then represent the absorption frequency of the substance.

The combined influence of the atomic binding and the polarization may be treated by introducing an effective frequency ω_A defined by

$$\omega_A^2 = \omega_a^2 + \nu^2 \tag{4.4}$$

to replace ω_a in formulae deduced for isolated atoms. In particular, the stopping power may be obtained in this manner from the non-relativistic approximation of (3.9).

In order to estimate the significance of the atomic interaction effects in stopping problems, we must thus compare ν with the atomic frequency ω_a. From (4.1) we have, introducing the electronic velocity v_0 and the radius a_0 of the hydrogen atom,

$$\nu^2 = 4\pi n a_0^3 \left(\frac{v_0}{a_0}\right)^2. \tag{4.5}$$

Now, $\frac{v_0}{a_0}$ represents the order of magnitude of the frequencies of the most loosely bound electrons in atoms and since, even in dense materials, $n a_0^3$ is always smaller than unity, it follows that, compared with atomic frequencies, ν will never be very large and, in most cases, actually quite small. It is just for this reason that, in the non-relativistic problem which we have hitherto considered, the atomic interaction effects are usually of only secondary importance for the stopping power. Still, as already mentioned in the Introduction, there are exceptions to this rule. In fact, for the free electrons in metals or ionized substances, the binding frequency vanishes and, in this case, which we shall discuss more closely in § 5, the polarization effects become of decisive importance.

In the present paragraph, we shall further show how the stopping power of a substance may be directly described as a force with which the medium acts on the moving particle[1]. This alternative way of approach also allows of a simple deduction of the stopping formula which corresponds to (3.9) when due account is taken of the polarization effects. For illustration we shall, however, first briefly consider the analogous problem for the two-body collision.

1) This method has been outlined in a more qualitative way by N. Bohr (1948, § 3.1).

Instead of calculating the energy loss of the particle from the momentum transfer to the electron, one might in fact directly have estimated the reactive force of the struck electron. Thus, in the non-relativistic case considered here, the displacement of the electron implies that, taking the particle to be positive, the decelerative force in the last half of the collision more than compensates the acceleration in the first half. That part of the reactive force, directed against the motion of the particle, which is produced by the electronic displacement is given by

$$\delta K = -\eta \frac{\partial}{\partial p} \frac{z_1 e^2 v t}{(p^2 + v^2 t^2)^{3/2}} = \frac{3 z_1 e^2 \eta p v t}{(p^2 + v^2 t^2)^{5/2}} \tag{4.6}$$

and, by introducing η from (3.3), putting $\gamma = 1$, one finds for the resulting decrease in kinetic energy of the particle

$$\int_{-\infty}^{\infty} \delta K \, v \, dt = 3 \frac{z_1^2 e^4}{\mu v^2} v^3 \int_{-\infty}^{\infty} \frac{t^2 \, dt}{(p^2 + v^2 t^2)^{5/2}} = T \tag{4.7}$$

as given by (3.4).

In case of a particle penetrating through a substance, it is in a similar way the polarization which acts as a brake on the particle. If the medium is homogeneous and isotropic, however, no free charges will be generated (div $\boldsymbol{P} = 0$) except at the position of the particle. Inside the medium, therefore, each volume element remains neutral and gives rise to no resultant force, but along the path of the particle opposite charge will be accumulated. Of course, such considerations depending on average quantities like free charge cannot be applied to the material in the immediate neighbourhood of the particle but, for the purpose of considering the interaction between the particle and the medium at distances large compared with atomic dimensions, we may imagine removed a cylindrical tube of radius $q \gg a_0$ around the path of the particle. The force S_q with which the more distant part of the medium acts on the particle may then be calculated from the attraction of the free charges induced on the inner surface of this cylindrical tube.

The surface density σ of these charges equals $-e n \eta$. For the value of η, however, we may not use the simple formula (3.3),

since we must take into account the presence of a harmonic force of frequency ω_A. If, however, we choose $q \ll \frac{v}{\omega_A}$, an electron at the surface will, during the time when the direct force of the particle is active, behave as if it were free and, assuming it to be at rest before the encounter, we get from (3.3)

$$\sigma(x) - \sigma(-x) = 2en\frac{z_1e^2}{\mu v^2}\frac{x}{q}, \tag{4.8}$$

where $x = -vt$ denotes the distance of the electron from the instantaneous position of the particle, measured in the direction of v. The expression (4.8) will hold for $|x| \ll \frac{v}{\omega_A}$ but, for larger values of $|x|$, the harmonic force becomes of importance. Since, however, at such large distances the direct influence of the particle on the electronic motion perpendicular to the path is negligible, (4.8) may be simply generalized to

$$\sigma(x) - \sigma(-x) = 2en\frac{z_1e^2}{\mu v^2}\frac{v}{\omega_A q}\sin\left(\frac{x\omega_A}{v}\right). \tag{4.9}$$

For the force acting on the particle, we thus have

$$S_q = z_1 e\int_0^\infty \frac{\sigma(x) - \sigma(-x)}{(x^2+q^2)^{3/2}}\,2\pi q\,x\,dx = B\frac{v}{\omega_A}\int_0^\infty \frac{x\sin\left(\frac{x\omega_A}{v}\right)}{(x^2+q^2)^{3/2}}\,dx, \tag{4.10}$$

where B is given by (3.6). This integral can be expressed in terms of a Hankel function and gives asymptotically for $q \ll \frac{v}{\omega_A}$

$$S_q = B\log\frac{kv}{\omega_A q}, \tag{4.11}$$

corresponding to (3.9) for $v \ll c$, if only ω_a is replaced by ω_A.

The results of this paragraph, expressed by the formulae (4.1), (4.4), and (4.11), correspond for non-relativistic velocities to those obtained by the more general treatment of Fermi (1940), who, in order to cover the case of $v \sim c$, proceeds by a formally rather different method in which S_q is estimated as the flux of the Poynting vector through the surface of the cylinder of radius q.

§ 5. Stopping Power of Materials Containing Free Electrons.

As already mentioned, the atomic interaction effects are, for non-relativistic particle velocities, of special importance if the substance contains free electrons. Of particular interest in this respect is the stopping power of metals, where the conduction electrons may to a large extent be regarded as free (cf. § 10a).

A few remarks would seem required to justify an application of the considerations in the previous paragraph to problems of free electrons. Indeed, we have here in a sense to do with infinitely large atoms and the very definition of distant collisions, as encounters with impact parameter large compared with atomic dimensions, is therefore, strictly speaking, ambiguous. Still, to our purpose, it is not essential that the electrons are able to move freely throughout space, but we may imagine them confined within limited volumes of linear dimensions a, if only the corresponding oscillation frequency, which will be of the order of $\frac{\hbar}{\mu a^2}$, is small compared with ω_A. This condition may be fulfilled and a at the same time chosen small in comparison with the screening distance $\frac{v}{\omega_A}$, provided $\mu v^2 \gg \hbar \omega_A$. For smaller particle velocities, the stopping mechanism here considered is of only minor significance (cf. the concluding passage in § 2).

In the estimate of the stopping power, it must be taken into account that also other effects than the polarization will tend to restrain the electrons from moving freely. In fact, during the encounter with the incident particle, the electron may collide with ions or electrons in the medium. The influence of these collisions may be compared with the effect of a frictional force $-\mu \omega_\varrho \dot{\xi}$, where $\dot{\xi}$ is the velocity vector and where $\frac{1}{\omega_\varrho}$ is a measure of the time interval in which the electronic momentum is substantially changed. In particular for metals, it is well known from the theory of conduction that

$$\omega_\varrho = \frac{ne^2}{\mu} \varrho, \tag{5.1}$$

where ϱ is the specific resistance.

In an early treatment of the stopping power of metals, by v. WEIZSÄCKER (1933), it was actually suggested that the limit of effective interaction between the particles and the free electrons was determined by the resistance. As pointed out by KRAMERS (1947), however, such effects will, in general, be of only very small influence as compared with that of the polarization of the medium. In fact, since the momentum transfer from the particle to a free electron is comparable with the force of the particle multiplied by the effective collision time $\frac{p}{v}$, it follows that a frictional force can influence the collisions only for $p \gtrsim d_\varrho = \frac{v}{\omega_\varrho}$. Now, in metals at ordinary temperatures, $\omega_\varrho \ll \nu$ and, thus, $d_\varrho \gg d_\nu$ given by (4.2). Consequently, the effective adiabatic limit is primarily determined by the polarization.

A closer estimate of the influence of the friction on the stopping power may be obtained in complete analogy to the considerations leading to (4.11), the only difference being that (4.9) must now represent a damped oscillation. Thus, we merely have to add an extra factor $\exp\left\{-\frac{\omega_\varrho}{2v}x\right\}$ and substitute for ω_A the effective oscillation frequency which, for $\omega_a = 0$, will be equal to $\sqrt{\nu^2 - \frac{1}{4}\omega_\varrho^2}$. Evaluating S_q, one thereby finds asymptotically, for q small compared with the adiabatic limit,

$$S_q = B\left\{\log\frac{kv}{q\nu} - \frac{\omega_\varrho}{\sqrt{4\nu^2-\omega_\varrho^2}}\operatorname{arctg}\frac{\sqrt{4\nu^2-\omega_\varrho^2}}{\omega_\varrho}\right\}. \qquad (5.2)$$

This formula is equivalent to that obtained by KRAMERS by a somewhat different method and also coincides with the non-relativistic approximation of FERMI's formula[1]. For $\omega_\varrho \ll \nu$, the last term in the brackets in (5.2) has the approximate value $-\frac{\pi}{4}\frac{\omega_\varrho}{\nu}$, and the stopping formula therefore reduces to (4.11) for $\omega_A = \nu + \frac{\pi}{4}\omega_\varrho$. In the opposite extreme case of $\omega_\varrho \gg \nu$, the last

[1] In the case of bound electrons, there may likewise be a damping to take into account, e. g., due to radiative forces. In this more general case we get, of course, an expression for S_q which follows from (5.2) by simply replacing ν with ω_A given by (4.4) and ω_ϱ with the damping constant (cf. FERMI 1940).

term in the brackets in (5.2) has the asymptotic value $\log \frac{v}{\omega_Q}$ so that (5.2) now coincides with (4.11) for $\omega_A = \omega_Q$, just corresponding to the result of v. Weizsäcker.

It may be noted that, in the above calculations, we have assumed the electrons to be at rest before the collision with the particle, whereas in metals or ionized materials the electrons actually have quite considerable velocities, often greatly surpassing the velocity changes induced by the particle. However, this circumstance should have no essential effect on the average energy transfer. In fact, if we denote by $\boldsymbol{w}$ the initial velocity, and by $\boldsymbol{u}$ the velocity alteration, the increase in kinetic energy is given by

$$T = \frac{1}{2}\mu(\boldsymbol{w}+\boldsymbol{u})^2 - \frac{1}{2}\mu w^2 = \frac{1}{2}\mu u^2 + \mu \boldsymbol{w}\boldsymbol{u} \qquad (5.3)$$

and, averaged over all directions of $\boldsymbol{w}$, the last term vanishes.

Still, of course, it must be assumed that the electrons, during the actual collisions, do not move over distances comparable with the impact parameter and that, therefore, w must be small compared with the particle velocity. In most cases of importance, this condition is amply fulfilled but, e. g. in ionized media at very high temperatures, the thermal velocities may exceed v even for "fast" particles and, under such circumstances, the whole stopping phenomenon acquires an essentially different character. However, we shall not here enter more closely on this problem.

§ 6. Atomic Interaction for Relativistic Particle Velocities.

The preceding considerations regarding the polarization effects were confined to particle velocities small compared with that of light. While, in this case, it was seen that, with the few exceptions discussed in § 5, the atomic interaction is of only minor importance, being in general of small influence compared with that of the internal binding forces, the situation is essentially different for relativistic velocities. In fact, for sufficiently large values of $\gamma = \left(1 - \frac{v^2}{c^2}\right)^{-1/2}$, the radius of action of the particle is,

as shown by FERMI (1940), always determined by the polarization effects.

As regards collisions with single atoms, the modifications to be taken into account for $v \gtrsim c$ are of very simple character. Thus, as long as we are within the adiabatic limit, the energy transfer in distant collisions is, according to (3.4), independent of relativity effects. In fact, the retardation merely implies a contraction by a factor γ of the field of the incident particle in the direction of motion and an intensification of the field in the same ratio, and, therefore, does not affect the total momentum transfer. On account of the contraction of the field and the resulting shortening of the collision time, however, the adiabatic limit is increased by a factor γ, as also follows from (3.8).

It may be added that the influence of resistive forces discussed in § 5 is modified in a similar manner. Since a frictional force $-\mu\omega_\varrho\dot{\boldsymbol{\xi}}$ is comparable with the force from the particle only if the collision time is of the order of or larger than $\frac{1}{\omega_\varrho}$, the screening distance corresponding to such effects will be given by

$$d_\varrho = \frac{v}{\omega_\varrho}\gamma, \tag{6.1}$$

which, for velocities small compared with that of light, reduces to the estimate in § 5.

An analysis of the atomic interaction effects in the relativistic case presents, however, a somewhat more intricate problem. In particular, we may no longer, like for $v \ll c$, compare the polarization force with a simple harmonic restitutional force. In fact, in contrast to the screening effect of a force of this type, one finds that the adiabatic limit for a material in which the electrons are free, and where the polarization is determining for the stopping effect, is uninfluenced by retardation effects. This result, which follows from FERMI's formula and which, as we shall see, can also be obtained by more elementary considerations, shows that in the relativistic case the mutual influence of the electrons is much stronger than corresponding to the electrostatic forces considered in § 4. Indeed, as was to be expected, all interaction effects become, for $\gamma \gg 1$, primarily of electromagnetic character.

In order to illustrate this latter point, it is instructive to consider a simple two-body collision from the point of view of the reaction of the struck electron on the incident particle. This problem was treated in § 4 for $v \ll c$, but is essentially modified by retardation effects. In fact, the particle will not "know" that the electron has been perturbed before the pulse caused by this perturbance catches up with the particle and, for velocities very close to c, this will happen a comparatively long time after the actual collision is initiated. Thus, a signal emitted by the electron at $t = 0$ will reach the particle at a distance $p\gamma$. Now, the periods characterizing the electronic motion will be comparable with the collision time $\frac{p}{v}\frac{1}{\gamma}$ and, for $v \lesssim c$, the field which this motion produces will, thus, mainly contain harmonic components of wave-lengths of the order of $\frac{p}{\gamma}$. Since such wave-lengths are small compared with the distances in question, it follows that the reaction of the electron on the particle is primarily determined by the electromagnetic wave field emitted by the accelerating electron. The electrostatic part of the field which depends on the electronic displacement and which, in the non-relativistic case, is responsible for the reaction, is here of only secondary importance.

The following estimate may serve to illustrate that the acceleration of the electron, for $\gamma \gg 1$, is actually determining for the reaction. In fact, the electric field intensity produced by an accelerated electron is, at large distances r, asymptotically given by

$$E(t) = \frac{e\ddot{\eta}(t')}{c^2 r} \sin\varphi, \tag{6.2}$$

where φ is the angle between the acceleration and the radius vector and where, as indicated, $\ddot{\eta}$ is to be taken at the retarded time $t' = t - \frac{r}{c}$. Since this field is transverse, i. e. perpendicular to r, the corresponding force acting on the particle against the direction of motion will be

$$\delta K(t) = \frac{z_1 e^2}{c^2} \frac{\ddot{\eta}(t')}{r} \sin\varphi \cos\varphi. \tag{6.3}$$

Now, during the actual collision, $\ddot{\eta}$ is, according to (3.1), comparable with $\frac{z_1 e^2 \gamma}{p^2}$ and since, as already mentioned, the r-values in question are of the order of $p\gamma$, we may, for $\gamma \gg 1$, put $\sin \varphi = 1$ and $\cos \varphi = \frac{1}{\gamma}$. Furthermore, the pulse given out by the accelerated electron, although it has a spatial extension of about $\frac{p}{\gamma}$, will act on the particle through a distance comparable with $p\gamma$, since the velocities of pulse and particle only differ by a relative amount of the order of γ^{-2}. It will thus be seen that the force component (6.3) gives rise to an energy loss just of the order of T given by (3.4).

A more accurate analysis of the reaction in the two-body collision is given in Appendix I, but the above cursory considerations suffice to illustrate the decisive part played by the radiation field. It is also just this circumstance which is manifested in the peculiar radiation effects which accompany the passage of very fast particles through matter and which will be discussed more closely in the next paragraph.

On similar lines as the simple analysis of the two-body collision, one may obtain an estimate of the mutual interaction

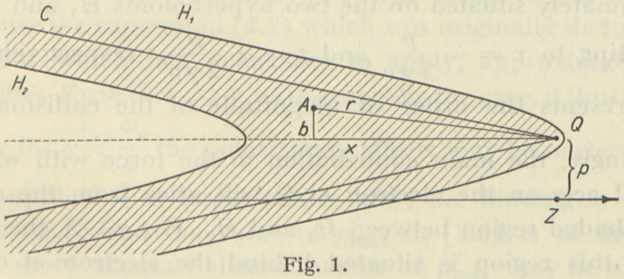

Fig. 1.

between the electrons in the penetrated substance. To this purpose, consider an electron at point Q (see Fig. 1), which is colliding with the particle Z passing at distance p. At the same time, the electron is acted upon by the surrounding electrons, and the major contribution will come from those electrons which, at the retarded time $t' = t - \frac{r}{c}$, were themselves accelerated, i. e. were colliding with the particle. Now, an electron at point A will, at the retarded

time, be in a phase of collision which, as compared with that of the electron at Q at the instant considered, is earlier by a time interval τ given by

$$\tau = \frac{r}{c} - \frac{x}{v}, \tag{6.4}$$

where x is the projected distance from Q to A measured against the direction of motion of the particle. Introducing $r^2 = x^2 + b^2$ (see the figure), one gets from (6.4)

$$\frac{(x + v\tau\gamma^2)^2}{v^2\tau^2\gamma^2(\gamma^2 - 1)} - \frac{b^2}{c^2\tau^2(\gamma^2 - 1)} = 1, \tag{6.5}$$

which shows that the points of constant τ are situated on a hyperboloid. In particular, the electrons which at the retarded time were in the same stage of collision as the electron at Q, will be found on the conical surface C extending backwards from Q and having an opening angle ϑ for which $\sin\frac{\vartheta}{2} = \frac{1}{\gamma}$. This surface intersects the path of the particle at the distance $x = \frac{v}{c}\gamma p$.

In the figure, the electron at Q is, at the instant considered, at the peak of collision. The electrons which, at the retarded time, were "beginning" or "concluding" their collisions are, thus, approximately situated on the two hyperboloids H_1 and H_2, corresponding to $\tau = -\frac{p}{2\gamma v}$ and $\tau = +\frac{p}{2\gamma v}$, respectively, since $\frac{p}{\gamma v}$ represents the order of magnitude of the collision time[1]. Accordingly, the main contribution to the force with which the material acts on the electron at Q will arise from the electrons in the shaded region between H_1 and H_2. For $\gamma \gg 1$, the essential part of this region is situated behind the electron at distances of the order of or smaller than $p\gamma$. In fact, further away, we have contributions from electrons accelerated in all directions, and therefore the total field of these electrons is small.

According to (6.2), the field from each electron is inversely proportional to r; furthermore, since $\sin\varphi \sim 1$ and since the majority

1) Strictly speaking, it should be taken into account that the collision time varies with the impact parameter. For the present purpose of estimating orders of magnitude, however, the more cursory considerations should suffice, since the major part of the polarization force arises from atoms with impact parameters comparable with that of the atom at Q.

of the electrons in question have accelerations comparable with that of the electron at Q, the resulting polarization force K will be of the order of magnitude of

$$K \sim \frac{e^2}{c^2} \ddot{\eta} p^2 n \tag{6.6}$$

and directed against $\ddot{\eta}$. This force is evidently small compared with the total force $\mu \ddot{\eta}$ acting on the electron, only if

$$p \ll \frac{c}{\nu}, \tag{6.7}$$

where ν is given by (4.1). This upper limit should, therefore, represent the screening distance d_ν corresponding to the atomic interaction effects. The estimate of the polarization force is, of course, of a rather cursory character but, due to the complicated calculations which would be implied, we shall not attempt a detailed analysis from the microscopic point of view. The above considerations suffice, however, to bring out the essential point that, for $v \to c$, the distance d_ν approaches a constant value of the order of c/ν.

In estimating the stopping power of a substance we now have to compare d_ν with the adiabatic limit d_a corresponding to the effect of the binding and given by (3.8). As to the former distance, we may use the expression (4.2) which was originally deduced for $v \ll c$, but which has been seen to apply, approximately, for all velocities. Even if $\omega_a \gg \nu$, as is generally the case, it thus follows that only for $\gamma < \frac{\omega_a}{\nu}$ the polarization effects may be neglected and (3.9) be applied. For larger values of γ, the binding is of little influence on S, and the value of $p_{\max}$ in (3.5) is of the order of d_ν. A more accurate determination of $p_{\max}$ may be obtained by noting that the stopping power of a substance containing free electrons (cf. p. 27) is not affected by retardation. For large γ, we thus have the asymptotic expression.

$$S_q = B \log \frac{kv}{p\nu} \tag{6.8}$$

corresponding to (4.11) for $\omega_A = \nu$.

We have here neglected the possible influence of frictional forces which may become significant if d_ϱ given by (6.1) is

smaller than both d_a and d_v. Under such circumstances, the stopping formula is obtained from (3.9) by substituting ω_ϱ for ω_a.

These results are in complete agreement with the more rigorously deduced formulae given by FERMI (1940). Only in the transitional cases, in which neither of the three distances d_a, d_v or d_ϱ is very much smaller than the two others, certain refinements have to be introduced in analogy to the more detailed expressions given in § 4 and § 5 for non-relativistic velocities. Such corrections, however, amount at most to only a few per cent of the stopping power.

§ 7. Čerenkov Effect and its Relation to the Stopping Problem.

As already mentioned in the Introduction, the passage of very fast particles through dense matter is accompanied by a peculiar radiation (Čerenkov effect). An analysis of this phenomenon was first given by FRANK and TAMM (1937), who pointed out its immediate connection with the circumstance that the phase velocity of light in the substance may be smaller than the speed of the particle. In fact, the Čerenkov radiation presents a close analogue to familiar acoustical and hydrodynamical phenomena produced by an object moving with a velocity exceeding that of the wave velocities in the medium (TAMM 1939).

Since the phase velocity of electromagnetic waves is given by $c/\sqrt{\varepsilon}$, where ε is the dielectric constant, the radiation will take place over spectral regions for which

$$\sqrt{\varepsilon} > \frac{c}{v}. \tag{7.1}$$

Moreover, since the waves must be stationary with respect to the moving particle, the angle of emission for a frequency for which (7.1) is fulfilled is given by

$$\cos \Theta = \frac{c}{v\sqrt{\varepsilon}}, \tag{7.2}$$

where Θ is measured from the direction of motion of the particle.

In the present paragraph, we shall discuss, by means of simple arguments, some of the general characteristics of the Čerenkov effect and, in particular, its relation to stopping theory.

In order to obtain a survey of the various aspects of the phenomenon, it is of interest to consider the problem from the microscopic as well as from the macroscopic point of view. In the former case, we have immediate connections to the considerations of § 6, while the latter approach is more in analogy to that of FRANK and TAMM, and of FERMI.

From the microscopic point of view, the Čerenkov effect simply originates in the circumstance that part of the energy transferred from the penetrating particle to the electrons in the substance may be subsequently emitted as coherent radiation. Thus, it was not necessary in the previous paragraph to take the effect explicitly into account since, in problems of stopping power, one need, in the first instance, consider only the behaviour of the struck electrons during the actual collision with the particle. In fact, the energy loss of the particle may be said to be decided within this short time interval and is not affected by the question of the later distribution of the energy transferred to the electrons. In particular it is, from such considerations, immediately evident that the Čerenkov effect corresponds to part of the stopping power estimated in § 6 and should not be regarded as an additional source of energy loss (cf. FERMI 1940).

Some of the main features of the radiation may also be understood from an analysis like that in § 6. Thus, an emission of coherent radiation will demand the fulfilment of proper phase relations between the wavelets originating from the individual electrons, and this condition leads immediately to (7.2). Moreover, the spectral distribution is correlated to the rate at which the energy of the electronic oscillations is dissipated into radiation. For an isolated atom, this rate is very low, but it may be strongly increased by the influence of surrounding atoms. In fact, just due to the phase relations, the superposition of the electromagnetic fields of the individual oscillators may lead to greatly enhanced radiative effects.

In order to estimate the influence of atomic interaction on the Čerenkov spectrum, we may consider the two extreme cases, $d_\nu \gg d_a$ and $d_\nu \ll d_a$, in which, according to the considerations in § 6, the interaction forces may be regarded as, respectively, very weak and very strong compared with the binding forces. In the former case, we should expect the atoms to perform a large number of oscillations before their energy is radiated, and the

emitted spectrum to consist of a narrow line around the proper frequency of oscillation. In the latter case, however, the atoms will not be able to perform even a single oscillation and the frequency distribution should bear no simple resemblance to a spectral line.

Such general features of the radiation are just in accordance with those implied by the condition (7.1) for the spectrum. In fact, the dispersion law corresponding to the simple atomic model considered, involving only a single proper frequency ω_a, may be written

$$\varepsilon = 1 + \frac{\nu^2}{\omega_a^2 - \omega^2}, \tag{7.3}$$

where ν is given by (4.1). Furthermore, according to (3.8) and (4.2), the two cases in question correspond to $\nu\gamma \ll \omega_a$ and $\nu\gamma \gg \omega_a$, respectively. It is, therefore, seen that, in the former case, (7.1) is fulfilled only in a narrow region around ω_a while, in the latter case, it holds for all frequencies smaller than ω_a.

From the macroscopic point of view, the energy loss of the particle appears to take place in two essentially different modes. In fact, neglecting absorption due to damping forces, energy may either be radiated or it may be absorbed by the matter, giving rise to oscillations persisting in the medium after the passage of the particle. For the distinction between these two mechanisms, it is convenient to divide the electromagnetic field produced by the particle in the substance into a transverse (divergence-free) and a longitudinal (irrotational) component. The radiative part of the field is obviously of the transverse character, while the residual oscillations, left in the "wake" of the particle, must correspond to a longitudinal field. In fact, in the absence of electric currents, a divergence-free field consists of free electromagnetic radiation which propagates to infinite distances.

The longitudinal component just represents the field calculated with neglect of retardation effects and is, therefore, simply that considered in § 4, where the velocity of light was regarded as infinite. It is thus immediately seen that the energy absorbed by the medium in the neighbourhood of the path of the particle is given by the non-relativistic stopping formula[1].

1) It must be noted that, when damping is taken into account, also some part of the transverse field energy may be absorbed by the medium close to the particle (cf. § 8).

The relativistic increase of the stopping effect is due to the transverse field and, hence, represents the radiated energy. Moreover, it is evident from such considerations that, while the energy stored in the medium corresponds to that transferred to the atoms within the non-relativistic adiabatic limit, the radiation is emitted by the atoms at larger distances from the path of the particle.

In particular, it is of interest to note that, for substances containing free electrons ($\omega_a = 0$), it follows from (7.3) that ε is always smaller than unity, and the condition (7.1) can, thus, never be fulfilled. Consequently, no radiation occurs and the stopping power must, therefore, as already mentioned in § 6, for all velocities be given simply by the expression originally deduced for $v \ll c$.

For the residual field left in the medium after the passage of the particle, we have, of course, $\boldsymbol{D} = 0$ since, from the macroscopic point of view, no "true" charges are present. The dielectric constant of the medium must, therefore, vanish for the oscillation frequency concerned and, according to (7.3), this condition will just be fulfilled for $\omega = \omega_A$ given by (4.4), which was seen in § 4 to represent the proper frequency of the substance. It may be added that, from the very circumstance that we have to do with the excitation of oscillators of proper frequency corresponding to $\varepsilon = 0$, it may immediately be concluded that their energy absorption is unaffected by retardation effects. In fact, this energy depends, as is well known, exclusively on the resonance component of the exciting field, for which the phase velocity of light, $c/\sqrt{\varepsilon}$, is infinite.

In the evaluation of the radiated energy, Frank and Tamm (1937) and Fermi (1940) expand the electromagnetic field produced by the particle in harmonic components with respect to time-dependence. It is, however, also possible to adapt to the case of ponderable media the well-known method of radiation theory in which the field is dissolved in plane waves. In Appendix II, we shall consider the application of this formalism to the problems of stopping power and Čerenkov radiation. The method sheds some light on the phenomena in question and, in addition, is illustrative of the difference in approach between ordinary procedures of classical electromagnetic theory and the formalism which has become the conventional tool in quantum electrodynamics.

§ 8. The Atom as a General Dispersive System.

The preceding considerations have been based on a highly simplified atomic model in which the virtual oscillators were considered to have all the same frequency. This simplification was made in order to bring out as clearly as possible the principal points regarding the atomic interaction effects, but in a more detailed treatment, the atom should be compared with an ensemble of oscillators corresponding to the different excitation possibilities (cf. § 2). The proper frequencies of these oscillators will be denoted by ω_i, and their relative strengths by f_i normalized per electron $\left(\sum_i f_i = 1\right)$. If the atoms are bound together, this model is still adequate if only the oscillators represent the transition possibilities of the electrons in the molecules or in the lattice.

Such refinements are readily accounted for in the usual stopping theory. In fact, if the oscillators can be regarded as independent, formula (3.9) is simply to be replaced by

$$S_q = B \sum_i f_i \left(\log \frac{kv\gamma}{q\,\omega_i} - \frac{1}{2}\frac{v^2}{c^2} \right), \tag{8.1}$$

where the electron density n entering in the expression (3.6) for B is equal to $z_2 N$, if z_2 denotes the atomic number of the substance and N the number of atoms per unit volume.

The polarization phenomena, however, introduce a coupling between the different oscillators. In principle, this effect presents no great difficulties, since the calculation of FERMI (1940), or a procedure like that used in Appendix II, may be immediately generalized by replacing the simplified dispersion law (7.3) by

$$\varepsilon = 1 + \sum_i \frac{f_i\, \nu^2}{\omega_i^2 - \omega^2}, \tag{8.2}$$

corresponding to the atomic model on which (8.1) is based. Still, exact calculations by means of such methods lead to rather complicated expressions[1] and it is, therefore, of interest that, on the

1) The case of two dispersion frequencies has been considered by HALPERN and HALL (1940). The more general model corresponding to (8.2) has been treated by STERNHEIMER (1946), but an evaluation of the expressions deduced is difficult and has been attempted only under simplifying assumptions. The accuracy involved seems, therefore, hardly to go beyond that of the more simple analysis given here, the results of which also coincide in essentials with those obtained by STERNHEIMER.

See also Postscript (i), p. 50.

basis of considerations analogous to those in § 6, it is possible to obtain simple formulae representing a degree of accuracy sufficient for most purposes.

In such a microscopic treatment, the influence of the polarization on the stopping effect may be estimated by comparing the distance d_v with the adiabatic limits d_i, corresponding to the various atomic frequencies ω_i and given by (3.8) for $\omega_a = \omega_i$. The value of d_v will be given by an expression of the type of (4.2), but an essential point will be to estimate the effective electronic density determining for the polarization. In fact, due to the influence of the binding forces, this density will decrease with increasing distance from the path of the particle.

At distances comparable with d_i, the number of electrons per unit volume which contribute materially to the polarization will be equal to nF_i, where F_i represents the sum of the oscillator strengths, corresponding to atomic frequencies equal to or smaller than ω_i. According to the estimates in § 6, the atomic interaction will therefore be effective, provided $\gamma v F_i^{1/2} > \omega_i$, where v is given by (4.1) for $n = z_2 N$. For a survey of the problem, it will thus be convenient to introduce a critical frequency ω_c defined by

$$\omega_c = \gamma v F_c^{1/2}, \tag{8.3}$$

where

$$F_c = \sum_{\omega_i \leqq \omega_c} f_i. \tag{8.4}$$

In general, we may assume that equation (8.3) has only a single root, a point to which we shall return briefly in § 9, where approximate expressions for the frequency distribution of the oscillators are considered.

In this case, the situation is especially simple, and it is seen that the limit of free energy transfer will be determined primarily by the binding forces or the polarization, according as $\omega_i > \omega_c$ or $\omega_i < \omega_c$, respectively. The contribution to the stopping power of the former oscillators will approximately be given by the respective terms in (8.1), while for the latter oscillators the expression (6.8) for an effective electron density nF_c will apply.

The total stopping power of distant collisions may, thus, be written

$$S_q = B\left\{F_c \log\frac{kv}{q\nu F_c^{1/2}} + \sum_{\omega_i > \omega_c} f_i\left(\log\frac{kv\gamma}{q\omega_i} - \frac{1}{2}\frac{v^2}{c^2}\right)\right\}. \qquad (8.5)$$

In particular, it may be noted that, for very large velocities for which γv exceeds the largest significant atomic frequencies, we have $F_c \approx 1$ and, in this case, the stopping formula will be especially simple, being practically independent of the atomic frequencies. The latitude involved in (8.5) arises mainly from the estimate of the contribution of the oscillators with $\omega_i \sim \omega_c$, for which, of course, the polarization as well as the binding forces have a significant influence. The accuracy of the above approximation would, however, seem to be quite high since, as already mentioned in § 6, even in the case where all frequencies are equal and, therefore, may all fall in the transition region, the necessary corrections will never exceed a few per cent[1].

The part of the energy loss which is radiated to large distances may, according to the considerations in § 7, be readily estimated, provided the absorption due to damping effects can be disregarded. In this case, the radiated energy, in fact, simply represents the difference between (8.5) and the stopping power which would be obtained by disregarding relativity effects. Actually, however, we have to do with a considerable absorption in the spectral region extending from the lowest proper frequency of the substance to the highest relevant atomic frequencies, and an estimate shows that, in this region, by far the greater part of the radiation will, in not too dilute materials, be reabsorbed close to the path of the particle. It would thus seem that, to a first approximation, an actual emission of radiation, easily accessible to observation, will be confined to the region below the first absorption band. For such frequencies, which in generally comprise primarily the visible and infrared region and possibly part of the ultraviolet, the radiation spectrum may be calculated from formula (12) in Appendix II by introducing the proper values for the dielectric constant.

Finally, we shall consider briefly the influence of atomic interaction on the number of ions produced by the particle along the path. This problem involves in principle a detailed investigation of the distribution of the energy loss on the various atomic

[1]) Cf. Postscript (ii), p. 50.

oscillators, but it appears that the relationship between stopping power and ionization is not essentially affected by the polarization effects, and recourse may therefore be taken to the results of ordinary penetration theory. In the analysis of the problem, we may conveniently make use of the considerations in § 6 and § 7 and shall, in particular, divide the field surrounding the particle into a longitudinal and a transverse part.

The former part, corresponding to the energy loss calculated with neglect of retardation, will (cf. § 4) be only little influenced by the polarization, especially in case of dilute materials like gases, where the ionization problem is of particular importance. For this part of the interaction between particle and matter, we may thus immediately use the result, derived for collisions with isolated atoms, that in distant encounters the contribution of any bound electron to the number of primary ionization processes is closely proportional to the corresponding contribution to the stopping power. In the simplest case, of hydrogen, it follows in particular from the detailed calculations of BETHE (1930) that the number of ions produced per unit path, in collisions with impact parameter greater than q, is given by

$$P_q = S_q \frac{0.285}{\hbar\omega_0}. \tag{8.6}$$

For heavier substances, generalized approximate expressions may be given (cf. N. BOHR 1948, § 3.4).

The relativistic increase in the energy loss was seen to be correlated to the transverse part of the field, but it is of importance that, according to the above considerations, only a negligible part of the energy transfer due to the interaction with the ionization oscillators will be emitted as radiation to larger distances, since this energy is mainly concentrated in frequency regions of strong absorption.

A detailed investigation of the energy absorbed by the various oscillators from the transverse field is rendered difficult by the circumstance that the radiation emitted by one type of oscillators may, as discussed in § 7, contain frequencies extending over a wide interval and may, consequently, be absorbed by oscillators of a different type. However, just in case of gases, where v is very small compared with atomic frequencies, this "mixing" effect

should be rather insignificant. In fact, even in case of $d_i \gg d_v$, where the frequency distribution of the emitted radiation is most strongly spread out, it may be shown that, for $v \ll \omega_i$, the larger part of the energy is concentrated on frequencies which differ from ω_i by an amount small in comparison with ω_i itself. The mixing will, therefore, primarily take place between very close lying levels and should not essentially affect the relative number of ionization processes.

Relations of the type of (8.6) must thus, in general, be expected to be only little influenced by the atomic interaction effects. As regards the total ionization, including primary as well as secondary processes, one may likewise conclude that, as has been deduced for collisions with isolated atoms (cf., e. g., FANO 1946), the average energy expenditure per ion is largely independent of the particle velocity.

§ 9. Estimate of Stopping Power for Heavy Substances.

It follows from the considerations in the previous paragraph that the influence of atomic interaction may imply a considerable simplification in the stopping formula since, for very large values of $v\gamma$ corresponding to $F_c \approx 1$, the stopping becomes independent of the atomic frequencies and is determined only by the electronic density of the substance. In order, however, to evaluate S_q in the transition region where the polarization gradually becomes effective, it is necessary to investigate the distribution of the atomic oscillator frequencies involved in expressions like (8.5). In the case of heavy substances, a detailed analysis of this problem is complicated[1]), but more cursory estimates, sufficient for many purposes, may be derived on the basis of simplifying assumptions regarding the frequency distribution.

In penetration problems, one thus often obtains an approximate account of general features (cf. N. BOHR 1948, § 3.5) by representing the sum F of the oscillator strengths corresponding to $\omega_i \leq \omega$ by an expression of the simple type

$$F = \left(\frac{\omega}{z_2^s\,\omega_0}\right)^{1/2}, \tag{9.1}$$

[1]) Cf. Postscript (iii), p. 51.

where ω_0 denotes the Rydberg frequency. Of course, such a relation needs modification for the most loosely as well as the most firmly bound electrons in the atom. While the corrections in the low frequency region are of only minor significance in the present connection, it will be necessary to make adjustments in

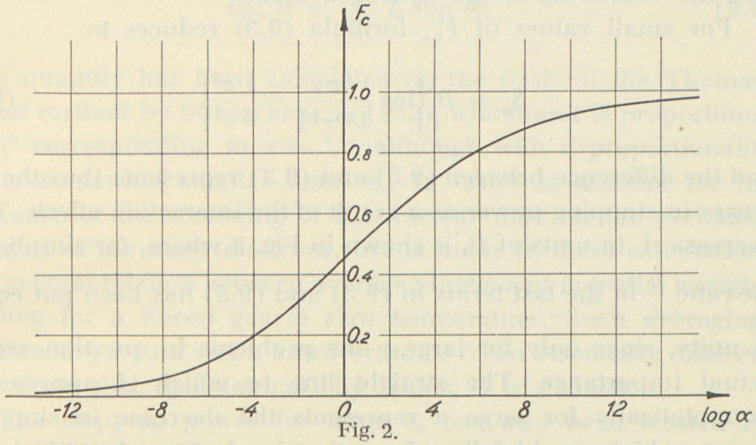

Fig. 2.

the high frequency region so as to take into account that the total oscillator strength equals unity. To this purpose, it would seem natural to put tentatively

$$F = \frac{\left(\frac{\omega}{z_2^s \omega_0}\right)^{1/2}}{1 + \left(\frac{\omega}{z_2^s \omega_0}\right)^{1/2}} \tag{9.2}$$

as a simple function which corresponds to (9.1) for $F \ll 1$ and gives $F = 1$ for large ω.

In particular, it may be noted that, for distributions of the type (9.1) or (9.2), the equation (8.3) determining for the interaction effects will have only a single root. The stopping power will, thus, be given by (8.5) and one finds, by replacing the sum by an integral and introducing (9.2),

$$S_q = B \left\{ \log \frac{k v F_c^{3/2}}{q \nu} - \frac{1}{2} (1 - F_c) \frac{v^2}{c^2} \right\} \tag{9.3}$$

as a simple approximate formula involving only F_c. The variation of this quantity in the transition region is shown in Fig. 2 which gives F_c as a function of α defined by

$$a = \left(\frac{\gamma \nu}{z_2^s \omega_0}\right)^2 = 16 \pi \gamma^2 N a_0^3 z_2^{1-2s}, \tag{9.4}$$

where the ratio between ν, given by (4.1), and the Rydberg frequency ω_0 has, for convenience, been written in terms of N and the radius a_0 of the hydrogen atom.

For small values of F_c, formula (9.3) reduces to

$$S_q = B \left\{ \log \frac{k v \gamma}{q \omega_0 z_2^s} - \frac{1}{2} \frac{v^2}{c^2} \right\} \tag{9.5}$$

and the difference between (9.5) and (9.3) represents thus the decrease in stopping power as a result of the interaction effects. This decrease Δ, in units of B, is shown in Fig. 3 where, for simplicity, the ratio $\frac{v}{c}$ in the last terms in (9.3) and (9.5) has been put equal to unity, since only for large γ the problems in question are of actual importance. The straight line to which Δ approaches asymptotically for large a represents the decrease in stopping power, which would follow from the simple formula (6.8) to be applied when the polarization effects have reached full efficiency.

In order to estimate the exponent s in (9.2) which gives the best fit to the actual frequency distribution of the atomic oscillators, we may compare (9.5) with theoretical and experimental deter-

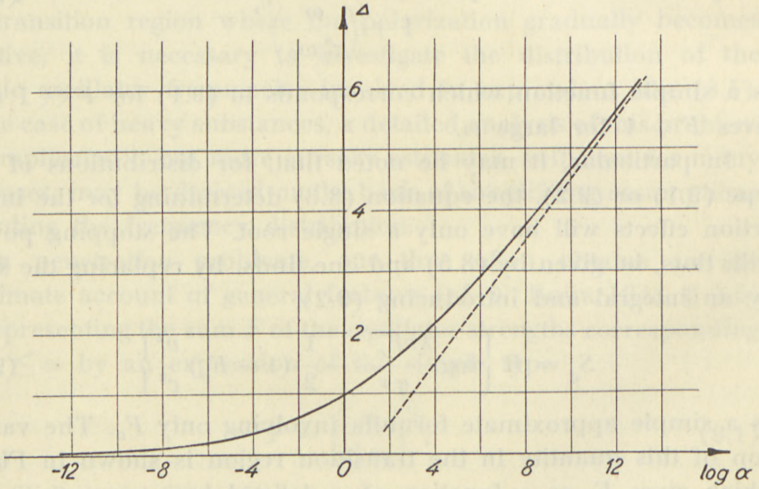

Fig. 3.

minations of the stopping power for heavy atoms in cases where the polarization effects are negligible. The expression (9.5) corresponds to (8.1) for $\overline{\omega} = \omega_0 z_2^s$, where $\overline{\omega}$ represents the average excitation frequency defined by

$$\log \overline{\omega} = \sum_i f_i \log \omega_i. \tag{9.6}$$

This quantity has been calculated on the basis of the Thomas-Fermi method by SOMMERFELD (1932), who found $\overline{\omega}$ proportional to $z_2^{4/3}$ corresponding to $s = 4/3$, although with a proportionality factor somewhat smaller than ω_0. In order to account for the influence of the screening of the nuclear field on the excitation energies of the inner electrons, use is made in these calculations of a general relation between average kinetic and potential energies holding for a Fermi gas at zero temperature. Such averagings (arithmetic) would seem, however, to be of an essentially different type from that (geometrical) by which $\overline{\omega}$ is defined.

The stopping power for large z_2 has also been treated by BLOCH (1933b) who, likewise, compared the atom with a Fermi gas, but considered explicitly its dynamic properties. Although the details of the distribution of the proper frequencies involved highly complicated calculations, it was found that F depends only on the ratio ωz_2^{-1}, a result which leads to $\overline{\omega}$ proportional to z_2. Later, the problem has been reconsidered by H. JENSEN (1937), who pointed out minor corrections to the results of BLOCH, but these refinements are of little importance in the present connection.

The estimate of BLOCH is confirmed by experiments of WILSON (1941) on the stopping power of protons which, in the region where the polarization effects are insignificant, is found to be in good agreement with the theory, if $\overline{\omega}$ is taken proportional to z_2. Moreover, the proportionality factor is estimated to be very nearly equal to ω_0 and the results, therefore, just correspond to (9.5) for $s = 1$. This circumstance may perhaps be taken as an indication of the approximate adequacy of the procedure used in the present paragraph to estimate the polarization effects in the transition region.

§ 10. Comparison with Experimental Evidence.

a) Non-relativistic velocities.

Considering, first, the case of particle velocities small compared with that of light, it was seen in § 4 and § 5 that the atomic interaction effects are of particular importance when the substance penetrated contains free electrons. Of special interest in this respect is the problem of metals.

According to the dispersion theory of metals (cf., e. g., KRONIG 1929, 1931), the behaviour of the valence electrons may be represented by a series of oscillators the first of which has zero frequency, corresponding to free electrons, and the remainder of which represent the transitions of the electrons between different bands (Brillouin zones). The most prominent of these transitions will have frequencies of the order of

$$\omega_b = \frac{\pi^2 \hbar}{2 \mu b^2} \tag{10.1}$$

if, for simplicity, we compare the lattice with a cubic structure of spacing $b = N^{-1/3}$. Denoting the number of valence electrons per atom by $z_2 F_v$, we have thus, by means of (4.1),

$$\frac{F_v \nu^2}{\omega_b^2} = \frac{16}{\pi^3} \frac{b}{a_0} z_2 F_v \tag{10.2}$$

and since, in general, b will be equal to 2 or 3 Å units, while $a_0 = \frac{1}{2}$ Å, it follows that, even for monovalent metals, the interaction between the valence electrons will overshadow the binding in the lattice. Since, furthermore, for the electrons in the interior atomic shells, the polarization is negligible, formula (8.5) should represent a fair approximation if F_c is simply put equal to F_v[1].

For the effective average excitation potential $I = \hbar \bar{\omega}$, we thus have (cf. (9.6))

$$I = F_v \log \hbar \nu F_v^{1/2} + \sum_i{}' f_i \log \hbar \omega_i, \tag{10.3}$$

where the summation is to be extended to the transition possibilities of the electrons bound in the atomic shells lying below the conduction band.

[1]) Cf., however, Postscript (ii), p. 50.

The most favourable circumstances for testing this formula are found in the lightest metals like lithium and beryllium, where the relative number of conduction electrons is largest. In Li, we have $F_v = \frac{1}{3}$ and $\hbar v F_v^{1/3} = 7.6\ eV$ while, for Be, one obtains $F_v = \frac{1}{2}$ and $\hbar v F_v^{1/3} = 18\ eV$. For comparison, it may be mentioned that $\hbar \omega_b$ is about 4.5 eV and 9 eV in Li and Be, respectively, and the corrections to the effective frequency of the valence electrons due to the lattice binding may, thus, from expressions like (4.4), be estimated to be only of the order of 5 %. It is, however, of interest to note that, in the gaseous state, where the polarization is negligible, we must reckon with effective excitation energies for the valence electrons of the order of the ionization potentials, which are 5.4 eV for Li and 9.3 eV for Be. The atomic stopping power of the metals must, therefore, be expected to be appreciably smaller than for the corresponding gases.

An evaluation of the sum in (10.3) involves, of course, a detailed analysis of the binding of the inner electrons, but just in case of Li and Be the problem is comparatively simple, since the terms represent only the excitations of the K-electrons. An estimate of the average excitation potentials for the K-shell has been made by LIVINGSTON and BETHE (1937, p. 264), who give 110 eV and 205 eV for Li and Be, respectively. By means of (10.3) these values lead to $I_{Li} = 45\ eV$ and $I_{Be} = 60\ eV$. It may be noted that we here assume the total oscillator strength $\sum' f_i$ for the K-electrons to be equal to $\frac{2}{z_2}$. This value should actually be somewhat decreased since the presence of outer electrons may prevent certain transitions from the K-shell (LIVINGSTON and BETHE, 1937). For Li and Be, however, the effect would appear negligible; in fact, not only is the number of L-electrons very small compared with the cases considered by LIVINGSTON and BETHE, but the effect even vanishes in the approximation in which the binding of the outer electrons can be represented by s-states.

The stopping power of Li has been determined by ROSENBLUM (1928), whose results indicate a value of I of about 40 eV (cf. MANO 1933). However, the experimental uncertainty of about 10 % in the stopping power corresponds to a latitude in

I_{Li} of 50 %. For Be, no reliable measurements appear available, but empirical evidence would be of considerable interest due to the high density of valence electrons which should imply a comparatively small stopping power[1].

It may be added that the influence of the metallic resistance is in general quite negligible (cf. KRAMERS 1947). Thus, the value of ω_ϱ given by (5.1) corresponds, in the case of Li at normal temperatures, to $\omega_\varrho = 0.01\, v F_v^{1/2}$. The use of (5.2) for the valence electrons may, thus, be estimated to increase the above value for I_{Li} by less than 1 %. On the other hand, v. WEIZSÄCKER's theory in which ω_ϱ is assumed to determine the adiabatic limit for the oscillator of zero frequency leads to $I_{Li} = 10\ eV$, which is decidedly at variance with the empirical data. Furthermore, this theory predicts a considerable temperature dependence of the stopping power which, for a decrease in resistance by a factor 100, should increase by about 20 % in the case of fast α-rays. Experiments by GERRITSEN (1946) have shown that no such temperature variation occurs.

Also in other substances than those actually containing free electrons, the polarization effect may be of some significance for the stopping already for $v \ll c$. In fact, in solid or liquid materials, the values of $\hbar v F^{1/2}$ will, even for $F z_2 \sim 1$, most frequently be of the order of 10 eV and may, therefore, exceed the excitation energies of the most loosely bound electrons. In many cases, one may accordingly put $z_2 F_c$ in (8.5) equal to the number of bonding electrons, and it is of interest that the atomic interaction phenomena thus not only imply a certain reduction in stopping power, but also entail a simplification in the theoretical estimate of S. Indeed, under such circumstances, it is not necessary to consider details of the rather complicated mechanism of molecular binding or lattice structure, since the electrons involved will give practically the same contribution to S as if they were free.

b) Relativistic velocities.

As often mentioned in the preceding, the polarization phenomena become of special importance in the domain of relativistic

[1] Note added in proof. A recent investigation of the stopping power of protons in metallic Be (C. B. MADSEN and P. VENKATESWARLU, Phys. Rev. **74**. 648 (1948)) has given $I_{Be} = 64 \pm 5\ eV$ in good agreement with the above estimate.

velocities where, for sufficiently large values of γ, they imply a considerable reduction of the stopping power. In the original treatment of FERMI, attention was in particular called to the implications of this effect on the interpretation of measurements of fast cosmic ray particles.

A direct experimental test of the influence of atomic interaction on the stopping power is made difficult by the large energies required, but some evidence is given by the measurements of CRANE, OLESON and CHAO (1940) of the stopping in carbon of 10 *MeV* electrons. These investigators found an energy loss appreciably smaller than corresponding to formula (8.1), but (cf. HALPERN and HALL 1940) in good agreement with expression (6.8) which may be applied for the velocity in question. In fact, we have $F_c \approx 1$ since the value of $\hbar\nu\gamma$ is about 900 *eV* and, therefore, exceeds $z_2^2 \hbar\omega_0 \sim 500$ *eV*, representing the order of magnitude of the largest significant excitation energies of carbon.

Moreover, the influence of the polarization effects has been observed by ionization measurements. While it was shown by HAZEN (1945) in experiments with cosmic ray electrons that, for not too large values of γ, the ionization increases logarithmically with γ, corresponding to (8.1), some indication was obtained by HAYWARD (1947) that, for very large γ, the ionization reaches a constant value. Compared with the minimum in the ionization for $\gamma \sim 1$, the limiting value represents a relative increase which was found to conform, within the experimental latitude, with the theoretical estimate of the increase in stopping power, given by (6.8) and (8.1).

This evidence agrees with the considerations of § 8, according to which the atomic interaction, although of importance for the absolute values of ionization and stopping power, should have only minor influence on the ratio between these two quantities. In particular, it may be noted that this relationship rests on the assumption that the major part of the radiative energy loss correlated with the ionization oscillators is absorbed close to the path of the particle. Since the radiation represents the relativistic increase in the stopping effects, the observations of HAZEN, as well as those of HAYWARD, thus confirm the expected strong absorption.

As regards the interpretation of ionization measurements, it

may under circumstances be necessary to take into account that the average energy expenditure per ion, although largely independent of velocity, must still be expected to increase somewhat with γ due to the increasing importance of distant collisions relative to close collisions (cf. FANO 1946). As regards the measurements of HAYWARD, however, the increase in energy loss per ion from $\gamma \sim 1$ to very large γ may be estimated, from FANO's expressions, to be of the order of only 1 % in a He gas at normal pressure.

Finally, it may be recalled that the atomic interaction manifests itself very conspicuously in the radiative effects accompanying the penetration of fast particles, a phenomenon which has been investigated in detail since its discovery by ČERENKOV (1934). Thus, the general properties of the radiation, such as its polarization and the relation (7.2) between frequency and angle of emission, have been tested by ČERENKOV (1937, 1938) and by COLLINS and REILING (1938), and also the intensity of the radiation was shown by the latter investigators to be in accordance with theory. Recently, attempts have been made to use the radiation as a velocity indicator by applying the simple relation (7.2) for the directions in which the emission occurs (GETTING 1947, FURRY 1947, DICKE 1947).

Appendix I.

Reaction in Relativistic Two-body Collision.

In § 6, it was indicated in outline how the collision between two point charges may in classical mechanics be analyzed by tracing the reaction of the struck particle on the incident particle. We shall here consider this problem in some greater detail, confining ourselves, as in the text, to the treatment of distant collisions or, to be more specific, to the case of $p \gg \frac{z_1 e^2}{\mu v^2}$. In this approximation, the displacement, during the collision, of the struck particle, referred to as the electron, is small compared with p and its velocity remains negligible in comparison with c. Moreover, we may disregard the change of velocity of the incident particle.

The force which acts on the particle at time t depends on

the motion and position of the electron at the retarded time t' for which, on account of the simplifications mentioned, we have

$$t' = t - \frac{r}{c} = t - \frac{1}{c}\sqrt{p^2 + v^2 t^2}. \tag{I.1}$$

In the first approximation, the force is simply given by the static field corresponding to the electron at rest in its original position. Since, however, this field gives rise to no resultant energy transfer to the particle, we disregard it in the present connection. In higher approximations, we have reactive forces depending on the electronic displacement and motion. In the case of distant collisions, we need consider only linear terms in η, of which there will firstly be the force corresponding to a uniform motion of the electron. This force may simply be obtained from (4.6) by replacing $\eta(t)$ by $\eta(t') + (t - t')\dot{\eta}(t')$, representing the position which would have been reached by the electron at time t if it had proceeded from time t' with uniform velocity. Secondly, the acceleration of the electron at time t' produces a field given by (6.2).

For the total effective force of reaction one thus obtains, by means of (I.1),

$$\delta K(t) = \frac{z_1 e^2}{r^3} v t p \left\{ \frac{3\eta}{r^2} + \frac{3\dot{\eta}}{rc} + \frac{\ddot{\eta}}{c^2} \right\}, \tag{I.2}$$

where η and its derivatives are to be taken at the retarded time t'. This expression might, of course, also have been found from the general formula for the field produced by a point charge in arbitrary motion (cf., e. g., M. Abraham, Theorie der Elektrizität, 3rd ed., Leipzig and Berlin 1914, p. 92). The energy decrease of the particle is given by

$$T = \int_{-\infty}^{+\infty} \delta K \, v dt = T_1 + T_2 + T_3, \tag{I.3}$$

corresponding to the three terms in (I.2).

By a partial integration one finds

$$T_1 = z_1 e^2 p \int_{-\infty}^{\infty} \frac{1}{r^3} \frac{d\eta}{dt} dt = z_1 e^2 p \int_{-\infty}^{\infty} \frac{1}{r^3} \dot{\eta} \frac{dt'}{dt} dt, \tag{I.4}$$

where, according to (I.1),

$$\frac{dt'}{dt} = 1 - \frac{v}{c}\frac{vt}{r}. \tag{I.5}$$

Consequently, we have

$$T_1 + T_2 = z_1 e^2 p \int_{-\infty}^{\infty} \frac{\dot{\eta}}{r^3}\left(1 + 2\frac{v}{c}\frac{vt}{r}\right) dt \tag{I.6}$$

and, by another partial integration, again making use of (I.5),

$$T_1 + T_2 = \frac{z_1 e^2}{p}\left[\dot{\eta}\,\frac{t}{r}\right]_{t=-\infty}^{t=\infty} - T_3 - \frac{z_1 e^2}{p}\int_{-\infty}^{\infty} \ddot{\eta}\,\frac{t - \frac{r}{c}}{r}\,dt. \tag{I.7}$$

Now, from (I.1) it follows that $\frac{dt}{r} = \gamma\, dt'\,(\gamma^2 v^2 t'^2 + p^2)^{-1/2}$ and it is therefore seen, by a transformation of the last term in (I.7) to an integral over t', that this term vanishes, since $\ddot{\eta}$ is an even function of t' and since $t - \frac{r}{c} = t'$. Applying (3.2) for $\dot{\eta}$, one thus finds from (I.7) that $T = T_1 + T_2 + T_3$ coincides with the value given by (3.4).

An evaluation of T_1, T_2, and T_3, separately, involves somewhat more lengthy calculations which lead to rather complicated expressions, indicating that the division of T into three parts in the above manner is not of a very significant character. Putting $\beta = \frac{v}{c}$, one obtains

$$\begin{aligned} T_1 &= T\,(1-\beta) \\ T_2 &= T\left[-\frac{3}{\beta}(1-\beta^2) + \frac{3}{2}\frac{1-\beta^2}{\beta^2}\log\frac{1+\beta}{1-\beta}\right] \\ T_3 &= T\left[\frac{1}{\beta}(3-2\beta^2) - \frac{3}{2}\frac{1-\beta^2}{\beta^2}\log\frac{1+\beta}{1-\beta}\right]. \end{aligned} \tag{I.8}$$

In particular, it is seen that, as stressed in § 6, the term T_3, depending on the acceleration of the electron, becomes dominating for $\beta \to 1$.

So far, we have considered only the problem of the energy transfer but, for the sake of completeness, we shall briefly examine also how the momentum transfer in the relativistic two-body collision is described. The component perpendicular to the path of the incident particle presents no special problems; in fact, the momentum transferred in this direction to the electron was analyzed already in § 3, and the corresponding reactive force is, of course, simply the electrostatic force of the electron considered approximately at rest. It is of interest, however, that the latter circumstance is sufficient to show that, in distant collisions, the momentum transfer in this direction and, consequently, the total energy transfer is uninfluenced by relativity effects.

The problem of the component parallel to the path requires somewhat more detailed considerations. It is true that, in distant collisions, the momentum transfer in this direction is very small compared with that perpendicular to the path but, still, corresponding to the slowing down of the particle, there must, of course, be such a momentum transfer of magnitude $\frac{1}{v} T$. From the point of view of the reaction of the electron on the particle, this momentum is just that transferred by the force δK, given by (I.2).

In the non-relativistic case where actio equals reactio, the corresponding transfer of momentum from the particle to the electron is accounted for by the difference, due to the electronic displacement, in the electric force of the particle, in the first and last half of the collision. In the relativistic case, however, this force in the direction parallel to the path is given by

$$-eE_x = \frac{z_1 e^2 \gamma v t}{(p^2 + \gamma^2 v^2 t^2)^{3/2}} \tag{I.9}$$

and, by a simple calculation, one obtains from (3.3)

$$\int_{-\infty}^{\infty} e \frac{\partial E_x}{\partial p} \eta \, dt = \frac{1}{v} T (1 - \beta^2), \tag{I.10}$$

where T is given by (3.4). Thus, for $\beta \approx 1$, the electric field accounts for only a small part of the momentum transfer.

The remaining part is transferred by magnetic interaction. In fact, the magnetic field of the particle, which is directed perpendicular to the plane containing the electron and the path of the particle, equals βE_y, where E_y is the component of the electric field perpendicular to v. The transfer of momentum through magnetic forces is, thus, given by

$$\int_{-\infty}^{\infty} \frac{e\dot{\eta}}{c} \beta E_y \, dt = \frac{1}{v} T\beta^2 \tag{I.11}$$

since the integral of $e E_y \dot{\eta} \, dt$ just represents the energy transfer.

It should be stressed that the decisive part played by the radiative field of the struck electron in the slowing down of the particle, of course, in no way implies that the energy actually radiated during the encounter constitutes a major part of the energy transfer. In fact, this energy will be given by

$$W = \frac{2}{3} \frac{e^2}{c^3} \int_{-\infty}^{\infty} |\ddot{\boldsymbol{\xi}}|^2 \, dt, \tag{I.12}$$

neglecting the acceleration of the incident particle, the mass of which we may, for simplicity, consider to be very large. Introducing for $\ddot{\boldsymbol{\xi}}$ the force divided by μ, one obtains by a simple integration

$$W = \frac{2}{3} \frac{e^2}{c^3} \frac{z_1^2 e^4 \gamma^2}{\mu^2} \int_{-\infty}^{\infty} \frac{p^2 + v^2 t^2}{(p^2 + \gamma^2 v^2 t^2)^3} \, dt = T \frac{\pi}{8} \cdot \frac{e^2}{\mu c^2 p} \beta\gamma \left(1 + \frac{1}{3\gamma^2}\right). \tag{I.13}$$

Since, in distant collisions, p is extremely large compared with the classical electron radius $\frac{e^2}{\mu c^2}$, the value of W will thus be negligible compared with T. For excessively large values of γ, where the field of the particle at distance p is contracted to dimensions comparable with $\frac{e^2}{\mu c^2}$, the situation would be different, but such problems lie outside the scope of the simple classical picture of two colliding point charges.

Appendix II.

Application to Penetration Problems of Formalism of Radiation Theory.

As mentioned in § 7, it is possible to treat also ponderable media by the method, particularly well known from quantum electrodynamics (cf., e. g., W. HEITLER, Theory of Radiation I. 6, Oxford 1944), of dissolving the field in plane waves, and we shall here consider its application to the problems of stopping power and Čerenkov radiation. This method implies an expansion in Fourier components with respect to the spatial variation of the field and may, therefore, not always be well adapted to the case of dispersive media. Just for a field produced by a uniformly moving charge, however, the spatial components will also be harmonic in time.

We shall first treat the Čerenkov effect which is the more naturally suited to the formalism[1]. Since this phenomenon is connected with the rotational part of the field, we consider the transverse part of the vector potential which we expand in the familiar manner

$$\boldsymbol{A}_{tr} = \sum_{\lambda} q_\lambda \boldsymbol{A}_\lambda + q_\lambda^* \boldsymbol{A}_\lambda^* \quad \boldsymbol{A}_\lambda = \sqrt{4\pi c^2}\, \Omega^{-1/2} \boldsymbol{e}_\lambda\, e^{i(\boldsymbol{\varkappa}_\lambda \boldsymbol{r})}, \quad \text{(II.1)}$$

where q^* and $\boldsymbol{A}^*$ denote the complex conjugates of q and $\boldsymbol{A}$. The field is here assumed to be enclosed in a volume Ω, and the unit vector $\boldsymbol{e}_\lambda$ gives the direction of polarization. We follow the usual procedure in which terms corresponding to both $\boldsymbol{\varkappa}_\lambda$ and $-\boldsymbol{\varkappa}_\lambda \equiv \boldsymbol{\varkappa}_{-\lambda}$ are contained in the summation. The amplitudes q are then not uniquely defined by (II.1), but are determined by certain extra conditions imposed on their time dependence.

On account of the aforementioned difficulties in treating quite generally the case of dispersive media, we assume in the first instance the substance to have a constant value of ε. Neglecting specific magnetic properties of the medium, the field is given by

$$\Delta \boldsymbol{A} - \frac{\varepsilon}{c^2} \frac{\partial^2}{\partial t^2} \boldsymbol{A} = -\frac{4\pi \boldsymbol{i}}{c}, \quad \text{(II.2)}$$

where $\boldsymbol{i}$ denotes the current density corresponding to the moving particle. Multiplying this equation by $\boldsymbol{A}_\lambda^*$, and integrating over Ω, one thus finds

[1] Cf. Postscript (iv), p. 51.

$$(\ddot{q}_\lambda + \ddot{q}^*_{-\lambda}) + \omega_\lambda^2 (q_\lambda + q^*_{-\lambda}) = \frac{z_1 e}{\varepsilon c} (v, A^*_\lambda(x)), \qquad \text{(II.3)}$$

where x denotes the position of the particle, considered to be a point charge. The frequency ω_λ is given by

$$\omega_\lambda = \frac{\varkappa_\lambda c}{\sqrt{\varepsilon}}. \qquad \text{(II.4)}$$

We now require that the free waves associated with q_λ must have the time dependence $e^{-i\omega_\lambda t}$, which condition leads to

$$\ddot{q}_\lambda + \omega_\lambda^2 q_\lambda = \frac{z_1 e}{2\varepsilon c} \left(1 + \frac{i}{\omega_\lambda} \frac{d}{dt}\right) (v, A^*_\lambda(x)), \qquad \text{(II.5)}$$

an equation describing an oscillator in forced vibration.

If the particle moves with constant velocity, we may put $x = vt$ and the right hand side of (II.5) is harmonic with frequency $(\varkappa_\lambda, v)$. The equation (II.5) then reduces to

$$\ddot{q}_\lambda + \omega_\lambda^2 q_\lambda = \frac{z_1 e}{2 c \varepsilon \{(\varkappa_\lambda, v)\}} \left(1 + \frac{(\varkappa_\lambda, v)}{\omega_\lambda}\right) (v, A^*_\lambda(vt)). \qquad \text{(II.6)}$$

In this particular case, there is no difficulty in treating dispersive media; as indicated in (II.6), one simply inserts for ε the value corresponding to the frequency $(\varkappa_\lambda, v)$.

In vacuum, it follows from (II.4) that ω_λ is numerically greater than $(\varkappa_\lambda, v)$, since $v < c$. The solutions to (II.6) are, therefore, simple forced vibrations of constant amplitude. However, in a ponderable medium (or in the imaginary case of $v > c$) we may for certain wave numbers have $\omega_\lambda = (\varkappa_\lambda, v)$, corresponding to resonance between the exciting force and the oscillator. In this case, the oscillator will continue to absorb energy, corresponding to an actual emission of radiation. This effect just represents the Čerenkov radiation and it is also seen that, according to (II.4), the condition for resonance is identical with (7.2).

The treatment of an oscillator in resonance presents certain mathematical intricacies which may be overcome by introducing, formally, an infinitesimal damping. A more convenient representation is obtained, however, by making use of the Dirac δ-function. The general solution to (II.6) may thus be written, symbolically,

$$q_\lambda = \frac{z_1 e}{2\,c\,\omega_\lambda}\frac{1}{\varepsilon\{(\varkappa_\lambda, v)\}}\left(\frac{1}{\omega_\lambda - (\varkappa_\lambda, v)} + i\pi\delta\,(\omega_\lambda - (\varkappa_\lambda v))\right)(v, \boldsymbol{A}^*_\lambda\,(vt))\,, \quad \text{(II.7)}$$

as may be easily verified[1].

In particular, we shall use the expression (II.7) to determine the force $\boldsymbol{S}_{tr}$ acting on the particle. For symmetry reasons, the Lorentz force obviously vanishes and we have, thus,

$$\boldsymbol{S}_{tr} = -\frac{z_1 e}{c}\dot{\boldsymbol{A}}_{tr}\,(vt) = -\frac{z_1 e}{c}\sum_\lambda \dot{q}_\lambda \boldsymbol{A}_\lambda(vt) + \dot{q}^*_\lambda \boldsymbol{A}^*_\lambda(vt) \quad \text{(II.8)}$$

which gives, by means of (II.7) and (II.1),

$$\boldsymbol{S}_{tr} = -4\,\pi^2 z_1^2 e^2\,\Omega^{-1}\sum_\lambda \boldsymbol{e}_\lambda\,(\boldsymbol{e}_\lambda, v)\frac{(\varkappa_\lambda, v)}{\omega_\lambda\,\varepsilon\{(\varkappa_\lambda, v)\}}\,\delta(\omega_\lambda - (\varkappa_\lambda, v)). \quad \text{(II.9)}$$

Summing first over the two directions of polarization and introducing $(\varkappa_\lambda, v) = \varkappa_\lambda v y$, we get in the usual manner in the limit of infinitely large volumes Ω

$$S_{tr} = z_1^2 e^2 \int_0^\infty \varkappa^2\,d\varkappa \int_{-1}^{+1} dy\,\frac{\varkappa v^2 y}{\omega\,\varepsilon\{\varkappa v y\}}\,(1-y^2)\,\delta(\omega - \varkappa v y), \quad \text{(II.10)}$$

where S_{tr} is the component of $\boldsymbol{S}_{tr}$ directed against v. The other components vanish for symmetry reasons.

In evaluating the integral (II.10) it is convenient to change to the new variables ω, defined by (II.4), and $z = \frac{v}{c}\,y\sqrt{\varepsilon\{\varkappa v y\}}$. Since $v\,d\varkappa\,dy = d\omega\,dz$, one finds

$$S_{tr} = \frac{z_1^2 e^2}{c^2}\int_0^\infty \omega\,d\omega \int z\,dz\left(1 - \frac{c^2}{v^2\varepsilon\{\omega z\}}\right)\delta(1-z), \quad \text{(II.11)}$$

where the last integral is to be extended over values of z for

1) It may be shown that the equation $\ddot{x} + \omega_0^2 x = k(t)$ with the boundary condition $x = \dot{x} = 0$ for $t = -\infty$, in a Fourier expansion has the solution

$$x^\omega = k^\omega\,\frac{1}{2\,\omega_0}\left[\frac{1}{\omega_0 - \omega} + i\,\pi\,\delta\,(\omega_0 - \omega) + \frac{1}{\omega_0 + \omega} - i\,\pi\,\delta\,(\omega_0 + \omega)\right],$$

where $x(t) = \int_{-\infty}^{\infty} x^\omega\,e^{-i\,\omega\,t}\,d\omega$ and similarly for $k(t)$.

which $-1 < \dfrac{c\,z}{v\sqrt{\varepsilon\{\omega z\}}} < 1$. This integral vanishes, except for frequencies for which $z = 1$ is contained in the integration interval, i. e. for which $v\sqrt{\varepsilon\{\omega\}} > c$.

Thus, one gets finally

$$S_{tr} = \frac{z_1^2 e^2}{c^2} \int_{v\sqrt{\varepsilon}>c} \left(1 - \frac{c^2}{\varepsilon v^2}\right) \omega \, d\omega, \tag{II.12}$$

which is just the expression given by FRANK and TAMM (1937) for the Čerenkov radiation and its spectral distribution. For the simple dispersion formula (7.3) the expression (II.12) may easily be evaluated, and one finds the values given by FERMI (1940) which, as mentioned in § 7, represent the relativistic increase in the stopping formula.

The non-relativistic part of the stopping power is, as discussed in § 7, determined by the irrotational part of the field. It should be emphasized that the application to this problem of a formalism analogous to that used for the Čerenkov effect is somewhat artificial but, for the sake of completeness, we shall give a brief account of the procedure.

Choosing, for convenience, a gauge in which the vector potential is purely transverse, the longitudinal part of the field is given by the scalar potential φ, for which we have

$$\Delta \varphi = -\frac{4\pi\varrho}{\varepsilon}, \tag{II.13}$$

where ϱ denotes the charge density of the particle and where, like for the transverse field, we consider first the case of constant ε. Expanding φ, one gets, in analogy to (II.1),

$$\varphi = \sum_\sigma q_\sigma \Phi_\sigma + q_\sigma^* \Phi_\sigma^* \qquad \Phi_\sigma = \sqrt{4\pi c^2 \Omega^{-1}}\, e^{i(\varkappa_\sigma, r)} \tag{II.14}$$

and may obtain, by considerations similar to those leading to (II.5),

$$\varepsilon q_\sigma = \frac{z_1 e}{2\varkappa_\sigma^2 c^2}\left(1 + \frac{i}{\omega_A}\frac{d}{dt}\right)\Phi_\sigma^*(x), \tag{II.15}$$

where ω_A represents the effective frequency defined by (4.4). As

discussed in § 7, only free oscillations of this particular frequency can be excited in the medium, and we have, accordingly, defined the variables q_σ so as to contain terms corresponding to free waves of the type $e^{-i\omega_A t}$, only. In case of a uniformly moving particle, we get from (II.15),

$$\varepsilon\{(\varkappa_\sigma v)\}\, q_\sigma = \frac{z_1 e}{2\,\varkappa_\sigma^2 c^2}\left(1+\frac{(\varkappa_\sigma, v)}{\omega_A}\right)\Phi_\sigma^*(vt) \qquad \text{(II.16)}$$

where, like in (II.6), we have taken into account the dispersion.

Now, the force acting on the particle is given by

$$S_{\text{long}} = -z_1 e\,\text{grad}\,\varphi = -z_1 e \sum_\sigma i\varkappa_\sigma (q_\sigma \Phi_\sigma(vt) - q_\sigma^* \Phi_\sigma^*(vt)) \qquad \text{(II.17)}$$

and, therefore, vanishes except for the contribution from the singularity in the terms representing wave-numbers for which $\varepsilon = 0$. It was to be expected, however, that only these components give rise to a stopping force, since the energy transfer to the medium takes place over the frequency ω_A for which just $\varepsilon = 0$ (cf. § 7).

In the neighbourhood of $\omega = \omega_A$ we may write the dispersion formula (7.3), by means of (4.4),

$$\varepsilon \approx -\frac{\omega_A^2 - \omega^2}{v^2} \qquad \text{(II.18)}$$

and, in complete analogy to the symbolism used in (II.7), we thus get

$$q_\sigma \approx -\frac{z_1 e}{2\,\omega_A}\frac{v^2}{\varkappa_\sigma^2 c^2}\left(\frac{1}{\omega_A - (\varkappa_\sigma, v)} + i\pi\delta(\omega_A - (\varkappa_\sigma, v))\right)\Phi_\sigma^*(vt). \qquad \text{(II.19)}$$

Introducing in (II.17) one finally gets, similarly to (II.10),

$$S_{\text{long}} = z_1^2 e^2 v^2 \int_0^\infty \varkappa\, d\varkappa \int_{-1}^{1} y\, dy \frac{1}{\omega_A}\delta(\omega_A - \varkappa v y) = \frac{z_1^2 e^2 v^2}{v^2}\int_{\frac{1}{v}\omega_A}^\infty \frac{d\varkappa}{\varkappa}. \qquad \text{(II.20)}$$

This expression, however, ceases to be valid for very large $\varkappa$,

since the whole procedure applies to distant collisions only. In analogy to § 4, where we considered the medium outside a certain distance q from the path of the particle, we may here introduce a cut-off at some wave number $\varkappa_{\max}$. Choosing $\varkappa_{\max} \sim \frac{1}{q}$ it is seen, by means of (3.6) and (4.1), that (II.20) coincides with (4.11) as closely as could be expected, considering the arbitrariness in cut-off procedure.

The present investigation has been carried out at the Institute for Theoretical Physics, Copenhagen, and the writer wishes to acknowledge the great benefit he has derived from the continual interest of Professor NIELS BOHR in the work. He is also grateful to Professor C. MØLLER for helpful discussions and to M. Sc. BØRGE MADSEN for preparing the figures.

Postscript Added in Proof.

Since the completion of the present manuscript, a number of investigations dealing with the same topics have come to the notice of the writer; some of these have been published only quite recently, while others were published already during the war, but the respective periodicals were not available in Copenhagen at the time in question.

(i) G. C. WICK (Ric. Scient. **11**, 273 (1940), ibid. **12**, 858 (1941), and Il Nuovo Cimento **9**, no. 3 (1943)) has considered the extension of FERMI's calculations to the multi-frequency model (cf. § 8) and, on the basis of a dispersion formula of the type (8.2), has worked out an expression for the reduction in stopping power, easily susceptible to numerical calculation for any given set of dispersion frequencies. The result had been obtained independently by O. HALPERN and H. HALL (Phys. Rev. **73**, 477 (1948)), the publication of whose work was delayed by the war. These latter authors moreover have deduced an explicit formula for the stopping power, valid under certain simplifying assumptions which are fulfilled in most cases of interest. This formula just coincides with (8.5); in fact, the approximation involved is equivalent to that underlying the analysis in § 8. It may be noted that the authors start from a dispersion law which, in contrast to (8.2), takes into account the Lorentz-Lorenz correction (cf. p. 12), but it would seem that, in the approximation considered, this correction may be neglected.

(ii) HALPERN and HALL (loc. cit.) consider also the influence of the damping of conduction electrons and point out that the effect, although in general negligible, may be of significance in special cases like that of carbon, where the resistance is excessively large. From the line of

approach adopted in § 8, this effect is readily taken into account; in fact, it follows from (6.1) that, as regards the stopping power, the conduction electrons are equivalent to dispersion oscillators of effective frequency ω_0. Thus, the phenomenon may be said to be actually covered by (8.5).

(iii) The influence of the polarization on the stopping power has been computed for various substances by HALPERN and HALL (loc. cit.) on the basis of approximate dispersion-conduction models derived from X-ray ionization data. As pointed out by these authors, this procedure involves a certain latitude but, due to the relative insensitivity of the stopping effect on the exact model, the results may be expected to be reliable within a few per cent. More detailed estimates have been made, for a number of substances, by WICK (loc. cit.), who has employed X-ray data as well as theoretical calculations on the basis of the Hartree method in the establishment of appropriate sets of oscillators for the atoms in question.

(iv) V. I. GINSBURG (Journ. of Physics II, 441 (1940)) has treated the Čerenkov radiation by a Hamiltonian formalism which is very similar to the procedure applied in Appendix II. Such a formalism can be immediately quantized in the usual manner, and GINSBURG has developed a quantum electrodynamics which describes, in a phenomenological way, the radiation field in a ponderable medium. In particular, GINSBURG verifies that the average radiated energy is practically equal to that given by the classical formula, a result which was to be expected from quite general arguments (cf. § 2).

REFERENCES

H. A. Bethe, Ann. d. Phys. 5, **5**, 325 (1930).
F. Bloch, Ann. d. Phys. 5, **16**, 285 (1933a).
— ZS. f. Phys. **81**, 363 (1933b).
N. Bohr, Phil. Mag. **25**, 10 (1913).
— Phil. Mag. **30**, 581 (1915).
— Kgl. Danske Vidensk. Selskab, Mat.-fys. Medd. **18**, 8 (1948).
P. Čerenkov, C. R. Acad. Sci. URSS **2**, 451 (1934).
— Phys. Rev. **52**, 378 (1937).
— C. R. Acad. Sci. URSS **20**, 651 and **21**, 116, 339 (1938).
G. B. Collins and V. G. Reiling, Phys. Rev. **54**, 499 (1938).
D. R. Corson and R. B. Brode, Phys. Rev. **53**, 773 (1938).
H. R. Crane, N. L. Oleson and K. T. Chao, Phys. Rev. **57**, 555(A), (1940).
C. G. Darwin, Proc. Roy. Soc. **A 146**, 17 (1934).
R. H. Dicke, Phys. Rev. **71**, 737 (1947).
U. Fano, Phys. Rev. **70**, 44 (1946).
E. Fermi, Phys. Rev. **56**, 1242 (1939).
— Phys. Rev. **57**, 485 (1940).
I. Frank and Ig. Tamm, C. R. Acad. Sci. URSS **14**, 109 (1937).
W. H. Furry, Phys. Rev. **72**, 171 (A) (1947).
A. N. Gerritsen, Physica **12**, 311 (1946).
I. A. Getting, Phys. Rev. **71**, 123 (1947).
O. Halpern and H. Hall, Phys. Rev. **57**, 459 (1940).
E. Hayward, Phys. Rev. **72**, 937 (1947).
W. E. Hazen, Phys. Rev. **67**, 269 (1945).
H. Jensen, ZS. f. Phys. **106**, 620 (1937).
H. A. Kramers, Atti Congr. Int. di Fisica, Como (1927).
— Physica **13**, 401 (1947).
R. de L. Kronig, Proc. Roy. Soc. **A 124**, 409 (1929).
— Proc. Roy. Soc. **A 133**, 255 (1931).
M. G. Mano, C. R. **197**, 319 (1933).
N. F. Mott, Proc. Camb. Phil. Soc. **27**, 553 (1931).
A. Sommerfeld, ZS. f. Phys. **78**, 283 (1932).
M. Stanley Livingston and H. A. Bethe, Rev. Mod. Phys. **9**, 245 (1937).
R. M. Sternheimer, Diss., Univ. of Chicago, March 1946 (unpublished).
W. F. G. Swann, J. Franklin Inst. **226**, 598 (1938).
Ig. Tamm, Journ. of Phys. USSR **I**, 439 (1939).
C. F. v. Weizsäcker, Ann. d. Phys. 5, **17**, 869 (1933).
R. R. Wilson, Phys. Rev. **60**, 749 (1941).

Indleveret til Selskabet den 23. januar 1948.
Færdig fra trykkeriet den 15. januar 1949.

DET KGL. DANSKE VIDENSKABERNES SELSKAB
MATEMATISK-FYSISKE MEDDELELSER, BIND XXIV, NR. 20

ON A GEOMETRICAL INTERPRETATION OF ENERGY AND MOMENTUM CONSERVATION IN ATOMIC COLLISIONS AND DISINTEGRATION PROCESSES

BY

J. BLATON †

KØBENHAVN
I KOMMISSION HOS EJNAR MUNKSGAARD
1950

CONTENTS

Printed in Denmark.
Bianco Lunos Bogtrykkeri

INTRODUCTION

In every collision and disintegration process we have to do with two kinds of relations, *viz.*, those which result from pure conservation laws and are valid both in classical and in quantum theory, and others which for the different processes allowed by the conservation laws give the probabilities resulting from quantum-mechanical considerations.

In almost all collision and disintegration processes one or two particles are present in the initial state; it is not necessary to treat separately the case of one particle (spontaneous decay) since it is a special case of a process with two initial particles, one of which has a vanishing mass and momentum. The final state comprises two or more particles. In the following, however, we shall consider processes with two particles only in the final state; a certain extension to the case of three particles will be given in the last section.

The present paper deals only with relations that can be derived from the conservation laws for energy and momentum. The conservation laws are treated in the relativistic form, and only for some of the applications do we go over to the non-relativistic domain. The conservation laws allow an interpretation, by means of a simple geometrical picture, from which it is possible, for every collision or disintegration process, to obtain a qualitative and quantitative survey regarding the possible momenta and energies of the particles in the final state.

For the special case of elastic collisions, this picture was given by LANDAU and LIFSCHITZ [1], but it can easily be extended to all kinds of collision and disintegration processes[1].

[1] Such a picture was also given by WATAGHIN [2] in the discussion of meson production by collision of nucleons.

As will be shown in § 1, the geometrical picture in question consists of a certain prolate ellipsoid of revolution with the major axis in the direction of the total momentum of the system, together with two points, A_1 and A_2, lying on its major axis at a distance apart equal to the total momentum of the system (Fig. 1). This ellipsoid will be called the momentum ellipsoid. If A_1 is taken as the origin of the momentum of one of the two particles in the final state (denoted as particle 1), all possible end points B of this momentum vector lie on the surface of the momentum ellipsoid. The corresponding momentum of particle 2 in the final state will then be given by the vector from B to A_2.

The parameters describing the momentum ellipsoid (e. g., the semi-minor axis and the eccentricity) are easily found from the total energy and the total momentum of the system and the rest masses m_1 and m_2 of the particles 1 and 2, respectively. For a given ellipsoid, these two masses, m_1 and m_2, determine the positions, relative to the ellipsoid, of the corresponding points A_1 and A_2, respectively. The point A_1 may lie inside or outside the momentum ellipsoid or on its surface; this is also true for the point A_2. Consequently, from our geometrical picture, there are several different possibilities regarding the directions of flight of the outcoming particles.

In § 2, the useful relations between corresponding quantities in the laboratory system and the mass centre frame of reference (m.c.f.) are derived from the geometrical properties of the momentum ellipsoid. Directly, we find formulae for the momentum and the energy values of a particle as functions of the angle ϑ between the direction of flight of the particle and the total momentum of the system. Moreover the relation between the angular distributions of the outcoming particles in the m.c.f. and in the laboratory system is derived. Especially simple is the connection between the angular distribution in the m.c.f. and the energy distribution in the laboratory system.

In all practical applications, we can assume that one of the particles in the initial state is at rest; the elements of the geometrical picture for this case are given in § 3. In the following four sections (§ 4 — § 7), the geometrical picture is applied to the discussion of some physically important cases.

Elastic collisions are discussed in § 4. In this case, point A_2,

referring to that particle which is at rest before the collision, lies on the surface of the momentum ellipsoid, while the point A_1 lies inside or outside the ellipsoid, depending upon whether the mass of the incident particle is smaller or larger than the mass of the target particle.

The discussion of nuclear reactions in § 5 is simplified by the fact that, here, we have generally to do with nonrelativistic energies for which the momentum ellipsoid goes over into a sphere. This allows a simple geometrical representation of the square roots of the kinetic energies of the outgoing particles.

Photo-disintegration is treated in § 6. It is characteristic of this process (as of all endothermic processes) that the energy and the possible directions of flight of the disintegration products change rapidly for relatively small variations of energy of the incident photon in the neighbourhood of the threshold energy.

§ 7 deals with the spontaneous decay of a meson into two particles. This problem is of particular interest in connection with the discovery, by POWELL and collaborators [3], of the heavy meson. Energy and angular distribution of the secondary particles for a given primary meson energy are calculated.

Finally, in § 8, it is shown that the method can be extended to the case of three particles in the final state and, as an example, is given the geometrical picture for the β-decay of a nucleus.

§ 1. Geometrical Picture of the Conservation Laws.

In any process which results in the presence of only two particles the conservation laws for energy and momentum may be easily interpreted geometrically. We consider, in particular, an initial state in which there are two free particles, *I* and *II*, with rest masses m_I and m_{II} and momenta $\vec{k}_I$ and $\vec{k}_{II}$ (momentum and mass will throughout be measured in energy units, i.e. $\vec{k}$ denotes the momentum in usual units times the velocity of light c, and m is the mass in usual units times c^2). The case of a spontaneous decay with one particle only in the initial state can be described by putting $m_{II} = 0$, $\vec{k}_{II} = 0$. The two free particles *1* and *2*, present in the final state, are not necessarily of the same kind as those in the initial state; let their rest masses be m_1 and m_2 and their momenta $\vec{k}_1$ and $\vec{k}_2$.

Denoting the total energy of the system by E, and the total momentum by $\vec{K}$, we have when considering the initial state

$$E = \sqrt{m_I^2 + k_I^2} + \sqrt{m_{II}^2 + k_{II}^2} \tag{1,1}$$

$$\vec{K} = \vec{k}_I + \vec{k}_{II}, \tag{1,2}$$

and, according to the conservation laws,

$$E = \sqrt{m_1^2 + k_1^2} + \sqrt{m_2^2 + k_2^2} \tag{1,3}$$

$$\vec{K} = \vec{k}_1 + \vec{k}_2. \tag{1,4}$$

For any Lorentz frame of reference, the quantity

$$N = \sqrt{E^2 - K^2} \tag{1,5}$$

is an invariant giving the energy of the system in the m.c.f. The velocity of the mass centre in units of light velocity is given by

$$\vec{\beta} = \frac{\vec{K}}{E}. \tag{1,6}$$

In the initial as well as in the final state, the particles move relative to the m.c.f. in opposite directions and have equal absolute values of momentum. For the final state, the momentum value in the m.c.f., which we shall denote by b, is readily computed from the energy conservation law in the m.c.f., and is equal to

$$b = \frac{1}{2N}\sqrt{\{N^2-(m_1+m_2)^2\}\{N^2-(m_1-m_2)^2\}}. \qquad (1,7)$$

The corresponding energies

$$e_1^* = \sqrt{m_1^2+b^2} \text{ and } e_2^* = \sqrt{m_2^2+b^2} \qquad (1,8)$$

of the particles *1* and *2* in the m.c.f. are then

$$e_1^* = \frac{N}{2}\left(1+\frac{m_1^2-m_2^2}{N^2}\right), \quad e_2^* = \frac{N}{2}\left(1+\frac{m_2^2-m_1^2}{N^2}\right), \qquad (1,9)$$

the asterisk referring to the m.c.f.

On performing a Lorentz transformation which brings us back to the laboratory frame, with the z-axis in the direction of the total momentum vector $\vec{K}$, we find the following equation for the components of $\vec{k}_1$:

$$\frac{k_{1x}^2+k_{1y}^2}{b^2}+\frac{(k_{1z}-\alpha_1)^2}{a^2} = 1, \qquad (1,10)$$

where

$$a = \frac{b}{\sqrt{1-\beta^2}} \qquad (1,11)$$

$$\alpha_1 = \frac{\beta}{\sqrt{1-\beta^2}}e_1^*. \qquad (1,12)$$

An analogous equation in wich α_1 is replaced by

$$\alpha_2 = \frac{\beta}{\sqrt{1-\beta^2}}e_2^* = K-\alpha_1 \qquad (1,12\,a)$$

holds for the components of the momentum $\vec{k}_2$.

Equation (1,10) represents a prolate ellipsoid of revolution with the symmetry axis in the direction of $\vec{K}$, and with the centre displaced by the distance α_1 in the direction of $\vec{K}$ from the origin A_1 of the $\vec{k}_1$ vector[1]. Any vector from A_1 to an arbitrary point B on the surface of the ellipsoid represents, therefore, a possible momentum of the particle *1* in the final state, and vice versa. On the other side of the centre of the ellipsoid, in a distance α_2 from it, lies the point A_2, and the vector from B to A_2 represents the corresponding momentum $\vec{k}_2$ of the particle *2*. The ellipsoid defined by (1,10) will be called the momentum ellipsoid.

The semi-minor axis of the momentum ellipsoid is equal to the common value b of the momentum of both particles in the m.c.f. as determined by (1,7), whereas the semi-major axis a is given by (1,11). The eccentricity of the ellipsoid is, therefore, equal to the velocity β of the mass centre, i. e.

$$\beta = \frac{f}{a}, \tag{1,13}$$

where

$$f = \sqrt{a^2 - b^2} \tag{1,14}$$

is half the distance between the foci (Fig. 1).

The considerations in this and the following section are equally valid for both particles *1* and *2* and we, thus, denote all quantities referring to one of these particles by the index n ($n = 1, 2$).

The distance α_n can, on account of (1,12), (1,8), (1,13), and (1,11), also be written in the form

$$\alpha_n = \frac{f}{b}\sqrt{b^2 + m_n^2} \tag{1,15}$$

1) According to a remark by Professor O. KLEIN, the ellipsoid (1,10) can be considered to be the section in $\vec{k}_1$ space of a 4-dimensional ellipsoid of revolution in a $(\vec{k}_1, x_4)$ space. The equation of this 4-dimensional ellipsoid is

$$\sqrt{\vec{k}_1^2 + (x_4 - m_1)^2} + \sqrt{(\vec{k}_1 - \vec{K})^2 + (x_4 - m_2)^2} = E.$$

Putting $x_4 = 0$, we have an equation which follows immediately from (1,3) and (1,4). The foci of this 4-dimensional ellipsoid lie in the $\vec{K}, x_4$-plane and have there the coordinates $(0, m_1)$ and (K, m_2), respectively; the major axis is equal to E.

and it is seen that, for a given momentum ellipsoid, the distance α_n is entirely determined by the corresponding mass m_n. From (1,15) results the construction of A_n given in Fig. 2. Hence, we have always

$$\alpha_n \geq f.$$

Equality between α_n and f is established only when $m_n = 0$.

Regarding the possible directions of the momentum of particle n in the final state, we have to distinguish between two cases, *viz.* $\alpha_n \geq a$ and $\alpha_n < a$. In the first case, the vector $\vec{k}_n$ always forms, with the direction of $\vec{K}$, an acute angle ϑ_n which is smaller than or equal to a certain angle $\vartheta_{n\max}$, whereas, in the second case no such limitation exists. To distinguish these two cases we introduce

$$\gamma_n = \frac{\alpha_n}{a}. \qquad (1,16)$$

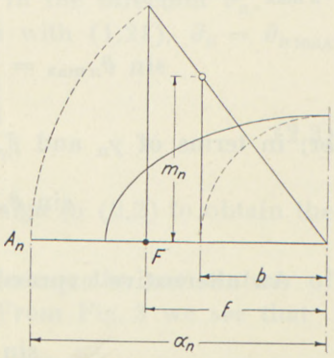

Fig. 2. Geometrical determination of the point A_n (origin of the $\vec{k}_n$ vector) as given by the proportion $\alpha_n : \sqrt{b^2 + m_n^2} = f : b$.

Thus, the first case is characterized by the relation $\gamma_n \geq 1$ and the second case by the relation $\gamma_n < 1$. The quantity γ_n has a simple physical meaning. As seen from (1,11) and (1,12),

$$\gamma_n = \beta \frac{e_n^*}{b}. \qquad (1,17)$$

Taking into account that the velocity β_n^* (in units of light velocity) of the particle n relative to the m.c.f. is equal to

$$\beta_n^* = \frac{b}{e_n^*} \qquad (1,18)$$

we obtain

$$\gamma_n = \frac{\alpha_n}{a} = \frac{\beta}{\beta_n^*}. \qquad (1.19)$$

In the first case, ($\gamma_n \geq 1$), the velocity of the mass centre is, therefore, greater than or equal to the velocity of the particle relative to the m.c.f. and, in the second case, ($\gamma_n < 1$), it is smaller than the velocity of the particle relative to the m.c.f. We have always

$$\gamma_n \geq \beta. \tag{1,20}$$

Equality exists only when $m_n = 0$.

From Fig. 1 we can easily compute the maximum angle $\vartheta_{n\,\max}$ occurring in the case $\gamma_n \geq 1$:

$$\sin \vartheta_{n\,\max} = \frac{b}{\sqrt{\alpha_n^2 - f^2}}, \qquad \vartheta_{n\,\max} \leq \frac{\pi}{2}$$

or, in terms of γ_n and β,

$$\sin \vartheta_{n\,\max} = \sqrt{\frac{1-\beta^2}{\gamma_n^2 - \beta^2}}. \tag{1,21}$$

An alternative expression for (1,21) is

$$\sin \vartheta_{n\,\max} = \frac{b^2}{f m_n}. \tag{1,22}$$

§ 2. Relations between Corresponding Quantities in Laboratory System and m. c. f.

The geometrical interpretation of the energy and momentum conservation leads immediately to a geometrical construction connecting the value and direction of the momentum of a particle in the m.c.f. with the corresponding values in the laboratory frame of reference and shown in Fig. 3.

From Fig. 3 we see that

$$\operatorname{tg} \vartheta_n = \frac{b \sin \vartheta_n^*}{\alpha_n + a \cos \vartheta_n^*} = \sqrt{1-\beta^2}\, \frac{\sin \vartheta_n^*}{\gamma_n + \cos \vartheta_n^*}, \tag{2,1}$$

the asterisk referring to the m.c.f.

From (2,1) we can also express the angle ϑ_n^* in terms of ϑ_n and obtain

$$\cos\vartheta_n^* = \frac{1}{1-\beta^2\cos^2\vartheta_n}\left\{-\gamma_n\sin^2\vartheta_n \pm (1-\beta^2)\sqrt{1-\frac{\gamma_n^2-\beta^2}{1-\beta^2}\sin^2\vartheta_n}\cos\vartheta_n\right\}. \quad (2,2)$$

The function $\cos\vartheta_n^*$ is, for $\gamma_n > 1$, double-valued since, as it can directly be seen from Fig. 3, the line drawn from A_n at an angle ϑ_n with $\vec{K}$ will, for every angle ϑ_n smaller than $\vartheta_{n\max}$, have two points of intersection with the momentum ellipsoid giving, thus, two possible values for ϑ_n^* and two possible momenta in the laboratory system. The plus sign in (2,2) belongs to the greater possible value of momentum in the direction ϑ_n.

As seen from (2,2) in connection with (1,21), $\vartheta_n = \vartheta_{n\max}$ corresponds to ϑ_{n0}^* given by

$$\cos\vartheta_{n0}^* = -\frac{1}{\gamma_n}. \quad (2,3)$$

For $\gamma_n \leq 1$, we need take only the + sign in (2,2) to obtain the correct value ϑ_n^*.

From (2,2) we can also easily deduce the momentum of particle n going in the direction ϑ_n. From Fig. 3 we see that

$$k_n(\vartheta_n) = a\frac{\gamma_n + \cos\vartheta_n^*}{\cos\vartheta_n} \quad (2,4)$$

so that, according to (2,2),

$$k_n(\vartheta_n) = \frac{p}{1-\beta^2\cos^2\vartheta_n}\left\{\gamma_n\cos\vartheta_n \pm \sqrt{1-\frac{\gamma_n^2-\beta^2}{1-\beta^2}\sin^2\vartheta_n}\right\}, \quad (2,5)$$

where

$$p = b\sqrt{1-\beta^2} \quad (2,6)$$

is the parameter of the ellipsoid. As regards the sign, the same conditions are valid as for (2,2).

The energy $e_n = \sqrt{k_n^2 + m_n^2}$ of the particle n can also be expressed as a function of ϑ_n. The transformation equation for the energy from the m.c.f. to the laboratory system is given by

$$e_n = \frac{e_n^*}{\sqrt{1-\beta^2}} + f\cos\vartheta_n^*. \quad (2,7)$$

From this equation it follows immediately that the energy range

of each particle in the final state is given by the distance $2f$ between the foci, i. e.

$$e_{n\max} - e_{n\min} = 2f \tag{2,8}$$

with

$$e_{n\max} = \frac{\alpha_n}{\beta} + f, \quad e_{n\min} = \frac{\alpha_n}{\beta} - f. \tag{2,9}$$

Expressing $\cos \vartheta_n^*$ by means of (2,4), we obtain

$$e_n = \sqrt{1-\beta^2}\, e_n^* + \beta k_n \cos \vartheta_n = \frac{p}{f}\alpha_n + \beta k_n \cos \vartheta_n. \tag{2,10}$$

Apart from the constant $\frac{p}{f}\alpha_n$, the energy of a particle in the final state is, therefore, given by the product of its momentum component in the direction of the total momentum times the eccentricity of the ellipse.

By means of (2,2), we can easily find the connection between the angular distribution of the particles in the laboratory system and in the m.c.f. If we denote by $\sigma_n(\vartheta_n, \varphi)$ and $\sigma_n^*(\vartheta_n^*, \varphi)$ the probability per unit solid angle of finding the particle n in a certain direction in the laboratory system and in the m.c.f., respectively, we have

$$\sigma_n(\vartheta_n, \varphi) = \sigma_n^*(\vartheta_n^*, \varphi) \frac{d\cos \vartheta_n^*}{d\cos \vartheta_n}. \tag{2,11}$$

We have here also, in analogy to (2,2) and (2,5), to distinguish between two cases, *viz.* $\gamma_n > 1$ and $\gamma_n \leq 1$. In the first case, $\cos \vartheta_n$ as a function of $\cos \vartheta_n^*$ has a minimum value $\cos \vartheta_{n\max}$. Therefore, $\cos \vartheta_n^*$ as well as $\frac{d\cos \vartheta_n^*}{d\cos \vartheta_n}$ is a double-valued function of $\cos \vartheta_n$, and $\frac{d\cos \vartheta_n^*}{d\cos \vartheta_n}$ becomes infinite for $\vartheta_n = \vartheta_{n\max}$. For the two branches (which correspond to different absolute values of momentum), $\frac{d\cos \vartheta_n^*}{d\cos \vartheta_n}$ has different signs. The sign is positive for the particles moving in the direction ϑ_n with a higher value of momentum, and negative for those moving with lower momentum in the same direction. In the latter case, the probability density is given by $|\sigma|$.

For $\gamma_n \leq 1$, $\cos \vartheta_n^*$ is a single-valued function of $\cos \vartheta_n$ and $\frac{d\cos\vartheta_n^*}{d\cos\vartheta_n}$ is single-valued, finite, and positive.

Carrying out the differentiation, we obtain from (2,11), (2,2), and (2,5)

$$\sigma_n(\vartheta_n \varphi) = \pm \sigma^*(\vartheta_n^*, \varphi)\left(\frac{k_n}{b}\right)^2 \frac{1}{\sqrt{1 - \frac{\gamma_n^2 - \beta^2}{1-\beta^2}\sin^2\vartheta_n}}, \quad (2,12)$$

where k_n in terms of ϑ_n is given by (2,5). As regards the sign, the same conditions are valid as in (2,2) and (2,5). We see from (2,12) that, in the case $\gamma_n > 1$, and for a spherical symmetric angular distribution in the m.c.f., the probability density for a given angle ϑ_n is, due to the factor k_n^2, always greater for the particles with the greater than for those with the smaller of the two possible momentum values.

In the case $\gamma_n = 1$ which is, for example, realized in an elastic collision when the particle under consideration is, before the collision, at rest in the laboratory system (cf. § 4), (2,12) is simplified, on account of (2,5), to

$$\sigma_n = \sigma_n^* \frac{4(1-\beta^2)}{(1-\beta^2\cos^2\vartheta_n)^2}\cos\vartheta_n.$$

A very simple relation exists between the angular distribution in the m.c.f. and the energy distribution $\sigma_n(e_n)$ per unit energy range in the laboratory system, which follows directly from (2,7). From this equation, we obtain by differentiation

$$de_n = f d\cos\vartheta_n^*.$$

Since $\sigma_n^*(\vartheta_n^*, \varphi)$ will in general not depend upon the azimuth φ so that $\sigma_n^*(\vartheta_n^*, \varphi) = \sigma_n^*(\vartheta_n^*)$, we get, after integration over the azimuth φ, for $\sigma_n(e_n)$,

$$\sigma_n(e_n) = \frac{2\pi}{f}\sigma_n^*(\vartheta_n^*), \quad e_{n\min} \leq e_n \leq e_{n\max},$$

where we have to express ϑ_n^* in $\sigma_n^*(\vartheta_n^*)$ by e_n in using the formula (2,7):

$$\cos \vartheta_n^* = \frac{1}{f}\left(e_n - \frac{\alpha_n}{\beta}\right).$$

If the angular distribution in the m.c.f. is spherically symmetrical ($\sigma^* = \frac{1}{4\pi}$), the probability $\sigma_n(e_n)$ per unit range of energy is constant and equal to

$$\sigma_n(e_n) = \frac{1}{2f} \qquad e_{n\,\min} \leq e_n \leq e_{n\,\max}$$

which is well known in the non-relativistic case [4].

§ 3. Collisions with One Particle Originally at Rest.

In all cases of practical importance, we may assume that in the laboratory system one of the two particles in the initial state is at rest. In the following applications (§§ 4—8), particle II will always be considered as being at rest ($\vec{k}_{II} = 0$). It then follows from (1,1) and (1,2) that

$$\vec{K} = \vec{k}_I, \qquad E = \sqrt{m_I^2 + K^2} + m_{II} \tag{3,1}$$

and, for the energy N of the system in the m.c.f.,

$$N = \sqrt{M_i^2 + 2\, m_{II}\, W_i}, \tag{3,2}$$

where the index i refers to the initial state of the system, W is the kinetic energy (defined as the total energy minus the rest energy) of the system

$$W_i = \sqrt{m_I^2 + K^2} - m_I, \tag{3,3}$$

and M is the sum of the rest masses of the particles present:

$$M_i = m_I + m_{II}, \tag{3,4}$$

$$M_f = m_1 + m_2, \tag{3,5}$$

the index f referring to the final state of the system.

The reaction energy Q released in the process is then equal to

$$Q = M_i - M_f, \tag{3,6}$$

which is positive for exothermic and negative for endothermic processes. If

$$M = \frac{1}{2}(M_i + M_f) \tag{3,7}$$

is the arithmetical mean of the sum of the rest masses in the initial and the final state, we can write the value b of the semi-minor axis of the momentum ellipsoid in the form

$$b = \sqrt{\frac{(QM + m_{II} W_i)(QM + m_{II} W_i + 2 m_1 m_2)}{M_i^2 + 2 m_{II} W_i}}. \tag{3,8}$$

For endothermic processes ($Q < 0$), we obtain from this equation the threshold energy $W_i = \delta$ from the condition that b must be real,

$$\delta = \frac{M}{m_{II}} |Q| \tag{3,9}$$

and, for this value of W_i we have $b = a = 0$.

Using (3, 6), we get

$$\delta = \frac{M_f^2 - M_i^2}{2 m_{II}}. \tag{3,10}$$

§ 4. Elastic Scattering.

In this particular case, the rest masses of the two particles remain unchanged throughout the process ($m_1 = m_I$, $m_2 = m_{II}$ and, consequently, $M = M_i = M_f$). The momentum ellipsoid is determined by its eccentricity β (= mass centre velocity) computed from (1,6), (3,3), (3,1), and (3,4):

$$\beta = \frac{\sqrt{W_i (2 m_1 + W_i)}}{M + W_i}. \tag{4,1}$$

and the parameter $p = b\sqrt{1 - \beta^2}$, according to (4,1), (3,8), and (3,6), is given by

$$p = m_2 \beta . \tag{4,2}$$

The semi-minor and semi-major axes are then

$$b = \frac{m_2 \beta}{\sqrt{1-\beta^2}}, \quad a = \frac{m_2 \beta}{1-\beta^2}. \tag{4,3}$$

The distances α_1 and α_2 are, according to (1,12), (1,9), (3,2), and (4,3),

$$\alpha_1 = \frac{W_i + \frac{m_1}{m_2} M}{W_i + M} a, \quad \alpha_2 = a. \tag{4,4}$$

From (4,4) and (1,16) we see at once that $\gamma_1 \geq 1$ for $m_1 \geq m_2$ and $\gamma_1 < 1$ for $m_1 < m_2$, while $\gamma_2 = 1$, since the particle which is at rest before the collision has the velocity $\beta_1^* = \beta$ relative to the m.c.f. in the initial as well as in the final state.

The three possible cases, *viz.* $m_1 = m_2$, $m_1 > m_2$, and $m_1 < m_2$, are illustrated in Figs. 4, 5, and 6.

From the geometrical picture we can easily deduce the following results for elastic collisions:

(1) The momentum of the target particle moving after the collision in the direction ϑ_2 is, from (2,5),

$$k_2 = \frac{2 m_2 \beta \cos \vartheta_2}{1 - \beta^2 \cos^2 \vartheta_2}. \tag{4,5}$$

(2) The maximum momentum $k_{2\max}$ transferred in an elastic collision to the struck particle is given by the major axis ($= 2a$) of the ellipsoid as determined by (4, 3).

(3) The kinetic energy transferred in the collision to the target particle is, from (2,10), (4,2), and (4,4),

$$w_2 = \beta k_2 \cos \vartheta_2 \tag{4,6}$$

and is, therefore, given by the product of the momentum component of the target particle in the primary direction times the eccentricity of the ellipse.

(4) The maximum amount of energy is transferred when $\vartheta_2 = 0$ and is

$$(w_2)_{\max} = 2\,m_2 \frac{\beta^2}{1-\beta^2} = 2f, \tag{4,7}$$

$(w_2)_{\max}$ is, therefore, equal to the distance between the foci, as is also seen directly from (2,8).

(5) The angle ϑ_2 between the motion of the target particle and the primary direction of the incident particle is, from (4,6),

$$\cos\vartheta_2 = \frac{1}{\beta}\sqrt{\frac{w_2}{w_2+2\,m_2}}. \tag{4,8}$$

(6) The range of angles ϑ_2 for the target particle, for a given energy transfer w_2, is from (4,8)

$$\vartheta_2(w_2) < \Theta_2(w_2) \text{ where } \operatorname{ctg}\Theta_2 = \sqrt{\frac{w_2}{2\,m_2}}. \tag{4,9}$$

This limiting angle Θ_2 is independent of the mass and the energy of the incident particle. From (4,9) it follows that the path of a particle which receives a relativistic energy in an elastic collision ($w_2 \gg m_2$) always forms a very small angle with the primary direction. Further, for a given angle ϑ_2, we have $\frac{w_2}{m_2} < 2\operatorname{ctg}^2\vartheta_2$. [5]

(7) The mass m_1 of the incident particle can be determined from the knowledge of its primary momentum K (or its magnetic rigidity) and the direction of flight and momentum of a struck particle of known mass [6]. By means of (1,6) and (4,6) we can determine the total energy of the system $E = \frac{K}{\beta} = K\frac{k_2\cos\vartheta_2}{w_2}$ and, therefore, also m_1 which, according to (3,1), is given by

$$m_1^2 = \left(\frac{K k_2\cos\vartheta_2}{w_2} - m_2\right)^2 - K^2.$$

This formula becomes simpler in the case $m_1 \gg m_2$, for instance for collisions of mesons with electrons.

(8) The kinetic energy W_i of the incident particle which makes an elastic collision with another particle of equal mass ($m_1 = m_2 = m$) can be determined solely from the two directions after the collision (from the ellipse in Fig. 4):

$$\frac{W_i}{2m} + 1 = \operatorname{ctg}\vartheta_1 \operatorname{ctg}\vartheta_2. \tag{4,10}$$

For kinetic energies small compared with the rest energy, we have $\vartheta_1 + \vartheta_2 \sim \frac{\pi}{2}$, as is well known for non-relativistic velocities. Formula (4,10) is, therefore, convenient only for the energy determination of fast particles. It has been checked experimentally by CHAMPION [7] for collisions between two electrons.

(9) The angle ψ between the particles after the collision, in the case $m_1 > m_2$, can vary between 0 and $\frac{\pi}{2}$, but for $m_1 = m_2$ there is a lower limit $\psi_{\min}$ for this angle, given by

$$\cos\psi_{\min} = \frac{W_i}{W_i + 4m}.$$

The minimum value is attained for $\vartheta_1 = \vartheta_2$.

(10) The momentum k_1 of a photon of original momentum K, scattered through an angle ϑ_1 by a particle of mass m_2, is given by the standard form of the equation for an ellipse in polar coordinates

$$k_1 = \frac{m_2\beta}{1 - \beta\cos\vartheta_2} \tag{4,11}$$

$$\beta = \frac{K}{m_2 + K}. \tag{4,12}$$

This equation represents the well-known Compton formula.

The energy determination of a photon by measuring the momentum (or energy) of the Compton electron is often used [8]. From (4,11), (4,12) and (4,6) we have

$$K = \frac{m_2}{\frac{k_2}{w_2}\cos\vartheta_2 - 1}.$$

For $\vartheta_2 = 0$, in which direction the probability for the motion

of the electron is highest, we have from the figure

$$K = a + f = \frac{1}{2}(k_2 + w_2).$$

(11) In the case $m_1 > m_2$, the maximum deflection angle $\vartheta_{1\max}$ of the incident particle is, from (1,22) and (4,3), given by

$$\sin \vartheta_{1\max} = \frac{m_2}{m_1}.$$

§ 5. Nuclear Reactions.

For the application of the geometrical picture of energy-momentum conservation to nuclear reactions, we may confine ourselves to the non-relativistic domain and treat only the case in which the kinetic energy both in the initial and the final state is small compared with the rest energy of any of the particles under consideration. The momentum ellipsoid goes then over into a sphere with the radius, given from (3,8),

$$a = b = \frac{1}{M}\sqrt{2\, m_1 m_2 (m_{II} W_i + M Q)}. \tag{5,1}$$

The distance α_n is found from (1,12), by putting

$$e_n^* = m_n, \quad \beta = \frac{K}{M},$$

to be equal to

$$\alpha_n = \frac{m_n}{M} K.$$

Also for physical reasons, this formula is clear, α_n now representing that part of the momentum of particle n which comes from the motion of the mass centre, as seen in Fig. 7.

Expressing α_n in terms of the kinetic energy W_i of the incident particle, we obtain

$$\alpha_n = \frac{m_n}{M}\sqrt{2\, m_I W_i}. \tag{5,2}$$

For the discussion of the different cases, it is convenient to introduce the quantity

$$\delta' = \frac{M}{m_{II}} Q \tag{5,3}$$

which, in the special case of endothermic processes, represents the threshold energy δ with negative sign.

The directions in which particles *1* and *2* in the final state can move are determined by γ_1 and γ_2 which, according to (1,16), (5,1), (5,2), and (5,3), are given by

$$\gamma_1 = \frac{\alpha_1}{a} = \sqrt{\frac{m_1}{m_2}\frac{m_I}{m_{II}}\frac{W_i}{W_i + \delta'}}, \quad \gamma_2 = \frac{\alpha_2}{a} = \sqrt{\frac{m_2}{m_1}\frac{m_I}{m_{II}}\frac{W_i}{W_i + \delta'}}. \tag{5,4}$$

For $\gamma_n \geq 1$ the direction of the outgoing particle n forms with the primary direction an acute angle smaller than or equal to $\vartheta_{n\max}$ which, according to (1,21), in the non-relativistic case considered here, is given by

$$\sin \vartheta_{n\max} = \frac{1}{\gamma_n}. \tag{5,5}$$

From now on, we shall for convenience ascribe the index *1* to that of the two particles in the final state which has the smaller mass, i. e.

$$m_1 \leq m_2.$$

In almost all nuclear reactions[1] $m_I \leq m_{II}$. Obviously,

$$\sqrt{\frac{W_i}{W_i + \delta'}} < 1 \; (> 1)$$

for exothermic (endothermic) reaction and increases (decreases) with increasing W_i. With the aid of these data we can, from (5,4), derive the following results.

Exothermic reactions.

(1) The quantity γ_1 is always smaller than unity; consequently, the direction of motion of the lighter particle, or of both particles if they have equal masses, is not limited.

1 In fact, the only exception is presented by the bombardment of deuterium with α-particles.

(2) The quantity γ_2 is greater than or equal to unity only in reactions in which $m_I > m_1$ (i. e. in (d, p), (d, n), (α, p), and (α, n) reactions) and in which the energy W_i satisfies the condition

$$W_i \geq \frac{m_1}{m_I - m_1} Q.$$

The direction of motion of the recoil nucleus is then limited by (5,5).

Endothermic reactions.

(1) At the threshold energy $W_i = \delta$, it is apparent that $a = 0$ ($\gamma_1 = \gamma_2 = \infty$). Both particles in the final state move in the primary direction, with energies $m_1 \frac{m_I}{M m_{II}} Q$ and $m_2 \frac{m_I}{M m_{II}} Q$ for particles *1* and *2*, respectively.

(2) The quantity γ_1 is smaller than or equal to unity, according as the energy W_i of the incident particle exceeds the threshold energy δ by an amount greater than or equal to

$$\frac{m_1 m_I}{M (m_2 - m_I)} \delta.$$

Hence, the direction of motion of the light particle is limited only when the energy W_i lies in the small interval given by this expression. For $\gamma_1 = 1$, the maximum kinetic energy of particle *1* is about four times greater than the energy which it receives at the threshold.

(3) The quantity γ_2 is smaller than or equal to unity only in reactions in which $m_1 > m_I$ (for instance, $^{14}N\,(n\,\alpha)\,^{11}B$), and in which the energy W_i exceeds the threshold energy δ by an amount greater than or equal to

$$\frac{m_2 m_I}{M (m_1 - m_I)} \delta.$$

In order to obtain directly the energies of the outgoing particles by a graphical construction, it is convenient to introduce for each

particle (*1* and 2) a separate scale for the drawing of a and α. Thus, we introduce

$$a_1 = \frac{a}{\sqrt{2\,m_1}} = \frac{\sqrt{m_2\,m_{II}}}{M}\sqrt{W_i+\delta'}, \quad c_1 = \frac{\alpha_1}{\sqrt{2\,m_1}} = \frac{\sqrt{m_1\,m_I}}{M}\sqrt{W_i}$$

for particle 1, and

$$a_2 = \frac{a}{\sqrt{2\,m_2}} = \frac{\sqrt{m_1\,m_{II}}}{M}\sqrt{W_i+\delta'}, \quad c_2 = \frac{\alpha_2}{\sqrt{2\,m_2}} = \frac{\sqrt{m_2\,m_I}}{M}\sqrt{W_i}$$

for particle 2. The quantity $(a_n)^2$ is then the energy which particle n receives in the m.c.f. The corresponding vectors in the geometrical picture will then give directly the square roots of the energies of the particles, as is illustrated Fig. 8.

§ 6. Photodisintegration.

In the discussion of photodisintegration, particle I is a photon ($m_I = 0$) of momentum $\vec{K}$, and particle II is a nucleus of the mass $m_{II} = m$. In the final state, we have a neutron of mass m_1 and the residual nucleus of mass m_2.

For the threshold energy δ of the photon, we obtain from (3,9), (3,6) and (3,7)

$$\delta = |Q|\left(1+\frac{|Q|}{2\,m}\right).$$

The threshold energy in this case exceeds the binding energy $|Q|$ of the nucleon only by the small amount $\frac{Q^2}{2\,m}$. For the deuteron ($|Q| = 2.2$ MeV) for example, the threshold for photodisintegration lies only 1.3 keV above the binding energy.

For photon energies small compared with the rest energy of the nucleus ($K \ll m$), we can confine ourselves, as before, to the non-relativistic approximation, and obtain from (3,8) and (3,9)

$$a = b = \sqrt{\frac{2\,m_1\,m_2}{m}(K-\delta)}$$

and, from (1,12),

$$\alpha_n = \frac{m_n}{m} K.$$

Measuring $K - \delta$ in units of the threshold value δ, i. e. introducing

$$x = \frac{K - \delta}{\delta},$$

we have for the ratios $\gamma_1 = \frac{\alpha_1}{a}$ and $\gamma_2 = \frac{\alpha_2}{a}$:

$$\gamma_1 = \sqrt{\frac{m_1 \delta}{2 m_2 m}} \frac{x+1}{\sqrt{x}}, \quad \gamma_2 = \sqrt{\frac{m_2 \delta}{2 m_1 m}} \frac{x+1}{\sqrt{x}}.$$

These ratios, being infinite at the threshold energy $x = 0$, decrease very rapidly in the neighbourhood of the threshold value and are equal to unity for

$$x_1 \cong \frac{m_1 \delta}{2 m_2 m}, \quad x_2 \cong \frac{m_2 \delta}{2 m_1 m}$$

for the particles *1* and *2*, respectively. Only for the photon energy corresponding to x_1 is it possible for the outgoing neutron to have a vanishing kinetic energy. The photon energy for this case was determined experimentally by WIEDENBECK and MARHOFER [9] for the deuteron (2.185 MeV) and the beryllium nucleus (1.630 MeV). For the deuteron, this energy exceeds the binding energy Q by an amount of ~ 2.5 keV.

A minimum value for γ_1 and γ_2 is reached when $x = 1$, i. e. when $K = 2\delta$. These minimum values of γ_1 and γ_2 are

$$\gamma_{1\,\min} = \sqrt{2 \frac{m_1}{m_2} \frac{\delta}{m}}, \quad \gamma_{2\,\min} = \sqrt{2 \frac{m_2}{m_1} \frac{\delta}{m}}$$

and are very small (due to the smallness of $\frac{\delta}{m}$); therefore, in this case, the two particles are moving nearly in opposite directions.

The three typical cases $K = \delta$, $\gamma_1 = 1$, $K = 2\delta$ are shown, for the deuteron, in Figs. 9a, b, c.

§ 7. Decay of a Meson into Two Particles.

In the initial state, we have a primary particle (meson) of mass $m_I = M$ and momentum $\vec{k}_I = \vec{K}$ ($m_{II} = 0$, $\vec{k}_{II} = 0$). In the final state resulting from the decay of the primary meson, we have two secondary particles of masses m_1 and m_2. Taking into account that in this process, according to (1,5), $N = M$, we obtain from (1,7) for the semi-minor axis of the momentum ellipsoid (= momentum of the secondary particle if the primary particle were at rest)

$$b = \frac{1}{2M}\sqrt{\{M^2-(m_1+m_2)^2\}\{M^2-(m_1-m_2)^2\}}. \tag{7,1}$$

The eccentricity of the ellipsoid is equal to the velocity β of the primary particle.

For the following considerations it will be convenient to introduce the abbreviations

$$\mathsf{K} = \frac{K}{M} = \frac{\beta}{\sqrt{1-\beta^2}} \tag{7,2}$$

$$\mathsf{K}_n^* = \frac{b}{m_n} = \frac{\beta_n^*}{\sqrt{1-\beta_n^{*2}}} \tag{7,3}$$

where the asterisk refers to the rest system of the primary particle. We can express K_n^* through the kinetic energy w_n^* which the secondary particle receives in the decay of a stopped meson:

$$\mathsf{K}_n^* = \sqrt{\frac{w_n^*}{m_n}\left(2+\frac{w_n^*}{m_n}\right)}. \tag{7,4}$$

From (1,9) it can be seen that, in the decay of a stopped meson, the kinetic energy w_n^* of the particle *1*, its mass m_1, and the mass ratio $\frac{M}{m_1}$ determine the mass m_2 of the other secondary particle:

$$\frac{m_2}{m_1} = \sqrt{\left(\frac{M}{m_1}-1\right)^2 - 2\frac{M}{m_1}\frac{w_1^*}{m_1}}.$$

The possible angles with which the secondary particle can move relative to the primary direction depend on the ratio

$$\gamma_n = \frac{\alpha_n}{\alpha} = \frac{\beta}{\beta_n^*}.$$

For $\beta > \beta_n^*$, the particle n always forms an acute angle with the primary direction, and the maximum value of this angle is found from (1,21), (7,2), and (7,3) to be:

$$\sin \vartheta_{n\max} = \frac{\mathsf{K}_n^*}{\mathsf{K}}. \tag{7,5}$$

Only for $\mathsf{K} \geq \mathsf{K}_n^*$ is the direction of flight limited by (7,5).

The momentum of the particle n emitted in the direction ϑ_n is given by (2,5) or, in our present notation, using (7,2) and (7,3), by the equation

$$\left.\begin{aligned} k_n(\vartheta_n) = \frac{m_n}{1+\mathsf{K}^2\sin^2\vartheta_n}\Bigg\{ & \mathsf{K}\sqrt{1+\mathsf{K}_n^{*2}}\cos\vartheta_n \pm \\ & \pm \mathsf{K}_n^*\sqrt{(1+\mathsf{K}^2)\left(1-\frac{\mathsf{K}^2}{\mathsf{K}_n^{*2}}\sin^2\vartheta_n\right)}\Bigg\}. \end{aligned}\right\} \tag{7,6}$$

As regards the sign, the same specifications hold as in the case of (2,5), *viz.* for $\mathsf{K} \leq \mathsf{K}_n^*$ we take the + sign, whereas for $\mathsf{K} > \mathsf{K}_n^*$ we have in every direction two possible momenta which differ with regard to sign in (7,6).

In order to observe in the cloud chamber the decay in flight of a meson with a lifetime τ_0, the mean free path for decay

$$l = \frac{\beta c}{\sqrt{1-\beta^2}}\tau_0 = K l_0, \quad l_0 = c\tau_0 \quad (c = \text{light velocity})$$

should be of the order 3—30 cm. For a lifetime $\tau_0 \sim 10^{-10}$ sec ($l_0 \sim 3$ cm) this gives K of the order 1—10, whereas for a lifetime $\tau_0 \sim 10^{-9}$ sec ($l_0 \sim 30$ cm) we must have K of the order 0.1—1.

The value K_n^* for the secondary particle observed in the decay of a π-meson can be estimated from the work of LATTES, OCCHIALINI and POWELL [3], who measured the range of the

secondary particles arising from the decay of stopped mesons in emulsions. Assuming particular values for the mass of the secondary particle, they obtain corresponding values for its kinetic energy w_n^* from which, by use of (7,4), K_1^* can be determined as follows:

Mass m_1 (in units of the electron mass)	100	150	200	250	300
w_1^* in MeV	3.0	3.6	4.1	4.5	4.85
K_1^*	0.35	0.31	0.29	0.27	0.25

We therefore expect that in all cases where $\mathsf{K} > 0.35$, the secondary particle in the laboratory system is emitted within a cone with a half angle given by (7,5).

In the rest system of the primary particle, the secondary particle can be emitted in every direction with the same probability. From the uniform angular distribution in the m.c.f. it follows, as mentioned in § 2, that the probability per unit energy range for the secondary particle having an energy e_n between the limits

$$e_{n\,\min} \leq e_n \leq e_{n\,\max}$$

is constant and equal to

$$\sigma_n(e_n) = \frac{1}{2f} = \frac{M}{2bK}.$$

The minimum and maximum energies of the secondary particle for a given momentum K of the primary particle are given by (2,9).

The angular distribution of the secondary particles is given by (2,12). In the case $\mathsf{K} > \mathsf{K}_n^*$, the direction of particle n lies within a cone of half angle $\vartheta_{n\,\max}$ and the probability per unit solid angle becomes infinite for $\vartheta_n = \vartheta_{n\,\max}$.

For this case, it is therefore more reasonable to calculate the integral probability $P(\vartheta_n)$ that the direction of the secondary particle lies inside a cone with the half angle ϑ_n. To the angle ϑ_n two angles ϑ_{n+}^* and ϑ_{n-}^* correspond in the m.c.f., and to the angle $\vartheta_n = 0$ correspond in the m.c.f. the angles $\vartheta_n^* = 0$ and $\vartheta_n^* = \pi$. Consequently, the solid angle in the m.c.f., which cor-

responds to the cone of half angle ϑ_n in the laboratory frame, is

$$2\pi (1 - \cos \vartheta^*_{n+}) + 2\pi (1 + \cos \vartheta^*_{n-}).$$

Dividing by 4π, we obtain the probability $P_n (\vartheta_n)$ from (2,2)

$$P(\vartheta_n) = 1 - \frac{\cos \vartheta_n}{1+\mathsf{K}^2 \sin^2 \vartheta_n} \sqrt{1 - \frac{\mathsf{K}^2}{\mathsf{K}^{*2}_n} \sin^2 \vartheta_n}.$$

For the decay of an ordinary meson ($M \sim 200\, m_e$) into an electron and a neutrino, we have for the electron, from (7,1) and (7,3),

$$\mathsf{K}^*_e \sim 100.$$

Therefore, the case discussed above, $\mathsf{K} > \mathsf{K}^*_e$, is only realized for $K > 100\, M$, i. e. for meson energies above $10^{10}\, eV$. For meson energies much lower than $10^{10}\, eV$ we can neglect $\mathsf{K}^2/\mathsf{K}^{*2}_e$ compared to 1 ($\gamma_e = \beta$) and obtain from (2,12) and (2,5) for the probability per unit solid angle of finding the decay electron at an angle ϑ, φ to the primary direction

$$\sigma(\vartheta, \varphi) = \frac{1}{4\pi} \frac{1-\beta^2}{(1-\beta \cos \vartheta)^2}. \tag{7,7}$$

The probability $P\left(\frac{\pi}{2}\right)$ that the electron goes in a forward direction is, from (7,7),

$$P\left(\frac{\pi}{2}\right) = \frac{1}{2}(1+\beta). \tag{7,8}$$

The formulae (7,7) and (7,8) are exactly valid when the secondary particle under consideration has a vanishing rest mass.

§ 8. β-Decay of Nuclei.

So far we have considered only processes with two free particles in the final state. In the case with three particles in the final state the conservation laws have the form

$$E = \sqrt{m_1^2 + k_1^2} + \sqrt{m_2^2 + k_2^2} + \sqrt{m_3^2 + k_3^2}$$

$$\vec{K} = \vec{k}_1 + \vec{k}_2 + \vec{k}_3 .$$

If we now fix the momentum of one of the three particles, say particle *3*, we have the same situation as in § 1 if, in all equations, $\vec{K}$ and E are replaced by $\vec{K}'$ and E' given by

$$\vec{K}' = \vec{K} - \vec{k}_3$$

$$E' = E - \sqrt{m_3^2 + k_3^2} .$$

The momentum ellipsoid together with the points A_1 and A_2, defined by $\vec{K}'$, E', m_1 and m_2, gives the possible momenta of the particles *1* and 2 for a chosen momentum of particle *3*. It may be noted that the m.c.f. in the preceding considerations is now no more the m.c.f. of the whole system, but only that of the two particles 1 and 2.

We shall now apply the geometrical picture to the β-decay of a nucleus of mass M at rest ($\vec{K} = 0$).[1] In the final state, we have three particles: an electron, a neutrino, and a recoil nucleus. We assume a vanishing rest mass for the neutrino. We shall use the picture for the determination of the possible momenta $\vec{k}_e$ and $\vec{k}_\nu$ of the electron and the neutrino for a given momentum $\vec{k}_r$ of the recoil nucleus. This momentum can vary between the limits $k_{r\min} = 0$ and a certain $\vec{k}_{r\max}$.

Denoting by m_r and w_r the mass and the kinetic energy of the recoil nucleus, we have

$$\vec{K}' = -\vec{k}_r , \qquad E' = \Delta - w_r , \tag{8,1}$$

where

$$\Delta = M - m_r$$

is the energy difference between the initial and the final nucleus. The energy N' of the system consisting of the electron and the neutrino, in the rest system of these two particles, is now

$$N' = \sqrt{E'^2 - K'^2} = \sqrt{\Delta^2 - 2 M w_r} .$$

1 The possibility of applying the geometrical picture to the problem of β-decay was suggested by mag. sc. O. KOFOED-HANSEN.

The semi-minor axis of the momentum ellipsoid is then, according to (1,7),

$$b = \frac{\Delta^2 - m_e^2 - 2 M w_r}{2 \sqrt{\Delta^2 - 2 M w_r}}. \tag{8,2}$$

Since b cannot be negative, we see that the maximum value of w_r is given by

$$w_{r\,\max} = \frac{\Delta^2 - m_e^2}{2 M}$$

and, consequently, Δ can be determined from a measurement of the maximum recoil energy [10].

For this maximum value of w_r, we have $b = 0$ and, therefore, $\alpha_\nu = f = 0$ (α_ν referring to the neutrino) so that the neutrino energy vanishes. Since the kinetic energy of the nucleus is very small we can put, with a sufficient degree of approximation,

$$k_r^2 = 2 M w_r$$

thus obtaining from (8,2)

$$b = \frac{k_{r\,\max}^2 - k_r^2}{2 \sqrt{\Delta^2 - k_r^2}}.$$

For the eccentricity of the ellipsoid we have, from (1,6) and (8,1),

$$\beta = \frac{k_r}{\Delta} \tag{8,3}$$

and for the semi-major axis, in the same approximation,

$$a = \Delta \frac{k_{r\,\max}^2 - k_r^2}{2 (\Delta^2 - k_r^2)}.$$

The momentum ellipsoid goes for $k_r = 0$ over in a sphere and reduces for $k_{r\,\max}$ to a point. The semi-major and semi-minor axes decrease with increasing k_r.

The origin A_e of the momentum vector of the electron is at the distance α_e apart from the centre of the ellipsoid

$$\alpha_e = \frac{k_r}{2}\left(1 + \frac{m_e^2}{\Delta^2 - k_r^2}\right), \tag{8,4}$$

while α_ν is given by

$$\alpha_\nu = f = \frac{k_r M}{(\Delta^2 - k_r^2)}(w_{r\max} - w_r) = \frac{k_r (k_{r\max}^2 - k_r^2)}{2(\Delta^2 - k_r^2)}. \tag{8,5}$$

The lower and upper limits of possible kinetic energies of the electron, for a given momentum of the recoil nucleus, are from (2,9) equal to

$$w_{e\min} = \frac{\alpha_e}{\beta} - m_e - f, \quad w_{e\max} = \frac{\alpha_e}{\beta} - m_e + f,$$

respectively. Putting for α_e, β and f the values given by (8,3), (8,4), and (8,5), we obtain

$$w_{e\min} = \frac{(\Delta - m_e - k_r)^2}{2(\Delta - k_r)}, \quad w_{e\max} = \frac{(\Delta - m_e + k_r)^2}{2(\Delta + k_r)}.$$

In carrying out integrations over the possible energies of the electron for a given energy of the recoil nucleus, it may be noticed that w_e can assume all values between $w_{e\min}$ and $w_{e\max}$ and that, since the point A_e lies outside the focus of the momentum ellipsoid, the angle ϑ_e is a single valued function of w_e.

This paper was written partly in the Institute for Theoretical Mechanics, Jagellonian University of Cracow, and partly in the Institute for Theoretical Physics, University of Copenhagen. I wish to express my sincere thanks to Professor Niels Bohr for the opportunity to work in his Institute and for stimulating discussions.

REFERENCES

1. L. Landau and E. Lifschitz, Theoretical Physics, vol. IV, Moscow 1941.
2. G. Wataghin, Acad. Bras. Sciencias, 1941.
3. C. M. G. Lattes, G. P. S. Occhialini, F. C. Powell, Nature **160**, 453, 486, 1947.
4. C. E. Mandeville, Journal of the Franklin Institute **244**, 385, 1947.
5. A. Rogozinski, Phys. Rev. **65**, 300, 1944.
6. L. Leprince Ringuet, S. Gorodetzky, E. Nageotte and R. Richard-Foy, Phys. Rev. **59**, 460, 1941.
7. F. C. Champion, Proc. Roy. Soc. A **136**, 630, 1932.
8. N. N. Das Gupta and S. K. Ghosh, Rev. Mod. Phys. **18**, 225, 1946.
9. M. L. Wiedenbeck and C. J. Marhoefer, Phys. Rev. **67**, 54, 1945.
10. J. C. Jacobsen and O. Kofoed-Hansen, Det Kgl. Danske Vidensk. Selskab, Mat.-fys. Medd. **23**, Nr. 12, 1945.

Indleveret til selskabet den 28. november 1947.
Færdig fra trykkeriet den 17. Marts 1950.

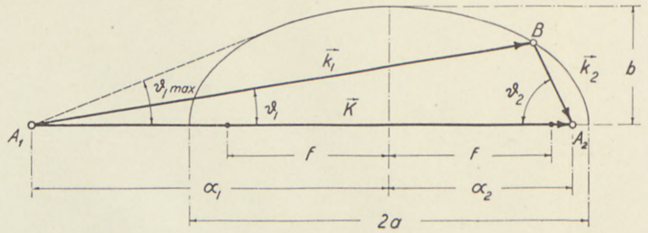

Fig. 1. Geometrical picture of energy-momentum conservation. The semi-minor axis of the ellipse is given by (1,7). The eccentricity is equal to the mass centre velocity of the system. $\vec{k}_1$, $\vec{k}_2$ are momenta of the particles in the final state.

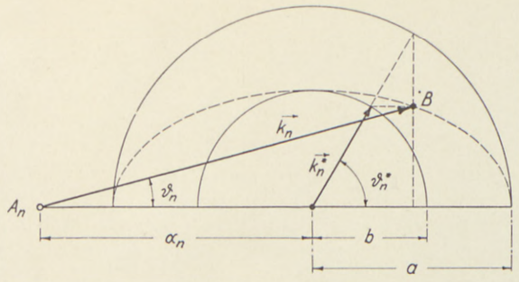

Fig. 3. Transition from the m.c.f. to the laboratory frame of reference. Quantities referring to the m.c.f. are denoted by an asterisk. The vector $\vec{k}_n^*$ with the origin in the centre of the ellipsoid has the length b and its component perpendicular to $\vec{K}$ is equal to the component of the vector $\vec{k}_n$ in the same direction, since $\vec{k}_n^*$ and $\vec{k}_n$ are connected by a Lorentz transformation with a relative velocity in the direction of $\vec{K}$.

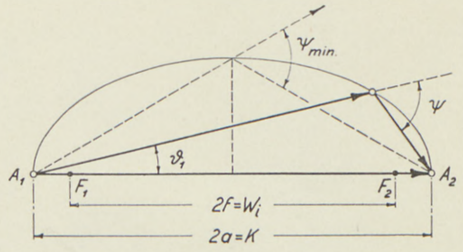

Fig. 4. Elastic collision between two particles of equal mass. The velocities after the collision form always an acute angle $\psi = \vartheta_1 + \vartheta_2$ which is larger than or equal to $\psi_{\min}\left(\cos\psi_{\min} = \frac{W_i}{W_i + 4\,m}\right)$. The distance $2\,f$ between the foci = kinetic energy W_i of the incident particle, and the major axis $2\,a = K$.

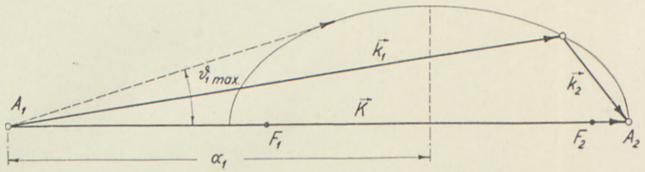

Fig. 5. Elastic collision in which the incident particle has a larger mass than the target particle ($m_1 > m_2$). Maximum deflection angle of the incident particle is given by $\sin\vartheta_{1\,\max} = \frac{m_2}{m_1}$. For instance, collision of a meson with an electron.

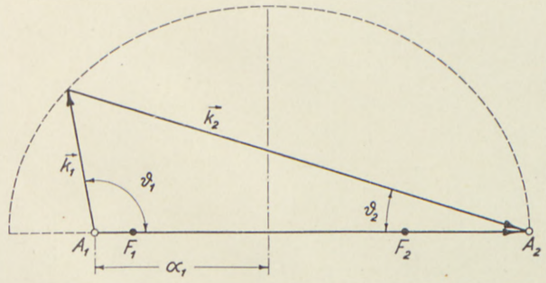

Fig. 6. Elastic collision in which the incident particle has a smaller rest mass than the target particle, for instance, scattering of photons by free electrons (in this case, A_1 coincides with F_1).

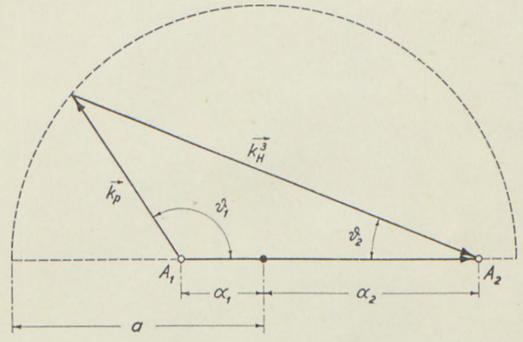

Fig. 7. Geometrical picture of the exothermic reaction $^2D\,(d,\,p)\,^3H$, ($Q \simeq 4\,MeV$) for an energy $W_i = 2\,MeV$ of the incident deuteron. $a = 83.5\,MeV$, $a_1 = 21.5\,MeV$, $a_2 = 3a_1$.

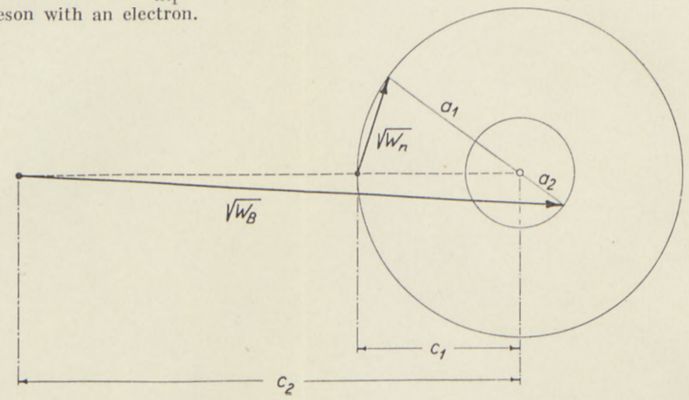

Fig. 8. Picture giving the energies of the outcoming particles in the endothermic reaction

$^9Be(p,n)^9B$ ($Q = -1{,}83\,MeV$, $\delta = 2{,}03\,MeV$, $a_1 = \frac{9}{10}\sqrt{W_i - 2{,}03}$, $a_2 = \frac{1}{3}a_1$, $c_1 = \frac{1}{10}\sqrt{W_i}$, $c_2 = 3c_1$)

for an energy W_i which is $25\,keV$ above the threshold where $a_1 = c_1 = 4.5\,\sqrt{keV}$. w_n and w_B represent the energies of the outgoing neutron and boron nucleus.

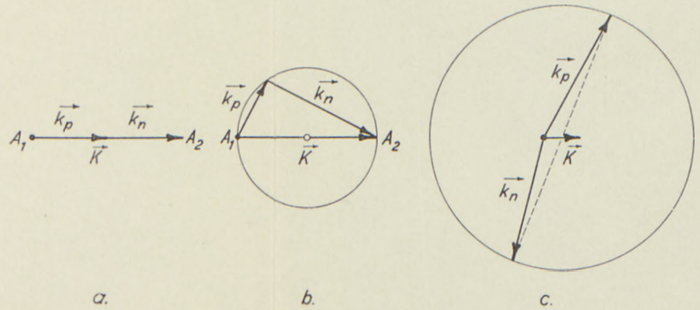

Fig. 9. Photodisintegration of the deuteron. a. $K = \delta$, $a = 0$. Exactly at the threshold ($1.3\,keV$ above the binding energy of the deuteron), the proton and the neutron are moving in the primary direction and have each an energy $0{,}65\,keV$. b. $K = \delta\left(1 + \frac{\delta}{2\,m}\right)$, $\gamma = 1$. At an energy $1.3\,keV$ above the threshold, the proton and the neutron paths form a right angle whatever their angle with the primary direction. c. $K = 2\delta$, $\gamma = 0.04$, the proton and the neutron are moving in nearly opposite directions.